

THESIS

METHODOLOGY FOR PREDICTING MAXIMUM VELOCITY AND SHEAR
STRESS IN A SINUOUS CHANNEL WITH BENDWAY WEIRS USING
1-D HEC-RAS MODELING RESULTS

Submitted by

Paul Sclafani

Department of Civil and Environmental Engineering

In partial fulfillment of the requirements

For the Degree of Master of Science

Colorado State University

Fort Collins, Colorado

Summer 2010

COLORADO STATE UNIVERSITY

June 4, 2010

WE HEREBY RECOMMEND THAT THE THESIS PREPARED UNDER OUR SUPERVISION BY PAUL SCLAFANI ENTITLED METHODOLOGY FOR PREDICTING MAXIMUM VELOCITY AND SHEAR STRESS IN A SINUOUS CHANNEL WITH BENDWAY WEIRS USING 1-D HEC-RAS MODELING RESULTS BE ACCEPTED AS FULFILLING IN PART REQUIREMENTS FOR THE DEGREE OF MASTER OF SCIENCE.

Committee on Graduate Work

Chester C. Watson

Ellen E. Wohl

Advisor: Christopher I. Thornton

Department Head: Luis A. Garcia

ABSTRACT OF THESIS

METHODOLOGY FOR PREDICTING MAXIMUM VELOCITY AND SHEAR STRESS IN A SINUOUS CHANNEL WITH BENDWAY WEIRS USING 1-D HEC-RAS MODELING RESULTS

The Middle Rio Grande is a 29-mi reach of the Rio Grande River in central New Mexico that extends from downstream of Cochiti Dam to Bernalillo, New Mexico. A series of anthropogenic factors including the construction of flood control levees and Cochiti Dam have altered the historically-braided morphology of the Middle Rio Grande to a more sinuous, degrading reach, with less overall channel migration within a natural floodplain area. Concentration of flow within an incised channel has caused areas of bank erosion and threatened riverside infrastructure, farmland productivity, irrigation systems, levee function, aquatic habitat, and riparian vegetation. Colorado State University (CSU) constructed an undistorted 1:12 Froude scale, fixed bed, physical model consisting of two channel bend geometries that are characteristic of the Middle Rio Grande reach below Cochiti Dam. Small rock structures extending from the outer bank of the bend into the main channel, referred to as bendway weirs, were constructed within each bend to research methods of stabilizing the outer bank with minimal disruption of sensitive habitat and riparian vegetation.

Bendway weirs deflect current from the bank in which they are installed to the center of the channel, thus, moving erosive forces away from a degrading bank, establishing a stable channel, and providing or maintaining aquatic habitat between weir structures. Placement of bendway weirs along a river bank effectively creates two zones of flow: 1) the main or constricted flow where the velocity, shear stresses, and potential for channel degradation are increased, and 2) the area between weirs where velocities and shear stresses are greatly reduced and sediment deposition is encouraged. Design criterion to predict increases in velocity and shear stress caused by placement of bendway weirs in a channel bend has not yet been established. Two-dimensional and three-dimensional computer models have been utilized to describe complex flow phenomena associated with bendway weirs in channel bends; however, such computer models may not be practical for typical design projects (Jia et al., 2005; Molls, et al., 1995; Abad *et al.*, 2008; Seed, 1997). Because of historic precedence, continual development, and prevalence in the engineering community, many engineers use one-dimensional (1-D) computer modeling tools, such as Hydrologic Engineering Center's River Analysis System (HEC-RAS), as a first choice in modeling channel flow.

1-D computer models were developed for the trapezoidal channel geometry present in the physical model and for fifteen weir configurations constructed during testing at CSU. Computed results from the 1-D models were compared to data collected from the Middle Rio Grande physical model. Regression relationships were developed to predict velocities and shear stresses in the trapezoidal channel constructed for physical testing at CSU, at the tips of the constructed bendway weirs, and along the inner bank opposite the constructed bendway weirs. From predictive regression relationships for the

velocity and shear stress in channel bends, with and without bendway weirs, a four-step design process was developed to provide practicing engineers with guidance that can be used to design bendway weir fields.

Paul Sclafani
Department of Civil and Environmental Engineering
Colorado State University
Fort Collins, CO 80523
Summer 2010

ACKNOWLEDGMENTS

Completion of this work would not have been possible without the support of many people for whom I am greatly indebted. I would like to, first, thank my advisor, Dr. Christopher Thornton for his support and guidance through this project and giving me the opportunity to work in the Hydraulics Laboratory during my Master's studies. I would like to thank my committee members Dr. Chester Watson and Dr. Ellen Wohl for their commitment and input in this and previous research on the Middle Rio Grande Projects.

Next, I would like to particularly thank Amanda Cox for her unremitting support, guidance, and commitment to my final product. It has been a pleasure working with her over the past few years, and I could not have completed this work without her support, counsel, and friendship.

I would also like to thank the support staff at the Engineering Research Center, for assisting me in various capacities along the way, including Jr. Garza, Tom Brisbane, Gloria Garza, and Jan Barman. Thank you, as well, to all the graduate students, present and past, that have helped me on this research and in my graduate work as a whole.

Finally, I would like to thank my family and friends for their support, patience, guidance, and sense of community that has allowed me to maintain some sanity throughout my studies.

TABLE OF CONTENTS

ABSTRACT OF THESIS	iii
ACKNOWLEDGMENTS	vi
LIST OF FIGURES	xi
LIST OF TABLES	xvii
LIST OF SYMBOLS	xx
1 INTRODUCTION	1
1.1 General Background.....	1
1.2 Project Background.....	2
1.3 Research Objectives	4
2 LITERATURE REVIEW	8
2.1 Introduction	8
2.2 Channel Patterns.....	9
2.3 Meander Geometry.....	15
2.4 Meander Flow Characteristics.....	17
2.4.1 Background.....	17
2.4.2 Research	28
2.4.2.1 Ippen <i>et al.</i> (1960a,b).....	28
2.4.2.2 Ippen and Drinker (1962).....	31
2.4.2.3 USBR (1964)	33
2.4.2.4 Yen (1965)	34
2.4.2.5 Heintz (2002)	37
2.5 Bendway Weir as an Erosion Countermeasure.....	44
2.5.1 Background.....	44
2.5.2 Bendway-weir Geometry.....	46
2.5.2.1 Weir Height.....	47
2.5.2.2 Orientation Angle.....	48
2.5.2.3 Weir Length	49
2.5.2.4 Cross Section	50
2.5.2.5 Permeability	50
2.5.2.6 Spacing Ratio	51
2.5.3 Flow Pattern.....	53
2.5.3.1 Background.....	53
2.5.3.2 Copeland (1983).....	57

2.5.3.3	Brown (1985).....	58
2.5.3.4	Seed (1997).....	61
2.5.3.5	Heintz (2002).....	65
2.5.3.6	Darrow (2004).....	69
2.5.3.7	Environmental Considerations.....	73
2.6	Computer Modeling.....	74
2.6.1	3-D Modeling.....	76
2.6.2	2-D Modeling.....	78
2.6.3	1-D Modeling.....	79
2.7	Summary.....	83
3	PHYSICAL MODEL DESCRIPTION.....	84
3.1	Introduction.....	84
3.2	Model Geometry.....	84
3.3	Model Construction.....	89
3.3.1	Introduction.....	89
3.3.2	Headbox.....	90
3.3.3	Test Section.....	91
3.3.4	Tailbox.....	93
3.4	Instrumentation.....	94
3.4.1	Flow-rate Measurement.....	95
3.4.2	Flow-depth Measurement.....	96
3.4.3	Velocity Measurement.....	97
3.4.4	Bed Shear Measurement.....	98
3.5	Model Calibration.....	101
3.6	Weir Design.....	103
3.6.1	Construction.....	103
3.6.2	Weir Geometry.....	106
3.6.2.1	Introduction.....	106
3.6.2.2	Spacing Ratio.....	108
3.6.2.3	Orientation Angle (θ).....	108
3.6.2.4	Weir Length.....	109
3.6.3	Test Program.....	110
3.6.4	Additional Instrumentation.....	112
4	DATABASE DEVELOPMENT.....	114
4.1	Introduction.....	114
4.2	Baseline Results.....	115
4.3	Weir Configuration Results.....	118
5	COMPUTER MODELING APPROACH.....	122
5.1	Baseline Modeling Approach.....	122
5.1.1	Introduction.....	122
5.1.2	Cross-section Geometry.....	123
5.1.3	Reach Length.....	123
5.1.4	Manning's Roughness Coefficient.....	124
5.1.5	Contraction and Expansion Coefficients.....	125

5.1.6	Baseline Model Results	125
5.2	Bendway-weir Modeling Approach	134
5.2.1	Introduction	134
5.2.2	Model Selection.....	134
5.2.2.1	Bendway-weir Computer Modeling Technique 1.....	135
5.2.2.2	Bendway-weir Computer Modeling Technique 2.....	137
5.2.2.3	Bendway-weir Computer Modeling Technique 3.....	140
5.2.2.4	Bendway-weir Computer Modeling Technique 4.....	143
5.2.2.5	Conclusion of Model Selection.....	147
5.2.2.6	Weir Model Results	150
6	BASELINE ANALYSIS.....	153
6.1	Introduction	153
6.2	Velocity	154
6.3	Boundary Shear Stress	158
6.4	Conclusion.....	161
7	WEIR CONFIGURATION ANALYSIS.....	165
7.1	Introduction.....	165
7.2	Analysis Approach	166
7.3	Velocity Analysis	170
7.3.1	MVR Inner.....	170
7.3.2	MVR Tip	175
7.3.3	MVR Center	180
7.3.4	Vr Inner	185
7.3.5	Vr Tip	189
7.4	Shear-stress Analysis.....	193
7.4.1	MTR Inner	193
7.4.2	MTR Tip.....	197
7.4.3	MTR Center.....	201
7.4.4	Tr Inner	205
7.4.5	Tr Tip.....	209
7.5	Summary	213
8	CONCLUSIONS AND RECOMMENDATIONS.....	215
8.1	Overview	215
8.2	Modeling Technique	216
8.3	Baseline Conditions.....	218
8.4	Weir Configurations.....	219
8.5	Recommendations for Further Research.....	224
9	REFERENCES	226
APPENDIX A	BASELINE SURVEY.....	236
APPENDIX B	PHYSICAL DATA.....	249

APPENDIX C	HEC-RAS DATA	266
APPENDIX D	STATISTICAL DATA	346
APPENDIX E	STATISTICAL THEORY	358

LIST OF FIGURES

Figure 1.1: Location Map of Project Reach (Figure 1.1 in Darrow (2004)).....	3
Figure 2.1: Definition of Sinuosity	9
Figure 2.2: Channel Pattern Classification Based on Schumm and Brakenridge (1987; Figure 1).....	10
Figure 2.3: Channel Pattern Relative to Grain Size and Unit Stream Power (Figure 3 in Van den Berg (1995)).....	13
Figure 2.4: Channel Pattern relative to Grain Size for Sand-bed Streams (Figure 3 in Bledsoe and Watson (2001)).....	14
Figure 2.5: Channel Pattern Relative to Grain Size for Gravel-bed Streams (Figure 6 in Bledsoe and Watson (2001))	14
Figure 2.6: Typical Trapezoidal Cross-section Characteristics	16
Figure 2.7: Subdivision of a Channel Cross Section within a Meander Bend (Figure 5.19 in Knighton (1998)).....	16
Figure 2.8: Planimetric Pattern Factors for a Typical Meander.....	17
Figure 2.9: Representation of Spiraling Flow through Meander Bends (Figure 5.19 in Knighton (1998)).....	19
Figure 2.10: Velocity Distribution through Meandering Bends (Figure 7.42 in Leopold <i>et al.</i> (1964)).....	20
Figure 2.11: Model of Velocity Direction through a Channel Bend (Figure 5.19 in Dietrich (1987)).....	21
Figure 2.12: Model of Shear-stress Distribution through Channel Meander (Figure 5.19 in Dietrich (1987)).....	23
Figure 2.13: Channel Migration versus Radius of Curvature over Top Width from a Study by Hickin and Nanson (1984; Figure 3) (Figure 5.21 in Julien (2002))	25
Figure 2.14: Cross-stream Flow as a Function of Tortuosity (Figure 4 in Welch and Wright (2005)).....	26
Figure 2.15: Schematic of Testing Facilities Used in Ippen <i>et al.</i> (1960a,b; Figure 3 in Ippen <i>et al.</i> (1960a)).....	29
Figure 2.16: Schematic of Test Facility Used in USBR (1964; Frame 1).....	33
Figure 2.17: Schematic of Test Facility Used in Yen (1965; Figure 2).....	35

Figure 2.18: Schematic of Testing Facility Used in Heintz (2002; Figure 3.11).....	38
Figure 2.19: Velocity Vectors through the Upstream Bend at 16 cfs, $y = 0.93$ ft (Figure 4.4 in Heintz (2002))	38
Figure 2.20: Outer Bank Velocity Comparison with Centerline Velocity (Figure 4.5 in Heintz (2002))	40
Figure 2.21: Inner Bank Velocity Comparison with Centerline Velocity (Figure 4.6 in Heintz (2002))	40
Figure 2.22: Upstream Shear-stress Distributions (Figure 4.7 in Heintz (2002)).....	41
Figure 2.23: Downstream Shear-stress Distributions (Figure 4.8 in Heintz (2002)).....	42
Figure 2.24: Outer Bank Shear-stress Comparison with Centerline Shear Stress (Figure 4.11 in Heintz (2002))	43
Figure 2.25: Inner Bank Shear-stress Comparison with Centerline Shear Stress (Figure 4.12 in Heintz (2002))	43
Figure 2.26: Variable Definition for Bendway Weirs	47
Figure 2.27: Weir Placement as a Function of Downstream Riffle/Insertion (NRCS; Figure 11 in Welch and Wright (2005)).....	52
Figure 2.28: Vortex Formation near Weir Tip (Figure 3.1.8 in Richardson and Simons (1974)).....	54
Figure 2.29: Siltation Patterns Associated with Upstream and Downstream Orientated Weirs (Figure 6.45 in Przedwojski <i>et al.</i> (1995)).....	55
Figure 2.30: Empirically-derived Plot of Limiting Velocity Based on Bed- material Grain Size (Figure 12 in Pemberton and Lara (1984)).....	57
Figure 2.31: Maximum Velocity off Weir Tip as a Function of Permeability and Weir Angle (Brown, 1985).....	59
Figure 2.32: Maximum Velocity off Weir Tip as a Function of Weir Length (Brown, 1985)	60
Figure 2.33: Maximum Outer Bank Velocity Ratio versus Spacing Ratio (Figure 4.20 in Heintz (2002))	67
Figure 2.34: Maximum Centerline Velocity Ratio versus Spacing Ratio (Figure 4.21 in Heintz (2002))	68
Figure 2.35: Maximum Inner Bank Velocity Ratio (Figure 4.23 in Heintz (2002))	69
Figure 2.36: Schematic of Computational Directions for 3-D, 2-D, and 1-D Models.....	75
Figure 3.1: Study Reach Planform Bend Geometry Curve Types (Figure 3.1 in Heintz (2002))	86
Figure 3.2: Aerial View of Horsetooth Reservoir and the ERC (adapted from Figure 3.3 in Heintz (2002)).....	88

Figure 3.3: Model Layout of the Type 1 and Type 3 Bends in Plan View	89
Figure 3.4: Schematic of the Physical Model Layout in the Hydromachinery Laboratory	90
Figure 3.5: Headbox Under Construction Including Pipe Manifold and Rock Baffle (Figure 3.5 in Heintz (2002))	91
Figure 3.6: Placement of Backfill between Model Sections During Construction.....	92
Figure 3.7: Placement and Roughening of the Concrete Cap.....	93
Figure 3.8: Discharge over Stop-log Configuration During Testing.....	94
Figure 3.9: Baseline Cross-section Layout Showing Physical Model Cross Sections	95
Figure 3.10: Electromagnetic Flow Meter.....	96
Figure 3.11: Location of Piezometer Taps Looking Downstream.....	97
Figure 3.12: Acoustic Doppler Velocity Meter	98
Figure 3.13: Preston-tube Schematic	99
Figure 3.14: Preston-tube Calibration Curve for a Concrete Channel.....	100
Figure 3.15: Layout of Survey Points, Cross Sections, and Benchmarks for Baseline Model.....	102
Figure 3.16: Stop-log Configuration for 8, 12, and 16 cfs.....	103
Figure 3.17: Weir Crest and Bottom Width Definitions.....	104
Figure 3.18: Plywood Shape Template for Weir Construction.....	105
Figure 3.19: Impermeable Bendway Weir during Testing	106
Figure 3.20: Geometric Properties Used in Weir Placement.....	107
Figure 3.21: Location of Additional Weir Data Points.....	113
Figure 4.1: Measured Depth Profiles for Baseline Physical Tests.....	115
Figure 4.2: Measured Velocity Profiles for Baseline Physical Tests.....	116
Figure 4.3: Measured Shear-stress Profiles for Baseline Physical Tests.....	117
Figure 4.4: Comparison of the Maximum Velocity Values for the Inner Bank and Weir Tip	120
Figure 4.5: Comparison of the Maximum Shear-stress Values for the Inner Bank and Weir Tip.....	121
Figure 5.1: Cross-section Spacing used for Baseline Model.....	123
Figure 5.2: Water-surface Profiles for Baseline Conditions.....	126
Figure 5.3: Velocity Profile at Piezometer C (right bank looking downstream) for Baseline Conditions.....	128

Figure 5.4: Velocity Profile at Piezometer D (channel center) for Baseline Conditions	129
Figure 5.5: Velocity Profile at Piezometer E (left bank looking downstream) for Baseline Conditions.....	129
Figure 5.6: Predicted Velocity versus Measured Velocity for Baseline Models.....	130
Figure 5.7: Shear-stress Profile for Piezometer C (right bank looking downstream) for Baseline Conditions.....	131
Figure 5.8: Shear-stress Profile for Piezometer D (channel center) for Baseline Conditions	132
Figure 5.9: Shear-stress Profile for Piezometer E (left bank looking downstream) for Baseline Conditions.....	132
Figure 5.10: Predicted Shear Stress versus Measured Shear Stress for Baseline Models.....	133
Figure 5.11: Schematic of Modeling Technique 1.....	135
Figure 5.12: Water-surface Profiles for Test W01 Using Modeling Technique 1.....	136
Figure 5.13: Water-surface Profile for Test W02 Using Technique 1.....	136
Figure 5.14: Water-surface Profile for Test W03 Using Technique 1.....	137
Figure 5.15: Schematic of Modeling Technique 2.....	138
Figure 5.16: Water-surface Profile for Test W01 Using Modeling Technique 2	139
Figure 5.17: Water-surface Profile for Test W02 Using Modeling Technique 2	139
Figure 5.18: Water-surface Profile for Test W03 Using Modeling Technique 2	140
Figure 5.19: Schematic of Modeling Technique 3.....	141
Figure 5.20: Water-surface Profile for Test W01 Using Modeling Technique 3	142
Figure 5.21: Water-surface Profile for Test W02 Using Modeling Technique 3	142
Figure 5.22: Water-surface Profile for Test W03 Using Modeling Technique 3	143
Figure 5.23: Schematic of Modeling Technique 4.....	144
Figure 5.24: Typical Example of Weir Geometry Incorporated into Baseline Cross-section Geometry	145
Figure 5.25: Water-surface Profile for Test W01 Using Modeling Technique 4	145
Figure 5.26: Water-surface Profile for Test W02 Using Modeling Technique 4	146
Figure 5.27: Water-surface Profile for Test W03 Using Modeling Technique 4	146
Figure 5.28: Average Percent Error between Computed and Measured Water-surface Elevations for each Modeling Technique	148
Figure 5.29: Average Percent Error between Computed and Measured Velocity and Shear Stress for each Modeling Technique	150

Figure 5.30: Comparisons between Predicted and Measured Velocity for Weir Models.....	151
Figure 5.31: Comparisons between Predicted and Measured Shear Stress for Weir Models.....	152
Figure 6.1: Radius of Curvature, R_c/Tw , Tw versus Bend Velocity Factor, $K_{BEND-VELOCITY}$	156
Figure 6.2: $K_{BEND-SHEAR}$ using Computed Shear Stress from HEC-RAS.....	160
Figure 7.1: Regression Analysis for MVR_{inner} Compared with Heintz (2002) and Darrow (2004).....	172
Figure 7.2: Residual Plot from MVR_{inner} Analysis.....	173
Figure 7.3: Quantile Plot of Residual from MVR_{inner} Analysis.....	173
Figure 7.4: MVR_{inner} Analysis Showing Outliers and Upper Envelope.....	175
Figure 7.5: Regression Analysis for MVR_{tip} Compared with Seed (1997).....	177
Figure 7.6: Residual Plot from MVR_{tip} Analysis.....	178
Figure 7.7: Quantile Plot of Residuals from MVR_{tip} Analysis.....	178
Figure 7.8: MVR_{tip} Analysis Showing Outliers and Upper Envelope.....	180
Figure 7.9: Regression Analysis for MVR_{center} Compared with Seed (1997), Heintz (2002), and Darrow (2004).....	182
Figure 7.10: Residual Plot from MVR_{center} Analysis.....	183
Figure 7.11: Quantile Plot of Residuals from MVR_{center} Analysis.....	183
Figure 7.12: MVR_{center} Analysis Showing Outliers and Upper Envelope.....	185
Figure 7.13: Residual Plot from $V_{r-inner}$ Analysis.....	187
Figure 7.14: Quantile Plot of Residuals from $V_{r-inner}$ Analysis.....	188
Figure 7.15: $V_{r-inner}$ Analysis Showing Outliers and Upper Envelope.....	189
Figure 7.16: Residual Plot from the V_{r-tip} Analysis.....	191
Figure 7.17: Quantile Plot of Residuals from the V_{r-tip} Analysis.....	192
Figure 7.18: V_{r-tip} Analysis Showing Outliers and Upper Envelope.....	193
Figure 7.19: Residual Plot from MTR_{inner} Analysis.....	195
Figure 7.20: Quantile Plot of Residuals from MTR_{inner} Analysis.....	196
Figure 7.21: MTR_{inner} Analysis Showing Outliers and Upper Envelope.....	197
Figure 7.22: Residual Plot from MTR_{tip} Analysis.....	199
Figure 7.23: Quantile Plot of Residuals from MTR_{tip} Analysis.....	200
Figure 7.24: MTR_{tip} Analysis Showing Outliers and Upper Envelope.....	201
Figure 7.25: Residual Plot from the MTR_{center} Analysis.....	203

Figure 7.26: Quantile Plot of Residuals from MTR_{center} Analysis	204
Figure 7.27: MTR_{center} Analysis Showing Outliers and Upper Envelope	205
Figure 7.28: Residual Plot from the $T_{r-inner}$ Analysis	207
Figure 7.29: Quantile Plot of the Residuals from the $T_{r-inner}$ Analysis	208
Figure 7.30: $T_{r-inner}$ Analysis Showing Outliers and Upper Envelope	209
Figure 7.31: Residual Plot of the T_{r-tip} Analysis	211
Figure 7.32: Quantile Plot of the Residuals from the T_{r-tip} Analysis	212
Figure 7.33: T_{r-tip} Analysis Showing Outliers and Upper Envelope	213
Figure 8.1: Summary of Cross-section Layout for Modeling Technique 4	217
Figure E.1: Example of a Simple Linear Model Showing Error Associated with Predicted Values	360
Figure E.2: Subdivision of the Total Error about the Mean (Chapman, 2006)	361

LIST OF TABLES

Table 2.1: Test Matrix for Ippen <i>et al.</i> (1960a,b)	30
Table 2.2: Summary of Shear-stress Distribution (Ippen <i>et al.</i> , 1960a,b)	30
Table 2.3: Summary of Shear-stress Distribution (Ippen and Drinker, 1962).....	32
Table 2.4: Summary of Boundary Shear Test Results for USBR (1964)	33
Table 2.5: Summary of Boundary Shear Test Results for Yen (1965).....	37
Table 2.6: Parameters Included in Scour-depth Equations from Various Sources (Copeland, 1983; Welch and Wright, 2005)	56
Table 2.7: Bend Characteristics for the Middle Rio Grande Physical Model (Heintz, 2002).....	65
Table 2.8: <i>MVR</i> Analysis from Heintz (2002).....	69
Table 2.9: Darrow (2004) C_p Values for Selected Regression Equations.....	72
Table 3.1: Similitude Scaling Used for the Physical Model (1:12 Froude Scale)	85
Table 3.2: Prototype Planform Geometry Characteristics (Heintz, 2002).....	86
Table 3.3: Model Planform Geometry Characteristics (Heintz, 2002).....	87
Table 3.4: Weir Dimensions that Remain Constant.....	104
Table 3.5: Configuration Matrix for Bendway-weir Testing.....	111
Table 4.1: Range of Depth Measurements for Baseline Physical Tests	116
Table 4.2: Range of Velocity Measurements for Baseline Physical Tests	117
Table 4.3: Range of Shear-stress Measurements for Baseline Physical Tests.....	118
Table 5.1: Cumulative Reach Length Used in HEC-RAS Model	124
Table 5.2: Average and Maximum Percent Error between Measured Baseline Data and Computed Baseline Results from HEC-RAS	127
Table 5.3: Percent Error for Modeling Technique 1	137
Table 5.4: Percent Error for Modeling Technique 2.....	140
Table 5.5: Percent Error for Modeling Technique 3.....	143
Table 5.6: Percent Error for Modeling Technique 4.....	147
Table 5.7: Average Percent Error between Computed and Measured Water- surface Elevations for Each Modeling Technique	147

Table 5.8: Average Percent Error Between Computed and Measured Velocity for Each Modeling Technique	149
Table 5.9: Average Percent Error Between Computed and Measured Shear Stress for Each Modeling Technique.....	149
Table 6.1: Velocity Results for Baseline Conditions.....	155
Table 6.2: Computed $K_{BEND-SHEAR}$ Factor for Baseline Data Using Computed Shear Stress from HEC-RAS	159
Table 7.1: Analysis Matrix for Velocity and Shear Stresses	167
Table 7.2: Model Parameters used in Statistical Analysis.....	169
Table 7.3: P-values for MVR_{inner} Regression Equation.....	171
Table 7.4: Outliers from MVR_{inner} Analysis.....	174
Table 7.5: P-values for MVR_{tip} Regression Equation.....	176
Table 7.6: Outliers from MVR_{tip} Analysis.....	179
Table 7.7: P-values for MVR_{center} Regression Equation.....	181
Table 7.8: Outliers from MVR_{center} Analysis.....	184
Table 7.9: P-values for $V_{r-inner}$ Regression Equation.....	186
Table 7.10: Outliers from the $V_{r-inner}$ Analysis.....	187
Table 7.11: P-values for V_{r-tip} Regression Equation	190
Table 7.12: Outliers from the V_{r-tip} Analysis.....	191
Table 7.13: P-values for MTR_{inner} Regression Equation	194
Table 7.14: Outliers from MTR_{inner} Analysis.....	195
Table 7.15: P-values for MTR_{tip} Regression Equation.....	198
Table 7.16: Outliers from MTR_{tip} Analysis	199
Table 7.17: P-values for MTR_{center} Regression Equation.....	202
Table 7.18: Outliers from the MTR_{center} Analysis	203
Table 7.19: P-values for $T_{r-inner}$ Regression Equation.....	206
Table 7.20: Outliers from the $T_{r-inner}$ Analysis.....	207
Table 7.21: P-values for T_{r-tip} Regression Equation.....	210
Table 7.22: Outliers from T_{r-tip} Analysis.....	211
Table 8.1: Summary Average Percent Error between Computed and Measured Water Surface, Velocity, and Shear Stress for Selected Modeling Technique	216
Table 8.2: Summary of $K_{BEND-VELOCITY}$ Analysis.....	218

Table 8.3: Summary of $K_{BEND-SHEAR}$ Analysis Using Computed HEC-RAS Shear Stress	219
Table 8.4: Summary of Velocity Analyses	220
Table 8.5: Summary of Shear-stress Analyses	221
Table 8.6: Velocity Coefficients for Regression Analyses	222
Table 8.7: Shear-stress Coefficients for Regression Analyses	222
Table A.1: Baseline Survey from Heintz (2002)	237
Table B.1: Baseline Depth Data from Physical Tests.....	250
Table B.2: Baseline Velocity and Shear-stress Data from Physical Tests.....	253
Table B.3: Depth Data for Weir Configuration Physical Tests	256
Table B.4: Velocity Data for Weir Configuration Physical Tests	258
Table B.5: Shear-stress Data for Weir Configuration Physical Tests.....	260
Table B.6: Maximum Velocity and Shear-stress Data for Weir Configuration Tests	262
Table C.1: Baseline Data from HEC-RAS	267
Table C.2: Data from Computer Simulation of Weir Fields in HEC-RAS	271
Table D.1: Model Parameters	347
Table D.2: Velocity Terms	351
Table D.3: Shear-stress Terms	355

LIST OF SYMBOLS

A	= total cross-sectional area of flow, m^2
A^*	= ratio of weir area to main channel area = $\frac{sA_g}{(A - sA_g)} \text{ for } 0.15 \leq A^* \leq 1.3$
A_c	= cross-sectional flow area, L^2
A_g	= area of weir below the water surface measured perpendicular to the flow, m^2
A_w	= projected weir area blocking the flow, L^2
α_m	= meander amplitude, L
b	= bottom width of channel, L
B_a	= effect of weir area on tip velocity = $0.13A^* + 0.05$ for $0.13 \leq A^* \leq 1.3$
B_n	= effect of channel roughness on tip velocity = $\begin{cases} F_n & \text{for rectangular weirs} \\ 1 & \text{for tapered weirs } (t^* > 0.5) \end{cases}$
B_s	= effect of weir spacing on tip velocity = $-0.02(S^* - 4)$ for $1.6 \leq S^* \leq 5$

B_t	= effect of crest angle on tip velocity =
	$\begin{cases} 0.8(t^* - 0.6) & \text{for } 0.6 \leq t^* \leq 1.0 \\ 0 & \text{for } 0.5 \leq t^* \leq 0.6 \end{cases}$
β_0	= mean value of Y if all x 's are 0
$\beta_1, \beta_2, \beta_n$	= change in mean value of Y for a unit change in x_n
β_i	= slope of the regression line for the i th independent variable
$C_{envelope}$	= envelope equation (upper/lower) developed to provide a conservative estimate
$C_{MTR-center}$	= coefficient for the maximum shear ratio associated with the center of the channel
$C_{MTR-inner}$	= coefficient for the maximum shear ratio associated with the inner bank of the channel across from the weir tip
$C_{MTR-tip}$	= coefficient for the maximum shear ratio associated with the weir tip
$C_{MVR-center}$	= coefficient for the maximum velocity ratio associated with the center of the channel
$C_{MVR-inner}$	= coefficient for the maximum velocity ratio associated with the inner bank of the channel across from the weir tip
$C_{MVR-tip}$	= coefficient for the maximum velocity ratio associated with the weir tip
$C_{Tr-inner}$	= modeling shear ratio associated with the inner bank across from the weir tip
C_{Tr-tip}	= modeling shear ratio associated with the weir tip

$C_{Vr-inner}$	= modeling velocity ratio associated with the inner bank across from the weir tip
C_{Tr-tip}	= modeling velocity ratio associated with the weir tip
C_z	= Chezy's coefficient $\approx 1.81 \frac{H^{1/6}}{n}$
dP	= differential pressure measured from Preston tube, L
$\Delta Width$	= change in width caused by placement of a weir, used in predictive equations for the weir tip scour hole, L
ε	= random deviation of the i^{th} variable (error)
F_n	= bed roughness correction factor = $2.12 \left[1 - \frac{1.303}{6 \ln \left(\frac{C_z}{26.72} \right) - 1} \right]$
ϕ	= crest angle
ϕ_m	= bend deflection angle, degrees
g	= gravitational acceleration, L/T ²
γ_w	= specific weight of water, ML ⁻² T ⁻²
h_w	= height of bendway weir, L
H	= depth, m
θ	= orientation angle of bendway weirs, degrees
θ_w	= angle between weirs, degrees
K_b	= correction for shear stress
K_{BEND}	= correction factor relationship

$K_{BEND-SHEAR}$	= ratio of shear stress in a bend to the straight channel shear stress (either approach or HEC-RAS), dimensionless
$K_{BEND-VELOCITY}$	= ratio of maximum measured velocity and average HEC-RAS velocity, dimensionless
$K_{BEND-VELOCITY (UPPER)}$	= upper envelope of $K_{BEND-VELOCITY}$, dimensionless
L_{arc}	= arc length between weirs along design waterline, L
L_{ch}	= channel length, L
L_{cw}	= length of weir crest measured from design flow water surface, L
$L_{proj,cw}$	= projected length of weir crest measured from the design flow water surface along the horizontal plane to a cross-section perpendicular to the flow, L
$L_{proj,w}$	= projected length of weir measured from the design flow water surface along the horizontal plane to a cross-section perpendicular to the flow, L
L_r	= length ratio scale factor, dimensionless
L_v	= valley length, L
L_w	= length of weir measured from design flow water surface, L
A_m	= channel meander length, L
$MaxV_{center}$	= maximum centerline bank velocity measured with bendway weirs along bend, L/T
$MaxV_{CenterBase}$	= maximum centerline velocity measured in baseline model, L/T

$MaxV_{inner}$	=	maximum inner bank velocity measured with bendway weirs along bend, L/T
$MaxV_{outer}$	=	maximum outer bank velocity measured with bendway weirs along bend, L/T
MTR	=	maximum shear-stress ratios
MTR_{center}	=	maximum shear-stress ratio at the channel center
$MTR_{center-envelope}$	=	envelope maximum shear-stress ratio at the channel center which incorporates all valid data
MTR_{inner}	=	maximum shear-stress ratio at the toe of the inner bank
$MTR_{inner-envelope}$	=	envelope maximum shear-stress ratio at the toe of the inner bank which incorporates all valid data
MTR_{tip}	=	maximum shear-stress ratio at the tip of the weir
$MTR_{tip-envelope}$	=	envelope maximum shear-stress ratio at the tip of the weir which incorporates all valid data
MVR	=	maximum velocity ratios
MVR_{center}	=	centerline maximum velocity ratio, dimensionless
$MVR_{center-envelope}$	=	envelope centerline maximum velocity ratio, dimensionless, which incorporates all valid data
MVR_{inner}	=	inner bank maximum velocity ratio, dimensionless
$MVR_{inner-envelope}$	=	envelope inner bank maximum velocity ratio, dimensionless, which incorporates all valid data
MVR_{outer}	=	outer bank maximum velocity ratio, dimensionless

MVR_{tip}	= maximum 1 ft (into channel from weir) velocity ratio, dimensionless
$MVR_{tip-envelope}$	= envelope weir tip maximum velocity ratio, dimensionless, which incorporates all valid data
μ_w	= dynamic viscosity of water, M/LT
n	= Manning's roughness coefficient
ν_w	= kinematics viscosity, L ² /T
$\pi_1, \pi_2, \pi_3, \pi_4, \pi_5$	= pi terms used in the evaluation of regression equations
Q	= flow rate, L ³ T ⁻¹
r/b	= relative curvature
R_c	= radius of curvature, L
ρ_w	= density of water, M/L ³
s	= index: 1 for weirs placed on one side of channel and 2 for weirs placed on both sides of channel
S	= spacing between weirs, L
S^*	= spacing ratio = $\frac{\text{longitudinal spacing of weirs}}{\text{weir length projected normal to flow}}$
S_o	= bed slope, L/L
S_r	= spacing ratio, dimensionless
S_{yx}	= strength of spiral flow, dimensionless
σ	= standard deviation of a dataset
t^*	= taper ratio = $\frac{\text{taper length}}{\text{weir length}}$

T_a	= effect of weir area on tip velocity = $0.87A^* + 0.61$ for $0.13 \leq A^* \leq 1.3$
T_n	= effect of channel roughness on tip velocity = $\begin{cases} \frac{1}{3}(2F_n + 1) \text{ for rectangular weirs} \\ F_n \text{ for tapered weirs} \end{cases}$
T_r	= shear ratio
T_{r-tip}	= shear-stress ratio at the weir tip
$T_{r-tip-envelope}$	= envelope shear-stress ratio at the weir tip
$T_{r-inner}$	= shear-stress ratio at the toe of the inner bank
$T_{r-inner-envelope}$	= envelope shear-stress ratio at the toe of the inner bank
T_s	= effect of weir spacing on tip velocity = $0.077(S^* - 4)$ for $1.6 \leq S^* \leq 6$
T_t	= effect of crest angle on tip velocity = $-0.04t^*$ for $t^* \leq 0.5$
T_w	= top width of channel at current flow rate, L
$T_{w_{testflow}}$	= top width of channel at test flow, ft
τ_o	= boundary shear stress, M/LT ²
τ_b	= shear stress measured in a meander bend, M/LT ²
$\tau_{max INNER}$	= maximum shear stress measured along the inner bank of the bend, M/LT ²
$\tau_{max TIP}$	= maximum shear stress measured at the weir tip, M/LT ²
V	= mean cross-sectional velocity, L/T
V_{avg}	= cross-section average velocity, L/T
$V_{AVG-APPROACH}$	= approach velocity computed from continuity, Q/A

V_{BANK}	= normalized bank velocity = $\frac{\text{velocity at the toe of the bank}}{\text{mean upstream velocity}}$
$V_{CHANNEL}$	= velocity in the main channel after placement of weirs, m/s
$V_{COMPUTED}$	= computed velocity from HEC-RAS, L/T
V_{MAX}	= maximum measured velocity, L/T
$V_{max INNER}$	= maximum measured inner bank velocity, L/T
$V_{max TIP}$	= maximum measured weir tip velocity, L/T
V_r	= velocity ratio
$V_{r-inner}$	= velocity ratio for the inner bank
$V_{r-inner-envelope}$	= envelope velocity ratio for the inner bank which incorporates all valid data
V_{r-tip}	= velocity ratio at the tip
$V_{r-tip-envelope}$	= envelope velocity ration at the weir tip, incorporates all valid data
V_{TIP}	= normalized tip velocity = $\frac{\text{velocity near the tip of weir}}{\text{mean approach velocity}}$
V_{yz}	= mean velocity vector projected on the lateral and vertical planes, L/T
W	= channel width, L
W_{bw}	= bottom width of weir, L
W_{cw}	= crest width of weir, L
W_m	= channel meander width, L
x	= independent variable
x_i	= the i^{th} independent variable

x_n	= n^{th} independent variable, here n is the total number of variables
y	= flow depth, L
\bar{y}	= computed mean
y_i	= the i^{th} dependent variable
Y	= prediction of population mean based on model parameters and an independent, x
z	= bank side-slope ratio, dimensionless
ω_s	= unit stream power, MT^{-3}
Ω	= channel sinuosity
Ω_s	= stream power, MLT^{-3}

1 INTRODUCTION

1.1 GENERAL BACKGROUND

As with every natural process, river morphology incorporates a complex and nuanced set of processes that combine to produce an infinite set of possible outcomes. Natural laws that govern natural systems cause rivers to react to changes in the environment in order to maintain equilibrium. Changes in hydraulics, sediment transport, and habitat help keep natural systems in balance. Natural reactions can be predictable, such as seasonal variations in weather patterns, or quite unpredictable, such as major flooding events or tectonic activity. Human impact to the environment is rarely subtle and often times can produce catastrophic changes to natural ecosystems. Virtually all watersheds within the continental United States have been impacted by increasing human population and development (Knighton, 1998; Wohl, 2004). As a result of such profound alterations to the environment, humans have been subjected to flooding, mudslides, droughts, and other extreme environmental processes.

Natural processes counteract man-made impacts in every type of environment from the desert southwest to the snow-covered peaks of Colorado. Riverine environments exhibit a unique set of processes whose main function is to move material, such as sediment, brush, and water, from a point of high-energy potential to a point of

lower energy potential. Natural channels maximize transport potential by perpetuating a continuous state of change.

From the earliest civilizations, mankind has sought to use rivers to benefit commerce and sustain communities. Technology has developed over history, to the point where mankind can drastically alter major riverine environments and perform magnificent feats of ingenuity. Technological evolution has rarely, however, adequately addressed natural impacts of such profound changes. As a result, recent efforts have focused on developing tools to predict geomorphic changes to natural riverine environments. Mathematical models have assisted in this effort, although current technology does not allow complete solutions of environmental hydraulic processes. Approximations must be made to predict characteristics of natural environments through the use of available practical tools in order to give adequate information for design purposes. One-dimensional (1-D) computer models, such as Hydrologic Engineering Centers River Analysis System (HEC-RAS), can be used to simulate flow conditions in channel bends with and without bank revetment measures and can be compared back to physically-measured data.

1.2 PROJECT BACKGROUND

The Middle Rio Grande is a 29-mi reach of the Rio Grande River in central New Mexico that extends from downstream of Cochiti Dam to Bernalillo, New Mexico. Figure 1.1 presents a map of the Middle Rio Grande reach. In recent years, the Middle Rio Grande has been the focus of channel-restoration techniques including the use of

native material and rock weir structures in attempts to control bank-erosion rates, channel-migration rates, and habitat degradation (Darrow, 2004).

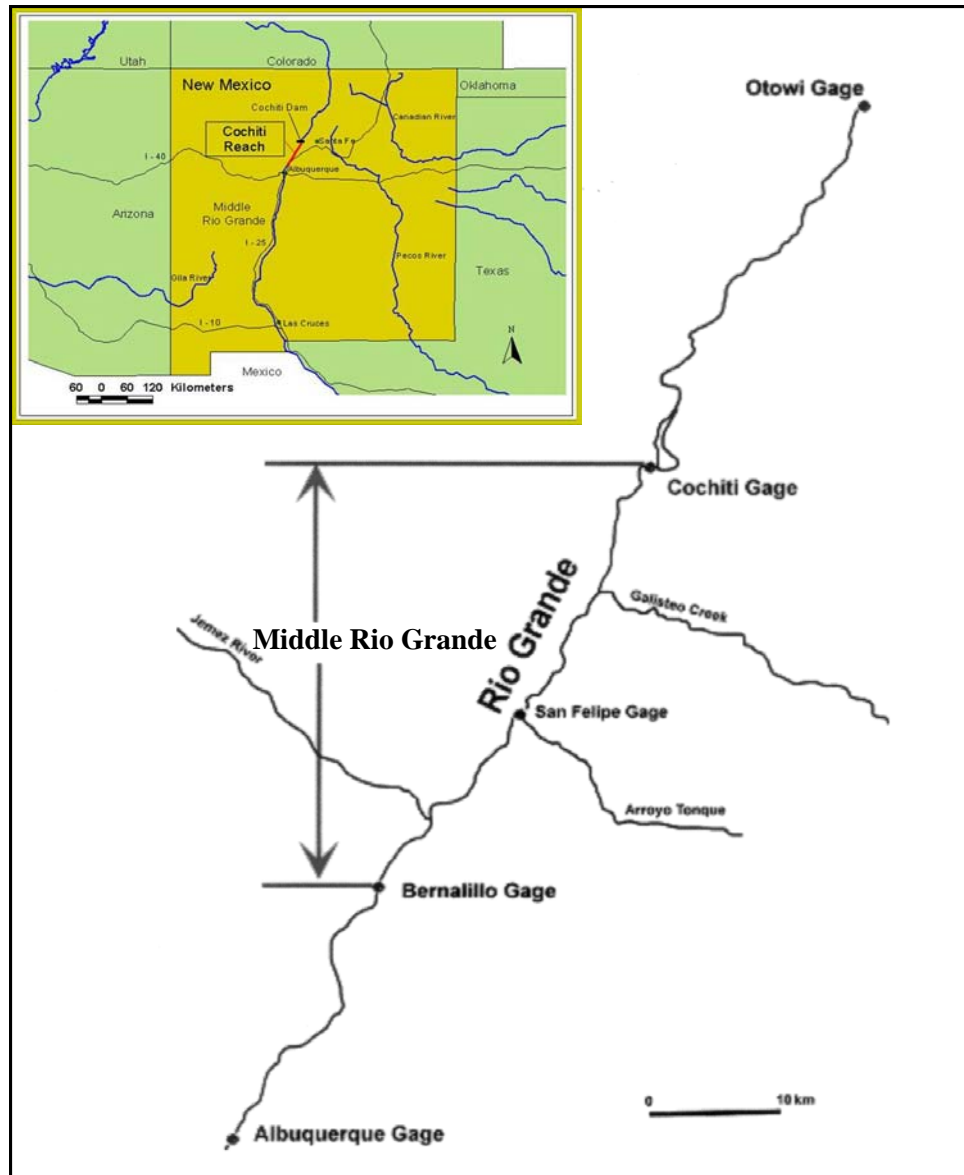


Figure 1.1: Location Map of Project Reach (Figure 1.1 in Darrow (2004))

For sediment and flood control reasons, the U.S. Army Corps of Engineers (USACE) commenced the construction of Cochiti Dam in 1965 (Heintz, 2002). The earth-filled embankment was completed in 1975, and is one of the largest earth-filled

dams in North America. Since the dam's construction, the downstream channel has undergone considerable changes. Historically, the river was a relatively-straight, braided system with a shifting sand bed and shallow banks. Since the construction of Cochiti Dam, the sinuosity of the stream has increased, average stream width has decreased from approximately 900 ft to about 300 ft, and degradation has been observed as far as 125 mi downstream (Schmidt, 2005). In general, the channel has been transformed from a braided channel to a meandering stream containing a pool/riffle system with a coarser gravel substrate than was historically present.

Channel degradation and migration along the Middle Rio Grande have caused the U.S. Department of the Interior, Bureau of Reclamation (USBR) to investigate ways to stabilize eroding banks, while preserving natural habitat. Traditional methods such as concrete riprap could be employed to stabilize the banks; however, such hard-armoring techniques are detrimental to the natural environment. Bendway weirs have been identified as appropriate structures to potentially protect the natural habitat and protect the vulnerable river banks. Impacts to the riverine environment caused by construction of bendway weirs, however, are not entirely known. As a result, Colorado State University (CSU) has been tasked to perform a series of studies to evaluate the hydraulic effects of bendway-weir installation in two prototypical meander bends of the Middle Rio Grande.

1.3 RESEARCH OBJECTIVES

A research program utilizing a rigid boundary model examined the effect of weir spacing, cross-sectional flow area blocked, planform angle, and crest slope on the flow characteristics observed in the constructed flume (Schmidt, 2005). Objectives of the

research included evaluating the effects of weir geometry on the hydraulics of a simulated channel bend and developing a method to predict flow velocity and shear stress as a function of weir field and bend geometry.

In practice, design of revetment measures such as bendway weirs requires some quantitative method to evaluate their impact on the environment in which they are installed. Typically, numerical models such as the USACE 1-D computer model HEC-RAS are used to simulate riverine conditions with and without the proposed design features in place. Use of simplified software, such as HEC-RAS, has offered enormous insight into the hydraulics associated with various riverine conditions; however, limitations and assumptions of such software is still a significant consideration for design engineers (USACE, 2008). When 1-D computer models are applied to complex flow conditions, it is useful to know how well the computer model is predicting certain key parameters including water-surface elevation (WSE), energy slope, velocity, and shear stress.

A comparative study was performed between the 1-D riverine computer model HEC-RAS and physical data collected from previous flume experiments reported by Heintz (2002) and Darrow (2004). Accuracy of the computer model to predict measured data was evaluated through the following scope of work:

- development of a baseline computer model of the constructed flume to accurately predict water-surface profiles in the test reach without bendway weirs,
- development of a modeling technique that can be used to modify the baseline computer model to represent fifteen different weir configurations,

- evaluation of baseline computer modeling to predict maximum velocity and shear stress in a channel bend,
- development of an adjustment factor that could be applied to results from a HEC-RAS computer model to predict the maximum expected velocity and shear stress in a channel bend without bendway weirs, and
- development of an adjustment factor that could be applied to the results from a HEC-RAS computer model to predict the maximum expected velocity and shear stress in a bend with bendway weirs.

Relationships developed from comparative studies between computed HEC-RAS results and measured results from physical model testing were used to develop a design procedure for modeling bendway weirs in a 1-D model. From comparisons between HEC-RAS computer model results and the physical data collected in the constructed flume, a design procedure for bendway weirs was developed into the following four steps:

1. Compile characteristics of site conditions such as bend radius of curvature, design flow rate, and slope.
2. Use relationships developed from comparisons between computed results and collected data in the physical model to select a suitable bendway-weir layout configuration.
3. Develop an appropriate computer model for the selected bendway-weir configuration.
4. Use relationships developed from comparisons between computed results and collected data in the physical model to predict maximum shear-stress and

velocity values for two key locations associated with the bendway weirs: at the weir tip and along the opposite bank across from the weir tip.

2 LITERATURE REVIEW

2.1 INTRODUCTION

The Middle Rio Grande has historically been a braided, slightly sinuous, aggrading river with a sand substrate (Whitney, 1996). A series of anthropogenic factors including the construction of flood control levees and the Cochiti Dam have altered the historic morphology of the Middle Rio Grande to a more sinuous, degrading reach, with less overall channel migration within a natural floodplain area. Concentration of flow within an incised channel has caused areas of bank erosion along with reduction in riparian vegetation. CSU has constructed a physical model of a fixed bed channel with two bends that represent the characteristically-sinuuous channel now found within the portion of the Middle Rio Grande below Cochiti Dam. With guidance from the USBR in Albuquerque, bank-stabilization methods have also been installed within the physical model. A thorough literature review has been conducted to explore general characterizations of flow in channel bends along with guidelines for predicting the anticipated increase in velocity due to centrifugal acceleration through channel bends. Characteristics of the erosion countermeasure studied in the Middle Rio Grande physical model will then be explained along with some construction methods which were used to create an appropriate test matrix.

2.2 CHANNEL PATTERNS

River systems can be described in terms of many characteristic parameters including channel slope, cross-sectional geometry, sediment load and size, and planform geometry. Changes to one variable often means that other river characteristics must be altered in order to reach some sort of equilibrium. Channel pattern is a river characteristic that often refers to planform geometry, the path that the river takes as it moves in the down gradient direction. Leopold *et al.* (1964) classified channel patterns as meandering, braided, and straight, but recognized that clear divisions between the classifications can not be made. Distinctions between channel patterns can often be thought of in terms of sinuosity (Ω), which is defined as the ratio of actual channel length (L_{ch}) to straight-line valley length (L_v) as shown in Figure 2.1.

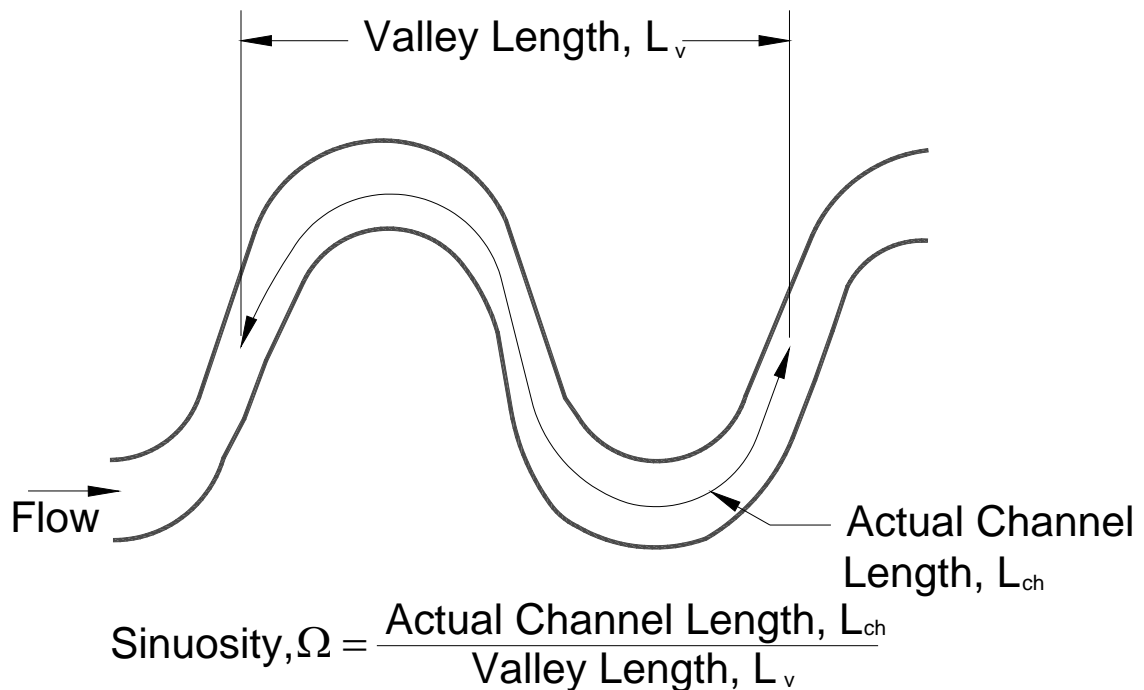


Figure 2.1: Definition of Sinuosity

Leopold *et al.* (1964) suggested that sinuosity values below 1.5 indicate a river that is relatively straight to slightly sinuous while rivers with sinuosity above 1.5 can be described as meandering. Limitations in this definition are apparent in that no indication is given for causal relationships between different channel pattern types. Schumm and Brakenridge (1987) recognized these limitations and presented a model of channel pattern formation indicated as a continuum based on key formation variables. Figure 2.2 shows a channel classification system presented in Schumm and Brakenridge (1987) that suggests channel formation to be a function of sediment size, sediment load, flow velocity, and stream power.

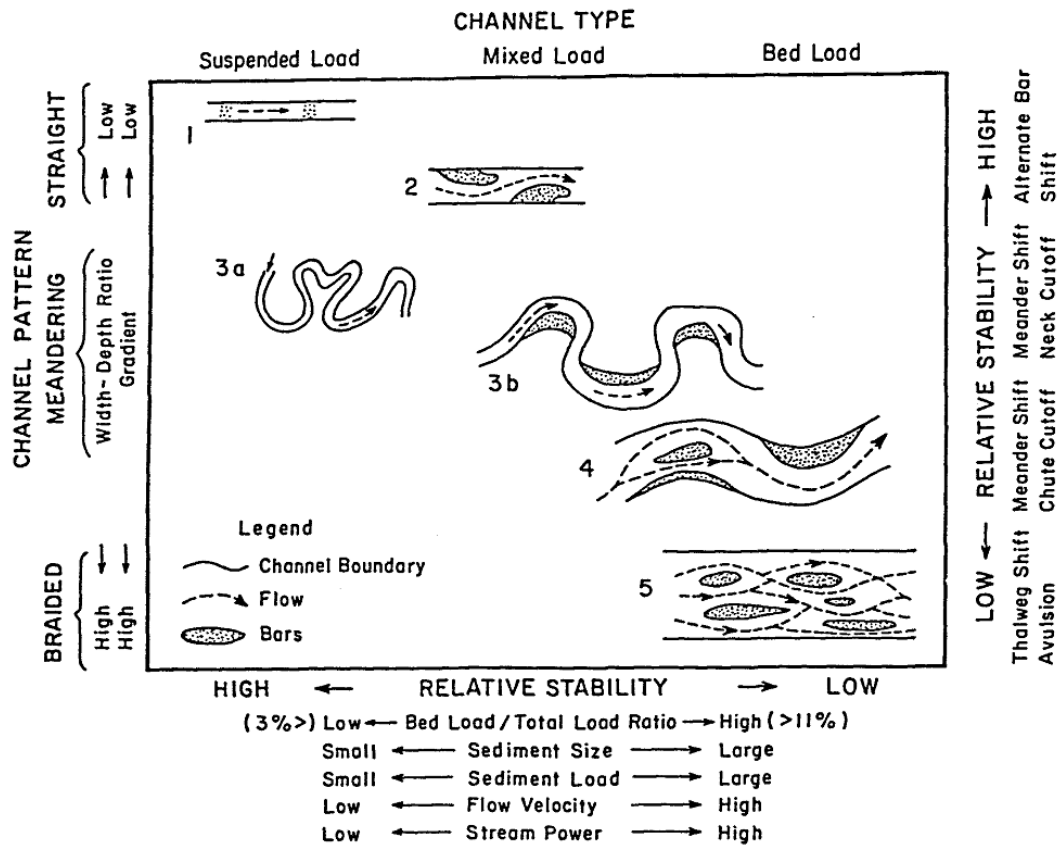


Figure 2.2: Channel Pattern Classification Based on Schumm and Brakenridge (1987; Figure 1)

Stream power and unit stream power are parameters developed by Bagnold (1960) that attempt to describe the overall energy of a stream. Stream power is defined as the product of the discharge and bed slope, Equation 2.1:

$$\Omega_s = \gamma_w Q S_o \quad \text{Equation 2.1}$$

where

Ω_s = stream power (ML/T³);

γ_w = specific weight of water (M/L²T²);

Q = discharge (L³/T); and

S_o = bed slope.

Unit stream power is defined in Equation 2.2 as the stream power of a river per unit width:

$$\omega_s = \frac{\gamma_w Q S_o}{W} \quad \text{Equation 2.2}$$

where

ω_s = unit stream power (M/T³);

γ_w = specific weight of water (M/L²T²);

Q = discharge (L³/T);

S_o = bed slope; and

W = channel width (L).

The continuum approach to channel classification illustrated in Figure 2.2 is valuable in understanding that a river is not merely defined as a single channel formation, but can at any time move through a range of channel patterns based on interactions of a

distinct set of continuous variables. Furthermore, a continuum approach to channel classification implies a direction of channel formation as the river seeks equilibrium. Knighton (1998) summarized the direction of channel pattern evolution in terms of increasing stream power beginning with a channel of no lateral migration moving to a channel with active meandering patterns and finally to a braided channel. Progression through planform characterizations from a straight channel to a braided channel is generally associated with the following characteristics (Knighton, 1998):

- a. increasing stream power;
- b. increasing discharge at a constant slope, increasing slope at a constant discharge, or a combination of the two;
- c. increasing width:depth ratio, which is generally associated with increasing bank erodibility and increasing bed-load transport; and
- d. increasing amount and size of bed load.

Two conditions are generally thought to be necessary for braided channels to persist: 1) a large bed-load transport at high discharge, and 2) easily erodible banks (van den Berg, 1995). Bed aggradation is typically cited as another characteristic of braiding streams, but less as a causal relationship and more as a systemic relationship. Van den Berg (1995) researched 192 rivers and related channel pattern to unit stream power and median grain size (Figure 2.3). Van den Berg's (1995) results indicate that as unit stream power increases, rivers tend toward a multiple-thread channel. The reverse could also be noted, as the stream power decreases, the river tends toward a single-thread channel.

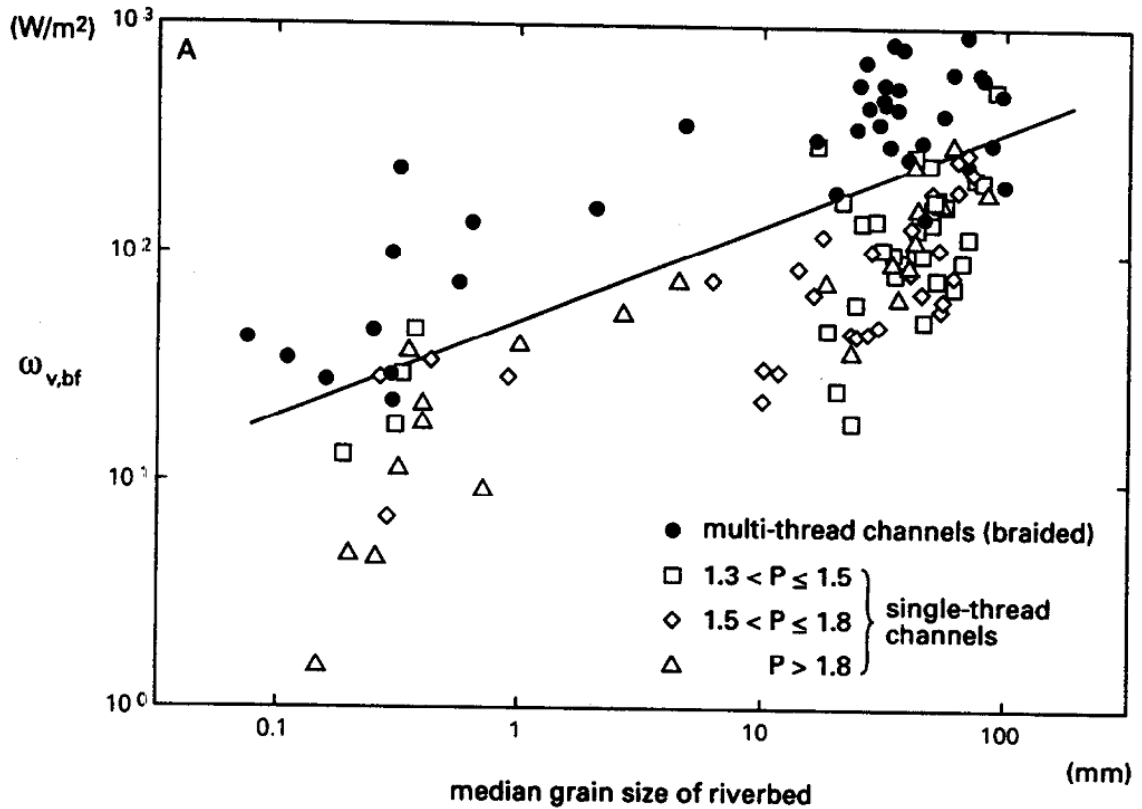


Figure 2.3: Channel Pattern Relative to Grain Size and Unit Stream Power (Figure 3 in Van den Berg (1995))

Bledsoe and Watson (2001) also found a direct correlation between stream power and channel pattern formation using a binary logistic regression for the dependent variable. A dataset of 270 rivers was compiled from various locales around the world. Streams were classified in terms of meandering, braiding, incising, or in a state of quasi-equilibrium. From Bledsoe and Watson's (2001) findings presented in Figure 2.4 and Figure 2.5, it is evident that braiding in rivers is associated with greater stream power than meandering rivers.

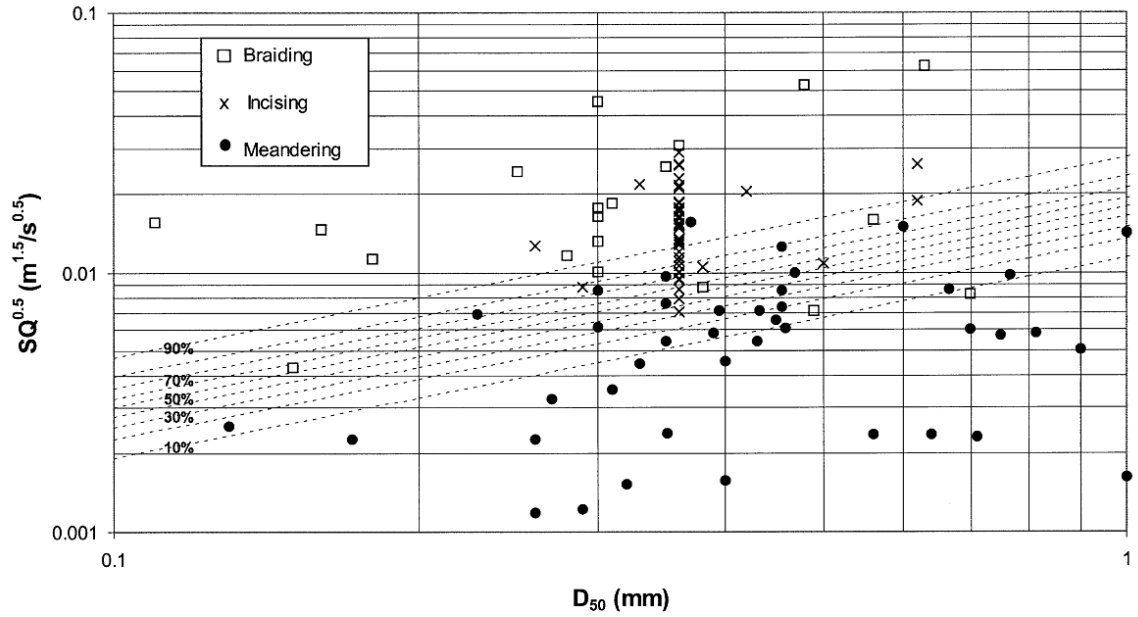


Figure 2.4: Channel Pattern relative to Grain Size for Sand-bed Streams (Figure 3 in Bledsoe and Watson (2001))

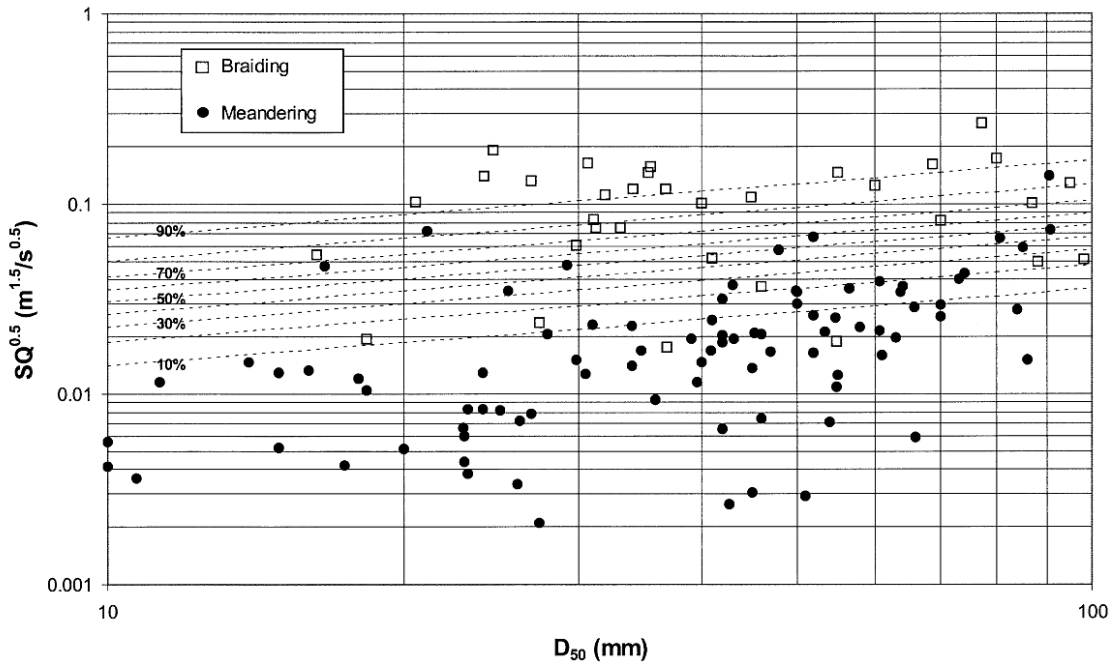


Figure 2.5: Channel Pattern Relative to Grain Size for Gravel-bed Streams (Figure 6 in Bledsoe and Watson (2001))

Based on the characteristic and magnitude of the perturbation to which the river is responding, the eventual pattern achieved may not necessitate covering the full spectrum of channel planforms. It also should be noted that direction of channel pattern evolution is not a one-way relationship. Perturbations can require a channel to move to a pattern of lower stream power as well as a channel pattern of greater stream power. Upon the construction of Cochiti Dam in 1965, sediment supply to the downstream reach was essentially cut off. In the immediate time scale, the river was able to carry much more sediment than was being transported as suspended load. Additional material was, therefore, picked up from the erodible channel banks and bed. As a result, the braided multiple-threaded channel was eroded to become an incised single channel. As the channel began to move toward equilibrium, the unit stream power decreased and the channel began to exhibit a meandering channel pattern. As a result, current research on using countermeasures along the Middle Rio Grande and construction of the physical model at CSU has focused exclusively on characterization of flow in single-thread meandering channels.

2.3 MEANDER GEOMETRY

Fundamentally, bend geometry can be grouped into four categories: 1) channel-geometry characteristics, 2) flow characteristics, and 3) fluid properties, and 4) sediment properties (Yen, 1965). Channel geometry characteristics include cross-sectional factors, planform pattern factors, and longitudinal profile factors. Cross-sectional factors include flow depth (y), top width (T_w), channel bottom width (b), and side-slope ratio (z) as shown in Figure 2.6.

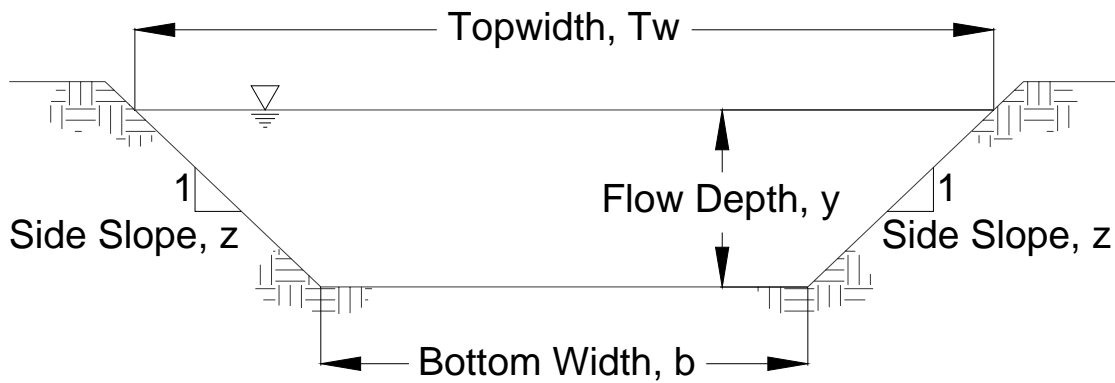


Figure 2.6: Typical Trapezoidal Cross-section Characteristics

Within meander bends, lateral secondary currents cause flow in the channel cross sections to become more complex than in straight channels. Subdivision of meandering channel cross sections into an inner-bank region, mid-channel region, and outer-bank region has been useful in analyses of shear stresses and velocities. Figure 2.7 illustrates sub-divisions used in cross sections within meander bends (Knighton, 1998).

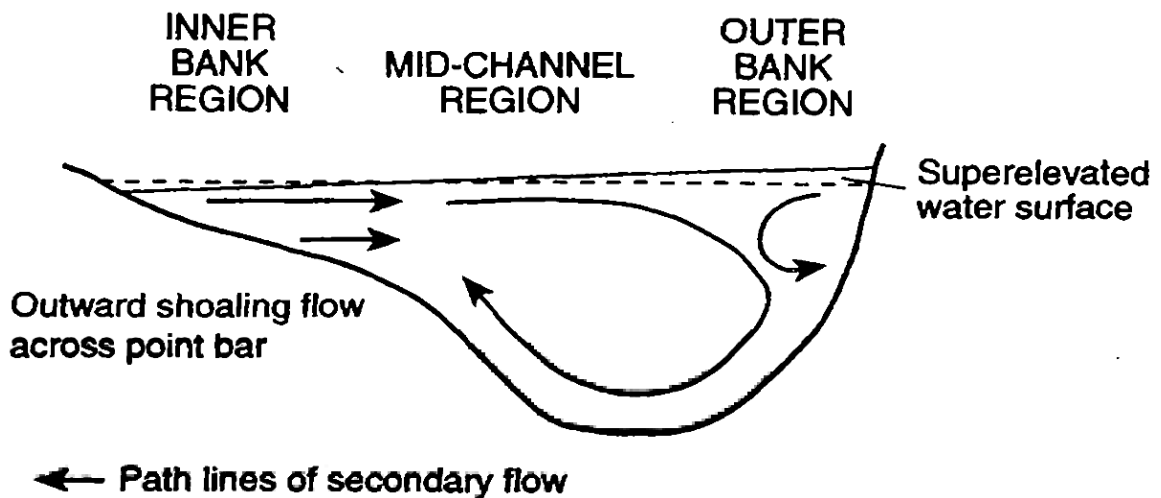


Figure 2.7: Subdivision of a Channel Cross Section within a Meander Bend (Figure 5.19 in Knighton (1998))

Planimetric pattern factors describe overall pattern of the channel meander. Planimetric pattern factors include the radius of curvature (R_c), bend deflection angle (ϕ_m), meander length (Λ_m), and meander amplitude (α_m). Figure 2.8 illustrates the characteristics of a typical channel meander.

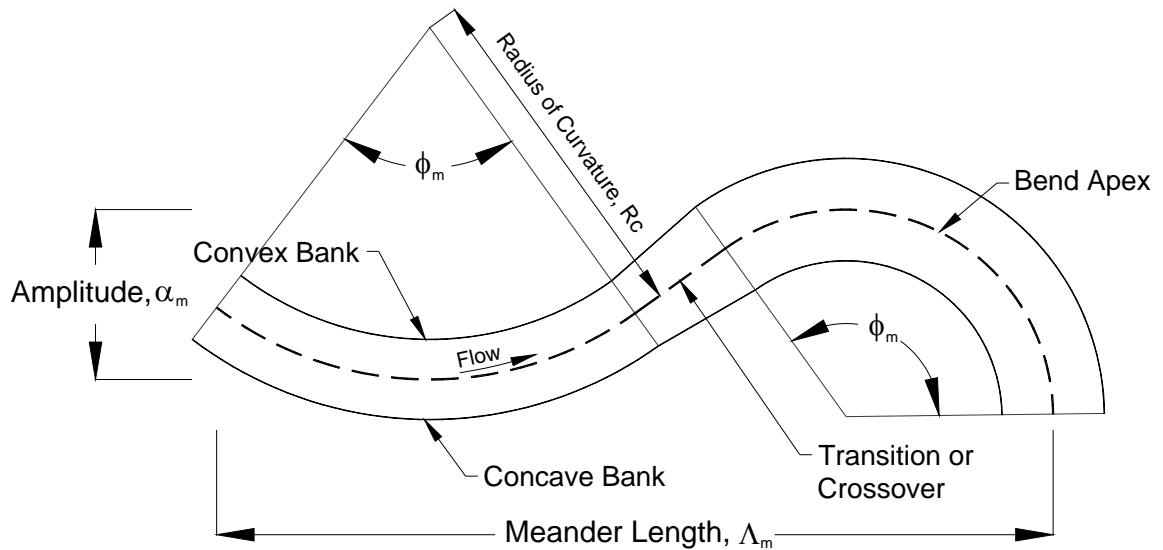


Figure 2.8: Planimetric Pattern Factors for a Typical Meander

2.4 MEANDER FLOW CHARACTERISTICS

2.4.1 BACKGROUND

Flow through meandering channels offers a complex set of challenges for scientists and design engineers. Presence of centripetal acceleration through meander bends causes super-elevation of the water surface, creation of spiraling motion, and modification of velocity and boundary shear distributions (Yen, 1965). Meander geometry amplifies the challenges of maintaining a stable channel design by subjecting the outer bank to intensified erosional forces. Development of meandering channels is exceedingly common; however, challenges to engineers seeking to provide bank

stabilization while maintaining a healthy riverine ecosystem remain profound. As a result of these challenges and the commonality of meandering channels, much research has been undertaken to understand and quantify flow patterns in channel bends.

Some researchers have suggested that interaction between flow through meander bends and erodible channel bed and bank material is the fundamental cause for the initiation of channel meanders, though complete explanations of the meander initiation do not yet exist (Knighton, 1998). It is clear, however, that increased shear forces and velocities exerted on an erodible outer bank contribute to channel instability.

Thompson (1876) introduced the notion that flow in channel bends creates a characteristic spiraling pattern. Initiation of spiraling motion in a channel results from a differential centripetal acceleration formed between the fluid near the water surface and the fluid near the channel boundary, which has been retarded due to boundary friction. Radial acceleration, manifested physically as super-elevation, causes low-velocity fluid near the channel bed to move toward the channel center and the surface flow, with greater momentum to move toward the outside of the bend (Ippen *et al.*, 1960a,b). Representation of spiraling flow and vector direction of velocity at cross sections through the meander bend is presented graphically in Figure 2.9 (Knighton, 1998).

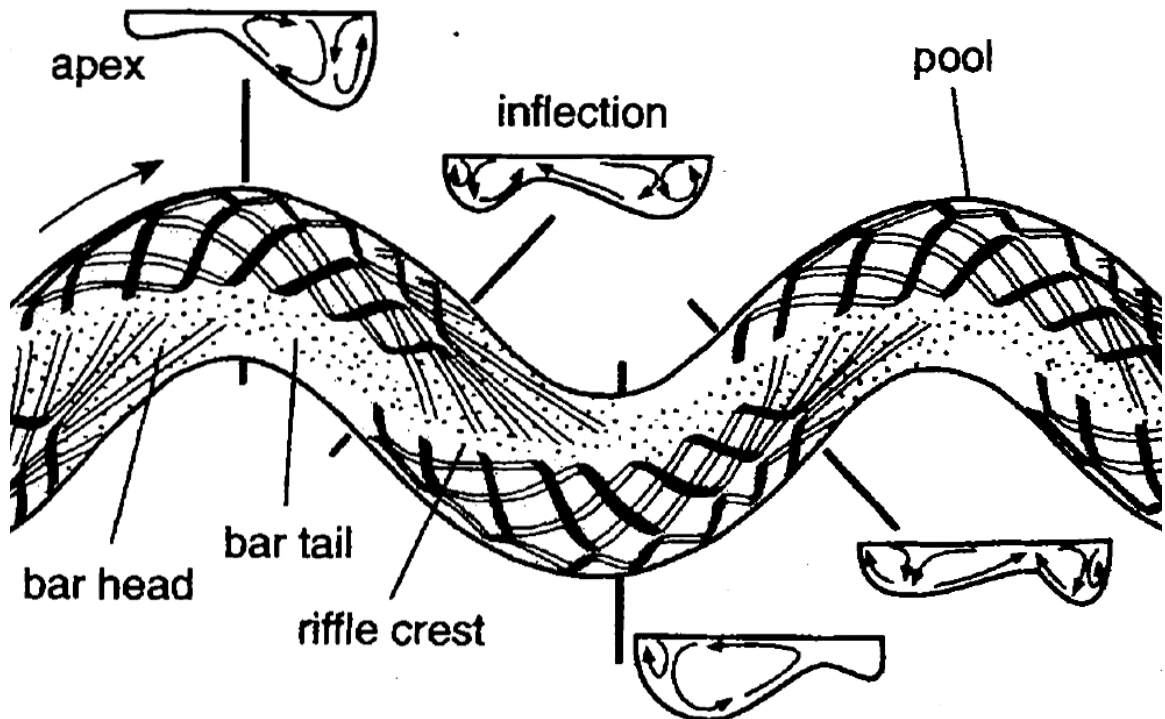


Figure 2.9: Representation of Spiraling Flow through Meander Bends (Figure 5.19 in Knighton (1998))

Black ribbons in Figure 2.9 indicate movement of flow patterns near the surface, while the white ribbons in Figure 2.9 indicate flow patterns near the channel bed. Flow paths continue along a general helical direction through the downstream half of the bend until the inside wall is reached.

Spiral flow through channel bends follows a helical direction whose strongest lateral currents occur close to the outer wall near the curve apex (Chow, 1959). Leopold *et al.* (1964) argued that the points of highest velocity along the outer bank of a meandering bend occur just downstream from the curve apex, where Leopold *et al.* (1964) suggested that most engineering revetment fails. Knighton (1998) characterized flow through meander bends as having three basic components: 1) super-elevation against the concave (outer) bank; 2) transverse flow directed towards the outer bank at

the surface and toward the inner bank at the bed; and 3) a maximum velocity flow moving from near the inner bank at the bend entrance to near the outer bank at the bend exit, crossing the channel through the zone of greatest curvature. The path of high velocity through bend meanders is presented graphically in Figure 2.10 (Leopold *et al.*, 1964).

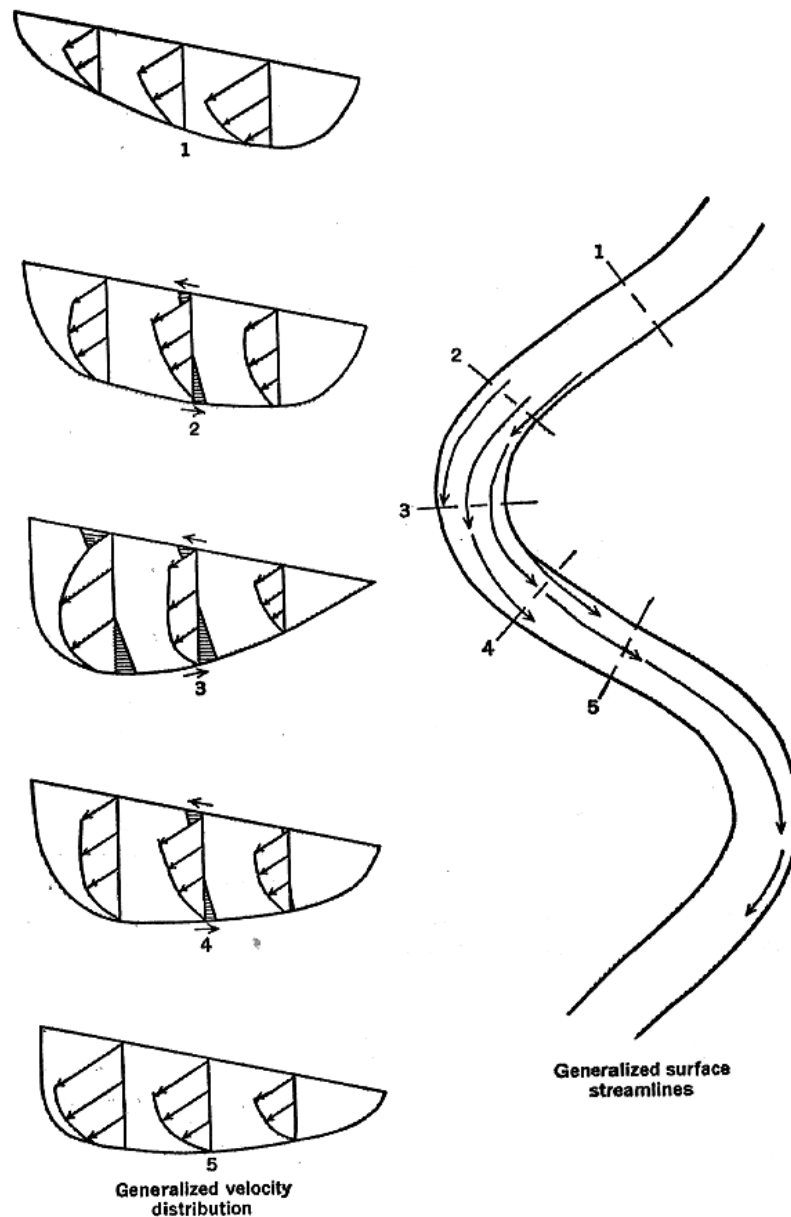


Figure 2.10: Velocity Distribution through Meandering Bends (Figure 7.42 in Leopold *et al.* (1964)).

Figure 2.10 illustrates how a fairly uniform velocity distribution entering a meander bend (Section 1) begins to shift towards the outer bend, causing the channel geometry to become more asymmetric. Secondary currents, indicated at Sections 2, 3, and 4, also facilitate the creation of a complex set of velocity vectors whose direction into the outer bank intensifies close to the outer wall just downstream of the apex. Dietrich (1987) presented an illustration of velocity vectors through meander bends that shows the point of maximum attack on the outer bank (Figure 2.11).

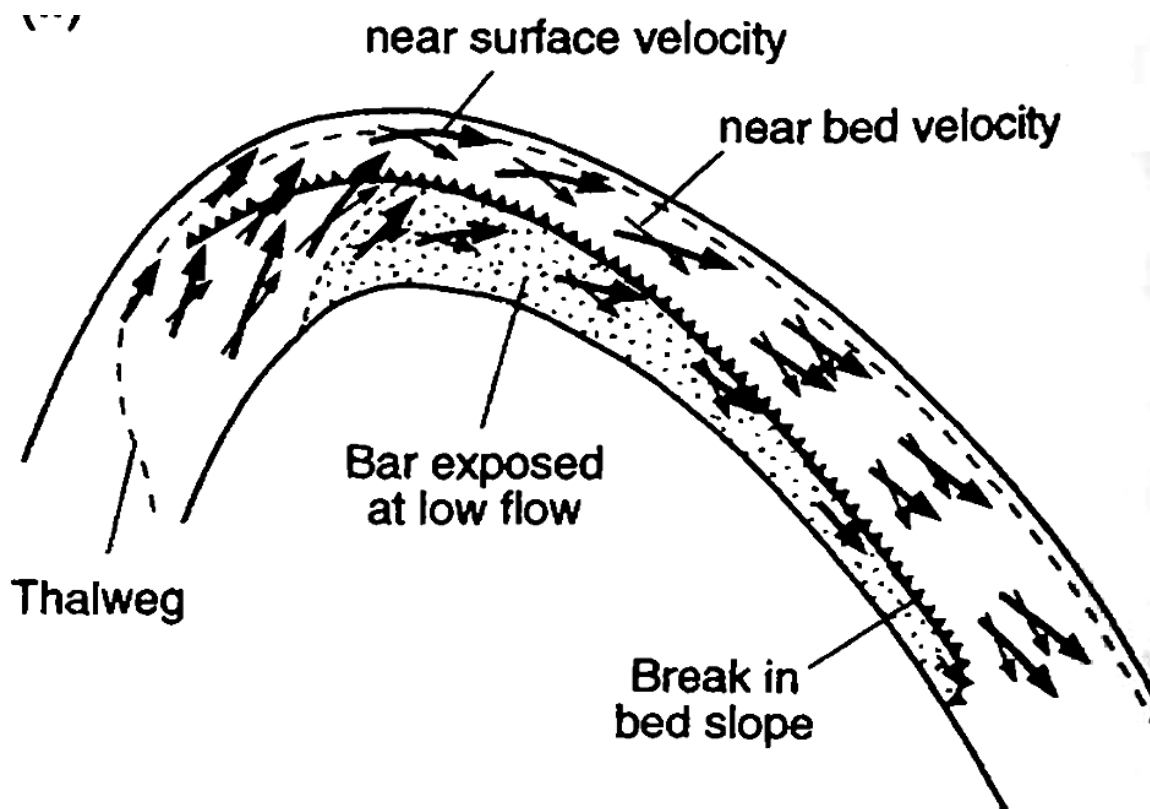


Figure 2.11: Model of Velocity Direction through a Channel Bend (Figure 5.19 in Dietrich (1987))

Figure 2.11 shows how maximum velocity vectors initiate at the entrance to the bend on the inner bank, then migrate towards the outer bank before being directed downstream. While surface velocity is migrating toward the outer bank, Figure 2.11 also

shows the bed velocity directed toward the inner bank of the bend, forming a bar of deposited material. Velocity distribution and angle of attack shown in Figure 2.11 are indicative of secondary currents associated with channel curvature. While Figure 2.11 shows the velocity's point of attack on the outer bank to be quite severe, it is typically the boundary shear stress that gives a more direct indication of bank erosion (Ippen *et al.*, 1960a,b). Ippen *et al.* (1960a,b), the USBR (1964), and Yen (1965) all found that the maximum boundary shear stress occurs at the inside bank of the entrance to the bend. Areas of high boundary shear stress tend to follow the same path as the areas of high velocity (USBR, 1964). Yen (1965) pointed out that although the maximum boundary shear stress found through the meander bend occurred along the inner bank of the bend entrance, significant erosion does not occur at this location because the orientation of the boundary shear stress tends to support bank stability. At a point downstream of the bend apex, high boundary shear stresses persist and boundary shear-stress direction is no longer supporting bank stabilization but actively removing material. Yen (1965) suggested that the point of high-erosion potential does not occur at the bend apex because of remnants of upstream boundary shear stresses supporting stabilization. Dietrich (1987) developed a graphical model indicating the relative magnitude of shear forces through meander bends (Figure 2.12).

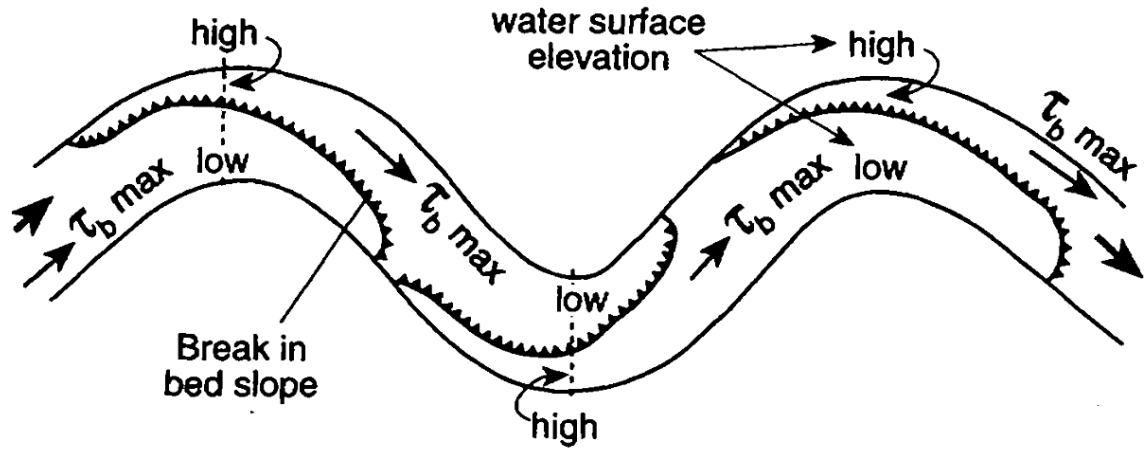


Figure 2.12: Model of Shear-stress Distribution through Channel Meander (Figure 5.19 in Dietrich (1987))

Once spiral currents are set up through a meander bend, they continue downstream for some distance after the exit of the bend. How far the effects from the bend extend downstream and how much damage the spiral flow causes on the outer bank are a function of the strength of the secondary currents which, in turn, depends on many variables including the size of the river, magnitude of flow, and the erodibility of the bank material.

Strength of the spiral flow was defined by Shukry (1950) as a ratio of the velocity projected on the lateral and vertical planes to the mean velocity in the cross section, Equation 2.3:

$$S_{yz} = \frac{V_{yz}^2}{V^2} \times 100 \quad \text{Equation 2.3}$$

where

S_{yz} = strength of spiral flow;

V_{yz} = mean velocity vector projected on the lateral and vertical planes (L/T);

and

V = mean cross-sectional velocity (L/T).

The ratio of the radius of curvature (R_c) to the channel top width (T_w) is considered a measure of a channel's tightness and has been found to be inversely related to the strength of secondary currents defined in Equation 2.3. Leopold *et al.* (1964) reported an average bend tightness value of approximately 2.7. Chang (1988) identified a median value of $R_c/T_w = 3.0$ (Welch and Wright, 2005). Shukry (1950) found that S_{yx} increases with increasing bend tightness (lower R_c/T_w) and that an increase in radial velocities occurs with increasing depth to width ratios. Resistance to flow through a bend has been found to be minimal at $R_c/T_w \approx 2$ (Knighton, 1998). Below $R_c/T_w \approx 2$, flow resistance increases very rapidly due to increasing flow separation and turbulence. Hickin and Nanson (1975, 1984) showed that the rate of channel erosion reaches a maximum when $2 < R_c/T_w < 3$ and decreases exponentially on either side of this range (Knighton, 1998). Figure 2.13 from Hickin and Nanson (1984) shows the relative migration of the channel, indicating bank erosion, versus the channel tightness (R_c/T_w).

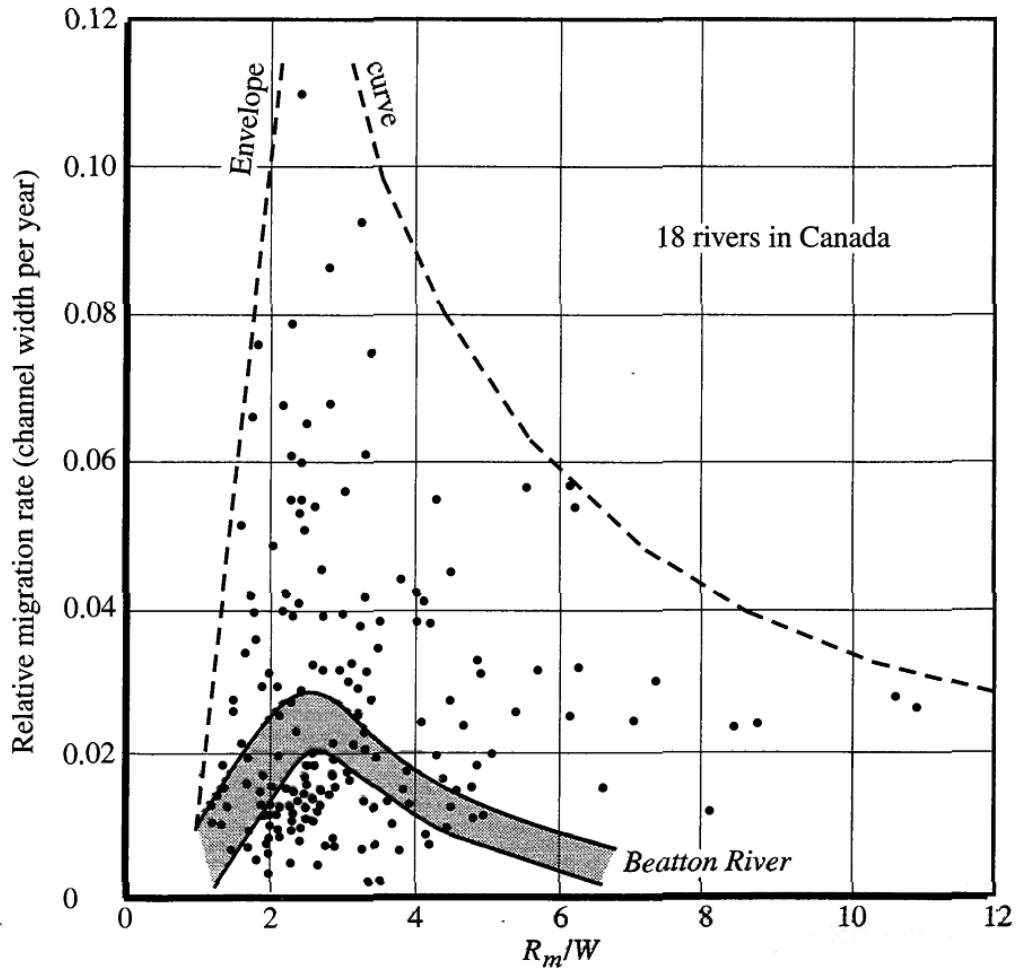


Figure 2.13: Channel Migration versus Radius of Curvature over Top Width from a Study by Hickin and Nanson (1984; Figure 3) (Figure 5.21 in Julien (2002))

Figure 2.13 shows a considerable degree of scatter, 70 percent of which could be the result of variations in stream power and sediment size (Nanson and Hickin, 1986). Biedenharn *et al.* (1989) indicated that although a general trend in migration rate decreases with increasing R_c/T_w , high degree of scatter in the data and system complexity do not rule out low-migration rates for low R_c/T_w , especially where resistive material is present. Maximum channel migration in Figure 2.13 occurs at approximately $R_c/T_w \approx 3$, below which the migration rate drops precipitously, which could be attributed to a

decrease in overall radial forces on the outer bank or a large increase in channel resistance (Knighton, 1998). For $R_c/T_w > 3$ there is again a drop off in channel migration, albeit somewhat shallower than for $R_c/T_w < 3$. Spiral flow, illustrated in Figure 2.9, has been identified as the primary design consideration for channel stability for $R_c/T_w > 3$. For tighter bends when the $R_c/T_w < 3$, both spiral flow and cross-stream flow need to be considered (Welch and Wright, 2005). Cross-stream flow refers to shifting downstream-directed flow across the channel centerline. As illustrated in Figure 2.14, cross-stream flow can be described as the redirection of downstream flow as a result of meander bend geometry. Change in downstream flow direction causes stream-bank abrasion, which is more significant when $R_c/T_w < 3$.

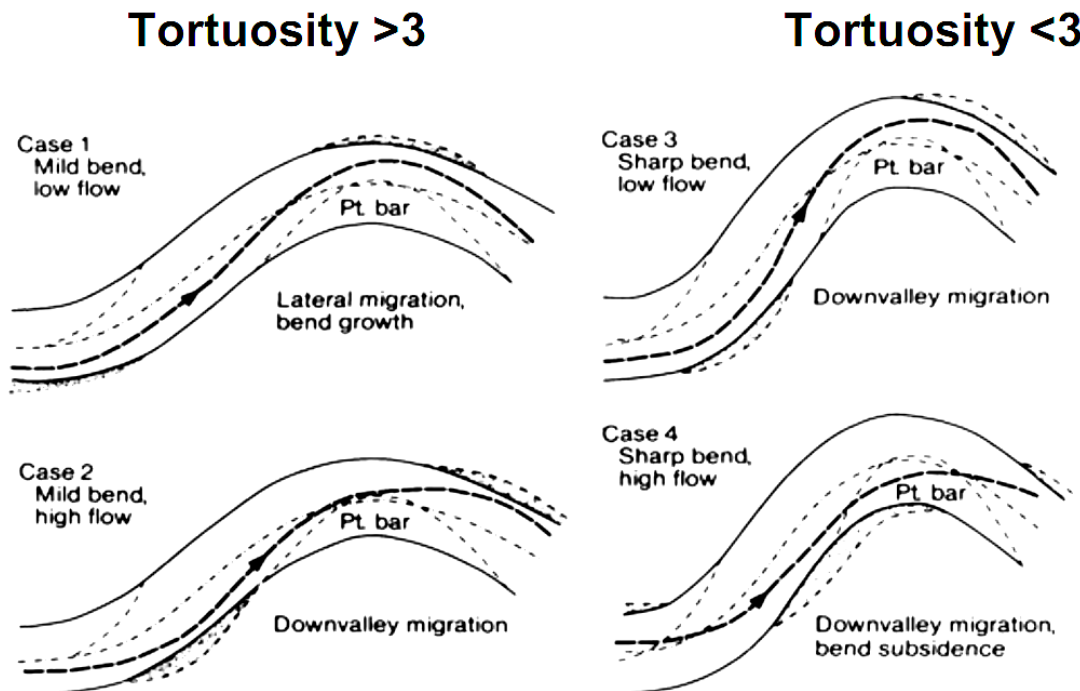


Figure 2.14: Cross-stream Flow as a Function of Tortuosity (Figure 4 in Welch and Wright (2005))

Understanding the mechanisms of channel pattern formation and meander initiation contributes to the overall understanding of riverine processes. Practical implications of riverine geomorphology include being able to design, or facilitate, healthy channel ecosystems while being able to counter specific points of instability. Several studies have been conducted to locate and quantify specific areas of maximum velocity and shear-stress patterns through meander bends. Design criteria provided in Kilgore and Cotton (2005) use an empirically-derived equation to predict the increase in shear stress associated with a meander bend. Equation 2.4 shows the relationship between the ratio of bend shear stress to the straight channel approach shear stress and R_c/T_w used in Kilgore and Cotton (2005):

$$\begin{aligned}
 K_{BEND-SHEAR} &= 2.0 && \left(\frac{R_c}{T_w} \right) \leq 2 \\
 K_{BEND-SHEAR} &= 2.38 - 0.206 \left(\frac{R_c}{T_w} \right) + 0.0073 \left(\frac{R_c}{T_w} \right)^2 && 2 < \left(\frac{R_c}{T_w} \right) < 10 \quad \text{Equation 2.4} \\
 K_{BEND-SHEAR} &= 1.05 && 10 \leq \left(\frac{R_c}{T_w} \right)
 \end{aligned}$$

where

$$\begin{aligned}
 K_{BEND-SHEAR} &= \text{ratio of shear stress in channel bend to straight channel} \\
 &\quad \text{approach shear stress at maximum depth;} \\
 R_c &= \text{radius of curvature of the bend to the channel centerline (ft); and} \\
 T_w &= \text{channel top (water surface) width (ft).}
 \end{aligned}$$

As the R_c/Tw decreases (the bend becomes tighter), the correction factor increases up to a maximum value of 2, corresponding to R_c/Tw of 2. A R_c/Tw value of 2 corresponds to the point of maximum migration in Figure 2.13. Equation 2.4 does not incorporate the reduced bend migration for R_c/Tw values < 2 and, therefore, provides some degree of conservatism.

2.4.2 RESEARCH

2.4.2.1 IPPEN *ET AL.* (1960a,b)

Ippen *et al.* (1960a,b) investigated velocity and boundary shear-stress distributions through a flume with a trapezoidal cross section for single curves and compound curve configurations. A 20-ft approach section preceded a 60-degree bend followed by a 10-ft exit section. The radius of curvature of the single bend was 60 in. and the channel slope was set at 0.00064 ft/ft. The trapezoidal cross section had a 24-in. bottom width with 2H:1V (Horizontal:Vertical) side slopes. Figure 2.15 shows a schematic of the testing facilities used in Ippen *et al.* (1960a,b).

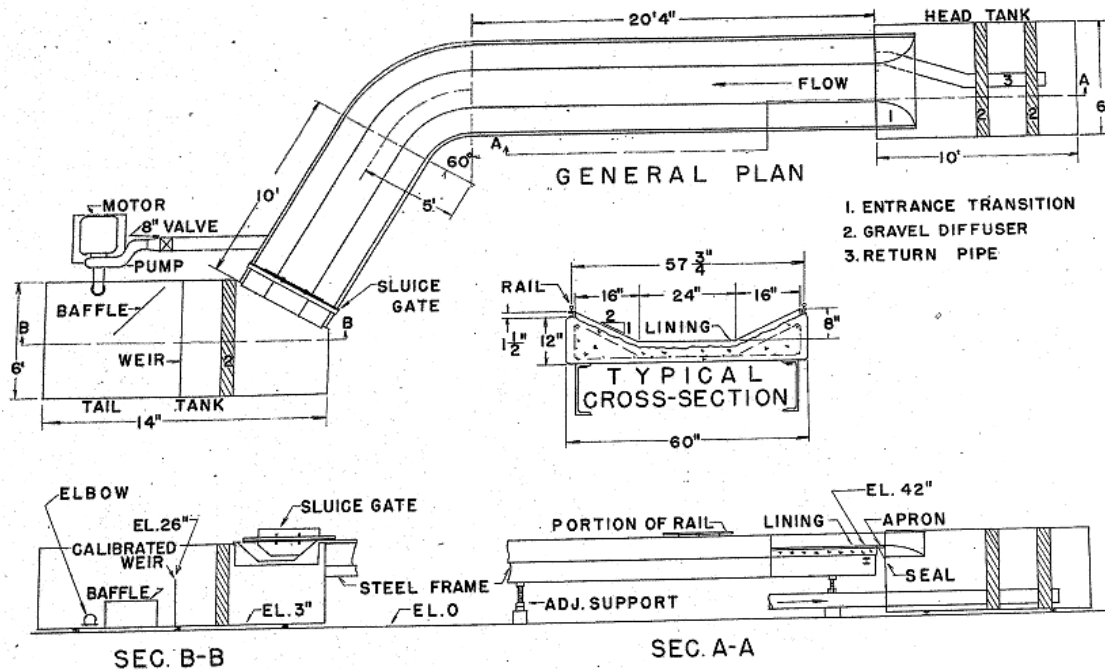


Figure 2.15: Schematic of Testing Facilities Used in Ippen *et al.* (1960a,b; Figure 3 in Ippen *et al.* (1960a))

Flow-depth, velocity profiles, and boundary shear-stress data were collected during a range of six tests that incorporate flow depths from 3 to 6 in. Flow depth was collected using a point gage mounted on an instrument cart. Velocity profiles were collected using a 5/16-in. Prandtl tube. Boundary shear-stress measurements were collected using a Preston tube, calibration for which was based on Preston (1954). Table 2.1 summarizes the tests performed in Ippen *et al.* (1960a,b).

Table 2.1: Test Matrix for Ippen *et al.* (1960a,b)

		Nominal Depth (in.)				
		Smooth Channel			Rough Channel	
		3	4*	5	6*	4
Actual Depth, y	ln	2.98	3.86	5.08	6.00	4.00
Top Width, T_w	ln	35.92	39.44	44.32	48.00	40.00
R_c/T_w		2.17	2.02	1.86	1.75	2.00
T_w/y		12.05	10.21	8.72	8.00	10.00
Q	cfs	0.85	1.27	2.02	2.86	0.96
V_{avg}	ft/s	1.36	1.50	1.67	1.91	1.08
Reynolds	$\times 10^5$	1.21	1.63	2.31	3.00	1.22
τ_o^{**}	lb/ft ²	0.0070	0.0087	0.0101	0.0148	0.0126

* Tests with 4-in. and 6-in. depths were run for single, double, and reverse curves

**Straight channel boundary shear stress (τ_o) was taken from data at the entrance to the bend

Boundary shear-stress data taken at ten cross sections were normalized with the approach straight-channel boundary shear stress and compiled in distribution plots showing contours of equal values along the bend (Table 2.2). Maximum values of measured boundary shear stress to straight-channel boundary shear stress, τ_b/τ_o , were denoted on the distribution plots.

Table 2.2: Summary of Shear-stress Distribution (Ippen *et al.*, 1960a,b)

Test Depth (in.)	Curve Configuration	R_c/T_w	T_w/y	Maximum
				τ_b/τ_o
3	Single-Smooth	2.17	12.05	2.00
4	Single-Smooth	2.02	10.21	1.78
5	Single-Smooth	1.86	8.72	2.20
6	Single-Smooth	1.75	8.00	2.40
4	Double-Smooth	1.86	8.72	2.22
6	Double-Smooth	1.75	8.00	2.40
4	Reverse-Smooth	1.86	8.72	2.86
6	Reverse-Smooth	1.75	8.00	3.00
4	Single-Rough	2.00	10.00	2.00

From the figures provided in Ippen *et al.* (1960a,b), it is evident that the shear pattern through the meander bend is directly associated with the velocity distribution, a result not unexpected due to the fact that shear stress is a function of the change in velocity with depth. Areas of high velocity are correlated with the areas of high shear stress and the distributions are generally similar. For the test configurations with 3-in. and 4-in. depths, the area of maximum shear-stress intensity occurs on the outer bank just downstream of the apex. As the flow depth increased for 5-in. and 6-in. tests, the area of the maximum shear-stress intensity moved toward the inner bank at the entrance to the bend. There is some evidence from Ippen *et al.*'s (1960a,b) data, that increasing flow depth results in the migration of maximum shear-stress intensity upstream. Thus, the distribution and the magnitude of the boundary shear stress appear to be governed by flow conditions, although the dataset is rather thin. Ippen *et al.* (1960a,b) concluded that for the range of R_o/Tw tested (1.75 to 2.2), the maximum τ_b/τ_o is approximately 2.0.

2.4.2.2 IPPEN AND DRINKER (1962)

In 1962, Ippen and Drinker expanded previous research to include tests with both a 24-in. bottom width trapezoidal section and a 12-in. bottom width trapezoidal section. The trapezoidal section with a 12-in. bottom width was constructed within the original 24-in. bottom width section and has a larger radius of curvature of 70 in. All other planimetric pattern factors remain the same as tests performed in Ippen *et al.* (1960a,b). Collection of data was also conducted in a similar manner as the Ippen *et al.* (1960a,b) tests, using a calibrated Preston tube for boundary shear-stress measurements. Seven configurations were tested; four included a single bend with a 24-in. trapezoidal section,

while three included a single bend with a 12-in. trapezoidal section. All tests were run within a smooth channel boundary. Tests 2, 3, and 4 were run twice because of minor changes to the surface pitot tubes (Ippen and Drinker, 1962). Test results and configurations for Ippen and Drinker (1962) are summarized in Table 2.3.

Table 2.3: Summary of Shear-stress Distribution (Ippen and Drinker, 1962)

Test Number	Test Depth (in.)	Curve Configuration	R_c/Tw	Tw/y	Maximum τ_b/τ_o
1	3	Single-Smooth; $b = 24$ -in.	1.670	12	2.000
2-A*	4	Single-Smooth; $b = 24$ -in.	1.521	10	1.782
2-B*	4	Single-Smooth; $b = 24$ -in.	1.500	10	1.784
3-A, 3-B*	5	Single-Smooth; $b = 24$ -in.	1.354	8.8	2.198
4-A	6	Single-Smooth; $b = 24$ -in.	1.354	8	2.198
4-B	6	Single-Smooth; $b = 24$ -in.	1.250	8	2.399
5	2	Single-Smooth; $b = 12$ -in.	1.251	10	2.400
6	3	Single-Smooth; $b = 12$ -in.	3.493	8	1.588
7	4	Single-Smooth; $b = 12$ -in.	2.907	7	1.600

* Additional runs for Tests 2, 3, and 4 were run to troubleshoot slight changes to instrumentation

Ippen and Drinker (1962) concluded, based on test results, that locations of maximum boundary shear stress are associated with areas of highest velocity and that the location of the maximum boundary shear is a function of flow conditions. For flow depths 5-in. and above, maximum boundary shear stress was located on the inner bank near the upstream end of the bend. For flow depths less than 5 in., the location of maximum shear stress was located on the outer bend, downstream of the apex. From the data in Table 2.3, the maximum relative boundary shear stress was measured to be 2.4.

2.4.2.3 USBR (1964)

The USBR (1964) investigated the velocity and shear-stress distribution in a 2-ft wide flume with 1.5H:1V side slopes, a radius of curvature of 16 ft, and a central bend angle of 15 degrees. A single test was run at 2.85 cfs and 0.75-ft depth (Table 2.4). A 30-ft straight entrance to the bend helped cultivate fully-developed flow and an 18-ft long exit section was placed downstream of the bend. Depth measurements were made with a point gage, velocity was measured with a Prandtl tube, and the boundary shear stress was measured with a Preston tube, calibration for which was based on Preston (1954). Data were taken at ten cross sections, shown in Figure 2.16.

Table 2.4: Summary of Boundary Shear Test Results for USBR (1964)

Test Depth (ft)	Curve Configuration	R_c / T_w	T_w / y	Maximum
				τ_b / τ_o
0.75	Single-Smooth; $b = 2$ ft	3.765	8.00	1.352

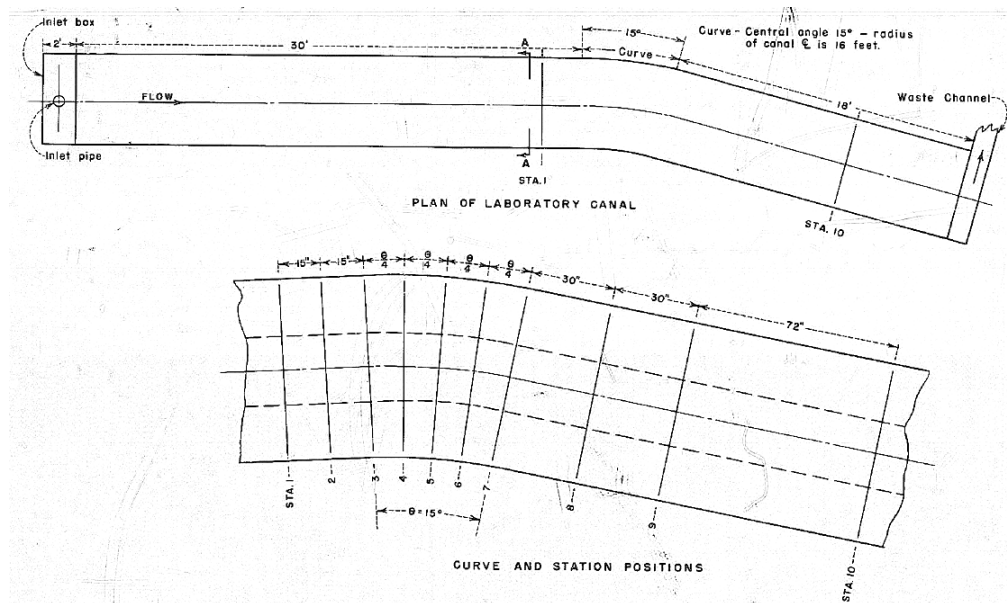


Figure 2.16: Schematic of Test Facility Used in USBR (1964; Frame 1)

From collected data, velocity distributions plotted for each cross section showed that a relatively uniform velocity profile at the upstream cross-section Station 1 becomes increasingly asymmetric through the meander bend near cross-section Stations 5 and 6, with the area of maximum velocity near the outer bank. Downstream of the bend apex, near cross-section Stations 7 and 8, the velocity profile begins to spread out across the entire cross section. At the approach section and through the bend, the maximum measured velocity is 1.3 ft/s and does not appear to increase in magnitude.

Shear-stress distributions through the bend were also created from the collected data. For the single test run, the point of maximum shear stress was located on the inner bank near the entrance to the bend. Since only one test was conducted, it is uncertain how this location might have shifted to the outer bank for varying flow conditions. A bend shear-stress correction factor, $K_{BEND-SHEAR}$, of 1.352 was computed using the maximum measured shear stress of 0.0073 lb/ft² and the centerline approach shear stress at cross section Station 1 of 0.0054 lb/ft².

2.4.2.4 YEN (1965)

Yen (1965) investigated velocity and shear-stress distributions in a 90-degree bend with a smooth trapezoidal cross section of 6-ft bottom width and 1H:1V side slopes. The radius of curvature for the test section was 28 ft. Two 90-degree bends were constructed, but only the second bend was used for data collection. A schematic of the testing facility is provided in Figure 2.17.

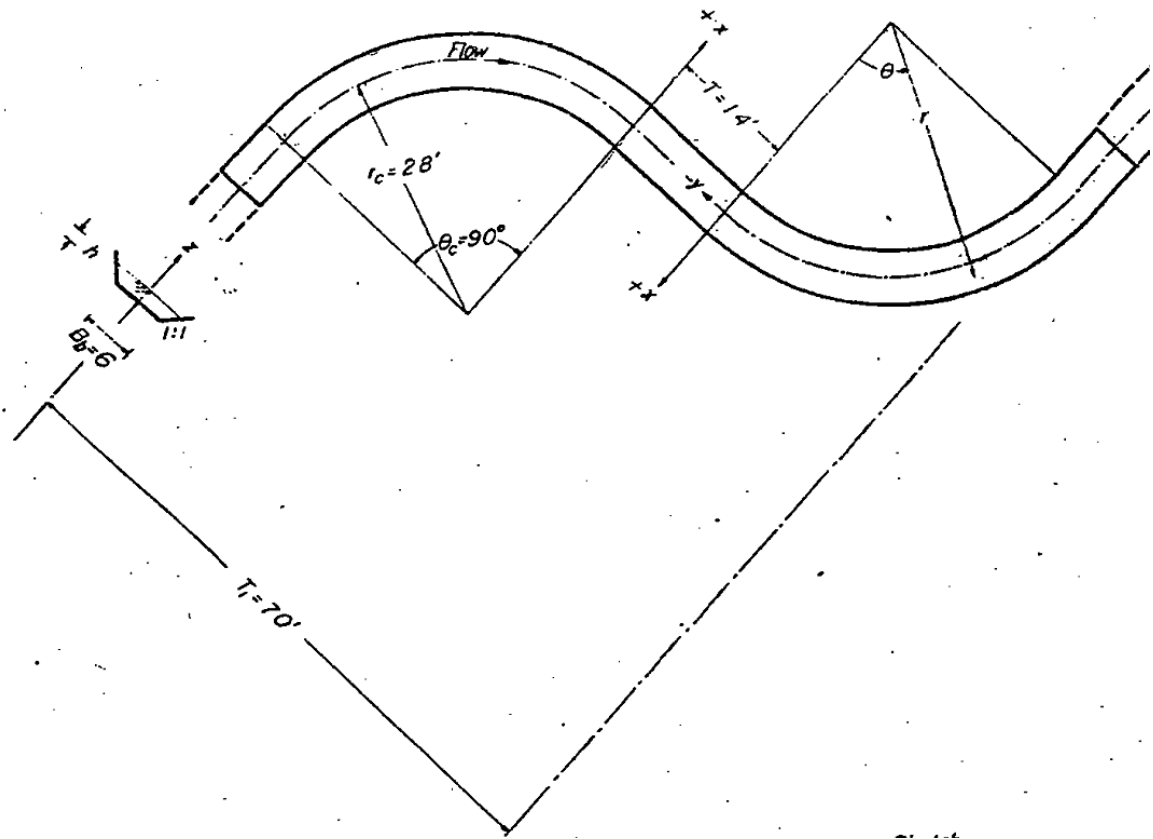


Figure 2.17: Schematic of Test Facility Used in Yen (1965; Figure 2)

Depth, velocity, and shear stress were measured at the entrance to the first bend, through the tangent reach, and every $\pi/16$ radian increment of θ in the second bend. A standard Prandtl tube was used to measure the velocity and a Preston tube, calibrated in a straight 3-ft wide, 90-ft long tilting flume of similar roughness, was used for the boundary shear-stress measurements. Five tests were conducted at varying depths, velocity, and width-to-depth ratios.

Velocity distributions entering the upstream bend from the straight reach follow a fairly uniform pattern. At the exit of the first bend, flow decelerates along the outside of the transition and speeds up on the opposite bank. Flow in the transition is affected both by residual vorticity from the upstream bend and super-elevation from the downstream

bend. It was found that maximum measured velocity near the entrance to the second bend was approximately 1.24 times the velocity measured in the straight reach upstream of the first bend. As flow moves through the bend, the areas of maximum velocity distribution shift from the inner to the outer bank and shift back again near the bend exit. Recovery of a uniform velocity distribution at the bend exit was found to be swift where the maximum measured centerline velocity was found to be 1.06 times that of the upstream straight reach.

Boundary shear-stress distribution was mapped through the bend in terms of a measured magnitude relative to the average boundary shear stress. Areas of maximum boundary shear stress at the entrance to the bend are located along the inner wall of the channel and follow a smooth arc through the bend until the latter section, where the maximum boundary shear stress shifts slightly toward the center. This general pattern is similar in all five tests. Although areas of maximum boundary shear stress follow the inner bank through the bend, it was thought that the orientation of the stresses and the spiral motion are in such a direction as to stabilize the inner bank rather than to scour it. Spiral motion along the outer bank directs the shear forces downward and thus facilitates the degradation of bank material. Location of the outer bank scour occurs mostly downstream of the apex due to residual spiral motion from upstream countering erosion forces at the apex. In general, Yen (1965) found that the highest velocity and shear stresses occur near the inner bank at the entrance of the curve. Table 2.5 summarizes the results from the shear-stress distribution analysis from Yen (1965). Values of the maximum τ_b/τ_o were obtained from the contour plots of the shear-stress distribution through the bend. Localized areas of maximum shear stress were not identified on these

plots and, therefore, the maximum τ_b/τ_o may, in fact, be slightly greater than the nearest contours indicate.

Table 2.5: Summary of Boundary Shear Test Results for Yen (1965)

Test Number	Test Depth (ft)	Curve Configuration	R_c/Tw	TW/y	Maximum
					τ_b/τ_o
1	0.354	Double-Smooth; $b = 6$ ft	4.175	20.1	1.199
2	0.465	Double-Smooth; $b = 6$ ft	3.998	15.0	1.301
3	0.475	Double-Smooth; $b = 6$ ft	3.986	14.8	1.301
4	0.477	Double-Smooth; $b = 6$ ft	3.983	14.8	1.296
5	0.675	Double-Smooth; $b = 6$ ft	3.732	11.1	1.298

2.4.2.5 HEINTZ (2002)

Heintz (2002) constructed an undistorted 1:12 Froude scale, fixed bed, physical model of a 29-mi reach of the Middle Rio Grande. The physical model consisted of two channel bend geometries that were characteristic of the Middle Rio Grande reach. An upstream bend had a 38.75-ft radius of curvature and a bend angle of 125 degrees had a trapezoidal section with a 10.2-ft bottom width and 3H:1V side slopes. The downstream bend had a 65.83-ft radius of curvature and a bend angle of 73 degrees had a trapezoidal section with a 6-ft bottom width and 3H:1V side slopes. Heintz (2002) collected flow-depth, three-dimensional (3-D) velocity, and boundary shear-stress data at seven points on each cross section for eighteen cross sections over the test reach for four different discharges (8, 12, 16, and 20 cfs). Velocity and shear-stress distributions were plotted for each cross section and measured values along the inner and outer banks for each cross section were compared to the measured values at the channel centerline for the same cross section. A schematic of the testing facility used in Heintz (2002) showing cross-section locations is provided in

Figure 2.18.

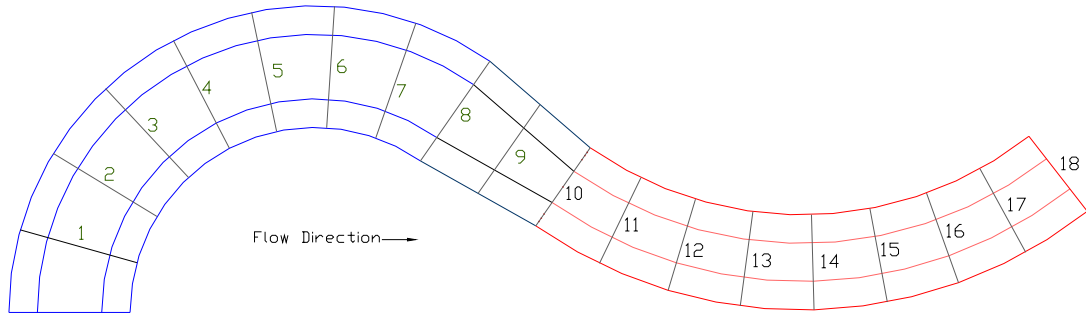


Figure 2.18: Schematic of Testing Facility Used in Heintz (2002; Figure 3.11)

Velocity distribution followed predictable patterns of being fairly uniform near the upstream entrance to the bends, with slightly higher velocities on the outer bank through the bend. Figure 2.19 shows a series of cross sections from upstream (top, Cross Section 17) to downstream (bottom, Cross Section 11) with velocity vectors plotted for 16 cfs.

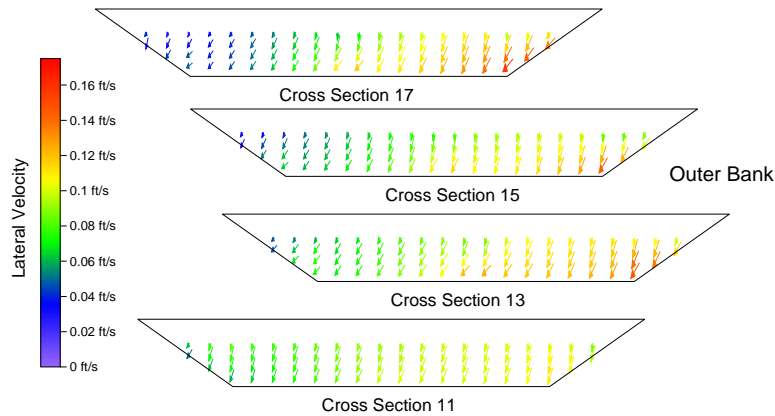


Figure 2.19: Velocity Vectors through the Upstream Bend at 16 cfs, $y = 0.93$ ft (Figure 4.4 in Heintz (2002))

Clearly, areas of high velocity exist on the outer bank but near the bend exit (Cross Section 11) velocity asymmetry disappears quickly, becoming uniform across the cross section. Inner and outer bank velocities were compared with centerline velocities and plotted with respect to cross-section station in Figure 2.20 and Figure 2.21,

respectively. Inner bank velocity near the entrance to the upstream cross section shows highest measured shear stress at approximately 1.27 times the centerline velocity. Moving through the bend, the inner bank velocity decreases dramatically and is approximately 0.75 times the centerline velocity at the bend exit. At the same time, the outer bank velocity remains approximately 1.1 ft/s throughout the bend. A similar trend can be seen on the downstream bend where the inner bank velocity begins 1.2 times the centerline velocity and reduces to 0.9 of the centerline velocity near the bend exit. The outer bank velocity on the downstream bend begins quite a bit lower than the upstream at 0.9 times the centerline velocity and increases to about 1.1 at the bend exit. It is likely that the low inner bank velocity, 0.75 times the centerline velocity, affects the low outer bank velocity at the downstream bend entrance. Although some equalization does occur in the transition, some spiraling motion persists at the entrance to the downstream bend.

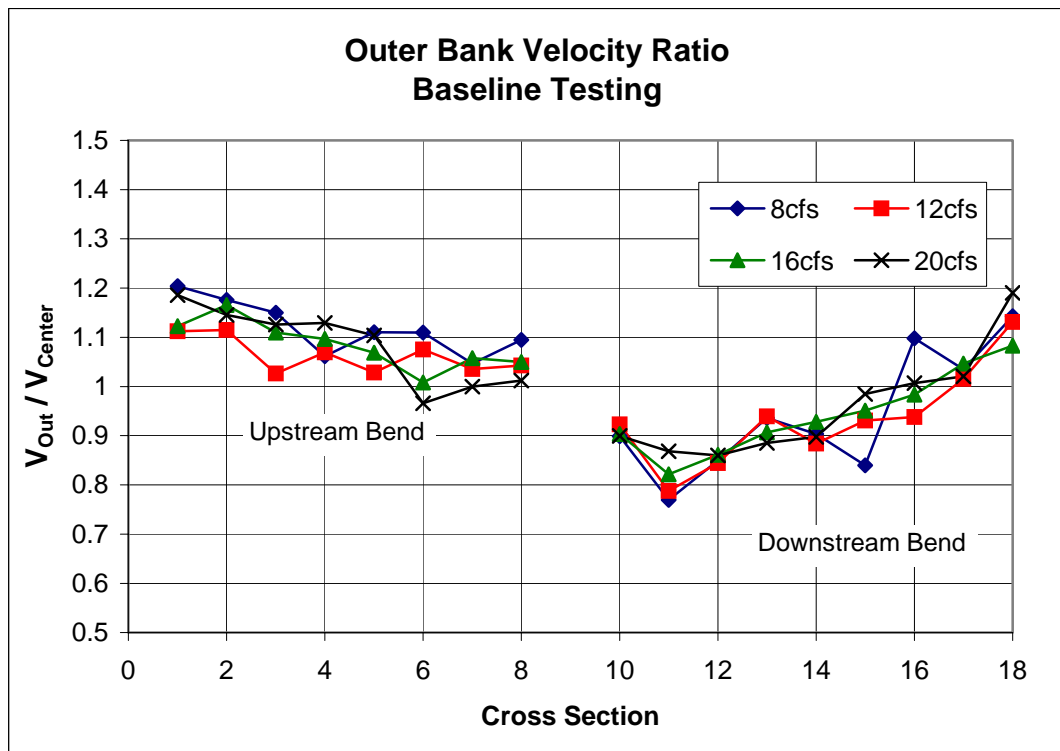


Figure 2.20: Outer Bank Velocity Comparison with Centerline Velocity (Figure 4.5 in Heintz (2002))

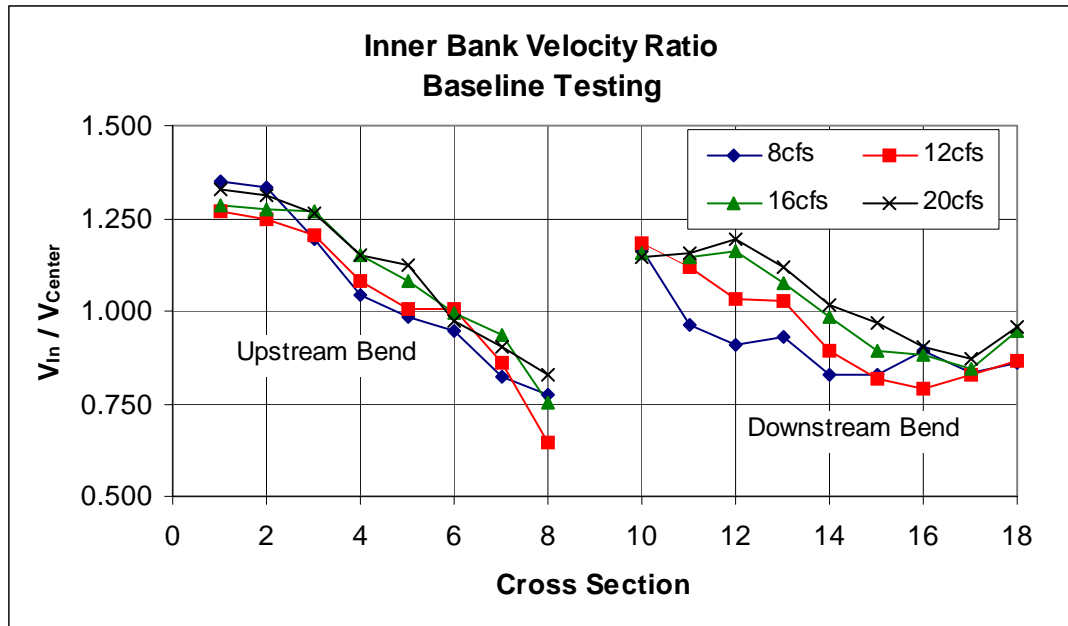


Figure 2.21: Inner Bank Velocity Comparison with Centerline Velocity (Figure 4.6 in Heintz (2002))

Boundary shear-stress distributions were plotted using contours of equal shear stress along the upstream (U/S) and downstream (D/S) bends in Figure 2.22 and Figure 2.23, respectively. Figure 2.22 and Figure 2.23 include shear-stress contour plots for 8, 12, and 16 cfs.

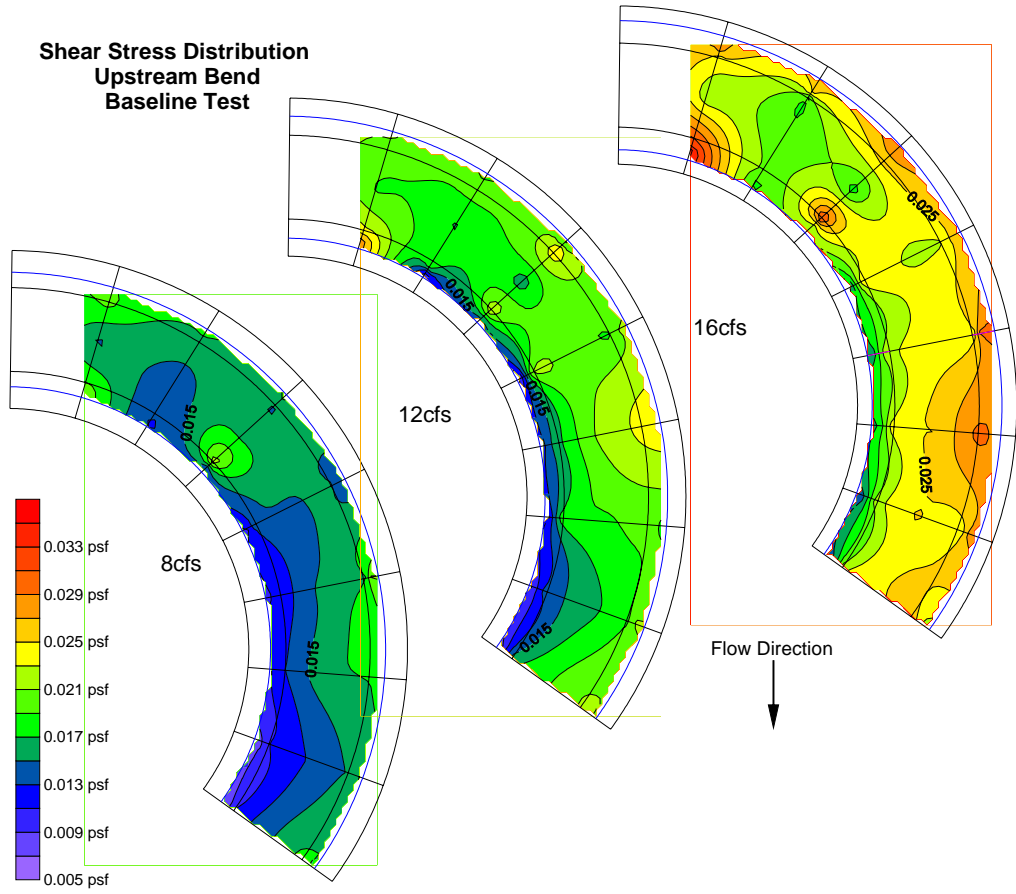


Figure 2.22: Upstream Shear-stress Distributions (Figure 4.7 in Heintz (2002))

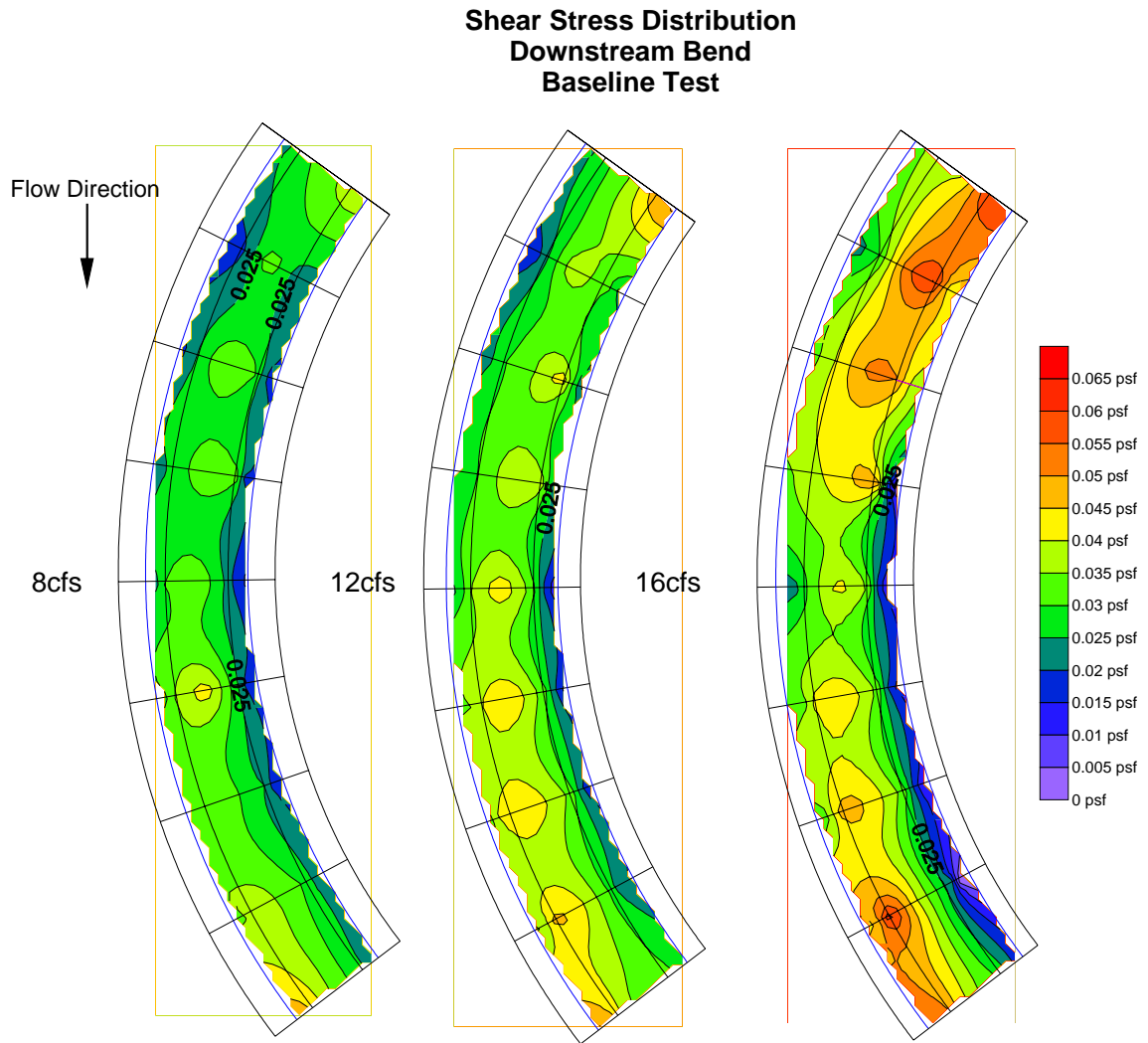


Figure 2.23: Downstream Shear-stress Distributions (Figure 4.8 in Heintz (2002))

Areas of maximum shear stress found in Heintz (2002) begin at the upstream end of the bend near the inner wall and migrate, through the bend, towards the outer wall past the apex, near the exit. Shear-stress distribution patterns found in Heintz (2002) agree with patterns found in Ippen and Drinker (1962; Ippen *et al.*, 1960a,b) for smaller depths. Measured outer and inner bank shear stresses were compared to centerline shear stress at each cross section in Figure 2.24 and Figure 2.25, respectively.

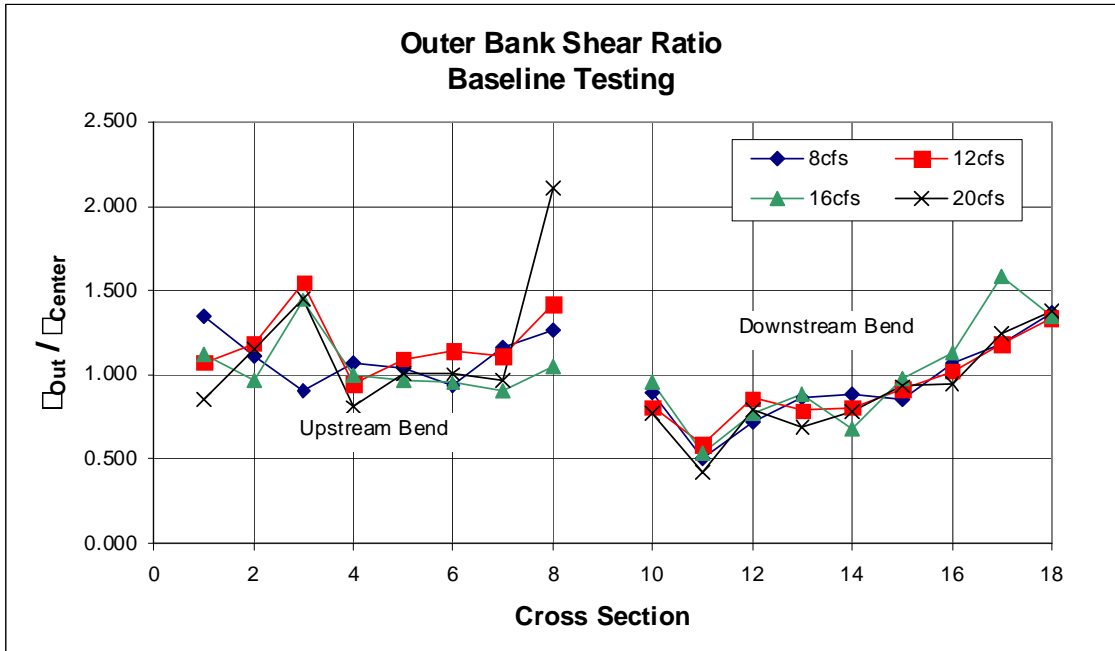


Figure 2.24: Outer Bank Shear-stress Comparison with Centerline Shear Stress (Figure 4.11 in Heintz (2002))

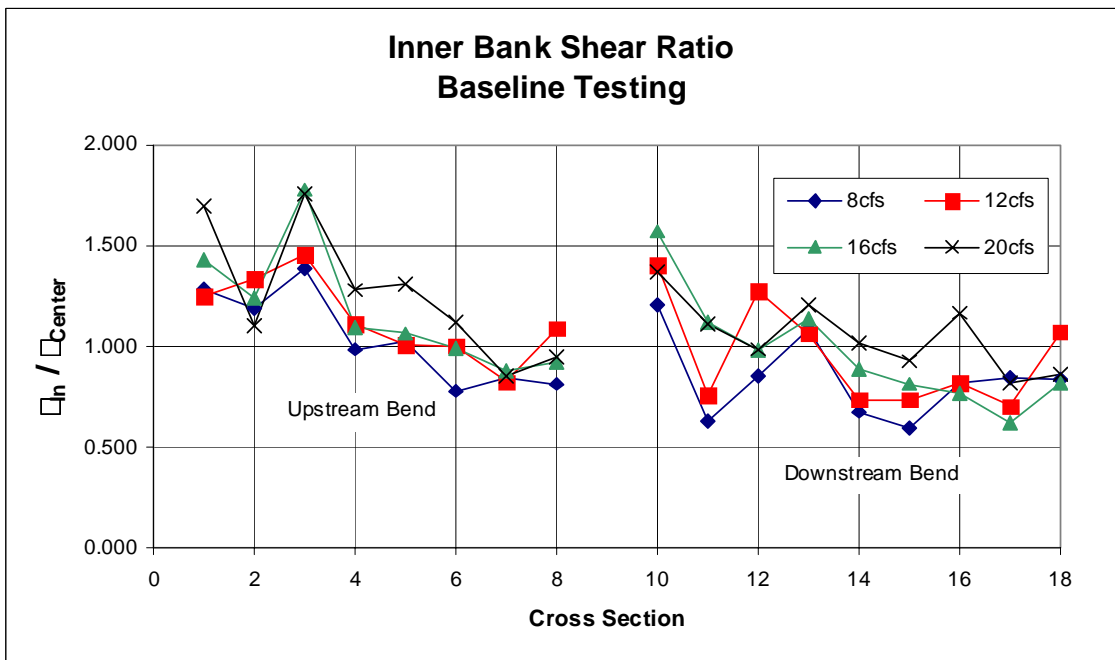


Figure 2.25: Inner Bank Shear-stress Comparison with Centerline Shear Stress (Figure 4.12 in Heintz (2002))

Boundary stress distribution through the upstream and downstream bends follows a similar pattern as the velocity distribution. Inner bank shear stresses begin at approximately 1.5 at the bend entrance and reduce to approximately 1.0 at the bend exit. Outer bank shear stresses at the entrance to the downstream bend are approximately 0.95 lb/ft², indicating correlation to the inner bank shear stress at the upstream bend exit. Outer bank shear stress in the upstream bend remains relatively constant at about 1.2 lb/ft². The outer bank shear stress at the entrance to the downstream bend increases more drastically than the upstream bend, starting out at approximately 1.0 lb/ft² and ending up at about 1.4 lb/ft². Both velocity and shear-stress distributions show some migration toward the outer bend, and from the velocity and shear-stress comparisons with the centerline values, there is some evidence that spiral flow from the upstream bend affects the hydraulics near the downstream bend.

2.5 BENDWAY WEIR AS AN EROSION COUNTERMEASURE

2.5.1 BACKGROUND

Geomorphic changes of the Middle Rio Grande River below Cochiti Dam have caused a traditionally-braided river to become a sinuous meandering river. Bank erosion caused from the Middle Rio Grande's morphological change to a meandering river pattern has threatened riverside infrastructure, farmland productivity, irrigation systems, levee function, aquatic habitat, and riparian vegetation (Heintz, 2002). Various bank stabilization measures have been researched by the USBR, but the endorsement of bendway weirs is the result of their unique ability to stabilize the bank while sustaining

sensitive habitat and riparian vegetation. The following section describes the bendway-weir functions, physical parameters, and use in practical applications.

CSU and the USBR have been conducting physical experiments on the use of bendway weirs since 2002. In the research program that CSU has developed with the USBR, a bendway weir refers to an elongated rock structure extending from the river bank at some defined angle and for some specified distance into the main stream flow. Structures of this type have, in previous research, been generally referred to as dikes, contracting dikes, transverse dikes, cross dikes, spur dikes, spurs, spur dams, cross dams, wing dams, jetties, barbs, and groins (groynes) (Richardson and Simons, 1974; USACE, 1980; Brown, 1985; Federal Highway Administration (FHWA), 2001; Welch and Wright, 2005).

Bendway weirs deflect current from the bank in which they are installed to the center of the channel, thus moving abrasive forces away from a degrading bank, establishing a stable channel for navigation, and providing or maintaining aquatic habitat between weir structures. Bendway weirs are traditionally used on sand-bed rivers, either single or multiple channel, and are not generally effective in mountainous gravel-bed rivers (Richardson and Simons, 1974), although Welch and Wright (2005) stated that weirs could be used on low-gradient alluvial river systems with cobble or gravel beds. Weirs are best used on rivers with sinuosity greater than 1.2, slope less than 2 percent, and width-to-depth ratio greater than 12. Use of bendway weirs is not recommended in narrow deep channels with width-to-depth ratios less than 10 (Knighton, 1998). Bendway weirs are best used for bank stabilization when erosion processes are dominated by abrasion and high-tractive stresses. Where bank instability is the result of

geotechnical slope failure, countermeasures other than bendway weirs are more appropriately applied (Welch and Wright, 2005).

Bendway weirs, being installed at discrete locations, have an advantage over riprap in that they are cheaper and easier to maintain. Failure on a riprap-protected bank is typically catastrophic in nature, whereas failure of bendway weirs does not threaten the stability of the entire structure (Richardson and Simons, 1974). Installation of bendway weirs also requires less construction right-of-way and less bank alteration than other countermeasures such as riprap (Brown, 1985). Bendway weirs are described based on their physical attributes, such as permeability, cross-section shape, or construction material. While no definitive design guidelines exist for bendway weirs, much research has been conducted on their various physical attributes.

2.5.2 BENDWAY-WEIR GEOMETRY

Physical elements used to describe bendway weirs need to be clearly and consistently defined before any meaningful discussions of model results can be made. Figure 2.26 provides geometric variable definitions used to characterize bendway weirs and will be used as a reference when discussing their various physical attributes.

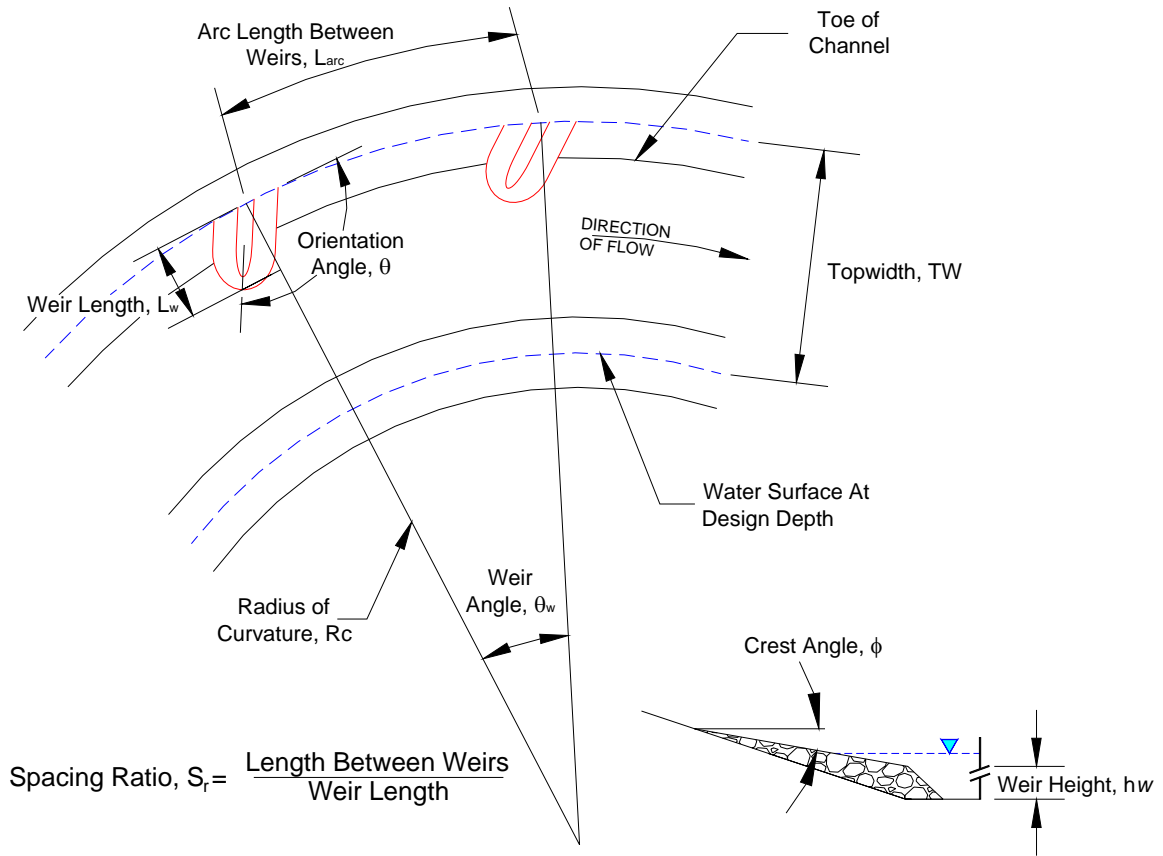


Figure 2.26: Variable Definition for Bendway Weirs

2.5.2.1 WEIR HEIGHT

Weir height depends almost entirely on the function of the weir and is, to some degree, related to weir permeability. Weir height set such that the structure is frequently overtopped can cause excessive erosion on the downstream face of the weir (Richardson and Simons, 1974). Overtopping impermeable weirs are especially vulnerable to erosion along the flank of the weir. For bank protection, weir height is typically set at bankfull elevation to prevent excessive bank erosion. Richardson and Simons (1974) recommended that weir height be set at 1 ft above bankfull in order to provide an adequate safety factor.

2.5.2.2 ORIENTATION ANGLE

Two types of bendway weirs are distinguished based on the orientation angle being greater or less than 90 degrees. Bendway weirs having deflection angles larger than 90 degrees are referred to as repelling weirs, while bendway weirs having angles less than 90 degrees are referred to as attracting weirs (Richardson and Simons, 1974). Richardson and Simons (1974) recommended attracting weirs with angles less than 90 degrees not be used due to their propensity to exacerbate bank erosion by directing the current toward the outer bank. In general, Richardson and Simons (1974) recommended weirs with deflection angles of 90 degrees be used and in cases where weirs are used to guide the flow, 100 to 110 degrees are appropriate.

Pokrefke (1990), however, reported improved performance from downstream-directed weirs. USACE (1980) recommended weir angles normal to the bank for most applications or slightly downstream at angles of 85 to 90 degrees. USACE (1980) reported excessive weir tip scour potential as the main reason upstream-oriented weirs are not recommended. Copeland (1983) presented arguments for both upstream- and downstream-oriented weirs. On one hand, upstream-facing weirs, while providing adequate bank protection by effectively redirecting water, induced additional scour in the vicinity of the tip and face of the weir. Because of increased scouring potential on upstream-facing weirs, additional protection is necessary, thus increasing cost of installation. Downstream-facing weirs have reduced scour potential due to the more streamlined orientation, and the fact that debris and trash are less likely to get caught on the weirs. However, downstream-oriented weirs redirect the current into the bank rather than away from the bank, resulting in the need for the weirs to be placed closer together

for additional bank protection to be installed. Arguments for and against upstream and downstream oriented weirs have caused Copeland (1983) to recommend a weir orientation angle of 90 degrees. Numerical simulations by Seed (1997) varied the orientation angle from 60 to 120 degrees and have shown that weirs with orientation angles of 90 degrees perform optimally. The Indian Central Board of Irrigation and Power (1971) recommends weir angles between 100 and 110 degrees (directed upstream). Welch and Wright (2005) advised that weir orientation angles should be between 150 to 160 degrees to avoid capturing too much cross-stream flow, resulting in flanking. Clearly, weir orientation is a subject of a great deal of debate, but, for the purposes of the Middle Rio Grande research program performed at CSU, weir angles varied from 90 degrees to 120 degrees.

2.5.2.3 WEIR LENGTH

Length of the bendway weir is generally a function of the desired channel contraction and the purpose of the weir. USACE (1980) denoted the limits of contraction as channel control lines or rectified channel lines. Because weir spacing is typically given in terms of some multiplier of the weir length, consideration of weir length must be evaluated in tandem with the distance between weirs (Richardson and Simons, 1974). Optimum channel flow, velocity, stage, sediment transport, and scour potential during bankfull, or design flow can be used to evaluate the amount of constriction that should be allowed. When hydraulic necessity does not dictate channel control lines, the United Nations (1953) recommended choosing a shorter length and extending the weir if the area behind the weir silts up. Richardson and Simons (1974) suggested that the maximum

length be less than 10 to 15 percent of the bankfull channel width. Brown (1985) recommended weir lengths for impermeable weirs to be less than 15 percent of the bankfull channel width and permeable weirs less than 25 percent of the channel width. Welch and Wright (2005) and FHWA (2001) advocate that the weir length should not exceed 1/3 the cross-section top width at bankfull stage and that the weir should be keyed into the bank from 1/4 to 1/3 of the weir length.

2.5.2.4 CROSS SECTION

A trapezoidal cross section is typically used for bendway-weir construction. Side slopes and tip slope should be determined for maximum stability and scour protection. Crest width is based on functionality and resistance to mobilization (USACE, 1980). Richardson and Simons (1974) recommended a minimum crest width of 3 ft, with larger widths being used for hauling and placement of stone, and side slopes of 2H:1V. USACE (1980) recommends a crest width of 10 ft when rock is delivered to the weir from a barge and 10 to 14 ft if the weir is to be constructed by trucks. Side-slope guidance varies from 1H:1V to 2H:1V for the sides of the weir and 5H:1V for the tip of the weir where erosion potential is greater.

2.5.2.5 PERMEABILITY

Bendway weirs can be either permeable or impermeable depending on the function of the weir. Permeable weirs have the advantage of equalizing pressures between the upstream and downstream faces. However, permeable weirs lack overall strength and have limited deflection ability (United Nations, 1953). Both permeable and

impermeable weirs will reduce sediment-carrying capacity near the bank and induce sediment deposition. However, the source of material deposited between impermeable weirs is primarily from overtopping flows which deliver significant amounts of suspended sediment that deposit as the flood stage withdraws (Brown, 1985). Some additional sediment sources for the area between impermeable weirs can be delivered from expanding flow as it moves past the weir tip (Brown, 1985). Permeable weirs allow sediment to flow freely through the structures, supplying significantly more material than what typically is available for impermeable weirs. Consequently, permeable weirs are able to induce much more sedimentation than impermeable weirs.

Care must be taken when designing impermeable weirs for overtopping. Scouring on the downstream face of impermeable weirs has been observed as a result of increased turbulence during overtopping. Because permeable weirs equalize pressure on either side of the weir, generation of turbulent conditions is not likely.

2.5.2.6 SPACING RATIO

Weir spacing is usually given in terms of some multiplier of the weir length. Both weir spacing and weir length must be considered simultaneously during design. The United Nations (1953) recommended spacing of one times the weir length for concave banks. Richardson and Simons (1974) recommended a spacing of 1.5 to 2 times the projected weir length for navigation purposes and 2 to 6 times the projected weir length for bank protection. Weir spacing between 0.75 and 2.5 have been suggested by the USACE (1980). The FHWA (2001) recommended that weir spacing be a function of the

weir length, radius of curvature, and channel width at design flow. Other studies have recommended spacing to be anywhere from 2 to 5 times the weir length.

Weir spacing can also be based on various other design criteria. Research by Winkler (2003) spaced weirs equally over the entire bend angle. Brown (1985), on the other hand, suggested that instead of a multiplier of weir length, weir placement should be determined by extending a tangent from the weir tip forward until the tangent intersects the bank, thus, bend geometry is inherently included in the weir design. Welch and Wright (2005) recommended a similar method, such that a weir is placed based on the extension of a riffle or downstream insertion point (Figure 2.27).

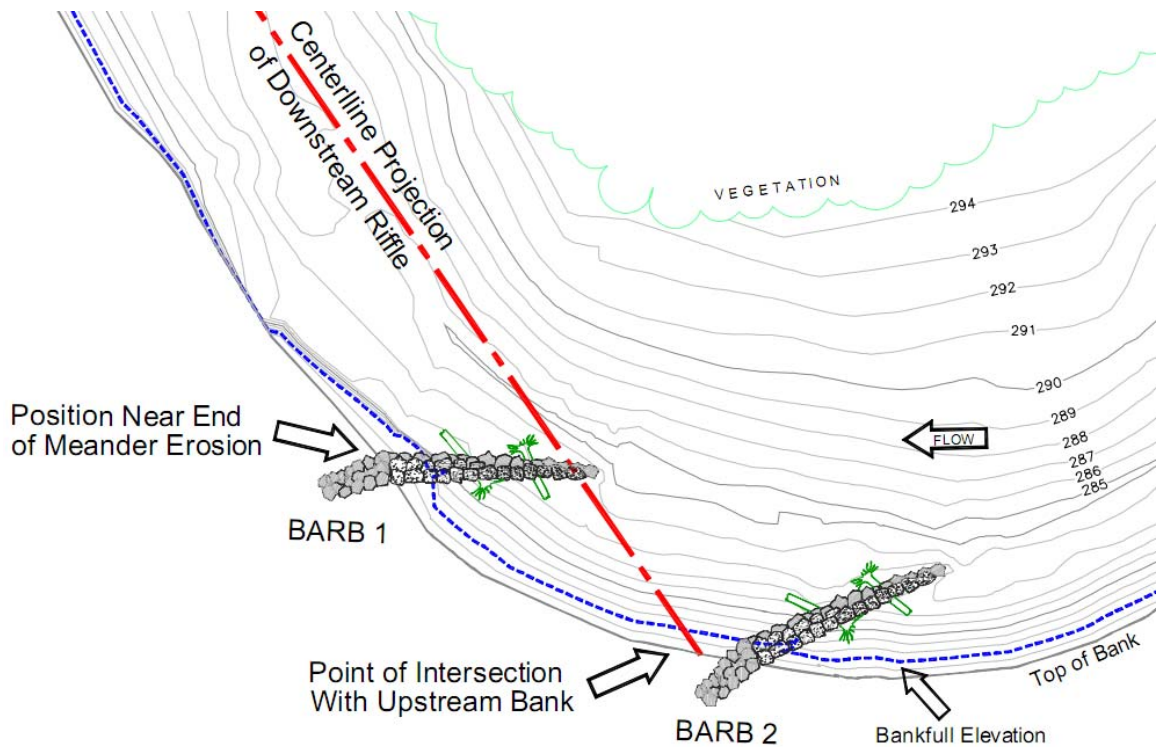


Figure 2.27: Weir Placement as a Function of Downstream Riffle/Insertion (NRCS; Figure 11 in Welch and Wright (2005))

Bendway weirs that are positioned too far apart will not effectively protect portions of the bank from erosion, and will allow the stream to meander into the bendway-weir field. Conversely, weirs that are positioned too close together duplicate functionality and add to the expense of the countermeasure.

2.5.3 FLOW PATTERN

2.5.3.1 BACKGROUND

Placement of bendway weirs along a river bank effectively creates two zones of flow; the main or constricted flow where the velocity, shear stresses, and potential for channel degradation are increased, and the area between weirs where velocities and shear stresses are greatly reduced and sediment deposition is encouraged. In laboratory experiments of impermeable weirs in a straight flume, Seed (1997) identified three areas of high velocity as key to the design of bendway weirs: 1) the maximum velocity in the main channel, 2) the maximum velocity near the weir tip, and 3) the velocity at the toe of the inner bank. Mobilization of the bed material and the size and depth of the scour hole at the tip of the weir depend on the stream power and the sediment distribution of the alluvial material. Degradation of the bed will increase the cross-sectional area, reducing velocities from initially high values and eventually reaching equilibrium (Richardson and Simons, 1974). Research by Knight *et al.* (1992) has shown that patterns of scour and deposition following construction with bendway weirs reach equilibrium after a period of about 2 yrs.

Local scour at the weir tip is caused from vortices of the fluid resulting from backwater on the upstream edge of the weir and subsequent acceleration of flow around the nose of the weir, shown in Figure 2.28 (Richardson and Simons, 1974).

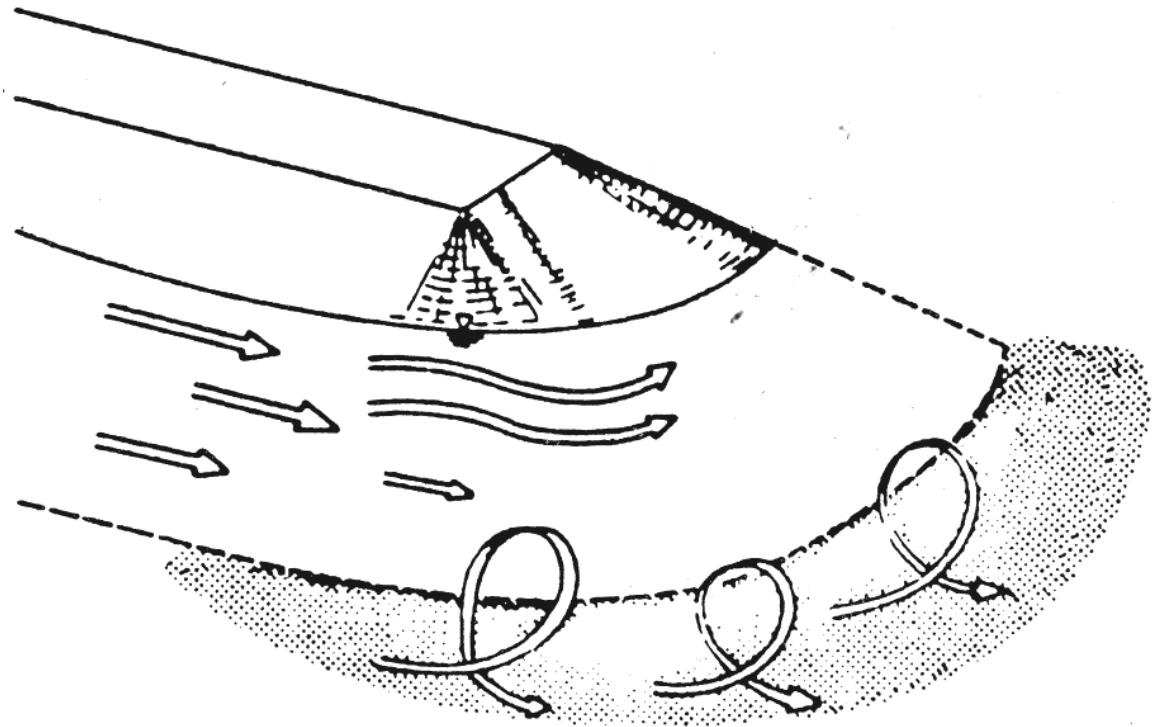


Figure 2.28: Vortex Formation near Weir Tip (Figure 3.1.8 in Richardson and Simons (1974))

Scour around weir tips has been found to be approximately 1.3 times the equilibrium scour depth in the overall channel (Richardson and Simons, 1974), but depends greatly on the position of the weir tips and the sediment size of the bed material. Silt and sand channels will encounter greater scour depths than channels with significant gravel or cobble size fractions (Brown, 1985). Upstream-angled weirs typically have greater scour potential at the weir tip and are more likely to induce sedimentation

upstream of the weir than downstream-oriented weirs (Przedwojski *et al.*, 1995). Figure 2.29 illustrates typical flow patterns associated with single weirs and weirs within a field.

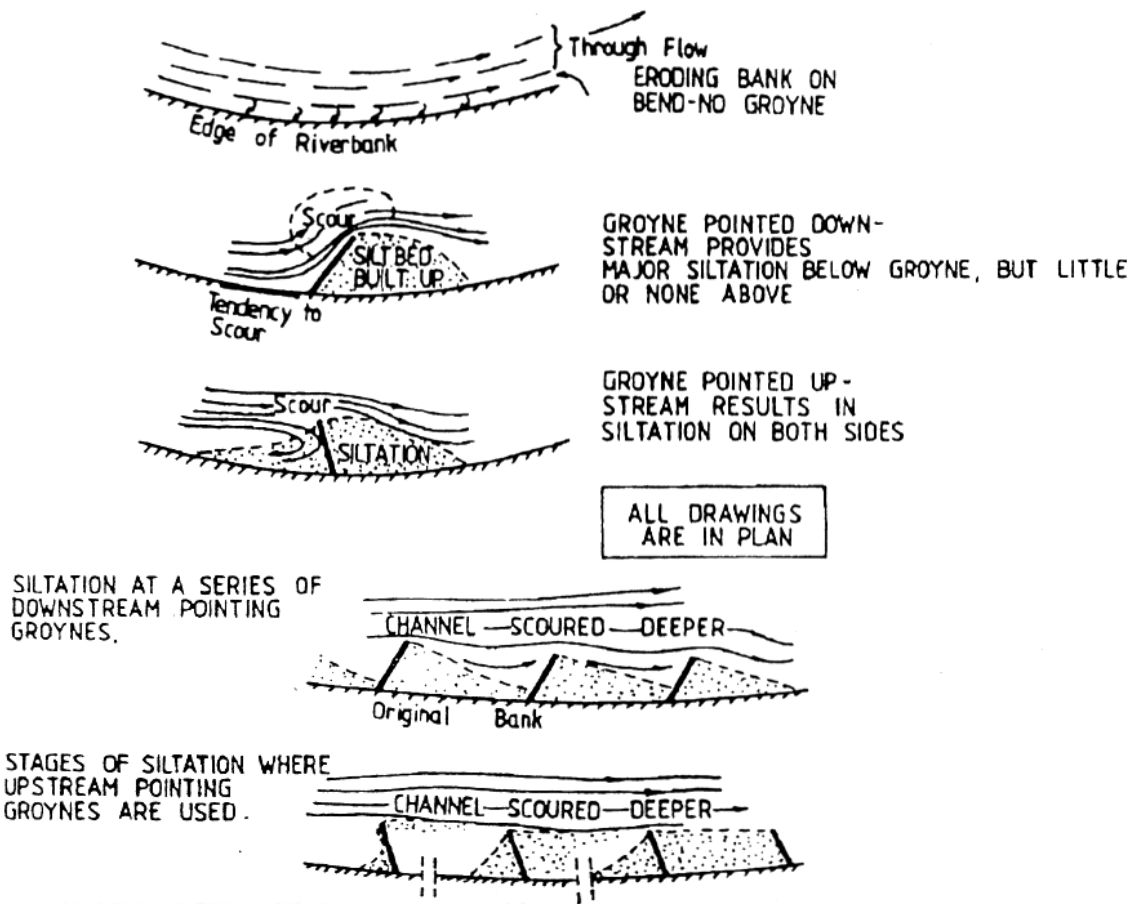


Figure 2.29: Siltation Patterns Associated with Upstream and Downstream Orientated Weirs (Figure 6.45 in Przedwojski *et al.* (1995))

Field data of scour depths associated with bendway weirs have generally been unavailable; therefore, laboratory experiments have been conducted to empirically derive predictive equations for scour depth. For each study, different opinions exist for what influences to include in the analytical prediction of scour depth. Table 2.6 includes a list of several scour-depth studies and indicates what parameters are included in their predictive scour-depth equation (Copeland, 1983).

Table 2.6: Parameters Included in Scour-depth Equations from Various Sources (Copeland, 1983; Welch and Wright, 2005)

Source	Upstream Depth	Velocity	Grain Size	Δ Width	Weir Length	Severity of Attack	Orientation Angle, θ
Inglis (1949)			✓			✓	
Blench <i>et al.</i> (1976)			✓			✓	
Ahmad (1953)						✓	
Garde <i>et al.</i> (1961)	✓	✓	✓	✓			✓
Liu <i>et al.</i> (1961)	✓	✓			✓		
Gill (1972)	✓		✓	✓			
Laursen (1962a,b)	✓				✓		✓
USBR (1977)	✓				✓		

All of the studies presented in Table 2.6 and their respective scour-depth equations, are empirically derived from laboratory experiments of a single weir in a straight flume. Correction factors are added to some of the equations to account for severity of attack and orientation angle as indicated in the last two columns of Table 2.6. Other methods of computing scour involve comparing computed velocity from hydraulic principles with empirically-derived limiting velocity based on grain size (Pemberton and Lara, 1984).

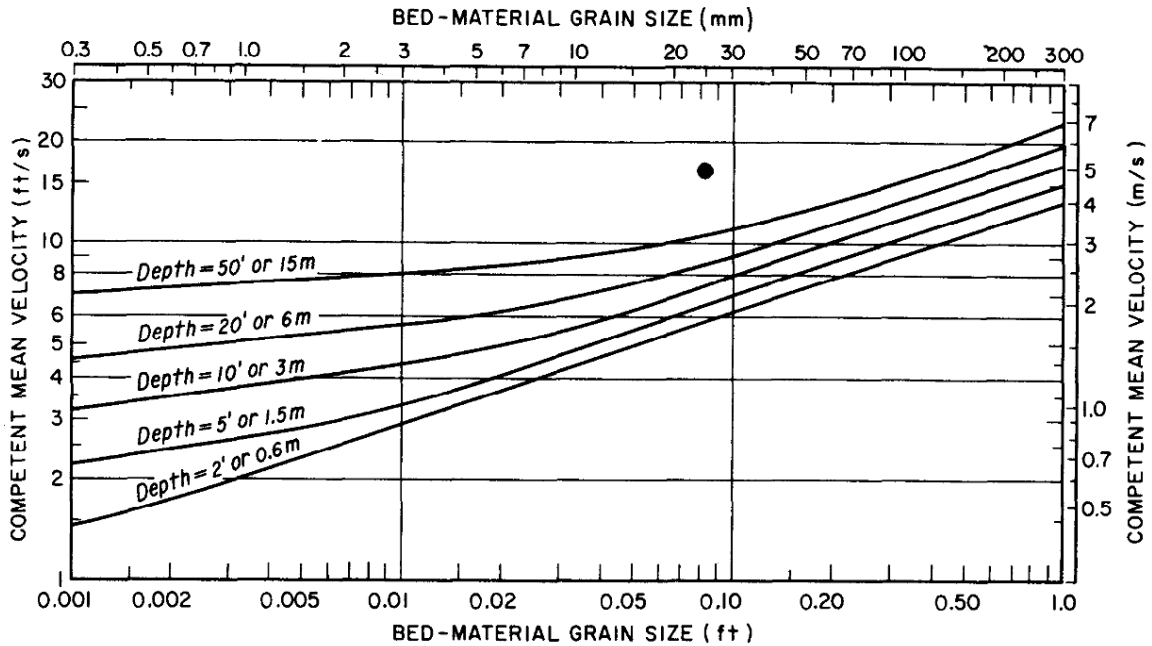


Figure 2.30: Empirically-derived Plot of Limiting Velocity Based on Bed-material Grain Size (Figure 12 in Pemberton and Lara (1984))

2.5.3.2 COPELAND (1983)

Copeland (1983) performed a series of studies in a sand-bed flume with three bends of sinuosity of 1.6, varying orientation angles from 60 to 120 degrees. Scour results were compared to the results from predictive equations from the studies shown in Table 2.6, but no conclusive recommendation was obtained. It was noted that each equation is derived from differing conditions, and that care needs to be used when computing predicted scour depth for design purposes. Additional tests by Copeland (1983) included rock aprons and gabion aprons at the toe of the weir. Both were found to be effective at preventing local scour immediately at the tip of the weir and both moved the point of maximum scour away from the weir tip and slightly downstream. Thus the

presence of a rock or gabion apron at the tip of the weir was found to dramatically increase the weir's stability.

Predicted equations from studies shown in Table 2.6 were typically developed for sand-bed streams. In some situations, where weirs are placed in streams with a gravel component to the bed material (*e.g.*, 10 percent coarse material which cannot be transported under constricted hydraulic conditions), armoring could develop as a natural byproduct of local scour (Pemberton and Lara, 1984). Where natural armoring is not likely to control local scour, placement of a stone blanket of sufficient size is necessary to armor the scour hole after it forms (Richardson and Simons, 1974). Additional stone protection is also required along the length of impermeable weirs if overtopping is expected. Rock sizing can be based on standard design equations for riprap on a sloped embankment. Riprap design equations are typically empirical in nature and solve for rock size as a function of a limiting velocity or limiting tractive force (Lagasse *et al.*, 2006; FHWA, 1989, 2006; USACE, 1991; Escarameia, 1998). While sizing rock riprap using limiting tractive force methodology is more academically correct, using limiting velocity is a generally more accepted design process (FHWA, 1989).

2.5.3.3 BROWN (1985)

Research by Brown (1985) was conducted in a straight flume with weir lengths at 20 percent of the channel width, for weirs of varied permeability and orientation angles. Maximum measured velocity near the weir tip was normalized with the average upstream cross-section velocity and plotted as a function of both percent permeable and spur angle in Figure 2.31.

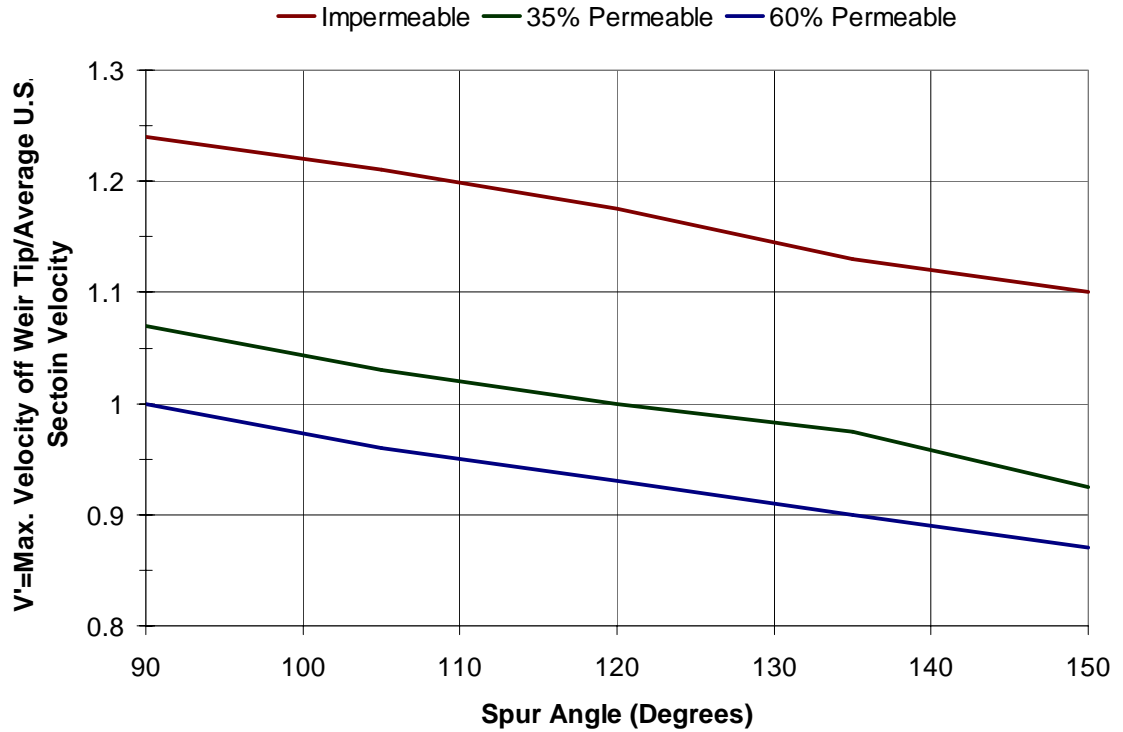


Figure 2.31: Maximum Velocity off Weir Tip as a Function of Permeability and Weir Angle (Brown, 1985)

Figure 2.31 shows that as the permeability decreases from 35 to 60 percent, there is a slight increase in the velocity off the weir tip. However, as the impermeability is entirely eliminated, there is more of a dramatic jump in velocity near the weir tip. Channel width was also compared to the maximum weir velocity as a function of permeability and similar patterns were found. Figure 2.32 shows the results from a single bend angle of 150 degrees.

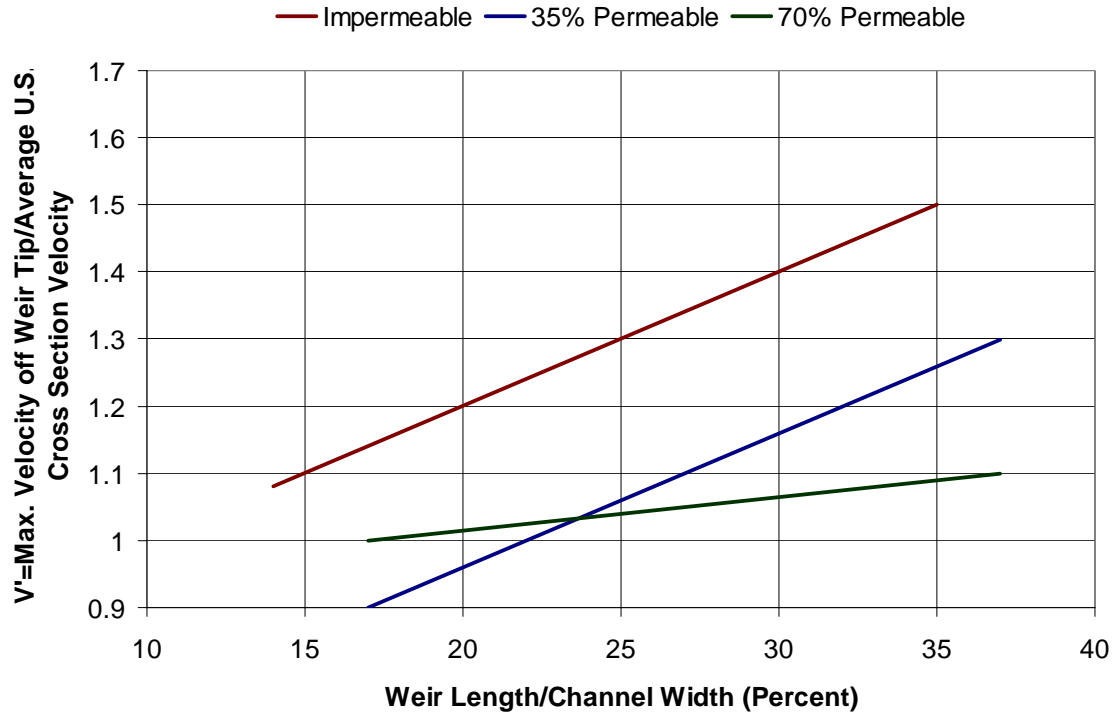


Figure 2.32: Maximum Velocity off Weir Tip as a Function of Weir Length (Brown, 1985)

Impermeable weirs and 35-percent permeability show similar patterns in velocity increase as the length of the weir increases, but 70-percent permeability shows a significant difference in velocity as the length of the weir is increased. Brown (1985) offered no explanation for this difference other than to note the overall trend of velocity increasing with decreasing permeability. Because tests were conducted in a straight flume, Brown (1985) indicated that the velocity ratio shown in Figure 2.31 is likely to be greater in a meandering channel bend where centrifugal acceleration affects the severity of attack.

2.5.3.4 SEED (1997)

Seed (1997) conducted a series of physical laboratory experiments and used the results to validate a 3-D computer model. Validation procedures indicated that the computer model was able to predict the velocities in the channel to ± 20 -percent accuracy for impermeable weirs. Once the computer model was validated, 3-D computer models of impermeable weirs along a uniform straight channel were created for weir fields to determine the effect of weir geometry, orientation, and spacing with different values of channel Manning's roughness. Four factors were found to significantly influence flow around a field of weirs: 1) area of the weir projected perpendicular to the flow, 2) weir spacing, 3) orientation angle, and 4) crest angle. A set of analytic equations for the depth-averaged velocity in the main channel (Equation 2.5), near-bed velocity near the weir tip (Equation 2.6), and near-bed velocity close to the bank toe (Equation 2.7) were developed from the results of the 3-D computer simulations:

$$V_{CHANNEL} = V_{AVG-APPROACH} (1.34A^* + 1) \quad \text{Equation 2.5}$$

where

$V_{CHANNEL}$ = velocity in the main channel after placement of weirs (m/s);

$V_{AVG-APPROACH}$ = approach velocity computed from continuity, Q/A ;

A^* = ratio of weir area to main channel area =

$$\frac{sA_g}{(A - sA_g)}; \text{ for } 0.15 \leq A^* \leq 1.3;$$

s = index: 1 for weirs placed on one side of channel and 2 for weirs placed on both sides of channel;

A_g = area of weir below the water surface measured perpendicular to the flow (m^2); and

A = total cross-sectional area of flow (m^2).

$$V_{TIP} = T_n(T_a + T_s + T_t) \quad \text{Equation 2.6}$$

where

V_{TIP} = normalized tip velocity = $\frac{\text{velocity near the tip of weir}}{\text{mean approach velocity}}$;

T_n = effect of channel roughness on tip velocity =

$$\begin{cases} \frac{1}{3}(2F_n + 1) & \text{for rectangular weirs;} \\ F_n & \text{for tapered weirs} \end{cases};$$

T_a = effect of weir area on tip velocity = $0.87A^* + 0.61$ for $0.13 \leq A^* \leq 1.3$;

T_s = effect of weir spacing on tip velocity = $0.077(S^* - 4)$ for $1.6 \leq S^* \leq 6$;

T_t = effect of crest angle on tip velocity = $-0.04t^*$ for $t^* \leq 0.5$;

A^* = ratio of weir area to main channel area = $\frac{sA_g}{(A - sA_g)}$;

s = index: 1 for weirs placed on one side of channel and 2 for weirs placed on both sides of channel;

A_g = area of weir below the water surface measured perpendicular to the flow (m^2);

A = total cross-sectional area of flow (m^2);

S^* = spacing ratio = $\frac{\text{longitudinal spacing of weirs}}{\text{weir length projected normal to flow}}$;

$$t^* = \text{taper ratio} = \frac{\text{taper length}}{\text{weir length}};$$

$$F_n = \text{bed roughness correction factor} = 2.12 \left[1 - \frac{1.303}{6 \ln \left(\frac{C_z}{26.72} \right) - 1} \right];$$

$$C_z = \text{Chezy's coefficient} \approx 1.81 \frac{H^{1/6}}{n};$$

$$H = \text{depth (m); and}$$

$$n = \text{Manning's roughness coefficient.}$$

$$V_{BANK} = B_n (B_a + B_s + B_t) \quad \text{Equation 2.7}$$

where

$$V_{BANK} = \text{normalized bank velocity} = \frac{\text{velocity at the toe of the bank}}{\text{mean upstream velocity}};$$

$$B_n = \text{effect of channel roughness on tip velocity} =$$

$$\begin{cases} F_n & \text{for rectangular weirs} \\ 1 & \text{for tapered weirs } (t^* > 0.5) \end{cases};$$

$$B_a = \text{effect of weir area on tip velocity} = 0.13A^* + 0.05 \text{ for}$$

$$0.13 \leq A^* \leq 1.3;$$

$$B_s = \text{effect of weir spacing on tip velocity} = -0.02(S^* - 4); \text{ for } 1.6 \leq S^* \leq 5$$

$$B_t = \text{effect of crest angle on tip velocity} = \begin{cases} 0.8(t^* - 0.6) & \text{for } 0.6 \leq t^* \leq 1.0 \\ 0 & \text{for } 0.5 \leq t^* \leq 0.6 \end{cases};$$

$$A^* = \text{ratio of weir area to main channel area} = \frac{sA_g}{(A - sA_g)};$$

s = index: 1 for weirs placed on one side of channel and 2 for weirs placed on both sides of channel;

A_g = area of weir below the water surface measured perpendicular to the flow (m^2);

A = total cross-sectional area of flow (m^2);

S^* = spacing ratio = $\frac{\text{longitudinal spacing of weirs}}{\text{weir length projected normal to flow}}$;

t^* = taper ratio = $\frac{\text{taper length}}{\text{weir length}}$;

F_n = bed roughness correction factor = $2.12 \left[1 - \frac{1.303}{6 \ln \left(\frac{C_z}{26.72} \right) - 1} \right]$;

C_z = Chezy's coefficient $\approx 1.81 \frac{H^{1/6}}{n}$;

H = depth (m); and

n = Manning's roughness coefficient.

Based on computer simulation results, Seed (1997) found that the weir tip velocities are approximately 1.2 times the average approach velocities. Parameter limitations of the design procedure presented by Seed (1997) are included in Equation 2.5, Equation 2.6, and Equation 2.7. Computer simulations and validation therein are based on impermeable weirs installed on a straight channel. Use of Seed's (1997) design equations for meandering or curved channels is likely to result in underestimating the respective velocities.

2.5.3.5 HEINTZ (2002)

Heintz (2002) constructed an undistorted 1:12 Froude scale, fixed brushed concrete bed, physical model of a 29-mi reach of the Middle Rio Grande. The physical model consisted of two channel bend geometries that were characteristic of the Middle Rio Grande reach. Bend characteristics used in the physical model are summarized in Table 2.7.

Table 2.7: Bend Characteristics for the Middle Rio Grande Physical Model (Heintz, 2002)

Bend Location	Channel Width ft (m)	Radius of Curvature ft (m)	Bend Angle Degrees	Relative Curvature <i>r/b</i>	Channel Length ft (m)
Upstream	19.2 (5.9)	38.75 (11.81)	125	2.02	84.5 (25.8)
Downstream	15.0 (4.6)	65.83 (20.06)	73	4.39	83.5 (25.5)

Heintz (2002) collected flow-depth, 3-D velocity, and boundary shear-stress data over the entire test reach with and without bendway weirs present. Successions of tests were conducted, varying the spacing ratio of the weirs from 3.4 to 8.4, while keeping height, length, and orientation angle of the weirs constant. Investigation of the outer bank, inner bank, and channel center velocities was based on the definition of three ratios defined in Equation 2.8:

$$MVR_{outer} = \frac{MaxV_{outer}}{MaxV_{CenterBase}}$$

$$MVR_{center} = \frac{MaxV_{center}}{MaxV_{CenterBase}}$$

Equation 2.8

$$MVR_{inner} = \frac{MaxV_{inner}}{MaxV_{CenterBase}}$$

where

$MaxV_{outer}$ = maximum outer bank velocity measured with bendway weirs along bend;

$MaxV_{center}$ = maximum centerline velocity measured with bendway weirs along bend;

$MaxV_{inner}$ = maximum inner bank velocity measured with bendway weirs along bend; and

$MaxV_{CenterBase}$ = maximum centerline velocity measured in baseline model.

Plotting the maximum outer bank velocity ratio (MVR_{outer}) versus the spacing ratio (Figure 2.33), Heintz (2002) showed that for spacing ratios between 3.4 and 8.4, placement of bendway weirs reduce the outer bank velocity by 40% from the maximum baseline velocity. Heintz (2002) reasoned that the maximum baseline velocity could come from a predictive computer model such as HEC-RAS, although her computations are based on measured baseline data.

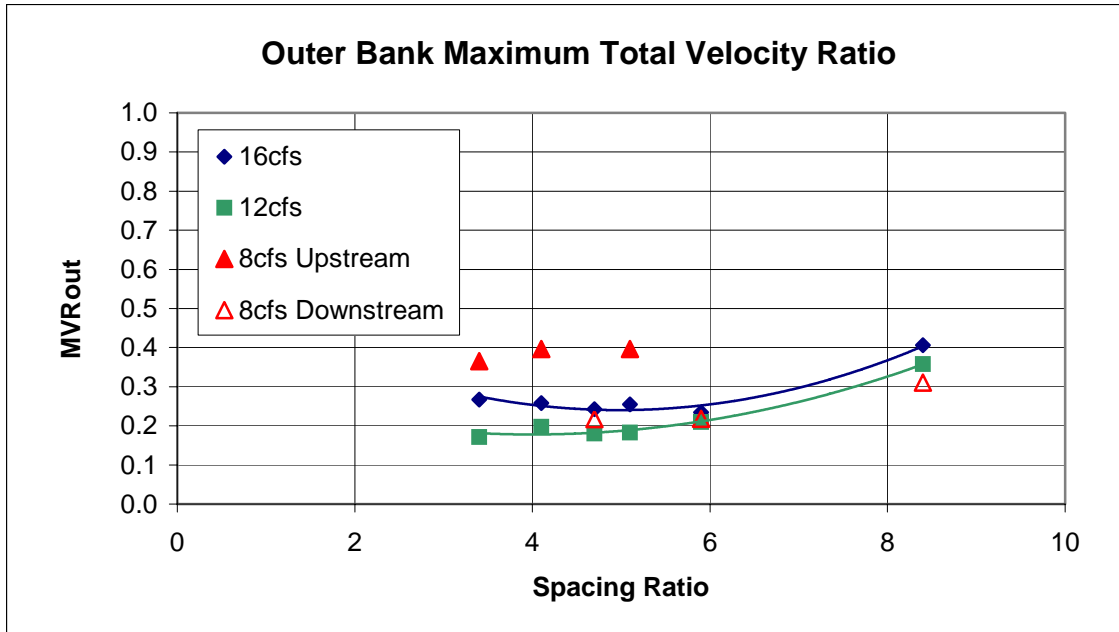


Figure 2.33: Maximum Outer Bank Velocity Ratio versus Spacing Ratio (Figure 4.20 in Heintz (2002))

Plotting the maximum centerline velocity ratio (MVR_{center}) versus the spacing ratio (Figure 2.34), Heintz (2002) showed that, for spacing ratios between 3.4 and 8.4, placement of a bendway-weir field could cause the centerline velocity to increase by 1.4 times the maximum pre-weir centerline velocity. Figure 2.34 also indicates that the maximum increase in centerline velocity was approximately 1.7 times the pre-weir centerline velocity.

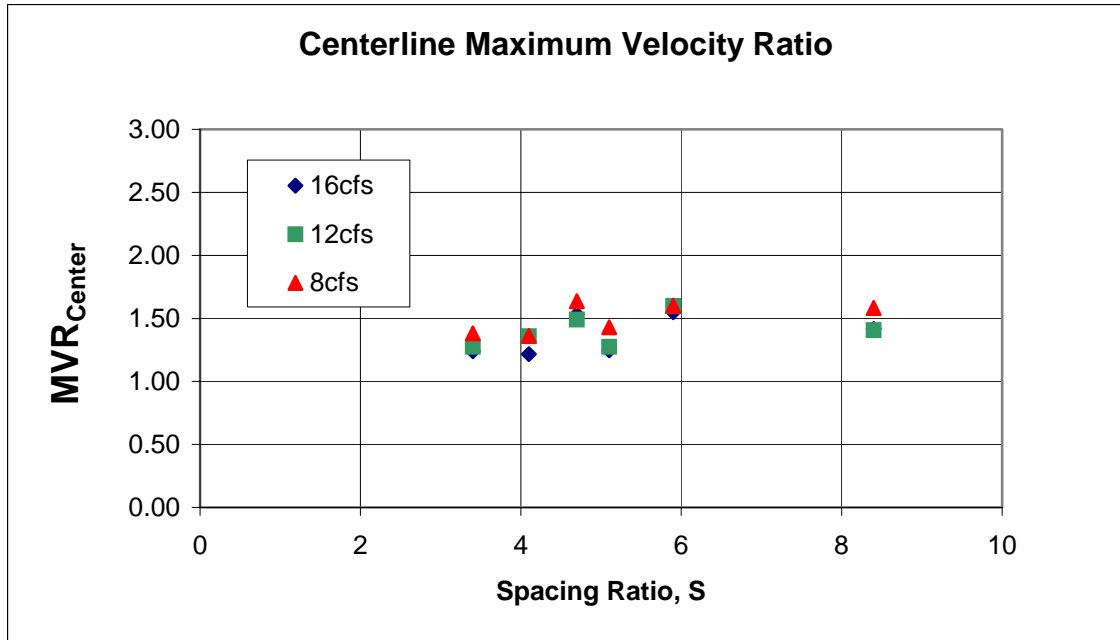


Figure 2.34: Maximum Centerline Velocity Ratio versus Spacing Ratio (Figure 4.21 in Heintz (2002))

Plotting the maximum inner bank velocity ratio (MVR_{inner}) versus the spacing ratio (Figure 2.35), Heintz (2002) showed that, for spacing ratios between 3.4 and 8.4, placement of a bendway-weir field could cause the inner bank velocity to increase by 1.478 times the maximum pre-weir inner bank velocity. Figure 2.35 also indicates that the maximum increase in inner bank velocity was approximately 1.56 times the pre-weir inner bank velocity.

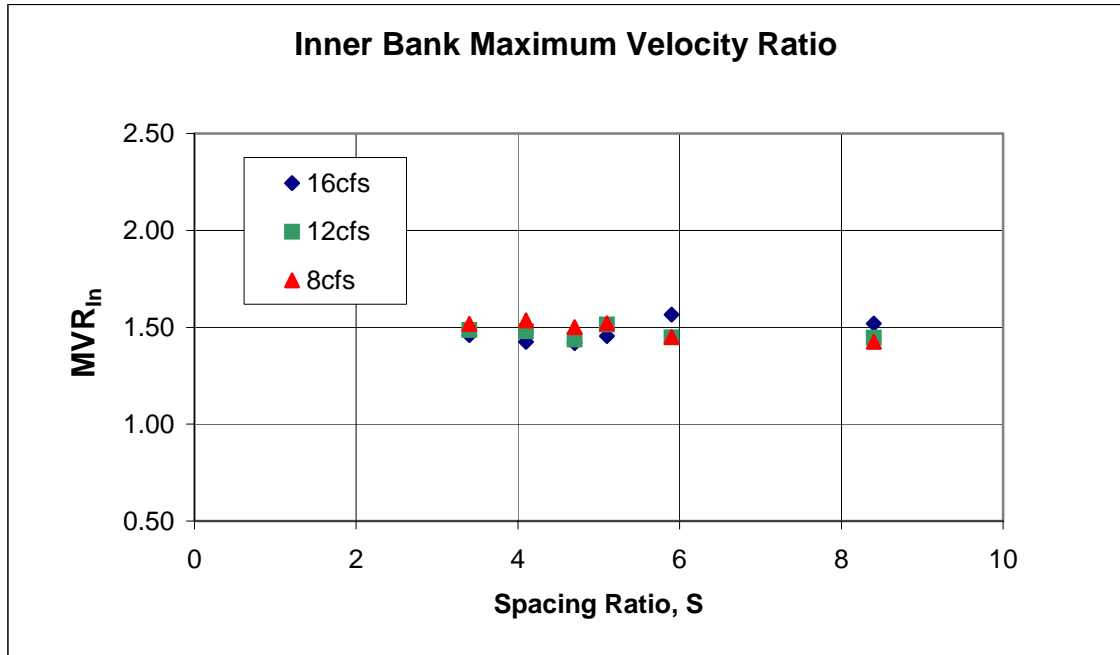


Figure 2.35: Maximum Inner Bank Velocity Ratio (Figure 4.23 in Heintz (2002))

Table 2.8 summarizes the results from the *MVR* analysis from Heintz (2002).

Table 2.8: *MVR* Analysis from Heintz (2002)

Location	Average <i>MVR</i>	Maximum <i>MVR</i>
Outer Bank	0.4	--
Centerline	1.422	1.69
Inner Bank	1.478	1.56

2.5.3.6 DARROW (2004)

Darrow (2004) continued the Heintz's (2002) research, using the same testing facility and instrumentation. Darrow (2004) investigated the effects of changing bendway-weir spacing ratios, weir lengths, and planform angles on flow conditions in a curved fixed-bed trapezoidal cross section. Darrow (2004) varied the spacing ratio from

3.4 to 7.62, the weir lengths from 15 percent to 28 percent of the design flow top width, and included planform angles of 90 and 60 degrees. Darrow (2004) developed statistically-relevant predictive equations for the *MVRs* defined by Heintz (2002). Regression equations developed by Darrow (2004) also included all data from Heintz (2002).

Darrow (2004) defined the *MVRs* for outer bank, centerline, and inner bank in the same way as shown in Equation 2.8. Darrow (2004) identified five pi terms that are summarized in Equation 2.9 and used in the evaluation of regression equations:

$$\begin{aligned}
 \pi_1: & \quad \frac{L_{arc}}{L_{proj,w}} \\
 \pi_2: & \quad \frac{y}{h_w} \\
 \pi_3: & \quad \frac{T_{W_{testflow}}}{L_{proj,cw}} \\
 \pi_4: & \quad \frac{L_{proj,cw}}{L_{cw}} \\
 \pi_5: & \quad \frac{A_w}{A_c}
 \end{aligned}
 \tag{Equation 2.9}$$

where

L_{arc} = arc length between weirs along design waterline (ft);

- $L_{proj,w}$ = projected length of weir to a cross section perpendicular to flow and passing through the point at which the centerline and waters edge meet at the design flow (ft);
- y = flow depth (ft);
- h_w = height of bendway weir (ft);
- $TW_{testflow}$ = top width of channel at test flow (ft);
- $L_{proj,cw}$ = projected length of weir crest to a cross section perpendicular to flow and passing through the point at which the centerline and waters edge meet at the design flow (ft);
- L_{cw} = length of weir crest measured along centerline (ft);
- A_w = projected weir area (ft²); and
- A_c = cross-sectional flow area (ft²).

Darrow's (2004) dataset consisted of fifty-four different tests with varying spacing ratios, weir lengths, planform angles, and flow rates for each location: inner bank, center, and outer bank. From this dataset, Darrow (2004) developed the regression equations shown in Equation 2.10:

$$MVR_{outer} = 0.019 \frac{\left(\frac{L_{arc}}{L_{proj,w}}\right)^{0.899} \left(\frac{L_{proj,cw}}{L_{cw}}\right)^{2.35}}{\left(\frac{A_w}{A_c}\right)^{0.859}}$$

$$MVR_{center} = 1.350 \left(\frac{L_{arc}}{L_{proj,w}}\right)^{0.160} \left(\frac{L_{proj,cw}}{L_{cw}}\right)^{0.567} \left(\frac{A_w}{A_c}\right)^{0.160}$$

Equation 2.10

$$MVR_{inner} = 2.153 \frac{\left(\frac{L_{proj,cw}}{L_{cw}}\right)^{0.700} \left(\frac{A_w}{A_c}\right)^{0.153}}{\left(\frac{L_{arc}}{L_{proj,w}}\right)^{0.109}}$$

where

L_{arc} = arc length between weirs along design waterline (ft);

$L_{proj,w}$ = projected length of weir to a cross section perpendicular to flow and passing through the point at which the centerline and waters edge meet at the design flow (ft);

$L_{proj,cw}$ = projected length of weir crest to a cross section perpendicular to flow and passing through the point at which the centerline and waters edge meet at the design flow (ft);

L_{cw} = length of weir crest measured along centerline (ft);

A_w = projected weir area (ft²); and

A_c = cross-sectional flow area (ft²).

Mallows' Cp criterion of the best subsets method was used to identify the relative significance of the pi terms and the final best-fit model. Table 2.9 summarizes the Cp values for the selected regression equations.

Table 2.9: Darrow (2004) Cp Values for Selected Regression Equations

Regression Equation	Mallow's Cp of Selected Regression Equation
MVR_{outer}	3.2
MVR_{center}	8.9
MVR_{inner}	3.5

2.5.3.7 ENVIRONMENTAL CONSIDERATIONS

Placement of bendway weirs on a meander bend tends to break up secondary currents that erode the outer bank. Since high-velocity currents are redirected toward the center of the channel, quiescent flow conditions between weirs cause bed material to accumulate in the near-bank region (Welch and Wright, 2005). To this end, bendway weirs act like reefs drawing lower members of the food chain, ultimately increasing fish habitat (USACE, 1980).

Bendway weirs have an environmental advantage over other revetment configurations in that they potentially promote development of habitat between weirs and move high shear stresses away from the bank, allowing for establishment of vegetation and terrestrial habitat (Brown, 1985). Initial construction of weirs would, of course, have negative impacts to habitat and water quality, but to a much lesser degree than what would be necessary for other revetment measures such as riprap where large portions of the bank would need to be exposed and altered before placement. In addition, placement of weirs creates additional pooling areas and provides increased length of stable stone shoreline (Knight *et al.*, 1992). Establishment of vegetation on the lower portions of the bank and on the berms that deposit between weirs has the dual effect of habitat rehabilitation and bank-erosion protection. Roots from vegetation penetrate the soil and tend to lock it in place while a substantial growth of vegetation will tend to retard any remaining excess flows. In some instances, bendway weirs have been installed accompanied by willow plantings on adjacent banks (Derrick, 1998), providing more habitat diversity and velocity shelters.

Formation of scour holes during high-flow conditions also provides additional low-flow habitat (Welch and Wright, 2005). Knighton (1998) found that addition of weirs corresponded to a shift toward larger and more dominant pool-dwelling fish and overall conditions indicative of less disturbed reaches. An increased fish population after bendway-weir installation was also reported by Rapp (1997) along thirteen bends in the Mississippi River near St. Louis. In another study, conducted by Ecological Specialists Inc. (1997), macro invertebrates were sampled upstream and downstream of the bendway-weir structures. Rocks used to construct the weirs were found to provide valuable habitat compared to adjacent fine-grained material.

Since the purpose of this research is basically a comparative analysis between computer modeling and physical data, environmental considerations were not fully investigated. However, hydraulic parameters used in design of the bendway weirs can be used to provide some insight into potential ecosystem development. Where environmental considerations are key, modification of weir design and subsequent evaluation of computer modeling could indicate net beneficial effects to habitat creation.

2.6 COMPUTER MODELING

Design of erosion countermeasures such as bendway weirs is based on knowledge obtained in two basic areas: 1) data from past installation, and 2) prediction of effects based on future installation. While significant progress has made in compiling data from previous installation of bendway weirs, predictive techniques are typically the only way to get a complete sense of impacts for a specific design. Predictive techniques can either be based on scaled physical models or numerical computer simulations. Physical models

are generally effective but are also expensive and not reasonable for every design project. As a result, computer modeling has been employed as a way to use fundamental hydraulic principles to predict effects of a particular design. Hydraulic computer models are broadly classified as 3-D, 2-D, or 1-D based on the complexity of the computational algorithm. Figure 2.36 shows a typical computational reach with 3-D, 2-D, and 1-D flow directions indicated.

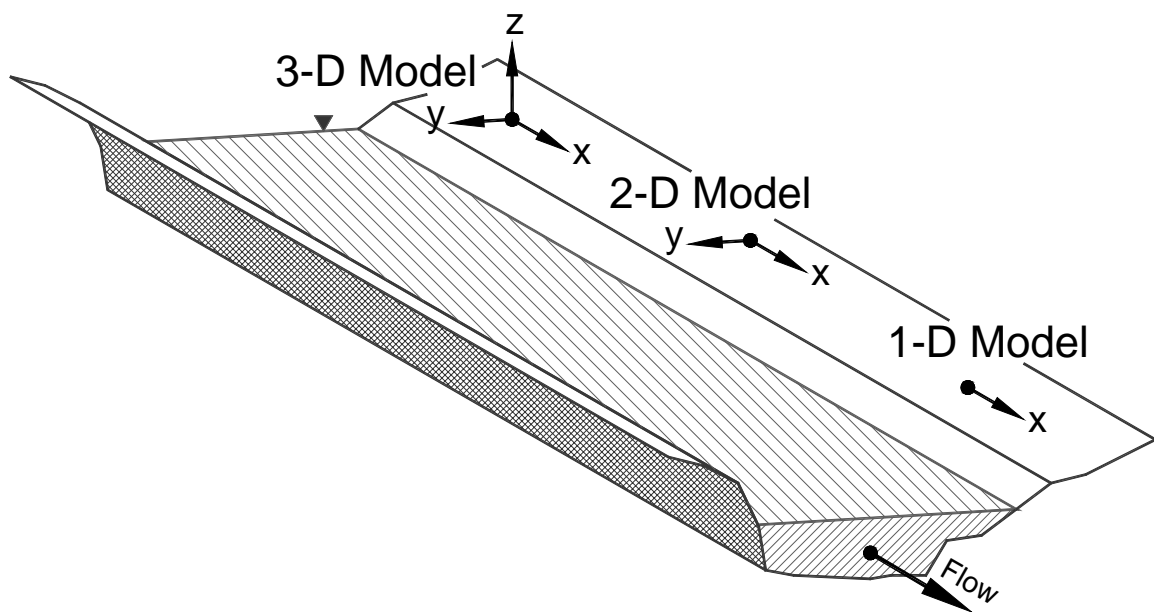


Figure 2.36: Schematic of Computational Directions for 3-D, 2-D, and 1-D Models

3-D and 2-D models typically use computational fluid dynamics principles to compute flow characteristics over a 3-D or 2-D grid, respectively. 1-D computer models assume an average water-surface elevation in the y-direction and z-direction. Although simplification from multi-dimensional model results in less detailed output, 1-D models are useful in that they are less computationally demanding and generally require less information to compile. Widespread use of 1-D models in the engineering and regulatory community as a whole has effectively overshadowed use of more complex models.

However, recent technological improvements have made 2-D and to some extent 3-D models more prevalent. Still, applications of 3-D models are still generally restricted to only specialized situations or academic research.

2.6.1 3-D MODELING

Streamlines associated with flow around weir tips and between weirs creates a complex 3-D system when trying to understand the intricacies of the flow characteristics associated with bendway weirs (Haltigin *et al.*, 2007). Most 3-D computer models use computational meshes that solve the fundamental Navier Stokes in a stepwise manner for one node or element at a time given known quantities from boundary conditions or previous computations. Sizing computational meshes is closely related to the type of flow expected and the amount of computational power available. Three different schemes can be used to solve Navier Stokes equations in a stepwise scheme: 1) finite volume method, 2) finite element method, and 3) finite difference method. The finite volume method solves the conservation form of the Navier-Stokes using appropriate boundary conditions for elemental volumes in the flow field. The iterative nature of this method causes convergence problems when applied in areas where flow characteristics are changing rapidly or highly irregular mesh is used (Wilcox, 2007). The finite element method uses a similar stepwise routine with appropriate boundary conditions on an irregular computational grid. Solutions to the Navier-Stokes partial differential equations are estimated on a stepwise elemental manner on a continuous domain with a discrete set of sub-domains or elements. A finite difference scheme approximates solutions to the differential form of the Navier-Stokes equation using a regularly-spaced grid. With any

stepwise procedure, accretion of small errors at each computational interval can result in erroneous results. Care and validation are necessary, therefore, when implementing stepwise computer models. A complete explanation of turbulence models and modeling schemes is beyond the scope of this research, but this discussion offers a basic sense of the considerations in implementing 3-D models.

Once the setup and compilation requirements of a 3-D model are overcome and quality of data is assured, the results of a 3-D model can provide substantial insight into characteristics of flow in channels with obstructions such as bendway weirs. For example, Haltigin *et al.* (2007) created a 3-D numerical simulation of a 4-m long by 0.4-m wide flume with bendway weirs installed along both banks. After validation of the computer model with physical data from laboratory experiments, various weir configurations were simulated with orientation angles varying from 45 to 135 degrees. Haltigin *et al.* (2007) used the computer simulations to predict the extent and depth of scour around bendway weirs. Once the computer model was set up, changing weir configurations was easier than creating additional physical models. Haltigin *et al.* (2007) was able to use results from various computer simulations to establish a relationship between simulated flow properties over a flat bed and resulting equilibrium scour geometry. Application of a 3-D finite element computer model on submerged bendway weirs by Jia *et al.* (2005) was found to adequately predict physical hydraulics. While the computer simulation enhanced the general understanding of flow around submerged weirs, extensive physical modeling was still necessary for validation purposes. Jia *et al.* (2005) and Abad *et al.* (2008) found that comparing velocity and depth results from computer simulations with physical data is adequate for validation.

After performing validation and performance analyses, Seed (1997) concluded that, although 3-D models provide a great deal of information regarding flow patterns around weirs, there are certain drawbacks to such models. Creation of 3-D models typically requires a great deal of data collection and development in terms of formulating an appropriate computational grid that is suitable for the specific flow conditions. Once a grid is created, convergence is not necessarily guaranteed, and a substantial trial-and-error process may be required. Once convergence is achieved, computation time can be significant and if changes are necessary the entire process may need to be reproduced. Utility of 3-D models is not necessarily disputed, but under typical design projects, the benefit from a 3-D model may not yet offset the cost of its creation.

2.6.2 2-D MODELING

The premise in using 2-D models is to eliminate a level of complexity by eliminating flow in one, less hydraulically significant, direction. Approximations inherent in using a 2-D model include assuming that computed average values sufficiently describe variables which vary over the flow depth (Molls *et al.*, 1995). 2-D simulation of spiral flow in a bend is limited due to the lack of a vertical component to the flow; but lateral flow characteristics and the main flow distribution have been found to be adequately simulated (Jia *et al.*, 2005). Computer modeling schemes used for 3-D models are applied in the same way for 2-D computer model and the characteristics of computational meshes must also be validated with physical data (Molls *et al.*, 1995). Where lateral flow distributions are of primary concern, 2-D models produce adequate results. Complexity in model creation and compilation still limits widespread use of 2-D

models, but commercially available software has enabled 2-D simulations to become more widely used than 3-D models.

2.6.3 1-D MODELING

1-D analysis of water-surface profiles involves several basic assumptions: 1) hydraulic characteristics of flow remain constant for the time interval under consideration, 2) hydrostatic pressure distribution prevails over the channel cross section, 3) small channel slope, 4) channel cross-section geometry is prismatic over the computational reach, 5) velocity coefficients are constant over the computational reach, and 6) locally uniform flow persists. A complete explanation of the hydraulic principles of 1-D flow can be found in USACE (2008), but it is clear that 1-D computational procedures require significant assumptions. Despite apparent limitations to 1-D models, their use is widely accepted by the engineering community at large. Consideration is given to the use of 1-D models for nearly all engineering projects that involve impacts to a flow conveyance channel. Many reasons exist as to why 1-D computational procedures persist in such an ubiquitous way, but historical precedence combined with the prevailing dissemination of practical modeling techniques has resulted in application of 1-D models in a wide variety of situations.

The use of 1-D models can be traced back to legislation passed in the late 1960's. On the recommendation of the Bureau of the Budget Task Force on Federal Flood Control, Congress passed the National Flood Insurance Act in 1968. Prior to 1968, the only source of financial assistance for flood victims was through disaster relief. Growing concerns regarding the rise in property damage and loss of life, combined with the

realization that private flood insurance was not economically feasible, led to the passing of the National Flood Insurance Act. Even after passage of the National Flood Insurance Act, communities had little incentive to participate in the government program of subsidized insurance. Continual rise in the cost of disaster relief led to passage of the Flood Disaster Protection Act of 1973. In this act, Congress mandated that Federal agencies and federally-insured or regulated lenders had to require flood insurance on all grants and loans for acquisition or construction of buildings in designated Special Flood Hazard Areas (SFHA) (Federal Emergency Management Agency (FEMA), 2002). SFHA was defined as land within the floodplain of a community subject to a 1 percent or greater chance of flooding in any given year, or the 100-yr floodplain. As a result of this act, communities where loans and grants were being obtained for the sale or construction of buildings needed to have a 100-yr floodplain delineated in order to determine which areas were in or out of the SFHA. Joining the National Flood Insurance Program meant that these floodplain boundaries, at least on an approximate level, would be delineated. Consequently, in the mid to late 1970s a large number of hydraulic studies across the United States were performed to delineate the SFHA, and the program used for these studies was most often a 1-D program developed by the USACE entitled HEC-2 (a precursor of HEC-RAS).

Over the past 30 yrs, communities all across the United States have gotten their floodplain areas mapped using 1-D computer software. Additionally, all development adjacent to the 100-yr floodplain needs to submit additional studies based on the original mapping, typically from a 1-D model. As a result, most engineering firms have some sort of in-house expertise in using 1-D computer modeling. While other factors have led to

the overwhelming use of 1-D modeling, none has been as prominent as the regulatory requirements.

Continuous improvements to the 1-D hydraulic model developed by the USACE (originally called HEC-2, updated to HEC-RAS in 1995) have dramatically improved its functionality and accuracy. While the hydraulic computational engine remains basically unchanged, many options and improvement have been added. Because of its continual development, and the fact the software is available for free downloads from the USACE website, many engineers use a 1-D model as a first choice with or without consideration of more complex computational algorithms. However, because of its relative simplicity and significant assumptions, academic research using HEC-RAS has been comparatively limited. In terms of bendway weirs, research has implied the use of 1-D hydraulic software through the development of predictive equations with respect to cross-section-averaged approach values. Brown (1985), for example, researched various bendway-weir characteristics against the ratio of maximum velocity near the tip of the weir to the cross-sectionally averaged approach velocity. Seed (1997) also studied the velocity associated with weir placement normalized using a cross-section-averaged approach velocity. Again, Heintz (2002) and Darrow (2004) developed relationships between the maximum velocity in a bend with bendway weirs and with average centerline velocity in meandering bends without bendway weirs. In addition, design criteria exist that predict velocity and shear stress in a bend as a function of the approach cross-sectional average velocity or shear stress, respectively (Kilgore and Cotton, 2005; USACE, 1991). In all these cases, average values or baseline values can be substituted with computed results from a 1-D computer analysis tool such as HEC-RAS. Development of predictive

equations as a function of computed values from a 1-D computer model does not necessarily imply accuracy or applicability of a 1-D computer model such as HEC-RAS; rather, there is a recognition of the pervasive use of 1-D models.

Kasper (2005) investigated the feasibility of using HEC-RAS to compute flow depths and total energy loss through meander bends with and without bendway weirs. Kasper's (2005) approach to evaluate HEC-RAS as a viable computer modeling tool for curved channels involved first evaluating the computer model results for baseline conditions, then incorporating bendway-weir design into the baseline model. Various modeling techniques were applied to the bendway-weir model and tested for overall accuracy. Selection of the appropriate technique was based on the quality of fit in terms of an overall percent difference between measured data and the computed profile.

Kasper (2005) investigated the viability of using HEC-RAS in a two meandering bends with and without bendway weirs. Kasper's (2005) research was performed on the Middle Rio Grande physical model, which consisted of a concrete trapezoidal channel with two bends as described in Table 2.7 and a 10:1 transition between the two bends. One weir configuration was imported into the baseline computer model and compared to collected physical data. Kasper (2005) found that, for baseline conditions, using a Manning's roughness of 0.013 for brushed concrete and a contraction coefficient of 0.6 in the 10:1 transition from the upstream bend to the downstream bend produced satisfactory results with less than 1-percent error. Kasper (2005) achieved similar results with the weir configuration computer model by adjusting the Manning's roughness coefficient and contraction coefficients as necessary at each cross section. As a result, Kasper's (2005) computer models of the bendway weirs contain roughness coefficients that varied from

0.013 to 0.090 from cross section to cross section. Contraction coefficients were likewise adjusted at each cross section, ranging from 0.1 to 6.8. Expansion coefficients were kept constant at 0.3 for all cross sections. While Kasper's (2005) research provided some indication of the suitability of using HEC-RAS for meandering bends with and without bendway weirs, adjustment of the Manning's roughness and contraction coefficients for each cross section is not necessarily a suitable design recommendation for general use in bendway weirs. Further, the number of weir configurations would need to be expanded before any relationships can be ascertained.

2.7 SUMMARY

Previous research projects on the Middle Rio Grande conducted at CSU serve as background for the procedures and objectives of this current research. Using research methodology outlined by Kasper (2005) and expanding on the *MVR* analysis performed by Heintz (2002) and Darrow (2004), this research will attempt to develop a computer model describing the physical model with and without various configurations of bendway weirs and develop relationships between the computer model results and data collected during physical model testing. Relationships developed from comparisons between computer model results and physical model data will provide the basis for developing a design procedure for bendway weirs.

3 PHYSICAL MODEL DESCRIPTION

3.1 INTRODUCTION

All data used in this study were obtained from Heintz (2002), Darrow (2004), Kinzli (2005), Kasper (2005), and Schmidt (2005). Initial research by Heintz (2002) included the construction of a physical model, representing the Middle Rio Grande section, as well as a specific set of bendway-weir configurations. Subsequent studies expanded variation of weir configurations within the Middle Rio Grande physical model. This section briefly describes the procedures used by Heintz (2002) in the original construction of the model as well as a description of subsequent weir configurations and related construction techniques.

3.2 MODEL GEOMETRY

For construction of the physical model, the Middle Rio Grande reach was scaled using a 1:12 Froude scale. Table 3.1 shows the scaling factors used for various physical parameters.

Table 3.1: Similitude Scaling Used for the Physical Model (1:12 Froude Scale)

Parameter	Scaling Factor (prototype/physical model)
Length, Depth, and Width	$12^1 = 12$
Velocity	$12^{1/2} = 3.46$
Discharge	$12^{5/2} = 500$
Slope	$12^0 = 1$
Roughness	$12^{1/6} = 1.51$

It was not the original intent of the research to construct an exact representation of the channel geometry for the entire 29-mi prototype reach. Instead, representative geometry was modeled to enable trends in hydraulic conditions to be examined within the prototype reach. To select typical geometric characteristics of the prototype model, relative curvature, R_c/Tw , was plotted against the channel width for the entire prototype reach under consideration. Bend geometry was generalized from Figure 3.1, into three types of curves. Type 1 and Type 3 bends were represented in the physical model constructed at CSU. Table 3.2 summarizes the geometric characteristics of each bend type.

Cochiti to Bernallilo
Radius of Curvature vs. Width
with Corresponding Arc Angle, After Hey (1976)

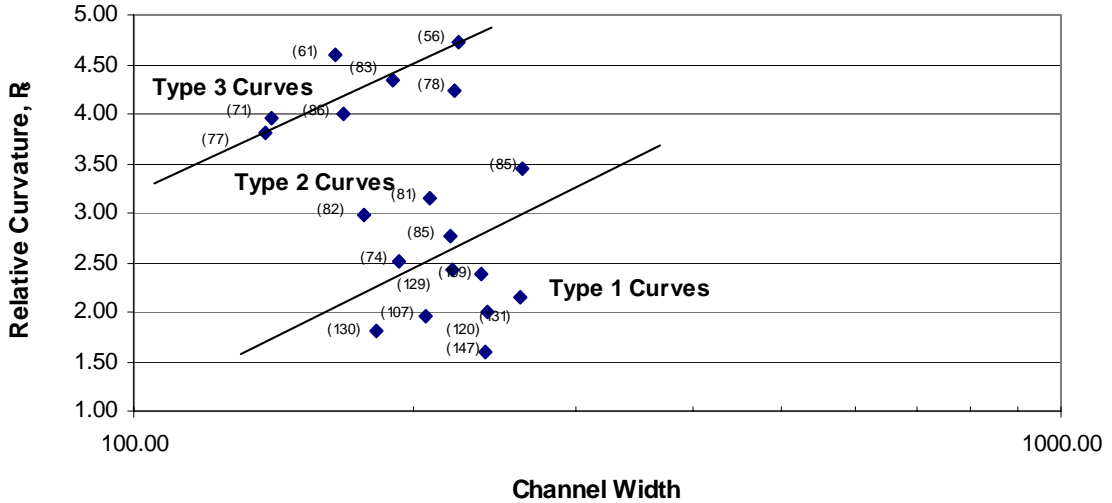


Figure 3.1: Study Reach Planform Bend Geometry Curve Types (Figure 3.1 in Heintz (2002))

Table 3.2: Prototype Planform Geometry Characteristics (Heintz, 2002)

Bend	Channel Width ft (m)	Radius of Curvature ft (m)	Bend Angle Degrees	Relative Curvature <i>r/b</i>	Channel Length ft (m)
Type 1	230.4 (70.2)	465 (141.73)	125	2.02	1014 (309)
Type 3	180 (54.86)	789.96 (240.77)	73	4.39	1002 (305)

Applying the similitude relationships presented in Table 3.1, the prototype curve geometry was scaled down to determined model dimensions. Table 3.3 summarizes the model utilized throughout the test program.

Table 3.3: Model Planform Geometry Characteristics (Heintz, 2002)

Bend	Channel Width ft (m)	Radius of Curvature ft (m)	Bend Angle Degrees	Relative Curvature r/b	Channel Length ft (m)
Type 1	19.2 (5.9)	38.75 (11.81)	125	2.02	84.5 (25.8)
Type 3	15 (4.6)	65.83 (20.06)	73	4.39	83.5 (25.5)

For testing purposes, natural prototype cross sections were represented in the physical model as a fixed-bed prismatic trapezoidal section with 3H:1V side slopes. A 10:1 transition was constructed between the upstream Type 1 curve and the downstream Type 3 curve. It was determined during the initial testing that placement of a 10:1 transition minimizes the influence of the downstream curve on the upstream hydraulics and vice versa. Since bed slope represents the ratio of elevation drop over channel distance, scaling of the prototype is not necessary. Therefore, the model was constructed to match the prototype bed slope of approximately 0.000863 ft/ft.

Three discharges were selected to simulate flow conditions of the Middle Rio Grande. Prototype flow conditions that were modeled include 4,000, 6,000, and 8,000 cfs (113, 170, 227 cms, respectively). Based on the similitude relationships presented in Table 3.1, the three prototype discharges were scaled, resulting in modeled discharges of 8, 12, and 16 cfs (0.23, 0.34, and 0.45 cms, respectively). Water for the simulations was supplied to the laboratory directly from the Horsetooth Reservoir, located just west of the Engineering Research Center (ERC), as shown in Figure 3.2.

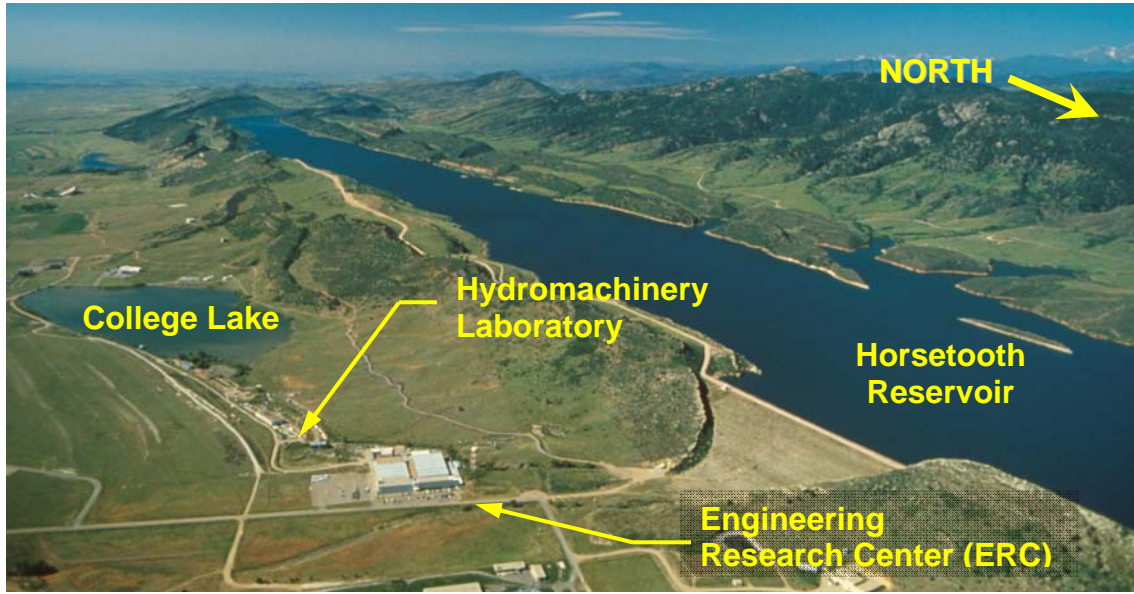


Figure 3.2: Aerial View of Horsetooth Reservoir and the ERC (adapted from Figure 3.3 in Heintz (2002))

Channel roughness in the prototype model was determined to range from 0.026 to 0.035 (Heintz, 2002). By scaling these coefficients using Table 3.1, the channel roughness in the model ranges from 0.017 to 0.023. In order to simulate this roughness, the concrete used to construct the physical model channel was brushed with a broom. Figure 3.3 displays a schematic summarizing the geometry of the physical model.

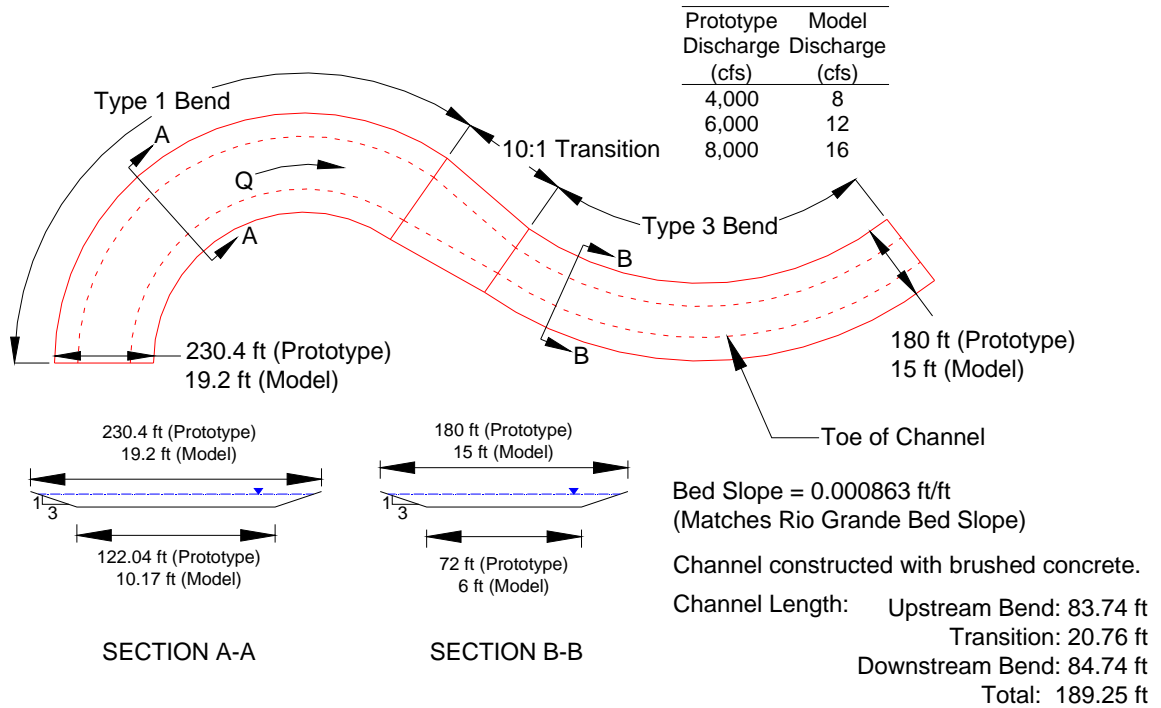


Figure 3.3: Model Layout of the Type 1 and Type 3 Bends in Plan View

3.3 MODEL CONSTRUCTION

3.3.1 INTRODUCTION

Construction of the physical model took place during an 8-month period, beginning in August 2000, within the Hydromachinery Laboratory at the ERC of CSU. Construction of the model consisted of three main components: 1) headbox, 2) test section, and 3) tailbox. A layout of the physical model within the Hydromachinery Laboratory is presented in Figure 3.4.

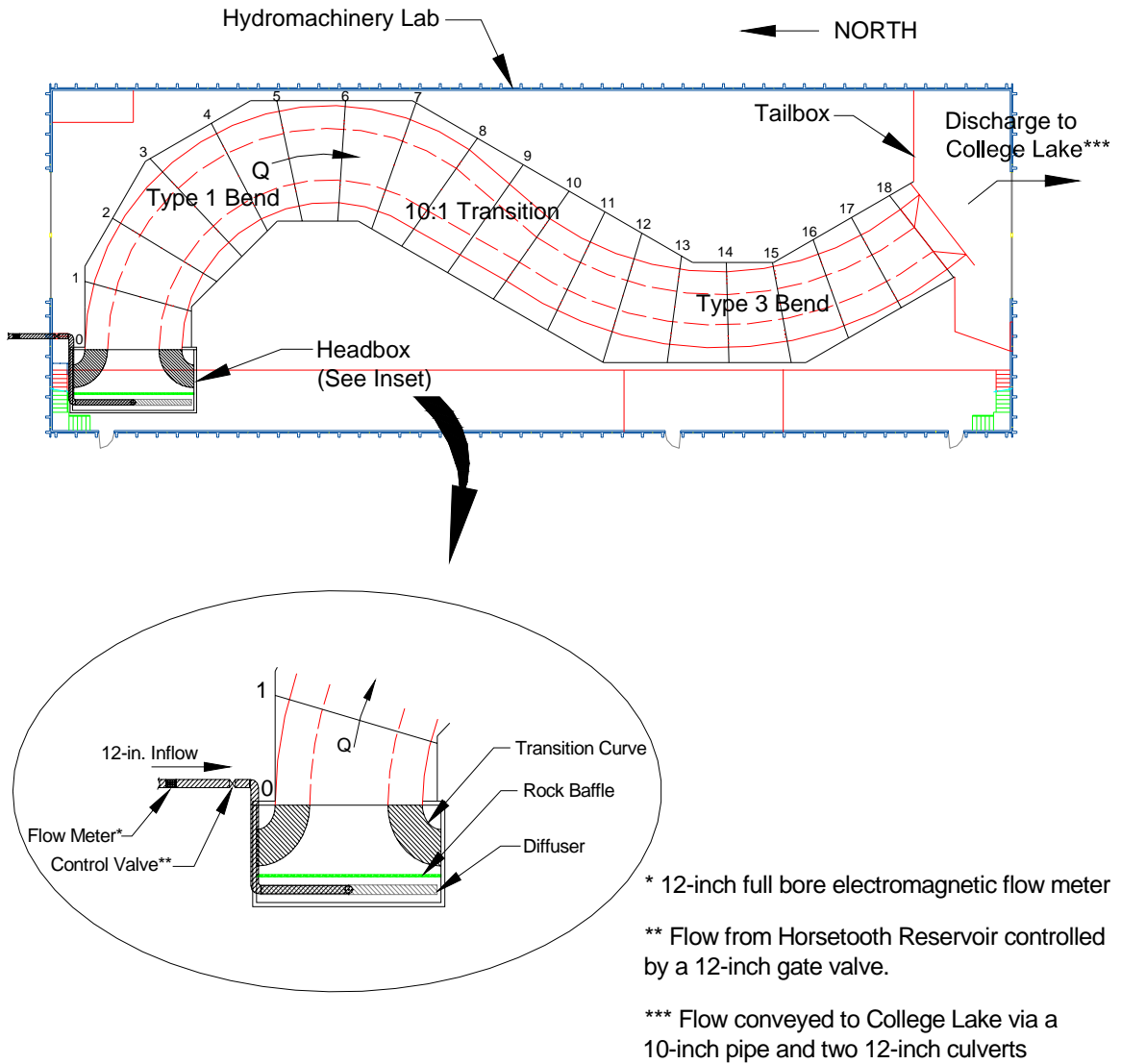


Figure 3.4: Schematic of the Physical Model Layout in the Hydromachinery Laboratory

3.3.2 HEADBOX

Water from Horsetooth Reservoir is delivered to the model through the headbox using a 12-in. line that enters at the northwest corner of the building. Discharge is

controlled by a 12-in. gate valve located just upline from the headbox. A 12-in. full bore electromagnetic flow meter was used to determine the flow rate in the pipe.

To prevent a concentration of inflow after the pipe discharged into the headbox, a rock baffle was constructed to diffuse the water across the entire channel width. Side and floor transitions were constructed to reduce the abrupt disturbances from the headbox to the upstream channel. Figure 3.5 shows the headbox including the rock baffle and the pipe manifold during construction.



Figure 3.5: Headbox Under Construction Including Pipe Manifold and Rock Baffle (Figure 3.5 in Heintz (2002))

3.3.3 TEST SECTION

Channel bends and geometry were constructed between two 4-ft high walls that were secured to the concrete floor of the laboratory. Each bend was segmented into eight

cross sections with two cross sections within the transition areas, for a total of eighteen cross sections. Templates, cut from plywood sheets, were used to outline each cross section. Placement of the section templates were also used to maintain the desired model slope of 0.000863 ft/ft. Each section was backfilled with sand. Leveled sand within the sections was saturated and compacted, as shown in Figure 3.6, before a final concrete cap was poured.



Figure 3.6: Placement of Backfill between Model Sections During Construction

A 2-in. concrete cap was poured on top of the finished sand. The concrete contained fiber and steel reinforcement (Heintz, 2002). Once poured, the concrete was leveled and then brushed with a broom to simulate the appropriate roughness. Brushing of the concrete cap is shown in Figure 3.7. Sealant was applied to the final concrete cap and all of the concrete seams.



Figure 3.7: Placement and Roughening of the Concrete Cap

3.3.4 TAILBOX

Near the southern wall of the laboratory, the test section discharged directly into a tailbox. To simulate a free-flowing outfall, the channel was constructed approximately 2 ft higher than the tailbox. Backwater was controlled through the use of stop logs that were placed within a steel frame. Stop-log configurations varied for each test depending on the flow rate. Calibration was performed by determining the appropriate stop-log configuration that produced the desired depth in the channel. Creation of backwater by the stop logs during testing is illustrated in Figure 3.8.



Figure 3.8: Discharge over Stop-log Configuration During Testing

3.4 INSTRUMENTATION

A movable measurement cart was fabricated to collect flow-depth, velocity, and shear-stress measurements at set locations along the entire length of the model. Flow-depth measurements were also taken using a series of piezometer taps along the channel bed. Each bend was divided into eight cross sections with two cross sections in the transition, for a total of eighteen cross sections, as shown in Figure 3.9. Data were collected at each cross section and around each weir, where appropriate. Detailed discussions of measurement techniques are provided in the following sections.

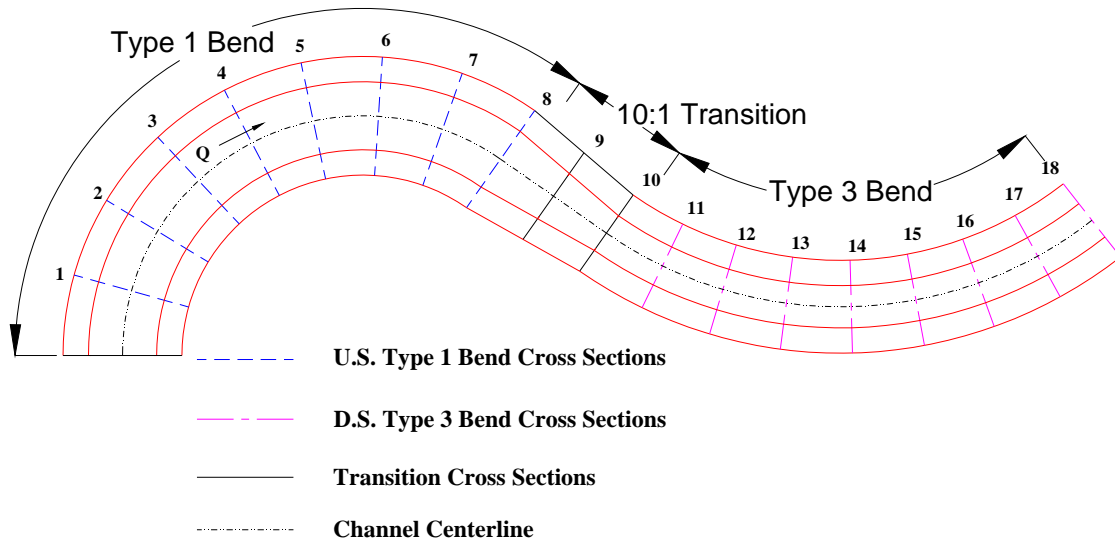


Figure 3.9: Baseline Cross-section Layout Showing Physical Model Cross Sections

3.4.1 FLOW-RATE MEASUREMENT

A 12-in. gate valve located just upstream of the testing facility controlled the delivery of water from Horsetooth Reservoir. A full bore electromagnetic flow meter, shown in Figure 3.10, measured the flow rate in the pipe with an accuracy of ± 5 percent by sending a DC voltage from 4 to 20 mA to a data-acquisition system installed on a personal computer. Flow rates were set using the gate valve, which was adjusted during testing as necessary.

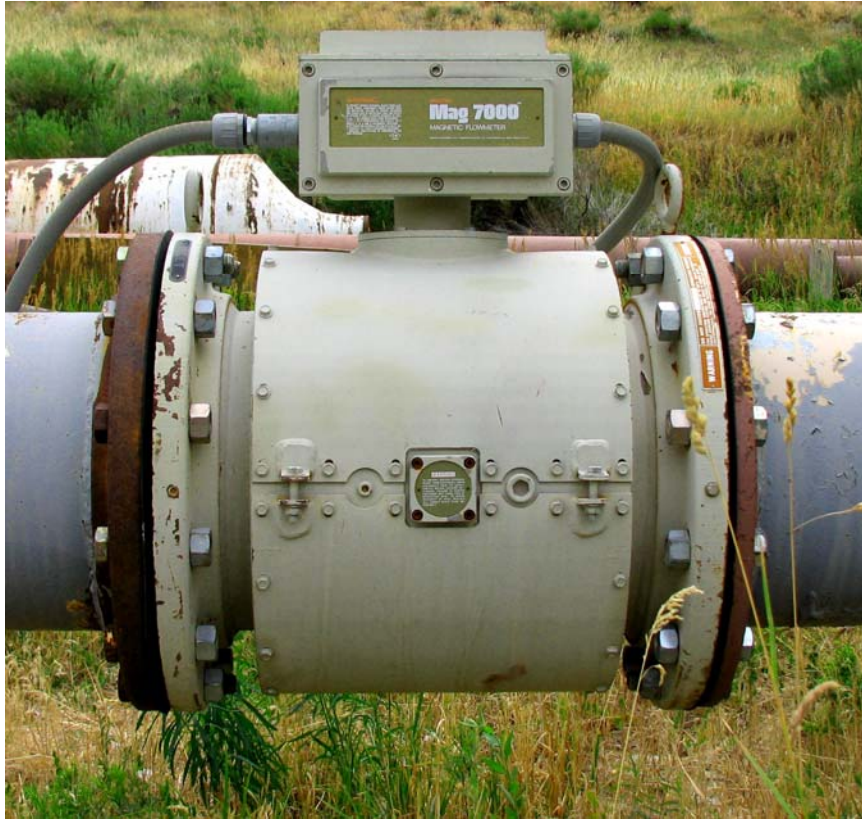


Figure 3.10: Electromagnetic Flow Meter

3.4.2 FLOW-DEPTH MEASUREMENT

Two methods were used to collect flow-depth measurements. A standard point gage mounted on the measurement cart, capable of measuring ± 0.001 ft (± 0.03 cm), allowed measurements at the water surface and at the bed along the length of the channel. In addition, seven piezometer taps (designated Piezometer A to Piezometer G) were installed at each of the eighteen cross sections. Three taps were installed along each side slope, and one tap was installed in the center of the channel. Figure 3.11 shows the placement of the taps along a typical cross section looking downstream.

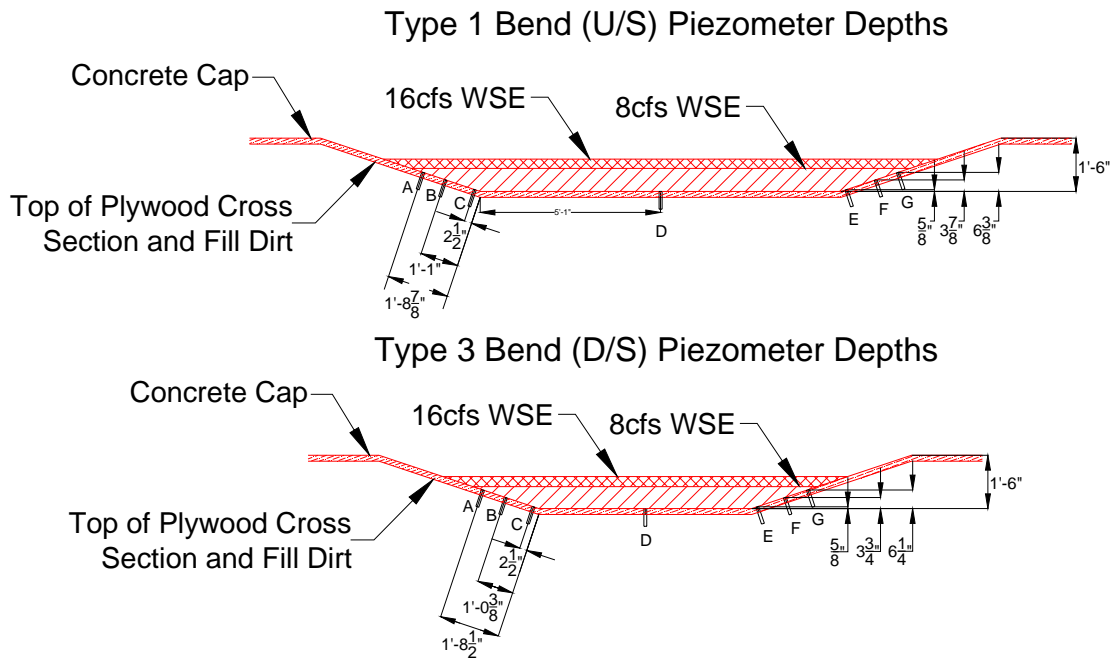


Figure 3.11: Location of Piezometer Taps Looking Downstream

Each of the 126 taps were connected to a stilling well comprised of a 2-in. polyvinyl chloride (PVC) pipe. The pipes for the stilling wells were mounted on a frame which facilitated the measurement of pressure head and, therefore, flow depth above the tap. Piezometric taps were installed in order to determine the extent of the super-elevation around the bend.

3.4.3 VELOCITY MEASUREMENT

An Acoustic Doppler Velocity (ADV) meter, accurate to ± 1 percent, was used to measure 3-D velocity profiles in the channel. The ADV probe was attached to a point gage on the measurement cart, shown in Figure 3.12, thus enabling velocity measurements at 10-percent depth increments at each of the piezometric taps for baseline tests, and at 60-percent depth for tests with installed weir configurations. Orientation of

positive x, y, and z directions of the probe corresponded to downstream flow direction, lateral flow to the right bank looking downstream, and vertical direction, respectively. 3-D velocity data were recorded in 30-sec durations at a rate of 10 Hz.



Figure 3.12: Acoustic Doppler Velocity Meter

3.4.4 BED SHEAR MEASUREMENT

Bed shear stress at each piezometric tap location for each cross section was measured using a Preston tube attached to a standard point gage. Differential pressure was measured using a Rosemount low-range and re-rangable differential pressure transducer, capable of reading pressures up to 3 in. (7.62 cm) of water. Figure 3.13 shows a schematic of the Preston tube and the general dimensions of the static and dynamic ports.

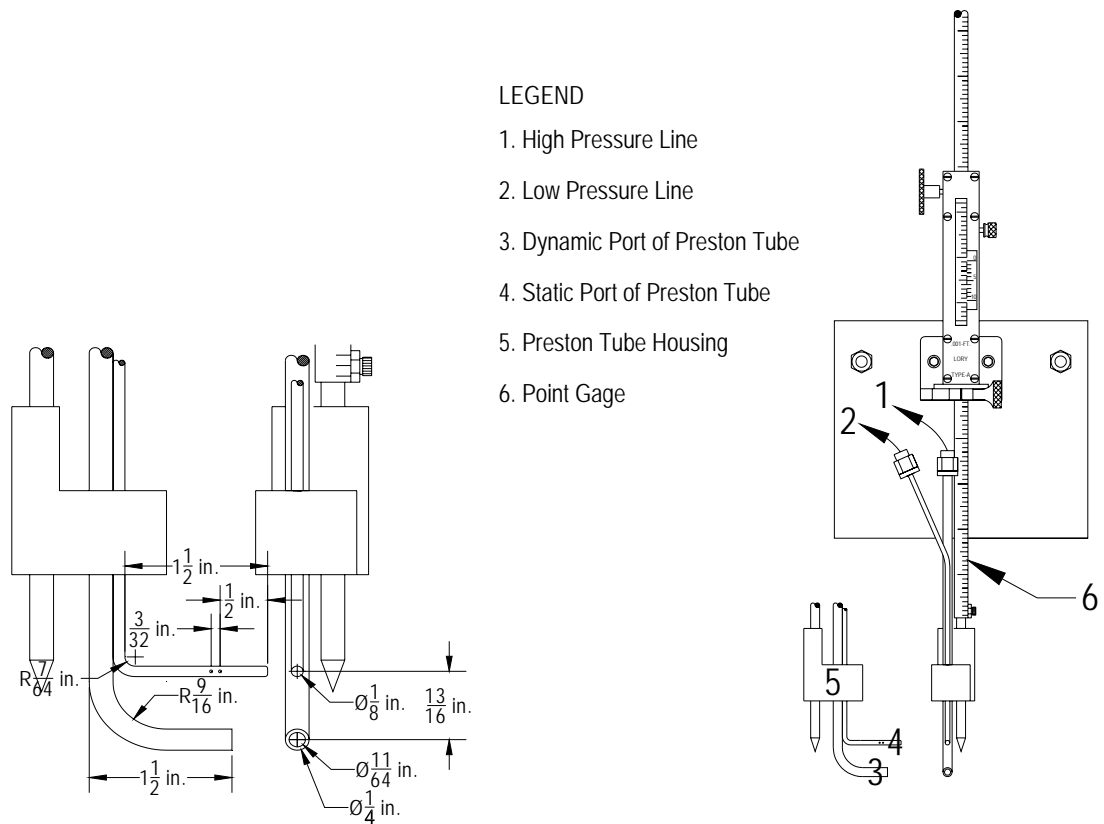


Figure 3.13: Preston-tube Schematic

Calibration of the Preston tube was performed in a 60-ft long, 4-ft wide flume with a concrete bed constructed to match exactly the conditions in the Middle Rio Grande physical model. Results of the Preston-tube calibration are shown in Figure 3.14.

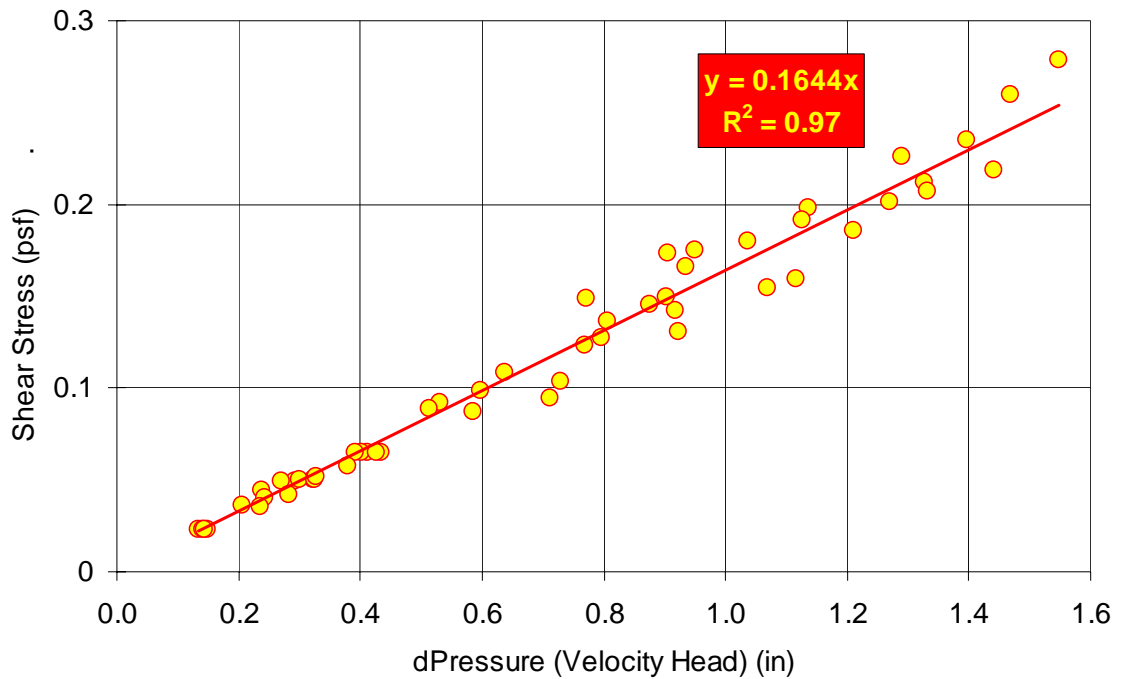


Figure 3.14: Preston-tube Calibration Curve for a Concrete Channel

Equation 3.1 presents the relationship, developed from the Preston-tube calibration study, relating differential pressure to shear stress. Equation 3.1 is used for this research and generally applies for brushed concrete channel surfaces of similar roughness as constructed in the physical model. Details regarding the Preston-tube calibration are on file at CSU (Sclafani, 2008):

$$\tau_o(\text{concrete cap}) = 0.1644dP \quad \text{Equation 3.1}$$

where

τ_o = boundary shear stress (lb/ft²); and

dP = Preston-tube measurement (differential pressure) (in.).

3.5 MODEL CALIBRATION

A survey compiled by Heintz (2002) served as a basis for the creation of a HEC-RAS baseline model. Nineteen cross sections were surveyed by Heintz; eight cross sections for each bend (Type 1 and Type 3), two cross sections in the transition, and one cross section at the downstream boundary. Cross sections in the physical model tests were denoted, from upstream to downstream, beginning with Cross Section 0 and ending with Cross Section 18. HEC-RAS requires the cross-section number begin downstream and increase moving upstream. Therefore, to create the HEC-RAS model, the cross-section order was reversed beginning with 0 for the downstream cross section; however, changing cross-section designation does not affect any hydraulic computation. Coordinates for this survey were based on an arbitrary point set at 5000, 5000, and elevation 100 ft. From this arbitrary point, two benchmarks were set to assist in subsequent surveys. A layout of survey points, cross sections, and benchmarks are illustrated in Figure 3.15. Cross-section nomenclature is shown for both the HEC-RAS model and Heintz (2002) survey. Survey data used to create the baseline HEC-RAS computer model are included in Appendix B.

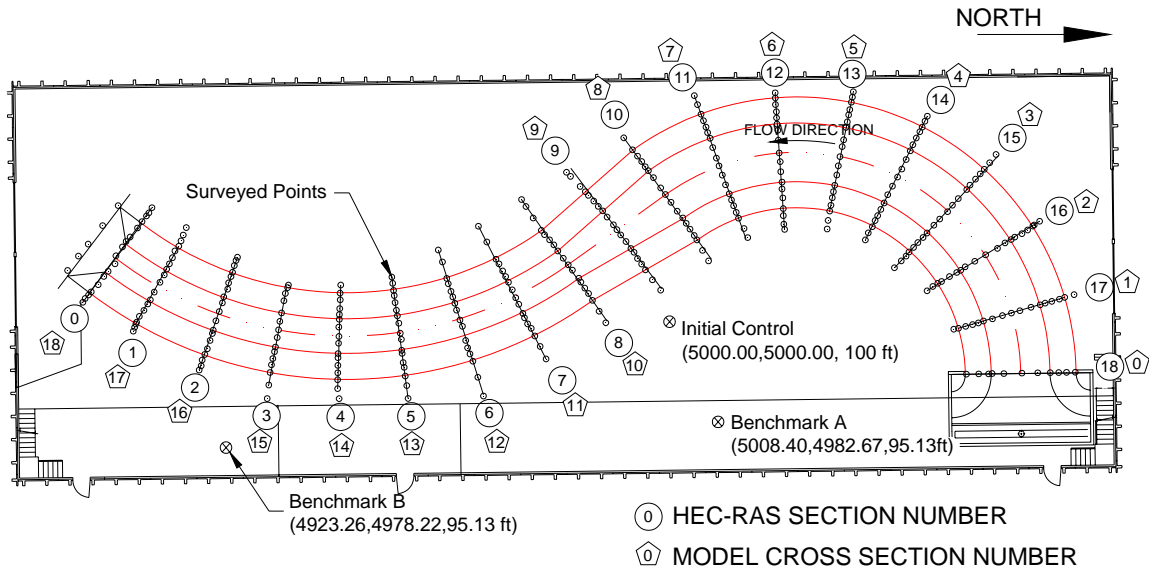


Figure 3.15: Layout of Survey Points, Cross Sections, and Benchmarks for Baseline Model

Comparisons were made between the results from the HEC-RAS model with free-flow downstream and the water-surface profile of the physical model. Manning's roughness coefficient was used to calibrate these two water-surface profiles. The final roughness coefficient of 0.018 falls within the desired range and corresponds to a prototype roughness of 0.027. A detailed description of this calibration is included in Heintz (2002). To accurately represent the prototype river depth, stop logs located at the downstream section were installed to backwater upstream into the flume. Various stop-log configurations were evaluated by comparing the resulting upstream water-surface profile to the HEC-RAS numerical model. Required flow-depth conditions were achieved by choosing a stop-log configuration that caused an upstream water-surface profile that matched the desired depth.

Figure 3.16 illustrates the final stop-log configuration for each flow condition.

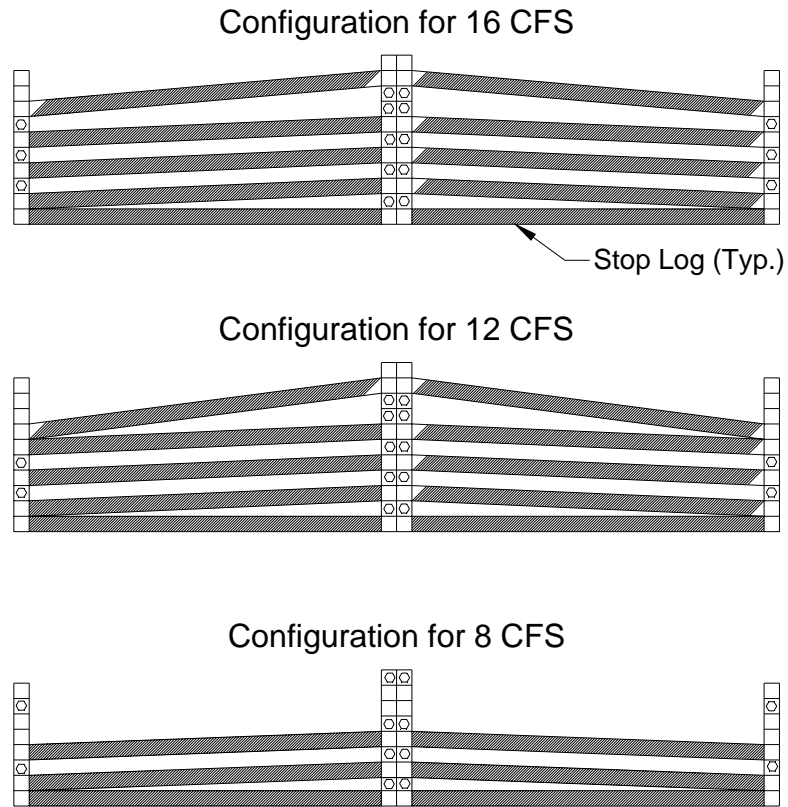


Figure 3.16: Stop-log Configuration for 8, 12, and 16 cfs

3.6 WEIR DESIGN

3.6.1 CONSTRUCTION

For all weir configurations modeled in the flume, consistency of data was maintained by changing one aspect of the weir geometry at a time, *e.g.*, spacing or orientation angle. Weir top width (W_{cw}), bottom width (W_{bw}), and height (h_w) were uniform for all tests included in this research. Figure 3.17 illustrates the constant geometry used in weir construction and Table 3.4 summarizes the respective geometric values.

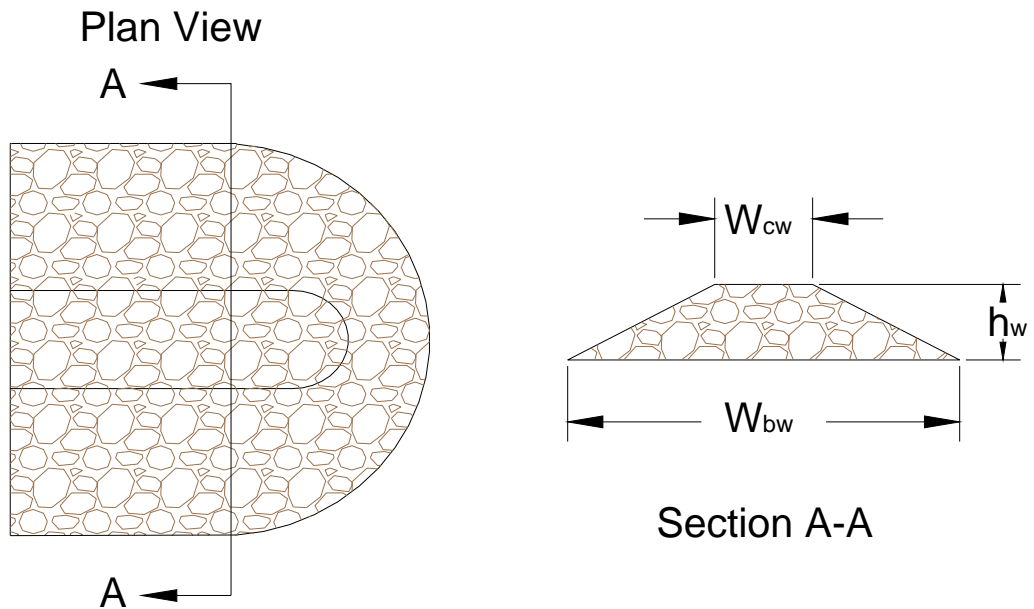


Figure 3.17: Weir Crest and Bottom Width Definitions

Table 3.4: Weir Dimensions that Remain Constant

Parameter		Type 1 Bend (upstream)	Type 3 Bend (downstream)
Top width	W_{cw}	1	1
Bottom Width	W_{bw}	4	4
Height	h_w	0.77	0.78

Hand-placed 3- to 6-in. angular rock was used to construct each weir. A plywood template was used as a shaping guide as shown in Figure 3.18.



Figure 3.18: Plywood Shape Template for Weir Construction

To render the weir impermeable to throughflow, a plywood core was inserted into its center. Inserting plywood in the weir also assisted in maintaining the shape of the weir. Figure 3.19 shows the plywood insert in the center of the weir during testing. Measurement of velocity in the region just downstream of the weir indicated that the plywood insert was effective at rendering the weir impermeable.



Figure 3.19: Impermeable Bendway Weir during Testing

3.6.2 WEIR GEOMETRY

3.6.2.1 INTRODUCTION

Construction of each weir was performed identically for all weir configurations. Weir configurations were established by identifying characteristic geometric properties of weir placement and varying selected properties to create a finite set of combinations. Parameters used to characterize the weirs are based on a prototype bankfull design flow of 6,000 cfs, which corresponds to a model discharge of 12 cfs. Characteristic geometric properties identified in weir placement are depicted in Figure 3.20. The following sections define the different properties selected to create the various combinations of test configurations.

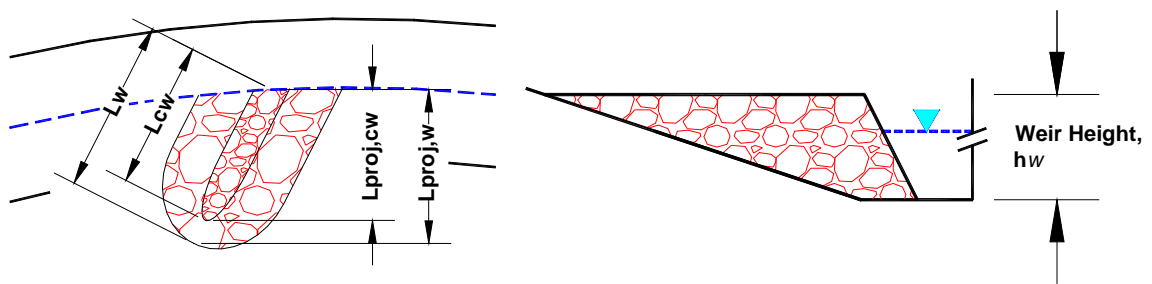
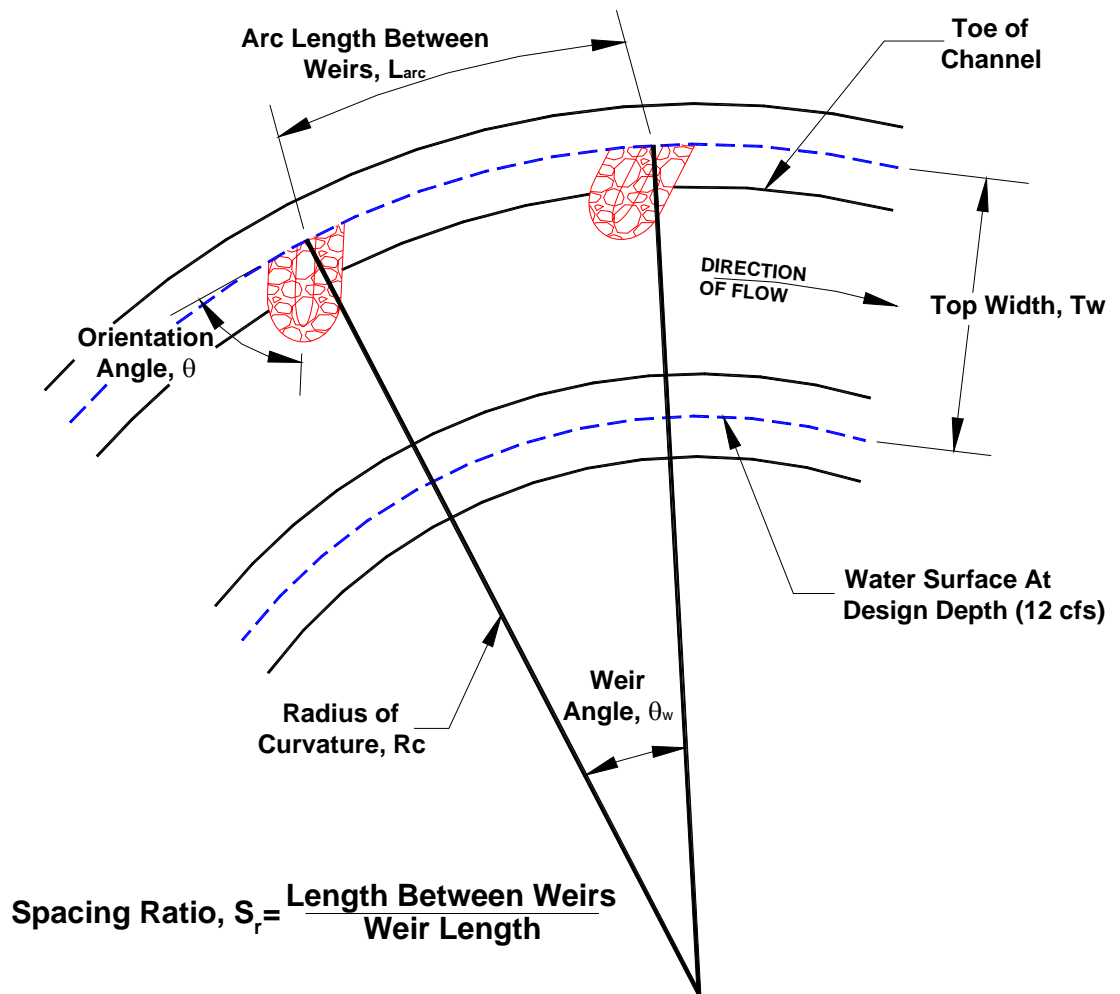


Figure 3.20: Geometric Properties Used in Weir Placement

3.6.2.2 SPACING RATIO

Spacing ratio refers to the distance between the weirs along the curve of the bank and is defined as the ratio between the distance separating weirs and their length, Equation 3.2:

$$S = \frac{L_{arc}}{L_{proj,w}} \quad \text{Equation 3.2}$$

where

S = spacing ratio;

L_{arc} = arc length between weirs (L); and

$L_{proj,w}$ = length of the weir projected perpendicular to the flow (L).

The spacing ratio was varied based on ranges suggested in current literature from 2.7 to 4.1 in the Type 1 bend and 5.5 to 8.4 in the Type 3 bend (Heintz, 2002). Based on Equation 3.2, the number of weirs located in the bend and the weir orientation angle (θ) will both have an effect on the spacing ratio. Increasing the number of weirs in a bend will decrease the distance between weirs and decreasing the orientation angle, θ , will decrease the projected length of the weir ($L_{proj,w}$). Therefore, a single spacing ratio may have multiple combinations of number of weirs and weir angles.

3.6.2.3 ORIENTATION ANGLE (θ)

The weir angle is the angle formed by a line tangent to the curve where the weir is installed and a line oriented along the weir. An angle that is between 0 and 90 degrees is consistent to a weir that is pointed in the upstream direction, whereas a 90- to

180-degree angle indicates a weir that is pointed in the downstream direction. For the tests included in this analysis, weir angles of 90, 60, and 75 were considered.

3.6.2.4 WEIR LENGTH

Weir length (L_w) is defined as length of the weir that is perpendicular to the flow. At weir angles of 90 degrees, the total length of the weir is equal to L_w . However, when the value of the weir angle is other than 90 degrees, the length of the weir must be projected onto a plane that is perpendicular to the flow, as shown in Equation 3.3:

$$L_{proj,w} = L_w \sin(\theta) \quad \text{Equation 3.3}$$

where

$L_{proj,w}$ = length of weir projected perpendicular to the flow (L);

L_w = total length of weir (L); and

θ = orientation angle.

To quantify the amount of constriction caused by the bendway weir, a length ratio is defined as the projected length of the weir and the top width at a given flow rate, presented in Equation 3.4:

$$L_r = \frac{L_{proj,w}}{TW} \quad \text{Equation 3.4}$$

where

L_r = length ratio;

$L_{proj,w}$ = weir length (L); and

TW = top width (L).

In addition to the total weir length, the crest length is defined in terms of the overall crest length (L_{cw}) and in terms of a crest length projected perpendicular to the flow.

3.6.3 TEST PROGRAM

Effects of bendway-weir variability were tested by systematically changing parameters discussed in Section 3.6.2. With a crest angle of 0 degrees, three separate weir angles were evaluated: 1) 90 degrees, 2) 60 degrees, and 3) 75 degrees. The length ratio ranges from 15 to 28 within each weir angle. For each length ratio, spacing ratios of 3.4, 4.1, and 5.1 were considered. For each weir angle, the length ratio ranged from 17 to 30 and the spacing ratio ranged from 2.6 to 3.19. Table 3.5 summarizes the variation of each test configuration. Each configuration listed in Table 3.5 was run with discharges of 8, 12, and 16 cfs. For each discharge and each test, data were collected in accordance with Section 3.4.

Table 3.5: Configuration Matrix for Bendway-weir Testing

Test System Identification	Reference	Orientation Angle, θ (degrees)	Estimated Area Blocked (%)	Upstream (Type 1 Bend)				Downstream (Type 3 Bend)				
				Number of Weirs	Length of Weirs, L_w (ft)	Nominal Spacing Ratio, S	Length Ratio	Number of Weirs	Length of Weirs, L_w (ft)	Nominal Spacing Ratio, S	Length Ratio	
0.	B01	Heintz (2002)	N/A	N/A	N/A	N/A	N/A	N/A	N/A	N/A	N/A	N/A
1.	W01	Heintz (2002)	90	27	5	4.9	4.1	28	4	3.8	5.9	28
2.	W02	Heintz (2002)	90	27	4	4.9	5.1	28	3	3.8	8.4	28
3.	W03	Heintz (2002)	90	27	6	4.9	3.4	28	5	3.8	4.7	28
4.	W04	Darrow (2004)	90	10.75	9	2.99	3.4	15	6	2.38	5.9	15
5.	W05	Darrow (2004)	90	10.75	8	2.99	4.1	15	5	2.38	7.62	15
6.	W06	Darrow (2004)	90	19.4	7	4.02	3.4	22	5	3.13	5.9	22
7.	W07	Darrow (2004)	90	19.4	6	4.02	4.1	22	4	3.13	7.62	22
8.	W08	Darrow (2004)	60	10.75	9	3.45	3.4	15	6	2.75	5.9	18
9.	W09	Darrow (2004)	60	10.75	8	3.45	4.1	15	5	2.75	7.62	18
10.	W10	Kinzli (2005)	60	19.4	7	4.52	3.4	22	5	3.49	5.9	22
11.	W11	Kinzli (2005)	60	19.4	6	4.52	4.1	22	4	3.49	7.62	22
12.	W12	Kinzli (2005)	60	27	6	5.54	3.4	28	4	4.29	5.9	28
13.	W13	Kinzli (2005)	60	27	5	5.54	4.1	28	3	4.29	7.62	28
14.	W14	Kasper (2005)	75	27	6	5.057	3.4	26	4	3.876	5.9	26
15.	W15	Schmidt (2005)	75	27	5	5.057	4.1	26	3	3.876	7.62	26

N/A = not available

3.6.4 ADDITIONAL INSTRUMENTATION

In addition to collecting data at each piezometric tap shown in Figure 3.9, flow-depth, 60-percent velocity, and Preston-tube data were collected at four additional points associated with each weir: 1) 1 ft upstream near the toe, 2) 1 ft downstream near the toe, 3) 1 ft from the tip, and 4) at the toe of the opposite bank. Additional data points were also taken at the toe of the inner and outer banks midway between each weir. Locations of the additional data points associated with each weir are shown schematically in Figure 3.21.

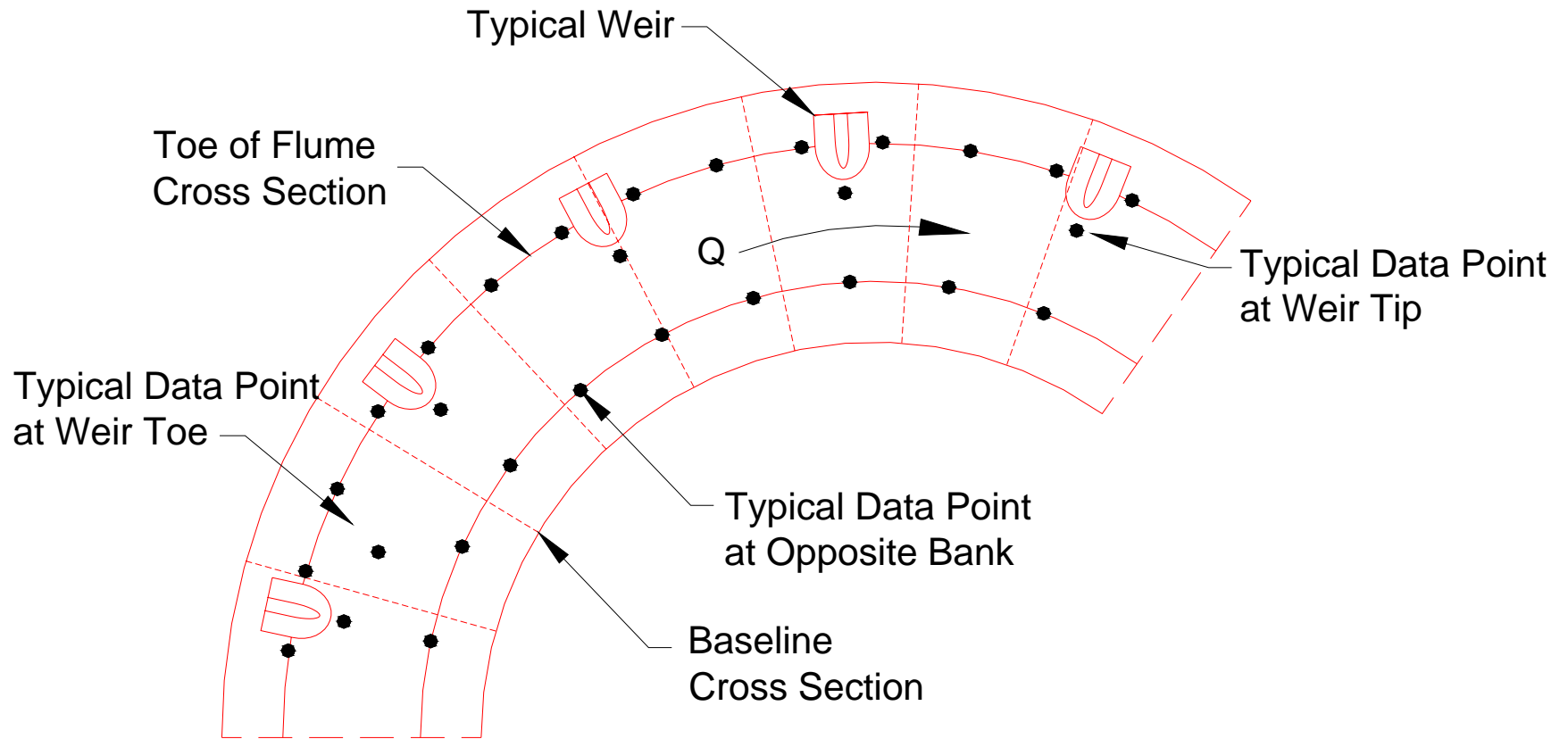


Figure 3.21: Location of Additional Weir Data Points

4 DATABASE DEVELOPMENT

4.1 INTRODUCTION

Upon completion of flume construction by Heintz (2002), tests were conducted. Depth, velocity, and shear-stress data collected at 8, 12, 16, and 20 cfs in the trapezoidal flume without weirs in place were used to establish baseline conditions. Subsequent to the baseline tests, bendway-weir fields were constructed in the trapezoidal channel. By varying the weir angle, crest slope, and spacing ratio, fifteen different bendway-weir configurations for each bend (as summarized in Table 3.5) were tested at 8, 12, and 16 cfs. Data that describe the associated hydraulic conditions are used in this research.

Each bend in the trapezoidal channel was divided into eight cross sections and each cross section contained seven piezometric taps. Depth, velocity, and shear-stress data were collected at each piezometric tap. In the weir configuration tests, velocity and shear-stress measurements were taken at additional locations with respect to the weir, as shown in Figure 3.21. Data at the weir tip and at the toe of the inner bank opposite each weir were used to describe conditions directly adjacent to the weir field. Appendix C contains all data collected in the physical tests that were used in this research.

4.2 BASELINE RESULTS

Initial tests in the trapezoidal section were conducted at 8, 12, 16, and 20 cfs. Measurements of depth in the middle of the channel were used to establish baseline depth profiles. Depths ranged from a maximum of 1.056 ft for the 20-cfs test in the smaller channel of the downstream bend to a minimum of 0.587 ft for the 8-cfs test in the larger upstream bend. Depth profiles are plotted in Figure 4.1 with respect to channel station for all four baseline discharges.

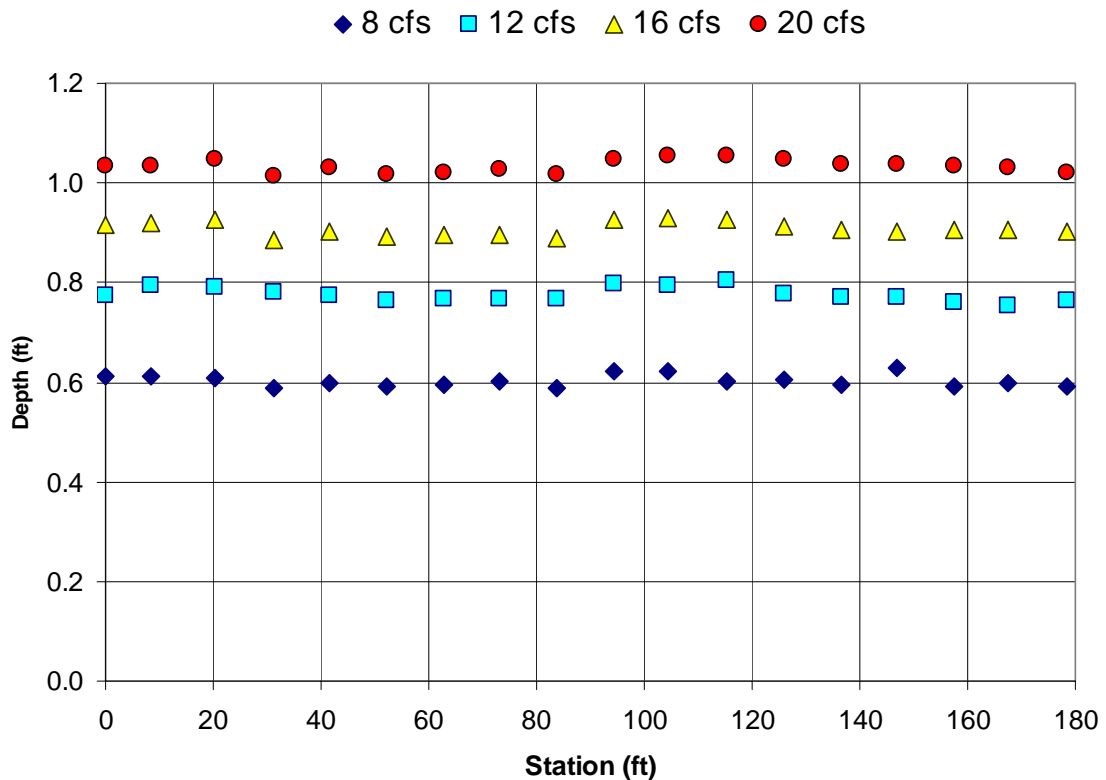


Figure 4.1: Measured Depth Profiles for Baseline Physical Tests

Average depth was computed and is shown along with maximum and minimum depths in Table 4.1 for the baseline tests.

Table 4.1: Range of Depth Measurements for Baseline Physical Tests

Discharge (cfs)	Bend Location in Channel	Minimum (ft)	Average Depth (ft)	Maximum (ft)
8	Upstream	0.591	0.604	0.629
8	Downstream	0.587	0.599	0.613
12	Upstream	0.754	0.775	0.805
12	Downstream	0.764	0.776	0.796
16	Upstream	0.903	0.912	0.929
16	Downstream	0.887	0.903	0.926
20	Upstream	1.040	1.021	1.056
20	Downstream	1.027	1.015	1.047

Measurements of velocity taken at 60 percent of the flow depth in the middle of the channel without any bendway weirs present were used to establish baseline velocity profiles. Figure 4.2 presents a plot of the measured velocity along the channel centerline at 60-percent depth for the baseline tests.

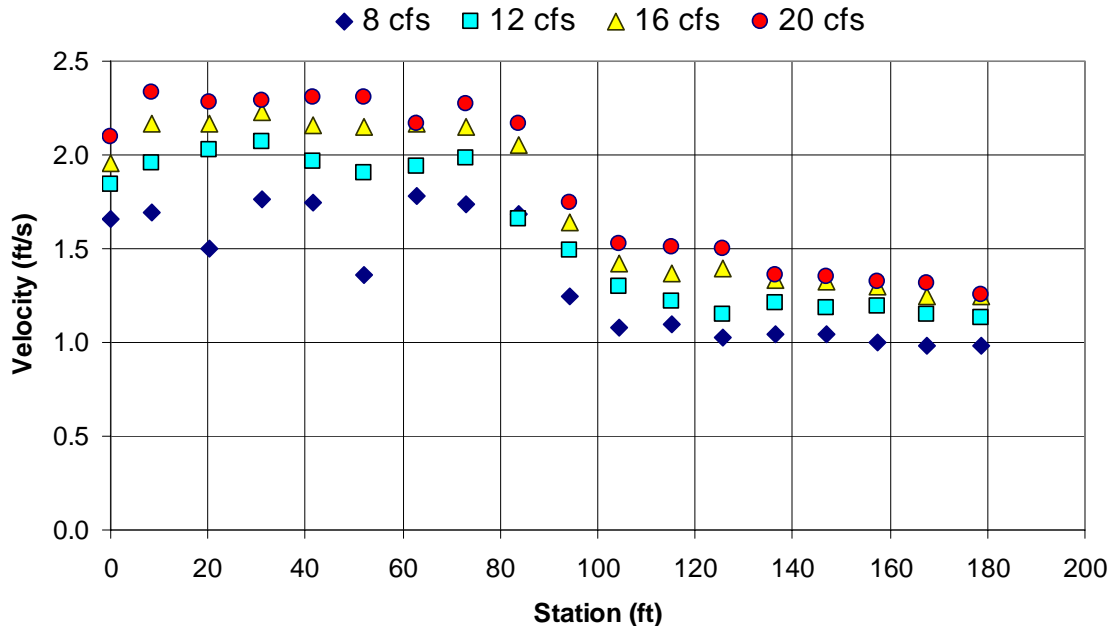


Figure 4.2: Measured Velocity Profiles for Baseline Physical Tests

Average velocities were computed for each profile in Figure 4.2 and are presented along with maximum and minimum velocities in Table 4.2.

Table 4.2: Range of Velocity Measurements for Baseline Physical Tests

Discharge (cfs)	Bend Location in Channel	Minimum (ft)	Average Velocity (ft/s)	Maximum (ft)
8	Upstream	0.979	1.030	1.094
8	Downstream	1.358	1.657	1.783
12	Upstream	1.132	1.191	1.295
12	Downstream	1.661	1.927	2.066
16	Upstream	1.241	1.328	1.425
16	Downstream	1.957	2.133	2.225
20	Upstream	1.254	1.392	1.527
20	Downstream	2.101	2.247	2.336

Shear-stress measurements taken at the channel boundary at the channel center for each cross section without any bendway weirs present in the physical model were used to establish baseline shear-stress profiles. Figure 4.3 presents a plot of the shear-stress profile for the baseline conditions.

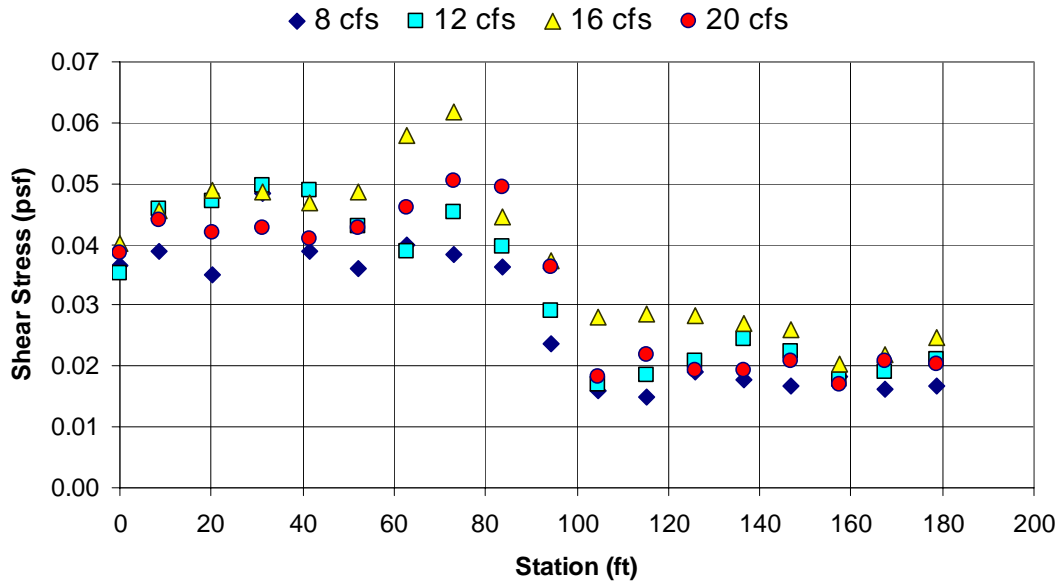


Figure 4.3: Measured Shear-stress Profiles for Baseline Physical Tests

Average shear-stress values were computed for each profile in Figure 4.3 and are presented along with maximum and minimum shear-stress values in Table 4.3.

Table 4.3: Range of Shear-stress Measurements for Baseline Physical Tests

Discharge (cfs)	Bend Location in Channel	Minimum (ft)	Average Shear Stress (lb/ft²)	Maximum (ft)
8	Upstream	0.0148	0.0169	0.0189
8	Downstream	0.0350	0.0387	0.0484
12	Upstream	0.0170	0.0202	0.0244
12	Downstream	0.0352	0.0437	0.0498
16	Upstream	0.0204	0.0256	0.0285
16	Downstream	0.0403	0.0492	0.0617
20	Upstream	0.0170	0.0197	0.0219
20	Downstream	0.0385	0.0441	0.0505

4.3 WEIR CONFIGURATION RESULTS

After baseline tests for 8, 12, 16, and 20 cfs were conducted in the physical model without any weirs present, a series of tests were conducted at 8, 12, and 16 cfs for various configurations of bendway-weir fields. Each weir configuration test included collection of depth, velocity, and shear-stress data at each cross section along the channel. Additional velocity and shear-stress data were collected in positions relative to the constructed weirs. For this research, velocity and shear-stress data collected at the weir tip and at the toe of the inner bank opposite the weir tip were used to support characterization of the hydraulic conditions for the various weir configurations.

Velocity measurements at the weir tip and at the toe of the inner bank across from the weir tip, both taken at 60 percent of the flow depth, were extracted from the physical weir configuration tests. Maximum weir tip and inner bank velocities were compiled for both bend geometries from each weir configuration physical test. The maximum velocity

in the downstream bend was experienced during weir configuration Test W12 (see Table 3.5), in which the inner bank velocity peaked at 3.35 ft/s. The maximum velocity experienced on the upstream bend occurred on the inner bank during weir configuration Test W03 (see Table 3.5) at a velocity of 2.08 ft/s. Figure 4.4 shows the relationship between the velocity measured at the weir tip and at the toe of the opposite bank across from the weir tip. Although the trendline shown in Figure 4.4 suggests that the velocity measured along the inner bank across from the weir is slightly greater than the maximum velocity measured at the weir tip, a clear relationship is not present. For velocities over 2 ft/s, Figure 4.4 shows that the velocity at the weir tip is generally greater than the velocity along the inner bank across from the weir tip. Conversely, for velocities below 2 ft/s, Figure 4.4 shows that the velocities along the inner bank across from the weir tip are generally greater than the velocities at the weir tip. Since, for a given test configuration, the maximum velocity could occur either at the weir tip or the inner bank across from the weir tip, both locations were used in comparisons made with results from the HEC-RAS computer model.

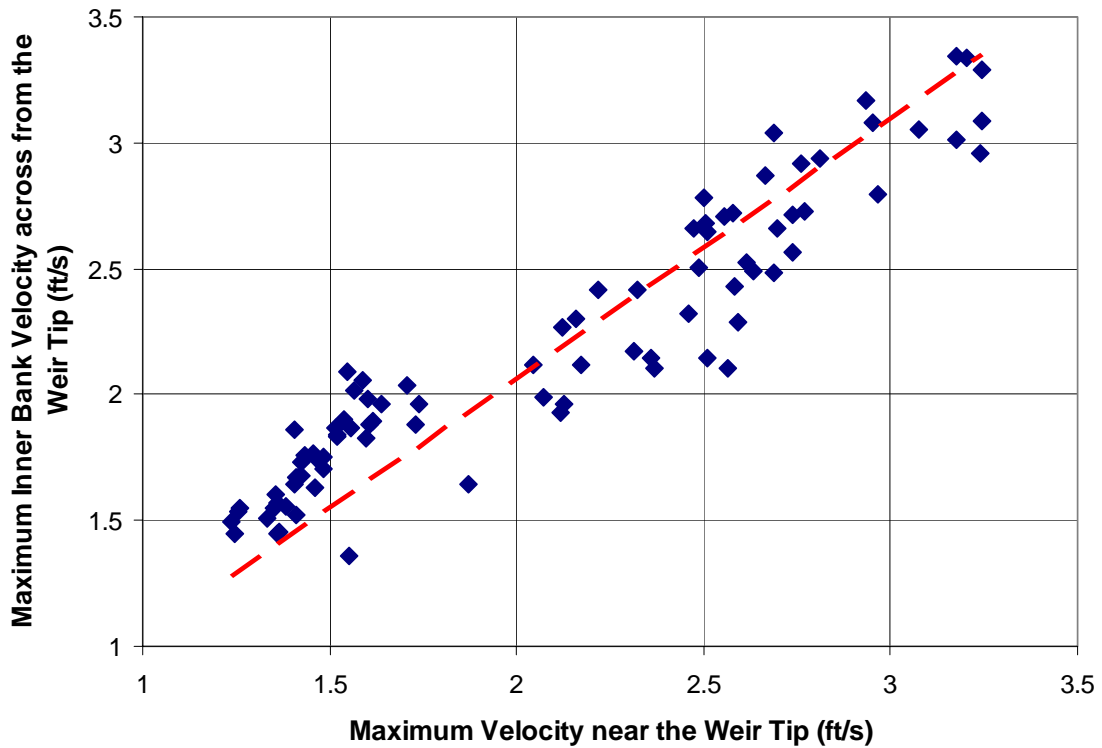


Figure 4.4: Comparison of the Maximum Velocity Values for the Inner Bank and Weir Tip

Shear-stress measurements were taken for each of the weir configuration tests at the same locations in the channel as the velocity measurements were taken. Inner bank and weir tip shear-stress measurements were extracted from the test results for the various weir configurations. Shear-stress measurements range from near 0 to 0.2 lb/ft². Maximum values for the shear stress along the inner bank and the weir tips were extracted for each test and each channel bend geometry. Shear stress varies greatly over the weir configuration tests. Maximum shear-stress values occur on the downstream bend along the inner bank during weir configuration Test W01 (see Table 3.5). Maximum shear-stress values for the upstream bend occur along the inner bank for weir configuration Test W08 (see Table 3.5). Figure 4.5 compares the maximum shear

stresses measured along the inner bank to the maximum measured shear stresses near the tip of the weir. No clear relationship between the shear stresses measured along the inner bank and shear stress measured at the weir tip was present. Comparisons of measured values with results from HEC-RAS computer models included both the shear stress measured at the weir tip and the shear stress measured across from the weir tip.

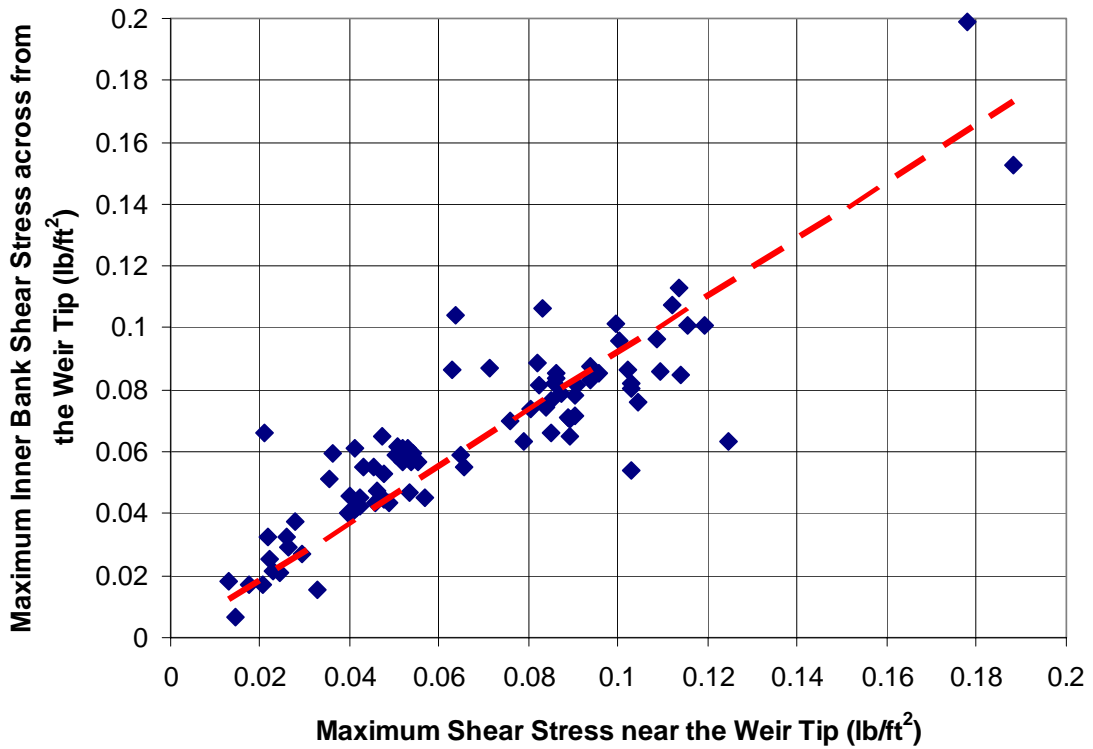


Figure 4.5: Comparison of the Maximum Shear-stress Values for the Inner Bank and Weir Tip

All of the measured depth, velocity, and shear-stress data presented in this section have been included in Appendix C.

5 COMPUTER MODELING APPROACH

5.1 BASELINE MODELING APPROACH

5.1.1 INTRODUCTION

As discussed in Chapter 2, the purpose of this research is to compare data collected from physical models of multiple bendway-weir configurations to results from a predictive numerical computer model. Due to its prevalence in the engineering community, the 1-D USACE model, HEC-RAS, was used as a platform for numerical simulation. Although previous research has shown that the flow associated with bendway weirs is not 1-D, it is thought that practicing engineers would seek to try to apply HEC-RAS to the complex hydraulic conditions created by placement of bendway weirs in river channels. Therefore, comparisons of the numerical models to the physical data are necessary to ascertain the relationship between the computed data and the collected physical data. Creation of a HEC-RAS model of the physical model's channel, with no bendway weirs present, represents the first step in the evaluation of the 1-D flow model and is subsequently referred to as the baseline model. Surveyed cross sections of the channel prepared by Heintz (2002) provide a basis for the baseline computer model.

5.1.2 CROSS-SECTION GEOMETRY

A survey compiled by Heintz (2002), as described in Section 3.5, served as a basis for the creation of a HEC-RAS baseline model. Cross sections of the trapezoidal flume from the Heintz (2002) survey were inputted directly into HEC-RAS, without weirs present, to represent a baseline conditions computer model.

5.1.3 REACH LENGTH

Reach length between cross sections is specified in HEC-RAS in terms of a left overbank, right overbank, and channel reach length. For the left and right overbanks, the 12-cfs water line was used for measurement. This line represents the mean reach length between the top and toe of the slope. Cross sections were spaced based on a uniform subdivision of the bend angle in eight segments. Figure 5.1 shows how cross-section spacing used for the baseline model relates to the overall bend angle.

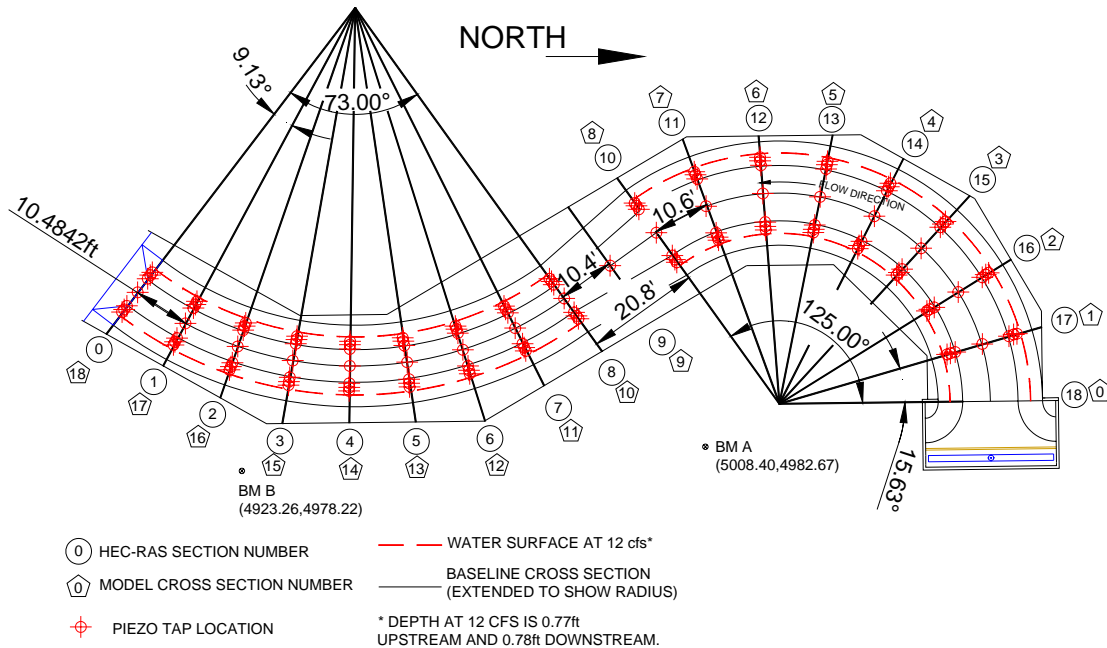


Figure 5.1: Cross-section Spacing used for Baseline Model

In terms of the channel centerline reach length, cross sections were spaced 10.6 ft apart for the upstream bend and 10.5 ft for the downstream bend. Cross sections in the transition were spaced 10.4 ft apart. Table 5.1 summarizes the cumulative reach lengths for the channel, left overbank, and right overbank.

Table 5.1: Cumulative Reach Length Used in HEC-RAS Model

HEC-RAS Cross-section Number	Left Bank Station	Channel Centerline Station	Right Bank Station
18	180.00	189.24	198.65
17	171.35	178.58	185.99
16	162.31	167.55	172.96
15	154.22	157.45	160.86
14	145.75	146.89	148.21
13	137.32	136.47	135.81
12	128.64	125.84	123.22
11	120.10	115.24	110.58
10	111.42	104.50	97.79
9	101.26	94.26	87.37
8	90.49	83.74	76.99
7	79.00	73.00	67.00
6	67.89	62.80	57.70
5	56.24	52.06	47.87
4	44.96	41.64	38.32
3	33.63	31.11	28.59
2	22.00	20.27	18.54
1	9.37	8.59	7.81
0	0.00	0.00	0.00

5.1.4 MANNING’S ROUGHNESS COEFFICIENT

Manning’s roughness coefficient is a parameter used to account for losses due to the roughness element of the channel surface. For the purposes of numerical simulation of the flume channel, the Manning’s roughness coefficient was set to 0.018 for all of the

cross sections. This value is consistent with the value reported in Heintz (2002) and the targeted value scaled from prototype conditions.

5.1.5 CONTRACTION AND EXPANSION COEFFICIENTS

Contraction and expansion coefficients are used in HEC-RAS to account for potential losses due to abrupt changes in cross-sectional geometry or change in cross-sectional area. Along the entire reach modeled in HEC-RAS, the transition between the upstream Type 1 bend and the downstream Type 3 bend is the only location of abrupt changes to cross-sectional geometry. With the exception of the transition cross sections, the contraction and expansion coefficients were kept at their default values of 0.1 and 0.3, respectively. At the location of the transition, the contraction coefficient was increased to 0.6 to account for the transition from the upstream Type 1 cross-sectional geometry to the smaller downstream Type 3 cross-sectional geometry based on Kasper (2005).

5.1.6 BASELINE MODEL RESULTS

Validity of baseline computer model results compared to measured data was determined before computer models of each weir configuration were created, as presented in Table 3.5. Measured baseline data were obtained from Heintz (2002), where depth, velocity, and boundary shear stress were measured for baseline conditions. Nineteen cross sections from a survey performed by Heintz (2002) formed the basis of the 1-D HEC-RAS baseline computer model. Comparisons between collected data and computed HEC-RAS modeling results for water-surface elevations, velocities, and

boundary shear stresses help support the validity of using the HEC-RAS baseline model as a platform for subsequent computer models of various weir configurations.

During baseline tests, as described in Section 4.2, depth was measured using piezometric taps installed on the channel surface at each cross section. Seven piezometric taps were installed at each cross section as shown previously in Figure 3.11. Three piezometric taps were installed at varying elevations on the cross-section side slopes and one piezometric tap, designated as Piezometer D, was installed at the center of the cross section. Because HEC-RAS is a 1-D model and assumes a constant water surface across the entire cross section, water-surface elevations measured at Piezometer D were used for comparing with elevations reported from HEC-RAS. Appendix D contains computed results from the HEC-RAS computer model. Figure 5.2 presents a plot of both measured and computed water-surface profiles for 8, 12, 16, and 20 cfs.

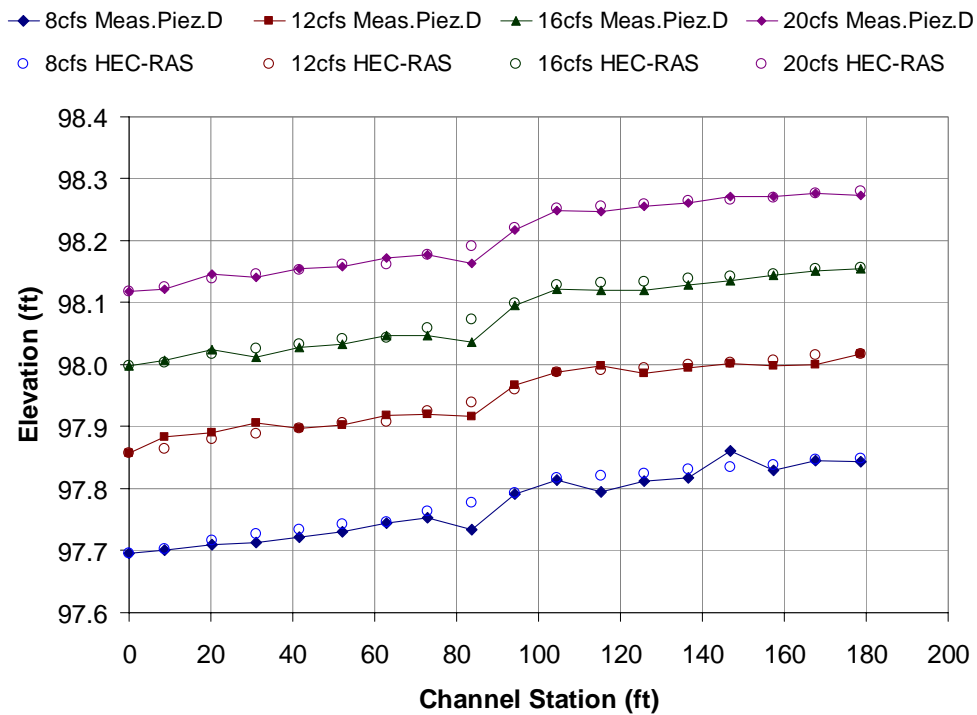


Figure 5.2: Water-surface Profiles for Baseline Conditions

Evaluation of the quality of fit between the measured and computed water-surface profiles was performed graphically by plotting the water-surface profiles and quantitatively by computing a percent error. Percent error was computed as the difference between measured water surfaces and computed water surfaces divided by the measured water surfaces. Table 5.2 summarizes the average and maximum computed percent error over each bend for 8, 12, 16, and 20 cfs.

Table 5.2: Average and Maximum Percent Error between Measured Baseline Data and Computed Baseline Results from HEC-RAS

Discharge (cfs)	Bend Location	Average Percent Error in Water- surface Elevation	Maximum Percent Error in Water- surface Elevation
8	Upstream	0.012%	0.028%
8	Downstream	0.011%	0.044%
12	Upstream	0.006%	0.016%
12	Downstream	0.010%	0.023%
16	Upstream	0.007%	0.014%
16	Downstream	0.010%	0.037%
20	Upstream	0.004%	0.010%
20	Downstream	0.007%	0.028%

Maximum percent error of 0.044 percent occurs on the downstream bend at 8 cfs. Overall, the average percent error over both bends and all the discharges was computed to be approximately 0.01 percent. From this analysis, the baseline computer model was considered appropriate to be used as a platform for the subsequent computer models of weir configurations.

Computed velocity obtained from HEC-RAS represents a cross-sectional average velocity. In order to make a valid comparison between measured and computed velocity, only baseline physical data taken at 60 percent of the flow depth were used for comparison. Computed velocity from HEC-RAS was plotted along with the measured

velocity at 60-percent depth at Piezometer C (right bank looking downstream), Piezometer D (channel center), and Piezometer E (left bank looking downstream) in Figure 5.3, Figure 5.4, and Figure 5.5, respectively.

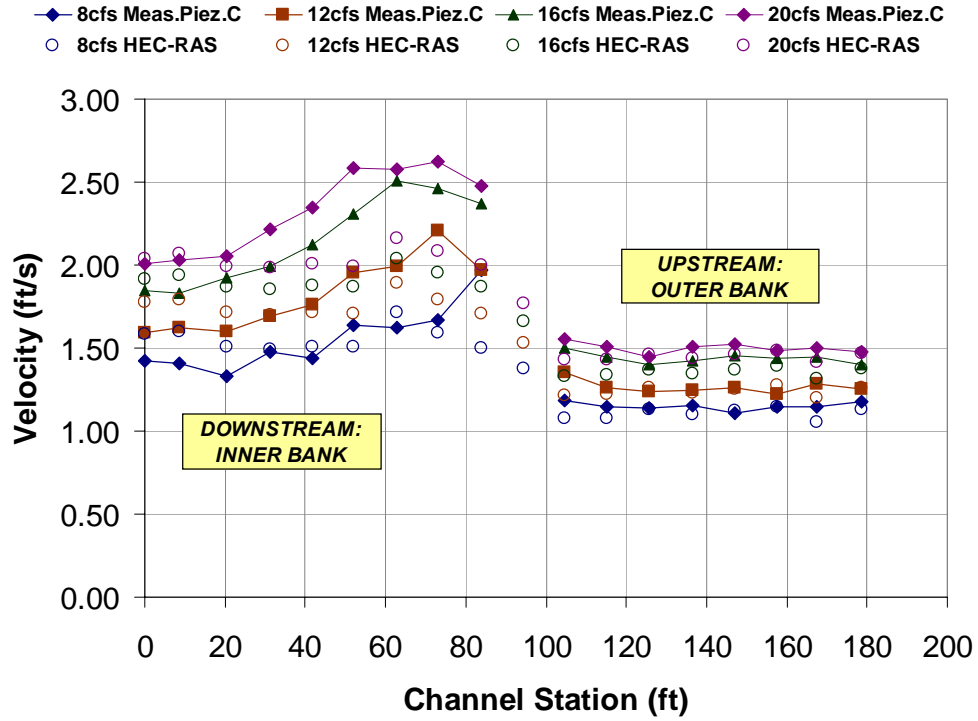


Figure 5.3: Velocity Profile at Piezometer C (right bank looking downstream) for Baseline Conditions

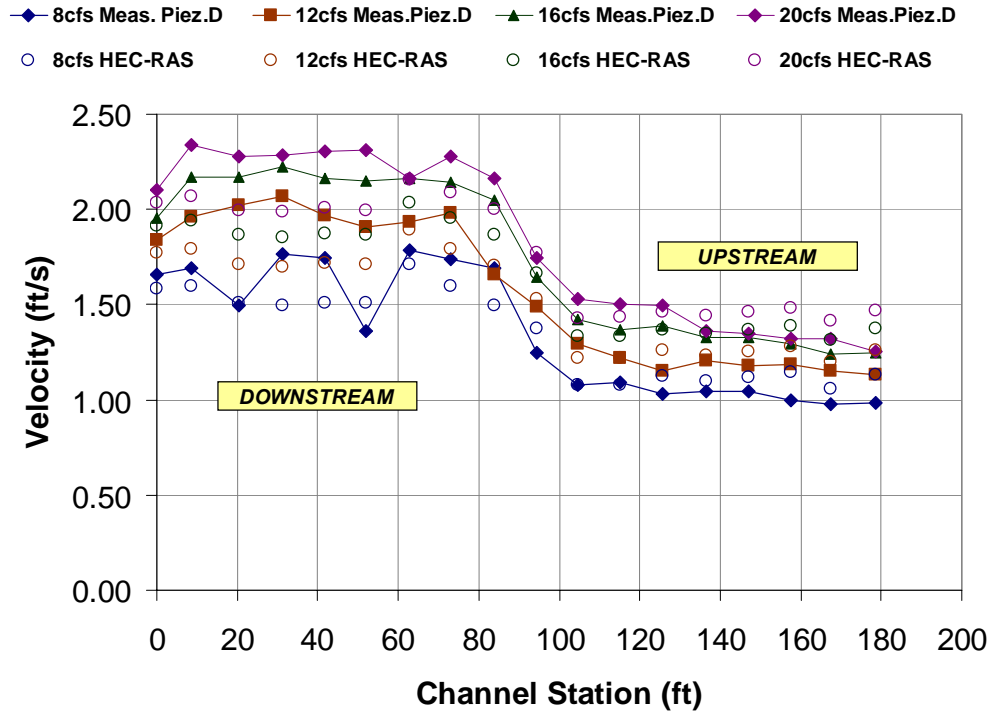


Figure 5.4: Velocity Profile at Piezometer D (channel center) for Baseline Conditions

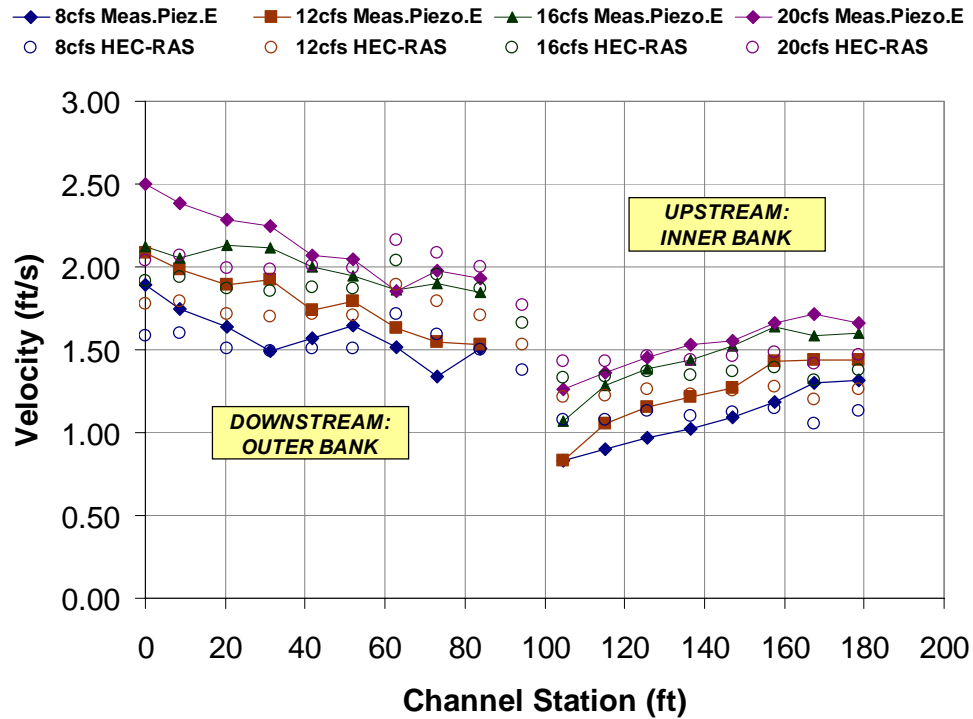


Figure 5.5: Velocity Profile at Piezometer E (left bank looking downstream) for Baseline Conditions

As can be seen in Figure 5.3, Figure 5.4, and Figure 5.5, discrepancies exist between the predicted velocity from HEC-RAS and the measured velocity from the physical model. Percent error of the predicted velocity was computed as the difference between the predicted HEC-RAS velocity and the measured velocity divided by the measured velocity. Error in the downstream bend averaged approximately 8 percent below what was measured, while the error associated with the predicted velocity in the upstream bend averaged approximately 5 percent. Figure 5.6 shows the relationship between the measured and the predicted velocity. Figure 5.6 shows that the ability of HEC-RAS to accurately predict velocity is affected by bend geometry.

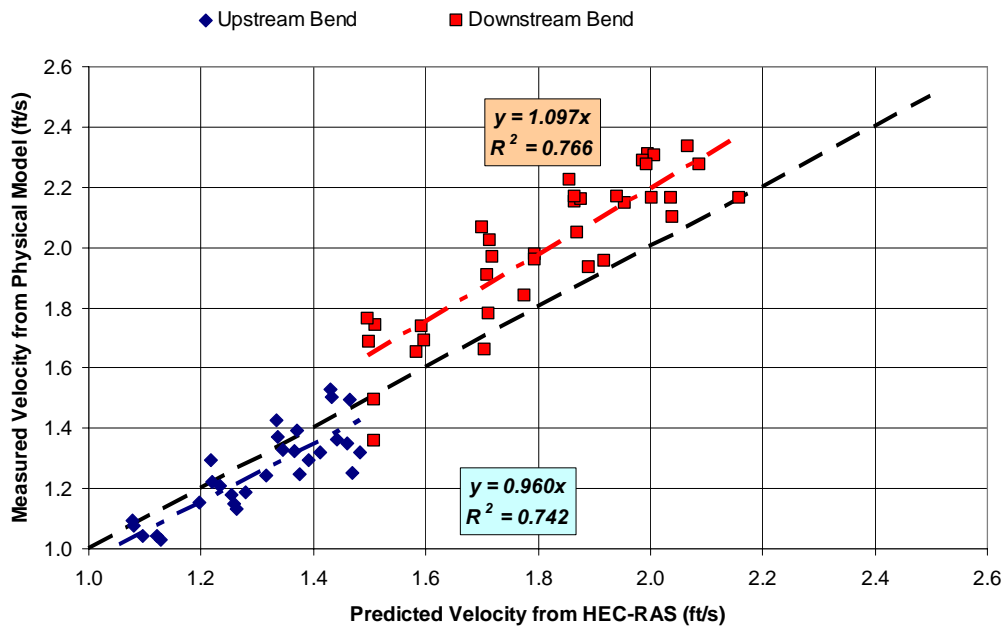


Figure 5.6: Predicted Velocity versus Measured Velocity for Baseline Models

Boundary shear stress was determined in the physical model through the use of a Preston tube placed at specific locations on the bottom surface of the channel cross section. Differential pressure measurements from the Preston tube were converted to

shear stress using Equation 3.1. Shear-stress values obtained from Preston-tube readings at Piezometers C, D, and E, were used to represent the right bank (looking downstream), channel center, and left bank (looking downstream), respectively. Measured shear-stress values were directly compared to computed cross-sectional averaged shear stress from the baseline HEC-RAS computer model. Figure 5.7, Figure 5.8, and Figure 5.9, present the shear-stress profiles for the right bank looking downstream, channel center, and left bank looking downstream, respectively.

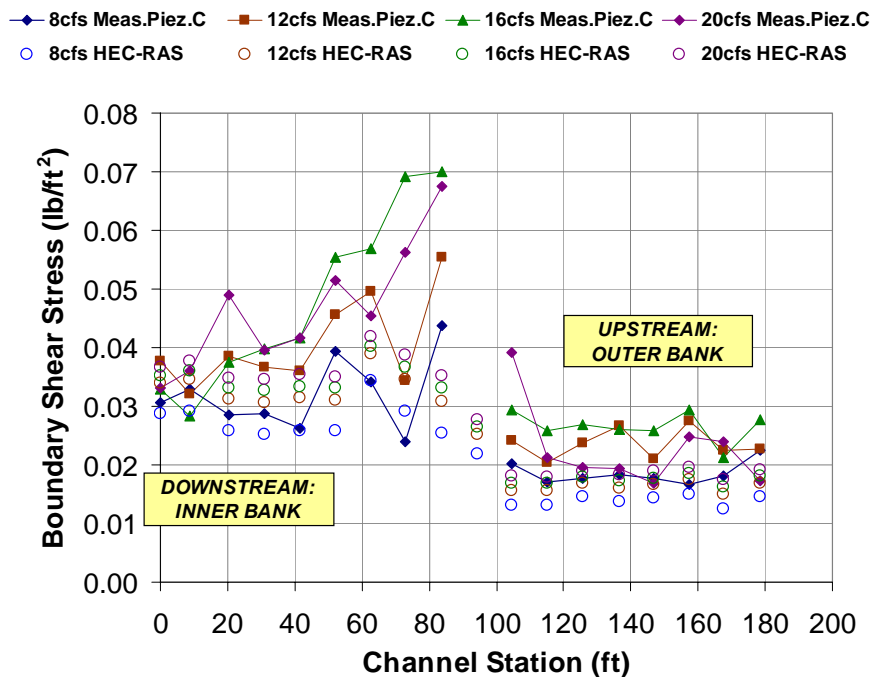


Figure 5.7: Shear-stress Profile for Piezometer C (right bank looking downstream) for Baseline Conditions

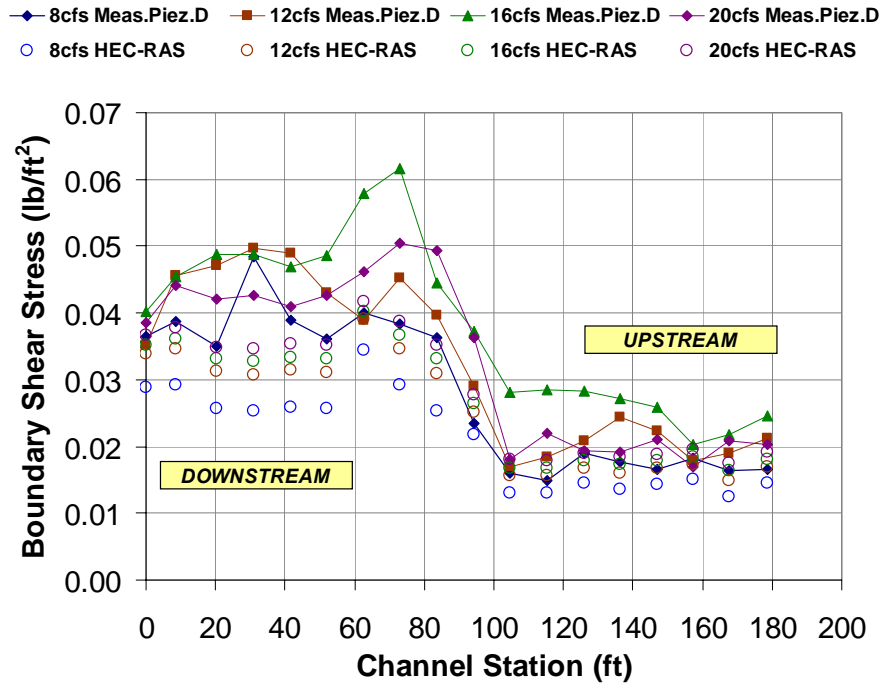


Figure 5.8: Shear-stress Profile for Piezometer D (channel center) for Baseline Conditions

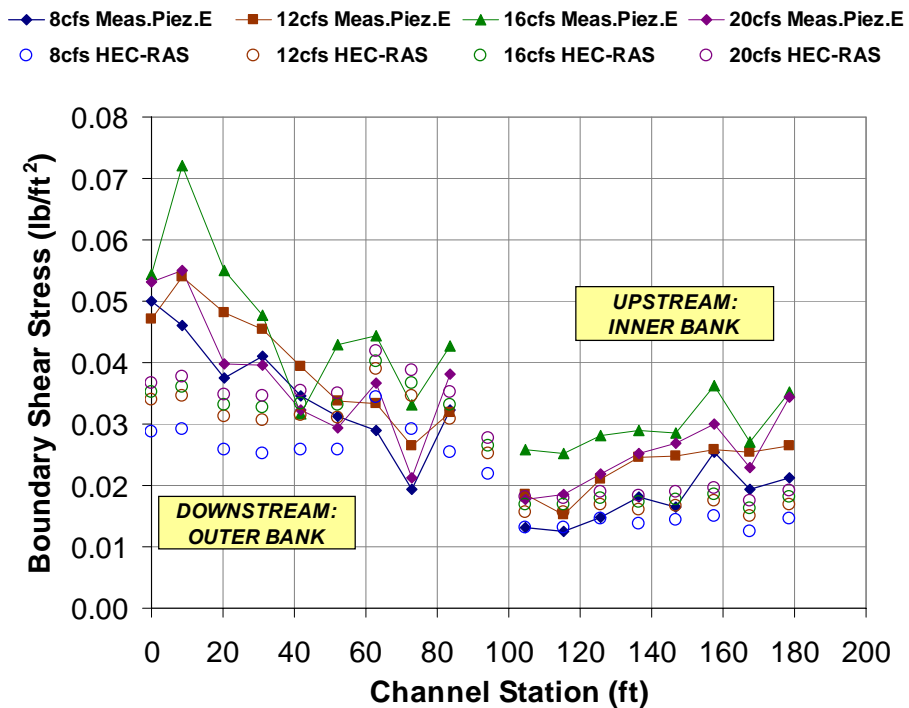


Figure 5.9: Shear-stress Profile for Piezometer E (left bank looking downstream) for Baseline Conditions

Figure 5.7, Figure 5.8, and Figure 5.9 show that HEC-RAS underpredicts measured shear stress for both upstream and downstream bends. Computing the percent difference between the measured shear stress and the predicted HEC-RAS shear stress shows that HEC-RAS, on average, underpredicts the shear stress by 18 percent in the upstream bend and 24 percent in the downstream bend. Figure 5.10 shows a comparison between the predicted and the measured shear stress for each bend. Considerable variation exists in the measured shear stress, particularly in the downstream bend. HEC-RAS's ability to predict shear stress is, however, affected by the bend geometry.

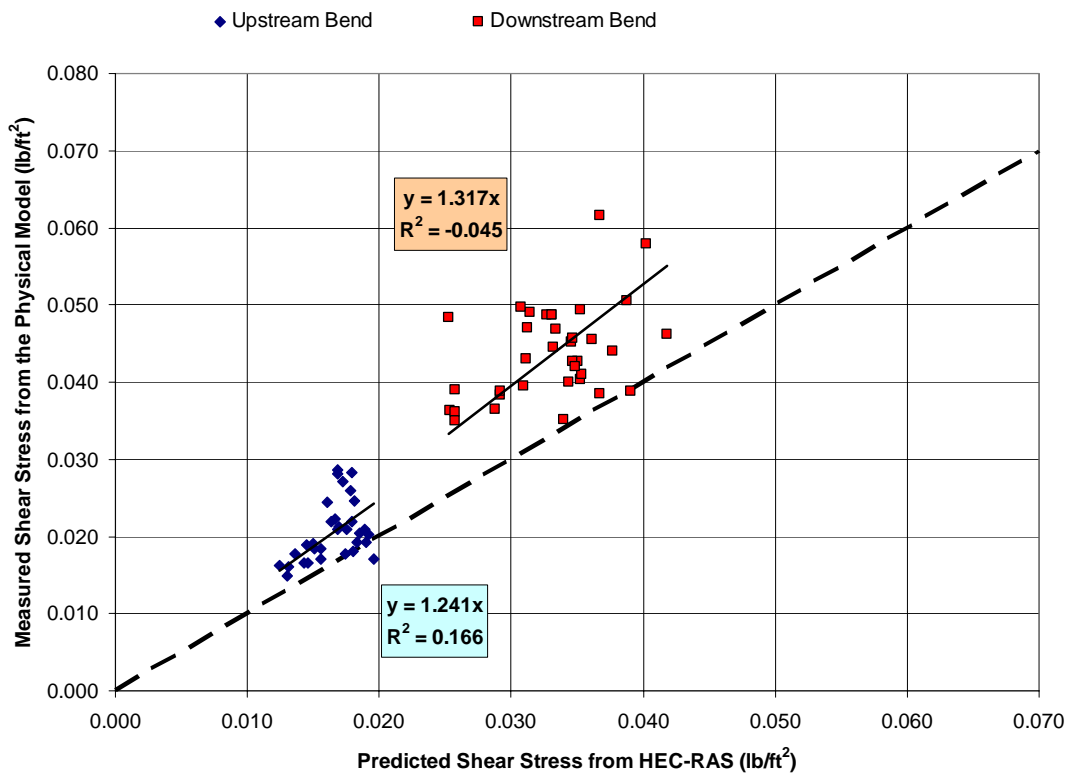


Figure 5.10: Predicted Shear Stress versus Measured Shear Stress for Baseline Models

Accuracy of HEC-RAS's prediction of water-surface profiles for baseline conditions supports the use of HEC-RAS to model subsequent weir configurations.

Discrepancies in both the velocity and shear-stress predictions and measured values stem from additional losses introduced by bend geometry. Additional adjustments to the predicted velocity and shear stress are necessary to accurately predict hydraulics in curved channels.

5.2 BENDWAY-WEIR MODELING APPROACH

5.2.1 INTRODUCTION

HEC-RAS computer models were created for each bendway-weir configuration presented in Table 3.5. Previously created geometry of the physical model without any weirs present was used as a platform to create new computer models for each weir configuration. Cross sections were inserted into the baseline HEC-RAS model using the *Cross Section Interpolation* routine within HEC-RAS (USACE, 2008). Location of interpolated cross sections depends on the modeling technique used to model the bendway weirs. Four unique modeling techniques were evaluated for the computer models of the weirs. A final modeling approach was selected based on which of the four cross-sectional layouts produced results that best fit the measured data.

5.2.2 MODEL SELECTION

Four different modeling techniques were evaluated for the simulation of the bendway weirs within the HEC-RAS computer models. Each of the four modeling techniques incorporates a unique cross-section layout or cross-sectional geometry. Selection of a modeling technique was based on which scenario produced the best overall fit to the measured data. Tests W01, W02, and W03, as defined in Table 3.5, were

chosen for the evaluation of each technique. The selected modeling technique was then applied to the computer models of all fifteen weir configurations.

5.2.2.1 BENDWAY-WEIR COMPUTER MODELING TECHNIQUE 1

The first computer modeling technique evaluated for a numeric representation of each bendway-weir configuration used the baseline cross-section layout shown in Figure 3.9, and interpolated a single cross section at each weir. Roughness, expansion, and contraction coefficients remained unchanged from the baseline model. Modeling Technique 1 is the simplest method of the four considered to model the weirs and is schematically represented in Figure 5.11.

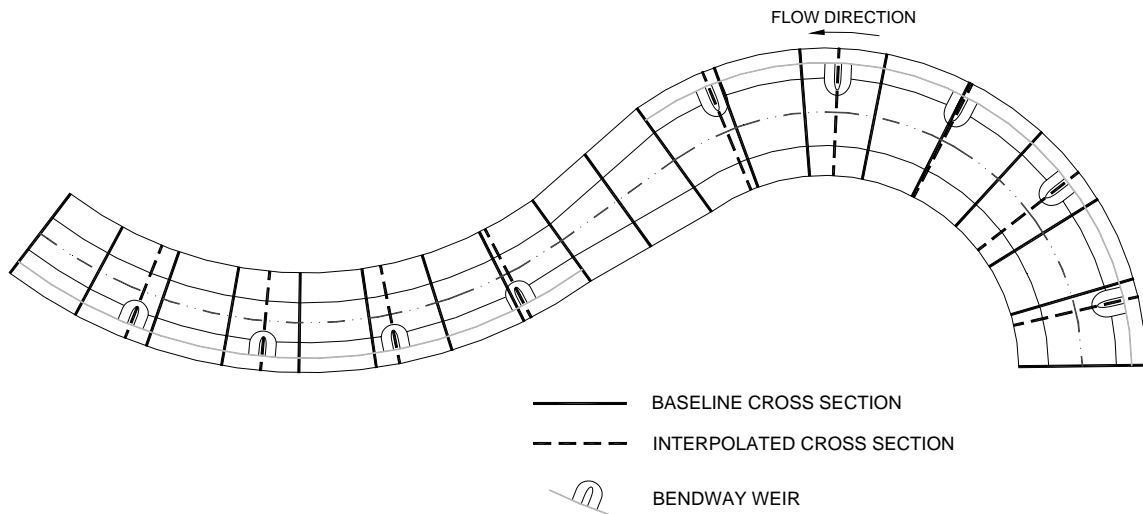


Figure 5.11: Schematic of Modeling Technique 1

Figure 5.12, Figure 5.13, and Figure 5.14 graphically display the results of the computed water-surface profiles for Tests W01, W02, and W03, respectively, for Modeling Technique 1 compared with the measured water-surface profiles collected in the physical model.

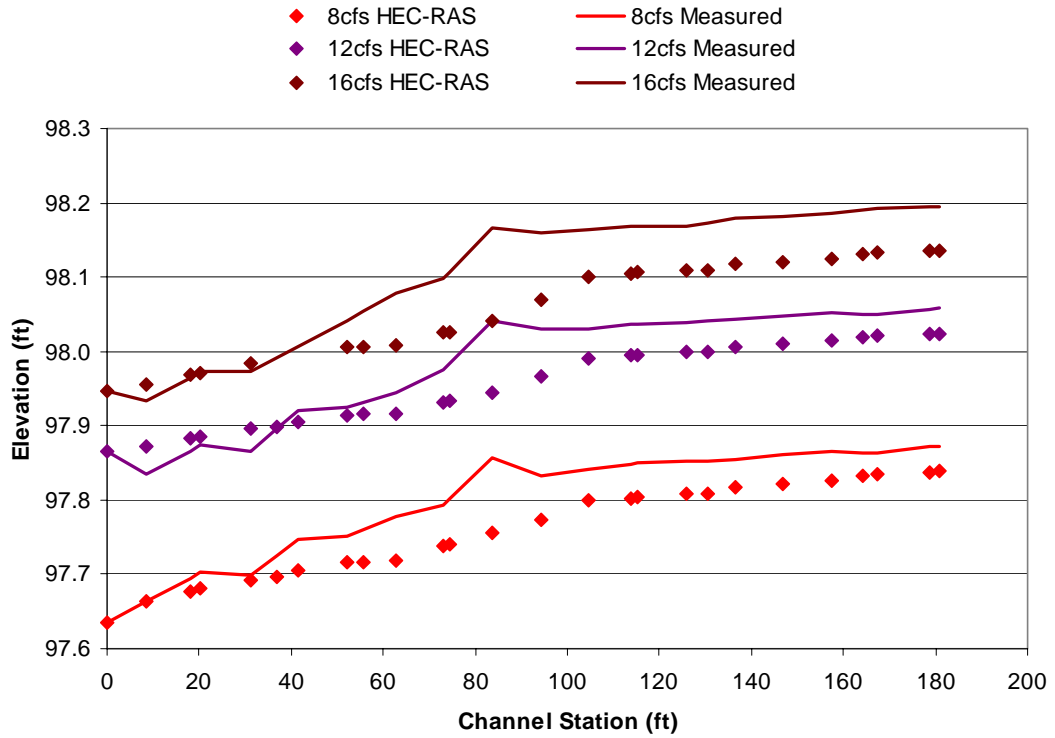


Figure 5.12: Water-surface Profiles for Test W01 Using Modeling Technique 1

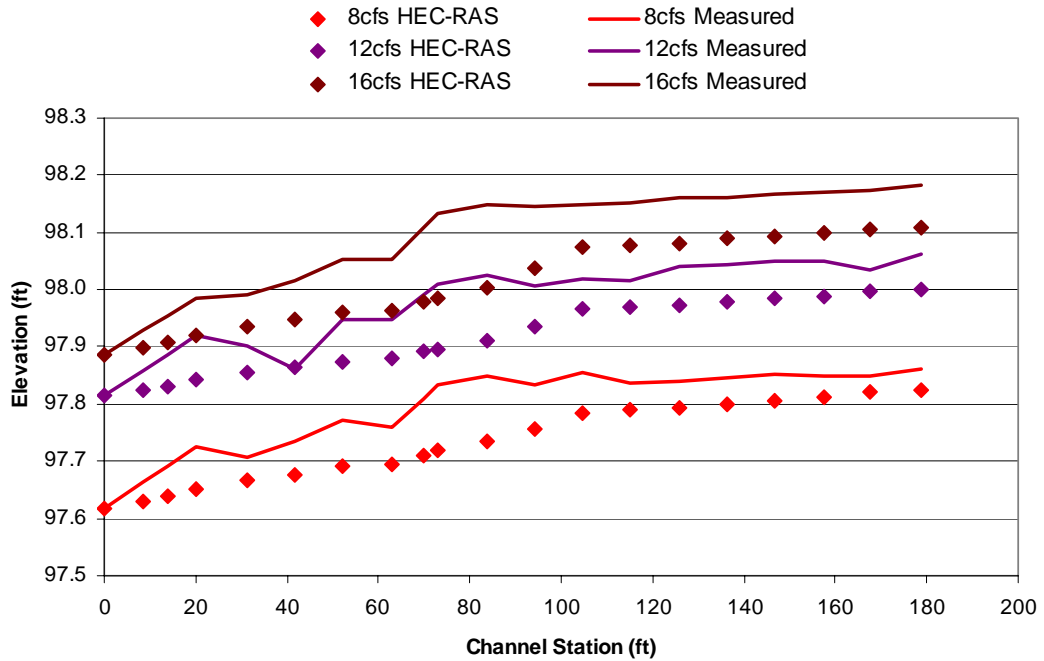


Figure 5.13: Water-surface Profile for Test W02 Using Technique 1

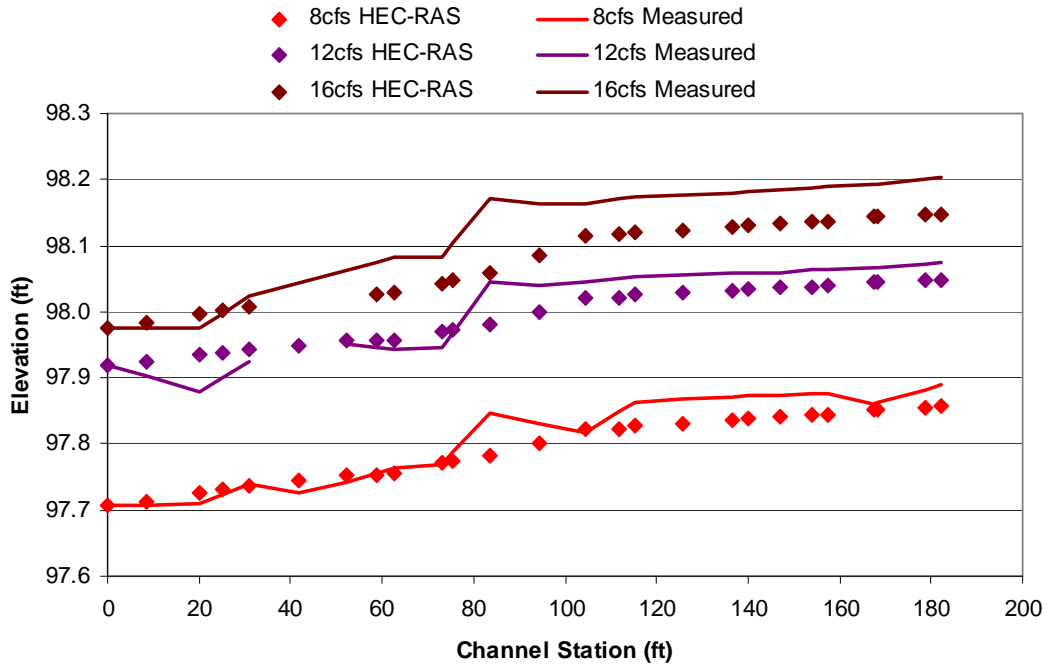


Figure 5.14: Water-surface Profile for Test W03 Using Technique 1

Table 5.3 summarizes the computed percent error between the measured water-surface profile and the computed water-surface profile for Modeling Technique 1.

Table 5.3: Percent Error for Modeling Technique 1

Test	Bend Location	Percent Error for Modeling Technique 1		
		8 cfs	12 cfs	16 cfs
W01	Downstream	5.27%	3.24%	4.15%
	Upstream	5.79%	4.39%	6.23%
W02	Downstream	9.70%	7.13%	8.12%
	Upstream	6.48%	7.00%	7.58%
W03	Downstream	2.02%	2.89%	3.85%
	Upstream	4.37%	2.90%	5.37%

5.2.2.2 BENDWAY-WEIR COMPUTER MODELING TECHNIQUE 2

For Modeling Technique 2, two cross sections, upstream and downstream of each weir, were added to the baseline model. Modeling Technique 2 attempted to capture

additional energy losses due to the weirs through the use of an additional cross section. The layout for Modeling Technique 2 is based on guidance from the HEC-RAS application manual (USACE, 2008) for placement of cross sections near abrupt changes in channel characteristics. No cross section was interpolated at the weir, and baseline cross sections were generally removed. Roughness, expansion, and contraction coefficients remained unchanged from the baseline model. Figure 5.15 schematically illustrates the general cross-section layout for Modeling Technique 2.

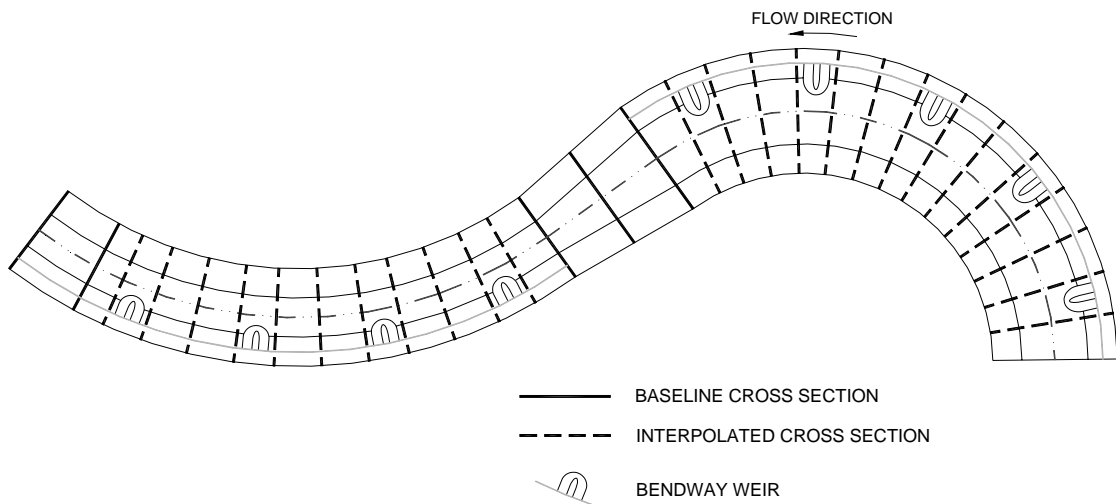


Figure 5.15: Schematic of Modeling Technique 2

Modeling Technique 2, shown in Figure 5.15, was applied to Tests W01, W02, and W03 and the results are presented in Figure 5.16, Figure 5.17, and Figure 5.18, respectively.

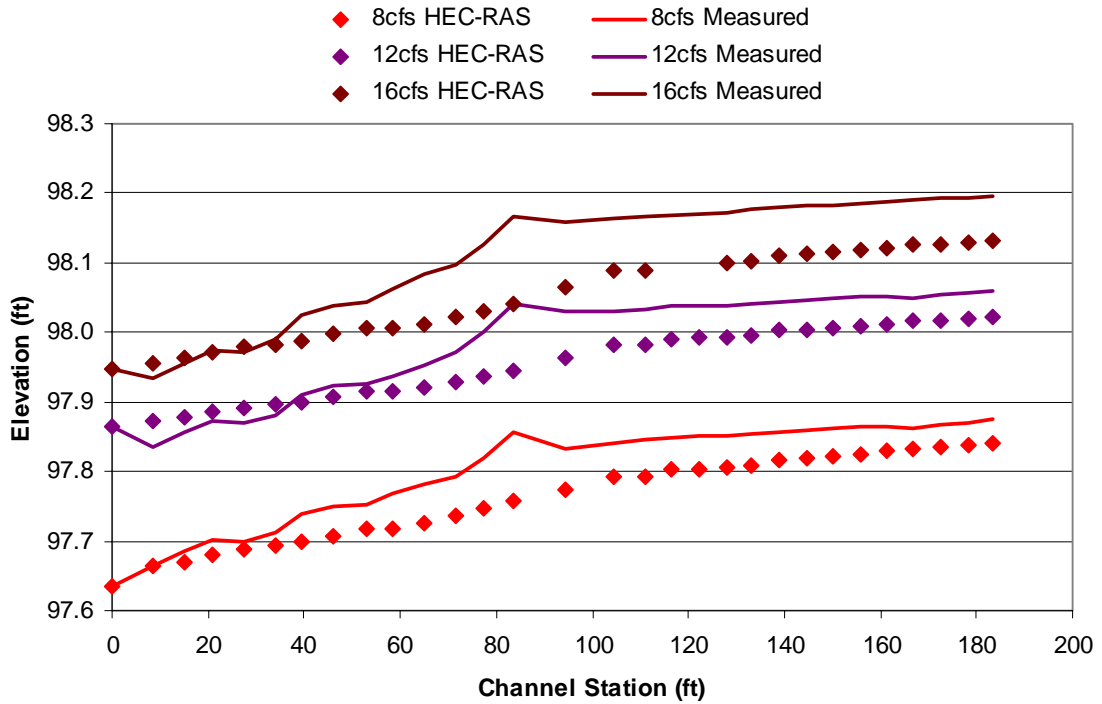


Figure 5.16: Water-surface Profile for Test W01 Using Modeling Technique 2

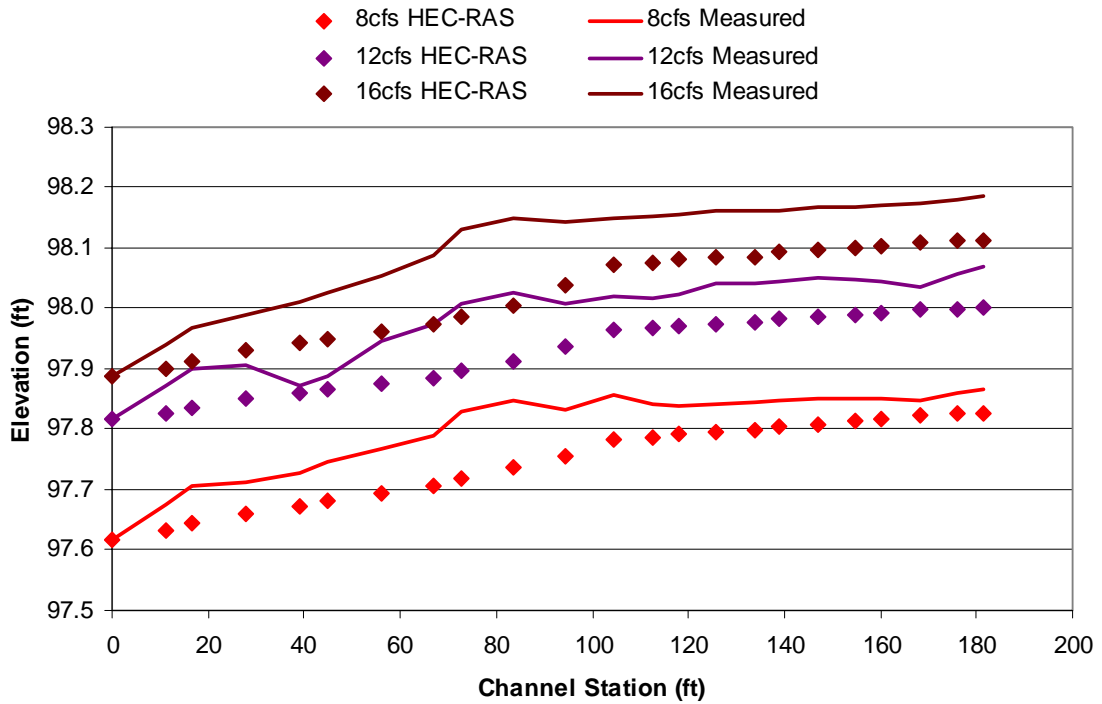


Figure 5.17: Water-surface Profile for Test W02 Using Modeling Technique 2

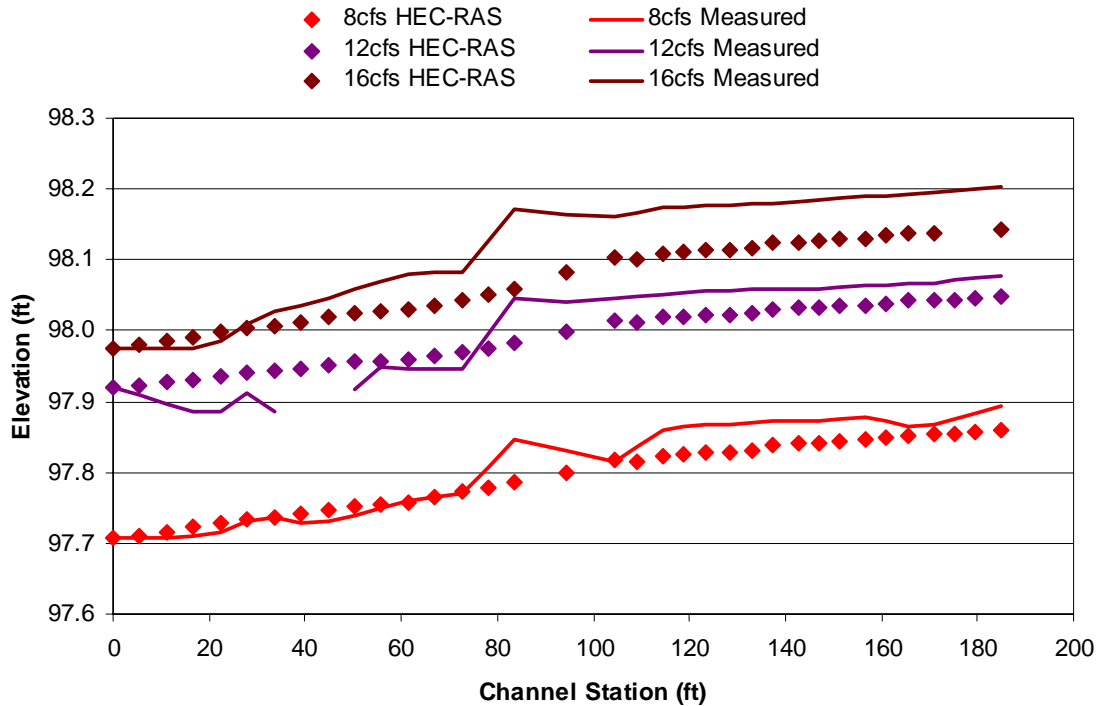


Figure 5.18: Water-surface Profile for Test W03 Using Modeling Technique 2

Table 5.4 summarizes the percent error between the computed water-surface elevation and the measured water-surface elevation for Modeling Technique 2.

Table 5.4: Percent Error for Modeling Technique 2

Test	Bend Location	Percent Error for Modeling Technique 2		
		8 cfs	12 cfs	16 cfs
W01	Downstream	5.38%	3.32%	4.17%
	Upstream	5.20%	4.11%	6.01%
W02	Downstream	9.64%	6.73%	8.15%
	Upstream	6.28%	6.92%	7.46%
W03	Downstream	1.80%	3.71%	3.50%
	Upstream	3.62%	2.63%	5.08%

5.2.2.3 BENDWAY-WEIR COMPUTER MODELING TECHNIQUE 3

Modeling Technique 3 incorporated three cross sections for each weir; one cross section upstream, one cross section downstream, and one cross section at the weir. An

additional cross section was interpolated between each weir. The layout for Modeling Technique 3 was derived from the layout of Modeling Technique 2 and using the additional cross sections to capture additional losses due to the weirs. Roughness, expansion, and contraction coefficients remained unchanged from the baseline model. Figure 5.19 illustrates the typical cross-section layout of Modeling Technique 3.

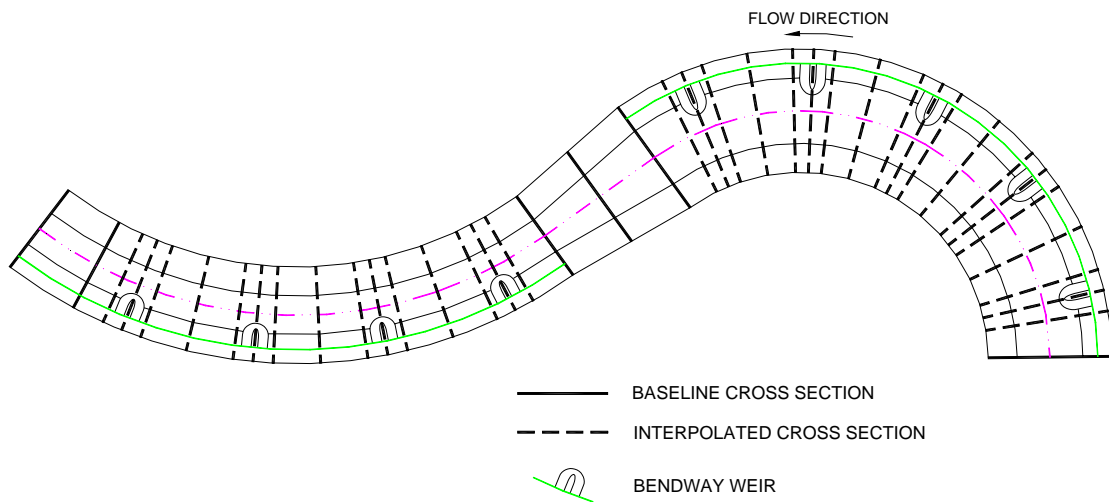


Figure 5.19: Schematic of Modeling Technique 3

Tests W01, W02, and W03 were modeled using Modeling Technique 3, and the results are shown in Figure 5.20, Figure 5.21, and Figure 5.22, respectively.

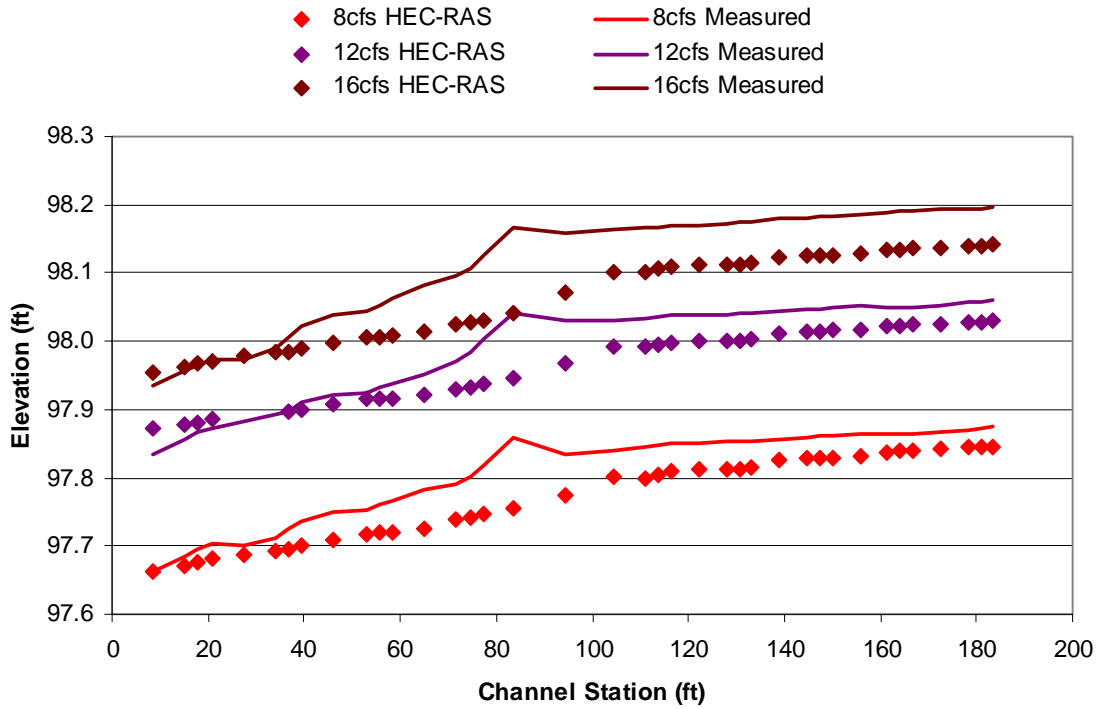


Figure 5.20: Water-surface Profile for Test W01 Using Modeling Technique 3

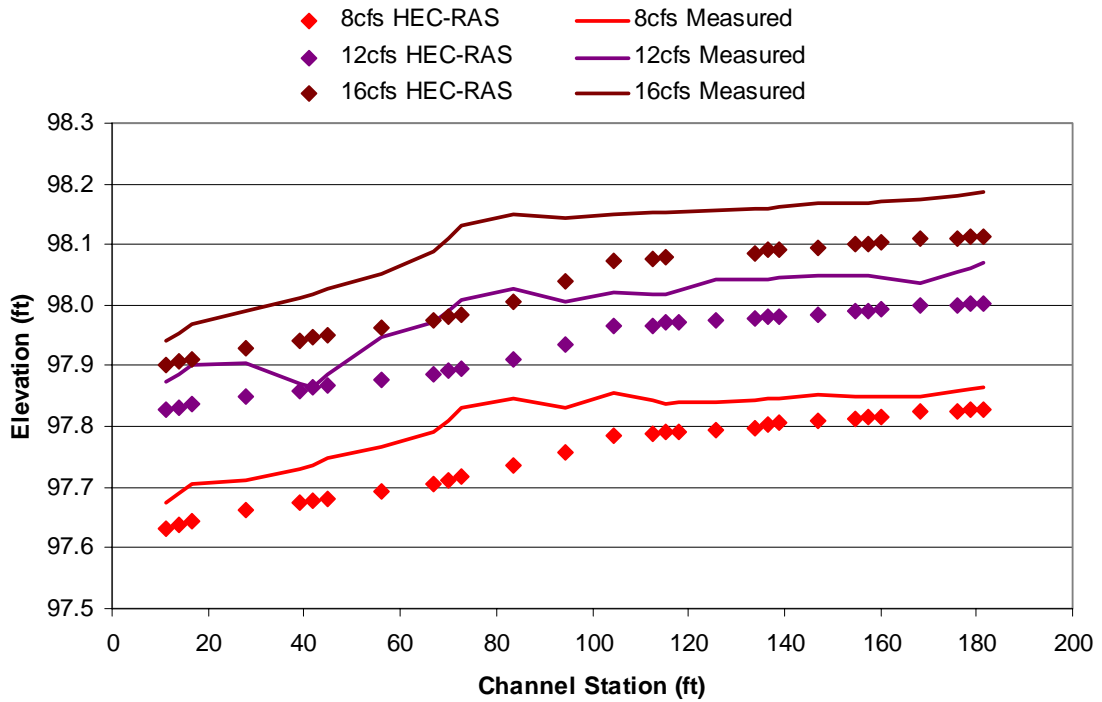


Figure 5.21: Water-surface Profile for Test W02 Using Modeling Technique 3

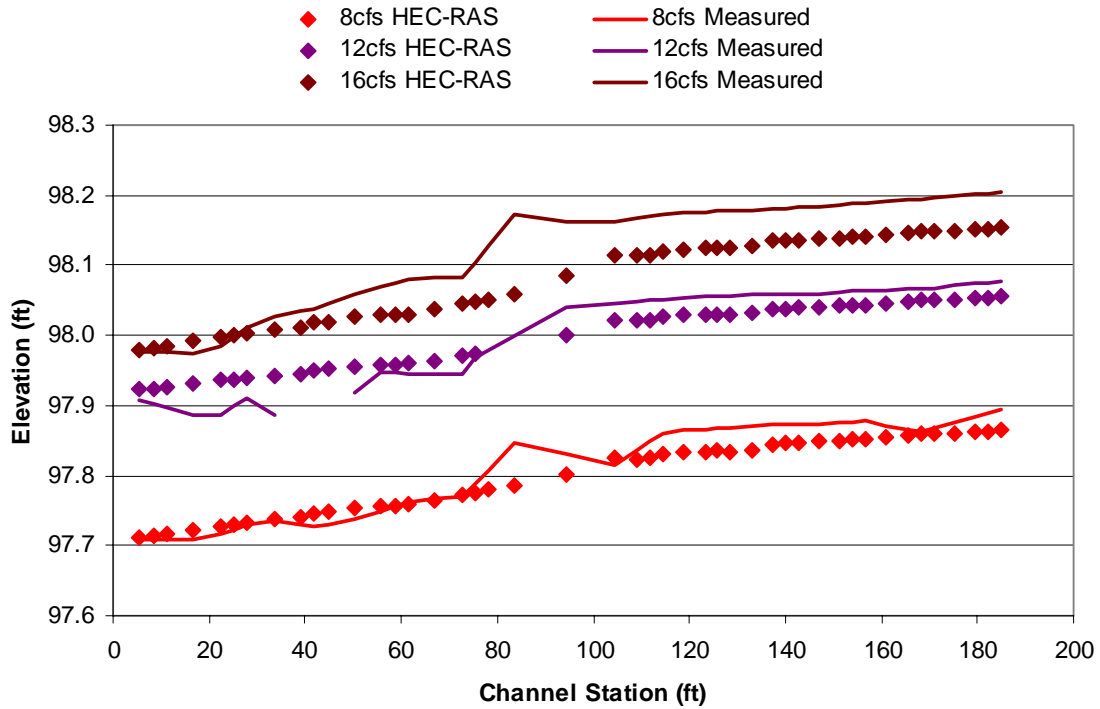


Figure 5.22: Water-surface Profile for Test W03 Using Modeling Technique 3

Percent error between the computed water-surface elevation and measured water-surface elevation was computed and is summarized in Table 5.5.

Table 5.5: Percent Error for Modeling Technique 3

Test	Bend Location	Percent Error for Modeling Technique 3		
		8 cfs	12 cfs	16 cfs
W01	Downstream	5.36%	3.09%	4.05%
	Upstream	5.04%	4.00%	5.90%
W02	Downstream	9.80%	6.56%	8.24%
	Upstream	6.24%	6.88%	7.41%
W03	Downstream	1.61%	3.19%	3.12%
	Upstream	3.50%	2.58%	5.01%

5.2.2.4 BENDWAY-WEIR COMPUTER MODELING TECHNIQUE 4

Computer Modeling Technique 4 used the same cross-section layout as Modeling Technique 3; three cross sections for each weir with an additional cross section between

the weirs. In addition to the interpolated cross sections, Modeling Technique 4 designates the area between the weirs as ineffective flow, or an area that is not contributing to the overall downstream flow in the main part of the channel. Prior research by Kinzli (2005) showed eddy formation and recirculation of flow in the areas between the weirs. Guidance from the *HEC-RAS Hydraulic Reference Manual* and the *User's Guide* (USACE, 2008) suggests the use of ineffective flow for areas in the channel dominated by eddies, reverse flow, or stagnant water. Removing these areas from the active downstream conveyance was thought to more accurately predict the observed hydraulics associated with the weir configurations. Roughness, expansion, and contraction coefficients remained unchanged from the baseline model. Figure 5.23 indicates this ineffective flow area for each bend.

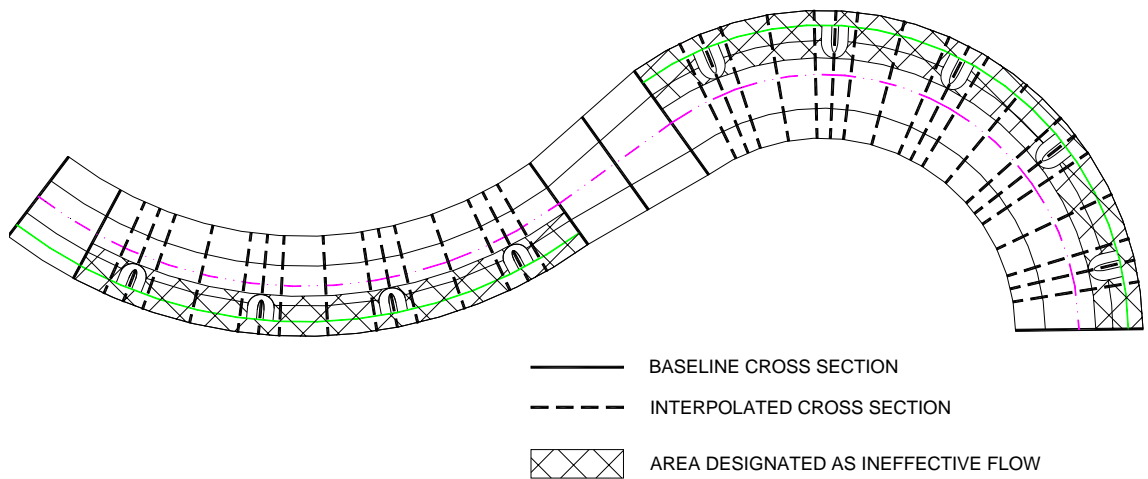


Figure 5.23: Schematic of Modeling Technique 4

Modeling Technique 4 also incorporates the geometry of the weirs at cross sections that fall at the weir location. Figure 5.24 shows a typical example of how the upstream and downstream weir geometry is incorporated into the baseline cross-section geometry.

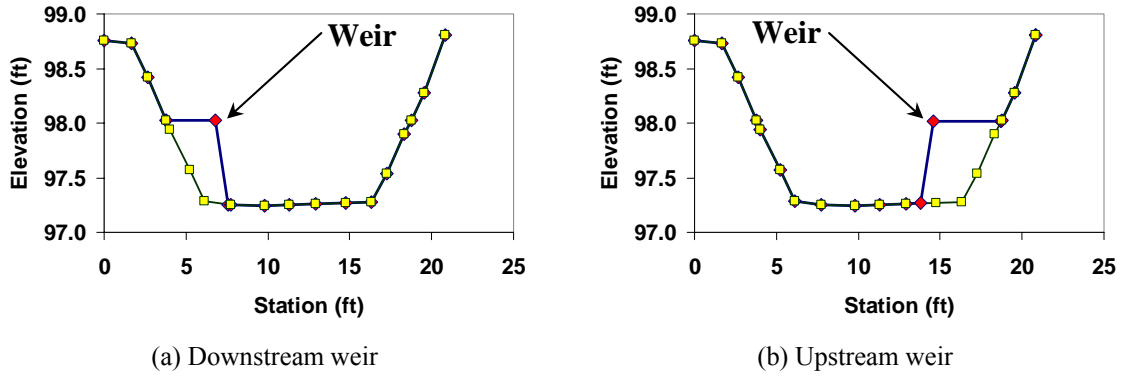


Figure 5.24: Typical Example of Weir Geometry Incorporated into Baseline Cross-section Geometry

Water-surface profiles were computed using Modeling Technique 4 for Tests W01, W02, and W03 and the results were compared to measured data, shown in Figure 5.25, Figure 5.26, and Figure 5.27, respectively.

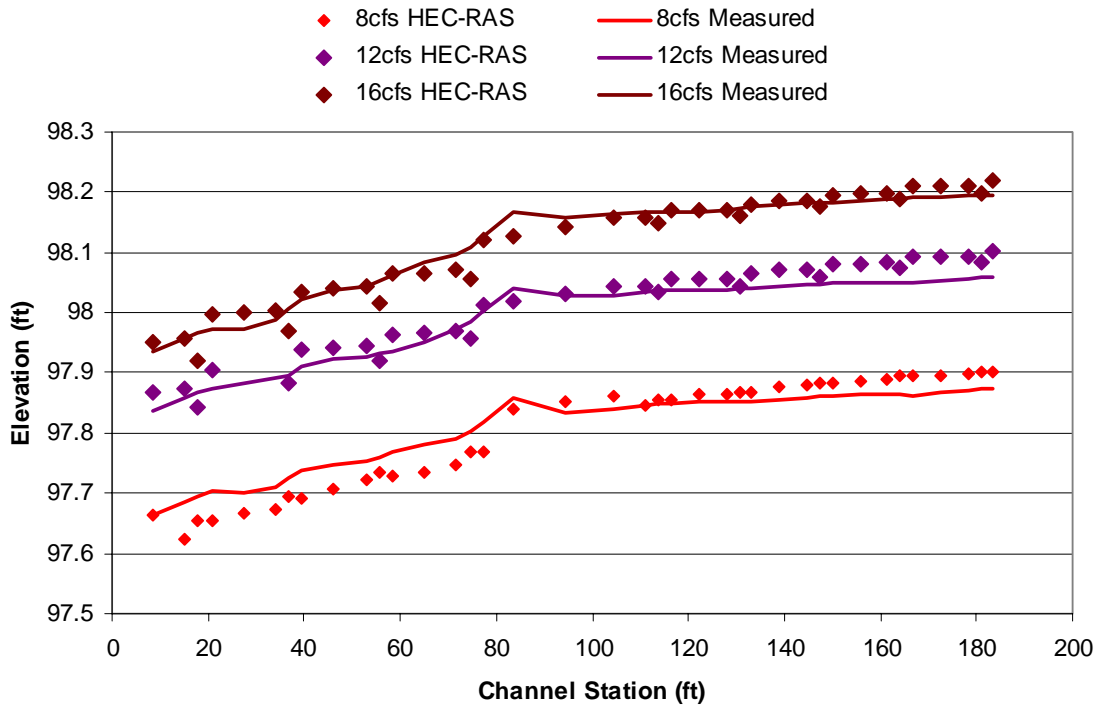


Figure 5.25: Water-surface Profile for Test W01 Using Modeling Technique 4

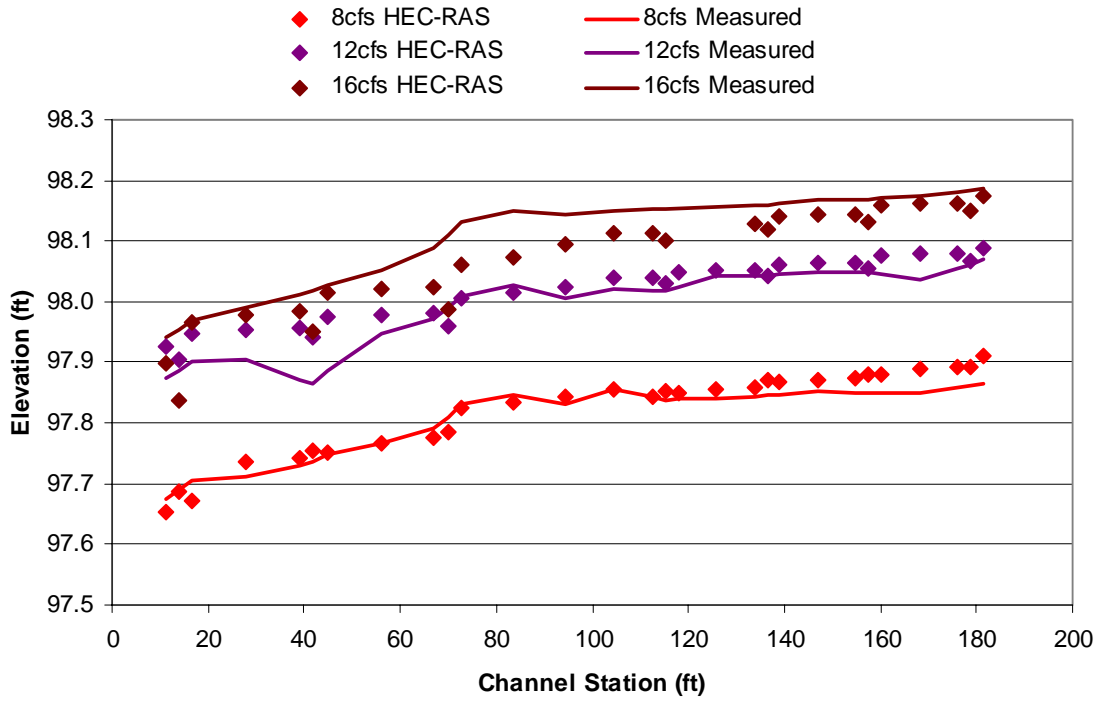


Figure 5.26: Water-surface Profile for Test W02 Using Modeling Technique 4

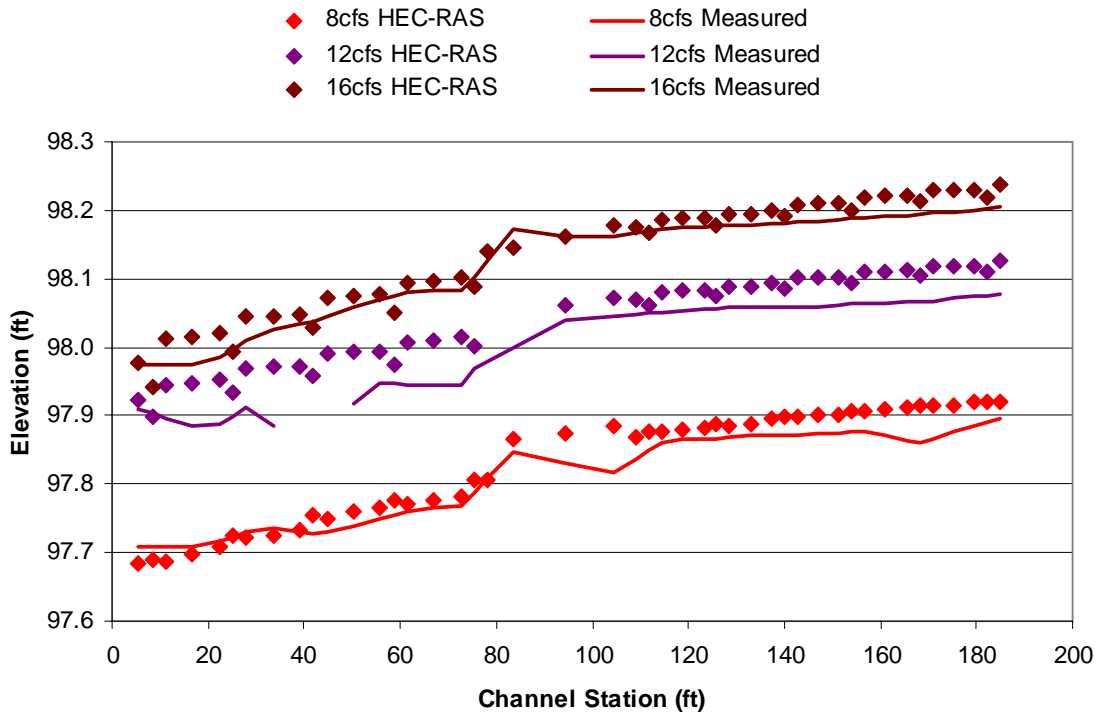


Figure 5.27: Water-surface Profile for Test W03 Using Modeling Technique 4

Computed water-surface elevations using Modeling Technique 4 were compared to measured data and percent difference was computed. Percent difference between the computed water-surface elevation and measured data is summarized in Table 5.6.

Table 5.6: Percent Error for Modeling Technique 4

	Bend Location	Percent Error for Modeling Technique 4		
		8 cfs	12 cfs	16 cfs
W01	Downstream	5.13%	2.47%	2.07%
	Upstream	3.13%	2.87%	1.02%
W02	Downstream	2.09%	4.62%	5.12%
	Upstream	3.64%	2.00%	2.87%
W03	Downstream	2.04%	5.28%	2.01%
	Upstream	4.46%	4.19%	2.05%

5.2.2.5 CONCLUSION OF MODEL SELECTION

Percent error between the computed and measured water-surface elevations was computed using four modeling techniques for Tests W01, W02, and W03. Table 5.3, Table 5.4, Table 5.5, and Table 5.6 summarize the percent error computations for Modeling Techniques 1, 2, 3, and 4, respectively. Percent error was averaged for each technique for Tests W01, W02, and W03, producing a parameter of overall quality of fit. Computed averaged percent errors are summarized in Table 5.7.

Table 5.7: Average Percent Error between Computed and Measured Water-surface Elevations for Each Modeling Technique

Modeling Technique	Average Percent Error		
	8 cfs	12 cfs	16 cfs
1	5.60%	4.59%	5.89%
2	5.32%	4.57%	5.73%
3	5.26%	5.05%	5.05%
4	3.42%	3.57%	2.52%

Results in Table 5.7 are shown graphically in Figure 5.28.

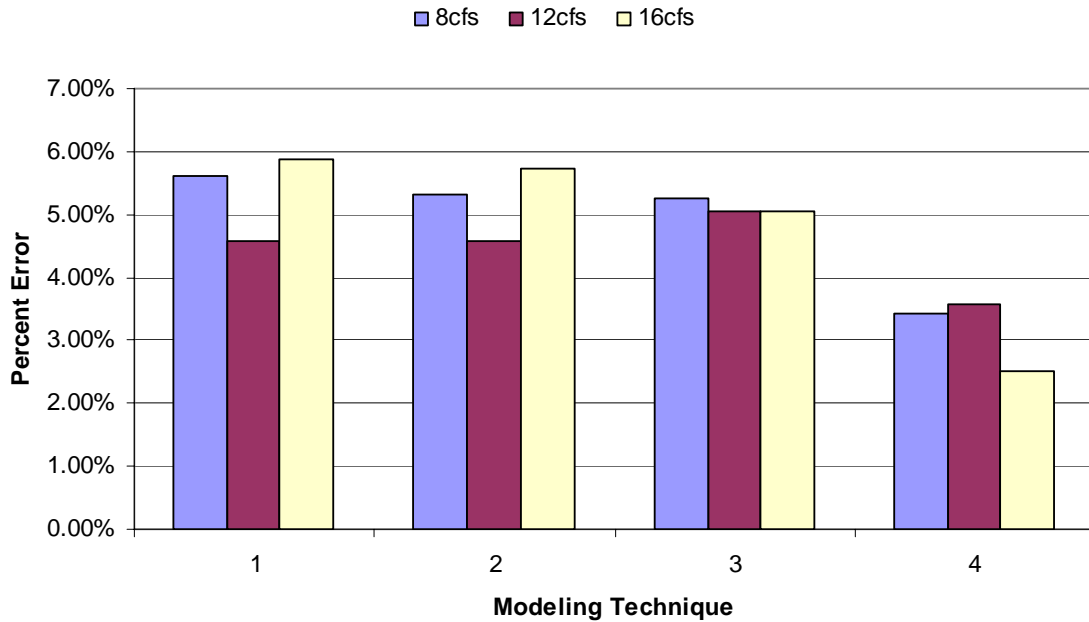


Figure 5.28: Average Percent Error between Computed and Measured Water-surface Elevations for each Modeling Technique

Considering the results presented in Table 5.7 and Figure 5.28, Modeling Technique 4 was chosen as the best overall technique to model weir configurations. From this analysis, the methodology from Modeling Technique 4 was applied to fifteen weir configurations. Modeling Technique 4 produced better results overall than the other techniques because it accounts for changes in flow pattern and areas of ineffective flow. Modeling Technique 4 is also the method that would be most likely chosen in practice due to its accuracy relative to flood stage.

In addition to water-surface elevation, the quality of fit of the velocity and shear stress were reviewed for each of the four techniques. Computation of the quality of fit was based on comparing the computed value from HEC-RAS to the measured maximum values for the weir tip and the inner bank opposite the weir. Table 5.8 and Table 5.9

show the percent errors in velocity and shear stress, respectively, based on the maximum measured values at the weir tip and the inner bank across from the weir tip.

Table 5.8: Average Percent Error Between Computed and Measured Velocity for Each Modeling Technique

	Modeling Technique	8 cfs	12 cfs	16 cfs
Percent Error in Velocity Based on Weir Tip	1	26.8%	29.9%	23.5%
	2	26.2%	29.3%	22.9%
	3	26.2%	29.3%	22.9%
	4	5.4%	29.4%	22.5%
Percent Error in Velocity Based on Inner Bank Opposite Weir	1	26.4%	32.8%	33.3%
	2	25.6%	32.2%	32.7%
	3	25.6%	32.2%	32.7%
	4	4.1%	32.0%	32.6%

Table 5.9: Average Percent Error Between Computed and Measured Shear Stress for Each Modeling Technique

	Modeling Technique	8 cfs	12 cfs	16 cfs
Percent Error in Shear Stress Based on Weir Tip	1	50.7%	50.7%	48.4%
	2	49.6%	49.8%	47.5%
	3	49.7%	49.8%	47.5%
	4	43.5%	63.8%	61.5%
Percent Error in Shear Stress Based on Inner Bank Opposite Weir	1	46.6%	52.5%	54.2%
	2	45.3%	51.5%	53.4%
	3	45.3%	51.5%	53.4%
	4	37.4%	64.6%	65.8%

As can be seen in Table 5.8 and Table 5.9, velocity results of Modeling Technique 4 produce the least amount of error, but shear stress for this technique produces slightly higher error than the other techniques. Although error in shear stress is greater for Modeling Technique 4, the purpose of the 1-D modeling was to predict the global hydraulic conditions of the channel; *i.e.*, water surface. Subsequent sections will present relationships to adjust the velocity and shear-stress values from the HEC-RAS model to

match the measured values. Modeling Technique 4 was, therefore, applied to all the weir configurations shown in Table 3.5.

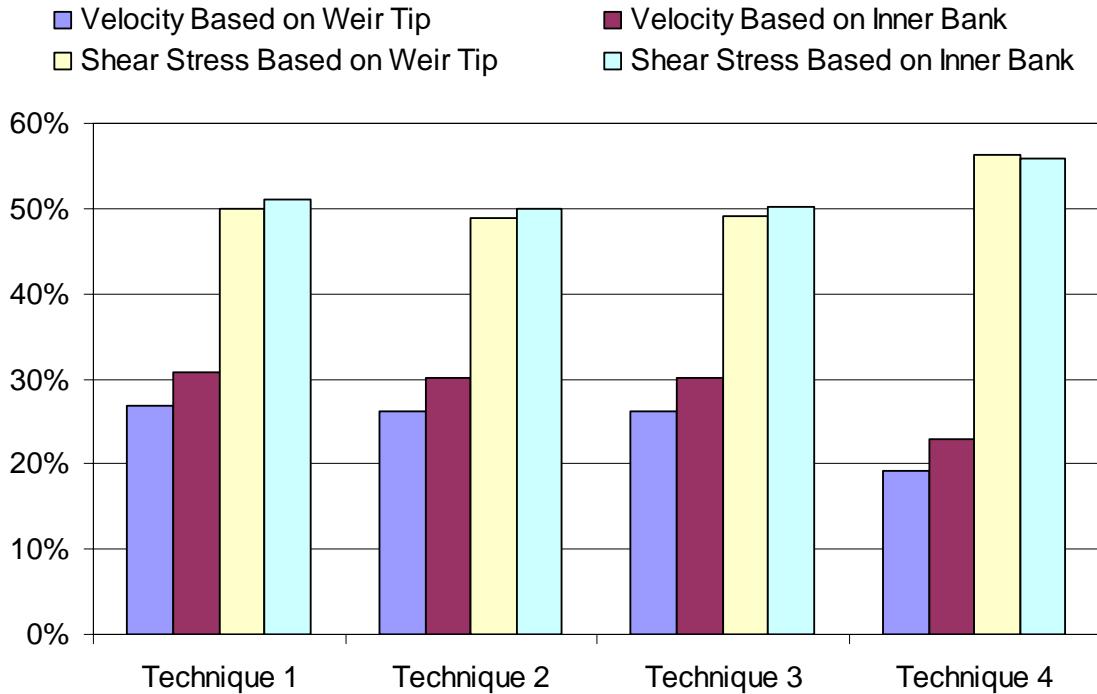


Figure 5.29: Average Percent Error between Computed and Measured Velocity and Shear Stress for each Modeling Technique

5.2.2.6 WEIR MODEL RESULTS

For each of the weir configurations listed in Table 3.5, a HEC-RAS model was created using Modeling Technique 4. Prior comparisons between the HEC-RAS results and measured values in Section 5.2.2.5 include only the first three weir configurations. Results from the HEC-RAS model for all of the weir configurations, including the first three, were compared to the measured data in order to evaluate how well HEC-RAS predicted physical data. Computed velocity and shear stress from HEC-RAS were averaged over each bend and compared with the maximum measured velocity and shear

stress along the bend. Two comparisons were made for the velocity and shear stress: 1) between HEC-RAS and the maximum measured values at the weir tip, and 2) comparison between HEC-RAS and the maximum measured values at the inner bank across from the weir tip. Comparisons between predicted velocity and measured velocity are shown in Figure 5.30, which show that HEC-RAS generally underpredicts the velocity by approximately 13 percent at the tip of the weir and by approximately 18 percent along the inner bank across from the weir tip. Appendix D contains computed results from the HEC-RAS computer modeling of weir configurations. Figure 5.30 includes data for all weir configurations, all bends, and each flow rate.

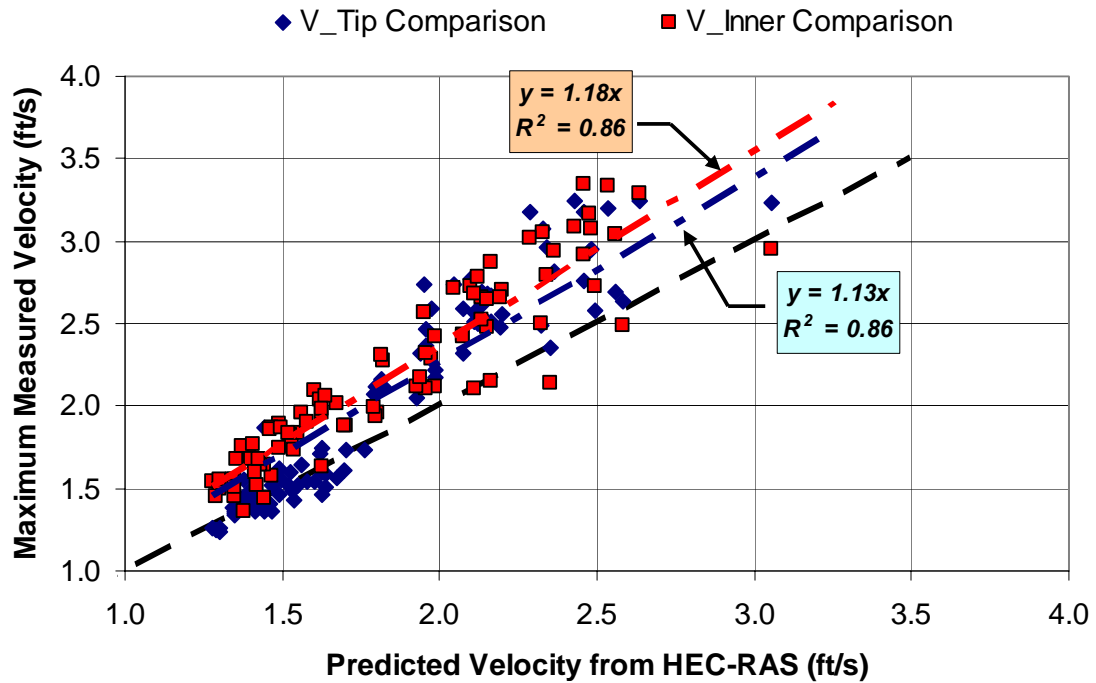


Figure 5.30: Comparisons between Predicted and Measured Velocity for Weir Models

Shear-stress comparisons between the predicted HEC-RAS values and the measured values, shown in Figure 5.31, indicate that, on average, HEC-RAS

underpredicts the measured shear stress by approximately 124 percent at the weir tip and approximately 108 percent along the inner bank across from the weir tip. Figure 5.31 includes shear-stress data for all weir configurations, each flow rate, and both bends.

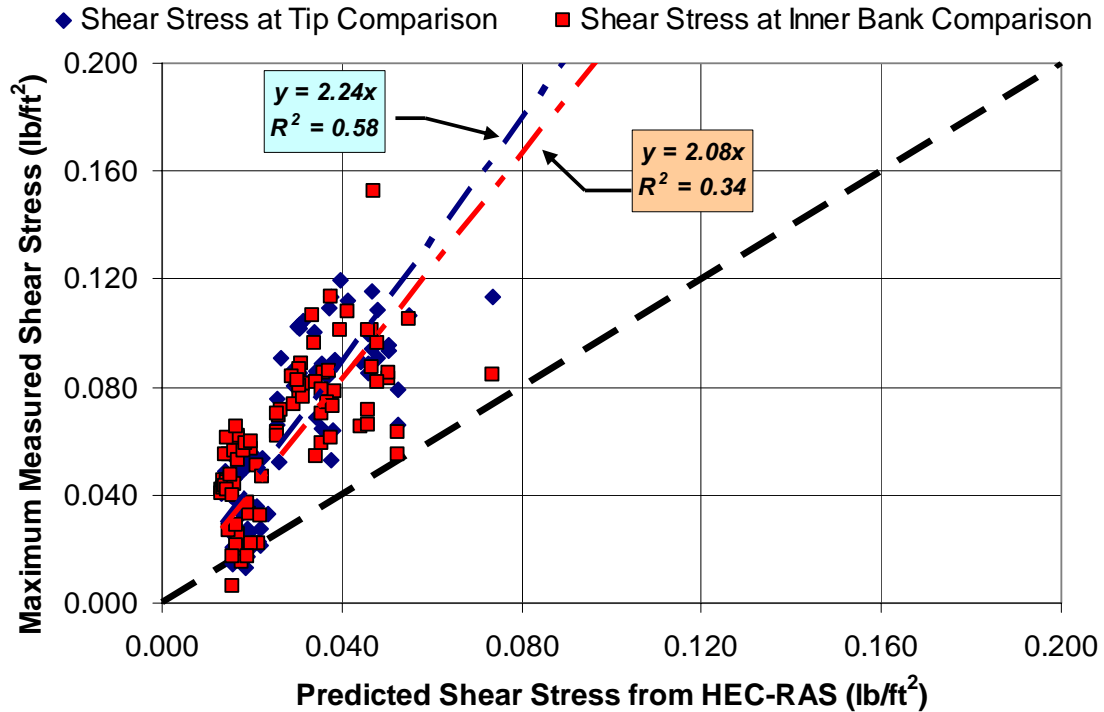


Figure 5.31: Comparisons between Predicted and Measured Shear Stress for Weir Models

From Figure 5.30 and Figure 5.31, it is clear that HEC-RAS is less effective at accurately predicting increased shear stress associated with bendway weirs than the increase in velocity. Inaccuracies of HEC-RAS predictions for both velocity and shear stress are likely dependent on the characteristics of the physical model, including the bend geometry, weir placement and construction, and hydraulic conditions associated with the weirs.

6 BASELINE ANALYSIS

6.1 INTRODUCTION

The inability of HEC-RAS to predict velocity and shear stress in a trapezoidal cross section through a bend is the result of HEC-RAS' inability to account for additional hydraulic losses due to channel bends. HEC-RAS results can be adjusted to account for additional bend losses through the use of regression equations derived from comparisons made between computer-modeling results and measured results from the physical tests. Regression equations used to adjust results from 1-D hydraulic computations have typically incorporated the bend geometric characteristic of radius of curvature divided by top width (Welch and Wright, 2005). Results from previous research by Ippen and Drinker (1962), USBR (1964), Yen (1965), and Kilgore and Cotton (2005, HEC-15) were compared with current CSU research, that was used to develop revised equations for predicting shear stress from 1-D flow hydraulic computations. No previous research exists to predict increased velocity through channel bends by adjusting 1-D hydraulic computations; however, regression equations were developed for this research by comparing results from the HEC-RAS computer model of the trapezoidal section to data measured during tests within the physical model.

6.2 VELOCITY

Practical comparisons between measured data and HEC-RAS computed results require an analysis of the ability of HEC-RAS to predict the maximum velocity of flow through meander bends. A predictive factor can be computed as the ratio of maximum measured velocity through the bend for a given discharge to the computed HEC-RAS velocity averaged over an individual bend at the same conditions, shown mathematically in Equation 6.1:

$$K_{BEND-VELOCITY} = \frac{V_{MAX}}{V_{COMPUTED}} \quad \text{Equation 6.1}$$

where

$K_{BEND-VELOCITY}$ = ratio of maximum measured velocity through bend to cross-sectional averaged velocity from HEC-RAS;

V_{MAX} = maximum measured velocity through a single bend for a given discharge (ft/s); and

$V_{COMPUTED}$ = computed velocity from HEC-RAS, averaged over a single bend for a given discharge (ft/s).

Maximum measured velocity along a single bend for a given discharge was obtained from the baseline velocity data across the entire channel at 60-percent flow depth. Velocity computed by HEC-RAS for each flow rate was averaged over each bend. Averages were computed as the mean of the velocity for each of the eight cross sections that make up the channel bend. Computation of the mean was performed for each bend and each discharge resulting in eight computed mean velocities. A summary

of both maximum measured velocity and average HEC-RAS velocity for each bend and discharge is compiled in Table 6.1.

Table 6.1: Velocity Results for Baseline Conditions

Discharge (cfs)	Bend Location	Tortuosity, R_c/Tw	Maximum Measured Velocity (ft/s)	Average HEC-RAS Velocity (ft/s)	$K_{BEND-VELOCITY}$
8	Upstream	2.80	1.31	1.10	1.19
8	Downstream	6.86	1.97	1.56	1.26
12	Upstream	2.61	1.44	1.24	1.16
12	Downstream	6.18	2.21	1.76	1.26
16	Upstream	2.47	1.64	1.35	1.21
16	Downstream	5.77	2.51	1.91	1.31
20	Upstream	2.36	1.72	1.45	1.19
20	Downstream	5.41	2.63	2.04	1.29

Tortuosity or the degree of bend curvature, as defined as the radius of curvature (R_c) divided by the top width (Tw) is included in Table 6.1 as a typical parameter used in practice to describe bend geometry (Welch and Wright, 2005). To compute the tortuosity reported in Table 6.1, the radius of curvature is based on the channel centerline and the top width is based on the measured depth in the trapezoidal section. Because the depth and top width both increase as the flow rate increases, the tortuosity decreases with increasing discharge. The bend velocity factor, $K_{BEND-VELOCITY}$, as shown in Table 6.1 is computed as the ratio of the maximum measured velocity within each bend for a given flow rate and the average computed velocity from HEC-RAS. Figure 6.1 shows a plot of the tortuosity versus the bend velocity factor.

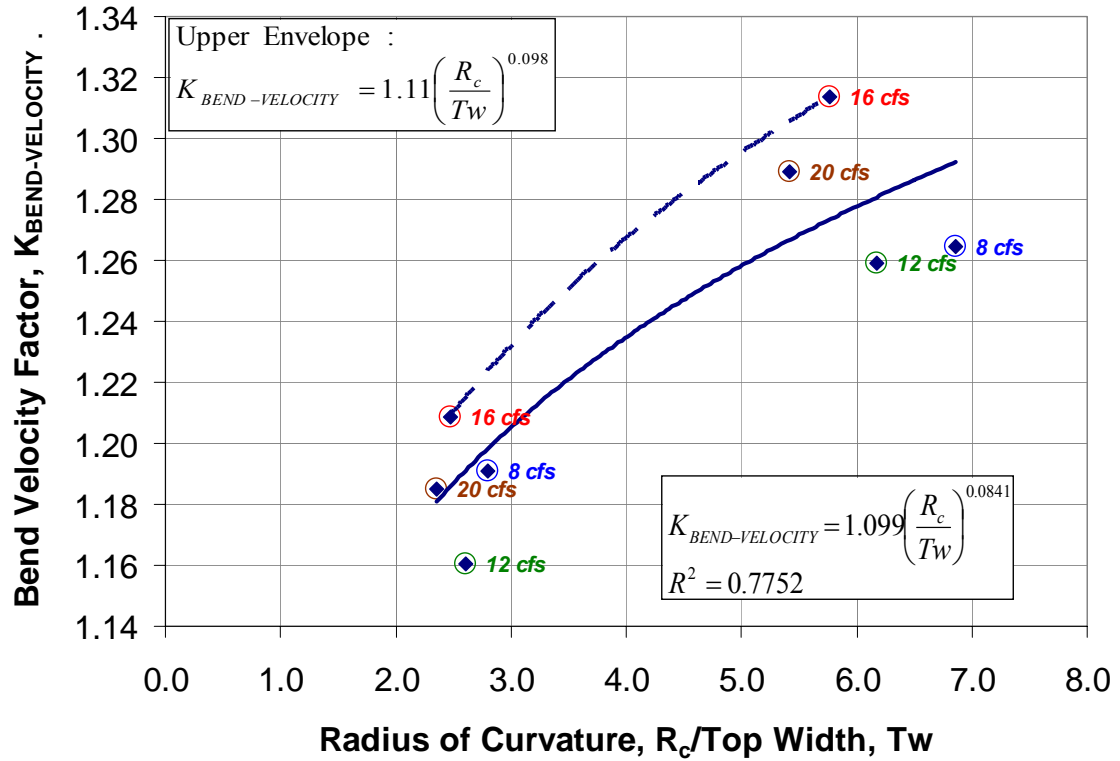


Figure 6.1: Radius of Curvature, R_c/T_w , T_w versus Bend Velocity Factor, $K_{BEND-VELOCITY}$

Equation 6.2 represents a best-fit regression equation through the baseline data shown in Table 6.1:

$$K_{BEND-VELOCITY} = 1.099 \left(\frac{R_c}{T_w} \right)^{0.0841} \quad \text{Equation 6.2}$$

where

$K_{BEND-VELOCITY}$ = ratio of maximum measured velocity through bend to cross-sectional averaged velocity from HEC-RAS;

R_c = radius of curvature (ft); and

T_w = top width measured for a specific flow rate (ft).

An upper envelope equation was also developed to incorporate 100 percent of the data. Both coefficients in Equation 6.2 were adjusted until all of the predicted values were greater than the data compiled in Table 6.1, resulting in Equation 6.3:

$$K_{BEND-VELOCITY(UPPER)} = 1.11 \left(\frac{R_c}{Tw} \right)^{0.098} \quad \text{Equation 6.3}$$

where

$K_{BEND-VELOCITY(UPPER)}$ = upper envelope; ratio of maximum measured velocity through bend to cross-sectional averaged velocity from HEC-RAS;

R_c = radius of curvature (ft); and

Tw = top width measured for a specific flow rate (ft).

Equation 6.3 represents a more conservative estimate of $K_{BEND-VELOCITY}$ than Equation 6.2; however, care should be taken when using either of these equations due to the limitation of the dataset to only two different curve configurations and four discharges.

Scatter in Figure 6.1 is the result of variability in the maximum measured velocity along the bend for each flow rate. Because computed cross-section-averaged velocity is computed in HEC-RAS assuming a straight channel, computed velocity from HEC-RAS is expected to vary consistently and linearly with discharge. Variation in $K_{BEND-VELOCITY}$, therefore, is the result of variation in measured velocity from baseline flume tests. Although the relationship presented in Equation 6.2 is based on limited data, Figure 6.1 shows that $K_{BEND-VELOCITY}$ generally increases by approximately 0.1 as the tortuosity increases from 3.0 to 6.0.

6.3 BOUNDARY SHEAR STRESS

Shear-stress profile plots in Figure 5.7, Figure 5.8, and Figure 5.9 indicate that HEC-RAS generally tends to underpredict measured boundary shear stress. Bend losses are not specifically accounted for in HEC-RAS. Instead, HEC-RAS accounts for channel meanders in terms of additional friction losses due to increased left- and right-bank reach lengths. Since bend losses are not accounted for in HEC-RAS, and overbank losses are minimal in the modeled trapezoidal section, computed shear stress from the baseline computer model was considered to represent a straight channel shear stress.

Prior research by Ippen and Drinker (1962), USBR (1964), Yen (1965), and Kilgore and Cotton (2005, HEC-15) has attempted to empirically find a multiplier that, once applied to computed shear stress in a straight approach section, could be used to accurately predict the increased shear stress due to the channel bend. This factor, termed here as $K_{BEND-SHEAR}$, represents the ratio of bend shear stress to straight approach channel shear stress. Equation 6.4, published in Kilgore and Cotton (2005, HEC-15), has been developed as a predictive equation for the $K_{BEND-SHEAR}$ factor as a function of the tortuosity, or radius of curvature divided by the measured top width:

$$\begin{aligned} K_{BEND-SHEAR} &= 2.0 && \left(\frac{R_c}{Tw}\right) \leq 2 \\ K_{BEND-SHEAR} &= 2.38 - 0.206\left(\frac{R_c}{Tw}\right) + 0.0073\left(\frac{R_c}{Tw}\right)^2 && 2 < \left(\frac{R_c}{Tw}\right) < 10 \\ K_{BEND-SHEAR} &= 1.05 && 10 \leq \left(\frac{R_c}{Tw}\right) \end{aligned} \quad \text{Equation 6.4}$$

where

$K_{BEND-SHEAR}$ = ratio of shear stress in channel bend to straight channel

approach shear stress at maximum depth;

R_c = radius of curvature of the bend to the channel centerline (ft); and

T_w = channel top (water surface) width (ft).

Although HEC-RAS subdivides the channel cross section into left, center, and right sub-divisions, bend losses are not specifically included in the hydraulic computations. As a result, while additional friction losses are considered along the bend (e.g., different reach lengths specified for left bank, channel center, and right bank), results from HEC-RAS are considered to be nearly equivalent to straight channel computations. Using computed cross-sectional average shear stresses from HEC-RAS and maximum measured shear stresses, $K_{BEND-SHEAR}$ was computed for each discharge modeled in the physical tests. Computed $K_{BEND-SHEAR}$ values are summarized in Table 6.2.

Table 6.2: Computed $K_{BEND-SHEAR}$ Factor for Baseline Data Using Computed Shear Stress from HEC-RAS

Discharge (cfs)	Bend Location	Tortuosity, R_c/T_w	Maximum Shear Stress in Bend (lb/ft ²)	Average HEC-RAS Shear Stress (lb/ft ²)	$K_{BEND-SHEAR}^*$
8	Upstream	2.803	0.0254	0.01385	1.833
8	Downstream	6.860	0.0438	0.02771	1.580
12	Upstream	2.610	0.0275	0.01625	1.693
12	Downstream	6.177	0.0555	0.03306	1.679
16	Upstream	2.473	0.0362	0.01745	2.075
16	Downstream	5.766	0.0700	0.03486	2.009
20	Upstream	2.357	0.0392	0.01857	2.111
20	Downstream	5.412	0.0674	0.03668	1.838

* USING COMPUTED HEC-RAS SHEAR STRESS

Data in Table 6.2 were plotted along with data from prior research in Figure 6.2. A best-fit regression equation was derived from relevant data presented along with a more conservative upper envelope regression equation that incorporates 100 percent of the data.

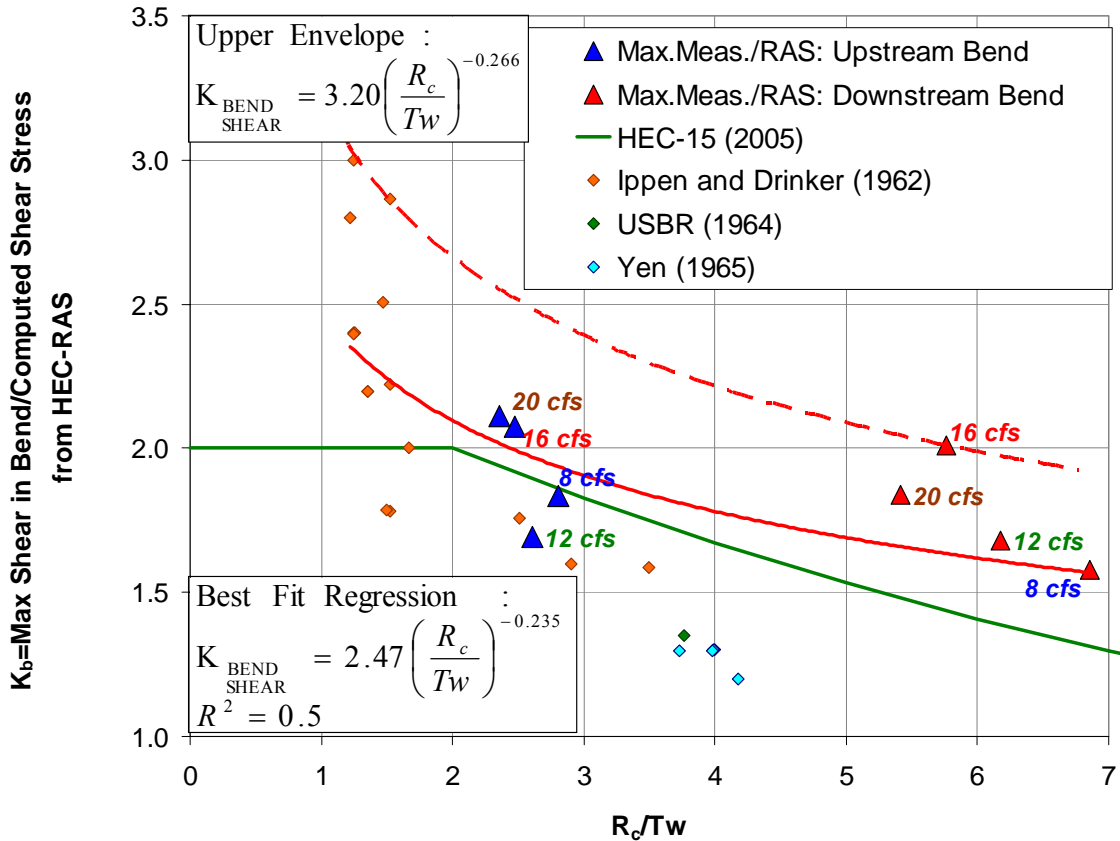


Figure 6.2: $K_{BEND-SHEAR}$ using Computed Shear Stress from HEC-RAS

Scatter in the computed $K_{BEND-SHEAR}$ values, shown in Figure 6.2, is the result of variability in the maximum measured shear stress along the bend for each flow rate. While it is expected that shear stress increases linearly with discharge, variability in measured data can be the result of complex flow characteristics created by the channel bend. Since variations in velocity do not appear to be as drastic as the variation in shear

stress, it is possible that shear stress is more sensitive than velocity to the complex flow conditions created by the channel bend. Based on the current data presented in Table 6.2, as the tortuosity increases from 3.0 to 6.0, the $K_{BEND-SHEAR}$ tends to decrease from approximately 2.0 to 1.8. Figure 6.2 further shows that $K_{BEND-SHEAR}$ appears to asymptotically approach 1.5 for increasing tortuosity.

6.4 CONCLUSION

Computed cross-sectional average velocity from the HEC-RAS model was compared with right bank, channel center, and left bank velocity measured at 60-percent flow depth from the physical model. Based on Figure 5.3, Figure 5.4, and Figure 5.5, the computed velocity from the HEC-RAS model generally underpredicted the maximum measured velocity along the bend. Investigation of a design factor, $K_{BEND-VELOCITY}$, resulted in a best-fit regression and an upper envelope regression (Equation 6.5):

Best Fit:

$$K_{BEND-VELOCITY} = 1.099 \left(\frac{R_c}{T_w} \right)^{0.0841}$$

Equation 6.5

Upper Envelope:

$$K_{BEND-VELOCITY(UPPER)} = 1.11 \left(\frac{R_c}{T_w} \right)^{0.092}$$

where

$K_{BEND-VELOCITY}$ = ratio of maximum measured velocity through bend to cross-sectional averaged velocity from HEC-RAS;

R_c = radius of curvature (ft); and

T_w = top width measured for a specific flow rate (ft).

As Equation 6.5 and Figure 6.1 suggest, HEC-RAS was better able to predict the shear stress in the upstream bend than the downstream bend. Although the radius of curvature in the upstream bend is approximately 60 percent smaller than the radius of curvature in the downstream bend, the cross-sectional area at the design discharge in the upstream bend is approximately 40 percent larger than the downstream cross-sectional area at the design flow, suggesting that the converging flow created by the reduction in cross-sectional area has a greater effect on raising the downstream velocity than the decreased radius of curvature in the upstream bend. The convergence of flow from the upstream bend to the downstream bend was accentuated by the application of uniform constriction with a uniform trapezoidal section. It is also possible that flow entering the upstream bend was considerably more distributed than flow entering the downstream bend. A dedicated rock baffle structure was constructed at the entrance to the upstream bend, while the downstream bend was separated from the upstream bend by approximately 21 ft, over which length the cross-sectional area was reduced by 40 percent. Additional tests would be necessary to confirm the validity of the relationships presented in Equation 6.5 as well as eliminate any error in the data resulting from test configurations.

Shear-stress profiles were presented in Figure 5.7, Figure 5.8, and Figure 5.9 for both measured data from the physical model and computed data from HEC-RAS. As with velocity, computed shear stresses from HEC-RAS generally underpredicted the maximum shear stress measured through the bend. A single design factor, $K_{BEND-SHEAR}$,

was computed as a ratio of the maximum measured shear stress through the bend and the average computed shear stress from HEC-RAS through the bend. Equation 6.6 presents the regression equations for $K_{BEND-SHEAR}$ computed with the computed HEC-RAS shear stress:

Best Fit:
$$K_{BEND-SHEAR} = 2.47 \left(\frac{R_c}{Tw} \right)^{-0.235}$$

Equation 6.6

Upper Envelope:
$$K_{BEND-SHEAR(UPPER)} = 3.20 \left(\frac{R_c}{Tw} \right)^{-0.266}$$

where

$K_{BEND-SHEAR}$ = ratio of maximum measured shear stress through the bend to cross-sectional averaged shear stress from HEC-RAS;

R_c = radius of curvature (ft); and

Tw = top width measured for a specific flow rate (ft).

Equation 6.6 has the advantage of being applicable to situations where HEC-RAS is used as a preliminary design tool and the $K_{BEND-SHEAR}$ factor is used to compute the maximum shear stress through the bend. For $R_c/Tw < 4$, Equation 6.5 agrees reasonably well with Equation 6.6; for $R_c/Tw > 4$, the two equations diverge somewhat. Equation 6.5 shows that the K_b correction for shear stress approaches unity for high values of R_c/Tw . Results from CSU research, however, show that for higher R_c/Tw , the K_b correction for shear stress asymptotically approaches a value of approximately 1.5. Overall, Equation 6.6, which includes the results from the CSU research, is a more conservative estimate of

the correction factor for the shear stress than Equation 6.5. An upper envelope regression equation was also developed to provide additional conservatism where increases in K_b due to complex channel curvature are likely.

7 WEIR CONFIGURATION ANALYSIS

7.1 INTRODUCTION

According to methodology presented in Section 5.2.2.4, Modeling Technique 4 was applied to the fifteen weir configurations presented in Table 3.5. Water-surface profiles for discharges of 8, 12, and 16 cfs were computed and compared to measured data collected in the Middle Rio Grande physical model. Appendix D and Appendix E contain summaries of HEC-RAS computer model results and data used in the weir configuration analyses, respectively.

Analyses presented herein represent an investigation of relationships between computed values of velocity and shear stress to corresponding measured values obtained from physical model tests. Since the main function of bendway weirs is to constrict the channel and move high shear stresses away from an unstable outer bank, it is expected that there will be some increase in velocity and shear stress in the main channel. Research has shown that the area in the vicinity of the weir tip is particularly vulnerable to increased velocity and shear stresses (Richardson and Simons, 1974; Seed, 1997; Knight *et al.*, 1992). For each weir configuration presented in Table 3.5, the increased velocity and shear stress measured in the physical model were compared with cross-sectional and depth averaged results from 1-D HEC-RAS computer simulations. HEC-RAS computer results were used as a basis for comparison because of the model's

widespread use in the engineering community at large. Results from this comparison can, in turn, be utilized by design engineers to present a more realistic idea of scour potential. From corrected velocity and shear-stress values, commonly applied design equations for riprap or other countermeasures can bolster areas of particular concern including in the vicinity of the weir tip.

7.2 ANALYSIS APPROACH

Comparisons of measured velocity and shear stress at specific points in the physical model were made with both the baseline HEC-RAS model results and the HEC-RAS weir configuration model results. Table 7.1 summarizes the ten analyses performed for velocity and shear stresses.

Table 7.1: Analysis Matrix for Velocity and Shear Stresses

Velocity Analyses

$$MVR_{inner} = \frac{\text{Maximum Velocity Measured at the Toe of the Inner Bank}}{\text{Average Centerline Velocity from the HEC - RAS Baseline Model}}$$

$$MVR_{tip} = \frac{\text{Maximum Velocity Measured at the Weir Tip}}{\text{Average Centerline Velocity from the HEC - RAS Baseline Model}}$$

$$MVR_{center} = \frac{\text{Maximum Velocity Measured in the Channel Centerline}}{\text{Average Centerline Velocity from the HEC - RAS Baseline Model}}$$

$$V_{r-inner} = \frac{\text{Maximum Velocity Measured at the Toe of the Inner Bank}}{\text{Maximum Velocity from Corresponding HEC - RAS Weir Configuration Model}}$$

$$V_{r-tip} = \frac{\text{Maximum Velocity Measured at the Weir Tip}}{\text{Maximum Velocity from Corresponding HEC - RAS Weir Configuration Model}}$$

Shear-stress Analyses

$$MTR_{inner} = \frac{\text{Maximum Shear Stress Measured at the Toe of the Inner Bank}}{\text{Average Centerline Shear Stress from the HEC - RAS Baseline Model}}$$

$$MTR_{tip} = \frac{\text{Maximum Shear Stress Measured at the Weir Tip}}{\text{Average Centerline Shear Stress from the HEC - RAS Baseline Model}}$$

$$MTR_{center} = \frac{\text{Maximum Shear Stress Measured in the Channel Centerline}}{\text{Average Centerline Shear Stress from the HEC - RAS Baseline Model}}$$

$$T_{r-inner} = \frac{\text{Maximum Shear Stress Measured at the Toe of the Inner Bank}}{\text{Maximum Shear Stress from Corresponding HEC - RAS Weir Configuration Model}}$$

$$T_{r-tip} = \frac{\text{Maximum Shear Stress Measured at the Weir Tip}}{\text{Maximum Shear Stress from Corresponding HEC - RAS Weir Configuration Model}}$$

Maximum velocity ratios, MVR , and maximum shear ratios, MTR , shown in Table 7.1 represent an extension of previous research performed by Heintz (2002) and Darrow (2004). Development of an MVR and MTR for the inner bank, channel center, and weir tip are based on the premise that there is an association between the baseline cross-sectional average velocity and the local increased velocity at the respective locations. For design engineers, the MVR and MTR are useful when trying to predict increased velocities associated with a bendway-weir field using a baseline computer model such as HEC-RAS. While useful, MVR s and MTR s do not indicate how well bendway weirs are modeled in HEC-RAS.

To determine if the increased velocity caused by bendway weirs can be predicted based on a 1-D numerical simulation of the weir field, another parameter was developed. The velocity ratio (V_r) and shear ratio (T_r) represent the ratios of the maximum measured velocities and shear stresses along a bend to the maximum computed velocities and shear stresses from a HEC-RAS model of the bendway weirs, respectively. The ratios (V_r and T_r) are useful as an indication of the adequacy of the 1-D computer model created using HEC-RAS. Use of V_r and T_r as design parameters subsequent to the MVR and MTR also serve to capture the complete range of variation in velocity and shear stress caused by complex flow fields developed around bendway weirs which were measured in physical tests.

For the fifteen weir configurations shown in Table 3.5, with three different discharge profiles and two bends, a dataset with a maximum of 90 points was compiled for each analysis (Table 7.1). From the compiled dataset, regression equations were developed using seven possible model parameters, five (P1 through P5) of which were

presented in Darrow (2004). Two (P6 and P7) parameters, radius of curvature over top width (R_c/Tw) and top width over depth (Tw/y), were added based on research described in Section 2.4, these parameters indicate that migration rates and bank abrasion were associated with the bend tightness and the level of channel incision, respectively. Table 7.2 presents the model parameters used in developing the regression equations for the velocity and shear-stress ratios shown in Table 7.1.

Table 7.2: Model Parameters used in Statistical Analysis

Parameter Designation	Model Parameter	Description
P1	$L_{arc}/L_{proj,w}$	Spacing ratio of bendway weirs
P2	y/h_w	Relative submergence of bendway weir
P3	$Tw/L_{proj,cw}$	Percent top width of the channel blocked by the bendway weir
P4	$L_{proj,cw}/L_{cw}$	Cosine of the angle between the weir and its perpendicular line to the flow direction
P5	A_w/A_c	Percent area blocked by the weir during the test
P6	R_c/Tw	Tightness of Bend
P7	Tw/y	Channel Incision

Model-selection procedures used to develop regression equations were based on standard forward, backward, and stepwise hierarchical routines as well as the Mallows Cp best-subset method. Model-selection procedures and basic statistical theory used in these analyses are presented in Appendix A. Preliminary regression analyses were performed

for each analysis in Table 7.1 using a complete dataset, from which outliers were identified with absolute R-student residual values greater than 2.0. Upper limits of the R-student residual value were set at a 95-percent level from a t-distribution with 90 data points and match similar outlier identification procedures used by Darrow (2004). Selected outliers were then removed from regression computations as necessary. The following analyses present the selected regression models with corresponding Mallow's Cp and R² values, and a summary of outliers removed from the regression model. Residual plots, normal quantile plot of residuals, and predicted versus observed plots are also presented to evaluate statistical assumptions and quality of regression predictions. Finally, in addition to the mean regression, envelope equations are provided to include 100 percent of the data points. Envelope equations are useful where conservatism in design is required.

7.3 VELOCITY ANALYSIS

7.3.1 MVR INNER

Using the measured dataset from physical tests, the MVR_{inner} was computed based on maximum measured velocity along the toe of the inner bank of the bend and the cross-sectional averaged baseline results from the HEC-RAS computer model. Equation 7.1 shows the result of the regression analysis (outliers excluded) using the model parameters defined in Table 7.2:

$$MVR_{inner} = 1.67 \left[\frac{\left(\frac{y}{h_w} \right)^{0.273} \left(\frac{A_w}{A_c} \right)^{0.083} \left(\frac{R_c}{Tw} \right)^{0.072}}{\left(\frac{L_{arc}}{L_{proj,w}} \right)^{0.095}} \right] \quad \text{Equation 7.1}$$

From the best-subset model-selection criterion, the Mallows's Cp was computed to be 4.81 and the R^2 was reported as 0.56. P-values for each parameter in Equation 7.1 are summarized in Table 7.3.

Table 7.3: P-values for MVR_{inner} Regression Equation

Parameter Designation	Model Parameter	P-value
P1	$L_{arc}/L_{proj,w}$	0.0024
P2	y/h_w	<0.0001
P3	$T_w/L_{proj,cw}$	Not Included
P4	$L_{proj,cw}/L_{cw}$	Not Included
P5	A_w/A_c	<0.0001
P6	R_c/T_w	0.0016
P7	T_w/y	Not Included

Equation 7.1 is presented graphically in Figure 7.1, which shows the current regression analysis along with results from Darrow (2004) and the multiplier from Heintz (2002).

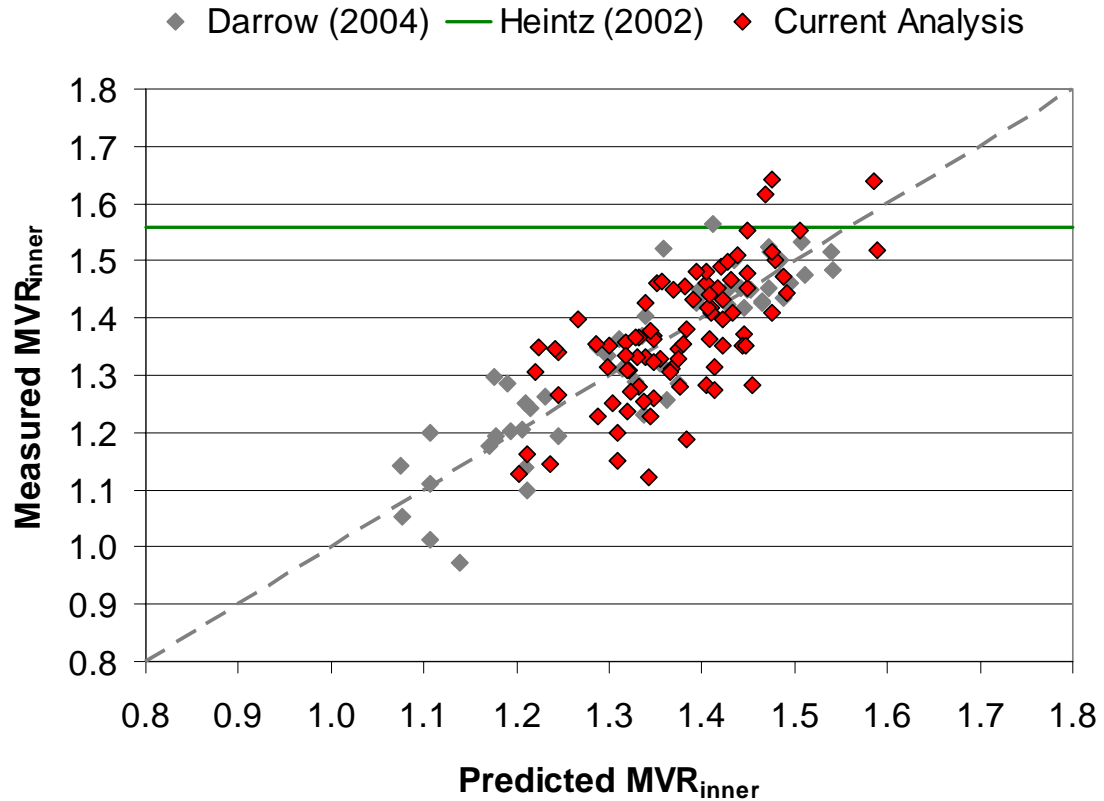


Figure 7.1: Regression Analysis for MVR_{inner} Compared with Heintz (2002) and Darrow (2004)

Testing statistical assumptions required the plotting of residuals against the predicted values and the quantile of residuals. Plotting residuals against the predicted values showed a reasonably scattered distribution about 0 with no significant trend. Normality was confirmed by a nearly 45-degree line in the quantile plot. Figure 7.2 and Figure 7.3, respectively, present the residual plot against predicted values and the quantile plot for the MVR_{inner} analysis.

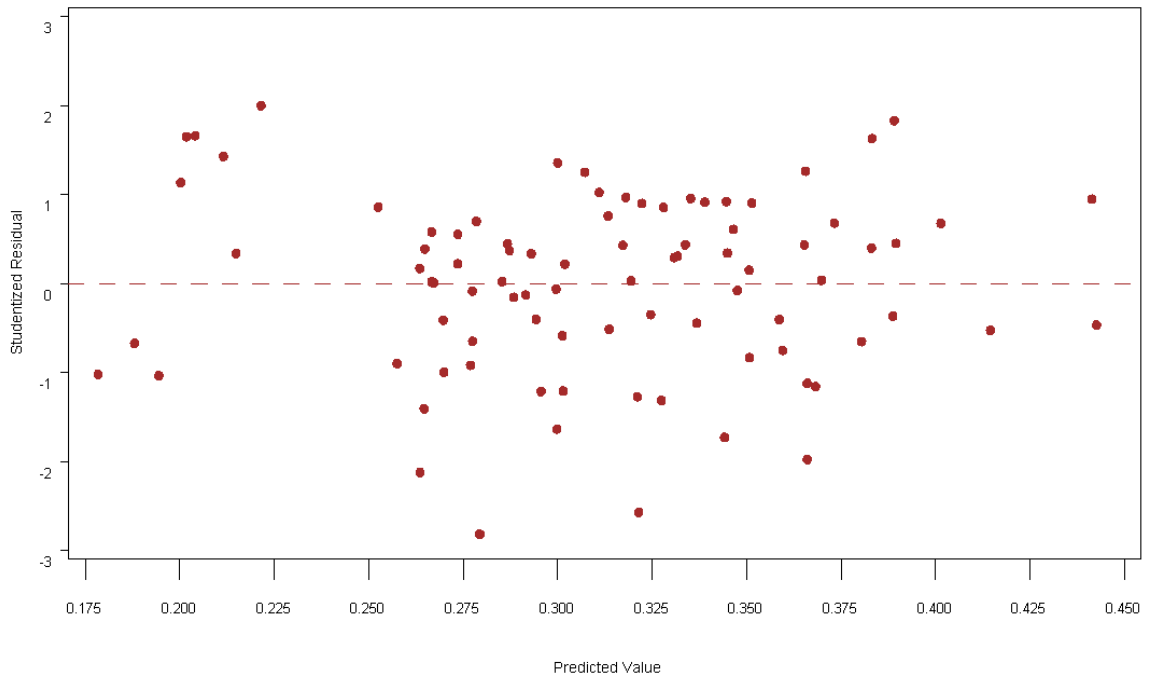


Figure 7.2: Residual Plot from MVR_{inner} Analysis

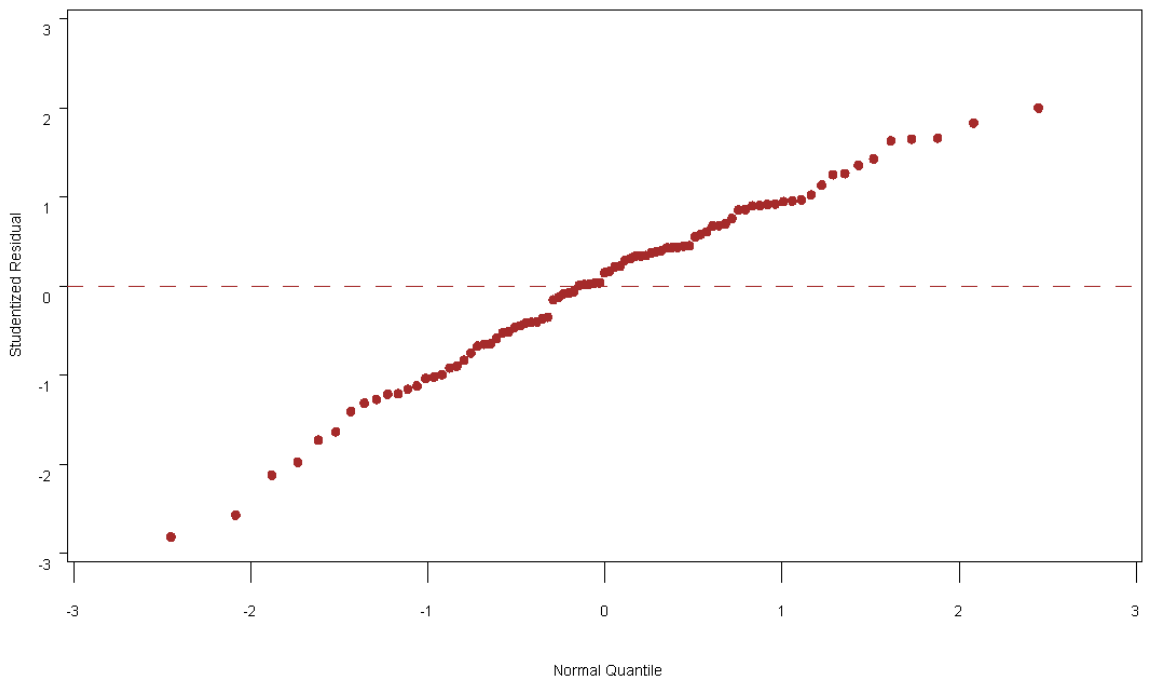


Figure 7.3: Quantile Plot of Residual from MVR_{inner} Analysis

Prediction of MVR_{inner} from Equation 7.1 incorporates additional data since Darrow (2004) and computes MVR_{inner} using common tools used in engineering practice; *i.e.*, HEC-RAS. From this analysis, engineers are provided with an equation derived from a dataset that includes HEC-RAS models, which can be directly applied to bendway-weir design.

A review of studentized residuals revealed five possible outliers from MVR_{inner} analysis. Outliers were identified as those points having R-student residual values greater than 2.0. The five outliers tabulated in Table 7.4 were removed from the regression analysis performed in Equation 7.1.

Table 7.4: Outliers from MVR_{inner} Analysis

Measured MVR_{inner}	Predicted MVR_{inner}	Residual	R-student Residual
1.187	1.383	-0.192	-2.660
1.284	1.338	-0.110	-2.009
1.122	1.450	-0.320	-2.941
1.150	1.310	-0.326	-2.166
1.397	1.235	-0.070	2.040

Equation 7.1 represented an average regression predictive equation for MVR_{inner} , and as a result does not represent the maximum range of velocity that might be experienced along the bend. Equation 7.2 shows upper and lower limits for the coefficient in Equation 7.1 such that the entire range of measured values are included in the regression equation:

$$MVR_{inner-envelope} = C_{envelope} \left[\frac{\left(\frac{y}{h_w} \right)^{0.273} \left(\frac{A_w}{A_c} \right)^{0.083} \left(\frac{R_c}{Tw} \right)^{0.072}}{\left(\frac{L_{arc}}{L_{proj,w}} \right)^{0.095}} \right] \quad \text{Equation 7.2}$$

where

$$C_{envelope} = 1.50 \text{ (lower) to } 1.87 \text{ (upper)}.$$

Figure 7.4 shows the results of the regression analysis for MVR_{inner} , including the upper envelope equation and outliers.

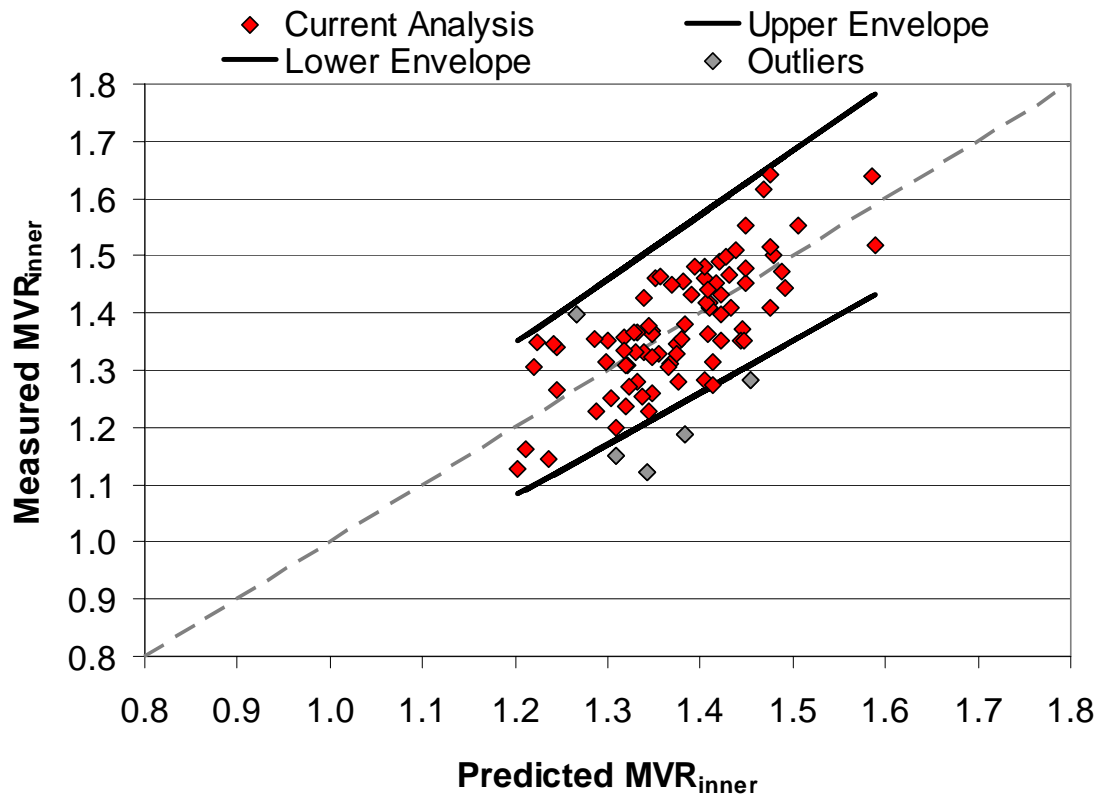


Figure 7.4: MVR_{inner} Analysis Showing Outliers and Upper Envelope

7.3.2 MVR TIP

Brown (1985) found that the velocity near the tip of bendway weirs ranges from 1.1 to 1.5 times the cross-sectional-average approach velocity. Seed (1997) extended this research and developed a design procedure for MVR_{tip} that incorporates roughness of the channel bed, area blocked by the weir, taper of the weir, and weir spacing. The design procedure presented by Seed (1997) was applied to the geometry tested in the Middle Rio

Grande physical model. Computed MVR_{tip} values from Seed (1997) design procedures ranged from 0.9 to 1.8.

Using all the test configurations presented in Table 3.5, a dataset was created for the MVR_{tip} , computed as the ratio of the maximum measured velocity at the weir tip and the maximum pre-weir velocity computed by HEC-RAS. Model selection was performed on the dataset resulting in the regression analysis (outliers excluded) shown in Equation 7.3:

$$MVR_{tip} = 1.17 \left[\left(\frac{y}{h_w} \right)^{0.103} \left(\frac{A_w}{A_c} \right)^{0.117} \left(\frac{R_c}{Tw} \right)^{0.211} \right] \quad \text{Equation 7.3}$$

From the best-subset model-selection criterion, the Mallows' C_p was computed to be 4.48 and the R^2 was reported as 0.79. P-values for each parameter in Equation 7.3 are summarized in Table 7.5.

Table 7.5: P-values for MVR_{tip} Regression Equation

Parameter Designation	Model Parameter	P-value
P1	$L_{arc} / L_{proj,w}$	Not Included
P2	y / h_w	0.0068
P3	$Tw / L_{proj,cw}$	Not Included
P4	$L_{proj,cw} / L_{cw}$	Not Included
P5	A_w / A_c	<0.0001
P6	R_c / Tw	<0.0001
P7	Tw / y	Not Included

Figure 7.5 shows the results from the statistical analysis compared with computation of MVR_{tip} computed using Seed (1997).

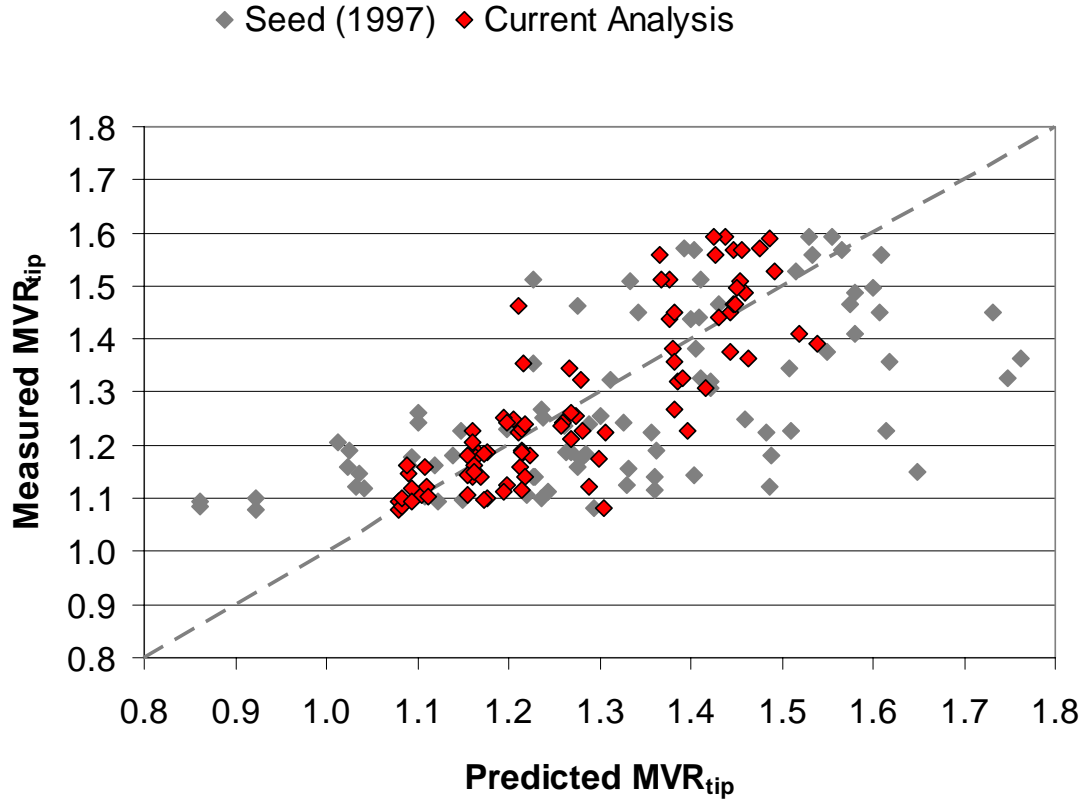


Figure 7.5: Regression Analysis for MVR_{tip} Compared with Seed (1997)

Equation 7.3, plotted in Figure 7.5, is not only simpler than Seed (1997), but also provides a better overall fit of the measured data. Since Equation 7.3 was derived from maximum velocities normalized with HEC-RAS data, it can be directly applied to the design of bendway weirs. Plotting residuals against the predicted values showed a reasonably even distribution about 0 with no significant trend. Normality was confirmed by a nearly 45-degree line in the quantile plot. Figure 7.6 and Figure 7.7 show the residual plot against predicted values and the quantile plot for the MVR_{tip} analysis, respectively.

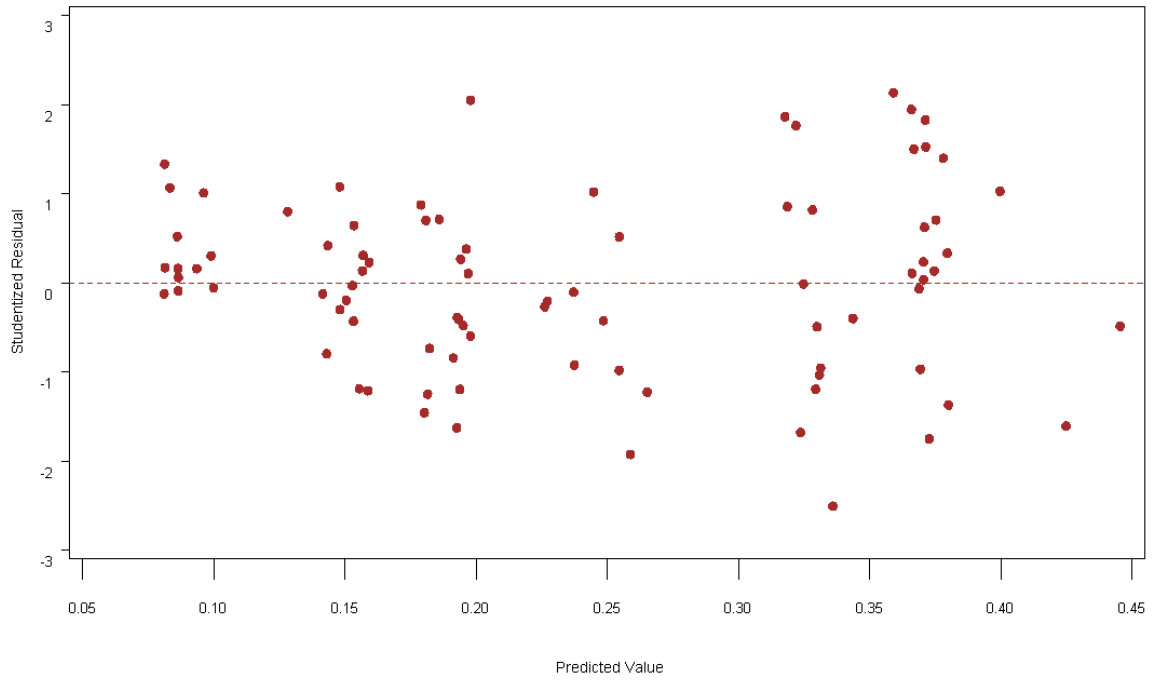


Figure 7.6: Residual Plot from MVR_{tip} Analysis

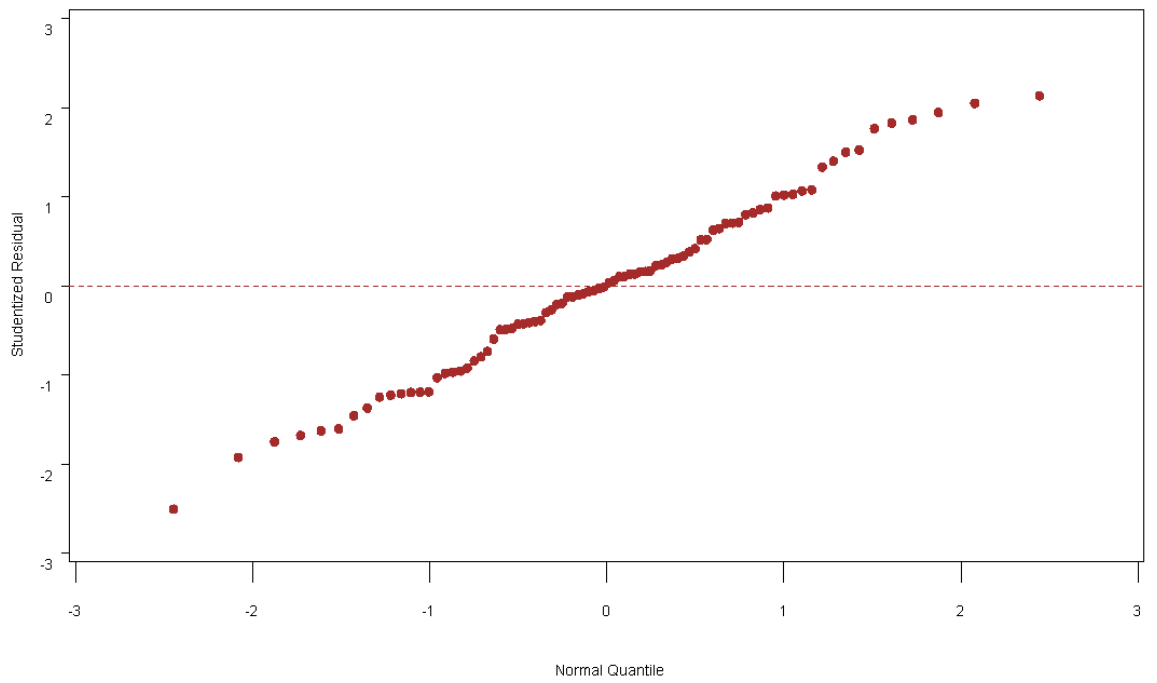


Figure 7.7: Quantile Plot of Residuals from MVR_{tip} Analysis

A review of studentized residuals revealed four possible outliers from MVR_{tip} analysis. Outliers were identified as those points having R-student residual values greater than 2.0. The four outliers tabulated in Table 7.4 were removed from the regression analysis performed in Equation 7.3.

Table 7.6: Outliers from MVR_{tip} Analysis

Measured MVR_{tip}	Predicted MVR_{tip}	Residual	R-student Residual
1.463	1.210	0.253	3.020
1.082	1.303	-0.221	2.909
1.122	1.289	-0.168	2.012
1.559	1.379	0.180	2.132

An envelope equation was developed to provide a conservative estimate for MVR_{tip} . The envelope equation for MVR_{tip} , shown in Equation 7.4, shows a range of values for the coefficient in Equation 7.3 such that all of the measured values are included in the envelope equation:

$$MVR_{tip-envelope} = C_{envelope} \left[\left(\frac{y}{h_w} \right)^{0.103} \left(\frac{A_w}{A_c} \right)^{0.117} \left(\frac{R_c}{T_w} \right)^{0.211} \right] \quad \text{Equation 7.4}$$

where

$$C_{envelope} = 1.0 \text{ (lower) to } 1.32 \text{ (upper).}$$

Figure 7.8 shows the regression equation (Equation 7.3) with the envelope equation (Equation 7.4) and the outliers which were removed from the analysis.

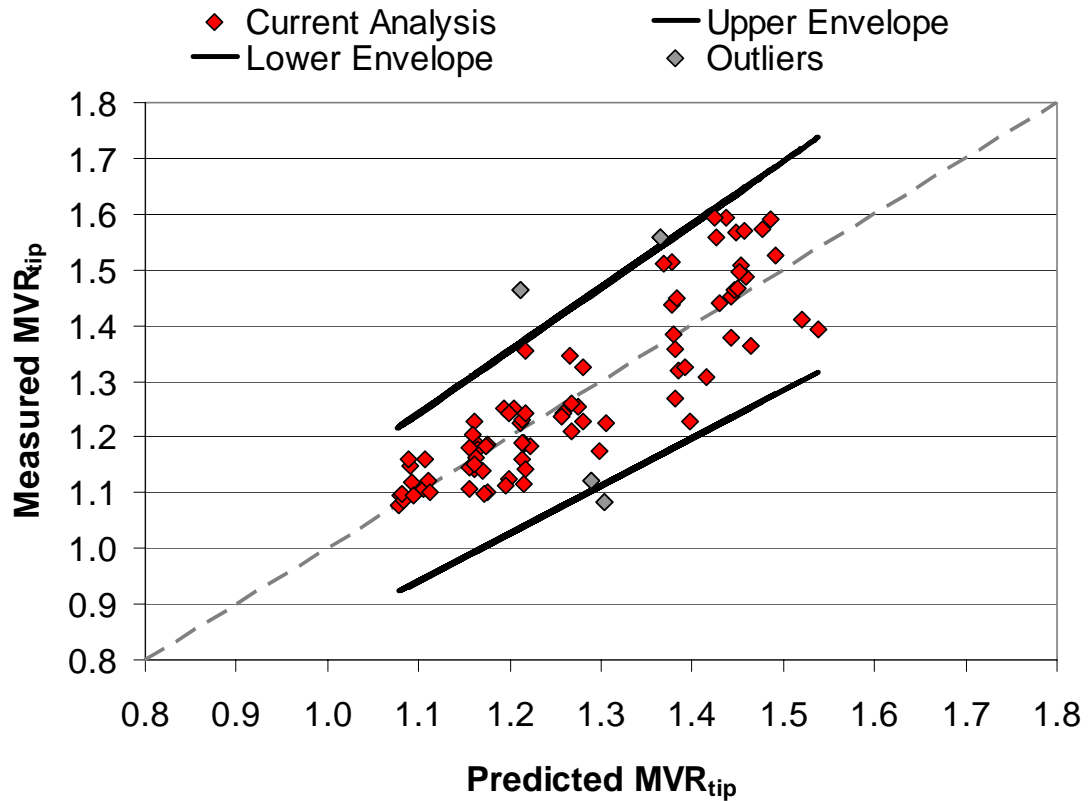


Figure 7.8: MVR_{tip} Analysis Showing Outliers and Upper Envelope

7.3.3 MVR CENTER

Constriction of the channel by bendway weirs results in overall channel degradation and a general increase in velocity in the main channel. As described in Section 2.5.3.5 and Section 2.5.3.6, Heintz (2002) and Darrow (2004), respectively, developed a measure of the increase in centerline velocities as a ratio of the maximum measured velocity in the channel centerline (with bendway weirs installed) to the maximum measured baseline velocity (without bendway weirs installed). Seed (1997) also conducted studies on the increased velocity in the channel center due to the presence of bendway weirs as a function of the cross-sectional-averaged approach velocity. Seed's design procedure to compute a MVR_{center} is presented in Section 2.5.3.4. Seed's (1997)

design procedure was applied to the bendway-weir configurations tested in the Middle Rio Grande physical model.

Using measured data from the physical test configurations in Table 3.5, the MVR_{center} was computed as the ratio of the maximum measured centerline velocity to the maximum computed velocity from the baseline HEC-RAS model. Regression analysis (outliers excluded) performed on this new dataset resulted in Equation 7.5:

$$MVR_{center} = 1.27 \left[\left(\frac{y}{h_w} \right)^{0.169} \left(\frac{A_w}{A_c} \right)^{0.142} \left(\frac{R_c}{Tw} \right)^{0.244} \right] \quad \text{Equation 7.5}$$

From the best-subset model-selection criterion, the Mallows' Cp was computed to be 2.12 and the R^2 was reported as 0.89. P-values for each parameter in Equation 7.5 are summarized in Table 7.7.

Table 7.7: P-values for MVR_{center} Regression Equation

Parameter Designation	Model Parameter	P-value
P1	$L_{arc} / L_{proj,w}$	Not Included
P2	y / h_w	<0.0001
P3	$Tw / L_{proj,cw}$	Not Included
P4	$L_{proj,cw} / L_{cw}$	Not Included
P5	A_w / A_c	<0.0001
P6	R_c / Tw	<0.0001
P7	Tw / y	Not Included

Figure 7.9 is a graphic presentation of the research results from Heintz (2002), Darrow (2004), and Seed (1997) compared with the predictive ability of Equation 7.5.

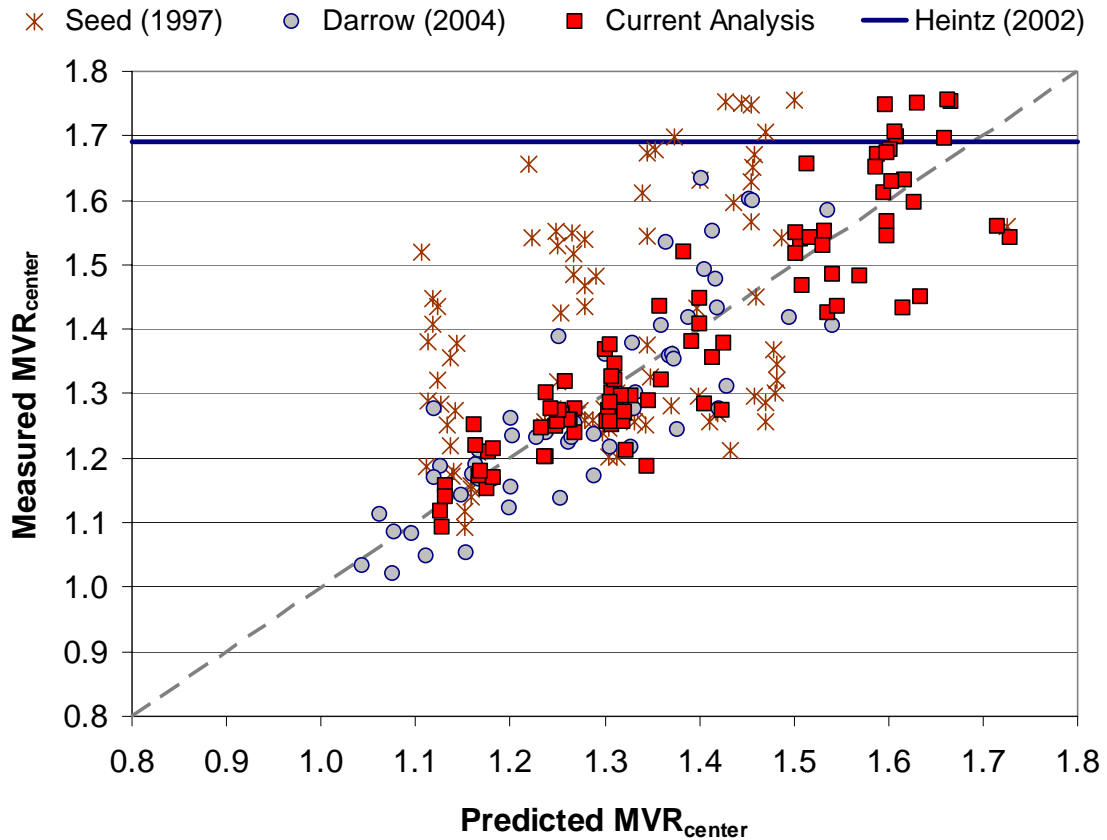


Figure 7.9: Regression Analysis for MVR_{center} Compared with Seed (1997), Heintz (2002), and Darrow (2004)

Equation 7.5 shows a reasonably good fit compared to previous studies and computed model-selection parameter C_p and the R^2 values indicate a better overall fit than Darrow (2004). The residual plot from the MVR_{center} shows a reasonably random scatter about 0 and the quantile plot indicates a satisfactory assumption of normality. Figure 7.10 and Figure 7.11 show the residual plot and quantile plot from the MVR_{center} analysis, respectively.

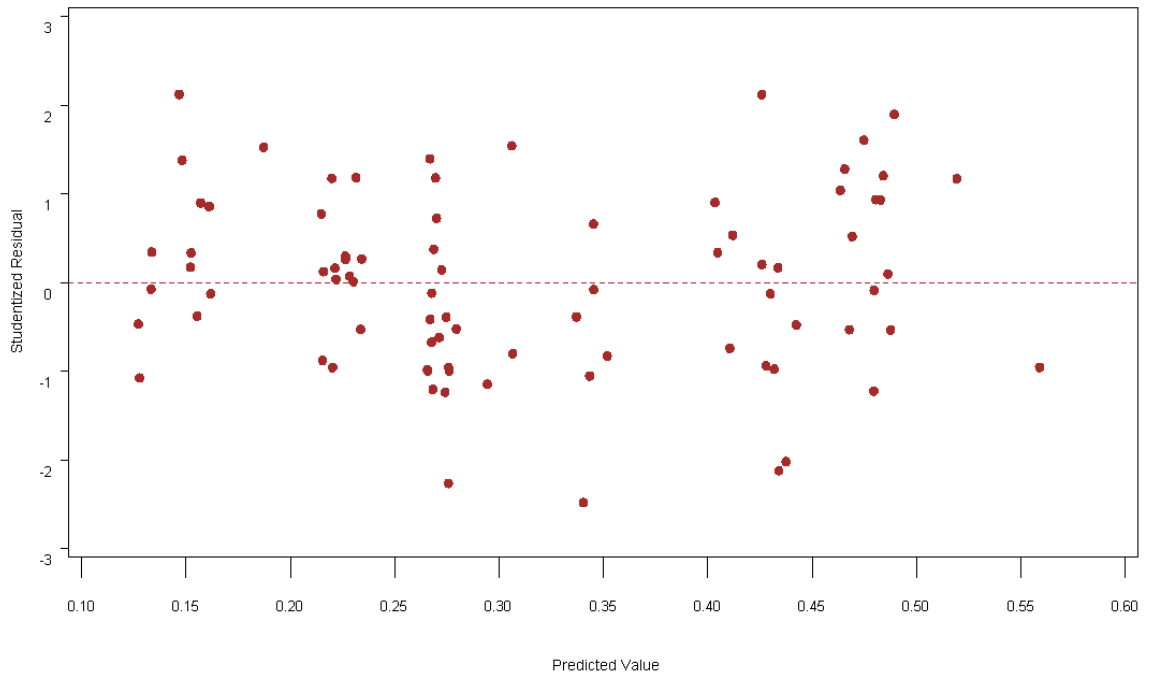


Figure 7.10: Residual Plot from MVR_{center} Analysis

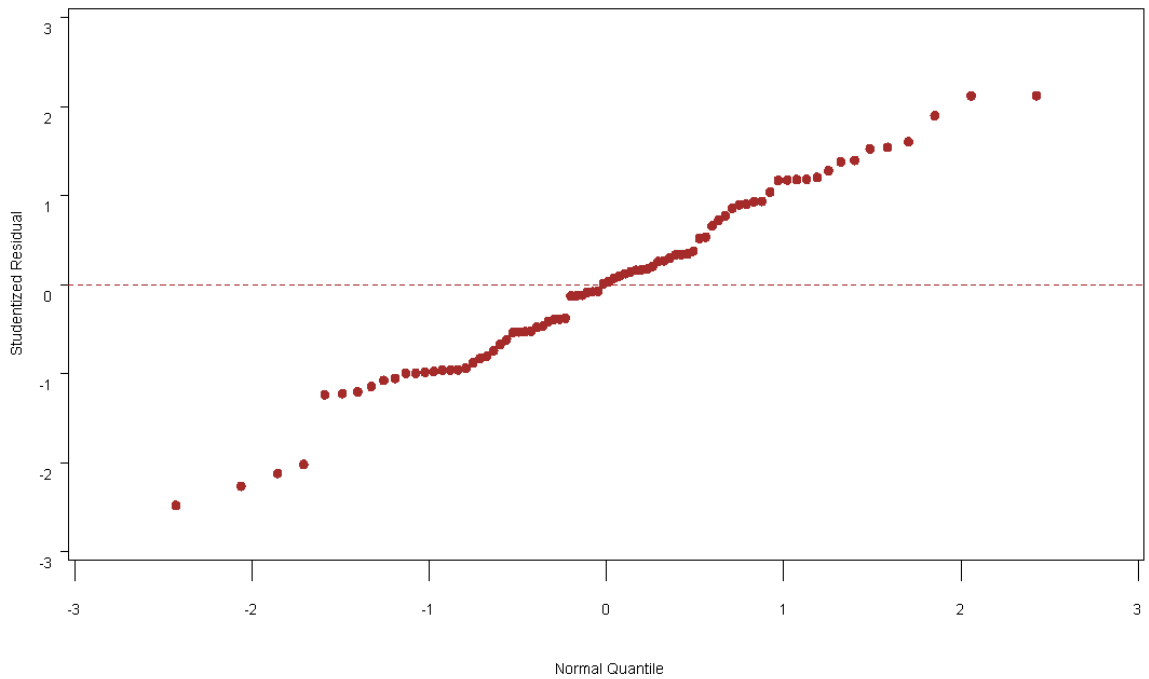


Figure 7.11: Quantile Plot of Residuals from MVR_{center} Analysis

A review of studentized residuals revealed eight possible outliers from MVR_{center} analysis. Outliers were identified as those points having R-student residual values greater than 2.0. The eight outliers tabulated in Table 7.8 were removed from the regression analysis performed in Equation 7.5.

Table 7.8: Outliers from MVR_{center} Analysis

Measured MVR_{center}	Predicted MVR_{center}	Residual	R-student Residual
1.753	1.594	0.159	2.153
1.187	1.332	-0.145	-2.573
1.520	1.387	0.133	2.009
1.275	1.413	-0.138	-2.226
1.747	1.586	0.161	2.084
1.449	1.619	-0.170	-2.400
1.560	1.713	-0.153	-2.036
1.433	1.610	-0.178	-2.538

An envelope equation for MVR_{center} , presented in Equation 7.6, shows a range of values for the coefficient in Equation 7.5 such that all of the measured values are included in the envelope equation:

$$MVR_{center-envelope} = C_{envelope} \left[\left(\frac{y}{h_w} \right)^{0.169} \left(\frac{A_w}{A_c} \right)^{0.142} \left(\frac{R_c}{Tw} \right)^{0.244} \right] \quad \text{Equation 7.6}$$

where

$$C_{envelope} = 1.12 \text{ (lower) to } 1.40 \text{ (upper)}.$$

Both Equation 7.5 and Equation 7.6 are plotted along with the outlier points that were removed from the regression analysis in Figure 7.12.

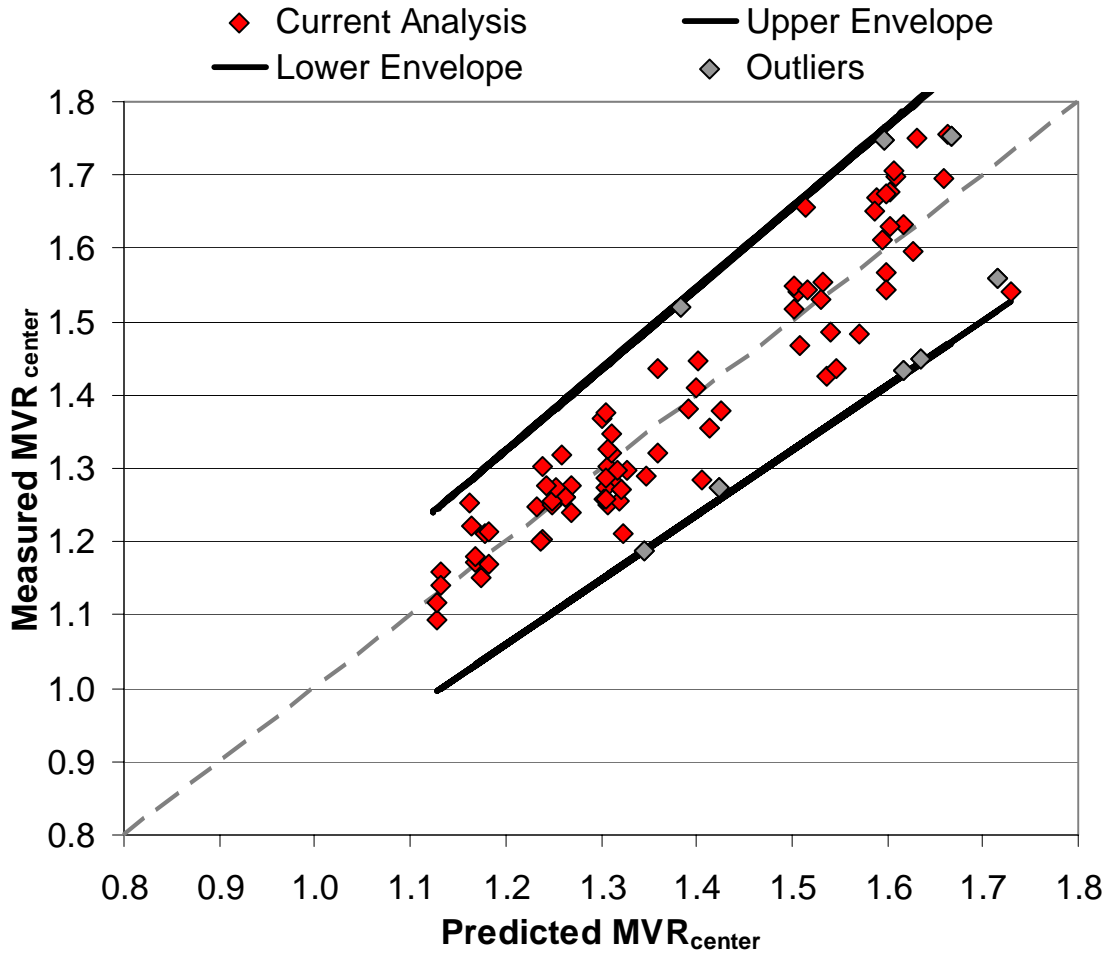


Figure 7.12: MVR_{center} Analysis Showing Outliers and Upper Envelope

7.3.4 VR INNER

Velocity ratio for the inner bank ($V_{r-inner}$) was computed as the ratio of the maximum measured velocity at the toe of the inner bank to the maximum computed velocity from a HEC-RAS computer simulation of the weir fields. All fifteen weir configurations shown in Table 3.5 were modeled in HEC-RAS and for each profile and each bend, a $V_{r-inner}$ was computed and used in a regression analysis (outliers excluded) to develop Equation 7.7:

$$V_{r-inner} = 1.035 \left[\frac{\left(\frac{y}{h_w} \right)^{0.256} \left(\frac{TW}{L_{proj,cw}} \right)^{0.461} \left(\frac{A_w}{A_c} \right)^{0.282} \left(\frac{R_c}{TW} \right)^{0.0923}}{\left(\frac{L_{arc}}{L_{proj,w}} \right)^{0.1045}} \right] \quad \text{Equation 7.7}$$

From the best-subset model-selection criterion, the Mallows' Cp was computed to be 5.50 and the R² was reported as 0.48. P-values for each parameter in Equation 7.7 are summarized in Table 7.9.

Table 7.9: P-values for $V_{r-inner}$ Regression Equation

Parameter Designation	Model Parameter	P-value
P1	$L_{arc}/L_{proj,w}$	0.0017
P2	y/h_w	<0.0001
P3	$TW/L_{proj,cw}$	0.0006
P4	$L_{proj,cw}/L_{cw}$	Not Included
P5	A_w/A_c	0.0012
P6	R_c/TW	0.0003
P7	TW/y	Not Included

A review of studentized residuals revealed eight possible outliers from $V_{r-inner}$ analysis. Seven outliers were identified as having R-student residual values greater than 2.0. A reported eighth data point had a computed R-studentized residual less than 2.0, but was eliminated based on its erroneous influence on the regression. A review of the source of the influential point revealed that it was an anomaly that was not representative of the mean and, therefore, should not be included in the predictive equation. All eight

outliers tabulated in Table 7.10 were removed from the regression analysis performed in Equation 7.7.

Table 7.10: Outliers from the $V_{r-inner}$ Analysis

Measured $V_{r-inner}$	Predicted $V_{r-inner}$	Residual	R-student Residual
1.219	1.044	0.174	2.967
0.957	1.107	-0.150	-2.320
1.017	1.186	-0.169	-2.549
1.256	1.098	0.158	2.106
1.031	1.202	-0.172	-2.578
0.998	1.138	-0.140	-2.028
1.257	1.502	-0.246	-3.147
0.964	0.950	0.0136	0.390

A plot of residuals in Figure 7.13 shows a reasonably random scatter about 0 and supports statistical assumptions. The quantile plot shown in Figure 7.14 illustrates a strong linear relationship and, therefore, supports the linearity assumption.

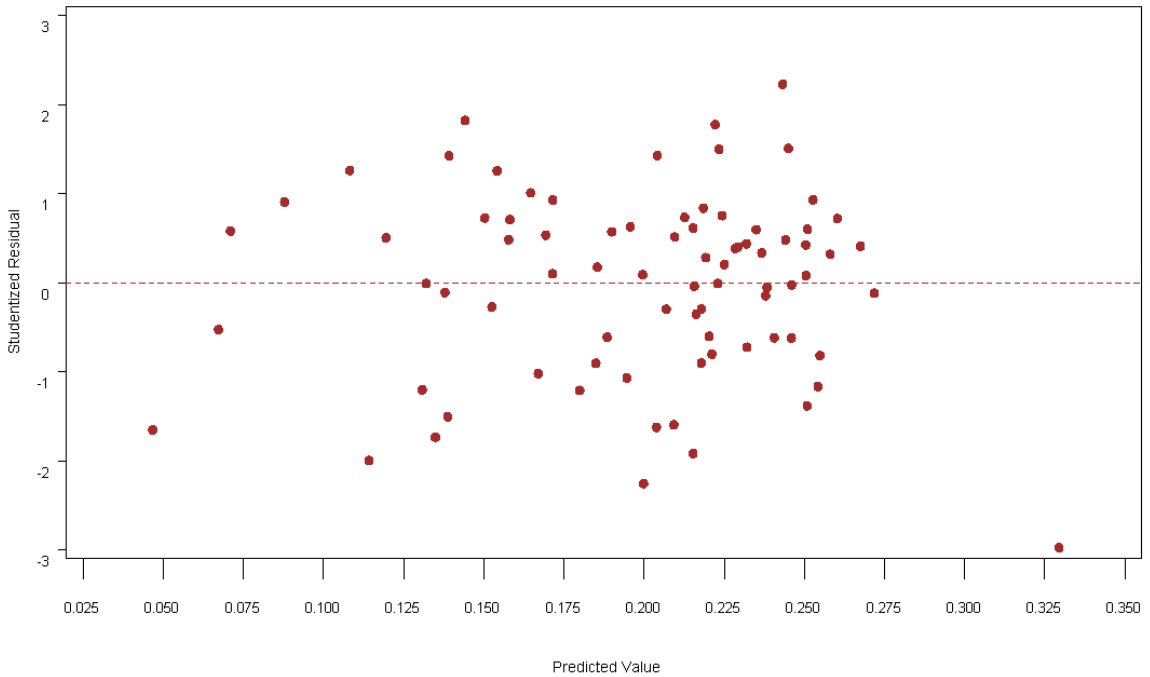


Figure 7.13: Residual Plot from $V_{r-inner}$ Analysis

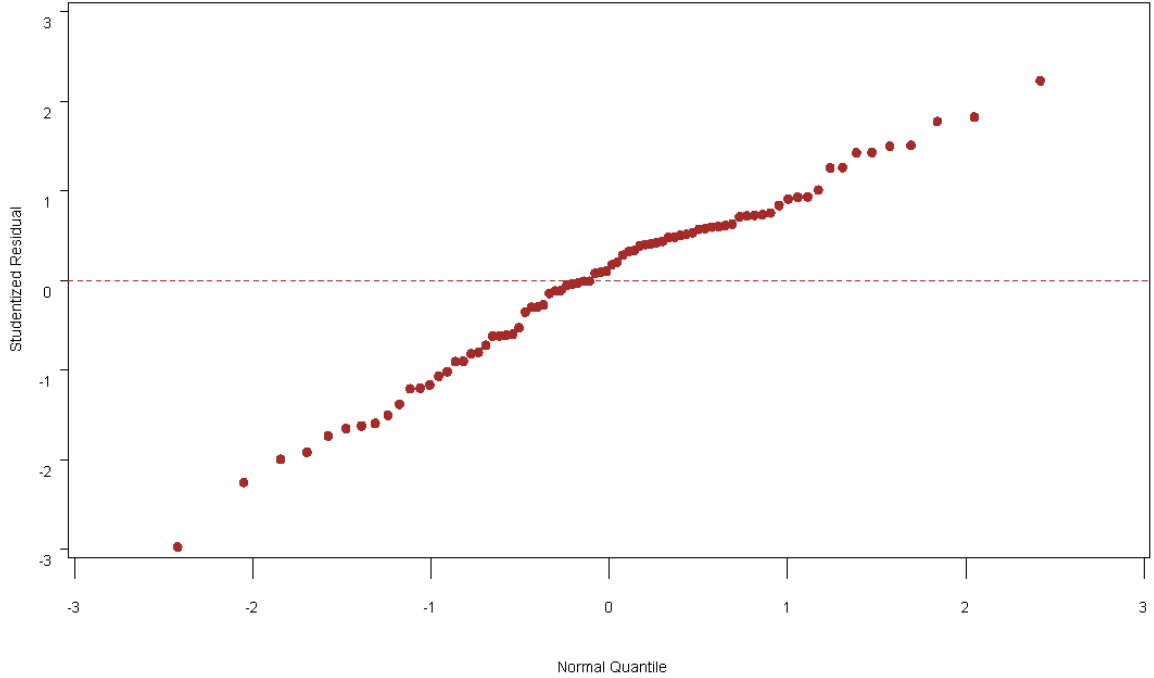


Figure 7.14: Quantile Plot of Residuals from $V_{r-inner}$ Analysis

An envelope equation was developed to provide a conservative estimate for $V_{r-inner}$. The envelope equation for $V_{r-inner}$, presented in Equation 7.8, shows a range of values for the coefficient in Equation 7.7 such that all of the measured values are included in the envelope equation:

$$V_{r-inner-envelope} = C_{envelope} \left[\frac{\left(\frac{y}{h_w} \right)^{0.256} \left(\frac{Tw}{L_{proj,cw}} \right)^{0.461} \left(\frac{A_w}{A_c} \right)^{0.282} \left(\frac{R_c}{Tw} \right)^{0.0923}}{\left(\frac{L_{arc}}{L_{proj,w}} \right)^{0.1045}} \right]$$

Equation 7.8

where

$$C_{envelope} = 0.87 \text{ (lower) to } 1.19 \text{ (upper).}$$

Both the average regression equation (Equation 7.7) and the upper envelope equation (Equation 7.8) were plotted with the outliers indicated (Figure 7.15).

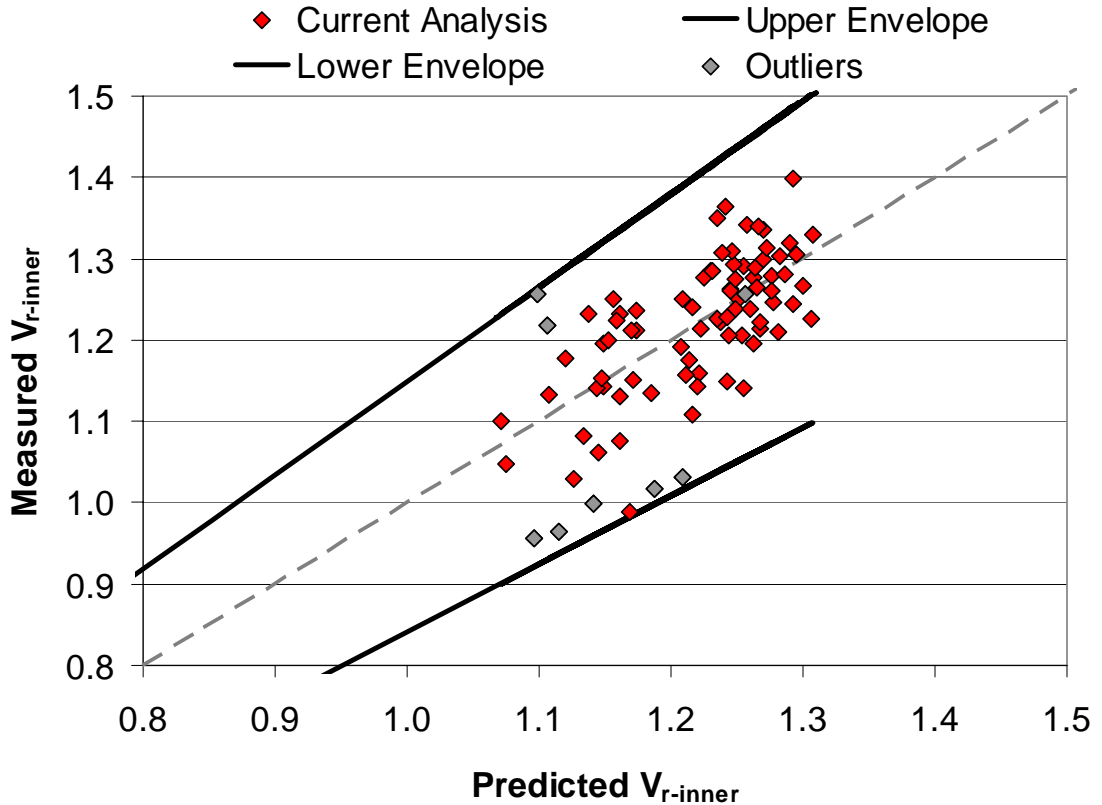


Figure 7.15: $V_{r-inner}$ Analysis Showing Outliers and Upper Envelope

7.3.5 VR TIP

Velocity ratio at the tip (V_{r-tip}) was computed as the ratio of the maximum measured tip velocity to the maximum computed velocity from a HEC-RAS computer simulation of the weir fields. All fifteen weir configurations shown in Table 3.5 were modeled in HEC-RAS and for each profile and each bend a V_{r-tip} was computed and used in a regression analysis (outliers excluded) to develop Equation 7.9:

$$V_{r-tip} = 0.763 \left[\frac{\left(\frac{y}{h_w} \right)^{0.179} \left(\frac{TW}{L_{proj,cw}} \right)^{0.077} \left(\frac{R_c}{TW} \right)^{0.288}}{\left(\frac{L_{arc}}{L_{proj,w}} \right)^{0.0975}} \right] \quad \text{Equation 7.9}$$

From the best-subset model-selection criterion, the Mallows' Cp was computed to be 7.54 and the R² was reported as 0.82. P-values for each parameter in Equation 7.9 are summarized in Table 7.11.

Table 7.11: P-values for V_{r-tip} Regression Equation

Parameter Designation	Model Parameter	P-value
P1	$L_{arc}/L_{proj,w}$	0.0006
P2	y/h_w	<0.0001
P3	$TW/L_{proj,cw}$	0.0004
P4	$L_{proj,cw}/L_{cw}$	Not Included
P5	A_w/A_c	Not Included
P6	R_c/TW	<0.0001
P7	TW/y	Not Included

A review of studentized residuals revealed five possible outliers from V_{r-tip} analysis. Outliers were identified as those points having R-student residual values greater than 2.0. The five outliers tabulated in Table 7.12 were removed from the regression analysis performed in Equation 7.9.

Table 7.12: Outliers from the V_{r-tip} Analysis

Measured V_{r-tip}	Predicted V_{r-tip}	Residual	R-student Residual
1.284	0.999	0.286	4.500
1.044	1.247	-0.203	-2.926
1.135	0.971	0.163	2.448
1.071	1.237	-0.166	-2.421
1.363	1.215	0.148	2.089

A plot of residuals in Figure 7.16 showed a reasonably random scatter about 0, with two major clumps of data. For linearity, the quantile plot in Figure 7.17 showed a linearity relationship.

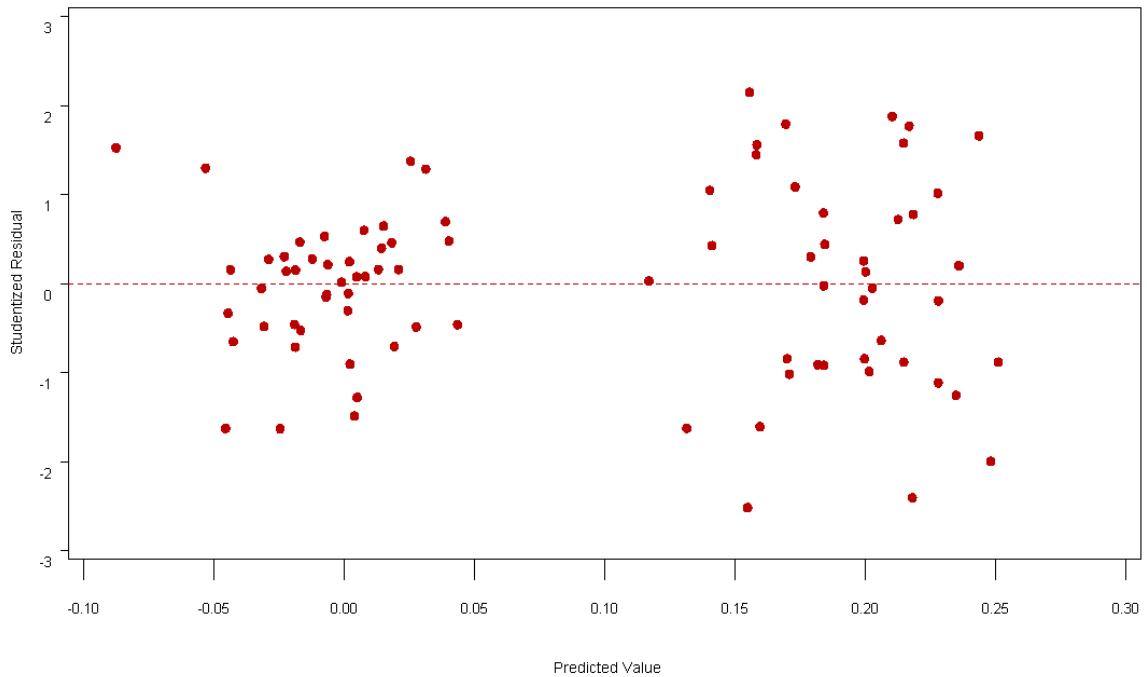


Figure 7.16: Residual Plot from the V_{r-tip} Analysis

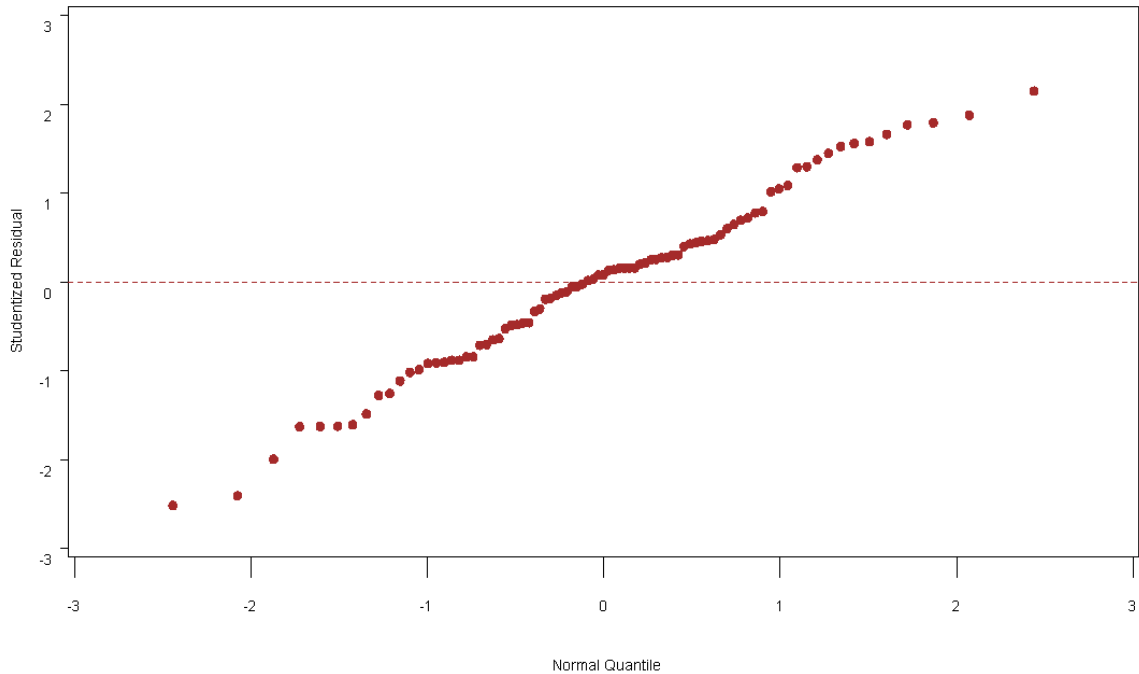


Figure 7.17: Quantile Plot of Residuals from the V_{r-tip} Analysis

An envelope equation was developed to provide a conservative estimate for V_{r-tip} . The envelope equation for V_{r-tip} , presented in Equation 7.10, shows a range of values for the coefficient in Equation 7.9 such that all of the measured values are included in the envelope equation:

$$V_{r-tip-envelope} = C_{envelope} \left[\frac{\left(\frac{y}{h_w} \right)^{0.179} \left(\frac{Tw}{L_{proj,cw}} \right)^{0.077} \left(\frac{R_c}{Tw} \right)^{0.288}}{\left(\frac{L_{arc}}{L_{proj,w}} \right)^{0.0975}} \right] \quad \text{Equation 7.10}$$

where

$$C_{envelope} = 0.65 \text{ (lower) to } 0.86 \text{ (upper).}$$

Both the average regression equation (Equation 7.9) and the upper envelope equation (Equation 7.10) were plotted with the outliers indicated in Figure 7.18.

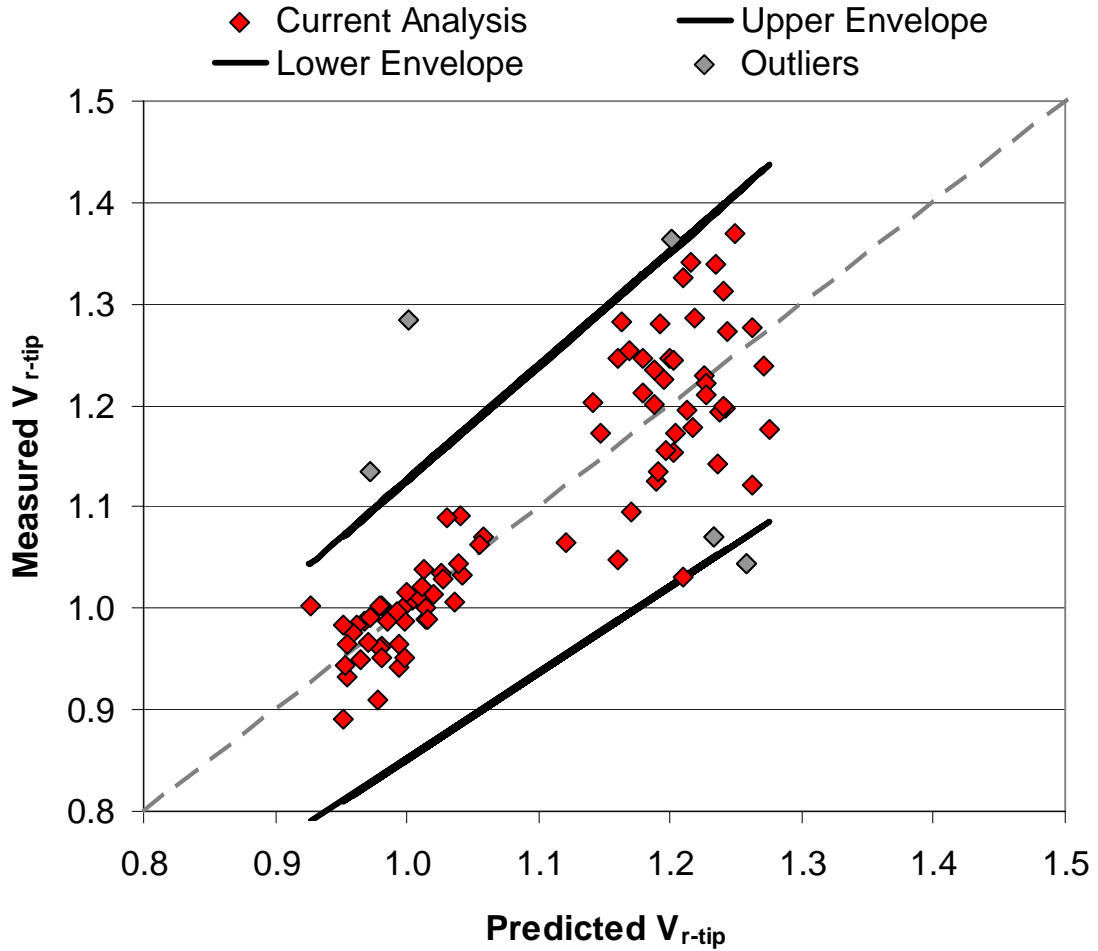


Figure 7.18: V_{r-tip} Analysis Showing Outliers and Upper Envelope

7.4 SHEAR-STRESS ANALYSIS

7.4.1 MTR INNER

Increase in shear stress at the toe of the inner bank over maximum computed shear stress from the baseline HEC-RAS model was measured using a maximum shear-stress ratio (MTR_{inner}). A MTR_{inner} was computed for each weir configuration in Table

3.5, for three discharges, and for each bend. From this dataset, the regression equation in Equation 7.11 was determined from regression analysis (excluded outliers):

$$MTR_{inner} = 1.346 \left[\frac{\left(\frac{TW}{L_{proj,cw}} \right)^{1.226} \left(\frac{A_w}{A_c} \right)^{0.586}}{\left(\frac{R_c}{TW} \right)^{0.181}} \right] \quad \text{Equation 7.11}$$

From the best-subset model-selection criterion, the Mallows' Cp was computed to be 1.5 and the R² was reported as 0.54. P-values for each parameter in Equation 7.11 are summarized in Table 7.13.

Table 7.13: P-values for MTR_{inner} Regression Equation

Parameter Designation	Model Parameter	P-value
P1	$L_{arc}/L_{proj,w}$	Not Included
P2	y/h_w	Not Included
P3	$TW/L_{proj,cw}$	0.0021
P4	$L_{proj,cw}/L_{cw}$	Not Included
P5	A_w/A_c	0.0181
P6	R_c/TW	0.0017
P7	TW/y	Not Included

A review of studentized residuals revealed six possible outliers from MTR_{inner} analysis. Outliers were identified as those points having R-student residual values greater than 2.0. The six outliers tabulated in Table 7.14 were removed from the regression analysis performed in Equation 7.11.

Table 7.14: Outliers from MTR_{inner} Analysis

Measured MTR_{inner}	Predicted MTR_{inner}	Residual	R-student Residual
0.430	2.443	-2.013	-5.957
0.876	2.823	-1.946	-2.604
0.997	2.416	-1.419	-2.412
1.175	2.595	-1.420	-2.241
1.145	2.369	-1.224	-3.106
1.578	2.496	-0.919	-3.762

Residuals, plotted in Figure 7.19, are relatively randomly scattered about 0 and the quantile plot of the residuals in Figure 7.20 indicates a linear relationship, both of which serve to validate statistical assumptions of multivariate regression.

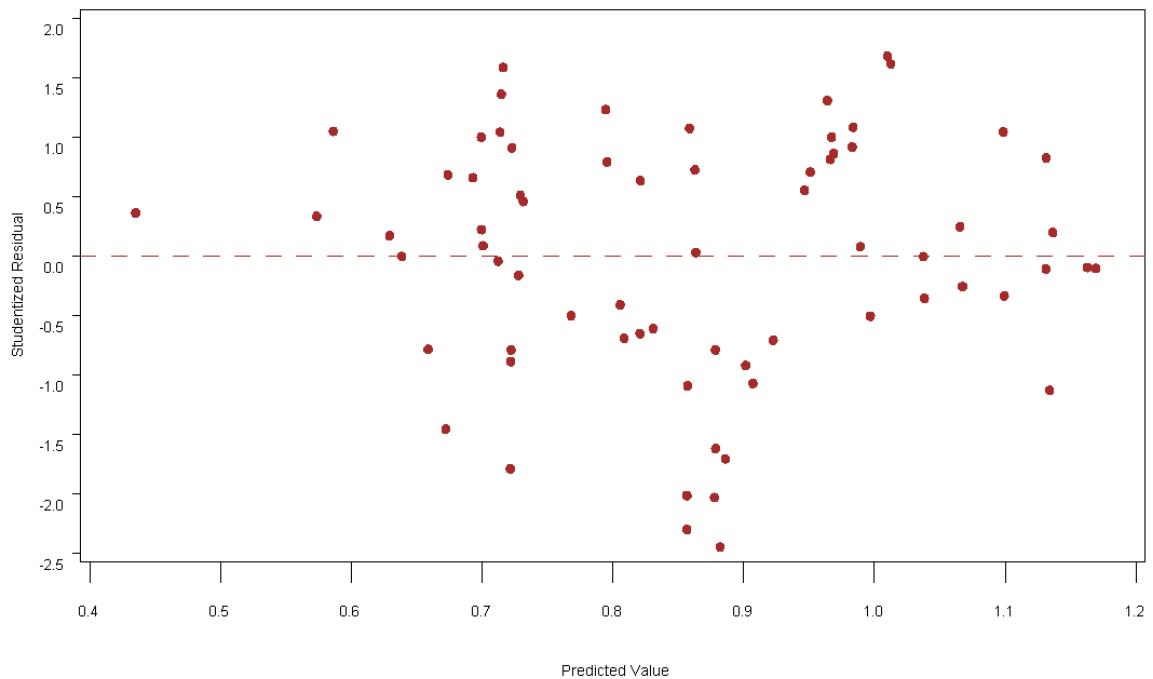


Figure 7.19: Residual Plot from MTR_{inner} Analysis

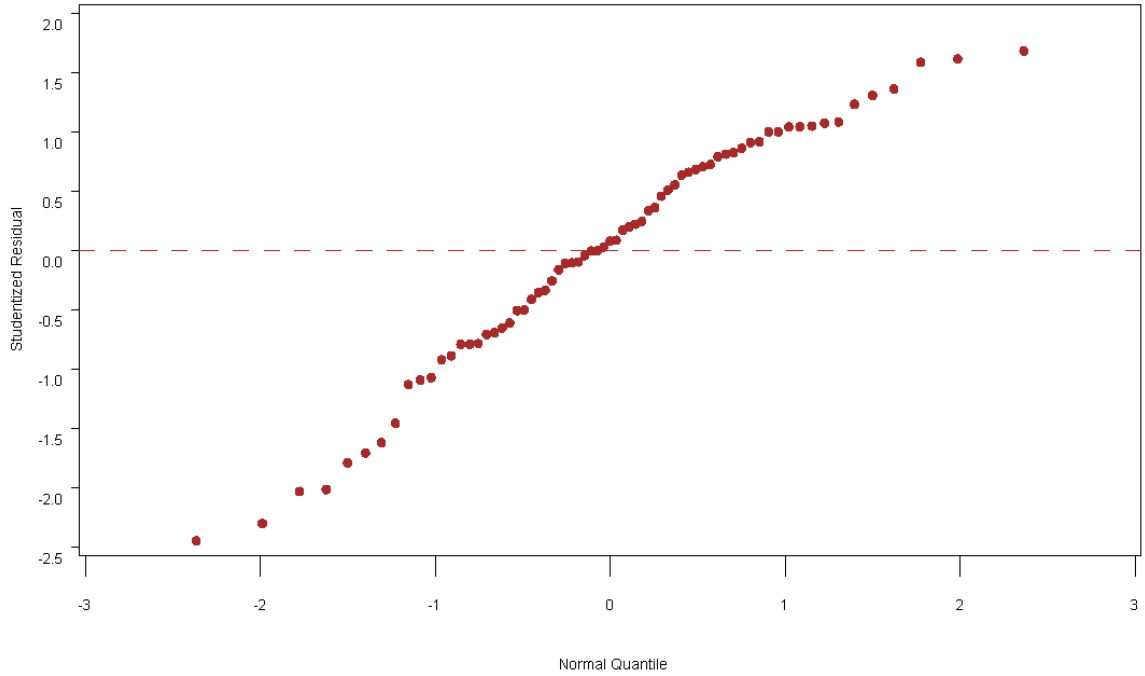


Figure 7.20: Quantile Plot of Residuals from MTR_{inner} Analysis

An envelope equation was developed to provide a conservative estimate for MTR_{inner} . The envelope equation for MTR_{inner} , presented in Equation 7.12, shows a range of values for the coefficient in Equation 7.11 such that all of the measured values are included in the envelope equation:

$$MTR_{inner-envelope} = C_{envelope} \left[\frac{\left(\frac{Tw}{L_{proj,cw}} \right)^{1.226} \left(\frac{A_w}{A_c} \right)^{0.586}}{\left(\frac{R_c}{Tw} \right)^{0.181}} \right] \quad \text{Equation 7.12}$$

where

$$C_{envelope} = 0.90 \text{ (lower) to } 1.75 \text{ (upper).}$$

Figure 7.21 shows the results of the MTR_{inner} regression analysis along with a plot of the upper envelope equation and the outliers, which are not included in Equation 7.11 or Equation 7.12.

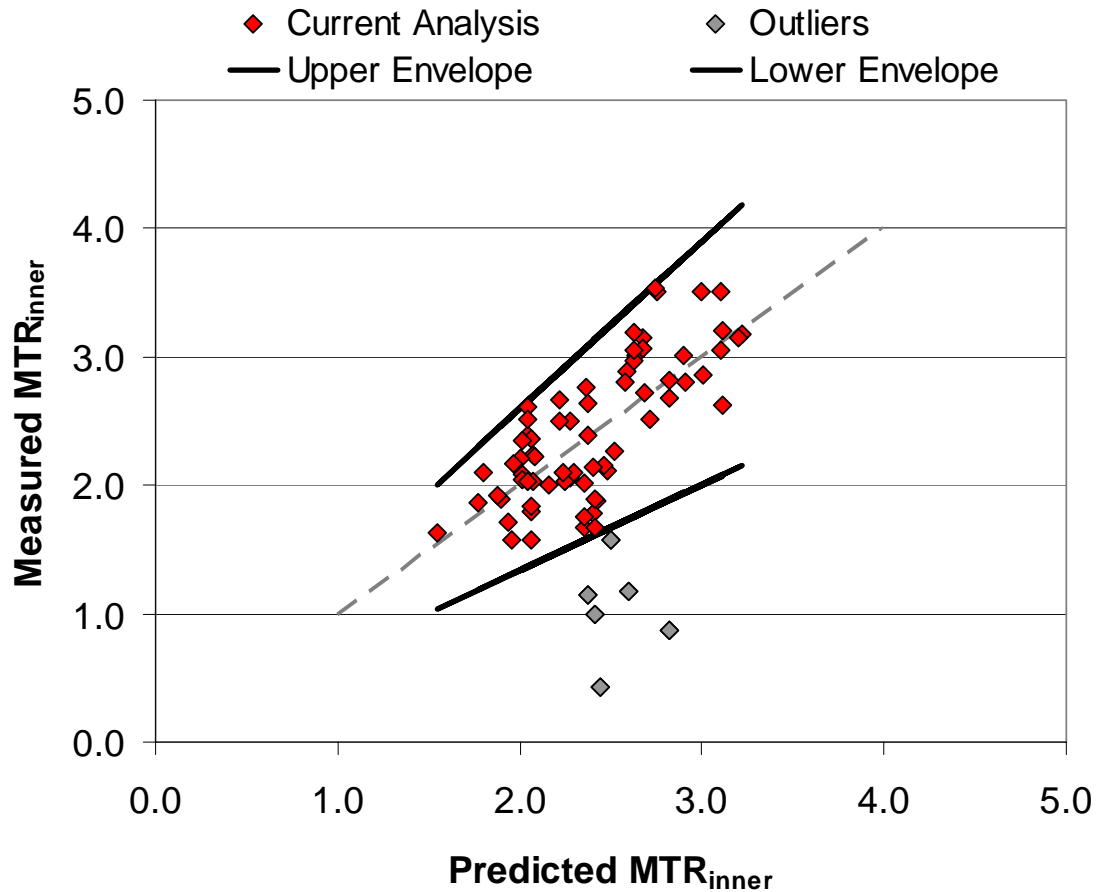


Figure 7.21: MTR_{inner} Analysis Showing Outliers and Upper Envelope

7.4.2 MTR TIP

Areas adjacent to the bendway-weir tip have been found to be particularly susceptible to attack by aggressive approach flows (Richardson and Simons, 1974; Seed, 1997). Scouring caused by increasing shear stresses can create instability in the weir structure if not addressed. Computation of the maximum shear-stress ratio MTR_{tip}

included data collected on the Middle Rio Grande physical model and results from a baseline HEC-RAS model. For fifteen weir configurations, three discharges, and two bends, the MTR_{tip} was computed as the ratio of the maximum shear stress measured at the tip of the weir through a bend and the maximum cross-sectional-averaged baseline shear stress. Equation 7.13 is the result of a regression analysis (outliers excluded) performed on the compiled MTR_{tip} data:

$$MTR_{tip} = 0.944 \left[\frac{\left(\frac{Tw}{L_{proj,cw}} \right)^{1.622} \left(\frac{A_w}{A_c} \right)^{0.873} \left(\frac{R_c}{Tw} \right)^{0.326}}{\left(\frac{L_{arc}}{L_{proj,w}} \right)^{0.323} \left(\frac{L_{proj,cw}}{L_{cw}} \right)^{0.860}} \right] \quad \text{Equation 7.13}$$

From the best-subset model-selection criterion, the Mallows' Cp was computed to be 5.92 and the R^2 was reported as 0.30. P-values for each parameter in Equation 7.13 are summarized in Table 7.15.

Table 7.15: P-values for MTR_{tip} Regression Equation

Parameter Designation	Model Parameter	P-value
P1	$\frac{L_{arc}}{L_{proj,w}}$	0.0154
P2	$\frac{y}{h_w}$	Not Included
P3	$\frac{Tw}{L_{proj,cw}}$	0.0030
P4	$\frac{L_{proj,cw}}{L_{cw}}$	0.0370
P5	$\frac{A_w}{A_c}$	0.0118
P6	$\frac{R_c}{Tw}$	0.0011
P7	$\frac{Tw}{y}$	Not Included

A review of studentized residuals revealed three possible outliers from MTR_{tip} analysis. Outliers were identified as those points having R-student residual values greater than 2.0. The three outliers tabulated in Table 7.16 were removed from the regression analysis performed in Equation 7.13.

Table 7.16: Outliers from MTR_{tip} Analysis

Measured MTR_{tip}	Predicted MTR_{tip}	Residual	R-student Residual
0.965	1.857	-0.893	-2.717
1.001	1.969	-0.968	-2.807
2.824	1.761	1.062	2.087

Plotting residuals against the predicted values showed a reasonably even distribution about 0 with no significant trend. Normality was confirmed by a nearly 45-degree line in the quantile plot. Figure 7.22 and Figure 7.23 show the residual plot against predicted values and the quantile plot for the MTR_{tip} analysis, respectively.

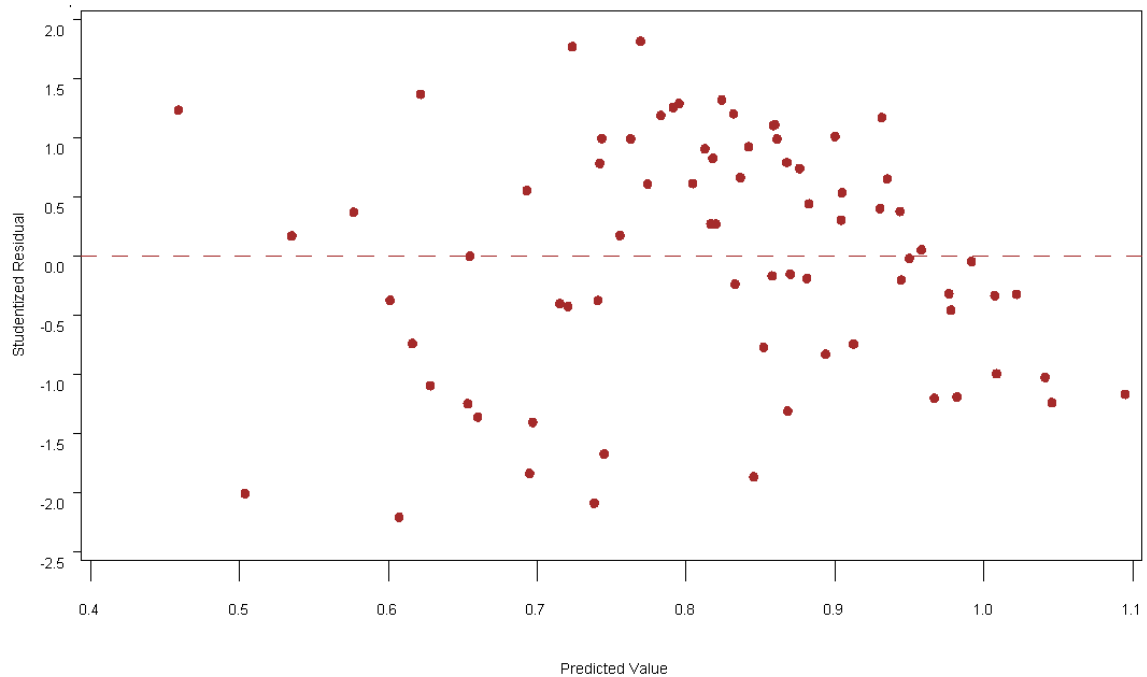


Figure 7.22: Residual Plot from MTR_{tip} Analysis

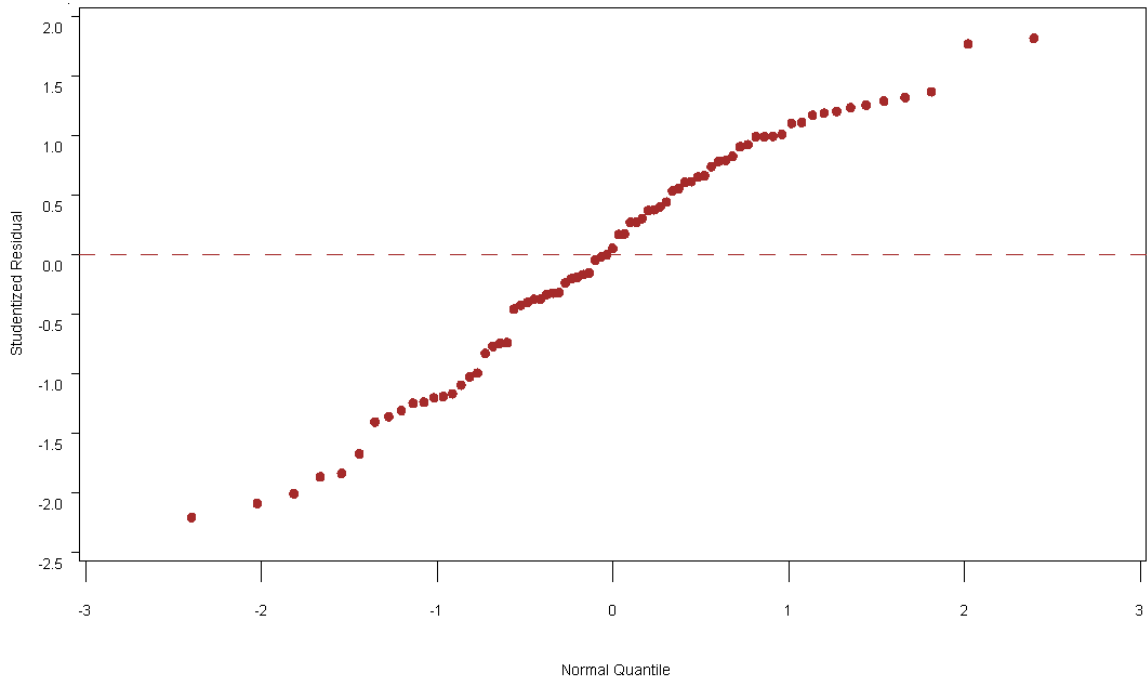


Figure 7.23: Quantile Plot of Residuals from MTR_{tip} Analysis

An envelope equation was developed to provide a conservative estimate for MTR_{tip} . The envelope equation for MTR_{tip} , presented in Equation 7.14, shows a range of values for the coefficient in Equation 7.13 such that all of the measured values are included in the envelope equation:

$$MTR_{tip-envelope} = C_{envelope} \left[\frac{\left(\frac{TW}{L_{proj,cw}} \right)^{1.622} \left(\frac{A_w}{A_c} \right)^{0.873} \left(\frac{R_c}{TW} \right)^{0.326}}{\left(\frac{L_{arc}}{L_{proj,w}} \right)^{0.323} \left(\frac{L_{proj,cw}}{L_{cw}} \right)^{0.860}} \right] \quad \text{Equation 7.14}$$

where

$$C_{envelope} = 0.60 \text{ (lower) to } 1.40 \text{ (upper).}$$

Figure 7.24 shows the regression equation for the MTR_{tip} along with the upper envelope equation and the outliers, which were not included in the regression analysis.

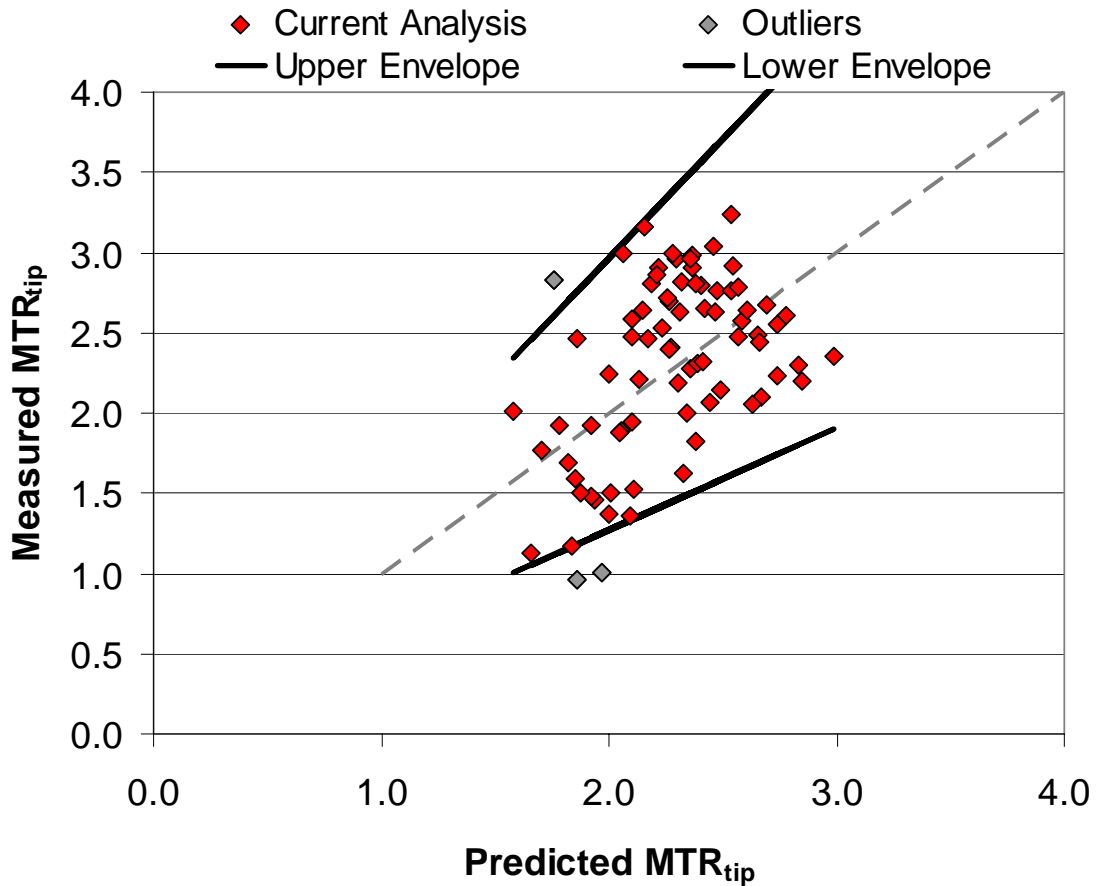


Figure 7.24: MTR_{tip} Analysis Showing Outliers and Upper Envelope

7.4.3 MTR CENTER

Maximum shear-stress ratio at the channel center (MTR_{center}) was computed as the ratio of the maximum measured shear stress along the meander bend in the physical model and the maximum computed shear stress from the baseline HEC-RAS model. MTR_{center} provides an estimate of the increased shear stress that might be encountered in the center of the channel due the installation of bendway weirs. MTR_{center} for all fifteen weir configurations were compiled into a regression analysis (outliers excluded), resulting in Equation 7.15:

$$MTR_{center} = 1.216 \left[\frac{\left(\frac{TW}{L_{proj,cw}} \right)^{1.476} \left(\frac{A_w}{A_c} \right)^{0.869} \left(\frac{R_c}{TW} \right)^{0.374}}{\left(\frac{L_{arc}}{L_{proj,w}} \right)^{0.294}} \right] \quad \text{Equation 7.15}$$

From the best-subset model-selection criterion, the Mallows' Cp was computed to be 6.54 and the R² was reported as 0.21. P-values for each parameter in Equation 7.15 are summarized in Table 7.17.

Table 7.17: P-values for MTR_{center} Regression Equation

Parameter Designation	Model Parameter	P-value
P1	$L_{arc} / L_{proj,w}$	0.0322
P2	y / h_w	Not Included
P3	$TW / L_{proj,cw}$	0.0049
P4	$L_{proj,cw} / L_{cw}$	Not Included
P5	A_w / A_c	0.0097
P6	R_c / TW	0.0004
P7	TW / y	Not Included

A review of studentized residuals revealed nine possible outliers from MTR_{center} analysis. Outliers were identified as those points having R-student residual values greater than 2.0. The nine outliers tabulated in Table 7.18 were removed from the regression analysis performed in Equation 7.15.

Table 7.18: Outliers from the MTR_{center} Analysis

Measured MTR_{center}	Predicted MTR_{center}	Residual	R-student Residual
0.527	1.933	-1.406	-5.737
5.232	2.635	2.597	2.358
0.998	2.443	-1.445	-2.024
1.060	2.823	-1.763	-2.025
1.142	2.416	-1.274	-2.014
1.077	2.595	-1.518	-3.206
1.407	2.058	-0.651	-3.120
1.559	2.071	-0.512	-2.406
3.827	2.746	1.081	2.192

A plot of residuals in Figure 7.25 shows a relatively scattered plot about 0 and the quantile plot in Figure 7.26 shows a linear relationship, both of which serve to validate statistical assumptions of multivariate regression.

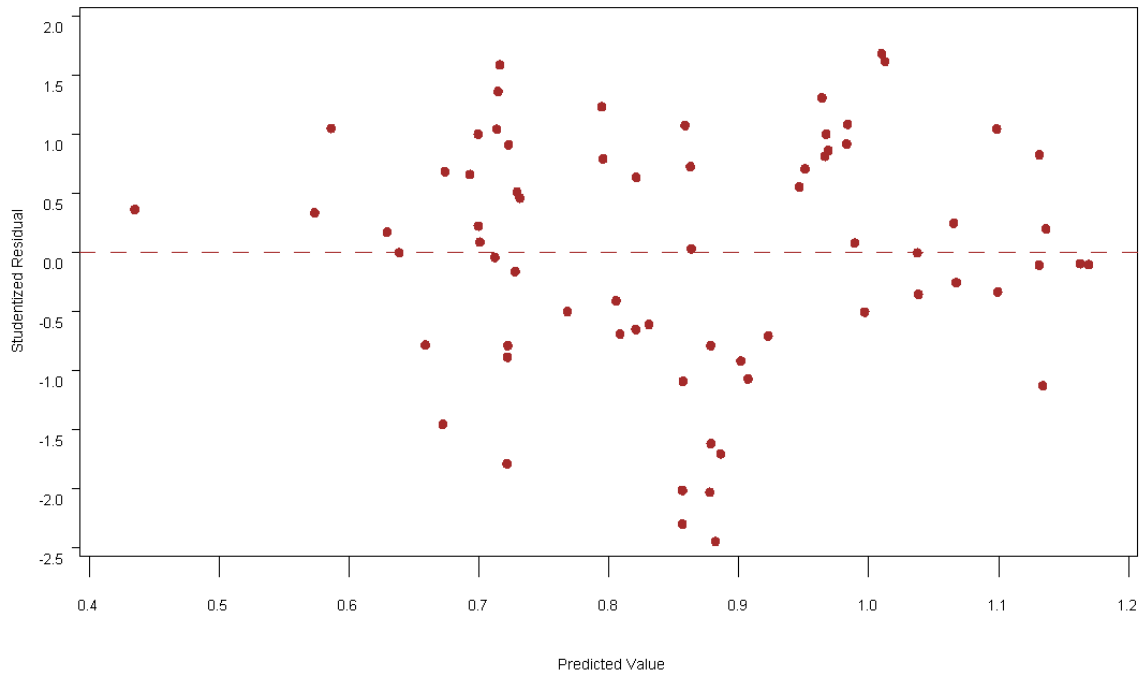


Figure 7.25: Residual Plot from the MTR_{center} Analysis

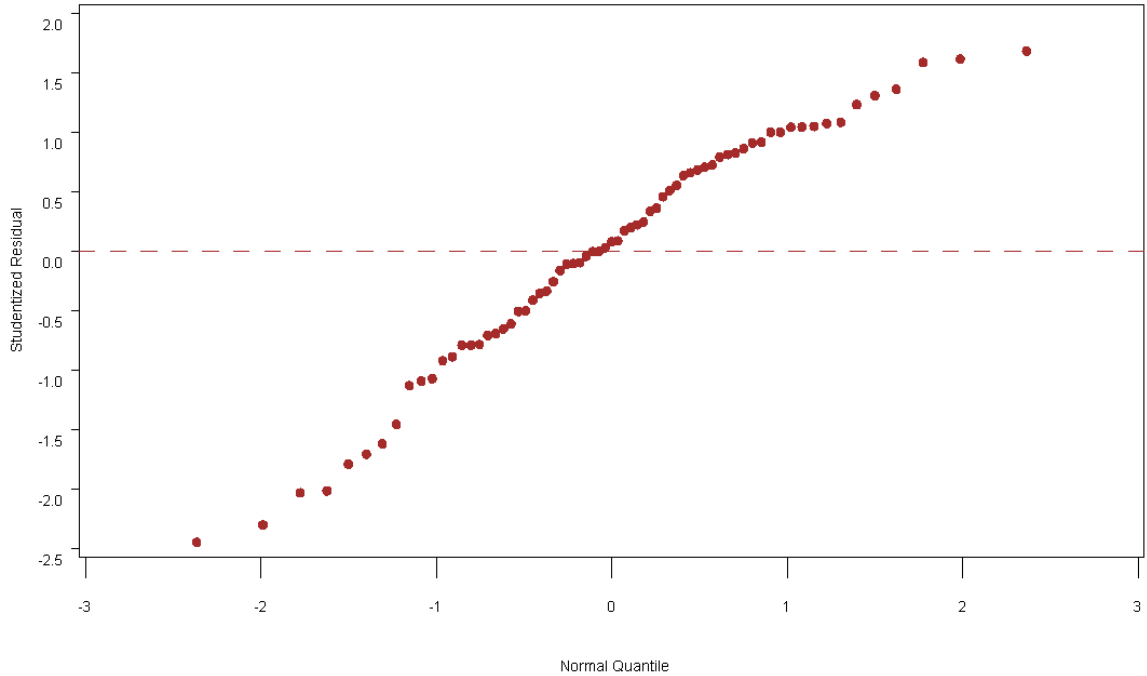


Figure 7.26: Quantile Plot of Residuals from MTR_{center} Analysis

An envelope equation was developed to provide a conservative estimate for MTR_{center} . The envelope equation for MTR_{center} , presented in Equation 7.16, shows a range of values for the coefficient in Equation 7.15 such that all of the measured values are included in the envelope equation:

$$MTR_{center-envelope} = C_{envelope} \left[\frac{\left(\frac{T_w}{L_{proj,cw}} \right)^{1.476} \left(\frac{A_w}{A_c} \right)^{0.869} \left(\frac{R_c}{T_w} \right)^{0.374}}{\left(\frac{L_{arc}}{L_{proj,w}} \right)^{0.294}} \right] \quad \text{Equation 7.16}$$

where

$$C_{envelope} = 0.85 \text{ (lower) to } 1.70 \text{ (upper)}.$$

Results of the MTR_{center} regression analysis are shown in Figure 7.27 along with the upper envelope equation and the outliers, which were not included in the regression analysis.

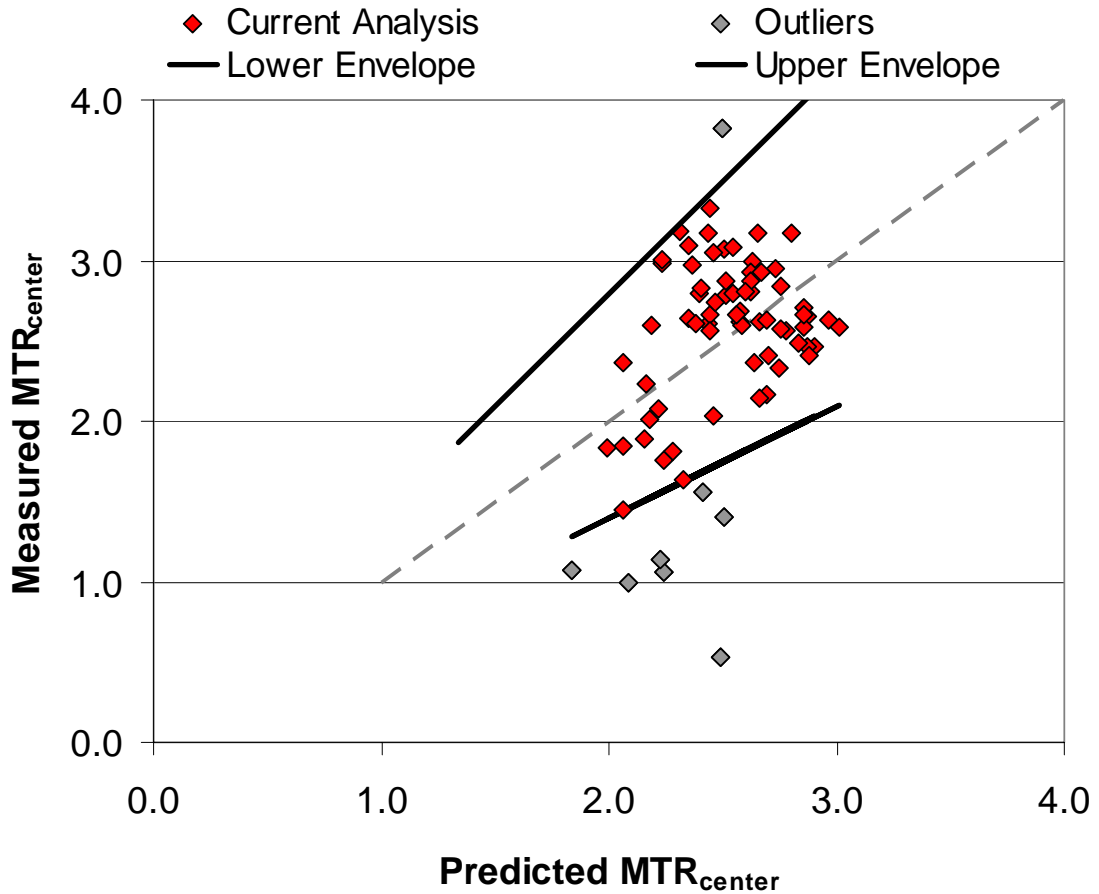


Figure 7.27: MTR_{center} Analysis Showing Outliers and Upper Envelope

7.4.4 TR INNER

Maximum measured increase in shear stress at the toe of the inner bank was evaluated against the maximum computed cross-sectional average shear stress from HEC-RAS computer models of the weir configurations in the shear-stress ratio, $T_{r-inner}$. The shear-stress ratio was computed for all of the fifteen weir configurations, three

discharges, and two channel bends. Shear-stress ratio data were compiled and a regression analysis (outliers excluded), was performed resulting in Equation 7.17:

$$T_{r-inner} = 0.668 \left[\frac{\left(\frac{TW}{L_{proj,cw}} \right)^{1.714} \left(\frac{A_w}{A_c} \right)^{0.588}}{\left(\frac{L_{arc}}{L_{proj,w}} \right)^{0.178} \left(\frac{y}{h_w} \right)^{0.323} \left(\frac{L_{proj,cw}}{L_{cw}} \right)^{0.841}} \right] \quad \text{Equation 7.17}$$

From the best-subset model-selection criterion, the Mallows' Cp was computed to be 7.9 and the R² was reported as 0.81. P-values for each parameter in Equation 7.17 are summarized in Table 7.19.

Table 7.19: P-values for $T_{r-inner}$ Regression Equation

Parameter Designation	Model Parameter	P-value
P1	$\frac{L_{arc}}{L_{proj,w}}$	0.0074
P2	$\frac{y}{h_w}$	0.0028
P3	$\frac{TW}{L_{proj,cw}}$	<0.0001
P4	$\frac{L_{proj,cw}}{L_{cw}}$	0.0021
P5	$\frac{A_w}{A_c}$	0.0086
P6	$\frac{R_c}{TW}$	Not Included
P7	$\frac{TW}{y}$	Not Included

A review of studentized residuals revealed eight possible outliers from $T_{r-inner}$ analysis. Outliers were identified as those points having R-student residual values greater than 2.0. The eight outliers tabulated in Table 7.20 were removed from the regression analysis performed in Equation 7.17.

Table 7.20: Outliers from the $T_{r\text{-inner}}$ Analysis

Measured $T_{r\text{-inner}}$	Predicted $T_{r\text{-inner}}$	Residual	R-student Residual
0.424	2.179	-1.756	-6.098
0.885	2.470	-1.585	-2.862
0.930	1.989	-1.059	-2.320
1.084	1.909	-0.825	-2.898
1.245	2.062	-0.817	-2.922
4.028	2.671	1.357	2.402
1.701	2.392	-0.691	-2.162
3.616	2.515	1.101	2.325

A plot of residuals in Figure 7.28 shows a relatively scattered plot about 0 and the quantile plot of the residuals in Figure 7.29 shows a linear relationship, both of which serve to validate statistical assumptions of multivariate regression.

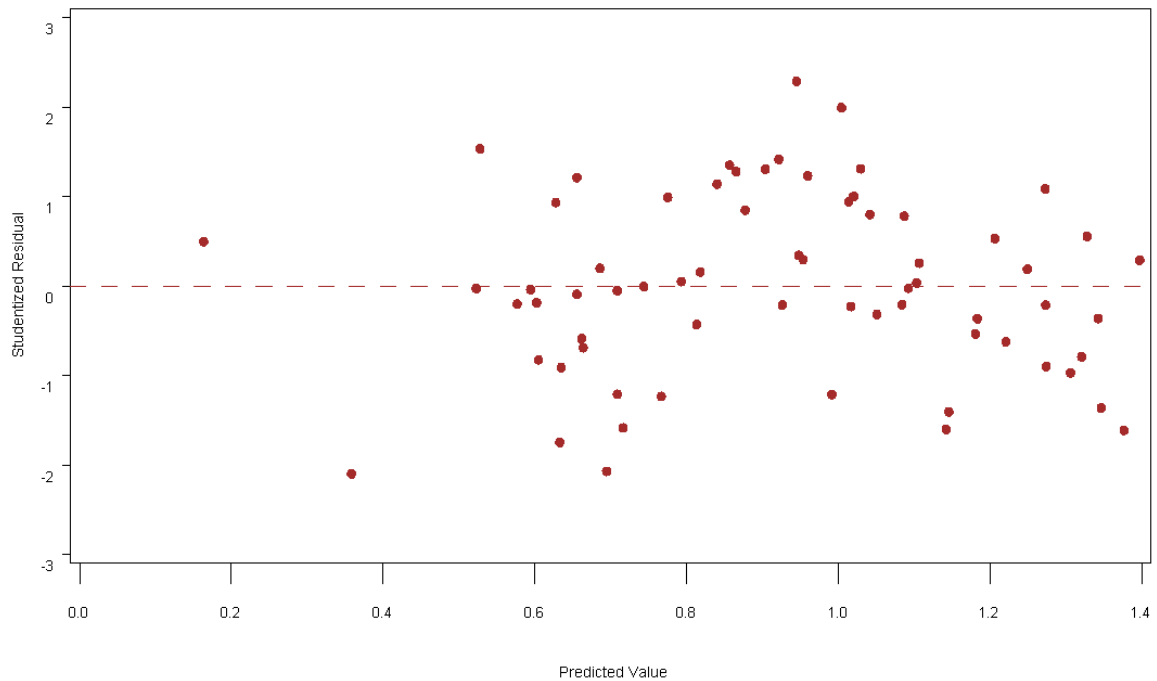


Figure 7.28: Residual Plot from the $T_{r\text{-inner}}$ Analysis

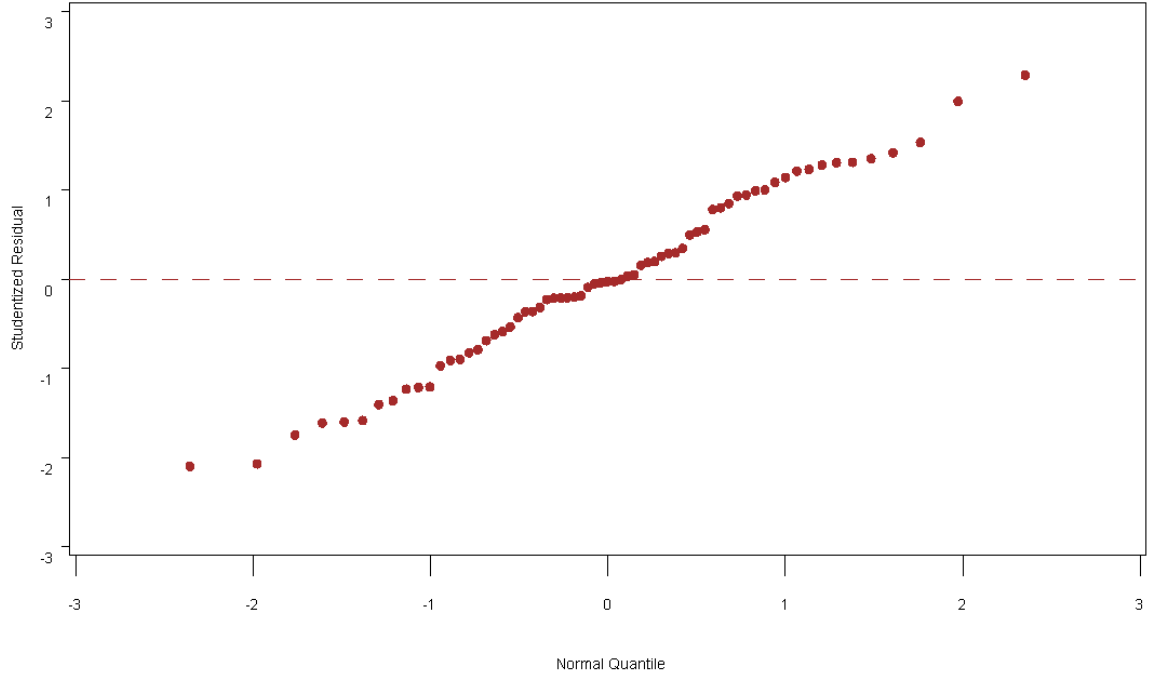


Figure 7.29: Quantile Plot of the Residuals from the $T_{r-inner}$ Analysis

An envelope equation was developed to provide a conservative estimate for $T_{r-inner}$. The envelope equation for $T_{r-inner}$, presented in Equation 7.18, shows a range of values for the coefficient in Equation 7.17 such that all of the measured values are included in the envelope equation:

$$T_{r-inner-envelope} = C_{envelope} \left[\frac{\left(\frac{T_w}{L_{proj,cw}} \right)^{1.714} \left(\frac{A_w}{A_c} \right)^{0.588}}{\left(\frac{L_{arc}}{L_{proj,w}} \right)^{0.178} \left(\frac{y}{h_w} \right)^{0.323} \left(\frac{L_{proj,cw}}{L_{cw}} \right)^{0.841}} \right] \quad \text{Equation 7.18}$$

where

$$C_{envelope} = 0.48 \text{ (lower) to } 0.88 \text{ (upper).}$$

Results of the $T_{r-inner}$ regression analysis are shown in Figure 7.30 along with the upper envelope equation and the outliers, which were not included in the regression analysis.

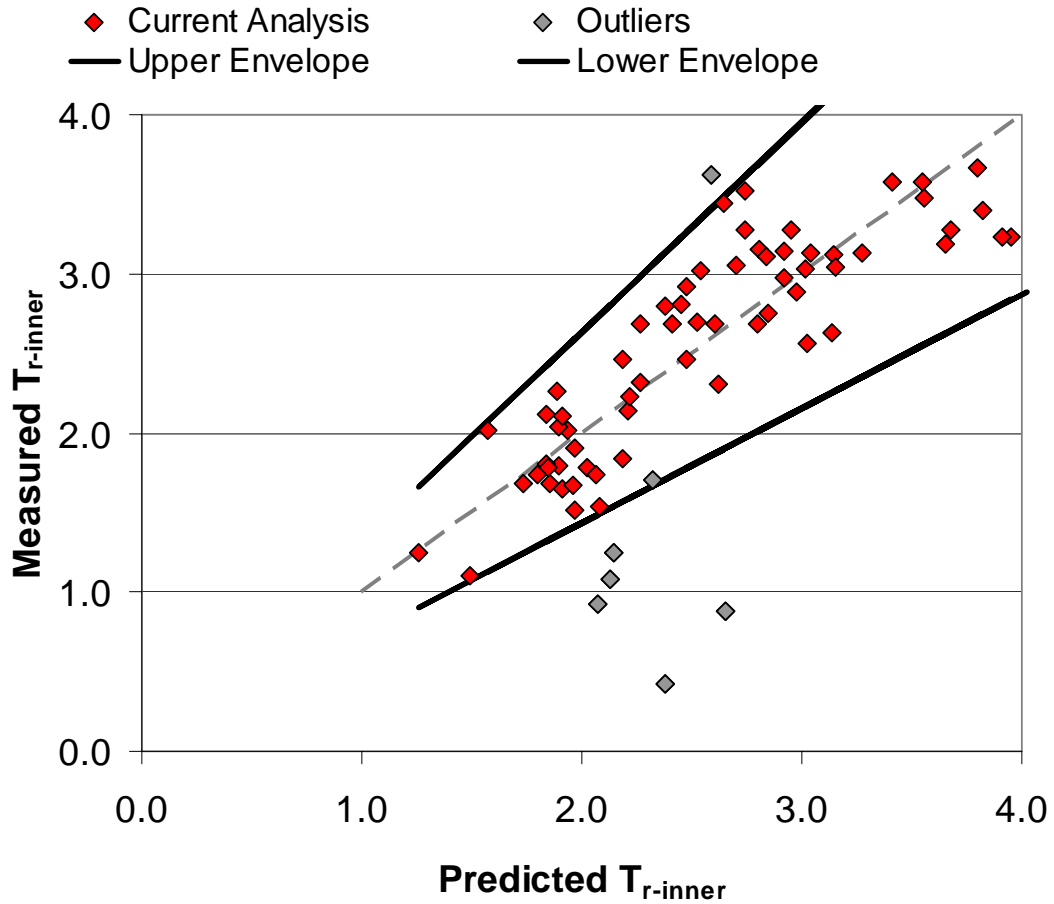


Figure 7.30: $T_{r-inner}$ Analysis Showing Outliers and Upper Envelope

7.4.5 TR TIP

Increase in shear stress near the tip of the weir is thought to be the best estimate of the scour potential associated with bendway weirs. A comparison was made between the maximum measured shear stress at the weir tip and the maximum cross-sectional-averaged shear stress computed from the HEC-RAS computer model of the bendway

weirs. The shear-stress ratio at the weir tip (T_{r-tip}) was computed for the fifteen weir configurations, three different discharges, and for each bend. Compiled T_{r-tip} values were used to create the regression analysis (outliers excluded) shown in Equation 7.19:

$$T_{r-tip} = 0.527 \left[\frac{\left(\frac{TW}{L_{proj,cw}} \right)^{1.866} \left(\frac{A_w}{A_c} \right)^{0.780}}{\left(\frac{L_{arc}}{L_{proj,w}} \right)^{0.252} \left(\frac{y}{h_w} \right)^{0.327} \left(\frac{L_{proj,cw}}{L_{cw}} \right)^{0.958} \left(\frac{R_c}{TW} \right)^{0.324}} \right] \quad \text{Equation 7.19}$$

From the best-subset model-selection criterion, the Mallows' Cp was computed to be 7.0 and the R^2 was reported as 0.60. P-values for each parameter in Equation 7.19 are summarized in Table 7.21.

Table 7.21: P-values for T_{r-tip} Regression Equation

Parameter Designation	Model Parameter	P-value
P1	$L_{arc}/L_{proj,w}$	0.039
P2	y/h_w	0.022
P3	$TW/L_{proj,cw}$	0.0001
P4	$L_{proj,cw}/L_{cw}$	0.0070
P5	A_w/A_c	0.0091
P6	R_c/TW	0.0006
P7	TW/y	Not Included

A review of studentized residuals revealed five possible outliers from T_{r-tip} analysis. Outliers were identified as those points having R-student residual values greater

than 2.0. The five outliers tabulated in Table 7.22 were removed from the regression analysis performed in Equation 7.19.

Table 7.22: Outliers from T_{r-tip} Analysis

Measured T_{r-tip}	Predicted T_{r-tip}	Residual	R-student Residual
0.807	2.082	-1.275	-3.63743
1.750	3.132	-1.382	-2.42829
0.923	1.845	-0.922	-2.60756
0.938	1.695	-0.757	-2.0696
1.011	1.713	-0.702	-1.44565

A plot of residuals in Figure 7.31 shows a scattered distribution in a band about 0 and the quantile plot in Figure 7.32 shows a linear relationship, both of which serve to validate statistical assumptions of multivariate regression.

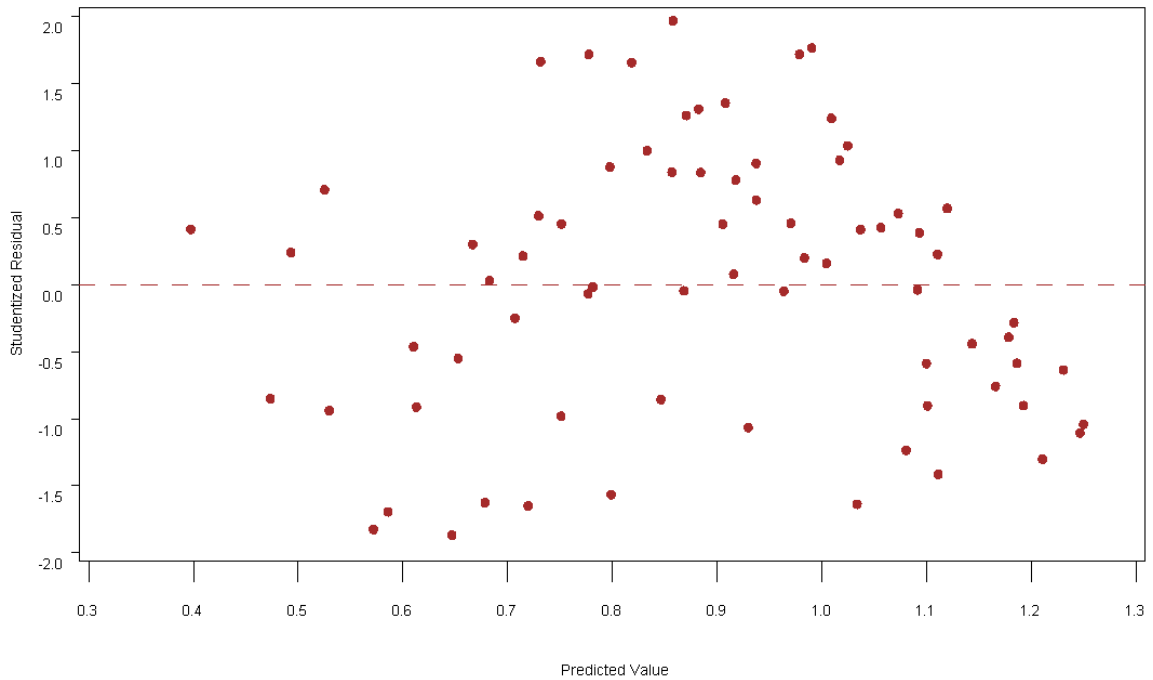


Figure 7.31: Residual Plot of the T_{r-tip} Analysis

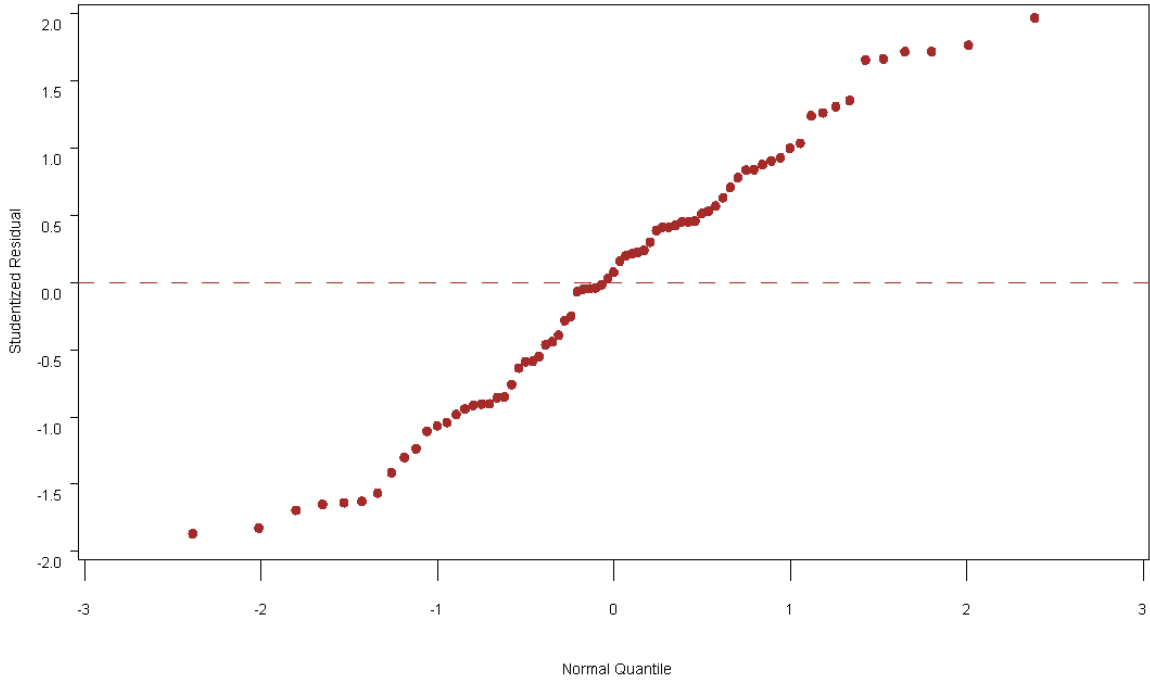


Figure 7.32: Quantile Plot of the Residuals from the T_{r-tip} Analysis

An envelope equation was developed to provide a conservative estimate for T_{r-tip} . The envelope equation for T_{r-tip} , presented in Equation 7.20, shows a range of values for the coefficient in Equation 7.19 such that all of the measured values are included in the envelope equation:

$$T_{r-tip-envelope} = C_{envelope} \left[\frac{\left(\frac{T_w}{L_{proj,cw}} \right)^{1.866} \left(\frac{A_w}{A_c} \right)^{0.780}}{\left(\frac{L_{arc}}{L_{proj,w}} \right)^{0.252} \left(\frac{y}{h_w} \right)^{0.327} \left(\frac{L_{proj,cw}}{L_{cw}} \right)^{0.958} \left(\frac{R_c}{T_w} \right)^{0.324}} \right]$$

Equation 7.20

where

$$C_{envelope} = 0.37 \text{ (lower) to } 0.76 \text{ (upper).}$$

Results of the T_{r-tip} regression analysis are shown in Figure 7.33 along with the upper envelope equation and the outliers, which were not included in the regression analysis.

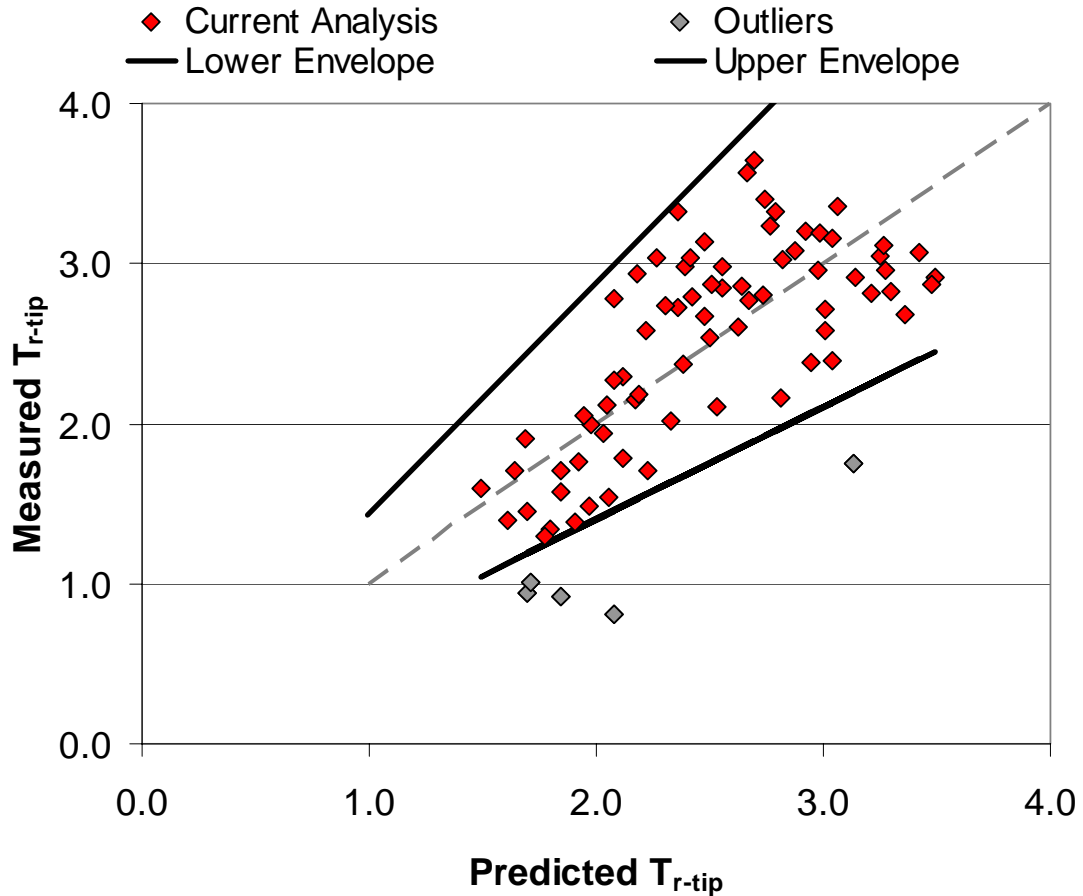


Figure 7.33: T_{r-tip} Analysis Showing Outliers and Upper Envelope

7.5 SUMMARY

By comparing velocity and shear-stress results from HEC-RAS computer models for each weir configuration to measured data, a total of ten regression equations were developed to assist in design of bendway weirs. Six of these regression equations relate the maximum measured velocity and shear stress to average centerline velocity and shear

stress from the HEC-RAS computer models. Four regression equations relate the maximum measured velocity and shear stress to the maximum computed velocity and shear stress from the HEC-RAS weir configuration models. Regression equations based on results from the HEC-RAS computer model provide a relationship for developing an appropriate weir field for given bend characteristics. Regression equations based on results from the HEC-RAS weir configuration computer models allow prediction of potential velocity or shear stresses for a given weir configuration and capture the entire variation in velocity and shear stress caused by the flow field around the bendway weirs. Prediction of the magnitude of velocity and shear stress increase based on a given bendway-weir geometry can then be used to properly design appropriate erosion countermeasures.

8 CONCLUSIONS AND RECOMMENDATIONS

8.1 OVERVIEW

The research presented has explored the use of the 1-D hydraulic software HEC-RAS to assist in the design of bendway weirs. Previous research has demonstrated that flow patterns associated with bendway weirs are characteristically 3-D, a fact that might preclude the use of such constrained software as HEC-RAS. However, complexity and resource needs of 3-D and 2-D hydraulic software renders them somewhat inaccessible by the engineering community as a whole. Its simplicity coupled with ubiquitous regulatory applications has caused HEC-RAS to become one of the hydraulic software programs most commonly used to model river systems. Understanding the fundamental dilemma of modeling a 3-D system on a 1-D platform, this research offers several tools to relate simplified cross-sectional and depth-averaged results from 1-D backwater computations to measured data at key locations associated with bendway weirs. Fundamentally, bendway weirs function by moving highly-abrasive flows away from the outer bank into the channel center. As a result, bendway weirs increase velocity and shear stresses in the constricted main channel. Research has shown that areas of particular concern are near the weir tips, in the inner bank opposite the weirs, and in the main channel where degradation is likely to occur. This research was completed in three main phases of effort:

1. finding a modeling scheme that could sufficiently be used to model bendway weirs in HEC-RAS,
2. comparisons of computed velocity and shear stress from baseline computer models to baseline physical data, and
3. comparisons of computed velocity and shear stress from physical data at the weir tip, inner bank opposite the weir tip, and in the channel center to computed HEC-RAS data (both baseline models and models of weir configurations).

8.2 MODELING TECHNIQUE

In the investigation of modeling techniques within HEC-RAS, it was assumed at the onset that chosen procedures were meant to replicate common engineering practices. While exploration of modeling schemes was not exhaustive, several of the most common approaches were investigated. Selection of a modeling scheme was based on how well the computed water-surface profile matched measured physical data. Table 8.1 summarizes the percent error for the chosen technique used to model the bendway weirs.

Table 8.1: Summary Average Percent Error between Computed and Measured Water Surface, Velocity, and Shear Stress for Selected Modeling Technique

Comparison	Average Percent Error		
	8 cfs	12 cfs	16 cfs
Water Surface	3.42%	3.57%	2.52%
Velocity at the Weir Tip	5.4%	29.4%	22.5%
Velocity at Inner Bank Across from Weir Tip	4.1%	32.0%	32.6%
Shear Stress at the Weir Tip	43.5%	63.8%	61.5%
Shear Stress at Inner Bank Across from Weir Tip	37.4%	64.6%	65.8%

In all, it was determined that the selected modeling scheme, generally shown in Figure 8.1 for one weir configuration, was adequate in modeling bendway-weir fields.

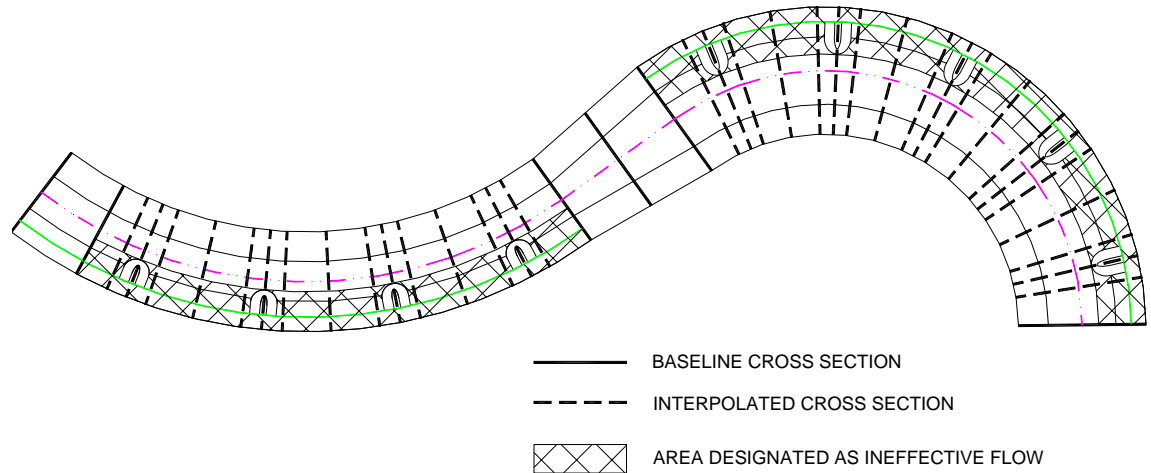


Figure 8.1: Summary of Cross-section Layout for Modeling Technique 4

In addition to the cross-section layout and ineffective flow areas around the weir fields shown in Figure 8.1, the weir geometry itself was modeled in the cross-section geometry. Roughness values were kept the same for all cross sections and no additional roughness was added to account for the weir material. Ineffective flow areas, shown in Figure 8.1, extended up to the design water-surface elevation. For water-surface elevations above the design flow elevation, ineffective areas were removed from hydraulic computations. Contraction and expansion coefficients were adjusted only in the transition area between the two bends based on the recommended values of 0.3 and 0.5, respectively.

8.3 BASELINE CONDITIONS

Baseline analysis consisted of first verifying the validity of the computed water-surface elevation from HEC-RAS and then comparing the cross-sectional averaged velocity and shear stress to the measured data collected within the meander bend. For all the discharges, the computed water-surface elevations matched the measured data within 1 percent and were generally adequate as a basis for creating subsequent weir models.

Overall, the computed velocity and shear stress from HEC-RAS were lower than measured in the physical model. A correction factor relationship, K_{BEND} , was computed to relate the HEC-RAS results to the measured data. For velocity, the K_{BEND} relationships, as a function of the radius of curvature (R_c) to top width (T_w) is shown in Table 8.2.

Table 8.2: Summary of $K_{BEND-VELOCITY}$ Analysis

Mean Regression	Upper Envelope
$K_{BEND-VELOCITY} = 1.099 \left(\frac{R_c}{T_w} \right)^{0.0841}$	$K_{BEND-VELOCITY(UPPER)} = 1.11 \left(\frac{R_c}{T_w} \right)^{0.098}$

Shear-stress K_{BEND} factors use the cross-sectional averaged HEC-RAS data as the normalizing factor. Table 8.3 shows K_{BEND} for shear stress as the ratio of the maximum measured shear stress in the bend to the cross-sectional average shear stress computed from HEC-RAS.

Table 8.3: Summary of $K_{BEND-SHEAR}$ Analysis Using Computed HEC-RAS Shear Stress

Mean Regression	Upper Envelope
$K_{BEND-SHEAR} = 2.47 \left(\frac{R_c}{Tw} \right)^{-0.235}$	$K_{BEND-SHEAR(UPPER)} = 3.20 \left(\frac{R_c}{Tw} \right)^{-0.266}$

Development of the K_{BEND} for shear stress was coupled with data from previous research, a total of thirty points, as compared to the eight points for the velocity relationships. Shear-stress equations show an inverse relationship between the K_{BEND} and the R_c/Tw , while the velocity equations show a direct relationship between K_{BEND} and R_c/Tw . Previous research suggested that the K_{BEND} for shear stress generally decreases towards unity for increasing R_c/Tw . Data collected from current tests at CSU, however, indicate that while the shear-stress K_{BEND} decreases with increasing R_c/Tw , K_{BEND} asymptotically approaches a value of 1.5 for high values of R_c/Tw . Further, current guidance published by Kilgore and Cotton (2005, *HEC-15*) potentially underpredicts K_{BEND} for high R_c/Tw . It is, therefore, concluded that the regression equations presented in Table 8.3 provide an estimate of K_{BEND} that is more conservative than methodology presented in Kilgore and Cotton (2005, *HEC-15*).

8.4 WEIR CONFIGURATIONS

Aside from the general layout of the bendway-weir field, the design engineer must sufficiently account for scouring forces at the weir tips and at the inner bank across from the weir tips. Knowing the increase in velocity and shear stress caused by installation of bendway weirs is fundamental to being able to design them effectively and counter abrasive forces. This research resulted in two sets of regression equations that

relate increased velocities and shear stresses caused by bendway weirs to results from 1-D computer software for baseline conditions and simulated weir fields. Table 8.4 summarizes the regression equations developed from velocity data and Table 8.5 summarizes the regression equations developed from shear-stress data.

Table 8.4: Summary of Velocity Analyses

$$MVR_{inner} = C_{MVR-inner} \left[\frac{\left(\frac{y}{h_w} \right)^{0.273} \left(\frac{A_w}{A_c} \right)^{0.083} \left(\frac{R_c}{Tw} \right)^{0.072}}{\left(\frac{L_{arc}}{L_{proj,w}} \right)^{0.095}} \right]$$

$$MVR_{tip} = C_{MVR-tip} \left[\left(\frac{y}{h_w} \right)^{0.103} \left(\frac{A_w}{A_c} \right)^{0.117} \left(\frac{R_c}{Tw} \right)^{0.211} \right]$$

$$MVR_{center} = C_{MVR-center} \left[\left(\frac{y}{h_w} \right)^{0.169} \left(\frac{A_w}{A_c} \right)^{0.142} \left(\frac{R_c}{Tw} \right)^{0.244} \right]$$

$$V_{r-inner} = C_{Vr-inner} \left[\frac{\left(\frac{y}{h_w} \right)^{0.256} \left(\frac{Tw}{L_{proj,cw}} \right)^{0.461} \left(\frac{A_w}{A_c} \right)^{0.282} \left(\frac{R_c}{Tw} \right)^{0.0923}}{\left(\frac{L_{arc}}{L_{proj,w}} \right)^{0.1045}} \right]$$

$$V_{r-tip} = C_{Vr-tip} \left[\frac{\left(\frac{y}{h_w} \right)^{0.179} \left(\frac{Tw}{L_{proj,cw}} \right)^{0.077} \left(\frac{R_c}{Tw} \right)^{0.288}}{\left(\frac{L_{arc}}{L_{proj,w}} \right)^{0.0975}} \right]$$

Table 8.5: Summary of Shear-stress Analyses

$$MTR_{inner} = C_{MTR-inner} \left[\frac{\left(\frac{Tw}{L_{proj,cw}} \right)^{1.226} \left(\frac{A_w}{A_c} \right)^{0.586}}{\left(\frac{R_c}{Tw} \right)^{0.181}} \right]$$

$$MTR_{tip} = C_{MTR-tip} \left[\frac{\left(\frac{Tw}{L_{proj,cw}} \right)^{1.622} \left(\frac{A_w}{A_c} \right)^{0.873} \left(\frac{R_c}{Tw} \right)^{0.326}}{\left(\frac{L_{arc}}{L_{proj,w}} \right)^{0.323} \left(\frac{L_{proj,cw}}{L_{cw}} \right)^{0.860}} \right]$$

$$MTR_{center} = C_{MTR-center} \left[\frac{\left(\frac{Tw}{L_{proj,cw}} \right)^{1.476} \left(\frac{A_w}{A_c} \right)^{0.869} \left(\frac{R_c}{Tw} \right)^{0.374}}{\left(\frac{L_{arc}}{L_{proj,w}} \right)^{0.294}} \right]$$

$$T_{r-inner} = C_{Tr-inner} \left[\frac{\left(\frac{Tw}{L_{proj,cw}} \right)^{1.714} \left(\frac{A_w}{A_c} \right)^{0.588}}{\left(\frac{L_{arc}}{L_{proj,w}} \right)^{0.178} \left(\frac{y}{h_w} \right)^{0.323} \left(\frac{L_{proj,cw}}{L_{cw}} \right)^{0.841}} \right]$$

$$T_{r-tip} = C_{Tr-tip} \left[\frac{\left(\frac{Tw}{L_{proj,cw}} \right)^{1.866} \left(\frac{A_w}{A_c} \right)^{0.780}}{\left(\frac{L_{arc}}{L_{proj,w}} \right)^{0.252} \left(\frac{y}{h_w} \right)^{0.327} \left(\frac{L_{proj,cw}}{L_{cw}} \right)^{0.958} \left(\frac{R_c}{Tw} \right)^{0.324}} \right]$$

For all the regression equations presented, envelope equations were developed in addition to the mean regression analysis. Envelope equations were developed by

modifying the mean regression equation to incorporate 100 percent of the data. Table 8.6 and Table 8.7 summarize the mean and the envelope coefficients used in the presented regression equations for the velocity and shear-stress relations, respectively.

Table 8.6: Velocity Coefficients for Regression Analyses

Analysis	Lower Envelope	Mean Regression	Upper Envelope
MVR_{inner}	1.50	1.67	1.87
MVR_{tip}	1.00	1.17	1.32
MVR_{center}	1.12	1.27	1.40
$V_{r-inner}$	0.87	1.035	1.19
V_{r-tip}	0.65	0.763	0.86

Table 8.7: Shear-stress Coefficients for Regression Analyses

Analysis	Lower Envelope	Mean Regression	Upper Envelope
MTR_{inner}	0.90	1.346	1.75
MTR_{tip}	0.60	0.944	1.40
MTR_{center}	0.85	1.216	1.70
$T_{r-inner}$	0.48	0.668	0.88
T_{r-tip}	0.37	0.527	0.76

Regression equations presented in Table 8.4 and Table 8.5 are meant to incorporate hydraulic conditions, bendway-weir layout parameters, and bend geometry in predictive equations that can be used by design engineers to give some indication of the increase in velocities and shear stresses at given locations.

From equations presented in Table 8.4 and Table 8.5, a procedure can be developed for the design of bendway weirs given characteristics of a channel bend. A design procedure developed from this research can be summarized in four steps:

1. Compile characteristics of site conditions such as bend radius of curvature, design flow rate, and slope.
2. Use MVR and MTR relationships presented in the first three rows of Table 8.4 and Table 8.5 to select a suitable bendway-weir layout configuration.
3. Develop a HEC-RAS computer model for the selected bendway-weir configuration based on the modeling technique described in Section 5.2.2.4.
4. Use V_r and T_r relationships in the last two rows of Table 8.4 and Table 8.5 to adjust the computed velocity and shear stress from the HEC-RAS computer model developed in Step 3 for the weir tip and along the opposite bank across from the weir tip.

From this four-step design procedure, a weir configuration can be selected and resulting increases in velocity and shear stresses can be countered with the appropriate river-armoring technique. Application of this design procedure is generally intended for conditions with $2 < R_c/Tw < 6$. Conservatism is provided in this design procedure through the selection of the leading coefficient for the regression equations and it is the judgement of the design engineer to understand and select appropriate values within the given range. It is recommended, however, that application of conservatism should be applied to the final step, Step 4, of the design procedure. The degree of conservatism chosen, either high or low, should be selected to match the specific physical characteristics of the application. Consideration should be given to the amount of scour expected through the constricted reach and the amount of sediment being transported from upstream sources through the design reach. Because the shear stress is shown in this research to be highly variable, it is possible that the envelope equations provided in

this design procedure may not provide enough conservatism in all potential practical applications. Care must, therefore, be given to the appropriate application of these results and employment of the design procedure should include a complete understanding of the data, data-collection methods, and physical limitations of this research.

8.5 RECOMMENDATIONS FOR FURTHER RESEARCH

In the analysis of data obtained from the physical model of the Middle Rio Grande, two bend configurations were investigated for three different discharges. Further research that includes additional bend geometries or weir configurations would supply valuable data and improve the quality of predictive regression models and support a more general application of design equations derived from regression analysis. Also, extension of the current research to include sloped weirs of various configurations might provide additional design equations for bendway weirs.

Presented baseline analyses focused primarily on velocity and shear-stress increase in the downstream direction. Further research could investigate strength of spiral flow in meander bends of varied geometries by using velocity data collected in the lateral (y) and vertical (z) directions. Comparison of strength of spiral flow with and without bendway weirs in place could provide some indication of the effectiveness of lateral flow disruption as well as locations of significant scour potential.

While this research focused on quantifying the magnitude of the velocity and shear-stress increase, no significant work was completed on the location of the maximum increase nor were the locations of the maximum baseline velocity and shear stress identified. Information as to the extent or specific location of the increased velocity and

shear stress could reduce the need for extensive erosion countermeasures. In addition, previous research has shown that the point of highest shear stress was located near the inner bank at the bend entrance; however, empirical evidence shows that the outer bank just downstream of the bend apex is most susceptible to failure. More research should be conducted to link these two observations, and to investigate the need for bank or bed protection at isolated points along the bend. Information on the location of the increased velocity and shear stress would be valuable in channels both with and without bendway weirs.

Finally, mobile-bed studies are necessary on bendway weirs to evaluate several characteristics associated with their main function of redirecting flow into the main channel from the outer bank. Previous research has stated that the increased scour potential caused by bendway weirs will tend to enlarge the main channel geometry, eventually reaching some sort of equilibrium. Mobile-bed studies are necessary to evaluate how long and to what extent this might be true. Further, research in a mobile-bed model is necessary to understand how various weir configurations affect local scour formation at critical locations, such as at the weir tips.

9 REFERENCES

- Abad, J.D., Rhoads, B.L., Guneralp, I., and Garcia, M.H. (2008). "Flow structure at different stages in a meander-bend with bendway weirs." *ASCE Journal of Hydraulic Engineering*, August:1052-1063.
- Ahmad, M. (1951). "Spacing and projection of spurs for bank protection." *Civil Engineering*, London, March: 172-174, April: 256-258.
- Ahmad, M. (1953). "Experiments on design and behavior of spur dikes." In: Proc. of the Minnesota International Hydraulics Convention, Minneapolis, MN, pp. 145-159.
- Bagnold, R.A. (1960). "Some aspects of the shape of river meanders." *U.S. Geological Survey Professional Paper 282E*, pp. 135-144.
- Biedenharn, D.S., Combs, P.G., Hill, G.J., Pinkard Jr., C.F., and Pinkiston, C.B. (1989). "Relationship between the channel migration and radius of curvature on the Red River." In: Proc. of the International Symposium on Sediment Transport and Modeling, ASCE, New York, pp. 536-541.
- Bledsoe, B.P. and Watson, C.C. (2001). "Logistic analysis of channel pattern thresholds: meandering, braiding, and incising." *Geomorphology*, 38(3-4):281-300.
- Brown, S.A. (1985). "Design of Spur-Type Streambank Stabilization Structures." *Report No. FHWA/RD-84/101*, Final Report, Federal Highway Administration, 98 p.

- Chang, H.H. (1988). "On the cause of river meandering." In: Proc. from the International Conference on River Regime, Hydraulics Research, Wallingford, UK, pp. 83-93.
- Chapman, P. (2007). "ST511 Design and Data Analysis for Researchers II." Colorado State University.
- Chapman, P. (2006). "ST511 Design and Data Analysis for Researchers I." Colorado State University.
- Chow, V.T. (1959). Open Channel Hydraulics. McGraw Hill, 680 pp.
- Copeland, R.R. (1983). "Bank Protection Techniques Using Spur Dikes." *Miscellaneous Paper HL-83-1*, U.S. Army Corps of Engineers, Waterways Experiment Station, 32 p.
- Darrow, J. (2004). "Effects of Bendway Weir Characteristics on Resulting Flow Conditions." M.S. Thesis, Colorado State University, Department of Civil Engineering, Fort Collins, CO.
- Derrick, D.L. (1998). "Four Years Later, Harland Creek Bendway Weir/Willow Post Bank Stabilization Demonstration Project." In: Proceedings of the 1998 International Water Resources Engineering Conference, Part 1 (of 2), August 3-7, Memphis, TN.
- Devore, J.L. (1995). Probability and Statistics for Engineering and the Sciences. International Thomson Publishing Inc., Belmont.
- Dietrich, W.E. (1987). "Mechanics of flow and sediment transport in river bends." In: Richards, K.S. (Ed.), River Channels: Environment and Process, Blackwell, Oxford, pp. 179-227.

- Ecological Specialists, Inc. (1997). "Macroinvertebrates Associated with the Carl Baer Bendway Weirs in the Mississippi River." Prepared for Parson Engineering Science Inc., under contract to the U.S. Army Corps of Engineers, St. Louis, MO.
- Escarameia, M. (1998). "River and channel revetments: A design manual." HR Wallingford, London, England.
- Federal Emergency Management Agency (2002). "National Flood Insurance Program." August.
- Federal Highway Administration (2006). "Design of Riprap Revetment." *Hydraulic Engineering Circular-14*, March.
- Federal Highway Administration (2001). "Highways in the River Environment." Engineering Research Center, Colorado State University, Prepared for U.S. Department of Transportation, Federal Highway Administration.
- Federal Highway Administration. (1989). "Design of Riprap Revetment." *Hydraulic Engineering Circular-11*, March.
- Garde, R.J., Subramanya, K., and Nambudripad, K.D. (1961). "Study of scour around spur-dikes." *Journal of the Hydraulics Division, Proceedings of the American Society of Civil Engineers*, 87(HY6):23-37.
- Gill, M.A. (1972). "Erosion of sand beds around spur dikes." *Journal of the Hydraulics Division, Proceedings of the American Society of Civil Engineers*, 98(HY9):1587-1602.
- Haltigin, T.W., Biron, P.M, and Lapointe, M.F. (2007). "Predicting equilibrium scour-hole geometry near angled stream deflectors using a three-dimensional numerical flow model." *ASCE Journal of Hydraulic Engineering*, August:983-988.

- Heintz, M.L. (2002). "Investigation of Bendway Weir Spacing." M.S. Thesis, Colorado State University, Department of Civil Engineering, Fort Collins, CO.
- Hey, R.D. (1976). "Geometry of river meanders." *Nature*, 262:482-484.
- Hickin, E.J. and Nanson, G.C. (1984). "Lateral migration rates of river bends." *Journal of Hydraulic Engineering*, 110:1557-1567.
- Hickin, E.J. and Nanson, G.C. (1975). "The character of channel migration on the Beatton River, north-east British Columbia, Canada." *Bulletin of the Geological Society of America*, 86:487-494.
- Indian Central Board of Irrigation and Power (ICBIP) (1971). "Manual on River Behavior, Control and Training." *Publication No. 60*, New Delhi, September.
- Inglis, C.C. (1949). "The Behavior and Control of Rivers and Canals." *Research Publication No. 13, Parts I and II*, Central Waterpower Irrigation and Navigation Research Station, Poona, India.
- Ippen, A.T. and Drinker, P.A. (1962). "Boundary shear stresses in curved trapezoidal channels." *ASCE Journal of the Hydraulics Division*, September:143-175.
- Ippen, A.T., Drinker, P.A., Jobin, W.R., and Shemdin, O.H. (1962). "Stream Dynamics and Boundary Shear Distributions for Curved Trapezoidal Channels." *Technical Report No. 47*, Department of Civil and Sanitary Engineering, Massachusetts Institute of Technology, January.
- Ippen, A.T., Drinker, P.A., Jobin, W.R., and Noutsopoulos, G.K. (1960a). "The Distribution of Boundary Shear Stresses in Curved Trapezoidal Channels." *Technical Report No. 43*, Department of Civil and Sanitary Engineering, Massachusetts Institute of Technology, October.

- Ippen, A.T., Drinker, P.A., Jobin, W.R., and Noutsopoulos, G.K. (1960b). "Basic Data Supplement to Technical Report 43: The Distribution of Boundary Shear Stresses in Curved Trapezoidal Channels." *Technical Report No. 43-S*, Department of Civil and Sanitary Engineering, Massachusetts Institute of Technology, October.
- Jia, Y., Scott, S., Xu, Y., Huang, S., and Wang, S.S. (2005). "Three-dimensional numerical simulation and analysis of flows around a submerged weir in a channel bendway." *ASCE Journal of Hydraulic Engineering*, August:682-693.
- Julien, P.Y. (2002). River Mechanics. Cambridge University Press, New York.
- Kasper, K. (2005). "Accuracy of HEC-RAS to Calculate Flow Depths and Total Energy Loss With and Without Bendway Weirs in a Meander Bend." M.S. Plan-B Report, Colorado State University, Department of Civil Engineering, Fort Collins, CO.
- Kilgore, R.T. and Cotton G.K. (2005). "Design of Roadside Channels with Flexible Linings." *HEC-15*, Federal Highway Administration, September.
- Kinzli, K. (2005). "Effects of Bendway Weir Characteristics on Resulting Eddy and Channel Flow Conditions." M.S. Thesis, Colorado State University, Department of Civil Engineering, Fort Collins, CO.
- Knight, Donald W., Yuan, Y.M., and Fares, Y.R. (1992) "Boundary Shear in Meandering Channels." International Symposium on Hydraulic Research in Nature and Laboratory, Nov. 17-20, 1992.
- Knighton, D. (1998). Fluvial Forms and Processes: A New Perspective. Oxford University Press Inc., New York, NY, 383 p.

- Lagasse, P.F., Clopper, P.E., Zevenbergen, L.W., and Ruff, J.F. (2006). "Riprap Design Criteria, Recommended Specifications, and Quality Control." *Report 568*, National Cooperative Highway Research Program, September.
- Lane, E.W. (1955). "Design of stable channels." *ASCE Trans.*, 120(2776):1234-1260.
- Laursen, E.M. (1962a). "Scour at bridge crossings." *ASCE Transactions*, Paper No. 3294, 127(Part I):166-180.
- Laursen, E.M. (1962b). "Discussion of 'Study of scour around spur dikes'." *Journal, Hydraulics Division, ASCE*, 89(HY3):225-228.
- Leopold, L.B., Wolman, M.G., and Miller, J.P. (1964). Fluvial Processes in Geomorphology. First published in 1964, W.H. Freeman and Company, San Francisco, CA (reprinted in 1992 by Dover Publications, Inc., New York, NY).
- Liu, H.K., Chang, F.M., and Skinner, M.M. (1961). "Effect of Bridge Construction on Scour and Backwater." *Report No. CER60-HKL22*, Department of Civil Engineering, Colorado State University, Fort Collins, CO.
- Molls, T., Chaudhry, M.H., and Khan, K.W. (1995). "Numerical simulation of two-dimensional flow near a spur dike." *Advances in Water Resources*, 18(4):227-236.
- Nanson, G.C. and Hickin, E.J. (1986). "A statistical examination of bank erosion and channel migration in western Canada." *Bulletin of the Geological Society of America*, 97:497-504.
- Ott, R.L. and Longnecker, M. (2001). An Introduction to Statistical Methods and Data Analysis. 5th Edition, Duxbury, Pacific Grove, CA.
- Pemberton, E.L. and Lara, J.M. (1984). "Computing Degradation and Local Scour." U.S. Bureau of Reclamation Technical Guideline, January.

- Pokrefke, T. (1990). "Historical Overview and Design of Stone Spur Dikes." U.S. Army Corps of Engineers, Waterways Experiment Station, Vicksburg, MS.
- Preston, J.H. (1954) "The determination of turbulent skin friction by means of pitot tubes." *Journal of the Royal Aeronautical Society*, 58:109-121.
- Przedwojski, B., Blazejewski, R., and Pilarczyk, K.W. (1995). River Training Techniques. Rotterdam, Netherlands, A.A. Balkema, 625 p.
- Rapp, J. (1997). "Sampling Shows Fish Find Homes in Bendway Weirs." U.S. Army Corps of Engineers, St. Louis District, July.
- Richardson, E.V. and Simons D.B. (1974). "Spur and Guide Banks." *Open File Report*, Colorado State University Engineering Research Center, Fort Collins, CO, February.
- Rouse, H. (1946). Elementary Fluid Mechanics. Dover Publications, Inc., New York.
- Rozovskii, I.L. (1957). Flow of Water in Bends of Open Channels. Academy of Sciences of the Ukrainian SSR, Kiev, 233 p.
- Sanchez V. and Baird D. (1997). "River Channel Changes Downstream of Cochiti Dam Middle Rio Grande, New Mexico." U.S. Department of Interior, Bureau of Reclamation, River Analysis Team, Albuquerque Area Office, Albuquerque, NM.
- Schmidt, P. (2005). "Effects of Bendway Weir Field Geometric Characteristics on Channel Flow Conditions." M.S. Thesis, Colorado State University, Department of Civil Engineering, Fort Collins, CO.
- Schumm, S.A. and Brakenridge, G.R. (1987). "River responses." In: W.F. Ruddiman and H.E. Wright Jr. (Eds.), North America and Adjacent Oceans During the Last Deglaciation, Geological Society of America, K-3, pp. 221-240.

- Sclafani, P. (2008). "Preston Tube Calibration." *Open File Report*, Colorado State University, Engineering Research Center, Fort Collins, Colorado, July.
- Seed, D.J. (1997). "Guidelines on the Geometry of Groynes for River Training." *Report SR 493HR*, Wallingford.
- Shukry, A. (1950). "Flow around bends in an open flume." *ASCE Transactions*, 115(2411):751-779.
- Thompson, J. (1876). "On the origin of windings of rivers in alluvial plains, with remarks on the flow of water round bends in pipes." *Proc. of the Royal Society of London*, 25:5-8.
- United Nations (1953). "River Training and Bank Protection." *Flood Control Series No. 4*, United Nations Economic Commission for Asia and the Far East, Bangkok.
- U.S. Army Corps of Engineers (USACE) (2008). "HEC-RAS River Analysis System." *Hydraulic Reference Manual – Version 3.1*, Hydrologic Engineering Center, U.S. Army Corps of Engineers, Davis, CA.
- U.S. Army Corps of Engineers (USACE) (1991). "Engineering and Design – Hydraulic Design of Flood Control Channels." *Engineering Manual EM-1110-2-1601*, Department of the Army, U.S. Army Corps of Engineers, Washington, DC, First published July 1, 1991 (reprinted June 30, 1994).
- U.S. Army Corps of Engineers (USACE) (1980). "Layout and Design of Shallow-Draft Waterways." *Engineering Manual EM 1110-2-1611*, U.S. Army Corps of Engineers Waterways Experiment Station Vicksburg, MS (<http://www.usace.army.mil/inet/usace-docs/eng-manuals/em1110-2-1611/entire.pdf>).

- U.S. Bureau of Reclamation (USBR) (1977). "Design of Small Dams." U.S. Department of Interior, U.S. Government Printing Office.
- U.S. Bureau of Reclamation (USBR) (1964). "Progress Report I Boundary Shear Distribution around a Curve in a Laboratory Canal." *Report No. Hyd-526*, June.
- Van den Berg, J.H. (1995). "Prediction of alluvial channel pattern of perennial rivers." *Geomorphology*, 12(1995):259-279.
- Watson, C.C., Biedenharn, D.S., and Thorne, C.R. (2004). Channel Rehabilitation. Colorado State University.
- Welch S. and Wright, S. (2005). "Design of Stream Barbs." *Technical Note 23*, Natural Resource Conservation Service, Portland, OR, April.
- Whitney, J.C. (1996). "The Middle Rio Grande: Its ecology and management." In: Proc. Desired Future Conditions for the Southwestern Riparian Ecosystems: Bringing Interest and Concerns Together, U.S. Department of Agriculture, *General Technical Report RM-GTR-272*, pp. 4-21.
- Wilcox, D.C. (2007). Basic Fluid Mechanics. 3rd Edition, DCW Industries.
- Willkerson, C.A. (1972). "Stone dikes for river channels." *The Military Engineer*, March-April.
- Winkler, M.F. (2003). "Defining Angle and Spacing of Bendway Weirs." U.S. Army Corps of Engineers, Coastal Hydraulics Laboratory.
- Wohl, E. (2004). Disconnected Rivers, Linking Rivers to Landscapes. Yale University Press, New Haven.

Yen, B.C. (1965). "Characteristics of Subcritical Flow in a Meandering Channel." Ph.D
Dissertation, University of Iowa, Department of Mechanics and Hydraulics, Iowa
City, IA, June.

APPENDIX A BASELINE SURVEY

Table A.1: Baseline Survey from Heintz (2002)

Point Number	Northing	Easting	Elevation	Description	Heintz (2002) Cross-section Number
0	5000	5000	100	START	Control
1	5060.74	5037.01	95.60	SE corner of electrical pad.	Control
2	5077.41	4975.62	103.23	NW corner of building	Control
3	5008.40	4982.67	95.13	Control Point A	Control
4	4923.26	4978.22	95.13	Control Point B	Control
5	5051.371097	4990.925927	98.658515	RTOPBANK XS#0	0
6	5053.49415	4990.971138	97.95746	WS XS#0	0
7	5055.204244	4990.968198	97.402225	WS XS#0	0
8	5055.816427	4991.034152	97.219145	RREBAR XS#0	0
9	5057.836997	4991.029944	97.238458	WS XS#0	0
10	5060.964426	4991.110404	97.221128	WS XS#0	0
11	5063.715484	4991.15864	97.223829	WS XS#0	0
12	5065.875743	4991.173423	97.224255	LREBARXS#0	0
13	5067.336986	4991.20905	97.700467	WS XS#0	0
14	5068.682756	4991.239317	98.175036	WS XS#0	0
15	5070.20088	4991.263107	98.684697	LTOPBANK XS#0	0
338	5049.18154	4998.710176	98.800494	WS XS#1	1
339	5049.983478	4998.86173	98.804061	RTOPBANK XS#1	1
340	5051.238724	4999.190446	98.280128	WS XS#1	1
341	5052.435931	4999.502407	97.896076	WS XS#1	1
342	5053.446652	4999.794066	97.537247	WS XS#1	1
343	5054.320276	5000.123006	97.277466	RREBAR XS#1	1
344	5055.86827	5000.491546	97.265503	WS XS#1	1
345	5057.602173	5001.059827	97.264421	WS XS#1	1
346	5059.15489	5001.491407	97.25472	WS XS#1	1
347	5060.618316	5001.909132	97.244354	WS XS#1	1
348	5062.545948	5002.500745	97.252407	WS XS#1	1

Point Number	Northing	Easting	Elevation	Description	Heintz (2002) Cross-section Number
349	5064.125675	5002.92983	97.283794	LREBARXS#0	1
350	5064.989595	5003.216034	97.570209	WS XS#1	1
351	5066.143708	5003.529689	97.939002	WS XS#1	1
352	5067.46258	5003.899228	98.417736	LTOPBANK XS#1	1
353	5068.366866	5004.21999	98.734583	WS XS#1	1
354	5069.992411	5004.690431	98.756596	WS XS#1	1
54	5064.033718	5017.380001	98.71073	WS XS#2	2
55	5063.092154	5016.7281	98.72637	WS XS#2	2
56	5062.854446	5016.564869	98.72292	LTOPBANK XS#2	2
57	5061.963232	5015.877646	98.349358	WS XS#2	2
58	5060.976585	5015.242595	97.944115	WS XS#2	2
59	5059.7309	5014.636773	97.486983	WS XS#2	2
60	5059.10849	5014.223839	97.24806	WS XS#2	2
61	5058.049748	5013.639643	97.229185	LREBARXS#2	2
62	5056.736934	5012.693119	97.218476	WS XS#2	2
63	5054.694383	5011.577084	97.211572	WS XS#2	2
64	5052.815363	5010.464721	97.219931	WS XS#2	2
65	5051.143434	5009.501262	97.208455	WS XS#2	2
66	5050.377478	5008.894142	97.233527	RREBAR XS#2	2
67	5049.699781	5008.517357	97.46336	WS XS#2	2
68	5048.435829	5007.815215	97.948098	WS XS#2	2
69	5047.063349	5006.965462	98.503504	WS XS#2	2
70	5046.408213	5006.642212	98.738245	RTOPBANK XS#2	2
71	5045.555484	5006.100606	98.750975	WS XS#2	2
72	5044.561362	5005.34632	98.74337	WS XS#2	2
95	5038.908111	5009.341776	98.764265	WS XS#3	3
96	5040.096348	5010.528063	98.774994	WS XS#3	3
97	5040.926116	5011.35271	98.758156	WS XS#3	3
98	5041.448517	5012.07367	98.741205	RTOPBANK XS#3	3

Point Number	Northing	Easting	Elevation	Description	Heintz (2002) Cross-section Number
99	5042.226099	5012.856672	98.386759	WS XS#3	3
100	5042.964975	5013.70164	98.009989	WS XS#3	3
101	5043.864575	5014.576104	97.625584	WS XS#3	3
102	5044.552877	5015.351489	97.275238	RREBAR XS#3	3
103	5045.737699	5016.70367	97.24075	WS XS#3	3
104	5046.740346	5017.768956	97.244441	WS XS#3	3
105	5048.105328	5019.041052	97.243908	WS XS#3	3
106	5048.957006	5020.165682	97.252598	WS XS#3	3
107	5049.956288	5021.306068	97.258961	WS XS#3	3
108	5051.422302	5022.863173	97.262104	LREBARXS#3	3
109	5051.982781	5023.63306	97.563809	WS XS#3	3
110	5052.942624	5024.668317	98.019239	WS XS#3	3
111	5053.748742	5025.575866	98.427066	WS XS#3	3
112	5054.461082	5026.374862	98.7615	LTOPBANK XS#3	3
113	5055.394754	5027.503538	98.727575	WS XS#3	3
114	5056.493109	5028.940843	98.735354	WS XS#3	3
134	5033.877416	5014.151844	98.742005	WS XS#4	4
135	5034.391278	5015.376563	98.729589	WS XS#4	4
136	5035.089116	5016.439765	98.730264	RTOPBANK XS#4	4
137	5035.569049	5017.502743	98.35056	WS XS#4	4
138	5036.00968	5018.356538	98.01879	WS XS#4	4
139	5036.555279	5019.436983	97.62939	WS XS#4	4
140	5037.126461	5020.54839	97.248484	RREBAR XS#4	4
141	5037.746147	5021.976476	97.22343	WS XS#4	4
142	5038.575563	5023.463043	97.243499	WS XS#4	4
143	5039.455078	5025.033313	97.239339	WS XS#4	4
144	5040.188716	5026.41378	97.250712	WS XS#4	4
145	5040.934762	5028.064082	97.23848	WS XS#4	4
146	5041.655208	5029.572457	97.252824	LREBARXS#4	4

Point Number	Northing	Easting	Elevation	Description	Heintz (2002) Cross-section Number
147	5042.095444	5030.62301	97.574664	WS XS#4	4
148	5042.6904	5031.792043	98.015817	WS XS#4	4
149	5043.308392	5032.869811	98.426796	WS XS#4	4
150	5043.716569	5033.670106	98.734546	LTOPBANK XS#4	4
151	5044.19389	5034.70023	98.712663	WS XS#4	4
152	5044.605971	5035.568516	98.705519	WS XS#4	4
172	5031.798467	5039.783709	98.658076	WS XS#5	5
173	5031.631788	5038.855698	98.684008	WS XS#5	5
174	5031.457593	5037.982388	98.725868	LTOPBANK XS#5	5
175	5031.185726	5036.70155	98.277838	WS XS#5	5
176	5030.988014	5035.786784	97.966801	WS XS#5	5
177	5030.759242	5034.57762	97.554997	WS XS#5	5
178	5030.524791	5033.617347	97.227286	LREBARXS#5	5
179	5030.119963	5031.480171	97.225023	WS XS#5	5
180	5029.86522	5030.29668	97.216596	WS XS#5	5
181	5029.488123	5028.554365	97.217779	WS XS#5	5
182	5029.195937	5026.975843	97.225853	WS XS#5	5
183	5028.937138	5025.391371	97.214595	WS XS#5	5
184	5028.586887	5023.605206	97.253858	RREBAR XS#5	5
185	5028.360588	5022.501828	97.58656	WS XS#5	5
186	5028.166032	5021.452013	97.921263	WS XS#5	5
187	5027.924584	5020.14335	98.383028	WS XS#5	5
188	5027.714523	5019.145893	98.736774	RTOPBANK XS#5	5
189	5027.433148	5017.5336	98.816105	WS XS#5	5
190	5027.270289	5016.04475	98.816974	WS XS#5	5
210	5018.277109	5039.605272	98.620738	WS XS#6	6
211	5018.290785	5038.713538	98.763638	WS XS#6	6
212	5018.330548	5037.568482	98.335591	LTOPBANK XS#6	6
213	5018.492483	5036.332888	97.896832	WS XS#6	6

Point Number	Northing	Easting	Elevation	Description	Heintz (2002) Cross-section Number
214	5018.515143	5035.278885	97.560122	WS XS#6	6
215	5018.593648	5034.199358	97.240522	LREBARXS#6	6
216	5018.74025	5033.135579	97.171832	WS XS#6	6
217	5018.81945	5031.427749	97.231952	WS XS#6	6
218	5018.972622	5029.206368	97.205918	WS XS#6	6
219	5019.150991	5027.693998	97.245656	WS XS#6	6
220	5019.242958	5025.95849	97.245673	WS XS#6	6
221	5019.466276	5024.155061	97.285479	RREBAR XS#6	6
222	5019.462778	5022.971941	97.609087	WS XS#6	6
223	5019.606843	5021.422673	98.126896	WS XS#6	6
224	5019.677984	5019.576131	98.757405	WS XS#6	6
225	5019.681673	5018.353724	98.786435	WS XS#6	6
226	5019.776111	5016.880933	98.805705	RTOPBANK XS#6	6
227	5019.914768	5015.973303	98.770985	WS XS#6	6
246	5004.284877	5039.116173	98.717158	WS XS#7	7
247	5004.843202	5037.555987	98.664141	WS XS#7	7
248	5005.453107	5035.905926	98.687125	LTOPBANK XS#7	7
249	5005.860107	5034.793965	98.300811	WS XS#7	7
250	5006.298246	5033.682257	97.926311	WS XS#7	7
251	5006.5839	5032.716869	97.496403	WS XS#7	7
252	5007.022898	5031.741006	97.229498	LREBARXS#7	7
253	5007.476688	5030.138088	97.138056	WS XS#7	7
254	5008.107469	5028.311799	97.238058	WS XS#7	7
255	5008.563364	5026.96492	97.146807	WS XS#7	7
256	5009.12925	5025.369029	97.262027	WS XS#7	7
257	5009.689647	5023.693787	97.240769	WS XS#7	7
258	5010.327157	5022.132962	97.211564	RREBAR XS#7	7
259	5010.721941	5021.068577	97.563134	WS XS#7	7
260	5011.085923	5020.076195	97.976125	WS XS#7	7

Point Number	Northing	Easting	Elevation	Description	Heintz (2002) Cross-section Number
261	5011.529451	5018.925464	98.359964	WS XS#7	7
262	5011.931066	5017.911323	98.697648	RTOPBANK XS#7	7
263	5012.886535	5016.127804	98.80697	WS XS#7	7
264	5013.523933	5014.559645	98.789403	WS XS#7	7
283	4992.081526	5031.81751	98.720035	WS XS#8	8
284	4993.585	5029.748027	98.712972	LTOPBANK XS#8	8
285	4994.464683	5028.644852	98.290335	WS XS#8	8
286	4995.191718	5027.718854	97.852927	WS XS#8	8
287	4995.791652	5026.811914	97.479981	WS XS#8	8
288	4996.336151	5026.133636	97.230185	LREBARXS#8	8
289	4997.219397	5024.92789	97.201026	WS XS#8	8
290	4998.468061	5023.157136	97.195903	WS XS#8	8
291	4999.280531	5022.008692	97.191028	WS XS#8	8
292	5000.250435	5020.669376	97.189397	WS XS#8	8
293	5001.324364	5019.128975	97.186765	WS XS#8	8
294	5002.296641	5017.963371	97.216059	RREBAR XS#8	8
295	5002.884257	5017.025473	97.560523	WS XS#8	8
296	5003.53946	5016.021008	97.956819	WS XS#8	8
297	5004.273111	5014.926388	98.415598	WS XS#8	8
298	5004.733087	5014.158346	98.733764	RTOPBANK XS#8	8
299	5005.705552	5012.349692	98.689916	WS XS#8	8
300	5006.75572	5010.520125	98.700225	WS XS#8	8
318	4998.468492	5005.464588	98.709333	WS XS#9	9
319	4997.043788	5007.258287	98.694595	WS XS#9	9
320	4995.829237	5008.973188	98.738773	RTOPBANK XS#9	9
321	4995.166897	5009.979485	98.298296	WS XS#9	9
322	4994.452126	5010.941857	97.902112	WS XS#9	9
323	4993.857457	5012.009742	97.506529	WS XS#9	9
324	4993.315575	5012.666358	97.213842	RREBAR XS#9	9

Point Number	Northing	Easting	Elevation	Description	Heintz (2002) Cross-section Number
325	4992.472119	5013.872197	97.20729	WS XS#9	9
326	4991.554458	5015.020233	97.210117	WS XS#9	9
327	4990.896556	5015.923575	97.197474	WS XS#9	9
328	4990.288472	5016.772411	97.206321	WS XS#9	9
329	4989.186779	5018.120603	97.203601	WS XS#9	9
330	4988.431104	5019.181627	97.208565	LREBARXS#9	9
331	4987.669388	5019.963361	97.547094	WS XS#9	9
332	4986.885251	5020.886304	98.007067	WS XS#9	9
333	4985.958328	5021.863405	98.421951	WS XS#9	9
334	4985.434553	5022.495907	98.700964	LTOPBANK XS#9	9
335	4984.534025	5023.406941	98.713068	WS XS#9	9
336	4982.867231	5025.152007	98.726641	WS XS#9	9
337	4982.176559	5025.862818	98.730304	WS XS#9	9
373	4988.979949	4999.81855	98.676517	WS XS#10	10
374	4987.822267	5001.814414	98.616168	WS XS#10	10
375	4986.666817	5003.697392	98.620328	RTOPBANK XS#10	10
376	4985.991261	5004.878115	98.180217	WS XS#10	10
377	4985.339615	5005.818271	97.783196	WS XS#10	10
378	4984.657925	5006.864719	97.350042	WS XS#10	10
379	4984.301355	5007.529049	97.124384	RREBAR XS#10	10
380	4983.189398	5008.928981	97.105064	WS XS#10	10
381	4982.469109	5009.844247	97.114387	WS XS#10	10
382	4981.605921	5010.988572	97.104748	WS XS#10	10
383	4980.660742	5012.242798	97.115604	WS XS#10	10
384	4979.985639	5013.292539	97.494467	WS XS#10	10
385	4979.248257	5014.171421	97.886911	LREBARXS#10	10
386	4978.372743	5015.063759	98.306034	WS XS#10	10
387	4977.822864	5015.809373	98.614662	WS XS#10	10
388	4976.402054	5017.944869	98.65323	WS XS#10	10

Point Number	Northing	Easting	Elevation	Description	Heintz (2002) Cross-section Number
389	4975.161236	5019.938836	98.662943	LTOPBANK XS#10	10
390	4974.396177	5021.145226	98.63514	WS XS#10	10
406	4978.636256	4993.55797	98.63992	WS XS#11	11
407	4977.611205	4995.72547	98.630698	WS XS#11	11
408	4976.697002	4997.535508	98.639875	LTOPBANK XS#11	11
409	4976.071583	4998.849668	98.156715	WS XS#11	11
410	4975.443161	4999.625262	97.76815	WS XS#11	11
411	4974.897143	5000.678538	97.378381	WS XS#11	11
412	4974.626627	5001.445375	97.14428	LREBARXS#11	11
413	4973.919675	5003.019816	97.126483	WS XS#11	11
414	4973.37896	5004.157244	97.116528	WS XS#11	11
415	4972.77872	5005.518567	97.127813	WS XS#11	11
416	4972.132377	5006.836035	97.13392	RREBAR XS#11	11
417	4971.635973	5007.81575	97.488493	WS XS#11	11
418	4971.131895	5008.780526	97.839755	WS XS#11	11
419	4970.491106	5010.009654	98.309459	WS XS#11	11
420	4969.970458	5010.823297	98.635978	RTOPBANK XS#11	11
421	4968.383933	5013.798235	98.646882	WS XS#11	11
422	4966.932135	5016.52667	98.64698	WS XS#11	11
438	4967.803676	4987.146973	98.65853	WS XS#12	12
439	4966.828334	4990.386696	98.614395	WS XS#12	12
440	4965.973308	4993.162326	98.614565	LTOPBANK XS#12	12
441	4965.463171	4994.421068	98.17686	WS XS#12	12
442	4965.066776	4995.476737	97.765329	WS XS#12	12
443	4964.724534	4996.760004	97.349143	WS XS#12	12
444	4964.165837	4999.20983	97.136319	LREBARXS#12	12
445	4963.741322	5000.301326	97.127793	WS XS#12	12
446	4963.141776	5002.009831	97.133138	WS XS#12	12
447	4962.854006	5003.191184	97.133719	RREBAR XS#12	12

Point Number	Northing	Easting	Elevation	Description	Heintz (2002) Cross-section Number
448	4962.497025	5004.289937	97.503311	WS XS#12	12
449	4962.186907	5005.251581	97.861884	WS XS#12	12
450	4961.706878	5006.569973	98.314713	WS XS#12	12
451	4961.442108	5007.490831	98.644135	RTOPBANK XS#12	12
452	4960.707459	5010.347014	98.668076	WS XS#12	12
453	4959.98172	5012.409609	98.670389	WS XS#12	12
467	4954.760671	4986.724713	98.608466	WS XS#13	13
468	4954.540218	4988.950206	98.582758	WS XS#13	13
469	4954.273229	4990.59724	98.571433	RTOPBANK XS#13	13
470	4954.084335	4992.112326	98.053859	WS XS#13	13
473	4953.91227	4992.931635	97.776102	WS XS#13	13
474	4953.735451	4994.515733	97.25858	WS XS#13	13
475	4953.671221	4995.059283	97.094858	RREBAR XS#13	13
476	4953.598831	4996.955037	97.073546	WS XS#13	13
477	4953.412726	4998.013237	97.07169	WS XS#13	13
478	4953.16061	4999.742474	97.072514	WS XS#13	13
479	4952.906129	5001.010125	97.09839	LREBARXS#13	13
480	4952.74162	5002.002312	97.413887	WS XS#13	13
481	4952.513358	5003.31086	97.864936	WS XS#13	13
482	4952.364688	5004.526294	98.311574	WS XS#13	13
483	4952.25211	5005.414365	98.600413	LTOPBANK	13
484	4952.092626	5006.646456	98.579479	WS XS#13	13
485	4951.948557	5007.730046	98.585189	WS XS#13	13
500	4942.831296	4986.691162	98.565342	WS XS#14	14
501	4942.576005	4988.423845	98.573695	WS XS#14	14
502	4942.570045	4989.959471	98.582958	RTOPBANK XS#14	14
503	4942.597574	4991.163961	98.162659	WS XS#14	14
504	4942.618075	4992.445965	97.73889	WS XS#14	14
505	4942.631452	4993.776713	97.284425	WS XS#14	14

Point Number	Northing	Easting	Elevation	Description	Heintz (2002) Cross-section Number
506	4942.652077	4994.485168	97.083501	RREBAR XS#14	14
507	4942.7342	4996.276823	97.075522	WS XS#14	14
508	4942.805632	4997.452882	97.067491	WS XS#14	14
509	4942.778414	4999.077532	97.055368	WS XS#14	14
510	4942.857676	5000.410229	97.081018	LREBARXS#14	14
511	4942.8713	5001.232366	97.321801	WS XS#14	14
512	4942.931086	5002.257492	97.703474	WS XS#14	14
513	4943.023076	5003.792886	98.230432	WS XS#14	14
514	4942.997319	5004.957607	98.579011	LTOPBANK XS#14	14
515	4943.110562	5006.347194	98.582891	WS XS#14	14
530	4930.387285	4986.704896	98.559556	WS XS#15	15
531	4930.658892	4989.052698	98.549216	WS XS#15	15
532	4930.886909	4991.217987	98.537122	RTOPBANK XS#15	15
533	4931.120147	4992.543357	98.128503	WS XS#15	15
534	4931.358001	4993.625613	97.731861	WS XS#15	15
535	4931.657158	4994.827139	97.322275	WS XS#15	15
536	4931.805875	4995.623295	97.061765	RREBAR XS#15	15
537	4932.115201	4997.265375	97.0522	WS XS#15	15
538	4932.353894	4998.592973	97.052677	WS XS#15	15
539	4932.571232	5000.060601	97.053446	WS XS#15	15
540	4932.871076	5001.521089	97.06926	LREBARXS#15	15
542	4933.278192	5003.628877	97.78017	WS XS#15	15
543	4933.525406	5004.88543	98.204202	WS XS#15	15
544	4933.923547	5005.904606	98.556359	LTOPBANK XS#15	15
545	4934.056088	5006.349924	98.55555	WS XS#15	15
561	4918.616852	4991.645945	98.58188	WS XS#16	16
562	4918.962874	4992.373594	98.57022	WS XS#16	16
563	4919.130154	4993.371998	98.557273	WS XS#16	16
564	4919.59692	4994.340935	98.558133	RTOPBANK XS#16	16

Point Number	Northing	Easting	Elevation	Description	Heintz (2002) Cross-section Number
565	4920.030774	4995.320188	98.221015	WS XS#16	16
566	4920.500699	4996.757948	97.70318	WS XS#16	16
567	4920.903523	4997.964531	97.268615	WS XS#16	16
568	4921.041023	4998.552716	97.079708	RREBAR XS#16	16
569	4921.520693	5000.156879	97.048188	WS XS#16	16
570	4922.101858	5001.763669	97.034969	WS XS#16	16
571	4922.639295	5003.260779	97.05605	WS XS#16	16
572	4922.863265	5004.299421	97.066448	LREBARXS#16	16
573	4923.545742	5005.635558	97.541223	WS XS#16	16
574	4923.707947	5006.72517	97.910192	WS XS#16	16
575	4924.113871	5007.811548	98.293615	WS XS#16	16
576	4924.385196	5008.560379	98.565959	LTOPBANK XS#16	16
577	4924.688003	5009.704244	98.578819	WS XS#16	16
578	4924.993866	5010.591399	98.57123	WS XS#16	16
579	4925.242952	5011.160712	98.566088	WS XS#16	16
595	4907.213842	4998.36235	98.579855	WS XS#17	17
596	4907.451129	4999.030847	98.572603	WS XS#17	17
597	4907.65682	4999.604605	98.558569	WS XS#17	17
598	4907.789069	4999.921105	98.558154	RTOPBANK XS#17	17
599	4908.263371	5000.929653	98.209539	WS XS#17	17
600	4909.048617	5001.960144	97.770969	WS XS#17	17
601	4909.72224	5003.070825	97.344312	WS XS#17	17
602	4910.160421	5003.778158	97.080876	RREBAR XS#17	17
603	4910.841844	5005.123566	97.056871	WS XS#17	17
604	4911.829807	5006.828103	97.064544	WS XS#17	17
605	4912.570444	5008.10382	97.069605	WS XS#17	17
606	4912.986036	5009.092601	97.085661	LREBARXS#17	17
607	4913.468938	5010.019439	97.423831	WS XS#17	17
608	4913.985761	5011.07635	97.823057	WS XS#17	17

Point Number	Northing	Easting	Elevation	Description	Heintz (2002) Cross-section Number
609	4914.419575	5012.246279	98.241911	WS XS#17	17
610	4915.093396	5013.077258	98.583179	LTOPBANK XS#17	17
611	4915.471633	5013.982869	98.579653	WS XS#17	17
612	4915.85999	5014.996469	98.572133	WS XS#17	17
613	4916.386151	5016.289225	98.571985	WS XS#17	17
629	4898.484851	5003.369063	98.608487	WS XS#18	18
630	4898.87528	5004.01673	98.592993	WS XS#18	18
631	4899.477027	5004.629614	98.570503	RTOPBANK XS#18	18
632	4899.93589	5005.170813	98.560518	WS XS#18	18
633	4901.139836	5006.411001	98.008714	WS XS#18	18
634	4902.123975	5007.844801	97.413891	WS XS#18	18
635	4902.863667	5008.719555	97.075533	RREBAR XS#18	18
636	4904.051429	5010.020553	97.057082	WS XS#18	18
637	4904.214958	5011.411207	97.068577	WS XS#18	18
638	4905.341575	5012.941097	97.076786	WS XS#18	18
639	4905.965303	5013.890685	97.090619	LREBARXS#18	18
640	4906.67416	5014.659831	97.429945	WS XS#18	18
641	4907.944626	5016.215068	98.12081	WS XS#18	18
642	4908.729748	5017.327617	98.584428	LTOPBANK XS#18	18
643	4909.499786	5018.303682	98.582494	WS XS#18	18
644	4909.914021	5018.836113	98.583658	WS XS#18	18
645	4910.44834	5019.731479	98.588652	WS XS#18	18
646	4895.849731	5008.870391	98.577359		
647	4897.724845	5011.357002	97.077359		
648	4899.401827	5013.435512	97.072427		
649	4901.913181	5016.632171	97.072132		
650	4904.598703	5020.090655	97.07243		

= number; L = left; NW = northwest; R = right; SE = southwest; WS = water surface; XS = cross section

APPENDIX B PHYSICAL DATA

Table B.1: Baseline Depth Data from Physical Tests

Cross Section	Mean Discharge (cfs)	Center-line Reach Length (ft)	Cumulative Channel Length (ft)	Baseline Piezometer C			Baseline Piezometer D			Baseline Piezometer E			Baseline Super-elevation	
				Elevation of Piezo (ft)	Meas. Depth (ft)	WSEL (ft)	Elevation of Piezo (ft)	Meas. Depth (ft)	WSEL (ft)	Elevation of Piezo (ft)	Meas. Depth (ft)	WSEL (ft)	c-d	e-d
1	8	11.039	178.585	97.307	0.541	97.848	97.252	0.591	97.843	97.317	0.534	97.851	0.0048	0.0075
2	8	10.091	167.545	97.299	0.547	97.846	97.246	0.599	97.845	97.264	0.561	97.825	0.0009	(0.0197)
3	8	10.564	157.454	97.301	0.540	97.841	97.238	0.592	97.830	97.284	0.552	97.836	0.0105	0.0054
4	8	10.423	146.890	97.285	0.563	97.848	97.232	0.629	97.861	97.291	0.544	97.835	(0.0132)	(0.0261)
5	8	10.632	136.468	97.293	0.500	97.793	97.222	0.596	97.818	97.277	0.540	97.817	(0.0250)	(0.0012)
6	8	10.600	125.836	97.265	0.563	97.828	97.208	0.605	97.813	97.269	0.549	97.818	0.0151	0.0054
7	8	10.731	115.236	97.261	0.540	97.801	97.193	0.601	97.794	97.250	0.553	97.803	0.0070	0.0086
8	8	10.242	104.505	97.241	0.562	97.803	97.193	0.621	97.814	97.235	0.551	97.786	(0.0114)	(0.0278)
9	8	10.518	94.263				97.170	0.621	97.791				(97.7905)	(97.7905)
10	8	10.742	83.744	97.191	0.543	97.734	97.148	0.587	97.735	97.200	0.554	97.754	(0.0002)	0.0198
11	8	10.206	73.003	97.205	0.541	97.746	97.152	0.601	97.753	97.215	0.543	97.758	(0.0062)	0.0057
12	8	10.741	62.796	97.198	0.535	97.733	97.150	0.594	97.744	97.213	0.538	97.751	(0.0116)	0.0069
13	8	10.413	52.055	97.187	0.540	97.727	97.139	0.592	97.731	97.197	0.553	97.750	(0.0034)	0.0188
14	8	10.529	41.642	97.175	0.547	97.722	97.123	0.599	97.722	97.178	0.548	97.726	(0.0001)	0.0044
15	8	10.846	31.113	97.183	0.533	97.716	97.126	0.587	97.713	97.179	0.544	97.723	0.0034	0.0099
16	8	11.682	20.267	97.154	0.546	97.700	97.099	0.610	97.709	97.162	0.550	97.712	(0.0090)	0.0030
17	8	8.586	8.586	97.155	0.553	97.708	97.088	0.613	97.701	97.156	0.552	97.708	0.0071	0.0063
18	8	0.000	0.000	97.131	0.534	97.665	97.083	0.612	97.695	97.140	0.557	97.697	(0.0299)	0.0023
1	12	11.039	178.585	97.307	0.718	98.025	97.252	0.765	98.017	97.317	0.706	98.023	0.0078	0.0055
2	12	10.091	167.545	97.299	0.715	98.014	97.246	0.754	98.000	97.264	0.741	98.005	0.0139	0.0053
3	12	10.564	157.454	97.301	0.715	98.016	97.238	0.759	97.997	97.284	0.716	98.000	0.0185	0.0024
4	12	10.423	146.890	97.285	0.731	98.016	97.232	0.770	98.002	97.291	0.714	98.005	0.0138	0.0029
5	12	10.632	136.468	97.293	0.723	98.016	97.222	0.772	97.994	97.277	0.714	97.991	0.0220	(0.0032)
6	12	10.600	125.836	97.265	0.736	98.001	97.208	0.779	97.987	97.269	0.752	98.021	0.0141	0.0344
7	12	10.731	115.236	97.261	0.722	97.983	97.193	0.805	97.998	97.250	0.734	97.984	(0.0150)	(0.0144)
8	12	10.242	104.505	97.241	0.728	97.969	97.193	0.794	97.987	97.235	0.729	97.964	(0.0184)	(0.0228)

Cross Section	Mean Discharge (cfs)	Center-line Reach Length (ft)	Cumulative Channel Length (ft)	Baseline Piezometer C			Baseline Piezometer D			Baseline Piezometer E			Baseline Super-elevation	
				Elevation of Piezo (ft)	Meas. Depth (ft)	WSEL (ft)	Elevation of Piezo (ft)	Meas. Depth (ft)	WSEL (ft)	Elevation of Piezo (ft)	Meas. Depth (ft)	WSEL (ft)	c-d	e-d
9	12	10.518	94.263				97.170	0.797	97.967				(97.9665)	(97.9665)
10	12	10.742	83.744	97.191	0.735	97.926	97.148	0.769	97.917	97.200	0.731	97.931	0.0098	0.0148
11	12	10.206	73.003	97.205	0.700	97.905	97.152	0.768	97.920	97.215	0.719	97.934	(0.0142)	0.0147
12	12	10.741	62.796	97.198	0.709	97.907	97.150	0.768	97.918	97.213	0.712	97.925	(0.0116)	0.0069
13	12	10.413	52.055	97.187	0.718	97.905	97.139	0.764	97.903	97.197	0.729	97.926	0.0026	0.0228
14	12	10.529	41.642	97.175	0.701	97.876	97.123	0.775	97.898	97.178	0.729	97.907	(0.0221)	0.0094
15	12	10.846	31.113	97.183	0.711	97.894	97.126	0.780	97.906	97.179	0.728	97.907	(0.0116)	0.0009
16	12	11.682	20.267	97.154	0.732	97.886	97.099	0.792	97.891	97.162	0.738	97.900	(0.0050)	0.0090
17	12	8.586	8.586	97.155	0.715	97.870	97.088	0.796	97.884	97.156	0.742	97.898	(0.0139)	0.0133
18	12	0.000	0.000	97.131	0.746	97.877	97.083	0.775	97.858	97.140	0.734	97.874	0.0191	0.0162
1	16	11.039	178.585	97.307	0.863	98.170	97.252	0.903	98.155	97.317	0.845	98.162	0.0148	0.0065
2	16	10.091	167.545	97.299	0.862	98.161	97.246	0.906	98.152	97.264	0.874	98.138	0.0089	(0.0137)
3	16	10.564	157.454	97.301	0.855	98.156	97.238	0.906	98.144	97.284	0.865	98.149	0.0115	0.0044
4	16	10.423	146.890	97.285	0.871	98.156	97.232	0.903	98.135	97.291	0.856	98.147	0.0208	0.0119
5	16	10.632	136.468	97.293	0.853	98.146	97.222	0.906	98.128	97.277	0.850	98.127	0.0180	(0.0012)
6	16	10.600	125.836	97.265	0.870	98.135	97.208	0.913	98.121	97.269	0.857	98.126	0.0141	0.0054
7	16	10.731	115.236	97.261	0.851	98.112	97.193	0.927	98.120	97.250	0.860	98.110	(0.0080)	(0.0104)
8	16	10.242	104.505	97.241	0.880	98.121	97.193	0.929	98.122	97.235	0.871	98.106	(0.0014)	(0.0158)
9	16	10.518	94.263				97.170	0.926	98.096				(98.0955)	(98.0955)
10	16	10.742	83.744	97.191	0.847	98.038	97.148	0.889	98.037	97.200	0.858	98.058	0.0018	0.0218
11	16	10.206	73.003	97.205	0.836	98.041	97.152	0.896	98.048	97.215	0.861	98.076	(0.0062)	0.0287
12	16	10.741	62.796	97.198	0.838	98.036	97.150	0.897	98.047	97.213	0.849	98.062	(0.0116)	0.0149
13	16	10.413	52.055	97.187	0.852	98.039	97.139	0.894	98.033	97.197	0.847	98.044	0.0066	0.0108
14	16	10.529	41.642	97.175	0.842	98.017	97.123	0.904	98.027	97.178	0.865	98.043	(0.0101)	0.0164
15	16	10.846	31.113	97.183	0.827	98.010	97.126	0.887	98.013	97.179	0.846	98.025	(0.0026)	0.0119
16	16	11.682	20.267	97.154	0.844	97.998	97.099	0.926	98.025	97.162	0.854	98.016	(0.0270)	(0.0090)
17	16	8.586	8.586	97.155	0.851	98.006	97.088	0.918	98.006	97.156	0.870	98.026	0.0001	0.0193

Cross Section	Mean Discharge (cfs)	Center-line Reach Length (ft)	Cumulative Channel Length (ft)	Baseline Piezometer C			Baseline Piezometer D			Baseline Piezometer E			Baseline Super-elevation	
				Elevation of Piezo (ft)	Meas. Depth (ft)	WSEL (ft)	Elevation of Piezo (ft)	Meas. Depth (ft)	WSEL (ft)	Elevation of Piezo (ft)	Meas. Depth (ft)	WSEL (ft)	c-d	e-d
18	16	0.000	0.000	97.131	0.871	98.002	97.083	0.915	97.998	97.140	0.858	97.998	0.0041	0.0003
1	20	11.039	178.585	97.307	0.978	98.285	97.252	1.021	98.273	97.317	0.963	98.280	0.0118	0.0065
2	20	10.091	167.545	97.299	0.985	98.284	97.246	1.031	98.277	97.264	0.981	98.245	0.0069	(0.0317)
3	20	10.564	157.454	97.301	0.984	98.285	97.238	1.033	98.271	97.284	0.983	98.267	0.0135	(0.0046)
4	20	10.423	146.890	97.285	1.009	98.294	97.232	1.039	98.271	97.291	0.950	98.241	0.0228	(0.0301)
5	20	10.632	136.468	97.293	0.990	98.283	97.222	1.038	98.260	97.277	0.977	98.254	0.0230	(0.0062)
6	20	10.600	125.836	97.265	1.006	98.271	97.208	1.048	98.256	97.269	0.979	98.248	0.0151	(0.0076)
7	20	10.731	115.236	97.261	0.985	98.246	97.193	1.053	98.246	97.250	0.987	98.237	(0.0000)	(0.0094)
8	20	10.242	104.505	97.241	0.982	98.223	97.193	1.056	98.249	97.235	0.979	98.214	(0.0264)	(0.0348)
9	20	10.518	94.263				97.170	1.048	98.218				(98.2175)	(98.2175)
10	20	10.742	83.744	97.191	0.967	98.158	97.148	1.016	98.164	97.200	0.970	98.170	(0.0052)	0.0068
11	20	10.206	73.003	97.205	0.956	98.161	97.152	1.026	98.178	97.215	0.981	98.196	(0.0162)	0.0187
12	20	10.741	62.796	97.198	0.966	98.164	97.150	1.022	98.172	97.213	0.973	98.186	(0.0086)	0.0139
13	20	10.413	52.055	97.187	0.964	98.151	97.139	1.019	98.158	97.197	0.981	98.178	(0.0064)	0.0198
14	20	10.529	41.642	97.175	0.984	98.159	97.123	1.032	98.155	97.178	0.983	98.161	0.0039	0.0064
15	20	10.846	31.113	97.183	0.960	98.143	97.126	1.015	98.141	97.179	0.991	98.170	0.0024	0.0289
16	20	11.682	20.267	97.154	0.972	98.126	97.099	1.047	98.146	97.162	0.989	98.151	(0.0200)	0.0050
17	20	8.586	8.586	97.155	0.991	98.146	97.088	1.034	98.122	97.156	0.965	98.121	0.0241	(0.0017)
18	20	0.000	0.000	97.131	0.992	98.123	97.083	1.036	98.119	97.140	0.979	98.119	0.0041	0.0003

c-d = WSEL difference between Piezotap C and Piezotap D; e-d = WSEL difference between Piezotap E and Piezotap D; Meas. = measured; Piezo = piezometer; WSEL = water-surface elevation

Table B.2: Baseline Velocity and Shear-stress Data from Physical Tests

Cross Section	Mean Discharge (cfs)	Centerline Reach Length (ft)	Cumulative Channel Length (ft)	Baseline Velocity Data			Baseline Shear Stress		
				Piezometer C	Piezometer D	Piezometer E	Piezometer C	Piezometer D	Piezometer E
1	8	11.039	178.585	1.180	0.982	1.315	0.022	0.017	0.021
2	8	10.091	167.545	1.150	0.979	1.298	0.018	0.016	0.019
3	8	10.564	157.454	1.145	0.996	1.188	0.017	0.018	0.025
4	8	10.423	146.890	1.109	1.043	1.090	0.018	0.017	0.016
5	8	10.632	136.468	1.157	1.042	1.024	0.018	0.018	0.018
6	8	10.600	125.836	1.142	1.030	0.973	0.018	0.019	0.015
7	8	10.731	115.236	1.145	1.094	0.901	0.017	0.015	0.013
8	8	10.242	104.505	1.183	1.077	0.831	0.020	0.016	0.013
9	8	10.518	94.263		1.246		0.000	0.024	0.000
10	8	10.742	83.744	1.968	1.688	1.511	0.044	0.036	0.032
11	8	10.206	73.003	1.672	1.739	1.335	0.024	0.038	0.019
12	8	10.741	62.796	1.626	1.783	1.514	0.034	0.040	0.029
13	8	10.413	52.055	1.635	1.358	1.643	0.039	0.036	0.031
14	8	10.529	41.642	1.442	1.743	1.568	0.026	0.039	0.035
15	8	10.846	31.113	1.474	1.763	1.496	0.029	0.048	0.041
16	8	11.682	20.267	1.335	1.496	1.639	0.029	0.035	0.038
17	8	8.586	8.586	1.410	1.690	1.748	0.033	0.039	0.046
18	8	0.000	0.000	1.426	1.655	1.891	0.031	0.037	0.050
1	12	11.039	178.585	1.256	1.132	1.435	0.023	0.021	0.027
2	12	10.091	167.545	1.285	1.153	1.439	0.023	0.019	0.025
3	12	10.564	157.454	1.222	1.189	1.431	0.027	0.018	0.026
4	12	10.423	146.890	1.260	1.180	1.273	0.021	0.022	0.025
5	12	10.632	136.468	1.244	1.208	1.216	0.027	0.024	0.025
6	12	10.600	125.836	1.238	1.151	1.155	0.024	0.021	0.021
7	12	10.731	115.236	1.262	1.221	1.054	0.020	0.018	0.015
8	12	10.242	104.505	1.354	1.295	0.833	0.024	0.017	0.019

Cross Section	Mean Discharge (cfs)	Centerline Reach Length (ft)	Cumulative Channel Length (ft)	Baseline Velocity Data			Baseline Shear Stress		
				Piezometer C	Piezometer D	Piezometer E	Piezometer C	Piezometer D	Piezometer E
9	12	10.518	94.263		1.488		0.000	0.029	0.000
10	12	10.742	83.744	1.966	1.661	1.531	0.056	0.040	0.032
11	12	10.206	73.003	2.211	1.979	1.549	0.034	0.045	0.026
12	12	10.741	62.796	1.993	1.935	1.632	0.050	0.039	0.033
13	12	10.413	52.055	1.956	1.907	1.791	0.046	0.043	0.034
14	12	10.529	41.642	1.760	1.967	1.736	0.036	0.049	0.039
15	12	10.846	31.113	1.691	2.066	1.923	0.037	0.050	0.045
16	12	11.682	20.267	1.603	2.024	1.895	0.039	0.047	0.048
17	12	8.586	8.586	1.626	1.959	1.986	0.032	0.046	0.054
18	12	0.000	0.000	1.592	1.840	2.082	0.038	0.035	0.047
1	16	11.039	178.585	1.397	1.248	1.601	0.028	0.025	0.035
2	16	10.091	167.545	1.446	1.241	1.582	0.021	0.022	0.027
3	16	10.564	157.454	1.435	1.294	1.637	0.029	0.020	0.036
4	16	10.423	146.890	1.454	1.325	1.527	0.026	0.026	0.028
5	16	10.632	136.468	1.422	1.330	1.438	0.026	0.027	0.029
6	16	10.600	125.836	1.403	1.391	1.385	0.027	0.028	0.028
7	16	10.731	115.236	1.449	1.371	1.284	0.026	0.029	0.025
8	16	10.242	104.505	1.500	1.425	1.072	0.029	0.028	0.026
9	16	10.518	94.263		1.642		0.000	0.037	0.000
10	16	10.742	83.744	2.370	2.049	1.845	0.070	0.045	0.043
11	16	10.206	73.003	2.462	2.146	1.900	0.069	0.062	0.033
12	16	10.741	62.796	2.508	2.163	1.863	0.057	0.058	0.044
13	16	10.413	52.055	2.309	2.151	1.948	0.055	0.049	0.043
14	16	10.529	41.642	2.126	2.160	2.002	0.042	0.047	0.032
15	16	10.846	31.113	1.990	2.225	2.114	0.040	0.049	0.048
16	16	11.682	20.267	1.922	2.171	2.132	0.037	0.049	0.055
17	16	8.586	8.586	1.830	2.170	2.056	0.028	0.046	0.072
18	16	0.000	0.000	1.847	1.957	2.120	0.033	0.040	0.054

Cross Section	Mean Discharge (cfs)	Centerline Reach Length (ft)	Cumulative Channel Length (ft)	Baseline Velocity Data			Baseline Shear Stress		
				Piezometer C	Piezometer D	Piezometer E	Piezometer C	Piezometer D	Piezometer E
1	20	11.039	178.585	1.480	1.254	1.661	0.017	0.020	0.034
2	20	10.091	167.545	1.502	1.318	1.718	0.024	0.021	0.023
3	20	10.564	157.454	1.484	1.321	1.659	0.025	0.017	0.030
4	20	10.423	146.890	1.523	1.349	1.556	0.017	0.021	0.027
5	20	10.632	136.468	1.504	1.363	1.534	0.019	0.019	0.025
6	20	10.600	125.836	1.448	1.497	1.455	0.020	0.019	0.022
7	20	10.731	115.236	1.506	1.505	1.364	0.021	0.022	0.019
8	20	10.242	104.505	1.557	1.527	1.263	0.039	0.018	0.018
9	20	10.518	94.263		1.746		0.000	0.036	0.000
10	20	10.742	83.744	2.479	2.163	1.934	0.067	0.049	0.038
11	20	10.206	73.003	2.626	2.276	1.974	0.056	0.050	0.021
12	20	10.741	62.796	2.579	2.164	1.856	0.045	0.046	0.037
13	20	10.413	52.055	2.581	2.309	2.042	0.052	0.043	0.029
14	20	10.529	41.642	2.348	2.307	2.069	0.042	0.041	0.032
15	20	10.846	31.113	2.219	2.288	2.250	0.040	0.043	0.040
16	20	11.682	20.267	2.055	2.277	2.286	0.049	0.042	0.040
17	20	8.586	8.586	2.034	2.336	2.382	0.036	0.044	0.055
18	20	0.000	0.000	2.007	2.101	2.498	0.033	0.039	0.053

Table B.3: Depth Data for Weir Configuration Physical Tests

Cross Section	Station (ft)	Discharge (cfs)	Depth at Piezometer D (ft)														
			W01	W02	W03	W04	W05	W06	W07	W08	W09	W10	W11	W12	W13	W14	W15
1	178.58	8	0.619	0.610	0.630	0.539	0.537	0.572	0.570	0.781	0.812	0.636	0.620	0.679	0.682	1.279	1.221
2	167.55	8	0.617	0.602	0.615	0.539	0.540	0.576	0.574	0.802	0.820	0.659	0.620	0.000	0.667	0.874	0.709
3	157.45	8	0.627	0.612	0.639	0.546	0.546	0.580	0.580	0.789	0.804	0.000	0.636	0.695	0.701	0.000	0.775
4	146.89	8	0.629	0.620	0.641	0.548	0.549	0.584	0.581	1.570	1.459	0.653	0.391	0.691	0.676	0.714	0.700
5	136.47	8	0.632	0.624	0.650	0.554	0.558	0.590	0.590	1.489	1.476	0.637	0.629	0.688	0.665	0.703	0.681
6	125.84	8	0.644	0.633	0.659	0.565	0.565	0.601	0.600	0.803	0.802	0.645	0.667	0.594	0.672	0.711	0.705
7	115.24	8	0.656	0.645	0.671	0.576	0.580	0.612	0.612	0.815	0.807	0.651	0.545	0.703	0.675	0.714	0.705
8	104.50	8	0.648	0.663	0.623	1.525	0.575	0.609	0.608	0.869	0.814	0.583	0.650	0.634	0.970	0.950	0.885
9	94.26	8	0.664	0.663	0.000	0.000	0.591	0.901	0.676	1.347	1.524	0.000	0.654	0.708	0.696	0.734	0.712
10	83.74	8	0.710	0.700	0.700	0.919	0.624	0.669	0.804	1.525	1.517	0.799	0.647	0.709	0.686	0.826	0.705
11	73.00	8	0.642	0.681	0.618	0.653	0.669	0.616	0.630	0.964	0.836	0.821	0.588	0.620	0.754	0.866	0.709
12	62.80	8	0.628	0.609	0.613	0.956	0.599	0.722	0.694	1.666	1.566	0.978	0.611	0.636	0.764	0.651	0.631
13	52.06	8	0.612	0.634	0.603	0.856	0.608	0.681	0.794	1.523	1.549	0.838	0.598	0.631	0.769	0.646	0.648
14	41.64	8	0.624	0.613	0.603	0.633	0.600	0.612	0.685	1.511	1.765	0.839	0.605	0.623	0.691	0.645	0.624
15	31.11	8	0.572	0.581	0.613	0.586	0.588	0.591	0.595	0.772	0.767	0.000	0.533	0.000	0.576	0.608	0.629
16	20.27	8	0.604	0.626	0.611	0.592	0.599	0.597	0.605	0.786	0.790	0.597	0.604	0.613	0.618	0.633	0.694
17	8.59	8	0.575	0.574	0.620	1.173	0.606	0.611	0.603	0.804	0.799	0.602	0.592	0.585	0.577	0.603	0.587
18	0.00	8	0.000	0.000	0.000	0.601	0.597	0.593	0.598	0.839	0.829	0.708	0.601	0.605	0.862	0.791	0.627
1	178.58	12	0.805	0.810	0.821	0.719	0.748	0.756	0.767	0.975	1.026	0.820	0.851	0.871	2.003	0.369	0.864
2	167.55	12	0.804	0.789	0.820	0.722	0.752	0.759	0.770	0.988	1.023	0.834	0.718	0.879	1.825	0.539	0.895
3	157.45	12	0.813	0.810	0.826	0.726	0.758	0.762	0.776	0.987	1.004	0.830	0.860	0.883	1.784	0.552	0.888
4	146.89	12	0.816	0.818	0.828	0.731	0.761	0.769	0.767	1.058	1.003	0.842	0.850	0.000	1.079	0.823	0.892
5	136.47	12	0.821	0.821	0.836	0.737	0.768	0.784	0.785	1.106	1.466	0.822	0.856	0.878	1.068	0.878	0.878
6	125.84	12	0.830	0.834	0.849	0.747	0.778	0.784	0.796	0.984	0.999	0.831	0.828	0.823	1.244	0.841	0.886
7	115.24	12	0.844	0.824	0.859	0.757	0.789	0.794	0.806	0.993	1.003	0.833	0.838	0.889	1.077	0.887	0.889
8	104.50	12	0.836	0.827	0.853	0.756	0.789	0.614	0.804	0.999	1.036	0.000	0.825	0.834	1.520	0.744	1.095
9	94.26	12	0.860	0.837	0.871	0.795	0.804	0.812	0.821	1.094	1.682	0.852	0.867	0.909	1.097	0.909	0.913

Cross Section	Station (ft)	Discharge (cfs)	Depth at Piezometer D (ft)														
			W01	W02	W03	W04	W05	W06	W07	W08	W09	W10	W11	W12	W13	W14	W15
10	83.74	12	0.894	0.879	0.898	0.803	0.827	0.847	0.853	1.771	1.532	0.000	0.871	0.920	0.898	0.837	0.900
11	73.00	12	0.824	0.859	0.794	0.771	0.864	0.803	0.807	1.017	1.038	0.799	0.774	0.862	0.905	0.581	0.905
12	62.80	12	0.795	0.796	0.794	0.763	0.810	0.792	0.801	1.899	1.775	0.791	0.826	0.782	0.824	0.585	0.828
13	52.06	12	0.785	0.808	0.812	0.784	0.833	0.779	0.797	1.754	1.762	0.784	0.817	0.812	0.876	0.813	0.842
14	41.64	12	0.798	0.739	0.630	0.774	0.835	0.784	0.801	1.803	1.972	0.783	0.827	0.732	0.816	0.808	0.832
15	31.11	12	0.740	0.774	0.799	0.745	0.807	0.762	0.788	0.952	0.966	0.770	0.644	0.765	0.841	0.651	0.809
16	20.27	12	0.775	0.820	0.779	0.764	0.819	0.768	0.799	0.980	0.990	0.777	0.830	0.775	0.842	0.798	0.855
17	8.59	12	0.747	0.771	0.814	0.771	0.830	0.785	0.810	0.980	0.997	0.782	0.828	0.758	0.803	0.775	0.808
18	0.00	12	0.782	0.000	0.000	0.776	0.834	0.765	0.800	1.229	1.012	0.790	0.840	0.785	0.000	0.827	0.847
1	178.58	16	0.942	0.931	0.948	0.853	0.836	0.872	0.881	0.930	0.936	0.967	1.114	0.000	0.000	1.277	1.137
2	167.55	16	0.946	0.929	0.948	0.792	0.834	0.871	0.881	0.943	0.946	0.977	0.987	1.598	1.522	1.017	1.015
3	157.45	16	0.948	0.931	0.951	0.857	0.836	0.875	0.886	0.943	0.945	0.974	0.982	1.222	1.296	1.015	1.008
4	146.89	16	0.950	0.935	0.952	0.860	0.837	0.881	0.888	0.844	0.946	0.980	1.001	1.232	1.005	1.020	1.009
5	136.47	16	0.957	0.938	0.958	0.864	0.845	0.885	0.897	0.834	1.065	0.966	0.976	1.214	0.994	1.007	0.994
6	125.84	16	0.961	0.953	0.969	0.874	0.852	0.896	0.906	0.941	0.938	0.972	0.980	1.221	1.003	1.015	1.003
7	115.24	16	0.975	0.959	0.981	0.883	0.872	0.903	0.916	0.942	0.942	0.973	0.984	1.231	1.000	1.011	1.004
8	104.50	16	0.971	0.957	0.969	1.067	0.859	0.900	0.911	0.954	0.950	0.000	0.994	1.512	0.000	1.199	1.222
9	94.26	16	0.989	0.975	0.993	0.962	0.872	0.917	0.884	0.946	1.090	0.988	0.998	1.241	1.021	1.028	1.021
10	83.74	16	1.019	1.002	1.024	0.922	0.921	1.035	0.926	0.827	1.060	0.000	0.985	1.434	1.012	1.023	1.030
11	73.00	16	0.947	0.982	0.931	0.889	0.879	0.899	0.892	0.901	1.043	0.924	0.935	1.839	1.226	0.974	1.011
12	62.80	16	0.928	0.903	0.932	0.878	0.858	0.900	0.810	0.000	0.975	0.914	0.927	1.154	1.186	0.929	0.927
13	52.06	16	0.902	0.914	0.924	0.882	0.843	0.868	0.785	0.875	0.979	0.902	0.911	1.139	0.000	0.912	0.941
14	41.64	16	0.913	0.894	0.914	0.875	0.842	0.864	0.807	0.615	1.290	0.894	0.913	1.138	0.908	0.909	0.916
15	31.11	16	0.846	0.866	0.898	0.867	0.832	0.838	0.855	0.871	0.877	0.876	0.878	1.522	0.000	0.869	0.899
16	20.27	16	0.874	0.886	0.876	0.872	0.831	0.836	0.859	0.892	0.893	0.885	0.896	1.094	0.922	0.887	1.054
17	8.59	16	0.846	0.840	0.887	0.880	0.843	0.851	0.867	0.875	0.901	0.885	0.887	1.063	0.868	0.848	0.877
18	0.00	16	0.864	0.000	0.000	0.885	0.941	0.822	0.851	0.906	0.910	0.892	0.907	1.369	0.909	1.054	0.920

Table B.4: Velocity Data for Weir Configuration Physical Tests

Cross Section	Station (ft)	Discharge (cfs)	Velocity (ft/s) at 60% Depth in Channel Center														
			W01	W02	W03	W04	W05	W06	W07	W08	W09	W10	W11	W12	W13	W14	W15
1	178.58	8	0.000	1.327	1.491	1.253	1.233	1.379	1.413	1.220	1.254	1.384	1.362	1.474	1.442	1.460	1.499
2	167.55	8	1.492	1.568	1.430	1.244	1.246	1.343	1.434	1.121	1.306	1.395	1.364	1.355	1.370	1.357	1.473
3	157.45	8	1.369	1.500	1.404	1.248	1.242	1.307	1.321	1.202	1.172	1.344	1.298	1.335	1.241	1.270	1.367
4	146.89	8	0.000	1.469	1.491	1.226	1.264	1.251	1.492	1.253	1.240	1.403	1.339	1.343	1.397	1.354	1.476
5	136.47	8	1.392	1.490	1.435	1.206	1.164	1.309	1.375	1.279	1.198	1.373	1.308	1.373	1.354	1.378	1.438
6	125.84	8	1.446	1.530	1.418	1.248	1.280	1.297	1.368	1.327	1.274	1.429	1.376	1.426	1.358	1.407	1.543
7	115.24	8	0.000	1.459	1.391	1.189	1.202	1.329	1.380	1.314	1.271	1.358	1.345	1.473	1.441	1.354	1.485
8	104.50	8	1.418	1.478	1.514	1.169	1.224	1.354	1.275	1.257	1.234	1.309	1.294	1.424	1.367	1.427	1.466
9	94.26	8	0.000	0.000	0.000	1.255	1.302	1.263	1.310	1.305	1.243	1.305	0.000	1.341	1.168	1.298	1.297
10	83.74	8	1.511	1.548	1.513	1.514	1.592	1.558	1.539	1.596	1.580	1.579	1.540	1.476	1.224	1.505	1.543
11	73.00	8	0.000	1.643	2.388	1.842	1.984	2.159	2.158	1.942	1.968	2.250	2.307	2.246	1.304	1.980	1.681
12	62.80	8	0.000	2.326	2.413	1.828	1.836	2.075	2.014	1.998	1.897	2.142	2.206	2.415	2.116	2.172	2.204
13	52.06	8	2.557	2.089	2.503	1.848	1.964	2.287	2.300	1.965	1.953	2.215	2.381	2.704	1.961	2.504	2.036
14	41.64	8	2.452	2.513	2.581	1.913	2.034	1.363	2.310	2.225	2.103	2.484	2.514	2.626	2.448	2.613	2.454
15	31.11	8	2.773	2.519	2.777	2.207	1.972	2.429	2.556	2.430	2.071	2.556	2.474	2.990	2.660	2.803	2.561
16	20.27	8	2.557	2.158	2.922	2.120	1.940	2.513	2.638	2.460	2.261	2.652	2.447	2.673	2.072	2.742	2.382
17	8.59	8	2.860	2.829	2.786	1.412	1.879	2.254	2.290	2.326	2.074	2.536	2.600	2.992	2.682	2.903	2.792
18	0.00	8	0.000	0.000	0.000	0.000	0.000	0.000	0.000	2.080	2.022	0.000	2.336	2.484	2.112	0.000	0.000
1	178.58	12	0.000	1.421	1.516	1.347	1.310	1.495	1.475	1.338	1.376	1.391	1.470	1.494	1.514	1.506	1.477
2	167.55	12	1.607	1.659	1.566	1.397	1.364	1.327	1.529	1.361	1.352	1.405	1.466	1.231	1.492	1.447	1.421
3	157.45	12	1.613	1.602	1.611	1.420	1.354	1.539	1.478	1.427	1.408	1.357	1.514	1.537	1.477	1.528	1.431
4	146.89	12	0.000	1.575	1.659	1.452	1.396	1.508	1.584	1.431	1.411	1.421	1.581	1.606	1.548	1.525	1.589
5	136.47	12	1.598	1.539	1.569	1.451	1.380	1.542	1.536	1.428	1.302	1.316	1.544	1.493	1.451	1.577	1.547
6	125.84	12	1.501	1.624	1.353	1.484	1.433	1.582	1.520	1.437	1.444	1.474	1.611	1.559	1.442	1.565	1.626
7	115.24	12	0.000	1.612	1.508	1.547	1.460	1.633	1.536	1.551	1.496	1.610	1.573	1.506	1.533	1.577	1.572
8	104.50	12	1.624	1.635	1.635	1.453	1.473	1.559	1.571	1.337	1.393	1.539	1.466	1.533	1.492	1.632	1.596
9	94.26	12	0.000	0.000	0.000	1.530	1.523	1.555	1.512	1.354	1.473	1.550	1.557	1.480	1.506	1.511	1.330

Cross Section	Station (ft)	Discharge (cfs)	Velocity (ft/s) at 60% Depth in Channel Center														
			W01	W02	W03	W04	W05	W06	W07	W08	W09	W10	W11	W12	W13	W14	W15
10	83.74	12	1.708	1.720	1.682	1.852	1.797	1.782	1.732	1.640	1.698	1.783	1.794	1.657	1.670	1.683	1.687
11	73.00	12	0.000	1.908	2.603	2.250	2.154	2.493	2.457	2.021	2.180	2.532	2.523	2.431	1.835	2.344	1.826
12	62.80	12	2.780	2.742	2.599	2.252	2.060	2.484	2.432	1.945	1.964	2.423	2.514	2.756	2.501	2.659	2.552
13	52.06	12	2.818	2.620	2.704	2.203	2.197	2.603	2.436	1.871	2.073	2.600	2.596	2.752	2.564	2.724	2.431
14	41.64	12	2.748	2.898	2.689	2.379	2.213	2.592	2.529	1.930	2.190	2.608	2.726	2.753	2.636	2.669	2.706
15	31.11	12	3.023	2.790	2.938	2.523	2.142	2.602	2.569	2.292	2.441	2.644	2.737	2.827	2.529	2.596	2.709
16	20.27	12	2.959	2.780	3.087	2.564	2.426	2.803	2.715	2.410	2.607	2.679	2.539	2.905	2.545	2.837	2.389
17	8.59	12	3.310	2.913	3.061	0.000	2.213	0.873	2.456	2.282	2.568	2.808	2.893	3.001	2.740	2.950	2.688
18	0.00	12	0.000	0.000	0.000	0.000	0.000	0.000	0.000	2.349	2.589	2.523	2.783	3.019	2.610	2.816	0.000
1	178.58	16	1.550	1.518	1.541	1.412	1.435	1.566	1.492	1.545	1.376	1.616	1.520	1.585	1.496	1.538	1.549
2	167.55	16	1.611	1.650	1.635	1.511	1.558	1.673	1.587	1.494	1.468	1.638	1.565	1.642	1.478	1.628	1.444
3	157.45	16	1.695	1.763	1.663	0.443	1.551	1.667	1.671	1.477	1.460	1.591	1.642	1.727	1.672	1.720	1.654
4	146.89	16	0.000	1.733	1.755	1.534	1.563	1.718	1.762	1.543	1.540	1.675	1.707	1.749	1.753	1.832	1.761
5	136.47	16	1.698	1.783	1.749	1.578	1.544	1.710	1.718	1.534	1.502	1.684	1.657	1.595	1.719	1.666	1.688
6	125.84	16	1.740	1.731	1.677	1.657	1.678	1.745	1.744	1.573	1.604	1.723	1.746	1.689	1.755	1.795	1.846
7	115.24	16	0.000	1.625	1.734	1.697	1.681	1.764	1.651	1.630	1.608	1.739	1.701	1.728	1.914	1.587	1.674
8	104.50	16	1.683	1.714	1.773	1.621	1.742	1.743	1.742	1.621	1.640	1.678	1.719	1.724	1.843	1.795	1.811
9	94.26	16	0.000	0.000	0.000	1.734	1.786	1.706	1.746	1.694	1.663	1.753	1.738	1.676	1.743	1.701	1.743
10	83.74	16	1.966	1.971	1.976	2.080	2.159	2.019	1.987	1.959	1.932	2.013	1.999	1.889	1.964	1.941	1.964
11	73.00	16	0.000	2.172	2.857	2.499	2.693	2.764	2.724	2.443	2.543	2.826	2.716	2.640	2.117	2.662	2.107
12	62.80	16	2.894	3.010	2.856	2.577	2.641	2.755	2.794	2.532	2.525	2.861	2.836	2.861	2.804	2.864	2.921
13	52.06	16	3.171	2.901	2.958	2.600	2.802	2.773	2.824	2.536	2.487	3.000	3.017	3.176	2.892	3.069	2.738
14	41.64	16	2.800	3.160	2.929	2.680	2.900	2.728	2.905	2.655	2.610	3.098	3.055	3.026	3.196	3.051	3.145
15	31.11	16	3.429	2.990	2.951	2.764	2.910	2.737	3.031	2.675	2.800	2.972	3.062	3.248	3.185	2.957	2.995
16	20.27	16	3.289	0.670	3.416	2.814	3.096	2.905	3.162	2.869	2.947	3.059	3.094	3.096	2.962	2.868	2.775
17	8.59	16	3.456	3.569	2.898	0.000	3.057	2.889	2.842	2.798	2.777	3.142	3.373	3.369	3.574	3.280	3.136
18	0.00	16	0.000	0.000	0.000	0.000	0.000	0.000	0.000	2.484	2.792	0.000	3.051	3.409	3.066	0.000	0.000

Table B.5: Shear-stress Data for Weir Configuration Physical Tests

Cross Section	Station (ft)	Dis-charge (cfs)	Shear Stress in Channel Center (lb/ft ²) (converted based on 0.1644)														
			W01	W02	W03	W04	W05	W06	W07	W08	W09	W10	W11	W12	W13	W14	W15
1	178.58	8	0.000	0.023	0.030	0.039	0.041	0.079	0.042	0.039	0.039	0.046	0.040	0.005	0.018	0.000	0.011
2	167.55	8	0.025	0.028	0.026	0.022	0.036	0.040	0.037	0.032	0.034	0.018	0.032	0.005	0.022	0.000	0.009
3	157.45	8	0.022	0.026	0.022	0.021	0.039	0.045	0.041	0.037	0.036	0.036	0.040	0.008	0.023	-0.002	0.006
4	146.89	8	0.000	0.024	0.026	0.035	0.042	0.048	0.046	-0.002	0.037	0.040	0.040	0.007	0.022	0.009	0.014
5	136.47	8	0.024	0.034	0.029	0.020	0.039	0.047	0.041	0.037	0.039	0.042	0.042	0.054	0.025	0.007	0.018
6	125.84	8	0.027	0.024	0.031	0.020	0.040	0.046	0.045	0.000	0.038	0.041	0.039	0.039	0.028	0.015	0.017
7	115.24	8	0.000	0.024	0.020	0.021	0.040	0.044	0.039	0.000	0.037	0.041	0.039	0.040	0.030	0.005	0.009
8	104.50	8	0.020	0.019	0.018	0.030	0.040	0.039	0.040	0.000	0.021	0.028	0.030	0.033	-0.002	-0.002	0.002
9	94.26	8	0.000	0.000	0.000	0.027	0.040	0.041	0.039	0.000	0.040	0.038	0.037	0.035	0.009	0.004	0.007
10	83.74	8	0.023	0.023	0.024	0.060	0.048	0.054	0.052	0.000	0.054	0.041	0.041	0.041	0.011	0.012	0.014
11	73.00	8	0.000	0.037	0.068	0.069	0.067	0.079	0.091	0.000	0.069	0.084	0.075	0.074	0.036	0.053	0.017
12	62.80	8	0.000	0.070	0.055	0.030	0.058	0.074	0.059	0.000	0.056	0.064	0.067	0.086	0.061	0.058	0.058
13	52.06	8	0.086	0.056	0.057	0.044	0.063	0.065	0.096	0.063	0.072	0.082	0.077	0.043	0.064	0.072	0.037
14	41.64	8	0.068	0.100	0.106	0.051	0.054	0.090	0.084	0.075	0.073	0.090	0.083	0.091	0.103	0.025	0.055
15	31.11	8	0.097	0.106	0.062	0.053	0.047	0.097	0.092	0.091	0.082	0.092	0.114	0.120	0.115	0.113	0.063
16	20.27	8	0.068	0.074	0.085	0.054	0.072	0.101	0.081	0.090	0.089	0.019	0.069	0.082	0.059	0.059	0.051
17	8.59	8	0.103	0.105	0.082	0.039	0.070	0.075	0.083	0.087	0.074	0.099	0.092	0.131	0.133	0.177	0.089
18	0.00	8	0.000	0.000	0.000	0.000	0.000	0.000	0.000	0.045	0.068	0.067	0.070	0.083	0.084	0.061	0.000
1	178.58	12	0.000	0.022	0.024	0.044	0.040	0.047	0.067	0.041	0.036	0.035	0.041	0.010	0.016	0.015	0.012
2	167.55	12	0.027	0.035	0.023	0.038	0.037	0.042	0.050	0.039	0.037	0.038	0.041	0.014	0.015	0.007	0.012
3	157.45	12	0.023	0.033	0.023	0.043	0.040	0.049	0.043	-0.002	0.042	0.044	0.041	0.007	0.016	0.016	0.005
4	146.89	12	0.000	0.026	0.028	0.044	0.041	0.048	0.045	0.043	0.038	0.017	0.044	0.010	0.019	0.006	0.015
5	136.47	12	0.031	0.027	0.027	0.046	0.040	0.049	0.044	0.043	0.038	0.045	0.049	0.017	0.019	0.011	0.020
6	125.84	12	0.027	0.023	0.025	0.044	0.042	0.042	0.047	0.038	0.042	0.045	0.046	0.031	0.019	0.018	0.018
7	115.24	12	0.000	0.028	0.022	0.044	0.045	0.044	0.040	0.043	0.040	0.045	0.046	0.015	0.024	0.010	0.017
8	104.50	12	0.026	0.024	0.021	0.039	0.038	0.055	0.036	0.038	0.036	0.035	0.033	0.011	0.010	0.004	0.002
9	94.26	12	0.000	0.000	0.000	0.047	0.044	0.042	0.046	0.044	0.041	0.043	0.044	0.007	0.015	0.007	0.012

Cross Section	Station (ft)	Dis-charge (cfs)	Shear Stress in Channel Center (lb/ft ²) (converted based on 0.1644)														
			W01	W02	W03	W04	W05	W06	W07	W08	W09	W10	W11	W12	W13	W14	W15
10	83.74	12	0.029	0.027	0.027	0.058	0.057	0.053	0.052	0.058	0.048	0.055	0.052	0.015	0.021	0.022	0.017
11	73.00	12	0.000	0.043	0.081	0.079	0.074	0.088	0.089	0.076	0.076	0.094	0.097	0.057	0.038	0.051	0.022
12	62.80	12	0.072	0.070	0.066	0.064	0.060	0.067	0.066	0.067	0.061	0.072	0.080	0.070	0.058	0.065	0.053
13	52.06	12	0.071	0.056	0.074	0.074	0.063	0.087	0.085	0.069	0.064	0.074	0.083	0.050	0.062	0.061	0.044
14	41.64	12	0.070	0.092	0.085	0.071	0.063	0.091	0.076	0.079	0.082	0.089	0.101	0.045	0.011	0.052	0.050
15	31.11	12	0.124	0.077	0.084	0.101	0.066	0.093	0.098	0.106	0.083	0.087	0.106	0.077	0.040	0.068	0.055
16	20.27	12	0.111	0.060	0.104	0.087	0.076	0.096	0.111	0.095	0.081	0.078	0.076	0.066	-0.002	0.054	0.030
17	8.59	12	0.112	0.075	0.093	0.000	0.085	0.022	0.076	0.094	0.084	0.087	0.110	0.110	0.034	0.104	0.044
18	0.00	12	0.000	0.000	0.000	0.000	0.000	0.000	0.000	0.069	0.073	0.074	0.079	0.063	0.029	0.021	0.000
1	178.58	16	0.032	0.026	0.025	0.044	0.044	0.047	0.050	0.046	0.042	0.047	0.046	0.015	0.021	0.010	0.015
2	167.55	16	0.024	0.025	0.027	0.043	0.043	0.047	0.048	0.045	0.041	0.042	0.043	0.011	0.031	0.019	0.012
3	157.45	16	0.034	0.031	0.027	0.044	0.047	0.049	0.052	0.043	0.041	0.041	0.054	-0.002	0.026	0.014	0.019
4	146.89	16	0.000	0.032	0.018	0.045	0.045	0.059	0.051	0.045	0.049	-0.002	0.051	0.011	0.015	0.010	0.023
5	136.47	16	0.028	0.026	0.035	0.046	0.047	0.057	0.052	0.047	0.047	0.052	0.056	0.010	0.022	0.017	0.018
6	125.84	16	0.033	0.025	0.028	0.048	0.053	0.043	0.059	0.050	0.041	0.055	0.053	0.009	0.019	0.020	0.027
7	115.24	16	0.000	0.034	0.029	0.049	0.093	0.043	0.052	0.046	0.046	0.050	0.052	0.018	0.033	0.019	0.020
8	104.50	16	0.027	0.019	0.022	0.045	0.046	0.032	0.043	0.043	0.044	0.038	0.035	0.033	0.022	0.014	0.011
9	94.26	16	0.000	0.000	0.000	0.048	0.061	0.071	0.051	0.049	0.047	0.051	0.045	0.015	0.026	0.017	0.025
10	83.74	16	0.028	0.031	0.041	0.070	0.076	0.052	0.061	0.075	0.062	0.060	0.055	0.043	0.034	0.021	0.032
11	73.00	16	0.000	0.058	0.090	0.090	0.105	0.024	0.113	0.092	0.096	0.118	0.099	0.081	0.033	0.064	0.039
12	62.80	16	0.094	0.069	0.071	0.084	0.086	0.032	0.089	0.077	0.085	0.091	0.083	0.056	0.072	0.062	0.093
13	52.06	16	0.087	0.059	0.094	0.082	0.088	0.031	0.106	0.075	0.085	0.096	0.108	0.074	0.097	0.082	0.056
14	41.64	16	0.074	0.100	0.089	0.055	0.103	0.030	0.092	0.094	0.077	0.095	0.097	0.066	0.093	0.077	0.090
15	31.11	16	0.104	0.087	0.080	0.103	0.105	0.029	0.096	0.095	0.103	0.101	0.110	0.099	0.086	0.085	0.059
16	20.27	16	0.085	0.073	0.073	0.091	0.124	0.104	0.107	0.092	0.094	0.097	0.088	0.157	0.050	0.059	0.041
17	8.59	16	0.118	0.120	0.070	0.000	0.085	0.095	0.106	-0.002	0.099	0.114	0.111	0.213	0.114	0.107	0.105
18	0.00	16	0.000	0.000	0.000	0.000	0.000	0.000	0.000	0.079	0.085	0.000	0.088	0.082	0.061	0.000	0.000

Table B.6: Maximum Velocity and Shear-stress Data for Weir Configuration Tests

Test Identification	Discharge (cfs)	Bend Location	V_{max} TIP (ft/s)	V_{max} INNER (ft/s)	τ_{max} TIP (lb/ft²)	τ_{max} INNER (lb/ft²)
W01	8	Downstream	2.4861	2.5026	0.089051	0.065148
W01	12	Downstream	2.8126	2.9368	0.09386	0.087456
W01	16	Downstream	3.2438	3.2888	0.17773	0.198927
W02	8	Downstream	2.3589	2.1445	0.084895	0.066262
W02	12	Downstream	2.631	2.4878	0.078707	0.06355
W02	16	Downstream	3.2377	2.956	0.113722	0.084713
W03	8	Downstream	2.5852	2.43	0.102901	0.054196
W03	12	Downstream	2.7694	2.7307	0.08899	0.070365
W03	16	Downstream	2.9356	3.1652	0.108452	0.096377
W04	8	Downstream	2.1279	1.9617	0.062822	0.086475
W04	12	Downstream	2.2194	2.418	0.081844	0.08856
W04	16	Downstream	2.5562	2.7062	0.086222	0.085136
W05	8	Downstream	2.1193	1.9315	0.124708	0.063316
W05	12	Downstream	2.1214	2.2703	0.071275	0.08699
W05	16	Downstream	2.7383	2.7128	0.102043	0.086609
W06	8	Downstream	2.1716	2.1163	0.082455	0.081403
W06	12	Downstream	2.4731	2.6629	0.090367	0.078098
W06	16	Downstream	2.6884	3.0362	0.093528	0.083002
W07	8	Downstream	2.3692	2.103	0.085138	0.076677
W07	12	Downstream	2.3232	2.4191	0.085629	0.081881
W07	16	Downstream	2.7616	2.9176	0.115348	0.100793
W08	8	Downstream	2.1604	2.3038	0.090422	0.071498
W08	12	Downstream	2.0461	2.1208	0.086069	0.083561
W08	16	Downstream	2.6969	2.6612	0.100218	0.096006
W09	8	Downstream	2.0737	1.989	0.07584	0.070223
W09	12	Downstream	2.3151	2.1736	0.080266	0.073821
W09	16	Downstream	2.5003	2.7839	0.083076	0.106399

Test Identification	Discharge (cfs)	Bend Location	V_{max} TIP (ft/s)	V_{max} INNER (ft/s)	τ_{max} TIP (lb/ft²)	τ_{max} INNER (lb/ft²)
W10	8	Downstream	2.5907	2.284	0.104328	0.076057
W10	12	Downstream	2.5067	2.6787	0.08734	0.079043
W10	16	Downstream	3.0776	3.0529	0.11203	0.107588
W11	8	Downstream	2.4621	2.3189	0.102989	0.080608
W11	12	Downstream	2.7396	2.5635	0.102706	0.082184
W11	16	Downstream	3.175	3.0155	0.119407	0.100719
W12	8	Downstream	2.6859	2.4824	0.109409	0.085928
W12	12	Downstream	2.9672	2.7958	0.088902	0.071348
W12	16	Downstream	3.1749	3.3463	0.188298	0.152705
W13	8	Downstream	2.5115	2.1459	0.113527	0.113196
W13	12	Downstream	2.5763	2.7242	0.065709	0.054835
W13	16	Downstream	3.2012	3.3379	0.095439	0.08548
W14	8	Downstream	2.6151	2.5232	0.083848	0.074535
W14	12	Downstream	2.6657	2.8696	0.063586	0.104073
W14	16	Downstream	3.2449	3.0879	0.09938	0.101286
W15	8	Downstream	2.5636	2.1022	0.064784	0.059112
W15	12	Downstream	2.5082	2.6439	0.05303	0.061371
W15	16	Downstream	2.9538	3.0771	0.090494	0.081638
W01	8	Upstream	1.3596	1.5702	0.021939	0.025154
W01	12	Upstream	1.52	1.832	0.025802	0.032743
W01	16	Upstream	1.5642	2.0181	0.035599	0.051197
W02	8	Upstream	1.4036	#N/A	0.02543	#N/A
W02	12	Upstream	1.5114	#N/A	0.027708	#N/A
W02	16	Upstream	1.7384	#N/A	0.032768	
W03	8	Upstream	1.5526	1.3603	0.029216	0.026729
W03	12	Upstream	1.8707	1.6415	0.026131	0.029207
W03	16	Upstream	1.5457	2.0888	0.027805	0.037228
W04	8	Upstream	1.2546	1.5377	0.041536	0.042129
W04	12	Upstream	1.4831	1.7031	0.045356	0.055237

Test Identification	Discharge (cfs)	Bend Location	V_{max} TIP (ft/s)	V_{max} INNER (ft/s)	τ_{max} TIP (lb/ft²)	τ_{max} INNER (lb/ft²)
W04	16	Upstream	1.5968	1.8241	0.053936	0.059466
W05	8	Upstream	1.2357	1.4952	0.042335	0.045356
W05	12	Upstream	1.4159	1.6714	0.042991	0.05493
W05	16	Upstream	1.6152	1.8944	0.053737	0.05652
W06	8	Upstream	1.3629	1.4567	0.056771	0.045204
W06	12	Upstream	1.5177	1.8673	0.051881	0.061153
W06	16	Upstream	1.7057	2.0389	0.051969	0.058381
W07	8	Upstream	1.3502	1.5484	0.047628	0.044756
W07	12	Upstream	1.4074	1.8615	0.050545	0.061639
W07	16	Upstream	1.5884	2.058	0.055383	0.056889
W08	8	Upstream	1.2444	1.4492	0.040207	0.040305
W08	12	Upstream	1.4343	1.76	0.041015	0.06107
W08	16	Upstream	1.5571	1.8702	0.047369	0.065009
W09	8	Upstream	1.26	1.5473	0.041509	0.042468
W09	12	Upstream	1.4092	1.6716	0.040005	0.045758
W09	16	Upstream	1.5217	1.8394	0.047712	0.052914
W10	8	Upstream	1.3815	1.5566	0.04866	0.043369
W10	12	Upstream	1.4045	1.6418	0.045901	0.043734
W10	16	Upstream	1.6407	1.9602	0.05185	0.056653
W11	8	Upstream	1.3337	1.5071	0.042246	0.042191
W11	12	Upstream	1.4578	1.7634	0.046133	0.047404
W11	16	Upstream	1.5403	1.8977	0.050369	0.059139
W12	8	Upstream	1.4112	1.5224	0.039509	0.040154
W12	12	Upstream	1.4823	1.7529	0.012984	0.018076
W12	16	Upstream	1.7403	1.9589	0.036227	0.059576
W13	8	Upstream	1.3621	1.4441	0.024343	0.021148
W13	12	Upstream	1.4592	1.6293	0.02267	0.02167
W13	16	Upstream	1.7283	1.8782	0.053458	0.046894
W14	8	Upstream	1.3563	1.6013	0.014511	0.006474

Test Identification	Discharge (cfs)	Bend Location	V_{max} TIP (ft/s)	V_{max} INNER (ft/s)	τ_{max} TIP (lb/ft²)	τ_{max} INNER (lb/ft²)
W14	12	Upstream	1.4638	1.7477	0.032844	0.015251
W14	16	Upstream	1.6009	1.9819	0.02088	0.066024
W15	8	Upstream	1.4225	1.677	0.020552	0.017231
W15	12	Upstream	1.4253	1.7292	0.017419	0.017351
W15	16	Upstream	1.6071	1.8783	0.021602	0.032479

#N/A = data not taken at this location

APPENDIX C HEC-RAS DATA

Table C.1: Baseline Data from HEC-RAS

Test Identification	Q (cfs)	Physical Model Cross Section	HEC-RAS Cross Section	Reach Length (ft)	Channel Station (ft)	WSE (ft)	Minimum Channel Elevation (ft)	Depth (ft)	V (ft/s)	Shear Stress (lb/ft ²)	Flow Area (ft ²)	Top Width, Tw (ft)
B01	8	1	17	11.039	178.585	97.849	97.244	0.605	1.130	0.015	7.080	13.871
B01	8	2	16	10.091	167.545	97.847	97.208	0.639	1.055	0.012	7.584	14.003
B01	8	3	15	10.564	157.454	97.839	97.241	0.598	1.146	0.015	6.980	13.730
B01	8	4	14	10.423	146.890	97.835	97.223	0.612	1.121	0.014	7.136	13.899
B01	8	5	13	10.632	136.468	97.831	97.215	0.616	1.097	0.014	7.291	13.913
B01	8	6	12	10.600	125.836	97.825	97.172	0.653	1.127	0.015	7.097	13.833
B01	8	7	11	10.731	115.236	97.822	97.138	0.684	1.077	0.013	7.428	13.791
B01	8	8	10	10.242	104.505	97.817	97.187	0.630	1.079	0.013	7.414	13.853
B01	8	9	9	10.518	94.263	97.794	97.197	0.597	1.375	0.022	5.817	11.632
B01	8	10	8	10.742	83.744	97.777	97.105	0.672	1.498	0.025	5.341	10.012
B01	8	11	7	10.206	73.003	97.763	97.117	0.646	1.594	0.029	5.019	9.877
B01	8	12	6	10.741	62.796	97.746	97.128	0.618	1.713	0.034	4.671	9.821
B01	8	13	5	10.413	52.055	97.743	97.072	0.671	1.508	0.026	5.307	10.019
B01	8	14	4	10.529	41.642	97.734	97.055	0.679	1.511	0.026	5.293	9.896
B01	8	15	3	10.846	31.113	97.726	97.052	0.674	1.496	0.025	5.349	10.011
B01	8	16	2	11.682	20.267	97.717	97.035	0.682	1.509	0.026	5.303	9.976
B01	8	17	1	8.586	8.586	97.703	97.057	0.646	1.596	0.029	5.011	9.815
B01	8	18	0	0.000	0.000	97.695	97.057	0.638	1.583	0.029	5.054	9.982
B01	12	1	17	11.039	178.585	98.018	97.244	0.774	1.263	0.017	9.502	14.916
B01	12	2	16	10.091	167.545	98.015	97.208	0.807	1.197	0.015	10.028	14.999
B01	12	3	15	10.564	157.454	98.008	97.241	0.767	1.279	0.017	9.386	14.806
B01	12	4	14	10.423	146.890	98.004	97.223	0.781	1.254	0.017	9.573	14.926

Test Identification	Q (cfs)	Physical Model Cross Section	HEC-RAS Cross Section	Reach Length (ft)	Channel Station (ft)	WSE (ft)	Minimum Channel Elevation (ft)	Depth (ft)	V (ft/s)	Shear Stress (lb/ft ²)	Flow Area (ft ²)	Top Width, Tw (ft)
B01	12	5	13	10.632	136.468	98.000	97.215	0.785	1.233	0.016	9.735	14.936
B01	12	6	12	10.600	125.836	97.994	97.172	0.822	1.259	0.017	9.531	14.847
B01	12	7	11	10.731	115.236	97.991	97.138	0.853	1.219	0.016	9.841	14.688
B01	12	8	10	10.242	104.505	97.987	97.187	0.800	1.218	0.016	9.853	14.831
B01	12	9	9	10.518	94.263	97.961	97.197	0.764	1.531	0.025	7.839	12.584
B01	12	10	8	10.742	83.744	97.939	97.105	0.834	1.705	0.031	7.039	10.958
B01	12	11	7	10.206	73.003	97.925	97.117	0.808	1.793	0.035	6.691	10.782
B01	12	12	6	10.741	62.796	97.909	97.128	0.781	1.891	0.039	6.347	10.746
B01	12	13	5	10.413	52.055	97.906	97.072	0.834	1.709	0.031	7.022	10.984
B01	12	14	4	10.529	41.642	97.897	97.055	0.842	1.718	0.031	6.983	10.864
B01	12	15	3	10.846	31.113	97.889	97.052	0.837	1.700	0.031	7.057	10.960
B01	12	16	2	11.682	20.267	97.880	97.035	0.845	1.713	0.031	7.004	10.939
B01	12	17	1	8.586	8.586	97.865	97.057	0.808	1.795	0.035	6.685	10.783
B01	12	18	0	0.000	0.000	97.858	97.057	0.801	1.775	0.034	6.759	10.932
B01	16	1	17	11.039	178.585	98.156	97.244	0.912	1.376	0.018	11.629	15.757
B01	16	2	16	10.091	167.545	98.154	97.208	0.946	1.315	0.016	12.168	15.806
B01	16	3	15	10.564	157.454	98.147	97.241	0.906	1.391	0.019	11.504	15.638
B01	16	4	14	10.423	146.890	98.143	97.223	0.920	1.366	0.018	11.714	15.756
B01	16	5	13	10.632	136.468	98.140	97.215	0.925	1.347	0.017	11.882	15.762
B01	16	6	12	10.600	125.836	98.135	97.172	0.963	1.371	0.018	11.670	15.664
B01	16	7	11	10.731	115.236	98.132	97.138	0.994	1.337	0.017	11.967	15.587
B01	16	8	10	10.242	104.505	98.128	97.187	0.941	1.334	0.017	11.995	15.612
B01	16	9	9	10.518	94.263	98.099	97.197	0.902	1.661	0.026	9.630	13.417

Test Identification	Q (cfs)	Physical Model Cross Section	HEC-RAS Cross Section	Reach Length (ft)	Channel Station (ft)	WSE (ft)	Minimum Channel Elevation (ft)	Depth (ft)	V (ft/s)	Shear Stress (lb/ft ²)	Flow Area (ft ²)	Top Width, Tw (ft)
B01	16	10	8	10.742	83.744	98.073	97.105	0.968	1.869	0.033	8.560	11.746
B01	16	11	7	10.206	73.003	98.059	97.117	0.942	1.954	0.037	8.189	11.523
B01	16	12	6	10.741	62.796	98.044	97.128	0.916	2.036	0.040	7.857	11.533
B01	16	13	5	10.413	52.055	98.042	97.072	0.970	1.866	0.033	8.576	11.773
B01	16	14	4	10.529	41.642	98.034	97.055	0.979	1.876	0.033	8.527	11.677
B01	16	15	3	10.846	31.113	98.027	97.052	0.975	1.856	0.033	8.620	11.760
B01	16	16	2	11.682	20.267	98.018	97.035	0.983	1.866	0.033	8.574	11.762
B01	16	17	1	8.586	8.586	98.004	97.057	0.947	1.942	0.036	8.241	11.606
B01	16	18	0	0.000	0.000	97.998	97.057	0.941	1.917	0.035	8.347	11.750
B01	20	1	17	11.039	178.585	98.279	97.244	1.035	1.469	0.019	13.615	16.503
B01	20	2	16	10.091	167.545	98.277	97.208	1.069	1.412	0.018	14.162	16.522
B01	20	3	15	10.564	157.454	98.270	97.241	1.029	1.484	0.020	13.479	16.373
B01	20	4	14	10.423	146.890	98.267	97.223	1.044	1.459	0.019	13.708	16.490
B01	20	5	13	10.632	136.468	98.264	97.215	1.049	1.441	0.018	13.880	16.493
B01	20	6	12	10.600	125.836	98.259	97.172	1.087	1.464	0.019	13.657	16.378
B01	20	7	11	10.731	115.236	98.256	97.138	1.118	1.434	0.018	13.951	16.382
B01	20	8	10	10.242	104.505	98.252	97.187	1.065	1.431	0.018	13.979	16.302
B01	20	9	9	10.518	94.263	98.220	97.197	1.023	1.769	0.028	11.306	14.174
B01	20	10	8	10.742	83.744	98.191	97.105	1.086	2.003	0.035	9.983	12.440
B01	20	11	7	10.206	73.003	98.177	97.117	1.060	2.087	0.039	9.583	12.180
B01	20	12	6	10.741	62.796	98.163	97.128	1.035	2.159	0.042	9.263	12.220
B01	20	13	5	10.413	52.055	98.162	97.072	1.090	1.996	0.035	10.019	12.454
B01	20	14	4	10.529	41.642	98.153	97.055	1.098	2.008	0.035	9.962	12.386

Test Identification	Q (cfs)	Physical Model Cross Section	HEC-RAS Cross Section	Reach Length (ft)	Channel Station (ft)	WSE (ft)	Minimum Channel Elevation (ft)	Depth (ft)	V (ft/s)	Shear Stress (lb/ft ²)	Flow Area (ft ²)	Top Width, Tw (ft)
B01	20	15	3	10.846	31.113	98.147	97.052	1.095	1.986	0.035	10.070	12.464
B01	20	16	2	11.682	20.267	98.138	97.035	1.103	1.994	0.035	10.029	12.477
B01	20	17	1	8.586	8.586	98.124	97.057	1.067	2.066	0.038	9.681	12.318
B01	20	18	0	0.000	0.000	98.119	97.057	1.062	2.038	0.037	9.812	12.479

Table C.2: Data from Computer Simulation of Weir Fields in HEC-RAS

Test Identification	River Station	Q (cfs)	Reach Length (ft)	Cumulative Channel Length (ft)	Minimum Channel Elevation (ft)	WSE (ft)	Depth (ft)	Flow Area (ft ²)	Top Width, Tw (ft)	Velocity (ft/s)	Shear Stress (lb/ft ²)
W01	18	8	5.69	189.25	97.2192	97.9228	0.7036	8.5429	14.3708	0.9364	0.006669
W01	17.4637	8	2.65	183.56	97.2327	97.8962	0.6635	5.2339	14.1925	1.5285	0.018147
W01	17.2138	8	2.65	180.91	97.239	97.8971	0.6581	5.5048	10.1599	1.4533	0.016664
W01	16.9694	8	5.74	178.25	97.2432	97.8948	0.6516	5.4275	14.1549	1.474	0.016737
W01	16.4526	8	5.74	172.51	97.2247	97.892	0.6673	5.4344	14.1937	1.4721	0.016641
W01	15.9225	8	2.65	166.78	97.211	97.8916	0.6806	5.7102	14.2552	1.401	0.014853
W01	15.6592	8	2.65	164.13	97.2195	97.8913	0.6718	5.8212	10.1369	1.3743	0.014628
W01	15.3958	8	5.74	161.48	97.228	97.8861	0.6581	5.4797	14.1098	1.4599	0.016317
W01	14.8352	8	5.74	155.74	97.2379	97.8816	0.6437	5.3354	14.0343	1.4994	0.017346
W01	14.2906	8	2.65	150	97.2285	97.8791	0.6506	5.3913	14.1187	1.4839	0.016964
W01	14.0391	8	2.65	147.34	97.2241	97.8796	0.6555	5.6184	10.1309	1.4239	0.01588
W01	13.7849	8	5.72	144.69	97.2215	97.8756	0.6541	5.3999	14.1572	1.4815	0.016892
W01	13.2309	8	5.72	138.97	97.2166	97.8721	0.6554	5.3522	14.1589	1.4947	0.017167
W01	12.6972	8	2.65	133.25	97.2016	97.8633	0.6617	5.0091	14.0911	1.5971	0.02003
W01	12.4489	8	2.65	130.6	97.191	97.8636	0.6726	5.2046	9.9973	1.5371	0.018881
W01	12.201	8	5.72	127.95	97.1804	97.8581	0.6777	4.9885	13.988	1.6037	0.020181
W01	11.6567	8	5.81	122.23	97.1602	97.8602	0.7	5.5161	14.0778	1.4503	0.016293
W01	11.1083	8	2.65	116.42	97.1417	97.8508	0.7091	5.1028	13.9709	1.5678	0.019015
W01	10.8611	8	2.65	113.77	97.1579	97.8502	0.6923	5.2007	9.7985	1.5383	0.018829
W01	10.6135	8	6.61	111.11	97.1569	97.8398	0.6829	4.7108	13.959	1.6982	0.022933
W01	10	8	10.24	104.5	97.1868	97.8564	0.6696	7.7293	14.0852	1.035	0.008117
W01	9	8	10.52	94.26	97.1975	97.8455	0.648	6.4255	11.9288	1.245	0.01219
W01	8	8	6.45	83.74	97.1048	97.8351	0.7304	5.8606	10.3487	1.3651	0.014123
W01	7.39875	8	2.81	77.3	97.1118	97.7603	0.6485	3.4541	9.8666	2.3161	0.042156
W01	7.13669	8	2.81	74.48	97.1149	97.76	0.6451	3.6238	7.0214	2.2076	0.039291
W01	6.86787	8	6.62	71.67	97.118	97.7376	0.6196	3.2818	9.7263	2.4377	0.047242
W01	6.21955	8	6.61	65.05	97.1253	97.7241	0.5988	3.2085	9.6772	2.4933	0.049761
W01	5.59241	8	2.81	58.44	97.105	97.7169	0.6118	3.3079	9.7345	2.4184	0.046478

Test Identification	River Station	Q (cfs)	Reach Length (ft)	Cumulative Channel Length (ft)	Minimum Channel Elevation (ft)	WSE (ft)	Depth (ft)	Flow Area (ft ²)	Top Width, Tw (ft)	Velocity (ft/s)	Shear Stress (lb/ft ²)
W01	5.33049	8	2.81	55.63	97.0903	97.7235	0.6332	3.6469	7.061	2.1936	0.038775
W01	5.06897	8	6.62	52.81	97.0756	97.7109	0.6353	3.4742	9.8138	2.3027	0.041676
W01	4.4276	8	6.61	46.19	97.0623	97.6918	0.6295	3.2656	9.6817	2.4498	0.047621
W01	3.80053	8	2.81	39.58	97.0547	97.6775	0.6228	3.182	9.583	2.5142	0.050476
W01	3.53123	8	2.81	36.77	97.0539	97.678	0.6241	3.3411	6.8581	2.3944	0.047079
W01	3.26223	8	6.61	33.95	97.053	97.6566	0.6036	3.0689	9.5461	2.6068	0.054893
W01	2.65695	8	6.62	27.34	97.0463	97.6476	0.6013	3.1378	9.5479	2.5495	0.052228
W01	2.05864	8	2.81	20.72	97.036	97.633	0.597	3.0788	9.4762	2.5984	0.054449
W01	1.79703	8	2.81	17.91	97.0394	97.6323	0.5929	3.2078	6.7656	2.4939	0.051527
W01	1.55756	8	6.51	15.09	97.0447	97.5971	0.5524	2.8027	9.2388	2.8544	0.067411
W01	1	8	8.59	8.59	97.0569	97.6403	0.5835	4.4052	9.4418	1.816	0.026988
W01	0	8			97.0571	97.634	0.5769	4.4587	9.6276	1.7943	0.02663
W01	18	12	5.69	189.25	97.2192	98.107	0.8878	11.29	15.4521	1.0629	0.008028
W01	17.4637	12	2.65	183.56	97.2327	98.1036	0.8709	10.664	15.4653	1.1253	0.009162
W01	17.2138	12	2.65	180.91	97.239	98.0839	0.8448	7.8	15.3384	1.5385	0.019039
W01	16.9694	12	5.74	178.25	97.2432	98.0945	0.8513	10.6612	15.3849	1.1256	0.009157
W01	16.4526	12	5.74	172.51	97.2247	98.0936	0.8689	10.7906	15.434	1.1121	0.008909
W01	15.9225	12	2.65	166.78	97.211	98.0934	0.8824	11.1718	15.4446	1.0741	0.008224
W01	15.6592	12	2.65	164.13	97.2195	98.075	0.8555	8.124	15.3028	1.4771	0.017309
W01	15.3958	12	5.74	161.48	97.228	98.084	0.856	10.7307	15.3198	1.1183	0.009007
W01	14.8352	12	5.74	155.74	97.2379	98.0821	0.8442	10.5478	15.2755	1.1377	0.009367
W01	14.2906	12	2.65	150	97.2285	98.0812	0.8526	10.6711	15.3472	1.1245	0.009131
W01	14.0391	12	2.65	147.34	97.2241	98.0618	0.8377	7.8254	15.2684	1.5335	0.018872
W01	13.7849	12	5.72	144.69	97.2215	98.0722	0.8507	10.6564	15.3422	1.1261	0.009159
W01	13.2309	12	5.72	138.97	97.2166	98.0713	0.8547	10.7648	15.3517	1.1147	0.008948
W01	12.6972	12	2.65	133.25	97.2016	98.0662	0.8646	9.9477	15.2882	1.2063	0.01073
W01	12.4489	12	2.65	130.6	97.191	98.0459	0.8549	7.4627	15.1498	1.608	0.021011
W01	12.201	12	5.72	127.95	97.1804	98.057	0.8766	9.927	15.2058	1.2088	0.010763
W01	11.6567	12	5.81	122.23	97.1602	98.0574	0.8972	10.5264	15.2162	1.14	0.009397

Test Identification	River Station	Q (cfs)	Reach Length (ft)	Cumulative Channel Length (ft)	Minimum Channel Elevation (ft)	WSE (ft)	Depth (ft)	Flow Area (ft ²)	Top Width, Tw (ft)	Velocity (ft/s)	Shear Stress (lb/ft ²)
W01	11.1083	12	2.65	116.42	97.1417	98.0568	0.9151	10.7526	15.0979	1.116	0.008928
W01	10.8611	12	2.65	113.77	97.1579	98.0345	0.8766	7.5935	14.9939	1.5803	0.020133
W01	10.6135	12	6.61	111.11	97.1569	98.0436	0.8867	9.7182	15.1238	1.2348	0.01129
W01	10	12	10.24	104.5	97.1868	98.0449	0.8581	10.7179	15.1494	1.1196	0.009002
W01	9	12	10.52	94.26	97.1975	98.0317	0.8342	8.7455	12.9986	1.3721	0.013764
W01	8	12	6.45	83.74	97.1048	98.0197	0.915	7.9392	11.4311	1.5115	0.01655
W01	7.39875	12	2.81	77.3	97.1118	98.0143	0.9025	7.7025	11.3177	1.5579	0.017692
W01	7.13669	12	2.81	74.48	97.1149	97.9568	0.8419	5.277	10.9694	2.274	0.042556
W01	6.86787	12	6.62	71.67	97.118	97.972	0.854	7.1835	11.0526	1.6705	0.020655
W01	6.21955	12	6.61	65.05	97.1253	97.9664	0.8411	7.0128	11.0657	1.7112	0.021846
W01	5.59241	12	2.81	58.44	97.105	97.9649	0.8599	7.2532	11.1771	1.6545	0.020264
W01	5.33049	12	2.81	55.63	97.0903	97.921	0.8307	5.2753	10.9899	2.2748	0.042611
W01	5.06897	12	6.62	52.81	97.0756	97.9466	0.871	7.4265	11.2032	1.6158	0.019201
W01	4.4276	12	6.61	46.19	97.0623	97.9423	0.88	7.3669	11.1648	1.6289	0.019535
W01	3.80053	12	2.81	39.58	97.0547	97.9375	0.8828	7.2773	11.1174	1.649	0.020072
W01	3.53123	12	2.81	36.77	97.0539	97.882	0.8281	4.9725	10.8185	2.4133	0.04864
W01	3.26223	12	6.61	33.95	97.053	97.911	0.858	7.0324	11.033	1.7064	0.021679
W01	2.65695	12	6.62	27.34	97.0463	97.9089	0.8626	7.2165	11.0818	1.6629	0.020447
W01	2.05864	12	2.81	20.72	97.036	97.9058	0.8698	7.2675	11.0882	1.6512	0.020125
W01	1.79703	12	2.81	17.91	97.0394	97.8426	0.8032	4.7901	10.7043	2.5052	0.052893
W01	1.55756	12	6.51	15.09	97.0447	97.8736	0.8289	6.7671	10.8722	1.7733	0.023595
W01	1	12	8.59	8.59	97.0569	97.8691	0.8122	6.7303	10.8058	1.783	0.023864
W01	0	12			97.0571	97.865	0.8079	6.8382	10.9753	1.7548	0.023111
W01	18	16	5.69	189.25	97.2192	98.2245	1.0054	13.1469	16.149	1.217	0.009647
W01	17.4637	16	2.65	183.56	97.2327	98.2207	0.988	12.5167	16.1516	1.2783	0.010817
W01	17.2138	16	2.65	180.91	97.239	98.2005	0.9614	9.6291	16.0354	1.6616	0.020028
W01	16.9694	16	5.74	178.25	97.2432	98.2115	0.9683	12.5019	16.0927	1.2798	0.010822
W01	16.4526	16	5.74	172.51	97.2247	98.2106	0.9859	12.6355	16.1231	1.2663	0.010574
W01	15.9225	16	2.65	166.78	97.211	98.2103	0.9993	13.0178	16.1249	1.2291	0.009875

Test Identification	River Station	Q (cfs)	Reach Length (ft)	Cumulative Channel Length (ft)	Minimum Channel Elevation (ft)	WSE (ft)	Depth (ft)	Flow Area (ft ²)	Top Width, Tw (ft)	Velocity (ft/s)	Shear Stress (lb/ft ²)
W01	15.6592	16	2.65	164.13	97.2195	98.1909	0.9714	9.9367	15.9817	1.6102	0.018611
W01	15.3958	16	5.74	161.48	97.228	98.2004	0.9724	12.5529	16.0062	1.2746	0.010713
W01	14.8352	16	5.74	155.74	97.2379	98.1983	0.9604	12.3624	15.9677	1.2943	0.01109
W01	14.2906	16	2.65	150	97.2285	98.1973	0.9688	12.4935	16.0375	1.2807	0.010839
W01	14.0391	16	2.65	147.34	97.2241	98.1772	0.9531	9.6273	15.9537	1.6619	0.020017
W01	13.7849	16	5.72	144.69	97.2215	98.1881	0.9666	12.4739	16.0291	1.2827	0.010879
W01	13.2309	16	5.72	138.97	97.2166	98.1871	0.9705	12.5824	16.036	1.2716	0.010665
W01	12.6972	16	2.65	133.25	97.2016	98.1815	0.9799	11.7493	15.9664	1.3618	0.012488
W01	12.4489	16	2.65	130.6	97.191	98.1609	0.9699	9.2438	15.8245	1.7309	0.021945
W01	12.201	16	5.72	127.95	97.1804	98.1722	0.9918	11.7176	15.8804	1.3655	0.012545
W01	11.6567	16	5.81	122.23	97.1602	98.1727	1.0125	12.3194	15.8814	1.2988	0.011174
W01	11.1083	16	2.65	116.42	97.1417	98.172	1.0303	12.536	15.858	1.2763	0.010659
W01	10.8611	16	2.65	113.77	97.1579	98.1488	0.9909	9.348	15.7147	1.7116	0.021282
W01	10.6135	16	6.61	111.11	97.1569	98.1582	1.0013	11.4882	15.7828	1.3927	0.013119
W01	10	16	10.24	104.5	97.1868	98.1597	0.9729	12.4937	15.7869	1.2806	0.010814
W01	9	16	10.52	94.26	97.1975	98.1431	0.9456	10.2325	13.6931	1.5636	0.016263
W01	8	16	6.45	83.74	97.1048	98.1272	1.0224	9.2017	12.063	1.7388	0.019948
W01	7.39875	16	2.81	77.3	97.1118	98.1209	1.0091	8.9411	11.9228	1.7895	0.021274
W01	7.13669	16	2.81	74.48	97.1149	98.0568	0.9419	6.4015	11.5256	2.4994	0.046424
W01	6.86787	16	6.62	71.67	97.118	98.0733	0.9553	8.3319	11.6148	1.9203	0.024932
W01	6.21955	16	6.61	65.05	97.1253	98.0671	0.9417	8.1559	11.6439	1.9618	0.026182
W01	5.59241	16	2.81	58.44	97.105	98.0657	0.9607	8.4088	11.7599	1.9028	0.024464
W01	5.33049	16	2.81	55.63	97.0903	98.0163	0.926	6.3492	11.5405	2.52	0.047358
W01	5.06897	16	6.62	52.81	97.0756	98.0451	0.9695	8.5591	11.7727	1.8694	0.02352
W01	4.4276	16	6.61	46.19	97.0623	98.0401	0.9778	8.4877	11.7399	1.8851	0.023936
W01	3.80053	16	2.81	39.58	97.0547	98.0346	0.9799	8.3854	11.6999	1.9081	0.024572
W01	3.53123	16	2.81	36.77	97.0539	97.9703	0.9164	5.9504	11.3403	2.6889	0.054856
W01	3.26223	16	6.61	33.95	97.053	98.0036	0.9506	8.079	11.5757	1.9805	0.026785
W01	2.65695	16	6.62	27.34	97.0463	98.001	0.9547	8.2618	11.6225	1.9366	0.025473

Test Identification	River Station	Q (cfs)	Reach Length (ft)	Cumulative Channel Length (ft)	Minimum Channel Elevation (ft)	WSE (ft)	Depth (ft)	Flow Area (ft ²)	Top Width, Tw (ft)	Velocity (ft/s)	Shear Stress (lb/ft ²)
W01	2.05864	16	2.81	20.72	97.036	97.9974	0.9614	8.3079	11.6335	1.9259	0.025152
W01	1.79703	16	2.81	17.91	97.0394	97.9195	0.8801	5.6312	11.1602	2.8413	0.062375
W01	1.55756	16	6.51	15.09	97.0447	97.9571	0.9124	7.6951	11.3677	2.0793	0.029925
W01	1	16	8.59	8.59	97.0569	97.9515	0.8946	7.6406	11.294	2.0941	0.030393
W01	0	16			97.0571	97.947	0.8899	7.7579	11.4538	2.0624	0.029514
W02	18	8	7.92	189.25	97.2192	97.9169	0.6977	8.4581	14.3359	0.9458	0.006821
W02	17.2545	8	2.65	181.33	97.2379	97.8912	0.6533	5.3174	14.1485	1.5045	0.017599
W02	17	8	2.65	178.68	97.2444	97.893	0.6487	5.7109	10.3338	1.4008	0.015382
W02	16.7696	8	7.92	176.02	97.2361	97.8883	0.6522	5.4472	14.1323	1.4686	0.016658
W02	16.0572	8	7.91	168.11	97.2105	97.8873	0.6768	5.7487	14.2344	1.3916	0.014691
W02	15.2705	8	2.65	160.2	97.232	97.8807	0.6487	5.4665	14.0503	1.4634	0.016463
W02	15	8	2.65	157.54	97.2408	97.8804	0.6397	5.5995	10.195	1.4287	0.016036
W02	14.7485	8	7.92	154.89	97.2364	97.8762	0.6398	5.3817	14.0167	1.4865	0.017075
W02	14	8	7.91	146.97	97.2234	97.8723	0.6488	5.4005	14.1283	1.4814	0.016935
W02	13.2417	8	2.65	139.06	97.2167	97.8694	0.6527	5.5353	14.1423	1.4453	0.016047
W02	13	8	2.65	136.41	97.2146	97.8701	0.6555	5.7823	10.3136	1.3835	0.014937
W02	12.7464	8	7.91	133.76	97.2038	97.8601	0.6563	5.1461	14.0773	1.5546	0.018974
W02	12	8	7.92	125.85	97.1718	97.8599	0.688	5.5732	14.0491	1.4354	0.015946
W02	11.2527	8	2.66	117.93	97.1466	97.85	0.7033	5.1669	14.0064	1.5483	0.018616
W02	11	8	2.64	115.27	97.1468	97.8516	0.7048	5.5119	9.9361	1.4514	0.016511
W02	10.7561	8	8.12	112.62	97.1499	97.841	0.691	4.9098	13.9003	1.6294	0.020942
W02	10	8	10.24	104.5	97.1868	97.8548	0.6681	7.7509	14.0763	1.0321	0.008087
W02	9	8	10.52	94.26	97.1975	97.8436	0.6461	6.4034	11.9181	1.2493	0.012285
W02	8	8	11.04	83.74	97.1048	97.8332	0.7285	5.842	10.3375	1.3694	0.014225
W02	6.97123	8	2.81	72.71	97.1169	97.7487	0.6318	3.3523	9.7895	2.3864	0.045039
W02	6.69556	8	2.81	69.9	97.12	97.7508	0.6308	3.5683	6.9952	2.242	0.040671
W02	6.42009	8	11.17	67.08	97.1231	97.7291	0.606	3.2303	9.6968	2.4765	0.04897
W02	5.35974	8	11.17	55.92	97.0919	97.715	0.6231	3.3271	9.7741	2.4045	0.045738
W02	4.28955	8	2.81	44.75	97.0601	97.6972	0.6371	3.3232	9.703	2.4073	0.045774

Test Identification	River Station	Q (cfs)	Reach Length (ft)	Cumulative Channel Length (ft)	Minimum Channel Elevation (ft)	WSE (ft)	Depth (ft)	Flow Area (ft ²)	Top Width, Tw (ft)	Velocity (ft/s)	Shear Stress (lb/ft ²)
W02	4.01567	8	2.81	41.94	97.0556	97.7022	0.6466	3.6121	6.9069	2.2148	0.03939
W02	3.75904	8	11.16	39.12	97.0546	97.6729	0.6182	3.1423	9.5608	2.5459	0.051937
W02	2.71495	8	11.17	27.96	97.0473	97.6558	0.6085	3.1854	9.595	2.5115	0.050476
W02	1.70445	8	2.81	16.79	97.0415	97.6193	0.5778	2.942	9.3801	2.7192	0.060354
W02	1.46485	8	2.81	13.98	97.0467	97.6181	0.5714	3.0663	6.6922	2.609	0.057015
W02	1.22549	8	11.17	11.17	97.0519	97.5712	0.5193	2.6144	9.0536	3.0599	0.078763
W02	0	8			97.0571	97.6163	0.5592	4.2892	9.5243	1.8652	0.029042
W02	18	12	7.92	189.25	97.2192	98.0676	0.8484	10.6858	15.2212	1.123	0.009078
W02	17.2545	12	2.65	181.33	97.2379	98.0629	0.825	10.0305	15.2165	1.1964	0.010508
W02	17	12	2.65	178.68	97.2444	98.0414	0.797	7.3993	15.0582	1.6218	0.021394
W02	16.7696	12	7.92	176.02	97.2361	98.0534	0.8173	10.0427	15.1631	1.1949	0.010468
W02	16.0572	12	7.91	168.11	97.2105	98.0529	0.8424	10.5278	15.2136	1.1398	0.009393
W02	15.2705	12	2.65	160.2	97.232	98.0493	0.8173	10.1387	15.0967	1.1836	0.010227
W02	15	12	2.65	157.54	97.2408	98.0243	0.7835	7.1654	14.9073	1.6747	0.022984
W02	14.7485	12	7.92	154.89	97.2364	98.0369	0.8005	9.8836	15.0185	1.2141	0.010834
W02	14	12	7.91	146.97	97.2234	98.0352	0.8118	10.046	15.1166	1.1945	0.010453
W02	13.2417	12	2.65	139.06	97.2167	98.0336	0.8169	10.189	15.1287	1.1777	0.010118
W02	13	12	2.65	136.41	97.2146	98.0112	0.7966	7.388	15.0033	1.6243	0.021448
W02	12.7464	12	7.91	133.76	97.2038	98.0207	0.8169	9.3416	15.0252	1.2846	0.012347
W02	12	12	7.92	125.85	97.1718	98.0205	0.8486	9.9203	14.9986	1.2096	0.010735
W02	11.2527	12	2.66	117.93	97.1466	98.019	0.8724	10.1077	14.9229	1.1872	0.010263
W02	11	12	2.64	115.27	97.1468	97.9966	0.8498	7.3586	14.7209	1.6307	0.021515
W02	10.7561	12	8.12	112.62	97.1499	98.006	0.8561	9.3505	14.8692	1.2833	0.012281
W02	10	12	10.24	104.5	97.1868	98.0063	0.8195	10.1373	14.9351	1.1838	0.010196
W02	9	12	10.52	94.26	97.1975	97.9909	0.7934	8.2209	12.7543	1.4597	0.015789
W02	8	12	11.04	83.74	97.1048	97.977	0.8723	7.4568	11.1803	1.6093	0.018998
W02	6.97123	12	2.81	72.71	97.1169	97.9671	0.8502	7.1457	11.0179	1.6793	0.020878
W02	6.69556	12	2.81	69.9	97.12	97.8991	0.7791	4.6498	7.592	2.5807	0.05077
W02	6.42009	12	11.17	67.08	97.1231	97.9339	0.8108	6.6908	10.8678	1.7935	0.024205

Test Identification	River Station	Q (cfs)	Reach Length (ft)	Cumulative Channel Length (ft)	Minimum Channel Elevation (ft)	WSE (ft)	Depth (ft)	Flow Area (ft ²)	Top Width, Tw (ft)	Velocity (ft/s)	Shear Stress (lb/ft ²)
W02	5.35974	12	11.17	55.92	97.0919	97.9307	0.8387	7.0403	11.0384	1.7045	0.02161
W02	4.28955	12	2.81	44.75	97.0601	97.9262	0.8661	7.2104	11.0586	1.6643	0.020453
W02	4.01567	12	2.81	41.94	97.0556	97.8699	0.8143	4.9316	10.703	2.4333	0.049352
W02	3.75904	12	11.16	39.12	97.0546	97.8978	0.8432	6.8202	10.8856	1.7595	0.02315
W02	2.71495	12	11.17	27.96	97.0473	97.8932	0.8459	7.0472	10.9881	1.7028	0.021523
W02	1.70445	12	2.81	16.79	97.0415	97.885	0.8435	6.9291	10.949	1.7318	0.022352
W02	1.46485	12	2.81	13.98	97.0467	97.8062	0.7595	4.3952	7.4403	2.7302	0.057414
W02	1.22549	12	11.17	11.17	97.0519	97.7601	0.7082	3.796	10.1787	3.1612	0.076389
W02	0	12			97.0571	97.8155	0.7584	6.3023	10.6866	1.9041	0.027703
W02	18	16	7.92	189.25	97.2192	98.1845	0.9653	12.5048	15.9078	1.2795	0.010787
W02	17.2545	16	2.65	181.33	97.2379	98.1794	0.9415	11.8438	15.9113	1.3509	0.012228
W02	17	16	2.65	178.68	97.2444	98.1576	0.9133	9.1911	15.7633	1.7408	0.022173
W02	16.7696	16	7.92	176.02	97.2361	98.1698	0.9337	11.849	15.8603	1.3503	0.0122
W02	16.0572	16	7.91	168.11	97.2105	98.1694	0.9589	12.3402	15.8944	1.2966	0.011122
W02	15.2705	16	2.65	160.2	97.232	98.1655	0.9335	11.9327	15.7845	1.3409	0.011991
W02	15	16	2.65	157.54	97.2408	98.1402	0.8994	8.9337	15.5988	1.791	0.023626
W02	14.7485	16	7.92	154.89	97.2364	98.1529	0.9165	11.6669	15.7095	1.3714	0.012613
W02	14	16	7.91	146.97	97.2234	98.1513	0.9279	11.8406	15.8055	1.3513	0.012216
W02	13.2417	16	2.65	139.06	97.2167	98.1497	0.933	11.9841	15.8145	1.3351	0.011882
W02	13	16	2.65	136.41	97.2146	98.1268	0.9122	9.1619	15.6857	1.7464	0.022332
W02	12.7464	16	7.91	133.76	97.2038	98.1364	0.9326	11.1188	15.7073	1.439	0.01411
W02	12	16	7.92	125.85	97.1718	98.1362	0.9644	11.6956	15.6738	1.368	0.012542
W02	11.2527	16	2.66	117.93	97.1466	98.1347	0.9881	11.8727	15.5906	1.3476	0.012094
W02	11	16	2.64	115.27	97.1468	98.1116	0.9648	9.094	15.458	1.7594	0.022515
W02	10.7561	16	8.12	112.62	97.1499	98.1213	0.9714	11.1023	15.5521	1.4411	0.014105
W02	10	16	10.24	104.5	97.1868	98.1217	0.9349	11.8977	15.5759	1.3448	0.012053
W02	9	16	10.52	94.26	97.1975	98.1029	0.9054	9.6872	13.4426	1.6517	0.018348
W02	8	16	11.04	83.74	97.1048	98.0846	0.9799	8.6937	11.8128	1.8404	0.022577
W02	6.97123	16	2.81	72.71	97.1169	98.0732	0.9563	8.346	11.6038	1.9171	0.024764

Test Identification	River Station	Q (cfs)	Reach Length (ft)	Cumulative Channel Length (ft)	Minimum Channel Elevation (ft)	WSE (ft)	Depth (ft)	Flow Area (ft ²)	Top Width, Tw (ft)	Velocity (ft/s)	Shear Stress (lb/ft ²)
W02	6.69556	16	2.81	69.9	97.12	97.9824	0.8624	5.5547	11.123	2.8805	0.047635
W02	6.42009	16	11.17	67.08	97.1231	98.0289	0.9058	7.749	11.4077	2.0648	0.02935
W02	5.35974	16	11.17	55.92	97.0919	98.0257	0.9337	8.115	11.5869	1.9717	0.026492
W02	4.28955	16	2.81	44.75	97.0601	98.0207	0.9606	8.2819	11.6186	1.9319	0.025261
W02	4.01567	16	2.81	41.94	97.0556	97.9533	0.8977	5.8452	11.1988	2.7373	0.056997
W02	3.75904	16	11.16	39.12	97.0546	97.9862	0.9316	7.8061	11.4127	2.0497	0.028873
W02	2.71495	16	11.17	27.96	97.0473	97.9811	0.9338	8.0359	11.5037	1.9911	0.027104
W02	1.70445	16	2.81	16.79	97.0415	97.9708	0.9293	7.8909	11.4593	2.0276	0.028242
W02	1.46485	16	2.81	13.98	97.0467	97.8225	0.7758	4.5172	7.5053	3.542	0.094904
W02	1.22549	16	11.17	11.17	97.0519	97.8964	0.8445	6.9935	10.9841	2.2878	0.035851
W02	0	16			97.0571	97.8867	0.8296	7.078	11.1021	2.2605	0.036343
W03	18	8	4.36	189.25	97.2192	97.9423	0.7231	8.8246	14.4861	0.9066	0.0062
W03	17.589	8	2.66	184.88	97.2295	97.9194	0.6899	5.5276	14.3384	1.4473	0.016048
W03	17.3388	8	2.65	182.23	97.2358	97.92	0.6842	5.7666	10.3396	1.3873	0.015042
W03	17.0894	8	4.39	179.58	97.2421	97.9198	0.6776	5.9012	14.3194	1.3557	0.014016
W03	16.6942	8	4.39	175.19	97.2334	97.9154	0.682	5.6876	14.3116	1.4066	0.015081
W03	16.2989	8	2.69	170.79	97.2192	97.9144	0.6952	5.7977	14.3548	1.3799	0.014402
W03	16.057	8	2.62	168.1	97.2105	97.916	0.7055	6.2215	10.3656	1.2859	0.012623
W03	15.7958	8	4.39	165.49	97.215	97.9124	0.6974	5.9365	14.3543	1.3476	0.013641
W03	15.3601	8	4.39	161.1	97.2291	97.9083	0.6792	5.7098	14.2409	1.4011	0.014885
W03	14.929	8	2.66	156.7	97.2395	97.9054	0.6659	5.6094	14.1677	1.4262	0.015523
W03	14.6771	8	2.65	154.05	97.2352	97.9059	0.6707	5.8464	10.2479	1.3684	0.014531
W03	14.4258	8	4.43	151.4	97.2308	97.9021	0.6713	5.6234	14.2369	1.4226	0.015433
W03	14.0054	8	4.35	146.97	97.2235	97.9004	0.6769	5.6457	14.2982	1.417	0.015297
W03	13.5856	8	2.66	142.62	97.2198	97.8994	0.6796	5.7585	14.3105	1.3892	0.014661
W03	13.3283	8	2.65	139.96	97.2175	97.8998	0.6823	5.9785	10.3282	1.3381	0.01383
W03	13.0719	8	4.39	137.31	97.2152	97.8965	0.6813	5.765	14.3173	1.3877	0.014601
W03	12.6676	8	4.39	132.92	97.2004	97.888	0.6876	5.2833	14.2343	1.5142	0.017788
W03	12.2572	8	2.69	128.53	97.1828	97.8856	0.7028	5.2915	14.1947	1.5118	0.017697

Test Identification	River Station	Q (cfs)	Reach Length (ft)	Cumulative Channel Length (ft)	Minimum Channel Elevation (ft)	WSE (ft)	Depth (ft)	Flow Area (ft ²)	Top Width, Tw (ft)	Velocity (ft/s)	Shear Stress (lb/ft ²)
W03	12	8	2.61	125.83	97.2059	97.8876	0.6816	5.6875	10.148	1.4066	0.015439
W03	11.7531	8	4.39	123.22	97.1635	97.8822	0.7187	5.3727	14.2001	1.489	0.017052
W03	11.3377	8	4.39	118.83	97.1495	97.8805	0.731	5.4246	14.1821	1.4748	0.016675
W03	10.9255	8	2.66	114.44	97.1417	97.8777	0.736	5.39	14.0123	1.4842	0.016872
W03	10.6772	8	2.65	111.78	97.1538	97.8767	0.7229	5.4309	10.0876	1.473	0.017169
W03	10.4302	8	4.63	109.13	97.1658	97.8699	0.7041	5.0684	14.1649	1.5784	0.019479
W03	10	8	10.24	104.5	97.1868	97.8845	0.6978	8.1353	14.2464	0.9834	0.007239
W03	9	8	10.52	94.26	97.1975	97.8749	0.6774	6.7792	12.0978	1.1801	0.01081
W03	8	8	5.44	83.74	97.1048	97.8665	0.7618	6.257	10.5316	1.2786	0.012464
W03	7.49355	8	2.81	78.3	97.1107	97.8051	0.6944	3.7594	10.1287	2.128	0.034868
W03	7.23155	8	2.81	75.49	97.1138	97.8054	0.6916	3.9562	7.2212	2.0222	0.032337
W03	6.96767	8	5.57	72.67	97.1169	97.7826	0.6657	3.534	9.991	2.2637	0.039937
W03	6.42191	8	5.57	67.1	97.123	97.7756	0.6526	3.524	9.9751	2.2702	0.040263
W03	5.88162	8	2.81	61.53	97.1212	97.7709	0.6497	3.5893	9.993	2.2289	0.038762
W03	5.61996	8	2.81	58.71	97.1065	97.7761	0.6696	3.9259	7.2322	2.0377	0.03292
W03	5.35804	8	5.57	55.9	97.0918	97.7643	0.6725	3.718	10.0681	2.1517	0.035779
W03	4.8316	8	5.57	50.32	97.0689	97.7594	0.6905	3.76	10.1095	2.1277	0.034839
W03	4.28962	8	2.82	44.75	97.0601	97.7495	0.6894	3.655	10.0099	2.1888	0.036966
W03	4.01486	8	2.81	41.93	97.0556	97.7544	0.6988	3.9927	7.1344	2.0037	0.031543
W03	3.75893	8	5.57	39.12	97.0546	97.7334	0.6788	3.5362	9.9156	2.2623	0.039861
W03	3.22591	8	5.57	33.55	97.0529	97.7258	0.6729	3.5095	9.958	2.2795	0.040583
W03	2.71633	8	2.81	27.98	97.0473	97.7215	0.6742	3.5912	9.9822	2.2277	0.038536
W03	2.46196	8	2.81	25.16	97.043	97.725	0.682	3.8554	7.1447	2.075	0.034219
W03	2.20798	8	5.57	22.35	97.0386	97.7088	0.6702	3.5395	9.9174	2.2602	0.03982
W03	1.70296	8	5.57	16.78	97.0415	97.6977	0.6562	3.4378	9.8427	2.3271	0.042529
W03	1.2285	8	2.81	11.2	97.0519	97.6858	0.6339	3.3332	9.7382	2.4001	0.04561
W03	0.976674	8	2.81	8.39	97.0569	97.6886	0.6317	3.5735	6.9888	2.2387	0.040545
W03	0.646123	8	5.57	5.57	97.0569	97.6836	0.6267	3.5274	9.7758	2.268	0.040619
W03	0	8			97.0571	97.7071	0.6501	5.1784	10.0543	1.5449	0.019065

Test Identification	River Station	Q (cfs)	Reach Length (ft)	Cumulative Channel Length (ft)	Minimum Channel Elevation (ft)	WSE (ft)	Depth (ft)	Flow Area (ft ²)	Top Width, Tw (ft)	Velocity (ft/s)	Shear Stress (lb/ft ²)
W03	18	12	4.36	189.25	97.2192	98.1316	0.9125	11.6725	15.5965	1.0281	0.007452
W03	17.589	12	2.66	184.88	97.2295	98.129	0.8995	11.1232	15.6141	1.0788	0.008332
W03	17.3388	12	2.65	182.23	97.2358	98.1125	0.8766	8.2904	15.5155	1.4475	0.016577
W03	17.0894	12	4.39	179.58	97.2421	98.1213	0.8791	11.0046	15.5523	1.0905	0.008534
W03	16.6942	12	4.39	175.19	97.2334	98.1206	0.8872	11.0944	15.5734	1.0816	0.008377
W03	16.2989	12	2.69	170.79	97.2192	98.1203	0.901	11.3182	15.5991	1.0602	0.008001
W03	16.057	12	2.62	168.1	97.2105	98.1072	0.8967	8.8189	15.5311	1.3607	0.014366
W03	15.7958	12	4.39	165.49	97.215	98.1145	0.8995	11.423	15.5511	1.0505	0.007826
W03	15.3601	12	4.39	161.1	97.2291	98.1128	0.8837	11.1551	15.4845	1.0757	0.008258
W03	14.929	12	2.66	156.7	97.2395	98.1113	0.8718	10.9728	15.4366	1.0936	0.008574
W03	14.6771	12	2.65	154.05	97.2352	98.0948	0.8596	8.2384	15.3733	1.4566	0.016778
W03	14.4258	12	4.43	151.4	97.2308	98.1037	0.8729	10.9837	15.462	1.0925	0.008558
W03	14.0054	12	4.35	146.97	97.2235	98.1031	0.8795	11.0834	15.5184	1.0827	0.00839
W03	13.5856	12	2.66	142.62	97.2198	98.1024	0.8826	11.1659	15.5262	1.0747	0.008248
W03	13.3283	12	2.65	139.96	97.2175	98.0866	0.8691	8.4017	15.4397	1.4283	0.016051
W03	13.0719	12	4.39	137.31	97.2152	98.0952	0.88	11.1701	15.4971	1.0743	0.008236
W03	12.6676	12	4.39	132.92	97.2004	98.0907	0.8903	10.2805	15.4291	1.1673	0.009968
W03	12.2572	12	2.69	128.53	97.1828	98.0897	0.9069	10.3255	15.3992	1.1622	0.009861
W03	12	12	2.61	125.83	97.2059	98.0758	0.8699	8.2446	15.3219	1.4555	0.016721
W03	11.7531	12	4.39	123.22	97.1635	98.0849	0.9214	10.9248	15.3807	1.0984	0.008649
W03	11.3377	12	4.39	118.83	97.1495	98.0844	0.9349	11.0545	15.3215	1.0855	0.008406
W03	10.9255	12	2.66	114.44	97.1417	98.0831	0.9414	10.9526	15.2906	1.0956	0.008586
W03	10.6772	12	2.65	111.78	97.1538	98.0643	0.9105	7.9924	15.2235	1.5014	0.017946
W03	10.4302	12	4.63	109.13	97.1658	98.0723	0.9065	10.1399	15.3195	1.1834	0.010268
W03	10	12	10.24	104.5	97.1868	98.074	0.8872	11.1605	15.3108	1.0752	0.008221
W03	9	12	10.52	94.26	97.1975	98.0621	0.8646	9.1437	13.1882	1.3124	0.012467
W03	8	12	5.44	83.74	97.1048	98.0513	0.9465	8.3033	11.6169	1.4452	0.014988
W03	7.49355	12	2.81	78.3	97.1107	98.0473	0.9366	8.0956	11.5168	1.4823	0.015847
W03	7.23155	12	2.81	75.49	97.1138	98.004	0.8902	5.8152	11.2412	2.0636	0.034207

Test Identification	River Station	Q (cfs)	Reach Length (ft)	Cumulative Channel Length (ft)	Minimum Channel Elevation (ft)	WSE (ft)	Depth (ft)	Flow Area (ft ²)	Top Width, Tw (ft)	Velocity (ft/s)	Shear Stress (lb/ft ²)
W03	6.96767	12	5.57	72.67	97.1169	98.0157	0.8988	7.6879	11.2869	1.5609	0.017761
W03	6.42191	12	5.57	67.1	97.123	98.0119	0.8889	7.5562	11.3109	1.5881	0.018496
W03	5.88162	12	2.81	61.53	97.1212	98.0091	0.8879	7.541	11.3588	1.5913	0.018606
W03	5.61996	12	2.81	58.71	97.1065	97.9753	0.8688	5.7225	11.2301	2.097	0.035494
W03	5.35804	12	5.57	55.9	97.0918	97.9953	0.9035	7.7667	11.4118	1.5451	0.017401
W03	4.8316	12	5.57	50.32	97.0689	97.9944	0.9255	7.9759	11.4914	1.5045	0.016394
W03	4.28962	12	2.82	44.75	97.0601	97.9917	0.9316	7.9473	11.4481	1.5099	0.016511
W03	4.01486	12	2.81	41.93	97.0556	97.9588	0.9032	5.9237	11.2317	2.0258	0.032761
W03	3.75893	12	5.57	39.12	97.0546	97.974	0.9194	7.6678	11.3394	1.565	0.017886
W03	3.22591	12	5.57	33.55	97.0529	97.9722	0.9193	7.7456	11.3978	1.5493	0.017501
W03	2.71633	12	2.81	27.98	97.0473	97.9709	0.9236	7.919	11.4436	1.5153	0.016647
W03	2.46196	12	2.81	25.16	97.043	97.9353	0.8923	5.7999	11.244	2.069	0.034419
W03	2.20798	12	5.57	22.35	97.0386	97.9525	0.9139	7.7485	11.3583	1.5487	0.017469
W03	1.70296	12	5.57	16.78	97.0415	97.9491	0.9076	7.6434	11.3301	1.57	0.018016
W03	1.2285	12	2.81	11.2	97.0519	97.9454	0.8935	7.5381	11.275	1.5919	0.018579
W03	0.976674	12	2.81	8.39	97.0569	97.9002	0.8433	5.3379	10.9951	2.2481	0.041478
W03	0.646123	12	5.57	5.57	97.0569	97.9222	0.8653	7.3694	11.1874	1.6284	0.019541
W03	0	12			97.0571	97.9203	0.8632	7.4536	11.2977	1.61	0.019091
W03	18	16	4.36	189.25	97.2192	98.2419	1.0228	13.4286	16.2537	1.1915	0.009228
W03	17.589	16	2.66	184.88	97.2295	98.2389	1.0094	12.8743	16.2466	1.2428	0.010188
W03	17.3388	16	2.65	182.23	97.2358	98.2207	0.9849	10.005	16.1584	1.5992	0.01842
W03	17.0894	16	4.39	179.58	97.2421	98.2303	0.9882	12.7365	16.2094	1.2562	0.010423
W03	16.6942	16	4.39	175.19	97.2334	98.2296	0.9962	12.8273	16.2228	1.2473	0.010258
W03	16.2989	16	2.69	170.79	97.2192	98.2292	1.01	13.0533	16.235	1.2257	0.009862
W03	16.057	16	2.62	168.1	97.2105	98.2147	1.0042	10.5223	16.1576	1.5206	0.016397
W03	15.7958	16	4.39	165.49	97.215	98.2228	1.0078	13.1425	16.1836	1.2174	0.0097
W03	15.3601	16	4.39	161.1	97.2291	98.2209	0.9918	12.8626	16.1226	1.2439	0.01018
W03	14.929	16	2.66	156.7	97.2395	98.2191	0.9796	12.6718	16.0793	1.2626	0.010529
W03	14.6771	16	2.65	154.05	97.2352	98.2009	0.9657	9.904	16.0055	1.6155	0.018813

Test Identification	River Station	Q (cfs)	Reach Length (ft)	Cumulative Channel Length (ft)	Minimum Channel Elevation (ft)	WSE (ft)	Depth (ft)	Flow Area (ft ²)	Top Width, Tw (ft)	Velocity (ft/s)	Shear Stress (lb/ft ²)
W03	14.4258	16	4.43	151.4	97.2308	98.2108	0.98	12.6737	16.0989	1.2625	0.010534
W03	14.0054	16	4.35	146.97	97.2235	98.2101	0.9866	12.7785	16.1537	1.2521	0.010348
W03	13.5856	16	2.66	142.62	97.2198	98.2094	0.9895	12.8603	16.1594	1.2441	0.010198
W03	13.3283	16	2.65	139.96	97.2175	98.1918	0.9743	10.0581	16.0614	1.5908	0.018182
W03	13.0719	16	4.39	137.31	97.2152	98.2014	0.9861	12.8484	16.1238	1.2453	0.010216
W03	12.6676	16	4.39	132.92	97.2004	98.196	0.9956	11.9392	16.0483	1.3401	0.012098
W03	12.2572	16	2.69	128.53	97.1828	98.195	1.0122	11.9789	16.0147	1.3357	0.011997
W03	12	16	2.61	125.83	97.2059	98.1797	0.9737	9.8671	15.9241	1.6216	0.018966
W03	11.7531	16	4.39	123.22	97.1635	98.1898	1.0263	12.5702	15.9857	1.2729	0.010729
W03	11.3377	16	4.39	118.83	97.1495	98.1892	1.0397	12.6925	15.9266	1.2606	0.010478
W03	10.9255	16	2.66	114.44	97.1417	98.1877	1.046	12.5871	15.9545	1.2711	0.01065
W03	10.6772	16	2.65	111.78	97.1538	98.1667	1.0129	9.5828	15.8366	1.6697	0.020255
W03	10.4302	16	4.63	109.13	97.1658	98.1756	1.0098	11.7513	15.8825	1.3616	0.012551
W03	10	16	10.24	104.5	97.1868	98.1776	0.9908	12.7767	15.8861	1.2523	0.01033
W03	9	16	10.52	94.26	97.1975	98.1621	0.9647	10.4945	13.8119	1.5246	0.015464
W03	8	16	5.44	83.74	97.1048	98.1472	1.0424	9.4442	12.1806	1.6942	0.018957
W03	7.49355	16	2.81	78.3	97.1107	98.1422	1.0315	9.2147	12.0653	1.7364	0.02002
W03	7.23155	16	2.81	75.49	97.1138	98.0887	0.9749	6.7882	11.7157	2.357	0.041
W03	6.96767	16	5.57	72.67	97.1169	98.1028	0.9859	8.6914	11.7674	1.8409	0.022879
W03	6.42191	16	5.57	67.1	97.123	98.0982	0.9752	8.5528	11.801	1.8707	0.023746
W03	5.88162	16	2.81	61.53	97.1212	98.0948	0.9736	8.5353	11.8558	1.8746	0.023884
W03	5.61996	16	2.81	58.71	97.1065	98.052	0.9455	6.601	11.6737	2.4239	0.043812
W03	5.35804	16	5.57	55.9	97.0918	98.0772	0.9854	8.7207	11.8847	1.8347	0.022792
W03	4.8316	16	5.57	50.32	97.0689	98.0762	1.0073	8.9353	11.9635	1.7906	0.021592
W03	4.28962	16	2.82	44.75	97.0601	98.0727	1.0126	8.8945	11.9242	1.7989	0.021787
W03	4.01486	16	2.81	41.93	97.0556	98.0292	0.9736	6.7292	11.6501	2.3777	0.041961
W03	3.75893	16	5.57	39.12	97.0546	98.0488	0.9942	8.5318	11.7889	1.8753	0.023958
W03	3.22591	16	5.57	33.55	97.0529	98.0464	0.9935	8.6078	11.8334	1.8588	0.023534
W03	2.71633	16	2.81	27.98	97.0473	98.0449	0.9976	8.7812	11.8772	1.8221	0.022505

Test Identification	River Station	Q (cfs)	Reach Length (ft)	Cumulative Channel Length (ft)	Minimum Channel Elevation (ft)	WSE (ft)	Depth (ft)	Flow Area (ft ²)	Top Width, Tw (ft)	Velocity (ft/s)	Shear Stress (lb/ft ²)
W03	2.46196	16	2.81	25.16	97.043	97.9953	0.9523	6.4853	11.5981	2.4671	0.045925
W03	2.20798	16	5.57	22.35	97.0386	98.021	0.9824	8.5403	11.7647	1.8735	0.023991
W03	1.70296	16	5.57	16.78	97.0415	98.0164	0.9749	8.4192	11.7304	1.9004	0.024784
W03	1.2285	16	2.81	11.2	97.0519	98.0113	0.9593	8.2934	11.6657	1.9292	0.025643
W03	0.976674	16	2.81	8.39	97.0569	97.942	0.8851	5.8025	11.2429	2.7574	0.059501
W03	0.646123	16	5.57	5.57	97.0569	97.9782	0.9213	8.0044	11.521	1.9989	0.027893
W03	0	16			97.0571	97.9756	0.9185	8.0879	11.6207	1.9783	0.02734
W04	18	8	3.27	189.25	97.2192	97.8606	0.6414	7.6609	14.0038	1.0443	0.008523
W04	17.6925	8	2.9	185.98	97.2269	97.8572	0.6303	7.1881	13.9655	1.113	0.009854
W04	17.4193	8	1.91	183.08	97.2338	97.8472	0.6134	6.014	13.8834	1.3302	0.013954
W04	17.2402	8	1.91	181.17	97.2383	97.8476	0.6093	6.2272	12.0375	1.2847	0.01319
W04	17.0596	8	2.36	179.26	97.2428	97.8461	0.6033	6.1429	13.8498	1.3023	0.013323
W04	16.8483	8	2.36	176.9	97.2389	97.8453	0.6064	6.1707	13.8529	1.2964	0.013179
W04	16.636	8	1.91	174.54	97.2313	97.8442	0.6129	6.1673	13.8702	1.2972	0.013172
W04	16.4644	8	1.91	172.63	97.2252	97.8449	0.6197	6.4286	12.044	1.2444	0.012249
W04	16.2928	8	2.58	170.72	97.219	97.8433	0.6243	6.3301	13.9212	1.2638	0.012404
W04	16.0601	8	2.13	168.14	97.2106	97.8433	0.6327	6.5039	13.9684	1.23	0.011649
W04	15.8467	8	1.91	166	97.2134	97.8425	0.6291	6.4946	13.9406	1.2318	0.011688
W04	15.6571	8	1.91	164.09	97.2195	97.8423	0.6228	6.5901	12.024	1.2139	0.01156
W04	15.4676	8	2.36	162.18	97.2256	97.8394	0.6137	6.3027	13.8344	1.2693	0.012517
W04	15.2335	8	2.36	159.82	97.2332	97.8376	0.6044	6.1984	13.7722	1.2907	0.013007
W04	15	8	1.91	157.46	97.2408	97.8359	0.5951	6.1064	13.7117	1.3101	0.013468
W04	14.8186	8	1.91	155.55	97.2376	97.8361	0.5985	6.2799	11.9331	1.2739	0.012902
W04	14.6373	8	2.36	153.64	97.2345	97.8334	0.5989	6.0836	13.7693	1.315	0.013562
W04	14.4134	8	2.36	151.28	97.2306	97.8328	0.6022	6.1427	13.8096	1.3024	0.013287
W04	14.1896	8	1.91	148.92	97.2267	97.8322	0.6055	6.2022	13.8491	1.2899	0.01302
W04	14.0086	8	1.91	147.01	97.2236	97.8324	0.6088	6.381	12.0295	1.2537	0.012463
W04	13.8264	8	2.27	145.1	97.2219	97.8301	0.6082	6.1955	13.8781	1.2913	0.013032
W04	13.6065	8	2.27	142.83	97.2199	97.8293	0.6094	6.2179	13.8813	1.2866	0.012921

Test Identifi- cation	River Station	Q (cfs)	Reach Length (ft)	Cumulative Channel Length (ft)	Minimum Channel Elevation (ft)	WSE (ft)	Depth (ft)	Flow Area (ft ²)	Top Width, Tw (ft)	Velocity (ft/s)	Shear Stress (lb/ft ²)
W04	13.3869	8	1.93	140.56	97.218	97.8287	0.6107	6.2595	13.8857	1.278	0.01273
W04	13.1996	8	1.89	138.63	97.2163	97.8291	0.6128	6.4769	12.0377	1.2352	0.012041
W04	13.0162	8	2.45	136.73	97.2147	97.8269	0.6122	6.2939	13.8898	1.2711	0.012566
W04	12.7956	8	2.45	134.28	97.2059	97.8203	0.6144	5.748	13.8339	1.3918	0.0155
W04	12.5668	8	1.91	131.83	97.1961	97.8165	0.6204	5.551	13.8016	1.4412	0.016796
W04	12.3878	8	1.91	129.92	97.1884	97.8169	0.6285	5.7462	11.8356	1.3922	0.015775
W04	12.2089	8	2.36	128.01	97.1808	97.8165	0.6357	5.8283	13.6824	1.3726	0.014957
W04	11.9822	8	2.36	125.65	97.1712	97.8166	0.6454	6.0182	13.7849	1.3293	0.013862
W04	11.7589	8	1.91	123.29	97.1637	97.8154	0.6517	6.0028	13.8036	1.3327	0.013944
W04	11.5783	8	1.91	121.37	97.1576	97.8159	0.6583	6.2166	11.839	1.2869	0.013177
W04	11.3979	8	2.36	119.46	97.1515	97.8135	0.662	6.0546	13.8353	1.3213	0.013676
W04	11.1744	8	2.36	117.1	97.1439	97.813	0.6691	6.1407	13.7998	1.3028	0.013225
W04	10.9536	8	1.91	114.74	97.1403	97.8119	0.6716	6.1238	13.687	1.3064	0.013291
W04	10.775	8	1.91	112.83	97.149	97.8098	0.6608	5.9966	11.7735	1.3341	0.014292
W04	10.5966	8	6.41	110.91	97.1577	97.8039	0.6462	5.5545	13.7477	1.4403	0.01667
W04	10	8	10.24	104.5	97.1868	97.8108	0.624	7.3255	13.8158	1.0921	0.009416
W04	9	8	10.52	94.26	97.1975	97.7955	0.598	5.8369	11.642	1.3706	0.015126
W04	8	8	7.23	83.74	97.1048	97.7838	0.679	5.4056	10.0495	1.4799	0.017252
W04	7.32771	8	2.09	76.52	97.1127	97.7547	0.642	4.2951	9.8325	1.8626	0.027054
W04	7.133	8	2.09	74.42	97.115	97.7547	0.6397	4.4541	8.4014	1.7961	0.025697
W04	6.9342	8	4.4	72.33	97.1173	97.7444	0.6271	4.1635	9.7646	1.9215	0.028977
W04	6.50363	8	4.4	67.93	97.1221	97.7386	0.6165	4.0951	9.7506	1.9536	0.030167
W04	6.07282	8	2.09	63.54	97.127	97.732	0.605	4.0046	9.7325	1.9977	0.031808
W04	5.87404	8	2.09	61.44	97.1207	97.7338	0.6131	4.2218	8.3922	1.8949	0.029029
W04	5.67926	8	4.4	59.35	97.1098	97.7298	0.62	4.1607	9.7932	1.9228	0.029167
W04	5.26983	8	4.4	54.95	97.0868	97.7298	0.643	4.3642	9.8826	1.8331	0.026121
W04	4.85386	8	2.09	50.55	97.0693	97.7276	0.6583	4.4425	9.9213	1.8008	0.025041
W04	4.65007	8	2.09	48.46	97.066	97.7285	0.6625	4.6192	8.4849	1.7319	0.023665
W04	4.44646	8	4.4	46.36	97.0627	97.7212	0.6585	4.3675	9.8563	1.8317	0.026

Test Identification	River Station	Q (cfs)	Reach Length (ft)	Cumulative Channel Length (ft)	Minimum Channel Elevation (ft)	WSE (ft)	Depth (ft)	Flow Area (ft ²)	Top Width, Tw (ft)	Velocity (ft/s)	Shear Stress (lb/ft ²)
W04	4.01851	8	4.4	41.97	97.0557	97.7188	0.6631	4.4286	9.8074	1.8064	0.025128
W04	3.61025	8	2.09	37.57	97.0541	97.7087	0.6546	4.1731	9.7909	1.9171	0.028816
W04	3.40982	8	2.09	35.47	97.0535	97.7107	0.6572	4.3946	8.386	1.8204	0.026437
W04	3.20969	8	4.4	33.38	97.0529	97.7066	0.6537	4.2974	9.8492	1.8616	0.026968
W04	2.80731	8	4.4	28.98	97.0489	97.7042	0.6553	4.3687	9.8811	1.8312	0.025929
W04	2.40968	8	2.09	24.58	97.0421	97.6996	0.6574	4.3327	9.8574	1.8464	0.026452
W04	2.22079	8	2.09	22.49	97.0388	97.7013	0.6625	4.5562	8.433	1.7559	0.024383
W04	2.03145	8	4.39	20.39	97.0355	97.6954	0.6599	4.3749	9.8458	1.8286	0.025901
W04	1.63729	8	4.41	16	97.0429	97.6886	0.6457	4.2303	9.7846	1.8911	0.027969
W04	1.26241	8	2.09	11.6	97.0511	97.6843	0.6332	4.2063	9.7326	1.9019	0.028358
W04	1.08389	8	2.09	9.5	97.055	97.6855	0.6304	4.394	8.362	1.8207	0.026482
W04	0.861618	8	7.41	7.41	97.0569	97.6799	0.623	4.2439	9.7082	1.885	0.027861
W04	0	8			97.0571	97.684	0.6269	4.9474	9.9194	1.617	0.021108
W04	18	12	3.27	189.25	97.2192	98.0487	0.8296	10.3999	15.1107	1.1539	0.009649
W04	17.6925	12	2.9	185.98	97.2269	98.0458	0.8189	9.9294	15.1039	1.2085	0.010737
W04	17.4193	12	1.91	183.08	97.2338	98.0441	0.8102	9.7421	15.1072	1.2318	0.011223
W04	17.2402	12	1.91	181.17	97.2383	98.0364	0.7981	8.6378	15.0571	1.3892	0.014908
W04	17.0596	12	2.36	179.26	97.2428	98.0403	0.7975	9.7877	15.0604	1.226	0.011095
W04	16.8483	12	2.36	176.9	97.2389	98.0398	0.8008	9.8265	15.0704	1.2212	0.010994
W04	16.636	12	1.91	174.54	97.2313	98.0392	0.8079	9.8665	15.0948	1.2162	0.010895
W04	16.4644	12	1.91	172.63	97.2252	98.0325	0.8073	8.8425	15.0622	1.3571	0.014118
W04	16.2928	12	2.58	170.72	97.219	98.0363	0.8173	10.0344	15.0958	1.1959	0.010476
W04	16.0601	12	2.13	168.14	97.2106	98.0363	0.8257	10.2728	15.1166	1.1681	0.009927
W04	15.8467	12	1.91	166	97.2134	98.0357	0.8223	10.2451	15.0966	1.1713	0.009986
W04	15.6571	12	1.91	164.09	97.2195	98.0281	0.8086	8.9796	15.024	1.3364	0.013614
W04	15.4676	12	2.36	162.18	97.2256	98.0311	0.8055	9.9651	15.0153	1.2042	0.010631
W04	15.2335	12	2.36	159.82	97.2332	98.0298	0.7966	9.8269	14.9754	1.2211	0.010974
W04	15	12	1.91	157.46	97.2408	98.0285	0.7877	9.6974	14.9326	1.2374	0.011309
W04	14.8186	12	1.91	155.55	97.2376	98.0206	0.783	8.5837	14.9119	1.398	0.015087

Test Identification	River Station	Q (cfs)	Reach Length (ft)	Cumulative Channel Length (ft)	Minimum Channel Elevation (ft)	WSE (ft)	Depth (ft)	Flow Area (ft ²)	Top Width, Tw (ft)	Velocity (ft/s)	Shear Stress (lb/ft ²)
W04	14.6373	12	2.36	153.64	97.2345	98.0245	0.79	9.7257	14.9612	1.2338	0.011238
W04	14.4134	12	2.36	151.28	97.2306	98.024	0.7934	9.773	14.9902	1.2279	0.011119
W04	14.1896	12	1.91	148.92	97.2267	98.0235	0.7968	9.8209	15.0194	1.2219	0.011
W04	14.0086	12	1.91	147.01	97.2236	98.0159	0.7923	8.7076	15.0003	1.3781	0.014619
W04	13.8264	12	2.27	145.1	97.2219	98.0197	0.7978	9.8495	15.0297	1.2183	0.010928
W04	13.6065	12	2.27	142.83	97.2199	98.0192	0.7993	9.8902	15.0329	1.2133	0.010825
W04	13.3869	12	1.93	140.56	97.218	98.0187	0.8007	9.9312	15.0367	1.2083	0.010722
W04	13.1996	12	1.89	138.63	97.2163	98.0113	0.7949	8.7933	14.998	1.3647	0.014289
W04	13.0162	12	2.45	136.73	97.2147	98.015	0.8003	9.9586	15.0251	1.205	0.010652
W04	12.7956	12	2.45	134.28	97.2059	98.0105	0.8046	9.29	14.9707	1.2917	0.012499
W04	12.5668	12	1.91	131.83	97.1961	98.0072	0.8111	8.9165	14.9293	1.3458	0.013735
W04	12.3878	12	1.91	129.92	97.1884	97.9995	0.8111	8.0715	14.8723	1.4867	0.017345
W04	12.2089	12	2.36	128.01	97.1808	98.0038	0.8229	9.1091	14.8915	1.3174	0.013059
W04	11.9822	12	2.36	125.65	97.1712	98.0051	0.8339	9.6917	14.9091	1.2382	0.011316
W04	11.7589	12	1.91	123.29	97.1637	98.0045	0.8408	9.7055	14.9086	1.2364	0.011277
W04	11.5783	12	1.91	121.37	97.1576	97.9966	0.839	8.576	14.8571	1.3993	0.015097
W04	11.3979	12	2.36	119.46	97.1515	98.0007	0.8492	9.7655	14.8516	1.2288	0.011105
W04	11.1744	12	2.36	117.1	97.1439	98.0004	0.8565	9.8728	14.7921	1.2155	0.010816
W04	10.9536	12	1.91	114.74	97.1403	97.9993	0.859	9.7892	14.7459	1.2258	0.011023
W04	10.775	12	1.91	112.83	97.149	97.9889	0.8399	8.3213	14.765	1.4421	0.016149
W04	10.5966	12	6.41	110.91	97.1577	97.9909	0.8332	8.9166	14.8306	1.3458	0.013707
W04	10	12	10.24	104.5	97.1868	97.9927	0.8059	9.9344	14.8594	1.2079	0.010674
W04	9	12	10.52	94.26	97.1975	97.9764	0.7789	8.0366	12.6726	1.4932	0.016619
W04	8	12	7.23	83.74	97.1048	97.9618	0.857	7.2865	11.0904	1.6469	0.020008
W04	7.32771	12	2.09	76.52	97.1127	97.9542	0.8415	7.0229	10.971	1.7087	0.021713
W04	7.133	12	2.09	74.42	97.115	97.9338	0.8188	6.0894	10.8412	1.9706	0.030338
W04	6.9342	12	4.4	72.33	97.1173	97.9378	0.8205	6.8198	10.8587	1.7596	0.023177
W04	6.50363	12	4.4	67.93	97.1221	97.9334	0.8113	6.6994	10.86	1.7912	0.024152
W04	6.07282	12	2.09	63.54	97.127	97.9286	0.8016	6.5735	10.8568	1.8255	0.025237

Test Identification	River Station	Q (cfs)	Reach Length (ft)	Cumulative Channel Length (ft)	Minimum Channel Elevation (ft)	WSE (ft)	Depth (ft)	Flow Area (ft ²)	Top Width, Tw (ft)	Velocity (ft/s)	Shear Stress (lb/ft ²)
W04	5.87404	12	2.09	61.44	97.1207	97.9106	0.7899	5.7859	10.7893	2.074	0.034055
W04	5.67926	12	4.4	59.35	97.1098	97.9209	0.811	6.7047	10.8998	1.7898	0.024133
W04	5.26983	12	4.4	54.95	97.0868	97.9211	0.8343	6.999	11.0055	1.7145	0.02191
W04	4.85386	12	2.09	50.55	97.0693	97.9197	0.8504	7.1382	11.0591	1.6811	0.020961
W04	4.65007	12	2.09	48.46	97.066	97.9043	0.8383	6.2729	10.9563	1.913	0.028382
W04	4.44646	12	4.4	46.36	97.0627	97.9104	0.8477	7.0126	10.977	1.7112	0.021788
W04	4.01851	12	4.4	41.97	97.0557	97.9087	0.853	7.1025	10.9339	1.6895	0.021138
W04	3.61025	12	2.09	37.57	97.0541	97.9027	0.8486	6.8344	10.9307	1.7558	0.023094
W04	3.40982	12	2.09	35.47	97.0535	97.8863	0.8328	6.0216	10.8622	1.9928	0.031093
W04	3.20969	12	4.4	33.38	97.0529	97.8945	0.8416	6.8906	10.9465	1.7415	0.022676
W04	2.80731	12	4.4	28.98	97.0489	97.8932	0.8443	7.0586	10.9861	1.7	0.02147
W04	2.40968	12	2.09	24.58	97.0421	97.89	0.8479	7.0143	10.9787	1.7108	0.021777
W04	2.22079	12	2.09	22.49	97.0388	97.8742	0.8354	6.1702	10.8931	1.9448	0.029436
W04	2.03145	12	4.39	20.39	97.0355	97.8815	0.846	7.0095	10.9463	1.712	0.021801
W04	1.63729	12	4.41	16	97.0429	97.8764	0.8335	6.8163	10.8939	1.7605	0.023217
W04	1.26241	12	2.09	11.6	97.0511	97.8724	0.8213	6.7297	10.8443	1.7831	0.023885
W04	1.08389	12	2.09	9.5	97.055	97.8549	0.7999	5.9015	10.728	2.0334	0.032526
W04	0.861618	12	7.41	7.41	97.0569	97.8626	0.8057	6.681	10.7943	1.7961	0.024267
W04	0	12			97.0571	97.859	0.8019	6.7727	10.9405	1.7718	0.02361
W04	18	16	3.27	189.25	97.2192	98.1717	0.9525	12.3021	15.8314	1.3006	0.011165
W04	17.6925	16	2.9	185.98	97.2269	98.1685	0.9416	11.8293	15.8412	1.3526	0.012213
W04	17.4193	16	1.91	183.08	97.2338	98.1668	0.933	11.6415	15.8391	1.3744	0.012681
W04	17.2402	16	1.91	181.17	97.2383	98.159	0.9207	10.5284	15.7888	1.5197	0.016109
W04	17.0596	16	2.36	179.26	97.2428	98.163	0.9202	11.6812	15.8013	1.3697	0.012567
W04	16.8483	16	2.36	176.9	97.2389	98.1625	0.9236	11.7213	15.809	1.365	0.012469
W04	16.636	16	1.91	174.54	97.2313	98.162	0.9307	11.7641	15.8245	1.3601	0.012373
W04	16.4644	16	1.91	172.63	97.2252	98.155	0.9298	10.7338	15.7951	1.4906	0.015399
W04	16.2928	16	2.58	170.72	97.219	98.159	0.94	11.9323	15.8271	1.3409	0.011971
W04	16.0601	16	2.13	168.14	97.2106	98.1591	0.9485	12.1728	15.8341	1.3144	0.011443

Test Identification	River Station	Q (cfs)	Reach Length (ft)	Cumulative Channel Length (ft)	Minimum Channel Elevation (ft)	WSE (ft)	Depth (ft)	Flow Area (ft ²)	Top Width, Tw (ft)	Velocity (ft/s)	Shear Stress (lb/ft ²)
W04	15.8467	16	1.91	166	97.2134	98.1584	0.945	12.1423	15.8137	1.3177	0.011505
W04	15.6571	16	1.91	164.09	97.2195	98.1505	0.931	10.8624	15.7441	1.473	0.014975
W04	15.4676	16	2.36	162.18	97.2256	98.1536	0.928	11.8494	15.739	1.3503	0.012151
W04	15.2335	16	2.36	159.82	97.2332	98.1522	0.919	11.7045	15.7009	1.367	0.012492
W04	15	16	1.91	157.46	97.2408	98.1508	0.9101	11.5691	15.6623	1.383	0.012823
W04	14.8186	16	1.91	155.55	97.2376	98.1428	0.9052	10.45	15.6395	1.5311	0.016344
W04	14.6373	16	2.36	153.64	97.2345	98.1468	0.9123	11.6005	15.6887	1.3792	0.01275
W04	14.4134	16	2.36	151.28	97.2306	98.1464	0.9157	11.6516	15.7172	1.3732	0.012629
W04	14.1896	16	1.91	148.92	97.2267	98.1459	0.9192	11.7035	15.7462	1.3671	0.012508
W04	14.0086	16	1.91	147.01	97.2236	98.1381	0.9145	10.5848	15.7261	1.5116	0.015897
W04	13.8264	16	2.27	145.1	97.2219	98.142	0.9201	11.7326	15.7548	1.3637	0.01244
W04	13.6065	16	2.27	142.83	97.2199	98.1415	0.9216	11.7737	15.7574	1.359	0.01234
W04	13.3869	16	1.93	140.56	97.218	98.141	0.923	11.8152	15.7601	1.3542	0.012241
W04	13.1996	16	1.89	138.63	97.2163	98.1334	0.917	10.6686	15.7192	1.4997	0.015609
W04	13.0162	16	2.45	136.73	97.2147	98.1373	0.9226	11.8399	15.7467	1.3514	0.01218
W04	12.7956	16	2.45	134.28	97.2059	98.1326	0.9267	11.1609	15.6909	1.4336	0.013953
W04	12.5668	16	1.91	131.83	97.1961	98.1291	0.933	10.7813	15.6472	1.484	0.015109
W04	12.3878	16	1.91	129.92	97.1884	98.1216	0.9332	9.9308	15.5932	1.6111	0.018339
W04	12.2089	16	2.36	128.01	97.1808	98.1258	0.945	10.9712	15.6108	1.4584	0.014492
W04	11.9822	16	2.36	125.65	97.1712	98.1273	0.9561	11.5574	15.6229	1.3844	0.012852
W04	11.7589	16	1.91	123.29	97.1637	98.1267	0.963	11.5713	15.6222	1.3827	0.012814
W04	11.5783	16	1.91	121.37	97.1576	98.1186	0.9609	10.4312	15.5609	1.5339	0.016403
W04	11.3979	16	2.36	119.46	97.1515	98.1228	0.9713	11.6226	15.5566	1.3766	0.012671
W04	11.1744	16	2.36	117.1	97.1439	98.1225	0.9786	11.7231	15.5089	1.3648	0.012398
W04	10.9536	16	1.91	114.74	97.1403	98.1214	0.9811	11.6375	15.5295	1.3749	0.012565
W04	10.775	16	1.91	112.83	97.149	98.1107	0.9617	10.1636	15.4848	1.5742	0.017359
W04	10.5966	16	6.41	110.91	97.1577	98.1129	0.9552	10.7673	15.5189	1.486	0.015139
W04	10	16	10.24	104.5	97.1868	98.1149	0.9281	11.7912	15.5379	1.3569	0.012272
W04	9	16	10.52	94.26	97.1975	98.0956	0.8981	9.5889	13.397	1.6686	0.018723

Test Identification	River Station	Q (cfs)	Reach Length (ft)	Cumulative Channel Length (ft)	Minimum Channel Elevation (ft)	WSE (ft)	Depth (ft)	Flow Area (ft ²)	Top Width, Tw (ft)	Velocity (ft/s)	Shear Stress (lb/ft ²)
W04	8	16	7.23	83.74	97.1048	98.0768	0.9721	8.6015	11.7668	1.8602	0.023036
W04	7.32771	16	2.09	76.52	97.1127	98.0685	0.9558	8.3145	11.6155	1.9243	0.024867
W04	7.133	16	2.09	74.42	97.115	98.0466	0.9316	7.3482	11.4688	2.1774	0.033324
W04	6.9342	16	4.4	72.33	97.1173	98.051	0.9336	8.0836	11.4843	1.9793	0.026493
W04	6.50363	16	4.4	67.93	97.1221	98.0464	0.9243	7.9622	11.4991	2.0095	0.027416
W04	6.07282	16	2.09	63.54	97.127	98.0414	0.9144	7.8354	11.51	2.042	0.028435
W04	5.87404	16	2.09	61.44	97.1207	98.0227	0.902	7.0322	11.4401	2.2753	0.036735
W04	5.67926	16	4.4	59.35	97.1098	98.0337	0.9239	7.9713	11.5528	2.0072	0.027356
W04	5.26983	16	4.4	54.95	97.0868	98.0342	0.9474	8.2812	11.6589	1.9321	0.025119
W04	4.85386	16	2.09	50.55	97.0693	98.0329	0.9636	8.4275	11.7154	1.8986	0.024152
W04	4.65007	16	2.09	48.46	97.066	98.0163	0.9503	7.5363	11.6121	2.1231	0.031452
W04	4.44646	16	4.4	46.36	97.0627	98.0229	0.9602	8.2844	11.6404	1.9313	0.025052
W04	4.01851	16	4.4	41.97	97.0557	98.021	0.9653	8.3686	11.6015	1.9119	0.024442
W04	3.61025	16	2.09	37.57	97.0541	98.0143	0.9602	8.0911	11.5946	1.9775	0.026414
W04	3.40982	16	2.09	35.47	97.0535	97.9968	0.9433	7.2578	11.5132	2.2045	0.034191
W04	3.20969	16	4.4	33.38	97.0529	98.0057	0.9528	8.1438	11.5968	1.9647	0.02606
W04	2.80731	16	4.4	28.98	97.0489	98.0045	0.9556	8.3171	11.6368	1.9238	0.024853
W04	2.40968	16	2.09	24.58	97.0421	98.001	0.9589	8.2697	11.6347	1.9348	0.025164
W04	2.22079	16	2.09	22.49	97.0388	97.9839	0.9451	7.4005	11.5437	2.162	0.032745
W04	2.03145	16	4.39	20.39	97.0355	97.9919	0.9564	8.2536	11.6026	1.9386	0.025263
W04	1.63729	16	4.41	16	97.0429	97.9863	0.9434	8.0495	11.547	1.9877	0.026723
W04	1.26241	16	2.09	11.6	97.0511	97.982	0.9309	7.9539	11.4947	2.0116	0.027439
W04	1.08389	16	2.09	9.5	97.055	97.9631	0.9081	7.0965	11.3691	2.2546	0.035975
W04	0.861618	16	7.41	7.41	97.0569	97.9715	0.9146	7.8909	11.4401	2.0276	0.027925
W04	0	16			97.0571	97.968	0.9109	7.9998	11.5764	2.0001	0.027197
W05	18	8	2.17	189.25	97.2192	97.8586	0.6395	7.6336	13.9923	1.048	0.008592
W05	17.7953	8	2.17	187.07	97.2243	97.8563	0.632	7.2879	13.9668	1.0977	0.00954
W05	17.591	8	1.89	184.91	97.2294	97.8465	0.6171	6.066	13.8937	1.3188	0.013678
W05	17.413	8	1.89	183.01	97.2339	97.8464	0.6125	6.2021	12.0266	1.2899	0.013308

Test Identification	River Station	Q (cfs)	Reach Length (ft)	Cumulative Channel Length (ft)	Minimum Channel Elevation (ft)	WSE (ft)	Depth (ft)	Flow Area (ft ²)	Top Width, Tw (ft)	Velocity (ft/s)	Shear Stress (lb/ft ²)
W05	17.2351	8	3.26	181.12	97.2384	97.844	0.6056	6.0227	13.8456	1.3283	0.013931
W05	16.9354	8	3.26	177.87	97.242	97.8433	0.6013	6.1379	13.8358	1.3034	0.013338
W05	16.6423	8	1.89	174.61	97.2315	97.842	0.6105	6.1541	13.8555	1.2999	0.013245
W05	16.4721	8	1.89	172.72	97.2254	97.8426	0.6172	6.3978	12.0351	1.2504	0.012384
W05	16.3018	8	2.47	170.83	97.2193	97.841	0.6217	6.3011	13.905	1.2696	0.012537
W05	16.0794	8	4.04	168.35	97.2113	97.8409	0.6296	6.4542	13.9496	1.2395	0.011853
W05	15.6788	8	1.89	164.31	97.2188	97.8387	0.6199	6.3491	13.8785	1.26	0.012293
W05	15.4916	8	1.89	162.42	97.2248	97.8387	0.6139	6.4757	11.9864	1.2354	0.012029
W05	15.3037	8	3.26	160.53	97.2309	97.8355	0.6046	6.1865	13.7745	1.2931	0.013056
W05	14.9827	8	3.26	157.27	97.2405	97.8334	0.5929	6.0921	13.6995	1.3132	0.013547
W05	14.6735	8	1.89	154.01	97.2351	97.8321	0.597	6.0969	13.7537	1.3121	0.013512
W05	14.4941	8	1.89	152.12	97.232	97.8324	0.6004	6.295	11.964	1.2709	0.01284
W05	14.3148	8	2.91	150.23	97.2289	97.8301	0.6012	6.1341	13.8118	1.3042	0.013336
W05	14.0388	8	3.53	147.32	97.2241	97.8286	0.6045	6.1098	13.8556	1.3094	0.013435
W05	13.7	8	1.89	143.79	97.2207	97.8277	0.607	6.2116	13.8682	1.2879	0.012966
W05	13.5167	8	1.89	141.9	97.2191	97.8281	0.609	6.4122	12.026	1.2476	0.012321
W05	13.3334	8	3.3	140.01	97.2175	97.8255	0.608	6.1995	13.8685	1.2904	0.012995
W05	13.0145	8	3.3	136.72	97.2147	97.8246	0.6099	6.2551	13.8755	1.279	0.012738
W05	12.7152	8	1.89	133.42	97.2024	97.8159	0.6135	5.5871	13.8066	1.4319	0.016535
W05	12.5337	8	1.89	131.53	97.1947	97.8152	0.6204	5.6334	11.8476	1.4201	0.016522
W05	12.3615	8	3.26	129.64	97.1873	97.8139	0.6266	5.627	13.7723	1.4217	0.016238
W05	12.0566	8	3.26	126.38	97.1743	97.8145	0.6402	5.9373	13.7007	1.3474	0.0143
W05	11.7432	8	1.89	123.12	97.1631	97.8133	0.6502	5.9803	13.7927	1.3377	0.014064
W05	11.5646	8	1.89	121.23	97.1571	97.8137	0.6566	6.1942	11.8314	1.2915	0.013286
W05	11.3862	8	3.26	119.34	97.1511	97.8114	0.6603	6.0349	13.8248	1.3256	0.013778
W05	11.0784	8	3.26	116.08	97.1407	97.8108	0.6701	6.1632	13.7626	1.298	0.013104
W05	10.7751	8	1.89	112.83	97.149	97.8059	0.6569	5.8084	13.6373	1.3773	0.015049
W05	10.5986	8	1.89	110.94	97.1576	97.8043	0.6467	5.738	11.8169	1.3942	0.015833
W05	10.4222	8	4.54	109.05	97.1662	97.8007	0.6345	5.5184	13.7466	1.4497	0.016972

Test Identification	River Station	Q (cfs)	Reach Length (ft)	Cumulative Channel Length (ft)	Minimum Channel Elevation (ft)	WSE (ft)	Depth (ft)	Flow Area (ft ²)	Top Width, Tw (ft)	Velocity (ft/s)	Shear Stress (lb/ft ²)
W05	10	8	10.24	104.5	97.1868	97.8084	0.6216	7.292	13.8014	1.0971	0.009514
W05	9	8	10.52	94.26	97.1975	97.7929	0.5954	5.8062	11.6269	1.3778	0.015306
W05	8	8	6.17	83.74	97.1048	97.781	0.6763	5.3778	10.0333	1.4876	0.017452
W05	7.42607	8	2.08	77.58	97.1115	97.7518	0.6403	4.2569	9.8193	1.8793	0.027568
W05	7.23228	8	2.08	75.5	97.1138	97.752	0.6382	4.432	8.3938	1.8051	0.025979
W05	7.03862	8	6.31	73.41	97.1161	97.7411	0.625	4.1282	9.7438	1.9379	0.029506
W05	6.42249	8	6.31	67.11	97.123	97.7315	0.6085	4.0075	9.7112	1.9962	0.031641
W05	5.81395	8	2.08	60.8	97.1174	97.7261	0.6087	4.0465	9.742	1.977	0.031049
W05	5.6202	8	2.08	58.72	97.1065	97.7294	0.6229	4.3377	8.4272	1.8443	0.02731
W05	5.4266	8	6.31	56.63	97.0956	97.725	0.6294	4.2509	9.8192	1.882	0.027749
W05	4.8319	8	6.31	50.33	97.0689	97.7227	0.6538	4.4055	9.8913	1.8159	0.025525
W05	4.21826	8	2.08	44.02	97.0589	97.7163	0.6574	4.3645	9.8097	1.833	0.02602
W05	4.01565	8	2.08	41.94	97.0556	97.7185	0.6629	4.625	8.3873	1.7297	0.023539
W05	3.82917	8	6.31	39.86	97.0548	97.707	0.6522	4.2241	9.7531	1.8939	0.028016
W05	3.22567	8	6.31	33.55	97.0529	97.7021	0.6492	4.2423	9.8198	1.8858	0.027749
W05	2.6504	8	2.08	27.24	97.0462	97.6985	0.6523	4.3437	9.8478	1.8417	0.026316
W05	2.46209	8	2.08	25.16	97.0429	97.6997	0.6568	4.5264	8.4243	1.7674	0.024742
W05	2.27377	8	6.31	23.08	97.0397	97.6926	0.6529	4.3005	9.8198	1.8602	0.026921
W05	1.70234	8	6.31	16.77	97.0415	97.6854	0.6439	4.2156	9.77	1.8977	0.028189
W05	1.16546	8	2.08	10.46	97.0532	97.6781	0.6249	4.1404	9.6863	1.9322	0.029341
W05	0.97571	8	2.08	8.38	97.0569	97.68	0.6231	4.3599	8.3468	1.8349	0.026953
W05	0.731156	8	6.3	6.3	97.0569	97.6761	0.6192	4.273	9.7129	1.8722	0.027531
W05	0	8			97.0571	97.68	0.6229	4.9079	9.8961	1.63	0.02149
W05	18	12	2.17	189.25	97.2192	98.0666	0.8475	10.6708	15.2154	1.1246	0.009109
W05	17.7953	12	2.17	187.07	97.2243	98.0647	0.8404	10.3298	15.2126	1.1617	0.009817
W05	17.591	12	1.89	184.91	97.2294	98.0632	0.8338	10.1092	15.2152	1.187	0.010321
W05	17.413	12	1.89	183.01	97.2339	98.0559	0.8219	8.9284	15.1806	1.344	0.013837
W05	17.2351	12	3.26	181.12	97.2384	98.0591	0.8207	9.9774	15.1922	1.2027	0.010637
W05	16.9354	12	3.26	177.87	97.242	98.0586	0.8166	10.1107	15.1725	1.1869	0.010313

Test Identification	River Station	Q (cfs)	Reach Length (ft)	Cumulative Channel Length (ft)	Minimum Channel Elevation (ft)	WSE (ft)	Depth (ft)	Flow Area (ft ²)	Top Width, Tw (ft)	Velocity (ft/s)	Shear Stress (lb/ft ²)
W05	16.6423	12	1.89	174.61	97.2315	98.0579	0.8264	10.1475	15.2055	1.1826	0.01023
W05	16.4721	12	1.89	172.72	97.2254	98.0518	0.8263	9.1305	15.1793	1.3143	0.013135
W05	16.3018	12	2.47	170.83	97.2193	98.0552	0.8359	10.3135	15.2083	1.1635	0.009852
W05	16.0794	12	4.04	168.35	97.2113	98.0552	0.8439	10.5376	15.2252	1.1388	0.009378
W05	15.6788	12	1.89	164.31	97.2188	98.0539	0.8351	10.4242	15.1807	1.1512	0.009607
W05	15.4916	12	1.89	162.42	97.2248	98.0468	0.822	9.1759	15.1135	1.3078	0.01297
W05	15.3037	12	3.26	160.53	97.2309	98.0496	0.8187	10.16	15.1031	1.1811	0.010182
W05	14.9827	12	3.26	157.27	97.2405	98.0481	0.8076	9.9951	15.0519	1.2006	0.010567
W05	14.6735	12	1.89	154.01	97.2351	98.0474	0.8123	10.0611	15.0918	1.1927	0.010415
W05	14.4941	12	1.89	152.12	97.232	98.0405	0.8085	8.961	15.0766	1.3391	0.013696
W05	14.3148	12	2.91	150.23	97.2289	98.044	0.815	10.098	15.1227	1.1884	0.010333
W05	14.0388	12	3.53	147.32	97.2241	98.0434	0.8193	10.1594	15.1591	1.1812	0.010197
W05	13.7	12	1.89	143.79	97.2207	98.0427	0.822	10.2243	15.1694	1.1737	0.010049
W05	13.5167	12	1.89	141.9	97.2191	98.036	0.8169	9.1063	15.1353	1.3178	0.01321
W05	13.3334	12	3.3	140.01	97.2175	98.0394	0.8219	10.2555	15.1603	1.1701	0.009976
W05	13.0145	12	3.3	136.72	97.2147	98.0387	0.824	10.3175	15.1653	1.1631	0.009839
W05	12.7152	12	1.89	133.42	97.2024	98.0335	0.8311	9.4794	15.0975	1.2659	0.011956
W05	12.5337	12	1.89	131.53	97.1947	98.025	0.8303	8.3502	15.032	1.4371	0.016079
W05	12.3615	12	3.26	129.64	97.1873	98.0284	0.841	9.2622	15.0412	1.2956	0.012601
W05	12.0566	12	3.26	126.38	97.1743	98.0295	0.8552	9.8734	15.047	1.2154	0.010867
W05	11.7432	12	1.89	123.12	97.1631	98.0293	0.8662	10.0799	15.0551	1.1905	0.010359
W05	11.5646	12	1.89	121.23	97.1571	98.0224	0.8653	8.965	15.0039	1.3385	0.013658
W05	11.3862	12	3.26	119.34	97.1511	98.026	0.8749	10.1483	14.9953	1.1825	0.010186
W05	11.0784	12	3.26	116.08	97.1407	98.0257	0.885	10.3034	14.9056	1.1647	0.00982
W05	10.7751	12	1.89	112.83	97.149	98.0215	0.8725	9.6194	14.9504	1.2475	0.011523
W05	10.5986	12	1.89	110.94	97.1576	98.0133	0.8557	8.4872	14.9565	1.4139	0.01547
W05	10.4222	12	4.54	109.05	97.1662	98.0161	0.8499	9.2928	15.0086	1.2913	0.012496
W05	10	12	10.24	104.5	97.1868	98.0182	0.8315	10.3158	15.0013	1.1633	0.009808
W05	9	12	10.52	94.26	97.1975	98.0036	0.8061	8.3826	12.8255	1.4315	0.015125

Test Identification	River Station	Q (cfs)	Reach Length (ft)	Cumulative Channel Length (ft)	Minimum Channel Elevation (ft)	WSE (ft)	Depth (ft)	Flow Area (ft ²)	Top Width, Tw (ft)	Velocity (ft/s)	Shear Stress (lb/ft ²)
W05	8	12	6.17	83.74	97.1048	97.9903	0.8856	7.6059	11.2584	1.5777	0.018196
W05	7.42607	12	2.08	77.58	97.1115	97.9846	0.873	7.3729	11.1522	1.6276	0.019493
W05	7.23228	12	2.08	75.5	97.1138	97.9675	0.8537	6.4622	11.0372	1.8569	0.026563
W05	7.03862	12	6.31	73.41	97.1161	97.971	0.8549	7.1933	11.0406	1.6682	0.020584
W05	6.42249	12	6.31	67.11	97.123	97.9654	0.8424	7.0364	11.0465	1.7054	0.021664
W05	5.81395	12	2.08	60.8	97.1174	97.962	0.8446	7.0607	11.103	1.6995	0.021525
W05	5.6202	12	2.08	58.72	97.1065	97.9501	0.8436	6.4052	11.0847	1.8735	0.027126
W05	5.4266	12	6.31	56.63	97.0956	97.9572	0.8616	7.2871	11.1749	1.6467	0.020044
W05	4.8319	12	6.31	50.33	97.0689	97.9562	0.8872	7.5412	11.2698	1.5913	0.01856
W05	4.21826	12	2.08	44.02	97.0589	97.9528	0.8939	7.5236	11.2113	1.595	0.018631
W05	4.01565	12	2.08	41.94	97.0556	97.9418	0.8862	6.7827	11.1304	1.7692	0.023808
W05	3.82917	12	6.31	39.86	97.0548	97.9458	0.891	7.3856	11.1644	1.6248	0.019422
W05	3.22567	12	6.31	33.55	97.0529	97.943	0.8901	7.4154	11.2266	1.6183	0.019272
W05	2.6504	12	2.08	27.24	97.0462	97.9411	0.8949	7.5758	11.271	1.584	0.018362
W05	2.46209	12	2.08	25.16	97.0429	97.9291	0.8861	6.7523	11.2074	1.7772	0.024079
W05	2.27377	12	6.31	23.08	97.0397	97.9343	0.8946	7.5278	11.2468	1.5941	0.018623
W05	1.70234	12	6.31	16.77	97.0415	97.9303	0.8888	7.4315	11.2185	1.6147	0.019171
W05	1.16546	12	2.08	10.46	97.0532	97.9261	0.8729	7.327	11.1558	1.6378	0.019781
W05	0.97571	12	2.08	8.38	97.0569	97.9135	0.8566	6.5495	11.0742	1.8322	0.025786
W05	0.731156	12	6.3	6.3	97.0569	97.9193	0.8624	7.3231	11.1542	1.6386	0.019811
W05	0	12			97.0571	97.917	0.8599	7.4171	11.2789	1.6179	0.019299
W05	18	16	2.17	189.25	97.2192	98.1883	0.9692	12.5661	15.931	1.2733	0.010653
W05	17.7953	16	2.17	187.07	97.2243	98.1863	0.962	12.2232	15.9341	1.309	0.011353
W05	17.591	16	1.89	184.91	97.2294	98.1847	0.9552	12.0021	15.9405	1.3331	0.011843
W05	17.413	16	1.89	183.01	97.2339	98.177	0.9431	10.8117	15.8996	1.4799	0.015188
W05	17.2351	16	3.26	181.12	97.2384	98.1804	0.942	11.8649	15.9166	1.3485	0.012159
W05	16.9354	16	3.26	177.87	97.242	98.18	0.938	11.9964	15.9058	1.3337	0.011844
W05	16.6423	16	1.89	174.61	97.2315	98.1793	0.9478	12.0365	15.9268	1.3293	0.011764
W05	16.4721	16	1.89	172.72	97.2254	98.1728	0.9474	11.0122	15.8994	1.4529	0.014551

Test Identification	River Station	Q (cfs)	Reach Length (ft)	Cumulative Channel Length (ft)	Minimum Channel Elevation (ft)	WSE (ft)	Depth (ft)	Flow Area (ft ²)	Top Width, Tw (ft)	Velocity (ft/s)	Shear Stress (lb/ft ²)
W05	16.3018	16	2.47	170.83	97.2193	98.1765	0.9572	12.2023	15.9291	1.3112	0.011397
W05	16.0794	16	4.04	168.35	97.2113	98.1766	0.9653	12.4277	15.9356	1.2874	0.010933
W05	15.6788	16	1.89	164.31	97.2188	98.1751	0.9563	12.3075	15.8911	1.3	0.011171
W05	15.4916	16	1.89	162.42	97.2248	98.1676	0.9428	11.044	15.8243	1.4488	0.01444
W05	15.3037	16	3.26	160.53	97.2309	98.1706	0.9397	12.03	15.8186	1.33	0.011757
W05	14.9827	16	3.26	157.27	97.2405	98.1689	0.9284	11.8575	15.7725	1.3494	0.012145
W05	14.6735	16	1.89	154.01	97.2351	98.1683	0.9332	11.9285	15.8113	1.3413	0.011988
W05	14.4941	16	1.89	152.12	97.232	98.1611	0.9291	10.8216	15.7935	1.4785	0.015127
W05	14.3148	16	2.91	150.23	97.2289	98.1647	0.9358	11.9676	15.8405	1.3369	0.011906
W05	14.0388	16	3.53	147.32	97.2241	98.1642	0.9401	12.0336	15.8762	1.3296	0.011765
W05	13.7	16	1.89	143.79	97.2207	98.1634	0.9427	12.0996	15.8849	1.3224	0.01162
W05	13.5167	16	1.89	141.9	97.2191	98.1564	0.9373	10.9716	15.848	1.4583	0.014671
W05	13.3334	16	3.3	140.01	97.2175	98.16	0.9425	12.1274	15.8736	1.3193	0.011556
W05	13.0145	16	3.3	136.72	97.2147	98.1594	0.9447	12.1898	15.8773	1.3126	0.011422
W05	12.7152	16	1.89	133.42	97.2024	98.1538	0.9514	11.3376	15.8059	1.4112	0.013496
W05	12.5337	16	1.89	131.53	97.1947	98.1451	0.9504	10.1984	15.7377	1.5689	0.017307
W05	12.3615	16	3.26	129.64	97.1873	98.1486	0.9613	11.1128	15.7493	1.4398	0.014119
W05	12.0566	16	3.26	126.38	97.1743	98.1498	0.9755	11.7263	15.7501	1.3645	0.012467
W05	11.7432	16	1.89	123.12	97.1631	98.1496	0.9865	11.9342	15.7534	1.3407	0.011972
W05	11.5646	16	1.89	121.23	97.1571	98.1423	0.9852	10.8059	15.6959	1.4807	0.015163
W05	11.3862	16	3.26	119.34	97.1511	98.1462	0.9951	11.9919	15.6887	1.3342	0.011825
W05	11.0784	16	3.26	116.08	97.1407	98.1458	1.0051	12.1401	15.685	1.3179	0.011427
W05	10.7751	16	1.89	112.83	97.149	98.1414	0.9923	11.4541	15.6757	1.3969	0.013122
W05	10.5986	16	1.89	110.94	97.1576	98.133	0.9754	10.3175	15.6326	1.5508	0.016849
W05	10.4222	16	4.54	109.05	97.1662	98.1359	0.9697	11.1304	15.6667	1.4375	0.014087
W05	10	16	10.24	104.5	97.1868	98.1382	0.9515	12.1561	15.6677	1.3162	0.011473
W05	9	16	10.52	94.26	97.1975	98.1205	0.923	9.9251	13.5525	1.6121	0.017351
W05	8	16	6.17	83.74	97.1048	98.1034	0.9986	8.9159	11.9229	1.7945	0.021314
W05	7.42607	16	2.08	77.58	97.1115	98.0969	0.9854	8.6616	11.7892	1.8472	0.022747

Test Identification	River Station	Q (cfs)	Reach Length (ft)	Cumulative Channel Length (ft)	Minimum Channel Elevation (ft)	WSE (ft)	Depth (ft)	Flow Area (ft ²)	Top Width, Tw (ft)	Velocity (ft/s)	Shear Stress (lb/ft ²)
W05	7.23228	16	2.08	75.5	97.1138	98.0781	0.9643	7.7161	11.656	2.0736	0.029922
W05	7.03862	16	6.31	73.41	97.1161	98.0819	0.9658	8.4511	11.6532	1.8933	0.024045
W05	6.42249	16	6.31	67.11	97.123	98.0759	0.9529	8.2912	11.6741	1.9298	0.025113
W05	5.81395	16	2.08	60.8	97.1174	98.0723	0.9549	8.3215	11.7429	1.9227	0.024928
W05	5.6202	16	2.08	58.72	97.1065	98.0597	0.9532	7.6541	11.7184	2.0904	0.030477
W05	5.4266	16	6.31	56.63	97.0956	98.0679	0.9723	8.5599	11.8146	1.8692	0.023396
W05	4.8319	16	6.31	50.33	97.0689	98.067	0.9981	8.8263	11.911	1.8128	0.021849
W05	4.21826	16	2.08	44.02	97.0589	98.0633	1.0044	8.7984	11.8646	1.8185	0.021954
W05	4.01565	16	2.08	41.94	97.0556	98.0509	0.9953	8.0326	11.7788	1.9919	0.027291
W05	3.82917	16	6.31	39.86	97.0548	98.0554	1.0006	8.6456	11.8218	1.8506	0.022825
W05	3.22567	16	6.31	33.55	97.0529	98.0525	0.9996	8.6799	11.8694	1.8434	0.022678
W05	2.6504	16	2.08	27.24	97.0462	98.0506	1.0044	8.8447	11.9141	1.809	0.021739
W05	2.46209	16	2.08	25.16	97.0429	98.037	0.9941	7.9969	11.8445	2.0008	0.027621
W05	2.27377	16	6.31	23.08	97.0397	98.043	1.0033	8.7849	11.8912	1.8213	0.022066
W05	1.70234	16	6.31	16.77	97.0415	98.0386	0.9971	8.6806	11.8622	1.8432	0.022665
W05	1.16546	16	2.08	10.46	97.0532	98.0338	0.9806	8.5635	11.7947	1.8684	0.023358
W05	0.97571	16	2.08	8.38	97.0569	98.0197	0.9628	7.7588	11.7037	2.0622	0.029567
W05	0.731156	16	6.3	6.3	97.0569	98.0263	0.9694	8.5504	11.792	1.8713	0.023449
W05	0	16			97.0571	98.024	0.9669	8.6572	11.9063	1.8482	0.022885
W06	18	8	5.91	189.25	97.2192	97.8924	0.6733	8.1096	14.1917	0.9865	0.007498
W06	17.4435	8	1.89	183.33	97.2332	97.8736	0.6404	5.695	14.0519	1.4047	0.01541
W06	17.2652	8	1.89	181.44	97.2377	97.8741	0.6364	5.9016	11.1046	1.3556	0.014572
W06	17.0869	8	3.85	179.55	97.2422	97.872	0.6298	5.7891	14.0124	1.3819	0.014863
W06	16.7398	8	3.85	175.7	97.235	97.8706	0.6356	5.823	14.023	1.3739	0.014646
W06	16.3929	8	1.89	171.84	97.2226	97.8696	0.647	5.9213	14.0642	1.3511	0.014079
W06	16.223	8	1.89	169.95	97.2165	97.8707	0.6542	6.2372	11.1243	1.2826	0.012822
W06	16.0532	8	3.85	168.06	97.2104	97.8693	0.6588	6.1569	14.1266	1.2993	0.012868
W06	15.6685	8	3.85	164.21	97.2192	97.8667	0.6475	6.0266	14.0479	1.3274	0.013498
W06	15.286	8	1.89	160.35	97.2315	97.8637	0.6322	5.8719	13.947	1.3624	0.014334

Test Identification	River Station	Q (cfs)	Reach Length (ft)	Cumulative Channel Length (ft)	Minimum Channel Elevation (ft)	WSE (ft)	Depth (ft)	Flow Area (ft ²)	Top Width, Tw (ft)	Velocity (ft/s)	Shear Stress (lb/ft ²)
W06	15.0986	8	1.89	158.46	97.2376	97.8636	0.626	5.9809	10.9922	1.3376	0.014084
W06	14.9164	8	3.74	156.57	97.2393	97.8602	0.6208	5.7319	13.8827	1.3957	0.015137
W06	14.5616	8	3.97	152.83	97.2331	97.8587	0.6255	5.7673	13.9417	1.3871	0.014934
W06	14.1854	8	1.89	148.87	97.2266	97.8572	0.6306	5.8218	14.0031	1.3741	0.014637
W06	14.006	8	1.89	146.97	97.2235	97.8579	0.6343	6.0497	11.0906	1.3224	0.013756
W06	13.825	8	3.85	145.08	97.2219	97.8552	0.6333	5.8679	14.0312	1.3633	0.014388
W06	13.4516	8	3.85	141.23	97.2186	97.8533	0.6347	5.8505	14.0342	1.3674	0.014451
W06	13.0785	8	1.89	137.38	97.2153	97.852	0.6367	5.903	14.0423	1.3553	0.014164
W06	12.9082	8	1.89	135.49	97.2107	97.8512	0.6405	5.9025	11.063	1.3554	0.014539
W06	12.7316	8	3.85	133.6	97.2031	97.8447	0.6416	5.4479	13.9849	1.4685	0.017065
W06	12.371	8	3.85	129.74	97.1877	97.8421	0.6544	5.4279	13.94	1.4739	0.017146
W06	12	8	1.89	125.89	97.1718	97.8413	0.6694	5.5741	13.9346	1.4352	0.016061
W06	11.8263	8	1.89	124	97.1878	97.8423	0.6544	5.8267	10.9115	1.373	0.014935
W06	11.6475	8	3.85	122.11	97.1599	97.8389	0.679	5.6133	13.9538	1.4252	0.01585
W06	11.2834	8	3.85	118.25	97.1476	97.837	0.6894	5.6222	13.9468	1.4229	0.015743
W06	10.9222	8	1.89	114.4	97.1418	97.8348	0.693	5.6	13.7792	1.4286	0.015849
W06	10.7458	8	1.89	112.51	97.1504	97.8342	0.6838	5.6436	10.8453	1.4175	0.016054
W06	10.5691	8	6.12	110.62	97.159	97.8281	0.6691	5.2608	13.9093	1.5207	0.018376
W06	10	8	10.24	104.5	97.1868	97.8389	0.6521	7.6709	13.9821	1.0429	0.008382
W06	9	8	10.52	94.26	97.1975	97.826	0.6285	6.194	11.8168	1.2916	0.013237
W06	8	8	5.57	83.74	97.1048	97.8156	0.7108	5.7152	10.2348	1.3998	0.015104
W06	7.48171	8	2.08	78.18	97.1108	97.768	0.6572	3.9279	9.9145	2.0367	0.032273
W06	7.28869	8	2.09	76.1	97.1131	97.7684	0.6553	4.1024	7.7094	1.9501	0.030305
W06	7.09453	8	6.46	74.01	97.1154	97.7516	0.6362	3.7432	9.811	2.1372	0.035888
W06	6.4666	8	6.46	67.56	97.1225	97.7431	0.6206	3.7074	9.7795	2.1579	0.036787
W06	5.84187	8	2.08	61.1	97.1189	97.7367	0.6178	3.7422	9.8001	2.1378	0.036114
W06	5.64812	8	2.08	59.02	97.1081	97.7408	0.6327	4.0219	7.7203	1.9891	0.03171
W06	5.45452	8	6.46	56.93	97.0972	97.7321	0.6349	3.8531	9.856	2.0763	0.033753
W06	4.8465	8	6.46	50.48	97.0692	97.7295	0.6603	4.0065	9.9327	1.9967	0.0309

Test Identification	River Station	Q (cfs)	Reach Length (ft)	Cumulative Channel Length (ft)	Minimum Channel Elevation (ft)	WSE (ft)	Depth (ft)	Flow Area (ft ²)	Top Width, Tw (ft)	Velocity (ft/s)	Shear Stress (lb/ft ²)
W06	4.21826	8	2.08	44.02	97.0589	97.7195	0.6606	3.8949	9.8286	2.054	0.032761
W06	4.01564	8	2.08	41.94	97.0556	97.7233	0.6677	4.1821	7.6488	1.9129	0.028917
W06	3.82915	8	6.46	39.86	97.0548	97.707	0.6522	3.7604	9.7529	2.1274	0.035447
W06	3.2113	8	6.46	33.4	97.0529	97.6996	0.6467	3.7448	9.8081	2.1363	0.035818
W06	2.62322	8	2.08	26.94	97.0457	97.6952	0.6495	3.853	9.8289	2.0763	0.033654
W06	2.43492	8	2.08	24.86	97.0424	97.6977	0.6553	4.0724	7.6719	1.9644	0.030778
W06	2.24663	8	6.46	22.78	97.0392	97.6864	0.6472	3.8056	9.7846	2.1022	0.034593
W06	1.66399	8	6.46	16.32	97.0423	97.675	0.6327	3.6777	9.7062	2.1753	0.037351
W06	1.11435	8	2.08	9.86	97.0544	97.6612	0.6068	3.5166	9.5801	2.2749	0.041231
W06	0.905209	8	2.08	7.78	97.0569	97.6663	0.6094	3.8075	7.5509	2.1011	0.035806
W06	0.66075	8	2.85	5.7	97.0569	97.661	0.6041	3.7275	9.6385	2.1462	0.036601
W06	0.325963	8	2.85	2.85	97.057	97.6776	0.6206	4.845	9.8096	1.6512	0.022082
W06	0	8			97.0571	97.676	0.6189	4.8682	9.8727	1.6433	0.021882
W06	18	12	5.91	189.25	97.2192	98.0779	0.8588	10.8432	15.2817	1.1067	0.008788
W06	17.4435	12	1.89	183.33	97.2332	98.0739	0.8407	10.2016	15.2899	1.1763	0.01012
W06	17.2652	12	1.89	181.44	97.2377	98.0606	0.8229	8.2191	15.2033	1.46	0.016798
W06	17.0869	12	3.85	179.55	97.2422	98.0678	0.8256	10.1836	15.2299	1.1784	0.010153
W06	16.7398	12	3.85	175.7	97.235	98.067	0.832	10.2571	15.2493	1.1699	0.009987
W06	16.3929	12	1.89	171.84	97.2226	98.0666	0.844	10.4153	15.2725	1.1522	0.009642
W06	16.223	12	1.89	169.95	97.2165	98.0553	0.8388	8.585	15.2141	1.3978	0.015183
W06	16.0532	12	3.85	168.06	97.2104	98.0622	0.8517	10.6738	15.2682	1.1242	0.00911
W06	15.6685	12	3.85	164.21	97.2192	98.0607	0.8415	10.5227	15.2201	1.1404	0.009407
W06	15.286	12	1.89	160.35	97.2315	98.0589	0.8274	10.2908	15.1556	1.1661	0.009895
W06	15.0986	12	1.89	158.46	97.2376	98.0446	0.807	8.1612	15.0437	1.4704	0.017024
W06	14.9164	12	3.74	156.57	97.2393	98.0518	0.8125	10.0677	15.0834	1.1919	0.010398
W06	14.5616	12	3.97	152.83	97.2331	98.0511	0.818	10.1442	15.1293	1.1829	0.010226
W06	14.1854	12	1.89	148.87	97.2266	98.0503	0.8237	10.2273	15.179	1.1733	0.010044
W06	14.006	12	1.89	146.97	97.2235	98.0371	0.8136	8.2459	15.1267	1.4553	0.016651
W06	13.825	12	3.85	145.08	97.2219	98.0443	0.8223	10.2206	15.1749	1.1741	0.010058

Test Identification	River Station	Q (cfs)	Reach Length (ft)	Cumulative Channel Length (ft)	Minimum Channel Elevation (ft)	WSE (ft)	Depth (ft)	Flow Area (ft ²)	Top Width, Tw (ft)	Velocity (ft/s)	Shear Stress (lb/ft ²)
W06	13.4516	12	3.85	141.23	97.2186	98.0435	0.8249	10.2916	15.1811	1.166	0.009899
W06	13.0785	12	1.89	137.38	97.2153	98.0428	0.8275	10.3639	15.1873	1.1579	0.009741
W06	12.9082	12	1.89	135.49	97.2107	98.0273	0.8166	8.0675	15.0838	1.4875	0.017488
W06	12.7316	12	3.85	133.6	97.2031	98.0331	0.83	9.5016	15.0966	1.263	0.011891
W06	12.371	12	3.85	129.74	97.1877	98.0306	0.8429	9.2883	15.0549	1.2919	0.012522
W06	12	12	1.89	125.89	97.1718	98.0323	0.8605	10.0984	15.0678	1.1883	0.010319
W06	11.8263	12	1.89	124	97.1878	98.0182	0.8303	8.0795	14.9886	1.4852	0.017405
W06	11.6475	12	3.85	122.11	97.1599	98.026	0.8661	10.0535	15.0341	1.1936	0.010418
W06	11.2834	12	3.85	118.25	97.1476	98.0254	0.8778	10.1879	14.968	1.1779	0.01009
W06	10.9222	12	1.89	114.4	97.1418	98.0238	0.882	10.0461	14.9096	1.1945	0.010413
W06	10.7458	12	1.89	112.51	97.1504	98.0079	0.8575	7.8721	14.8831	1.5244	0.018447
W06	10.5691	12	6.12	110.62	97.159	98.0138	0.8548	9.242	14.9665	1.2984	0.012646
W06	10	12	10.24	104.5	97.1868	98.0156	0.8288	10.2756	14.9864	1.1678	0.009894
W06	9	12	10.52	94.26	97.1975	98.0007	0.8032	8.3462	12.8095	1.4378	0.015272
W06	8	12	5.57	83.74	97.1048	97.9873	0.8826	7.5723	11.2409	1.5847	0.018375
W06	7.48171	12	2.08	78.18	97.1108	97.9819	0.8711	7.3529	11.1433	1.632	0.019611
W06	7.28869	12	2.09	76.1	97.1131	97.9422	0.8291	5.6244	10.9003	2.1336	0.036588
W06	7.09453	12	6.46	74.01	97.1154	97.9525	0.8371	6.9899	10.9423	1.7168	0.021939
W06	6.4666	12	6.46	67.56	97.1225	97.9464	0.8239	6.8344	10.9356	1.7558	0.023108
W06	5.84187	12	2.08	61.1	97.1189	97.9421	0.8232	6.8209	10.9805	1.7593	0.023243
W06	5.64812	12	2.08	59.02	97.1081	97.9099	0.8018	5.4374	10.8449	2.2069	0.03949
W06	5.45452	12	6.46	56.93	97.0972	97.9287	0.8315	6.9508	11.0031	1.7264	0.022261
W06	4.8465	12	6.46	50.48	97.0692	97.9276	0.8584	7.2241	11.1047	1.6611	0.020413
W06	4.21826	12	2.08	44.02	97.0589	97.9236	0.8647	7.199	11.0379	1.6669	0.02054
W06	4.01564	12	2.08	41.94	97.0556	97.8934	0.8377	5.6826	10.8426	2.1117	0.035667
W06	3.82915	12	6.46	39.86	97.0548	97.9069	0.8521	6.9557	10.9333	1.7252	0.022178
W06	3.2113	12	6.46	33.4	97.0529	97.9035	0.8506	6.9881	10.9986	1.7172	0.02198
W06	2.62322	12	2.08	26.94	97.0457	97.901	0.8553	7.1278	11.0362	1.6836	0.021015
W06	2.43492	12	2.08	24.86	97.0424	97.8679	0.8255	5.5473	10.847	2.1632	0.037722

Test Identification	River Station	Q (cfs)	Reach Length (ft)	Cumulative Channel Length (ft)	Minimum Channel Elevation (ft)	WSE (ft)	Depth (ft)	Flow Area (ft ²)	Top Width, Tw (ft)	Velocity (ft/s)	Shear Stress (lb/ft ²)
W06	2.24663	12	6.46	22.78	97.0392	97.8835	0.8443	6.9698	10.9466	1.7217	0.022083
W06	1.66399	12	6.46	16.32	97.0423	97.878	0.8357	6.8412	10.9051	1.7541	0.023029
W06	1.11435	12	2.08	9.86	97.0544	97.8726	0.8182	6.7455	10.8351	1.779	0.023755
W06	0.905209	12	2.08	7.78	97.0569	97.8303	0.7734	5.099	8.2012	2.3534	0.042
W06	0.66075	12	2.85	5.7	97.0569	97.851	0.7941	6.5857	10.7649	1.8221	0.025069
W06	0.325963	12	2.85	2.85	97.057	97.8495	0.7925	6.6176	10.8208	1.8134	0.024829
W06	0	12			97.0571	97.848	0.7909	6.6526	10.8762	1.8038	0.024566
W06	18	16	5.91	189.25	97.2192	98.191	0.9718	12.6082	15.9469	1.269	0.010608
W06	17.4435	16	1.89	183.33	97.2332	98.1865	0.9533	11.9608	15.9556	1.3377	0.011987
W06	17.2652	16	1.89	181.44	97.2377	98.1723	0.9346	9.9553	15.8694	1.6072	0.018477
W06	17.0869	16	3.85	179.55	97.2422	98.18	0.9378	11.9308	15.9061	1.3411	0.01204
W06	16.7398	16	3.85	175.7	97.235	98.1792	0.9442	12.0056	15.9193	1.3327	0.011872
W06	16.3929	16	1.89	171.84	97.2226	98.1788	0.9562	12.1663	15.9385	1.3151	0.011518
W06	16.223	16	1.89	169.95	97.2165	98.1666	0.9501	10.3144	15.874	1.5512	0.01702
W06	16.0532	16	3.85	168.06	97.2104	98.174	0.9636	12.4187	15.9215	1.2884	0.010989
W06	15.6685	16	3.85	164.21	97.2192	98.1724	0.9532	12.2595	15.8744	1.3051	0.01131
W06	15.286	16	1.89	160.35	97.2315	98.1703	0.9388	12.0171	15.8153	1.3314	0.011828
W06	15.0986	16	1.89	158.46	97.2376	98.155	0.9174	9.858	15.7002	1.6231	0.018848
W06	14.9164	16	3.74	156.57	97.2393	98.1627	0.9234	11.7773	15.7446	1.3585	0.012378
W06	14.5616	16	3.97	152.83	97.2331	98.162	0.9289	11.8585	15.7892	1.3492	0.012194
W06	14.1854	16	1.89	148.87	97.2266	98.1612	0.9346	11.9467	15.8376	1.3393	0.012
W06	14.006	16	1.89	146.97	97.2235	98.147	0.9235	9.9435	15.7787	1.6091	0.018512
W06	13.825	16	3.85	145.08	97.2219	98.1547	0.9328	11.9326	15.8298	1.3409	0.012034
W06	13.4516	16	3.85	141.23	97.2186	98.1539	0.9353	12.0035	15.8345	1.3329	0.011871
W06	13.0785	16	1.89	137.38	97.2153	98.1531	0.9378	12.0757	15.8389	1.325	0.01171
W06	12.9082	16	1.89	135.49	97.2107	98.1364	0.9257	9.7485	15.7287	1.6413	0.019355
W06	12.7316	16	3.85	133.6	97.2031	98.1426	0.9395	11.1899	15.7421	1.4299	0.01395
W06	12.371	16	3.85	129.74	97.1877	98.1399	0.9522	10.9687	15.699	1.4587	0.014597
W06	12	16	1.89	125.89	97.1718	98.1418	0.97	11.7838	15.7062	1.3578	0.012367

Test Identification	River Station	Q (cfs)	Reach Length (ft)	Cumulative Channel Length (ft)	Minimum Channel Elevation (ft)	WSE (ft)	Depth (ft)	Flow Area (ft ²)	Top Width, Tw (ft)	Velocity (ft/s)	Shear Stress (lb/ft ²)
W06	11.8263	16	1.89	124	97.1878	98.1266	0.9387	9.7385	15.6228	1.643	0.019381
W06	11.6475	16	3.85	122.11	97.1599	98.135	0.9751	11.7272	15.6631	1.3643	0.0125
W06	11.2834	16	3.85	118.25	97.1476	98.1344	0.9868	11.8536	15.597	1.3498	0.012176
W06	10.9222	16	1.89	114.4	97.1418	98.1326	0.9908	11.706	15.6052	1.3668	0.012485
W06	10.7458	16	1.89	112.51	97.1504	98.1154	0.965	9.506	15.5165	1.6831	0.020447
W06	10.5691	16	6.12	110.62	97.159	98.1218	0.9628	10.8907	15.5727	1.4691	0.014838
W06	10	16	10.24	104.5	97.1868	98.1238	0.9371	11.9308	15.5877	1.3411	0.012014
W06	9	16	10.52	94.26	97.1975	98.1052	0.9077	9.7179	13.4568	1.6465	0.018286
W06	8	16	5.57	83.74	97.1048	98.0871	0.9823	8.7224	11.8271	1.8344	0.022518
W06	7.48171	16	2.08	78.18	97.1108	98.0806	0.9698	8.4805	11.7051	1.8867	0.02399
W06	7.28869	16	2.09	76.1	97.1131	98.0333	0.9202	6.6405	11.4121	2.4095	0.042581
W06	7.09453	16	6.46	74.01	97.1154	98.0451	0.9297	8.0274	11.4562	1.9932	0.027172
W06	6.4666	16	6.46	67.56	97.1225	98.038	0.9155	7.86	11.455	2.0356	0.028516
W06	5.84187	16	2.08	61.1	97.1189	98.0331	0.9142	7.8442	11.5083	2.0397	0.028676
W06	5.64812	16	2.08	59.02	97.1081	97.9943	0.8862	6.3726	11.3328	2.5107	0.046809
W06	5.45452	16	6.46	56.93	97.0972	98.0168	0.9196	7.943	11.5122	2.0144	0.027905
W06	4.8465	16	6.46	50.48	97.0692	98.0158	0.9465	8.2258	11.6158	1.9451	0.025804
W06	4.21826	16	2.08	44.02	97.0589	98.0109	0.952	8.1848	11.556	1.9548	0.026038
W06	4.01564	16	2.08	41.94	97.0556	97.9726	0.917	6.5606	11.3136	2.4388	0.04382
W06	3.82915	16	6.46	39.86	97.0548	97.9892	0.9344	7.8756	11.4246	2.0316	0.028429
W06	3.2113	16	6.46	33.4	97.0529	97.9851	0.9322	7.9057	11.4762	2.0239	0.028261
W06	2.62322	16	2.08	26.94	97.0457	97.9819	0.9362	8.0398	11.5117	1.9901	0.027214
W06	2.43492	16	2.08	24.86	97.0424	97.9381	0.8957	6.3239	11.2618	2.5301	0.047901
W06	2.24663	16	6.46	22.78	97.0392	97.958	0.9188	7.8015	11.3883	2.0509	0.02917
W06	1.66399	16	6.46	16.32	97.0423	97.9509	0.9086	7.6517	11.3381	2.091	0.030486
W06	1.11435	16	2.08	9.86	97.0544	97.9436	0.8892	7.5303	11.2563	2.1248	0.031606
W06	0.905209	16	2.08	7.78	97.0569	97.8715	0.8146	5.5251	10.8389	2.8959	0.049748
W06	0.66075	16	2.85	5.7	97.0569	97.9089	0.852	7.219	11.1062	2.2164	0.03498
W06	0.325963	16	2.85	2.85	97.057	97.9068	0.8498	7.2479	11.1572	2.2075	0.034729

Test Identification	River Station	Q (cfs)	Reach Length (ft)	Cumulative Channel Length (ft)	Minimum Channel Elevation (ft)	WSE (ft)	Depth (ft)	Flow Area (ft ²)	Top Width, Tw (ft)	Velocity (ft/s)	Shear Stress (lb/ft ²)
W06	0	16			97.0571	97.905	0.8479	7.282	11.2088	2.1972	0.034423
W07	18	8	2.87	189.25	97.2192	97.8907	0.6715	8.085	14.1815	0.9895	0.007549
W07	17.7299	8	2.87	186.37	97.2259	97.8882	0.6622	7.6618	14.1536	1.0441	0.008544
W07	17.4598	8	1.89	183.5	97.2327	97.8715	0.6388	5.6327	14.0399	1.4203	0.015772
W07	17.2818	8	1.89	181.61	97.2372	97.8723	0.6351	5.869	11.0815	1.3631	0.01475
W07	17.1037	8	5.04	179.72	97.2417	97.8697	0.628	5.7124	13.9988	1.4005	0.015295
W07	16.6489	8	5.04	174.68	97.2318	97.8679	0.6361	5.7776	14.0172	1.3847	0.014884
W07	16.1961	8	1.89	169.65	97.2155	97.8673	0.6518	6.0106	14.0858	1.331	0.013593
W07	16.0263	8	1.89	167.76	97.2094	97.8686	0.6592	6.3665	11.1196	1.2566	0.012226
W07	15.8333	8	5.04	165.87	97.2139	97.8657	0.6518	6.1118	14.0788	1.309	0.013089
W07	15.3338	8	5.04	160.83	97.23	97.8611	0.6311	5.8443	13.9411	1.3689	0.014477
W07	14.8424	8	1.89	155.79	97.238	97.8575	0.6195	5.7054	13.8806	1.4022	0.015292
W07	14.6632	8	1.89	153.9	97.2349	97.8582	0.6233	5.9345	10.9887	1.3481	0.014341
W07	14.484	8	5.04	152.01	97.2318	97.8552	0.6234	5.735	13.9348	1.3949	0.015124
W07	14.0068	8	5.04	146.98	97.2235	97.8534	0.6299	5.8089	14.0122	1.3772	0.014717
W07	13.5209	8	1.89	141.94	97.2192	97.8514	0.6322	5.8417	14.0198	1.3695	0.014514
W07	13.3378	8	1.89	140.05	97.2176	97.8521	0.6345	6.0751	11.0703	1.3169	0.013613
W07	13.1546	8	5.04	138.16	97.216	97.8495	0.6335	5.8882	14.0233	1.3586	0.014259
W07	12.6873	8	5.04	133.12	97.2012	97.8405	0.6393	5.3705	13.9554	1.4896	0.017621
W07	12.2166	8	1.89	128.09	97.1811	97.838	0.6569	5.4182	13.8521	1.4765	0.017162
W07	12.0397	8	1.89	126.2	97.1873	97.8398	0.6525	5.7694	10.8797	1.3866	0.015272
W07	11.8552	8	5.04	124.3	97.1669	97.8356	0.6687	5.5046	13.9139	1.4533	0.016527
W07	11.3796	8	5.04	119.27	97.1509	97.8334	0.6825	5.5513	13.9435	1.4411	0.016216
W07	10.9062	8	1.89	114.23	97.1426	97.8305	0.6879	5.5311	13.7453	1.4464	0.016304
W07	10.7298	8	1.89	112.34	97.1512	97.8298	0.6786	5.5764	10.8236	1.4346	0.016496
W07	10.5536	8	5.95	110.45	97.1598	97.8237	0.6639	5.2071	13.8836	1.5364	0.018808
W07	10	8	10.24	104.5	97.1868	97.8349	0.6481	7.6605	13.9587	1.0443	0.008513
W07	9	8	10.52	94.26	97.1975	97.8214	0.624	6.1407	11.7909	1.3028	0.013496
W07	8	8	6.64	83.74	97.1048	97.811	0.7062	5.6813	10.2081	1.4081	0.015445

Test Identification	River Station	Q (cfs)	Reach Length (ft)	Cumulative Channel Length (ft)	Minimum Channel Elevation (ft)	WSE (ft)	Depth (ft)	Flow Area (ft ²)	Top Width, Tw (ft)	Velocity (ft/s)	Shear Stress (lb/ft ²)
W07	7.3823	8	2.08	77.11	97.112	97.7592	0.6472	3.8438	9.8604	2.0813	0.033867
W07	7.18856	8	2.08	75.02	97.1143	97.7602	0.6459	4.0569	7.7086	1.972	0.031098
W07	6.99416	8	8.95	72.94	97.1166	97.747	0.6304	3.7687	9.7777	2.1227	0.035454
W07	6.11792	8	8.95	64	97.1265	97.7319	0.6054	3.6222	9.7296	2.2086	0.038807
W07	5.27891	8	2.08	55.05	97.0874	97.7312	0.6438	3.9668	9.8889	2.0168	0.031689
W07	5.08523	8	2.08	52.97	97.0765	97.7346	0.6581	4.2479	7.8248	1.8833	0.028077
W07	4.88613	8	8.95	50.88	97.0698	97.7256	0.6557	3.9995	9.9112	2.0003	0.03105
W07	4.01566	8	8.95	41.94	97.0556	97.7152	0.6596	3.959	9.7861	2.0207	0.031619
W07	3.17228	8	2.08	32.99	97.0527	97.7049	0.6522	3.8952	9.847	2.0538	0.03294
W07	2.98147	8	2.08	30.91	97.0519	97.7092	0.6573	4.2107	7.7621	1.8999	0.028601
W07	2.79335	8	8.95	28.83	97.0486	97.6982	0.6496	3.924	9.8458	2.0387	0.032372
W07	1.96694	8	8.95	19.88	97.0357	97.6877	0.652	3.8868	9.7996	2.0583	0.033071
W07	1.20565	8	2.08	10.93	97.0524	97.6698	0.6174	3.6408	9.6408	2.1973	0.038281
W07	1.02837	8	2.08	8.85	97.0563	97.6729	0.6166	3.8669	7.5949	2.0688	0.034603
W07	0.786356	8	3.38	6.77	97.0569	97.6671	0.6102	3.7672	9.6477	2.1236	0.035721
W07	0.388886	8	3.38	3.38	97.057	97.6829	0.6259	4.8896	9.8267	1.6361	0.021628
W07	0	8			97.0571	97.681	0.6239	4.9178	9.9019	1.6267	0.021393
W07	18	12	2.87	189.25	97.2192	98.0756	0.8564	10.8077	15.268	1.1103	0.008853
W07	17.7299	12	2.87	186.37	97.2259	98.0732	0.8473	10.3845	15.2676	1.1556	0.009707
W07	17.4598	12	1.89	183.5	97.2327	98.0716	0.8389	10.1719	15.2755	1.1797	0.010186
W07	17.2818	12	1.89	181.61	97.2372	98.058	0.8208	8.1662	15.1887	1.4695	0.017047
W07	17.1037	12	5.04	179.72	97.2417	98.0653	0.8236	10.1346	15.2169	1.1841	0.010265
W07	16.6489	12	5.04	174.68	97.2318	98.0644	0.8326	10.2428	15.2433	1.1716	0.010018
W07	16.1961	12	1.89	169.65	97.2155	98.064	0.8485	10.5459	15.2679	1.1379	0.009367
W07	16.0263	12	1.89	167.76	97.2094	98.0534	0.844	8.7323	15.2196	1.3742	0.014598
W07	15.8333	12	5.04	165.87	97.2139	98.0592	0.8453	10.5948	15.2336	1.1326	0.009262
W07	15.3338	12	5.04	160.83	97.23	98.0568	0.8268	10.2842	15.1503	1.1668	0.009908
W07	14.8424	12	1.89	155.79	97.238	98.0549	0.8169	10.1331	15.1126	1.1842	0.010248
W07	14.6632	12	1.89	153.9	97.2349	98.0411	0.8062	8.1335	15.0559	1.4754	0.017164

Test Identification	River Station	Q (cfs)	Reach Length (ft)	Cumulative Channel Length (ft)	Minimum Channel Elevation (ft)	WSE (ft)	Depth (ft)	Flow Area (ft ²)	Top Width, Tw (ft)	Velocity (ft/s)	Shear Stress (lb/ft ²)
W07	14.484	12	5.04	152.01	97.2318	98.0486	0.8167	10.1255	15.1255	1.1851	0.010268
W07	14.0068	12	5.04	146.98	97.2235	98.0476	0.8241	10.2314	15.189	1.1729	0.010037
W07	13.5209	12	1.89	141.94	97.2192	98.0466	0.8274	10.3231	15.198	1.1624	0.009832
W07	13.3378	12	1.89	140.05	97.2176	98.0335	0.8158	8.3004	15.1251	1.4457	0.016396
W07	13.1546	12	5.04	138.16	97.216	98.0406	0.8246	10.3138	15.1722	1.1635	0.009848
W07	12.6873	12	5.04	133.12	97.2012	98.0348	0.8336	9.455	15.1023	1.2692	0.012029
W07	12.2166	12	1.89	128.09	97.1811	98.0336	0.8525	9.5411	15.0675	1.2577	0.011768
W07	12.0397	12	1.89	126.2	97.1873	98.0223	0.8349	8.0824	15.0059	1.4847	0.0174
W07	11.8552	12	5.04	124.3	97.1669	98.0302	0.8633	10.0752	15.0588	1.191	0.010372
W07	11.3796	12	5.04	119.27	97.1509	98.0293	0.8784	10.1999	15.0128	1.1765	0.01007
W07	10.9062	12	1.89	114.23	97.1426	98.0272	0.8846	10.0466	14.936	1.1944	0.010417
W07	10.7298	12	1.89	112.34	97.1512	98.0117	0.8605	7.9066	14.9101	1.5177	0.01827
W07	10.5536	12	5.95	110.45	97.1598	98.0176	0.8578	9.2926	14.9916	1.2914	0.012493
W07	10	12	10.24	104.5	97.1868	98.0194	0.8326	10.3334	15.0078	1.1613	0.009771
W07	9	12	10.52	94.26	97.1975	98.0048	0.8073	8.3986	12.8325	1.4288	0.015061
W07	8	12	6.64	83.74	97.1048	97.9916	0.8869	7.6206	11.2661	1.5747	0.018119
W07	7.3823	12	2.08	77.11	97.112	97.9854	0.8734	7.3757	11.1526	1.627	0.019476
W07	7.18856	12	2.08	75.02	97.1143	97.9481	0.8338	5.7068	10.925	2.1028	0.035395
W07	6.99416	12	8.95	72.94	97.1166	97.9578	0.8412	7.0484	10.9654	1.7025	0.021536
W07	6.11792	12	8.95	64	97.1265	97.9496	0.8231	6.8106	10.9757	1.762	0.023322
W07	5.27891	12	2.08	55.05	97.0874	97.949	0.8616	7.3026	11.165	1.6432	0.019941
W07	5.08523	12	2.08	52.97	97.0765	97.9252	0.8487	5.9777	11.0756	2.0075	0.031912
W07	4.88613	12	8.95	50.88	97.0698	97.9374	0.8676	7.3426	11.1634	1.6343	0.019689
W07	4.01566	12	8.95	41.94	97.0556	97.933	0.8774	7.372	11.0783	1.6278	0.019467
W07	3.17228	12	2.08	32.99	97.0527	97.9275	0.8748	7.2882	11.1464	1.6465	0.02002
W07	2.98147	12	2.08	30.91	97.0519	97.9033	0.8514	5.967	11.0417	2.0111	0.032027
W07	2.79335	12	8.95	28.83	97.0486	97.9156	0.867	7.3038	11.117	1.643	0.019907
W07	1.96694	12	8.95	19.88	97.0357	97.9111	0.8754	7.3299	11.1212	1.6371	0.019749
W07	1.20565	12	2.08	10.93	97.0524	97.9032	0.8508	7.069	11.0227	1.6975	0.021417

Test Identification	River Station	Q (cfs)	Reach Length (ft)	Cumulative Channel Length (ft)	Minimum Channel Elevation (ft)	WSE (ft)	Depth (ft)	Flow Area (ft ²)	Top Width, Tw (ft)	Velocity (ft/s)	Shear Stress (lb/ft ²)
W07	1.02837	12	2.08	8.85	97.0563	97.8701	0.8138	5.5227	10.8138	2.1728	0.038087
W07	0.786356	12	3.38	6.77	97.0569	97.886	0.8291	6.9465	10.947	1.7275	0.022265
W07	0.388886	12	3.38	3.38	97.057	97.8844	0.8274	6.99	11.0138	1.7167	0.021986
W07	0	12			97.0571	97.883	0.8259	7.0369	11.0804	1.7053	0.021688
W07	18	16	2.87	189.25	97.2192	98.1824	0.9633	12.4725	15.8956	1.2828	0.010893
W07	17.7299	16	2.87	186.37	97.2259	98.1797	0.9538	12.0446	15.9019	1.3284	0.011804
W07	17.4598	16	1.89	183.5	97.2327	98.1779	0.9452	11.8293	15.9045	1.3526	0.012314
W07	17.2818	16	1.89	181.61	97.2372	98.163	0.9258	9.7939	15.814	1.6337	0.019217
W07	17.1037	16	5.04	179.72	97.2417	98.171	0.9293	11.7767	15.8531	1.3586	0.012426
W07	16.6489	16	5.04	174.68	97.2318	98.17	0.9382	11.8863	15.8712	1.3461	0.01217
W07	16.1961	16	1.89	169.65	97.2155	98.1697	0.9542	12.1922	15.8933	1.3123	0.01148
W07	16.0263	16	1.89	167.76	97.2094	98.1577	0.9483	10.3518	15.8271	1.5456	0.016916
W07	15.8333	16	5.04	165.87	97.2139	98.1643	0.9504	12.2276	15.8468	1.3085	0.011403
W07	15.3338	16	5.04	160.83	97.23	98.1615	0.9314	11.9015	15.7686	1.3444	0.012117
W07	14.8424	16	1.89	155.79	97.238	98.1593	0.9213	11.7427	15.7344	1.3625	0.012491
W07	14.6632	16	1.89	153.9	97.2349	98.144	0.9091	9.7138	15.6682	1.6471	0.019544
W07	14.484	16	5.04	152.01	97.2318	98.1523	0.9205	11.7261	15.7425	1.3645	0.012538
W07	14.0068	16	5.04	146.98	97.2235	98.1512	0.9277	11.8375	15.8041	1.3516	0.012284
W07	13.5209	16	1.89	141.94	97.2192	98.1502	0.931	11.9287	15.8109	1.3413	0.01207
W07	13.3378	16	1.89	140.05	97.2176	98.1354	0.9178	9.8733	15.728	1.6205	0.018853
W07	13.1546	16	5.04	138.16	97.216	98.1434	0.9274	11.9053	15.7798	1.3439	0.012121
W07	12.6873	16	5.04	133.12	97.2012	98.1367	0.9355	11.0252	15.7024	1.4512	0.014468
W07	12.2166	16	1.89	128.09	97.1811	98.1354	0.9543	11.1062	15.6666	1.4406	0.014211
W07	12.0397	16	1.89	126.2	97.1873	98.1229	0.9356	9.6221	15.5949	1.6628	0.019978
W07	11.8552	16	5.04	124.3	97.1669	98.1318	0.9649	11.6353	15.6527	1.3751	0.012757
W07	11.3796	16	5.04	119.27	97.1509	98.1308	0.9799	11.7534	15.5986	1.3613	0.012453
W07	10.9062	16	1.89	114.23	97.1426	98.1284	0.9858	11.5901	15.5812	1.3805	0.012811
W07	10.7298	16	1.89	112.34	97.1512	98.111	0.9598	9.415	15.4902	1.6994	0.020966
W07	10.5536	16	5.95	110.45	97.1598	98.1176	0.9578	10.8191	15.5524	1.4789	0.015105

Test Identification	River Station	Q (cfs)	Reach Length (ft)	Cumulative Channel Length (ft)	Minimum Channel Elevation (ft)	WSE (ft)	Depth (ft)	Flow Area (ft ²)	Top Width, Tw (ft)	Velocity (ft/s)	Shear Stress (lb/ft ²)
W07	10	16	10.24	104.5	97.1868	98.1197	0.933	11.8669	15.5649	1.3483	0.012194
W07	9	16	10.52	94.26	97.1975	98.1008	0.9033	9.659	13.4295	1.6565	0.018604
W07	8	16	6.64	83.74	97.1048	98.0824	0.9776	8.6672	11.7996	1.846	0.02294
W07	7.3823	16	2.08	77.11	97.112	98.0747	0.9627	8.3936	11.6573	1.9062	0.024661
W07	7.18856	16	2.08	75.02	97.1143	98.0269	0.9126	6.5855	11.3651	2.4296	0.043616
W07	6.99416	16	8.95	72.94	97.1166	98.0389	0.9223	7.9548	11.4121	2.0114	0.02789
W07	6.11792	16	8.95	64	97.1265	98.0287	0.9022	7.6966	11.4324	2.0788	0.030095
W07	5.27891	16	2.08	55.05	97.0874	98.0284	0.941	8.2069	11.6233	1.9496	0.026074
W07	5.08523	16	2.08	52.97	97.0765	97.9973	0.9208	6.7916	11.4922	2.3559	0.040842
W07	4.88613	16	8.95	50.88	97.0698	98.013	0.9432	8.2027	11.601	1.9506	0.026139
W07	4.01566	16	8.95	41.94	97.0556	98.0072	0.9516	8.2102	11.5191	1.9488	0.026017
W07	3.17228	16	2.08	32.99	97.0527	98.0001	0.9474	8.1124	11.5705	1.9723	0.026827
W07	2.98147	16	2.08	30.91	97.0519	97.9666	0.9147	6.6774	11.41	2.3961	0.042589
W07	2.79335	16	8.95	28.83	97.0486	97.983	0.9344	8.0661	11.5113	1.9836	0.027221
W07	1.96694	16	8.95	19.88	97.0357	97.977	0.9413	8.0753	11.5138	1.9813	0.027159
W07	1.20565	16	2.08	10.93	97.0524	97.9659	0.9135	7.7728	11.3951	2.0585	0.029621
W07	1.02837	16	2.08	8.85	97.0563	97.9153	0.859	6.0176	11.0816	2.6589	0.054236
W07	0.786356	16	3.38	6.77	97.0569	97.9381	0.8812	7.5247	11.256	2.1263	0.032023
W07	0.388886	16	3.38	3.38	97.057	97.9359	0.8789	7.5646	11.3159	2.1151	0.031712
W07	0	16			97.0571	97.934	0.8769	7.6096	11.378	2.1026	0.031352
W08	18	8	2.69	189.25	97.2192	97.857	0.6379	7.6108	13.9827	1.0511	0.00865
W08	17.7473	8	2.68	186.56	97.2255	97.8541	0.6286	7.2024	13.9507	1.1107	0.009821
W08	17.4943	8	2.34	183.87	97.2319	97.8444	0.6125	6.0497	13.8742	1.3224	0.013793
W08	17.2743	8	2.34	181.53	97.2374	97.8442	0.6068	6.1881	11.9964	1.2928	0.013378
W08	17.0543	8	1.96	179.2	97.243	97.843	0.6	6.1628	13.8308	1.2981	0.013254
W08	16.8784	8	1.96	177.23	97.24	97.842	0.602	6.1423	13.8306	1.3025	0.013326
W08	16.7017	8	2.32	175.27	97.2337	97.8412	0.6075	6.1504	13.8421	1.3007	0.013277
W08	16.4928	8	2.32	172.95	97.2262	97.8415	0.6153	6.3813	12.0007	1.2537	0.012455
W08	16.2845	8	1.96	170.63	97.2187	97.8404	0.6217	6.3571	13.9046	1.2584	0.012312

Test Identifi- cation	River Station	Q (cfs)	Reach Length (ft)	Cumulative Channel Length (ft)	Minimum Channel Elevation (ft)	WSE (ft)	Depth (ft)	Flow Area (ft ²)	Top Width, Tw (ft)	Velocity (ft/s)	Shear Stress (lb/ft ²)
W08	16.1077	8	1.96	168.66	97.2123	97.84	0.6277	6.4288	13.9383	1.2444	0.011965
W08	15.9159	8	2.32	166.7	97.2112	97.8397	0.6285	6.4948	13.9402	1.2318	0.011689
W08	15.6855	8	2.32	164.38	97.2186	97.8393	0.6207	6.5737	11.9878	1.217	0.011623
W08	15.4557	8	1.96	162.06	97.226	97.8365	0.6105	6.3316	13.8142	1.2635	0.01242
W08	15.2607	8	1.96	160.09	97.2323	97.8345	0.6022	6.179	13.7582	1.2947	0.013104
W08	15.0659	8	2.32	158.13	97.2386	97.833	0.5944	6.0957	13.7068	1.3124	0.01352
W08	14.8439	8	2.32	155.81	97.238	97.8329	0.5948	6.2454	11.8908	1.2809	0.013062
W08	14.6244	8	1.96	153.49	97.2342	97.8307	0.5965	6.1204	13.7546	1.3071	0.013413
W08	14.4381	8	1.96	151.52	97.231	97.8301	0.5991	6.1489	13.7878	1.301	0.013279
W08	14.2519	8	2.32	149.56	97.2278	97.8294	0.6016	6.1777	13.8201	1.295	0.013146
W08	14.0319	8	2.32	147.24	97.224	97.8294	0.6054	6.3491	11.988	1.26	0.012604
W08	13.8091	8	1.96	144.92	97.2218	97.8274	0.6056	6.2205	13.8619	1.2861	0.012941
W08	13.6191	8	1.96	142.96	97.2201	97.8267	0.6066	6.2487	13.865	1.2803	0.012808
W08	13.4286	8	2.32	140.99	97.2184	97.8261	0.6077	6.2773	13.8685	1.2744	0.012676
W08	13.2043	8	2.32	138.67	97.2164	97.8262	0.6098	6.4493	11.9987	1.2404	0.012157
W08	12.9891	8	1.96	136.35	97.2141	97.8239	0.6097	6.2791	13.8701	1.2741	0.012662
W08	12.8052	8	1.96	134.39	97.2063	97.8173	0.611	5.731	13.8152	1.3959	0.015606
W08	12.6217	8	2.32	132.42	97.1985	97.8138	0.6153	5.5342	13.7911	1.4456	0.016927
W08	12.4049	8	2.32	130.1	97.1892	97.8137	0.6245	5.696	11.7999	1.4045	0.016088
W08	12.1881	8	1.96	127.78	97.1799	97.8136	0.6337	5.8537	13.6507	1.3667	0.014832
W08	12	8	1.96	125.82	97.1718	97.8135	0.6417	5.9849	13.7636	1.3367	0.01404
W08	11.8129	8	2.32	123.85	97.1655	97.8124	0.6469	5.9667	13.7796	1.3408	0.014137
W08	11.5938	8	2.32	121.53	97.1581	97.8127	0.6546	6.1828	11.7936	1.2939	0.013338
W08	11.3745	8	1.96	119.21	97.1507	97.8102	0.6595	6.0253	13.8193	1.3277	0.013829
W08	11.189	8	1.96	117.25	97.1444	97.8098	0.6654	6.0972	13.7867	1.3121	0.013443
W08	11	8	2.32	115.29	97.1381	97.8095	0.6715	6.1911	13.7308	1.2922	0.01296
W08	10.7884	8	2.32	112.97	97.1484	97.8066	0.6582	5.9801	11.7232	1.3378	0.014373
W08	10.5718	8	6.14	110.65	97.1589	97.8004	0.6415	5.5391	13.7292	1.4443	0.016815
W08	10	8	10.24	104.5	97.1868	97.8073	0.6205	7.2772	13.7951	1.0993	0.009557

Test Identification	River Station	Q (cfs)	Reach Length (ft)	Cumulative Channel Length (ft)	Minimum Channel Elevation (ft)	WSE (ft)	Depth (ft)	Flow Area (ft ²)	Top Width, Tw (ft)	Velocity (ft/s)	Shear Stress (lb/ft ²)
W08	9	8	10.52	94.26	97.1975	97.7917	0.5943	5.7928	11.6203	1.381	0.015385
W08	8	8	6.94	83.74	97.1048	97.7798	0.675	5.3656	10.0263	1.491	0.01754
W08	7.35391	8	2.38	76.8	97.1124	97.7506	0.6382	4.268	9.8098	1.8744	0.027449
W08	7.13234	8	2.38	74.42	97.115	97.7503	0.6353	4.4191	8.3494	1.8103	0.026139
W08	6.90553	8	4.11	72.04	97.1176	97.7385	0.6209	4.1006	9.73	1.9509	0.029969
W08	6.50322	8	4.11	67.93	97.1221	97.7351	0.613	4.1197	9.7288	1.9419	0.029861
W08	6.1005	8	2.38	63.82	97.1267	97.7278	0.6011	3.9971	9.706	2.0015	0.031994
W08	5.87338	8	2.38	61.43	97.1207	97.7289	0.6082	4.1861	8.3473	1.9111	0.029572
W08	5.65156	8	4.07	59.05	97.1082	97.7264	0.6182	4.1913	9.7787	1.9087	0.028766
W08	5.2727	8	4.07	54.98	97.087	97.7256	0.6386	4.3337	9.8567	1.846	0.026545
W08	4.88874	8	2.42	50.91	97.0699	97.7239	0.654	4.4326	9.9014	1.8048	0.025187
W08	4.65274	8	2.42	48.49	97.066	97.7243	0.6583	4.5858	8.4328	1.7445	0.024036
W08	4.417	8	4.11	46.06	97.0621	97.7171	0.655	4.3557	9.8299	1.8367	0.026184
W08	4.01731	8	4.11	41.95	97.0556	97.7145	0.6589	4.3959	9.7823	1.8199	0.025551
W08	3.63671	8	2.38	37.84	97.0542	97.7058	0.6516	4.1851	9.7697	1.9115	0.02869
W08	3.40893	8	2.38	35.46	97.0535	97.7065	0.653	4.3628	8.336	1.8337	0.026853
W08	3.18063	8	4.11	33.08	97.0528	97.7035	0.6507	4.3114	9.837	1.8555	0.0268
W08	2.80543	8	4.11	28.96	97.0489	97.7017	0.6528	4.4084	9.8662	1.8147	0.025485
W08	2.43363	8	2.37	24.85	97.0425	97.697	0.6544	4.3564	9.8418	1.8364	0.026196
W08	2.21979	8	2.37	22.48	97.0388	97.6977	0.6589	4.5308	8.3844	1.7657	0.024675
W08	1.98656	8	4.12	20.11	97.0353	97.6924	0.6571	4.3748	9.8285	1.8286	0.02593
W08	1.63562	8	4.12	15.99	97.043	97.6845	0.6415	4.1969	9.7603	1.9062	0.028473
W08	1.28508	8	2.37	11.86	97.0507	97.6809	0.6302	4.1932	9.714	1.9078	0.028587
W08	1.08303	8	2.37	9.49	97.0551	97.6815	0.6264	4.3623	8.313	1.8339	0.026898
W08	0.828077	8	3.56	7.12	97.0569	97.6783	0.6214	4.3052	9.7053	1.8582	0.027092
W08	0.409633	8	3.56	3.56	97.057	97.6837	0.6267	4.8955	9.8272	1.6342	0.021569
W08	0	8			97.0571	97.6818	0.6247	4.9251	9.9062	1.6243	0.021322
W08	18	12	2.69	189.25	97.2192	98.0575	0.8384	10.5329	15.1622	1.1393	0.009378
W08	17.7473	12	2.68	186.56	97.2255	98.0551	0.8296	10.1279	15.1576	1.1848	0.010266

Test Identifi- cation	River Station	Q (cfs)	Reach Length (ft)	Cumulative Channel Length (ft)	Minimum Channel Elevation (ft)	WSE (ft)	Depth (ft)	Flow Area (ft ²)	Top Width, Tw (ft)	Velocity (ft/s)	Shear Stress (lb/ft ²)
W08	17.4943	12	2.34	183.87	97.2319	98.0534	0.8215	9.9066	15.1611	1.2113	0.010806
W08	17.2743	12	2.34	181.53	97.2374	98.0458	0.8084	8.7762	15.1159	1.3673	0.014394
W08	17.0543	12	1.96	179.2	97.243	98.0494	0.8064	9.9286	15.1147	1.2086	0.010745
W08	16.8784	12	1.96	177.23	97.24	98.049	0.809	9.9636	15.1219	1.2044	0.010658
W08	16.7017	12	2.32	175.27	97.2337	98.0485	0.8148	9.9849	15.1423	1.2018	0.010608
W08	16.4928	12	2.32	172.95	97.2262	98.0418	0.8156	8.9681	15.1179	1.3381	0.013687
W08	16.2845	12	1.96	170.63	97.2187	98.0454	0.8267	10.1792	15.1509	1.1789	0.010145
W08	16.1077	12	1.96	168.66	97.2123	98.0454	0.8331	10.3555	15.1649	1.1588	0.009753
W08	15.9159	12	2.32	166.7	97.2112	98.0451	0.8339	10.4292	15.1622	1.1506	0.009594
W08	15.6855	12	2.32	164.38	97.2186	98.0377	0.8191	9.1416	15.0855	1.3127	0.013085
W08	15.4557	12	1.96	162.06	97.226	98.0403	0.8143	10.0981	15.0698	1.1883	0.01032
W08	15.2607	12	1.96	160.09	97.2323	98.0393	0.807	9.9831	15.0361	1.202	0.010592
W08	15.0659	12	2.32	158.13	97.2386	98.0383	0.7997	9.8743	15.001	1.2153	0.010858
W08	14.8439	12	2.32	155.81	97.238	98.0305	0.7925	8.7268	14.967	1.3751	0.014544
W08	14.6244	12	1.96	153.49	97.2342	98.0341	0.7999	9.8721	15.0197	1.2155	0.010868
W08	14.4381	12	1.96	151.52	97.231	98.0337	0.8026	9.912	15.0438	1.2107	0.010772
W08	14.2519	12	2.32	149.56	97.2278	98.0332	0.8054	9.9525	15.0679	1.2057	0.010676
W08	14.0319	12	2.32	147.24	97.224	98.0261	0.8021	8.8561	15.0575	1.355	0.014081
W08	13.8091	12	1.96	144.92	97.2218	98.0295	0.8077	10.001	15.0882	1.1999	0.01056
W08	13.6191	12	1.96	142.96	97.2201	98.0291	0.809	10.0365	15.0912	1.1956	0.010474
W08	13.4286	12	2.32	140.99	97.2184	98.0287	0.8103	10.0726	15.0943	1.1914	0.010388
W08	13.2043	12	2.32	138.67	97.2164	98.0215	0.8051	8.9491	15.0583	1.3409	0.013743
W08	12.9891	12	1.96	136.35	97.2141	98.0248	0.8107	10.0704	15.0818	1.1916	0.010391
W08	12.8052	12	1.96	134.39	97.2063	98.0211	0.8148	9.4699	15.0336	1.2672	0.01197
W08	12.6217	12	2.32	132.42	97.1985	98.0183	0.8198	9.1261	14.9994	1.3149	0.013032
W08	12.4049	12	2.32	130.1	97.1892	98.0103	0.8211	8.2128	14.9365	1.4611	0.016686
W08	12.1881	12	1.96	127.78	97.1799	98.0144	0.8344	9.3095	14.954	1.289	0.012431
W08	12	12	1.96	125.82	97.1718	98.0156	0.8438	9.8482	14.9705	1.2185	0.010917
W08	11.8129	12	2.32	123.85	97.1655	98.0151	0.8496	9.855	14.9708	1.2177	0.010898

Test Identification	River Station	Q (cfs)	Reach Length (ft)	Cumulative Channel Length (ft)	Minimum Channel Elevation (ft)	WSE (ft)	Depth (ft)	Flow Area (ft ²)	Top Width, Tw (ft)	Velocity (ft/s)	Shear Stress (lb/ft ²)
W08	11.5938	12	2.32	121.53	97.1581	98.0075	0.8494	8.7361	14.9219	1.3736	0.014489
W08	11.3745	12	1.96	119.21	97.1507	98.0113	0.8606	9.9333	14.9079	1.2081	0.010686
W08	11.189	12	1.96	117.25	97.1444	98.0111	0.8667	10.0228	14.8584	1.1973	0.010458
W08	11	12	2.32	115.29	97.1381	98.0109	0.8728	10.1321	14.8125	1.1844	0.010192
W08	10.7884	12	2.32	112.97	97.1484	98.0002	0.8518	8.5066	14.8247	1.4107	0.015372
W08	10.5718	12	6.14	110.65	97.1589	98.0018	0.8429	9.0641	14.8983	1.3239	0.013212
W08	10	12	10.24	104.5	97.1868	98.0036	0.8169	10.0975	14.9203	1.1884	0.010291
W08	9	12	10.52	94.26	97.1975	97.9881	0.7906	8.1848	12.7383	1.4661	0.015953
W08	8	12	6.94	83.74	97.1048	97.9741	0.8693	7.4235	11.1628	1.6165	0.0192
W08	7.35391	12	2.38	76.8	97.1124	97.9672	0.8548	7.1691	11.0462	1.6739	0.020743
W08	7.13234	12	2.38	74.42	97.115	97.9479	0.8329	6.2393	10.9196	1.9233	0.028756
W08	6.90553	12	4.11	72.04	97.1176	97.9515	0.8339	6.9641	10.9363	1.7231	0.022125
W08	6.50322	12	4.11	67.93	97.1221	97.9477	0.8256	6.8549	10.9406	1.7506	0.022951
W08	6.1005	12	2.38	63.82	97.1267	97.9435	0.8168	6.7411	10.9416	1.7801	0.023862
W08	5.87338	12	2.38	61.43	97.1207	97.9269	0.8062	5.9609	10.884	2.0131	0.031884
W08	5.65156	12	4.07	59.05	97.1082	97.9362	0.828	6.8924	10.9957	1.7411	0.022696
W08	5.2727	12	4.07	54.98	97.087	97.9364	0.8494	7.166	11.093	1.6746	0.020794
W08	4.88874	12	2.42	50.91	97.0699	97.9354	0.8655	7.3203	11.1515	1.6393	0.019823
W08	4.65274	12	2.42	48.49	97.066	97.9209	0.8549	6.4527	11.0551	1.8597	0.02667
W08	4.417	12	4.11	46.06	97.0621	97.9263	0.8642	7.1913	11.0693	1.6687	0.020606
W08	4.01731	12	4.11	41.95	97.0556	97.9248	0.8692	7.281	11.03	1.6481	0.020009
W08	3.63671	12	2.38	37.84	97.0542	97.9193	0.8651	7.0201	11.0259	1.7094	0.021759
W08	3.40893	12	2.38	35.46	97.0535	97.9042	0.8507	6.2146	10.9676	1.9309	0.028999
W08	3.18063	12	4.11	33.08	97.0528	97.9117	0.8589	7.105	11.0527	1.6889	0.021183
W08	2.80543	12	4.11	28.96	97.0489	97.9107	0.8618	7.2508	11.0882	1.655	0.02023
W08	2.43363	12	2.37	24.85	97.0425	97.9079	0.8654	7.2093	11.0835	1.6645	0.020494
W08	2.21979	12	2.37	22.48	97.0388	97.8935	0.8547	6.3808	11.0076	1.8807	0.027338
W08	1.98656	12	4.12	20.11	97.0353	97.8999	0.8646	7.2165	11.0562	1.6629	0.02044
W08	1.63562	12	4.12	15.99	97.043	97.8954	0.8524	7.0237	11.0065	1.7085	0.021726

Test Identification	River Station	Q (cfs)	Reach Length (ft)	Cumulative Channel Length (ft)	Minimum Channel Elevation (ft)	WSE (ft)	Depth (ft)	Flow Area (ft ²)	Top Width, Tw (ft)	Velocity (ft/s)	Shear Stress (lb/ft ²)
W08	1.28508	12	2.37	11.86	97.0507	97.892	0.8413	6.9419	10.9619	1.7286	0.022298
W08	1.08303	12	2.37	9.49	97.0551	97.8761	0.821	6.1251	10.8535	1.9592	0.029962
W08	0.828077	12	3.56	7.12	97.0569	97.8829	0.826	6.9061	10.9205	1.7376	0.022552
W08	0.409633	12	3.56	3.56	97.057	97.8812	0.8242	6.9515	10.9911	1.7263	0.022256
W08	0	12			97.0571	97.8797	0.8226	7	11.061	1.7143	0.021942
W08	18	16	2.69	189.25	97.2192	98.1839	0.9647	12.4953	15.9042	1.2805	0.011377
W08	17.7473	16	2.68	186.56	97.2255	98.1813	0.9558	12.0887	15.9097	1.3235	0.01228
W08	17.4943	16	2.34	183.87	97.2319	98.1795	0.9476	11.8667	15.9136	1.3483	0.01282
W08	17.2743	16	2.34	181.53	97.2374	98.1719	0.9345	10.7292	15.8671	1.4913	0.01628
W08	17.0543	16	1.96	179.2	97.243	98.1755	0.9324	11.8822	15.8762	1.3466	0.012777
W08	16.8784	16	1.96	177.23	97.24	98.175	0.935	11.9177	15.8814	1.3425	0.012689
W08	16.7017	16	2.32	175.27	97.2337	98.1745	0.9408	11.9408	15.8941	1.3399	0.012633
W08	16.4928	16	2.32	172.95	97.2262	98.1677	0.9415	10.9197	15.8684	1.4652	0.015626
W08	16.2845	16	1.96	170.63	97.2187	98.1714	0.9527	12.1356	15.9	1.3184	0.012168
W08	16.1077	16	1.96	168.66	97.2123	98.1714	0.9591	12.3129	15.9052	1.2995	0.011769
W08	15.9159	16	2.32	166.7	97.2112	98.1711	0.9599	12.3855	15.8959	1.2918	0.011609
W08	15.6855	16	2.32	164.38	97.2186	98.1634	0.9448	11.0843	15.8235	1.4435	0.015082
W08	15.4557	16	1.96	162.06	97.226	98.1661	0.9401	12.0396	15.8111	1.3289	0.012376
W08	15.2607	16	1.96	160.09	97.2323	98.165	0.9327	11.9194	15.7802	1.3424	0.012661
W08	15.0659	16	2.32	158.13	97.2386	98.1639	0.9253	11.8053	15.7488	1.3553	0.012941
W08	14.8439	16	2.32	155.81	97.238	98.156	0.918	10.6521	15.7146	1.502	0.016511
W08	14.6244	16	1.96	153.49	97.2342	98.1596	0.9254	11.8047	15.7666	1.3554	0.012946
W08	14.4381	16	1.96	151.52	97.231	98.1592	0.9282	11.8475	15.7902	1.3505	0.012844
W08	14.2519	16	2.32	149.56	97.2278	98.1588	0.931	11.8907	15.8139	1.3456	0.012741
W08	14.0319	16	2.32	147.24	97.224	98.1515	0.9275	10.7915	15.8021	1.4827	0.016046
W08	13.8091	16	1.96	144.92	97.2218	98.155	0.9332	11.9411	15.8321	1.3399	0.012622
W08	13.6191	16	1.96	142.96	97.2201	98.1546	0.9344	11.9764	15.8341	1.336	0.012536
W08	13.4286	16	2.32	140.99	97.2184	98.1541	0.9357	12.0124	15.8362	1.332	0.012449
W08	13.2043	16	2.32	138.67	97.2164	98.1468	0.9304	10.8818	15.7985	1.4703	0.015738

Test Identification	River Station	Q (cfs)	Reach Length (ft)	Cumulative Channel Length (ft)	Minimum Channel Elevation (ft)	WSE (ft)	Depth (ft)	Flow Area (ft ²)	Top Width, Tw (ft)	Velocity (ft/s)	Shear Stress (lb/ft ²)
W08	12.9891	16	1.96	136.35	97.2141	98.1502	0.936	12.0069	15.8217	1.3326	0.012459
W08	12.8052	16	1.96	134.39	97.2063	98.1462	0.9399	11.3975	15.7724	1.4038	0.014042
W08	12.6217	16	2.32	132.42	97.1985	98.1433	0.9448	11.0482	15.7343	1.4482	0.015081
W08	12.4049	16	2.32	130.1	97.1892	98.1355	0.9463	10.1295	15.6751	1.5795	0.018489
W08	12.1881	16	1.96	127.78	97.1799	98.1395	0.9596	11.2269	15.6898	1.4251	0.014517
W08	12	16	1.96	125.82	97.1718	98.1408	0.969	11.7678	15.7003	1.3596	0.013022
W08	11.8129	16	2.32	123.85	97.1655	98.1403	0.9748	11.7746	15.7019	1.3589	0.013004
W08	11.5938	16	2.32	121.53	97.1581	98.1325	0.9744	10.6467	15.6432	1.5028	0.016501
W08	11.3745	16	1.96	119.21	97.1507	98.1363	0.9856	11.8427	15.6296	1.351	0.012813
W08	11.189	16	1.96	117.25	97.1444	98.1361	0.9917	11.9255	15.5928	1.3417	0.012602
W08	11	16	2.32	115.29	97.1381	98.1359	0.9978	12.0335	15.6135	1.3296	0.012351
W08	10.7884	16	2.32	112.97	97.1484	98.125	0.9766	10.4022	15.5725	1.5381	0.01738
W08	10.5718	16	6.14	110.65	97.1589	98.1266	0.9677	10.9674	15.5992	1.4589	0.015299
W08	10	16	10.24	104.5	97.1868	98.1285	0.9417	12.0037	15.6136	1.3329	0.012415
W08	9	16	10.52	94.26	97.1975	98.1101	0.9126	9.7842	13.4875	1.6353	0.019072
W08	8	16	6.94	83.74	97.1048	98.092	0.9873	8.7811	11.8562	1.8221	0.023549
W08	7.35391	16	2.38	76.8	97.1124	98.0843	0.9719	8.5012	11.7071	1.8821	0.025279
W08	7.13234	16	2.38	74.42	97.115	98.0638	0.9488	7.5422	11.5642	2.1214	0.033487
W08	6.90553	16	4.11	72.04	97.1176	98.0675	0.9499	8.2695	11.5785	1.9348	0.026869
W08	6.50322	16	4.11	67.93	97.1221	98.0634	0.9413	8.1583	11.5951	1.9612	0.027733
W08	6.1005	16	2.38	63.82	97.1267	98.0589	0.9322	8.0422	11.6087	1.9895	0.028681
W08	5.87338	16	2.38	61.43	97.1207	98.0418	0.9211	7.2498	11.5507	2.207	0.036633
W08	5.65156	16	4.07	59.05	97.1082	98.0514	0.9432	8.1981	11.6626	1.9517	0.02747
W08	5.2727	16	4.07	54.98	97.087	98.0517	0.9647	8.4836	11.7588	1.886	0.025438
W08	4.88874	16	2.42	50.91	97.0699	98.0506	0.9807	8.6436	11.8183	1.8511	0.024397
W08	4.65274	16	2.42	48.49	97.066	98.0351	0.969	7.7523	11.7204	2.0639	0.031518
W08	4.417	16	4.11	46.06	97.0621	98.0407	0.9786	8.4959	11.7428	1.8833	0.025336
W08	4.01731	16	4.11	41.95	97.0556	98.039	0.9833	8.5783	11.708	1.8652	0.024765
W08	3.63671	16	2.38	37.84	97.0542	98.0328	0.9786	8.3103	11.7048	1.9253	0.026636

Test Identification	River Station	Q (cfs)	Reach Length (ft)	Cumulative Channel Length (ft)	Minimum Channel Elevation (ft)	WSE (ft)	Depth (ft)	Flow Area (ft ²)	Top Width, Tw (ft)	Velocity (ft/s)	Shear Stress (lb/ft ²)
W08	3.40893	16	2.38	35.46	97.0535	98.0168	0.9633	7.4869	11.6312	2.1371	0.034057
W08	3.18063	16	4.11	33.08	97.0528	98.0247	0.9719	8.3914	11.7135	1.9067	0.026057
W08	2.80543	16	4.11	28.96	97.0489	98.0234	0.9745	8.5376	11.7474	1.8741	0.025059
W08	2.43363	16	2.37	24.85	97.0425	98.0202	0.9777	8.4915	11.7467	1.8842	0.025369
W08	2.21979	16	2.37	22.48	97.0388	98.0046	0.9658	7.6403	11.6667	2.0942	0.032556
W08	1.98656	16	4.12	20.11	97.0353	98.0115	0.9762	8.4866	11.7205	1.8853	0.025396
W08	1.63562	16	4.12	15.99	97.043	98.0064	0.9634	8.2816	11.6661	1.932	0.026829
W08	1.28508	16	2.37	11.86	97.0507	98.0025	0.9518	8.1894	11.6175	1.9537	0.027501
W08	1.08303	16	2.37	9.49	97.0551	97.9852	0.9301	7.3448	11.5004	2.1784	0.035554
W08	0.828077	16	3.56	7.12	97.0569	97.9925	0.9356	8.1384	11.5715	1.966	0.027882
W08	0.409633	16	3.56	3.56	97.057	97.9906	0.9336	8.1893	11.6379	1.9538	0.027528
W08	0	16			97.0571	97.989	0.9319	8.2442	11.6989	1.9408	0.027149
W09	18	8	1.88	189.25	97.2192	97.8558	0.6367	7.5939	13.9755	1.0535	0.008694
W09	17.8236	8	1.88	187.37	97.2236	97.8462	0.6226	6.2395	13.9081	1.2822	0.01281
W09	17.6472	8	2.32	185.49	97.228	97.8443	0.6163	6.1094	13.8842	1.3095	0.013475
W09	17.4288	8	2.32	183.17	97.2335	97.8437	0.6102	6.177	11.9886	1.2951	0.013427
W09	17.2102	8	2.83	180.85	97.239	97.8417	0.6027	6.0641	13.8288	1.3192	0.013749
W09	16.9495	8	2.83	178.02	97.2425	97.8411	0.5986	6.1579	13.8211	1.2991	0.013265
W09	16.6953	8	2.32	175.19	97.2334	97.8396	0.6062	6.1314	13.833	1.3047	0.013369
W09	16.4866	8	2.32	172.87	97.2259	97.84	0.6141	6.3677	11.9987	1.2563	0.012516
W09	16.2777	8	2.83	170.55	97.2184	97.8388	0.6204	6.3413	13.8962	1.2616	0.012381
W09	16.0236	8	2.91	167.73	97.2093	97.8387	0.6294	6.5215	13.9491	1.2267	0.011593
W09	15.7369	8	2.32	164.82	97.217	97.8369	0.6198	6.4038	13.8806	1.2493	0.01208
W09	15.507	8	2.32	162.5	97.2244	97.8363	0.6119	6.4638	11.9549	1.2377	0.012078
W09	15.2771	8	2.83	160.18	97.2318	97.8331	0.6013	6.1834	13.7533	1.2938	0.01309
W09	15	8	2.83	157.35	97.2408	97.8313	0.5906	6.1117	13.6827	1.309	0.013474
W09	14.7296	8	2.32	154.52	97.236	97.8298	0.5938	6.0832	13.728	1.3151	0.013593
W09	14.5098	8	2.32	152.2	97.2322	97.8299	0.5977	6.2723	11.9291	1.2754	0.012945
W09	14.2899	8	2.83	149.88	97.2284	97.8275	0.5991	6.1253	13.8009	1.3061	0.013389

Test Identifi- cation	River Station	Q (cfs)	Reach Length (ft)	Cumulative Channel Length (ft)	Minimum Channel Elevation (ft)	WSE (ft)	Depth (ft)	Flow Area (ft ²)	Top Width, Tw (ft)	Velocity (ft/s)	Shear Stress (lb/ft ²)
W09	14.0215	8	2.83	147.05	97.2238	97.8266	0.6028	6.1592	13.8466	1.2989	0.01323
W09	13.7492	8	2.32	144.23	97.2212	97.8256	0.6044	6.1935	13.8534	1.2917	0.013061
W09	13.5248	8	2.32	141.91	97.2192	97.8258	0.6066	6.3936	11.9933	1.2512	0.012402
W09	13.3004	8	2.83	139.59	97.2172	97.8236	0.6063	6.2318	13.8573	1.2837	0.012867
W09	13.0266	8	2.83	136.76	97.2148	97.8225	0.6077	6.2453	13.8622	1.281	0.012792
W09	12.7699	8	2.32	133.93	97.2048	97.8149	0.6101	5.6458	13.7995	1.417	0.016148
W09	12.553	8	2.32	131.61	97.1955	97.8131	0.6176	5.6122	11.8248	1.4255	0.016662
W09	12.3359	8	2.83	129.29	97.1862	97.812	0.6258	5.6475	13.7605	1.4166	0.016116
W09	12.0718	8	2.83	126.46	97.1749	97.8126	0.6377	5.9309	13.675	1.3489	0.014354
W09	11.7989	8	2.32	123.63	97.165	97.8115	0.6465	5.9563	13.7753	1.3431	0.014193
W09	11.5799	8	2.32	121.31	97.1576	97.8118	0.6542	6.1762	11.7935	1.2953	0.013371
W09	11.3609	8	2.83	118.99	97.1502	97.8092	0.659	6.0196	13.8141	1.329	0.013859
W09	11.0937	8	2.83	116.16	97.1412	97.8087	0.6675	6.132	13.7566	1.3046	0.013259
W09	10.83	8	2.32	113.34	97.1463	97.8052	0.6589	5.8877	13.5738	1.3588	0.014586
W09	10.6136	8	2.32	111.02	97.1569	97.8024	0.6455	5.7333	11.7834	1.3954	0.015856
W09	10.3971	8	4.19	108.7	97.1674	97.7983	0.6309	5.4926	13.7318	1.4565	0.017148
W09	10	8	10.24	104.5	97.1868	97.8062	0.6194	7.2619	13.7885	1.1016	0.009603
W09	9	8	10.52	94.26	97.1975	97.7905	0.593	5.7787	11.6134	1.3844	0.01547
W09	8	8	5.85	83.74	97.1048	97.7785	0.6738	5.3527	10.0188	1.4946	0.017634
W09	7.45582	8	2.38	77.9	97.1112	97.751	0.6398	4.2916	9.816	1.8641	0.027125
W09	7.23422	8	2.38	75.51	97.1138	97.7505	0.6367	4.4217	8.3543	1.8093	0.026098
W09	7.01209	8	6.01	73.13	97.1164	97.7398	0.6234	4.1331	9.734	1.9356	0.029451
W09	6.42415	8	6.01	67.12	97.123	97.732	0.609	4.0611	9.7146	1.9699	0.030805
W09	5.84361	8	2.38	61.12	97.119	97.7264	0.6074	4.0663	9.7372	1.9674	0.030786
W09	5.62202	8	2.38	58.73	97.1066	97.729	0.6224	4.3375	8.3964	1.8444	0.027299
W09	5.40004	8	6.01	56.35	97.0941	97.7264	0.6323	4.3293	9.8336	1.8479	0.026708
W09	4.83347	8	6.01	50.34	97.069	97.7241	0.6551	4.4653	9.8999	1.7916	0.024825
W09	4.24908	8	2.38	44.34	97.0594	97.717	0.6576	4.3752	9.8163	1.8285	0.025897
W09	4.0173	8	2.38	41.95	97.0556	97.719	0.6633	4.6333	8.3537	1.7266	0.023434

Test Identification	River Station	Q (cfs)	Reach Length (ft)	Cumulative Channel Length (ft)	Minimum Channel Elevation (ft)	WSE (ft)	Depth (ft)	Flow Area (ft ²)	Top Width, Tw (ft)	Velocity (ft/s)	Shear Stress (lb/ft ²)
W09	3.8018	8	6.01	39.57	97.0547	97.7073	0.6526	4.2325	9.7577	1.8901	0.027929
W09	3.22728	8	6.01	33.56	97.0529	97.7036	0.6507	4.3066	9.8281	1.8576	0.02691
W09	2.67897	8	2.13	27.56	97.0466	97.7	0.6534	4.3833	9.8562	1.8251	0.02582
W09	2.48611	8	2.64	25.43	97.0433	97.7006	0.6573	4.538	8.3941	1.7629	0.024586
W09	2.24799	8	6.01	22.79	97.0392	97.6944	0.6552	4.3512	9.8314	1.8386	0.026268
W09	1.70375	8	6.01	16.79	97.0415	97.688	0.6465	4.2805	9.7854	1.8689	0.027305
W09	1.19261	8	2.38	10.78	97.0527	97.6808	0.6281	4.19	9.705	1.9093	0.028617
W09	0.977647	8	2.38	8.4	97.0569	97.6817	0.6248	4.38	8.3225	1.8265	0.026667
W09	0.697654	8	3.01	6.01	97.0569	97.6783	0.6214	4.312	9.733	1.8553	0.027008
W09	0.34449	8	3.01	3.01	97.057	97.6841	0.6271	4.907	9.8438	1.6303	0.021463
W09	0	8			97.0571	97.6825	0.6254	4.9325	9.9106	1.6219	0.021251
W09	18	12	1.88	189.25	97.2192	98.0492	0.83	10.4066	15.1133	1.1531	0.009635
W09	17.8236	12	1.88	187.37	97.2236	98.0474	0.8238	10.1037	15.1077	1.1877	0.010314
W09	17.6472	12	2.32	185.49	97.228	98.0459	0.8179	9.8898	15.1067	1.2134	0.010837
W09	17.4288	12	2.32	183.17	97.2335	98.0375	0.8039	8.6535	15.0659	1.3867	0.014854
W09	17.2102	12	2.83	180.85	97.239	98.0409	0.8018	9.7098	15.0811	1.2359	0.011306
W09	16.9495	12	2.83	178.02	97.2425	98.0405	0.798	9.8366	15.0604	1.2199	0.010968
W09	16.6953	12	2.32	175.19	97.2334	98.0397	0.8063	9.8548	15.0905	1.2177	0.010924
W09	16.4866	12	2.32	172.87	97.2259	98.0328	0.8069	8.8387	15.0627	1.3577	0.014141
W09	16.2777	12	2.83	170.55	97.2184	98.0365	0.8181	10.0515	15.0982	1.1938	0.010436
W09	16.0236	12	2.91	167.73	97.2093	98.0366	0.8273	10.3212	15.1223	1.1627	0.009821
W09	15.7369	12	2.32	164.82	97.217	98.0352	0.8182	10.175	15.0782	1.1794	0.010142
W09	15.507	12	2.32	162.5	97.2244	98.0273	0.8028	8.8933	14.9977	1.3493	0.013926
W09	15.2771	12	2.83	160.18	97.2318	98.0301	0.7983	9.8529	14.9837	1.2179	0.010908
W09	15	12	2.83	157.35	97.2408	98.0286	0.7878	9.6986	14.9331	1.2373	0.011306
W09	14.7296	12	2.32	154.52	97.236	98.0279	0.7919	9.7549	14.9684	1.2301	0.011162
W09	14.5098	12	2.32	152.2	97.2322	98.0203	0.7881	8.658	14.9546	1.386	0.01481
W09	14.2899	12	2.83	149.88	97.2284	98.0239	0.7955	9.8028	15.0077	1.2241	0.011044
W09	14.0215	12	2.83	147.05	97.2238	98.0233	0.7995	9.8608	15.0428	1.2169	0.010902

Test Identification	River Station	Q (cfs)	Reach Length (ft)	Cumulative Channel Length (ft)	Minimum Channel Elevation (ft)	WSE (ft)	Depth (ft)	Flow Area (ft ²)	Top Width, Tw (ft)	Velocity (ft/s)	Shear Stress (lb/ft ²)
W09	13.7492	12	2.32	144.23	97.2212	98.0227	0.8015	9.9114	15.0495	1.2107	0.010775
W09	13.5248	12	2.32	141.91	97.2192	98.0152	0.796	8.7957	15.0119	1.3643	0.014293
W09	13.3004	12	2.83	139.59	97.2172	98.0188	0.8016	9.952	15.0394	1.2058	0.010671
W09	13.0266	12	2.83	136.76	97.2148	98.0182	0.8034	10.0045	15.044	1.1995	0.010542
W09	12.7699	12	2.32	133.93	97.2048	98.0133	0.8085	9.2766	14.9839	1.2936	0.012544
W09	12.553	12	2.32	131.61	97.1955	98.0028	0.8073	8.0148	14.9022	1.4972	0.017647
W09	12.3359	12	2.83	129.29	97.1862	98.0065	0.8203	8.9594	14.9111	1.3394	0.013576
W09	12.0718	12	2.83	126.46	97.1749	98.0076	0.8327	9.5011	14.9177	1.263	0.01185
W09	11.7989	12	2.32	123.63	97.165	98.0076	0.8426	9.7447	14.9265	1.2314	0.011176
W09	11.5799	12	2.32	121.31	97.1576	97.9997	0.8421	8.6265	14.8755	1.3911	0.014907
W09	11.3609	12	2.83	118.99	97.1502	98.0037	0.8535	9.8261	14.861	1.2212	0.010949
W09	11.0937	12	2.83	116.16	97.1412	98.0034	0.8622	9.9631	14.7823	1.2044	0.010589
W09	10.83	12	2.32	113.34	97.1463	97.9997	0.8534	9.4215	14.8017	1.2737	0.012058
W09	10.6136	12	2.32	111.02	97.1569	97.9895	0.8326	8.1471	14.8186	1.4729	0.016973
W09	10.3971	12	4.19	108.7	97.1674	97.9925	0.8251	8.9601	14.8797	1.3393	0.013565
W09	10	12	10.24	104.5	97.1868	97.9949	0.8082	9.9676	14.8718	1.2039	0.010594
W09	9	12	10.52	94.26	97.1975	97.9788	0.7813	8.0668	12.686	1.4876	0.01648
W09	8	12	5.85	83.74	97.1048	97.9643	0.8595	7.3144	11.1052	1.6406	0.019839
W09	7.45582	12	2.38	77.9	97.1112	97.958	0.8468	7.0836	11.0048	1.6941	0.021303
W09	7.23422	12	2.38	75.51	97.1138	97.9374	0.8236	6.1289	10.8691	1.9579	0.029921
W09	7.01209	12	6.01	73.13	97.1164	97.9413	0.8249	6.868	10.8746	1.7472	0.022812
W09	6.42415	12	6.01	67.12	97.123	97.9349	0.8119	6.7025	10.8733	1.7904	0.024134
W09	5.84361	12	2.38	61.12	97.119	97.9309	0.8119	6.6977	10.9154	1.7917	0.024204
W09	5.62202	12	2.38	58.73	97.1066	97.9167	0.8101	6.0344	10.8907	1.9886	0.031011
W09	5.40004	12	6.01	56.35	97.0941	97.9256	0.8315	6.9556	10.9989	1.7252	0.022223
W09	4.83347	12	6.01	50.34	97.069	97.9243	0.8553	7.1857	11.0855	1.67	0.020655
W09	4.24908	12	2.38	44.34	97.0594	97.9205	0.8611	7.1573	11.0221	1.6766	0.020809
W09	4.0173	12	2.38	41.95	97.0556	97.9072	0.8516	6.4008	10.9251	1.8748	0.027109
W09	3.8018	12	6.01	39.57	97.0547	97.9116	0.8569	6.9918	10.9634	1.7163	0.021931

Test Identification	River Station	Q (cfs)	Reach Length (ft)	Cumulative Channel Length (ft)	Minimum Channel Elevation (ft)	WSE (ft)	Depth (ft)	Flow Area (ft ²)	Top Width, Tw (ft)	Velocity (ft/s)	Shear Stress (lb/ft ²)
W09	3.22728	12	6.01	33.56	97.0529	97.9085	0.8556	7.0311	11.0252	1.7067	0.021684
W09	2.67897	12	2.13	27.56	97.0466	97.9066	0.86	7.1917	11.067	1.6686	0.020603
W09	2.48611	12	2.64	25.43	97.0433	97.8917	0.8484	6.3358	10.986	1.894	0.027767
W09	2.24799	12	6.01	22.79	97.0392	97.8977	0.8585	7.126	11.0312	1.684	0.021026
W09	1.70375	12	6.01	16.79	97.0415	97.8931	0.8516	7.0186	10.9977	1.7097	0.021758
W09	1.19261	12	2.38	10.78	97.0527	97.8882	0.8354	6.9052	10.9328	1.7378	0.022558
W09	0.977647	12	2.38	8.4	97.0569	97.8722	0.8153	6.0964	10.8286	1.9684	0.03028
W09	0.697654	12	3.01	6.01	97.0569	97.8791	0.8222	6.8847	10.9234	1.743	0.022717
W09	0.34449	12	3.01	3.01	97.057	97.8777	0.8207	6.9224	10.9827	1.7335	0.022468
W09	0	12			97.0571	97.8763	0.8193	6.9631	11.0415	1.7234	0.022201
W09	18	16	1.88	189.25	97.2192	98.1781	0.9589	12.4037	15.8695	1.2899	0.011547
W09	17.8236	16	1.88	187.37	97.2236	98.1762	0.9526	12.0996	15.8732	1.3224	0.012233
W09	17.6472	16	2.32	185.49	97.228	98.1746	0.9466	11.8855	15.8795	1.3462	0.012754
W09	17.4288	16	2.32	183.17	97.2335	98.1663	0.9328	10.645	15.8361	1.5031	0.016566
W09	17.2102	16	2.83	180.85	97.239	98.1697	0.9307	11.702	15.8513	1.3673	0.013229
W09	16.9495	16	2.83	178.02	97.2425	98.1693	0.9268	11.8265	15.8395	1.3529	0.012908
W09	16.6953	16	2.32	175.19	97.2334	98.1685	0.9351	11.8476	15.8588	1.3505	0.012856
W09	16.4866	16	2.32	172.87	97.2259	98.1616	0.9357	10.8286	15.8321	1.4776	0.015922
W09	16.2777	16	2.83	170.55	97.2184	98.1653	0.9469	12.0456	15.8646	1.3283	0.012372
W09	16.0236	16	2.91	167.73	97.2093	98.1654	0.9561	12.317	15.8716	1.299	0.011754
W09	15.7369	16	2.32	164.82	97.217	98.164	0.9469	12.1644	15.8329	1.3153	0.012089
W09	15.507	16	2.32	162.5	97.2244	98.1559	0.9314	10.8709	15.7572	1.4718	0.015759
W09	15.2771	16	2.83	160.18	97.2318	98.1587	0.9269	11.8284	15.745	1.3527	0.012879
W09	15	16	2.83	157.35	97.2408	98.1571	0.9163	11.6667	15.6995	1.3714	0.013288
W09	14.7296	16	2.32	154.52	97.236	98.1564	0.9204	11.7274	15.733	1.3643	0.013137
W09	14.5098	16	2.32	152.2	97.2322	98.1488	0.9166	10.6296	15.7185	1.5052	0.016593
W09	14.2899	16	2.83	149.88	97.2284	98.1525	0.9241	11.7811	15.7712	1.3581	0.013008
W09	14.0215	16	2.83	147.05	97.2238	98.1519	0.9281	11.8435	15.8058	1.351	0.012858
W09	13.7492	16	2.32	144.23	97.2212	98.1512	0.93	11.8945	15.8112	1.3452	0.012732

Test Identification	River Station	Q (cfs)	Reach Length (ft)	Cumulative Channel Length (ft)	Minimum Channel Elevation (ft)	WSE (ft)	Depth (ft)	Flow Area (ft ²)	Top Width, Tw (ft)	Velocity (ft/s)	Shear Stress (lb/ft ²)
W09	13.5248	16	2.32	141.91	97.2192	98.1437	0.9245	10.7737	15.7724	1.4851	0.016098
W09	13.3004	16	2.83	139.59	97.2172	98.1473	0.9301	11.9335	15.7991	1.3408	0.012632
W09	13.0266	16	2.83	136.76	97.2148	98.1467	0.9319	11.986	15.8023	1.3349	0.012505
W09	12.7699	16	2.32	133.93	97.2048	98.1417	0.9369	11.248	15.7408	1.4225	0.01447
W09	12.553	16	2.32	131.61	97.1955	98.1315	0.936	9.9818	15.6597	1.6029	0.019124
W09	12.3359	16	2.83	129.29	97.1862	98.135	0.9488	10.9244	15.6689	1.4646	0.01546
W09	12.0718	16	2.83	126.46	97.1749	98.1361	0.9612	11.4663	15.6704	1.3954	0.01382
W09	11.7989	16	2.32	123.63	97.165	98.1361	0.9711	11.7111	15.6774	1.3662	0.013161
W09	11.5799	16	2.32	121.31	97.1576	98.1282	0.9706	10.5856	15.617	1.5115	0.016715
W09	11.3609	16	2.83	118.99	97.1502	98.1321	0.9819	11.7828	15.6024	1.3579	0.012958
W09	11.0937	16	2.83	116.16	97.1412	98.1317	0.9905	11.9109	15.5877	1.3433	0.012639
W09	10.83	16	2.32	113.34	97.1463	98.128	0.9817	11.3699	15.5874	1.4072	0.014074
W09	10.6136	16	2.32	111.02	97.1569	98.1182	0.9613	10.0997	15.5449	1.5842	0.018583
W09	10.3971	16	4.19	108.7	97.1674	98.1211	0.9537	10.9182	15.5875	1.4654	0.015455
W09	10	16	10.24	104.5	97.1868	98.1235	0.9367	11.925	15.5856	1.3417	0.012599
W09	9	16	10.52	94.26	97.1975	98.1047	0.9072	9.7117	13.454	1.6475	0.019389
W09	8	16	5.85	83.74	97.1048	98.0863	0.9815	8.7131	11.8225	1.8363	0.023956
W09	7.45582	16	2.38	77.9	97.1112	98.0794	0.9682	8.4614	11.6945	1.8909	0.025546
W09	7.23422	16	2.38	75.51	97.1138	98.0582	0.9444	7.4824	11.5454	2.1383	0.034085
W09	7.01209	16	6.01	73.13	97.1164	98.062	0.9456	8.2211	11.5405	1.9462	0.027212
W09	6.42415	16	6.01	67.12	97.123	98.0554	0.9324	8.0535	11.5577	1.9867	0.028549
W09	5.84361	16	2.38	61.12	97.119	98.0513	0.9322	8.0532	11.6131	1.9868	0.028594
W09	5.62202	16	2.38	58.73	97.1066	98.037	0.9304	7.3868	11.5868	2.166	0.035124
W09	5.40004	16	6.01	56.35	97.0941	98.0461	0.952	8.3227	11.6947	1.9224	0.026547
W09	4.83347	16	6.01	50.34	97.069	98.0448	0.9758	8.5628	11.7833	1.8685	0.02491
W09	4.24908	16	2.38	44.34	97.0594	98.0405	0.9811	8.5223	11.7327	1.8774	0.025151
W09	4.0173	16	2.38	41.95	97.0556	98.0265	0.9709	7.7464	11.634	2.0655	0.031538
W09	3.8018	16	6.01	39.57	97.0547	98.031	0.9762	8.3432	11.6777	1.9177	0.02638
W09	3.22728	16	6.01	33.56	97.0529	98.0277	0.9748	8.3867	11.7233	1.9078	0.026095

Test Identification	River Station	Q (cfs)	Reach Length (ft)	Cumulative Channel Length (ft)	Minimum Channel Elevation (ft)	WSE (ft)	Depth (ft)	Flow Area (ft ²)	Top Width, Tw (ft)	Velocity (ft/s)	Shear Stress (lb/ft ²)
W09	2.67897	16	2.13	27.56	97.0466	98.0253	0.9787	8.5472	11.764	1.872	0.025001
W09	2.48611	16	2.64	25.43	97.0433	98.0098	0.9665	7.6735	11.6821	2.0851	0.032234
W09	2.24799	16	6.01	22.79	97.0392	98.0159	0.9767	8.4713	11.7321	1.8887	0.025503
W09	1.70375	16	6.01	16.79	97.0415	98.0109	0.9694	8.3547	11.6978	1.9151	0.02631
W09	1.19261	16	2.38	10.78	97.0527	98.0054	0.9527	8.2276	11.6281	1.9447	0.027216
W09	0.977647	16	2.38	8.4	97.0569	97.9887	0.9318	7.3985	11.5194	2.1626	0.034988
W09	0.697654	16	3.01	6.01	97.0569	97.9959	0.939	8.2005	11.6172	1.9511	0.027427
W09	0.34449	16	3.01	3.01	97.057	97.9944	0.9374	8.244	11.6715	1.9408	0.027131
W09	0	16			97.0571	97.993	0.9359	8.291	11.7223	1.9298	0.026811
W10	18	8	2.88	189.25	97.2192	97.8884	0.6693	8.053	14.1681	0.9934	0.007617
W10	17.7296	8	2.88	186.37	97.226	97.8859	0.6599	7.6286	14.1397	1.0487	0.008628
W10	17.459	8	2.57	183.49	97.2328	97.8698	0.637	5.6766	14.0299	1.4093	0.015534
W10	17.2168	8	2.57	180.92	97.2389	97.8701	0.6312	5.8942	11.0849	1.3573	0.014616
W10	16.9787	8	3.02	178.35	97.2436	97.8683	0.6247	5.8269	13.9887	1.3729	0.01465
W10	16.7076	8	3.02	175.33	97.2338	97.8671	0.6333	5.8404	14.0048	1.3698	0.014575
W10	16.4362	8	2.57	172.31	97.2241	97.866	0.6419	5.8784	14.0354	1.3609	0.014325
W10	16.2048	8	2.57	169.74	97.2158	97.8671	0.6513	6.2332	11.1038	1.2835	0.012843
W10	15.9627	8	3.02	167.17	97.2097	97.8661	0.6564	6.2291	14.1105	1.2843	0.012565
W10	15.6636	8	3.02	164.15	97.2193	97.8633	0.644	6.048	14.026	1.3228	0.013421
W10	15.3643	8	2.57	161.13	97.229	97.8604	0.6314	5.8758	13.9434	1.3615	0.014317
W10	15.109	8	2.57	158.56	97.2372	97.8599	0.6227	5.9678	10.9745	1.3405	0.014159
W10	14.8612	8	3.02	155.99	97.2383	97.8564	0.6181	5.7383	13.8699	1.3941	0.015123
W10	14.5749	8	3.02	152.97	97.2334	97.8553	0.6219	5.7819	13.9185	1.3836	0.014881
W10	14.2885	8	2.63	149.95	97.2284	97.8542	0.6258	5.8269	13.966	1.373	0.014637
W10	14.0397	8	2.52	147.32	97.2241	97.8544	0.6303	6.0283	11.0673	1.3271	0.01387
W10	13.7981	8	3.01	144.8	97.2217	97.8519	0.6302	5.8903	14.0121	1.3582	0.014295
W10	13.5063	8	3.01	141.79	97.2191	97.8505	0.6314	5.8921	14.0152	1.3577	0.014266
W10	13.2145	8	2.57	138.78	97.2165	97.8493	0.6328	5.8956	14.0195	1.3569	0.014229
W10	12.9753	8	2.57	136.21	97.2135	97.8492	0.6357	6.0591	11.069	1.3203	0.013702

Test Identification	River Station	Q (cfs)	Reach Length (ft)	Cumulative Channel Length (ft)	Minimum Channel Elevation (ft)	WSE (ft)	Depth (ft)	Flow Area (ft ²)	Top Width, Tw (ft)	Velocity (ft/s)	Shear Stress (lb/ft ²)
W10	12.7349	8	3.02	133.63	97.2033	97.8411	0.6378	5.464	13.9636	1.4641	0.016996
W10	12.4526	8	3.02	130.62	97.1912	97.8387	0.6475	5.4201	13.9241	1.476	0.017279
W10	12.1709	8	2.57	127.6	97.1791	97.8382	0.6591	5.5558	13.8229	1.4399	0.016279
W10	11.9236	8	2.57	125.03	97.1887	97.8388	0.6501	5.8225	10.8945	1.374	0.014966
W10	11.6808	8	3.02	122.45	97.161	97.8355	0.6745	5.641	13.9308	1.4182	0.015713
W10	11.3955	8	3.02	119.44	97.1514	97.8337	0.6823	5.616	13.9475	1.4245	0.015835
W10	11.1106	8	2.57	116.42	97.1418	97.8325	0.6907	5.6504	13.8803	1.4158	0.015541
W10	10.8706	8	2.57	113.85	97.1443	97.832	0.6877	5.7542	10.7586	1.3903	0.015329
W10	10.6306	8	6.77	111.28	97.156	97.8244	0.6684	5.2654	13.8585	1.5193	0.018344
W10	10	8	10.24	104.5	97.1868	97.8348	0.648	7.6581	13.9577	1.0446	0.008519
W10	9	8	10.52	94.26	97.1975	97.8213	0.6238	6.1385	11.7898	1.3032	0.013507
W10	8	8	6.08	83.74	97.1048	97.8108	0.7061	5.6794	10.207	1.4086	0.015457
W10	7.4339	8	2.55	77.66	97.1114	97.7644	0.653	3.9557	9.8922	2.0224	0.031861
W10	7.19646	8	2.55	75.11	97.1142	97.7635	0.6493	4.0641	7.6497	1.9685	0.03093
W10	6.95614	8	5.69	72.55	97.117	97.7495	0.6325	3.7685	9.7949	2.1229	0.035429
W10	6.39878	8	5.69	66.86	97.1233	97.7423	0.619	3.7381	9.7776	2.1401	0.036203
W10	5.84876	8	2.55	61.17	97.1193	97.7361	0.6168	3.7436	9.7947	2.137	0.036105
W10	5.61086	8	2.55	58.62	97.1059	97.7399	0.634	4.0358	7.6896	1.9823	0.031448
W10	5.37336	8	5.69	56.06	97.0926	97.7347	0.6421	3.9683	9.8896	2.016	0.031693
W10	4.83611	8	5.69	50.37	97.069	97.7299	0.6609	4.0038	9.9341	1.9981	0.030941
W10	4.28229	8	2.55	44.68	97.06	97.7217	0.6617	3.9248	9.8465	2.0383	0.032254
W10	4.03396	8	2.56	42.13	97.0559	97.7245	0.6686	4.1908	7.6173	1.9089	0.02877
W10	3.80166	8	5.69	39.57	97.0547	97.7084	0.6537	3.7825	9.7644	2.115	0.035031
W10	3.25736	8	5.69	33.88	97.053	97.7021	0.6491	3.7703	9.8128	2.1219	0.035327
W10	2.73567	8	2.76	28.19	97.0477	97.6983	0.6506	3.8626	9.8464	2.0711	0.033442
W10	2.48591	8	2.35	25.43	97.0434	97.7004	0.657	4.0953	7.6457	1.9535	0.030383
W10	2.27392	8	5.69	23.08	97.0397	97.6907	0.651	3.8666	9.8091	2.069	0.033436
W10	1.75486	8	5.69	17.39	97.0403	97.684	0.6437	3.8357	9.7646	2.0856	0.034125
W10	1.27074	8	2.55	11.7	97.0509	97.6741	0.6231	3.7197	9.672	2.1507	0.036576

Test Identification	River Station	Q (cfs)	Reach Length (ft)	Cumulative Channel Length (ft)	Minimum Channel Elevation (ft)	WSE (ft)	Depth (ft)	Flow Area (ft ²)	Top Width, Tw (ft)	Velocity (ft/s)	Shear Stress (lb/ft ²)
W10	1.05313	8	2.55	9.14	97.0557	97.6742	0.6185	3.858	7.5319	2.0736	0.034736
W10	0.764896	8	3.29	6.59	97.0569	97.6696	0.6127	3.7959	9.667	2.1075	0.035136
W10	0.378183	8	3.29	3.29	97.057	97.6851	0.6281	4.9123	9.8422	1.6286	0.021408
W10	0	8			97.0571	97.6833	0.6262	4.9401	9.915	1.6194	0.021178
W10	18	12	2.88	189.25	97.2192	98.0842	0.8651	10.94	15.3188	1.0969	0.008615
W10	17.7296	12	2.88	186.37	97.226	98.082	0.856	10.5175	15.3203	1.141	0.009435
W10	17.459	12	2.57	183.49	97.2328	98.0804	0.8476	10.3058	15.3286	1.1644	0.009892
W10	17.2168	12	2.57	180.92	97.2389	98.0676	0.8287	8.3565	15.2415	1.436	0.016186
W10	16.9787	12	3.02	178.35	97.2436	98.0744	0.8308	10.353	15.2615	1.1591	0.009779
W10	16.7076	12	3.02	175.33	97.2338	98.0737	0.8399	10.367	15.2925	1.1575	0.009751
W10	16.4362	12	2.57	172.31	97.2241	98.0733	0.8492	10.489	15.3124	1.1441	0.009493
W10	16.2048	12	2.57	169.74	97.2158	98.0627	0.8469	8.7345	15.2595	1.3739	0.014608
W10	15.9627	12	3.02	167.17	97.2097	98.0691	0.8593	10.8218	15.3081	1.1089	0.008831
W10	15.6636	12	3.02	164.15	97.2193	98.0676	0.8483	10.6252	15.2596	1.1294	0.009205
W10	15.3643	12	2.57	161.13	97.229	98.0662	0.8372	10.4424	15.21	1.1492	0.009574
W10	15.109	12	2.57	158.56	97.2372	98.0524	0.8152	8.3046	15.0913	1.445	0.016375
W10	14.8612	12	3.02	155.99	97.2383	98.059	0.8207	10.1894	15.1339	1.1777	0.010122
W10	14.5749	12	3.02	152.97	97.2334	98.0584	0.825	10.2518	15.171	1.1705	0.009986
W10	14.2885	12	2.63	149.95	97.2284	98.0578	0.8294	10.3157	15.2087	1.1633	0.009851
W10	14.0397	12	2.52	147.32	97.2241	98.0451	0.821	8.3801	15.1692	1.432	0.016061
W10	13.7981	12	3.01	144.8	97.2217	98.0517	0.83	10.3399	15.2202	1.1605	0.009799
W10	13.5063	12	3.01	141.79	97.2191	98.0511	0.832	10.3957	15.2249	1.1543	0.009679
W10	13.2145	12	2.57	138.78	97.2165	98.0506	0.8341	10.4525	15.2296	1.1481	0.009558
W10	12.9753	12	2.57	136.21	97.2135	98.0374	0.8239	8.3901	15.1539	1.4303	0.016006
W10	12.7349	12	3.02	133.63	97.2033	98.0417	0.8384	9.6369	15.1475	1.2452	0.011519
W10	12.4526	12	3.02	130.62	97.1912	98.0393	0.8481	9.3773	15.1105	1.2797	0.012262
W10	12.1709	12	2.57	127.6	97.1791	98.0395	0.8604	9.7255	15.1024	1.2339	0.011265
W10	11.9236	12	2.57	125.03	97.1887	98.0286	0.8399	8.2575	15.0474	1.4532	0.016577
W10	11.6808	12	3.02	122.45	97.161	98.0356	0.8746	10.1897	15.0922	1.1777	0.010109

Test Identification	River Station	Q (cfs)	Reach Length (ft)	Cumulative Channel Length (ft)	Minimum Channel Elevation (ft)	WSE (ft)	Depth (ft)	Flow Area (ft ²)	Top Width, Tw (ft)	Velocity (ft/s)	Shear Stress (lb/ft ²)
W10	11.3955	12	3.02	119.44	97.1514	98.0352	0.8838	10.2816	15.0499	1.1671	0.009893
W10	11.1106	12	2.57	116.42	97.1418	98.0348	0.893	10.4217	14.9698	1.1514	0.009575
W10	10.8706	12	2.57	113.85	97.1443	98.0201	0.8758	8.1955	14.9015	1.4642	0.016823
W10	10.6306	12	6.77	111.28	97.156	98.0248	0.8688	9.4492	15.0129	1.2699	0.012023
W10	10	12	10.24	104.5	97.1868	98.0261	0.8393	10.4336	15.0448	1.1501	0.009561
W10	9	12	10.52	94.26	97.1975	98.0118	0.8144	8.4891	12.8751	1.4136	0.014705
W10	8	12	6.08	83.74	97.1048	97.999	0.8942	7.7037	11.3094	1.5577	0.017689
W10	7.4339	12	2.55	77.66	97.1114	97.9934	0.882	7.4736	11.2034	1.6057	0.018916
W10	7.19646	12	2.55	75.11	97.1142	97.9564	0.8422	5.7693	10.9718	2.08	0.034589
W10	6.95614	12	5.69	72.55	97.117	97.9648	0.8478	7.1188	11.0068	1.6857	0.021068
W10	6.39878	12	5.69	66.86	97.1233	97.9599	0.8365	6.9707	11.0163	1.7215	0.022122
W10	5.84876	12	2.55	61.17	97.1193	97.9565	0.8372	6.975	11.0623	1.7204	0.022119
W10	5.61086	12	2.55	58.62	97.1059	97.9286	0.8227	5.6626	10.9628	2.1192	0.036086
W10	5.37336	12	5.69	56.06	97.0926	97.9452	0.8526	7.1921	11.1192	1.6685	0.020633
W10	4.83611	12	5.69	50.37	97.069	97.9441	0.8751	7.4066	11.2	1.6202	0.019315
W10	4.28229	12	2.55	44.68	97.06	97.9407	0.8807	7.3735	11.1446	1.6275	0.019486
W10	4.03396	12	2.56	42.13	97.0559	97.9135	0.8576	5.8953	10.9636	2.0355	0.032887
W10	3.80166	12	5.69	39.57	97.0547	97.9252	0.8705	7.1419	11.0444	1.6802	0.020924
W10	3.25736	12	5.69	33.88	97.053	97.9224	0.8694	7.1613	11.1001	1.6757	0.020823
W10	2.73567	12	2.76	28.19	97.0477	97.921	0.8733	7.3562	11.15	1.6313	0.019596
W10	2.48591	12	2.35	25.43	97.0434	97.8913	0.8479	5.7974	10.9835	2.0699	0.034211
W10	2.27392	12	5.69	23.08	97.0397	97.9049	0.8652	7.1997	11.0726	1.6667	0.020553
W10	1.75486	12	5.69	17.39	97.0403	97.901	0.8607	7.1223	11.0473	1.6848	0.02106
W10	1.27074	12	2.55	11.7	97.0509	97.896	0.845	6.9862	10.9849	1.7177	0.021986
W10	1.05313	12	2.55	9.14	97.0557	97.859	0.8033	5.3736	10.7501	2.2331	0.040556
W10	0.764896	12	3.29	6.59	97.0569	97.8761	0.8192	6.8414	10.8926	1.754	0.02303
W10	0.378183	12	3.29	3.29	97.057	97.8745	0.8175	6.8823	10.9576	1.7436	0.022756
W10	0	12			97.0571	97.873	0.8159	6.9264	11.0221	1.7325	0.022463
W10	18	16	2.88	189.25	97.2192	98.2058	0.9866	12.8454	16.0362	1.2456	0.010144

Test Identification	River Station	Q (cfs)	Reach Length (ft)	Cumulative Channel Length (ft)	Minimum Channel Elevation (ft)	WSE (ft)	Depth (ft)	Flow Area (ft ²)	Top Width, Tw (ft)	Velocity (ft/s)	Shear Stress (lb/ft ²)
W10	17.7296	16	2.88	186.37	97.226	98.2033	0.9773	12.4208	16.0367	1.2882	0.010966
W10	17.459	16	2.57	183.49	97.2328	98.2017	0.9689	12.2083	16.0451	1.3106	0.011415
W10	17.2168	16	2.57	180.92	97.2389	98.1886	0.9496	10.2437	15.9644	1.5619	0.017279
W10	16.9787	16	3.02	178.35	97.2436	98.1956	0.952	12.2468	15.9954	1.3065	0.011311
W10	16.7076	16	3.02	175.33	97.2338	98.1949	0.9611	12.2638	16.0151	1.3047	0.011284
W10	16.4362	16	2.57	172.31	97.2241	98.1945	0.9704	12.3881	16.0292	1.2916	0.011029
W10	16.2048	16	2.57	169.74	97.2158	98.1835	0.9677	10.62	15.9733	1.5066	0.015896
W10	15.9627	16	3.02	167.17	97.2097	98.1901	0.9804	12.7182	16.0118	1.258	0.010384
W10	15.6636	16	3.02	164.15	97.2193	98.1886	0.9693	12.5138	15.9682	1.2786	0.010767
W10	15.3643	16	2.57	161.13	97.229	98.1871	0.9581	12.3235	15.9237	1.2983	0.011143
W10	15.109	16	2.57	158.56	97.2372	98.1727	0.9355	10.1637	15.8069	1.5742	0.017546
W10	14.8612	16	3.02	155.99	97.2383	98.1795	0.9412	12.0577	15.8526	1.327	0.011703
W10	14.5749	16	3.02	152.97	97.2334	98.179	0.9456	12.1246	15.8887	1.3196	0.011563
W10	14.2885	16	2.63	149.95	97.2284	98.1784	0.95	12.1931	15.9256	1.3122	0.011422
W10	14.0397	16	2.52	147.32	97.2241	98.1653	0.9412	10.2465	15.8829	1.5615	0.017251
W10	13.7981	16	3.01	144.8	97.2217	98.1722	0.9505	12.2169	15.9345	1.3097	0.011375
W10	13.5063	16	3.01	141.79	97.2191	98.1716	0.9525	12.273	15.9381	1.3037	0.011256
W10	13.2145	16	2.57	138.78	97.2165	98.1711	0.9546	12.33	15.9416	1.2976	0.011137
W10	12.9753	16	2.57	136.21	97.2135	98.1574	0.9439	10.2507	15.8622	1.5609	0.017226
W10	12.7349	16	3.02	133.63	97.2033	98.1618	0.9585	11.4987	15.8552	1.3915	0.013075
W10	12.4526	16	3.02	130.62	97.1912	98.1593	0.9681	11.2329	15.8148	1.4244	0.013795
W10	12.1709	16	2.57	127.6	97.1791	98.1596	0.9805	11.581	15.8063	1.3816	0.012847
W10	11.9236	16	2.57	125.03	97.1887	98.1485	0.9598	10.1031	15.7467	1.5837	0.017786
W10	11.6808	16	3.02	122.45	97.161	98.1558	0.9948	12.0445	15.7852	1.3284	0.01173
W10	11.3955	16	3.02	119.44	97.1514	98.1553	1.0039	12.131	15.7433	1.3189	0.011526
W10	11.1106	16	2.57	116.42	97.1418	98.1549	1.0131	12.2644	15.741	1.3046	0.011178
W10	10.8706	16	2.57	113.85	97.1443	98.1396	0.9953	10.0215	15.6564	1.5966	0.018026
W10	10.6306	16	6.77	111.28	97.156	98.1444	0.9884	11.2868	15.7015	1.4176	0.013619
W10	10	16	10.24	104.5	97.1868	98.146	0.9592	12.2774	15.7107	1.3032	0.011222

Test Identification	River Station	Q (cfs)	Reach Length (ft)	Cumulative Channel Length (ft)	Minimum Channel Elevation (ft)	WSE (ft)	Depth (ft)	Flow Area (ft ²)	Top Width, Tw (ft)	Velocity (ft/s)	Shear Stress (lb/ft ²)
W10	9	16	10.52	94.26	97.1975	98.1285	0.931	10.0337	13.6024	1.5946	0.016939
W10	8	16	6.08	83.74	97.1048	98.1118	1.0071	9.0171	11.9727	1.7744	0.020796
W10	7.4339	16	2.55	77.66	97.1114	98.1056	0.9942	8.7654	11.8396	1.8253	0.022162
W10	7.19646	16	2.55	75.11	97.1142	98.0651	0.9509	6.9954	11.5791	2.2872	0.037654
W10	6.95614	16	5.69	72.55	97.117	98.075	0.958	8.3651	11.6155	1.9127	0.024603
W10	6.39878	16	5.69	66.86	97.1233	98.0697	0.9464	8.2153	11.6413	1.9476	0.025636
W10	5.84876	16	2.55	61.17	97.1193	98.0663	0.947	8.2244	11.699	1.9454	0.02559
W10	5.61086	16	2.55	58.62	97.1059	98.0367	0.9308	6.8816	11.588	2.325	0.039035
W10	5.37336	16	5.69	56.06	97.0926	98.0547	0.9621	8.4437	11.7512	1.8949	0.02412
W10	4.83611	16	5.69	50.37	97.069	98.0537	0.9847	8.6686	11.8345	1.8457	0.022743
W10	4.28229	16	2.55	44.68	97.06	98.0499	0.9899	8.6255	11.7898	1.855	0.022951
W10	4.03396	16	2.56	42.13	97.0559	98.0198	0.9639	7.0945	11.5953	2.2553	0.036374
W10	3.80166	16	5.69	39.57	97.0547	98.0326	0.9779	8.3628	11.6878	1.9132	0.024584
W10	3.25736	16	5.69	33.88	97.053	98.0296	0.9766	8.3859	11.7294	1.908	0.024489
W10	2.73567	16	2.76	28.19	97.0477	98.0283	0.9806	8.5864	11.7789	1.8634	0.023222
W10	2.48591	16	2.35	25.43	97.0434	97.9954	0.952	6.9727	11.5976	2.2947	0.037933
W10	2.27392	16	5.69	23.08	97.0397	98.0103	0.9706	8.4002	11.6975	1.9047	0.02438
W10	1.75486	16	5.69	17.39	97.0403	98.006	0.9657	8.3154	11.6721	1.9241	0.024941
W10	1.27074	16	2.55	11.7	97.0509	98.0004	0.9495	8.1658	11.6044	1.9594	0.025972
W10	1.05313	16	2.55	9.14	97.0557	97.9594	0.9037	6.4824	11.3449	2.4682	0.044679
W10	0.764896	16	3.29	6.59	97.0569	97.9781	0.9212	7.9839	11.4985	2.004	0.027323
W10	0.378183	16	3.29	3.29	97.057	97.9765	0.9195	8.0305	11.5581	1.9924	0.02702
W10	0	16			97.0571	97.975	0.9179	8.081	11.6172	1.9799	0.026695
W11	18	8	2.8	189.25	97.2192	97.8891	0.67	8.0625	14.1721	0.9922	0.007597
W11	17.7368	8	2.79	186.45	97.2258	97.8866	0.6608	7.6471	14.1448	1.0462	0.00858
W11	17.4739	8	2.57	183.66	97.2324	97.8701	0.6376	5.6372	14.0322	1.4191	0.015753
W11	17.2321	8	2.57	181.08	97.2385	97.8704	0.6319	5.8608	11.0339	1.365	0.014789
W11	16.9934	8	4.14	178.51	97.2441	97.8691	0.625	5.8422	13.993	1.3693	0.014566
W11	16.6209	8	4.14	174.37	97.2308	97.867	0.6362	5.8264	14.0149	1.3731	0.014631

Test Identification	River Station	Q (cfs)	Reach Length (ft)	Cumulative Channel Length (ft)	Minimum Channel Elevation (ft)	WSE (ft)	Depth (ft)	Flow Area (ft ²)	Top Width, Tw (ft)	Velocity (ft/s)	Shear Stress (lb/ft ²)
W11	16.2485	8	2.6	170.23	97.2174	97.8662	0.6488	5.9818	14.0698	1.3374	0.013755
W11	16.0073	8	2.6	167.63	97.2087	97.8675	0.6588	6.3709	11.0722	1.2557	0.0122
W11	15.7507	8	4.17	165.03	97.2165	97.8636	0.6471	6.0418	14.0473	1.3241	0.013428
W11	15.3372	8	4.17	160.86	97.2299	97.8607	0.6308	5.9059	13.9392	1.3546	0.014173
W11	14.9281	8	2.57	156.7	97.2395	97.8575	0.618	5.7543	13.8634	1.3903	0.015036
W11	14.6844	8	2.57	154.12	97.2353	97.8574	0.6221	5.923	10.9425	1.3507	0.014397
W11	14.4406	8	4.16	151.55	97.231	97.8544	0.6234	5.7624	13.9381	1.3883	0.01498
W11	14.046	8	4.18	147.39	97.2242	97.8524	0.6282	5.7659	13.9994	1.3875	0.01495
W11	13.6439	8	2.57	143.22	97.2203	97.8512	0.6309	5.8593	14.0139	1.3654	0.014439
W11	13.395	8	2.57	140.64	97.2181	97.8514	0.6333	6.0595	11.0241	1.3202	0.013687
W11	13.1463	8	4.17	138.07	97.2159	97.8486	0.6327	5.8776	14.0181	1.3611	0.014316
W11	12.7603	8	4.17	133.9	97.2044	97.8412	0.6368	5.4399	13.9656	1.4706	0.017126
W11	12.3707	8	2.57	129.74	97.1877	97.8379	0.6502	5.3845	13.9149	1.4857	0.017463
W11	12.1303	8	2.57	127.16	97.1774	97.8392	0.6618	5.7179	10.8519	1.3991	0.01559
W11	11.8824	8	4.17	124.59	97.1679	97.8361	0.6682	5.5759	13.9144	1.4348	0.016091
W11	11.4885	8	4.17	120.42	97.1546	97.8332	0.6786	5.519	13.9373	1.4495	0.016434
W11	11.0951	8	2.57	116.26	97.1413	97.8322	0.6909	5.6552	13.8743	1.4146	0.015509
W11	10.8552	8	2.57	113.68	97.1451	97.8313	0.6862	5.6974	10.713	1.4041	0.015665
W11	10.6153	8	6.61	111.11	97.1568	97.8241	0.6673	5.2513	13.8641	1.5234	0.018456
W11	10	8	10.24	104.5	97.1868	97.8346	0.6478	7.613	13.9566	1.0508	0.008529
W11	9	8	10.52	94.26	97.1975	97.8214	0.6239	6.1397	11.7904	1.303	0.013501
W11	8	8	7.11	83.74	97.1048	97.8109	0.7061	5.6758	10.2074	1.4095	0.015396
W11	7.33814	8	2.55	76.63	97.1126	97.7624	0.6498	3.9207	9.8775	2.0405	0.032488
W11	7.1	8	2.55	74.08	97.1154	97.7618	0.6464	4.0526	7.6468	1.9741	0.031132
W11	6.85513	8	8.74	71.52	97.1182	97.7471	0.6289	3.7449	9.7851	2.1363	0.035933
W11	6	8	7.46	62.79	97.1278	97.7339	0.6061	3.6462	9.7493	2.1941	0.03828
W11	5.30622	8	2.55	55.33	97.0888	97.7338	0.645	3.9537	9.8988	2.0234	0.03189
W11	5.06849	8	2.55	52.78	97.0755	97.7374	0.6619	4.2617	7.7705	1.8772	0.027839
W11	4.82149	8	8.11	50.22	97.0688	97.7264	0.6576	3.9711	9.9124	2.0146	0.031507

Test Identification	River Station	Q (cfs)	Reach Length (ft)	Cumulative Channel Length (ft)	Minimum Channel Elevation (ft)	WSE (ft)	Depth (ft)	Flow Area (ft ²)	Top Width, Tw (ft)	Velocity (ft/s)	Shear Stress (lb/ft ²)
W11	4.03266	8	8.08	42.11	97.0559	97.7183	0.6624	3.9829	9.8059	2.0086	0.031208
W11	3.27176	8	2.55	34.03	97.0531	97.7067	0.6536	3.8499	9.8369	2.078	0.033795
W11	3.0273	8	2.55	31.47	97.0523	97.7112	0.6589	4.1935	7.6973	1.9077	0.028829
W11	2.80168	8	8.04	28.92	97.0488	97.7018	0.653	3.9582	9.8669	2.0211	0.03176
W11	2.07531	8	8.04	20.88	97.0363	97.6935	0.6572	3.9631	9.8327	2.0186	0.031717
W11	1.36817	8	2.61	12.84	97.0488	97.6765	0.6277	3.6913	9.6953	2.1672	0.037113
W11	1.14577	8	2.61	10.23	97.0537	97.6777	0.624	3.8826	7.5539	2.0605	0.034253
W11	0.886236	8	3.81	7.62	97.0569	97.6696	0.6127	3.7341	9.6411	2.1424	0.036329
W11	0.438757	8	3.81	3.81	97.057	97.6861	0.6291	4.9153	9.8346	1.6276	0.021373
W11	0	8			97.0571	97.684	0.6269	4.9474	9.9194	1.617	0.021108
W11	18	12	2.8	189.25	97.2192	98.0923	0.8731	11.063	15.3658	1.0847	0.008402
W11	17.7368	12	2.79	186.45	97.2258	98.0901	0.8643	10.6505	15.369	1.1267	0.009172
W11	17.4739	12	2.57	183.66	97.2324	98.0886	0.8562	10.4374	15.3775	1.1497	0.009614
W11	17.2321	12	2.57	181.08	97.2385	98.076	0.8375	8.4423	15.2928	1.4214	0.015822
W11	16.9934	12	4.14	178.51	97.2441	98.0827	0.8386	10.4819	15.3099	1.1448	0.009511
W11	16.6209	12	4.14	174.37	97.2308	98.0819	0.8511	10.5212	15.35	1.1406	0.009433
W11	16.2485	12	2.6	170.23	97.2174	98.0816	0.8642	10.7639	15.3691	1.1148	0.00895
W11	16.0073	12	2.6	167.63	97.2087	98.072	0.8633	9.0305	15.3299	1.3288	0.013541
W11	15.7507	12	4.17	165.03	97.2165	98.077	0.8605	10.8177	15.3264	1.1093	0.008841
W11	15.3372	12	4.17	160.86	97.2299	98.0751	0.8452	10.564	15.2586	1.1359	0.009329
W11	14.9281	12	2.57	156.7	97.2395	98.0735	0.834	10.393	15.211	1.1546	0.009682
W11	14.6844	12	2.57	154.12	97.2353	98.0608	0.8255	8.4187	15.1696	1.4254	0.01589
W11	14.4406	12	4.16	151.55	97.231	98.0674	0.8363	10.4218	15.2436	1.1514	0.009626
W11	14.046	12	4.18	147.39	97.2242	98.0666	0.8424	10.5115	15.2962	1.1416	0.009447
W11	13.6439	12	2.57	143.22	97.2203	98.0659	0.8456	10.5906	15.3084	1.1331	0.009286
W11	13.395	12	2.57	140.64	97.2181	98.0538	0.8357	8.5927	15.2439	1.3965	0.015174
W11	13.1463	12	4.17	138.07	97.2159	98.0601	0.8442	10.6136	15.2881	1.1306	0.009235
W11	12.7603	12	4.17	133.9	97.2044	98.0558	0.8514	9.8995	15.2332	1.2122	0.010841
W11	12.3707	12	2.57	129.74	97.1877	98.0532	0.8655	9.6294	15.188	1.2462	0.011547

Test Identification	River Station	Q (cfs)	Reach Length (ft)	Cumulative Channel Length (ft)	Minimum Channel Elevation (ft)	WSE (ft)	Depth (ft)	Flow Area (ft ²)	Top Width, Tw (ft)	Velocity (ft/s)	Shear Stress (lb/ft ²)
W11	12.1303	12	2.57	127.16	97.1774	98.0433	0.8659	8.3386	15.125	1.4391	0.016231
W11	11.8824	12	4.17	124.59	97.1679	98.0503	0.8824	10.3769	15.1765	1.1564	0.009708
W11	11.4885	12	4.17	120.42	97.1546	98.0496	0.895	10.4618	15.1505	1.147	0.00952
W11	11.0951	12	2.57	116.26	97.1413	98.0492	0.9079	10.6453	15.0507	1.1273	0.00913
W11	10.8552	12	2.57	113.68	97.1451	98.035	0.8899	8.3629	14.9987	1.4349	0.016082
W11	10.6153	12	6.61	111.11	97.1568	98.0395	0.8827	9.658	15.1004	1.2425	0.011448
W11	10	12	10.24	104.5	97.1868	98.0408	0.8541	10.6563	15.1268	1.1261	0.009119
W11	9	12	10.52	94.26	97.1975	98.0274	0.8299	8.69	12.972	1.3809	0.01396
W11	8	12	7.11	83.74	97.1048	98.0153	0.9105	7.8883	11.4049	1.5212	0.016787
W11	7.33814	12	2.55	76.63	97.1126	98.0094	0.8968	7.6383	11.2826	1.571	0.018022
W11	7.1	12	2.55	74.08	97.1154	97.9766	0.8611	5.9901	11.0759	2.0033	0.03179
W11	6.85513	12	8.74	71.52	97.1182	97.9841	0.8659	7.3154	11.1207	1.6404	0.019839
W11	6	12	7.46	62.79	97.1278	97.977	0.8492	7.0942	11.1421	1.6915	0.021314
W11	5.30622	12	2.55	55.33	97.0888	97.9774	0.8886	7.6012	11.3216	1.5787	0.018248
W11	5.06849	12	2.55	52.78	97.0755	97.9572	0.8817	6.3213	11.2643	1.8983	0.028198
W11	4.82149	12	8.11	50.22	97.0688	97.9674	0.8986	7.6658	11.3343	1.5654	0.017899
W11	4.03266	12	8.08	42.11	97.0559	97.964	0.9081	7.711	11.2638	1.5562	0.017627
W11	3.27176	12	2.55	34.03	97.0531	97.9588	0.9057	7.5598	11.3113	1.5874	0.01847
W11	3.0273	12	2.55	31.47	97.0523	97.9391	0.8868	6.3215	11.2438	1.8983	0.028189
W11	2.80168	12	8.04	28.92	97.0488	97.9496	0.9008	7.686	11.3157	1.5613	0.017781
W11	2.07531	12	8.04	20.88	97.0363	97.9461	0.9098	7.7137	11.3272	1.5557	0.017641
W11	1.36817	12	2.61	12.84	97.0488	97.94	0.8912	7.4766	11.2529	1.605	0.018921
W11	1.14577	12	2.61	10.23	97.0537	97.9132	0.8595	5.9698	11.0781	2.0101	0.032046
W11	0.886236	12	3.81	7.62	97.0569	97.9258	0.8689	7.3706	11.1639	1.6281	0.019521
W11	0.438757	12	3.81	3.81	97.057	97.9243	0.8673	7.4259	11.2385	1.616	0.019224
W11	0	12			97.0571	97.923	0.8659	7.4848	11.3139	1.6033	0.018915
W11	18	16	2.8	189.25	97.2192	98.2005	0.9814	12.7609	16.0044	1.2538	0.010346
W11	17.7368	16	2.79	186.45	97.2258	98.1981	0.9723	12.3444	16.0063	1.2961	0.011172
W11	17.4739	16	2.57	183.66	97.2324	98.1964	0.964	12.1288	16.0137	1.3192	0.01164

Test Identification	River Station	Q (cfs)	Reach Length (ft)	Cumulative Channel Length (ft)	Minimum Channel Elevation (ft)	WSE (ft)	Depth (ft)	Flow Area (ft ²)	Top Width, Tw (ft)	Velocity (ft/s)	Shear Stress (lb/ft ²)
W11	17.2321	16	2.57	181.08	97.2385	98.1825	0.944	10.105	15.9288	1.5834	0.017914
W11	16.9934	16	4.14	178.51	97.2441	98.1899	0.9458	12.1578	15.9597	1.316	0.011557
W11	16.6209	16	4.14	174.37	97.2308	98.189	0.9582	12.1996	15.986	1.3115	0.011478
W11	16.2485	16	2.6	170.23	97.2174	98.1887	0.9713	12.4447	16.0025	1.2857	0.010966
W11	16.0073	16	2.6	167.63	97.2087	98.1779	0.9692	10.6866	15.945	1.4972	0.015753
W11	15.7507	16	4.17	165.03	97.2165	98.1835	0.967	12.4839	15.949	1.2817	0.010883
W11	15.3372	16	4.17	160.86	97.2299	98.1813	0.9514	12.2181	15.8864	1.3095	0.011422
W11	14.9281	16	2.57	156.7	97.2395	98.1795	0.9399	12.0385	15.8428	1.3291	0.01181
W11	14.6844	16	2.57	154.12	97.2353	98.1654	0.9301	10.0379	15.7925	1.594	0.018157
W11	14.4406	16	4.16	151.55	97.231	98.1727	0.9417	12.0609	15.8704	1.3266	0.011769
W11	14.046	16	4.18	147.39	97.2242	98.1719	0.9477	12.1554	15.9215	1.3163	0.011572
W11	13.6439	16	2.57	143.22	97.2203	98.1711	0.9508	12.2341	15.9317	1.3078	0.011403
W11	13.395	16	2.57	140.64	97.2181	98.1576	0.9394	10.2059	15.8575	1.5677	0.017504
W11	13.1463	16	4.17	138.07	97.2159	98.1647	0.9488	12.244	15.9056	1.3068	0.01138
W11	12.7603	16	4.17	133.9	97.2044	98.1597	0.9553	11.5134	15.8458	1.3897	0.013112
W11	12.3707	16	2.57	129.74	97.1877	98.1567	0.969	11.2331	15.7968	1.4244	0.013871
W11	12.1303	16	2.57	127.16	97.1774	98.1459	0.9685	9.9207	15.7263	1.6128	0.018658
W11	11.8824	16	4.17	124.59	97.1679	98.1539	0.986	11.9808	15.7805	1.3355	0.011944
W11	11.4885	16	4.17	120.42	97.1546	98.1531	0.9985	12.0614	15.7481	1.3265	0.011755
W11	11.0951	16	2.57	116.26	97.1413	98.1526	1.0113	12.2372	15.7287	1.3075	0.011303
W11	10.8552	16	2.57	113.68	97.1451	98.1366	0.9915	9.919	15.6386	1.6131	0.018582
W11	10.6153	16	6.61	111.11	97.1568	98.1417	0.9849	11.2303	15.6847	1.4247	0.013867
W11	10	16	10.24	104.5	97.1868	98.1433	0.9565	12.2356	15.6959	1.3077	0.011381
W11	9	16	10.52	94.26	97.1975	98.1259	0.9285	9.9985	13.5862	1.6002	0.017217
W11	8	16	7.11	83.74	97.1048	98.1091	1.0043	8.9842	11.9565	1.7809	0.021169
W11	7.33814	16	2.55	76.63	97.1126	98.1018	0.9892	8.7054	11.8039	1.8379	0.022725
W11	7.1	16	2.55	74.08	97.1154	98.0608	0.9453	6.9424	11.5431	2.3047	0.038736
W11	6.85513	16	8.74	71.52	97.1182	98.0707	0.9525	8.2989	11.6014	1.928	0.025341
W11	6	16	7.46	62.79	97.1278	98.0621	0.9343	8.0635	11.6368	1.9843	0.027085

Test Identification	River Station	Q (cfs)	Reach Length (ft)	Cumulative Channel Length (ft)	Minimum Channel Elevation (ft)	WSE (ft)	Depth (ft)	Flow Area (ft ²)	Top Width, Tw (ft)	Velocity (ft/s)	Shear Stress (lb/ft ²)
W11	5.30622	16	2.55	55.33	97.0888	98.0629	0.9741	8.5908	11.8156	1.8625	0.023506
W11	5.06849	16	2.55	52.78	97.0755	98.0372	0.9616	7.2408	11.7264	2.2097	0.035329
W11	4.82149	16	8.11	50.22	97.0688	98.0499	0.9811	8.6212	11.8122	1.8559	0.023345
W11	4.03266	16	8.08	42.11	97.0559	98.0457	0.9897	8.6507	11.749	1.8496	0.023107
W11	3.27176	16	2.55	34.03	97.0531	98.0392	0.9861	8.4876	11.7831	1.8851	0.024194
W11	3.0273	16	2.55	31.47	97.0523	98.0128	0.9605	7.1659	11.6729	2.2328	0.036256
W11	2.80168	16	8.04	28.92	97.0488	98.0263	0.9775	8.5712	11.7644	1.8667	0.023696
W11	2.07531	16	8.04	20.88	97.0363	98.0218	0.9855	8.5884	11.778	1.863	0.023593
W11	1.36817	16	2.61	12.84	97.0488	98.0137	0.9649	8.3228	11.6906	1.9224	0.025332
W11	1.14577	16	2.61	10.23	97.0537	97.9768	0.9231	6.686	11.455	2.3931	0.042514
W11	0.886236	16	3.81	7.62	97.0569	97.9935	0.9366	8.14	11.5662	1.9656	0.026679
W11	0.438757	16	3.81	3.81	97.057	97.9916	0.9346	8.1957	11.6386	1.9522	0.026323
W11	0	16			97.0571	97.99	0.9329	8.2559	11.7048	1.938	0.025955
W12	18	8	2.28	189.25	97.2192	97.927	0.7079	8.6039	14.3959	0.9298	0.006563
W12	17.7859	8	2.27	186.97	97.2245	97.9242	0.6997	7.9928	14.3717	1.0009	0.007549
W12	17.5722	8	2.82	184.7	97.2299	97.9034	0.6735	5.4127	14.2401	1.478	0.016863
W12	17.3069	8	2.82	181.88	97.2366	97.9035	0.6669	5.6023	10.2283	1.428	0.016044
W12	17.0415	8	4.03	179.06	97.2433	97.9018	0.6585	5.571	14.2004	1.436	0.015849
W12	16.6801	8	4.03	175.03	97.2329	97.8993	0.6664	5.5284	14.2115	1.4471	0.01608
W12	16.3178	8	2.82	171	97.2199	97.8984	0.6785	5.6399	14.2537	1.4185	0.015338
W12	16.0643	8	2.82	168.18	97.2108	97.9	0.6892	6.0492	10.2543	1.3225	0.01344
W12	15.7831	8	4.03	165.36	97.2155	97.8968	0.6813	5.8349	14.2564	1.3711	0.014216
W12	15.3834	8	4.03	161.33	97.2284	97.8933	0.6649	5.6622	14.1523	1.4129	0.015223
W12	14.9854	8	2.82	157.3	97.2405	97.8892	0.6487	5.4703	14.054	1.4624	0.016445
W12	14.7182	8	2.82	154.48	97.2358	97.8894	0.6536	5.6733	10.131	1.4101	0.015538
W12	14.451	8	4.03	151.66	97.2312	97.8859	0.6547	5.511	14.1322	1.4516	0.016186
W12	14.0689	8	4.03	147.63	97.2246	97.8837	0.6591	5.4961	14.186	1.4556	0.016268
W12	13.6813	8	2.82	143.6	97.2206	97.8822	0.6616	5.5462	14.2019	1.4424	0.015944
W12	13.4085	8	2.82	140.78	97.2182	97.8828	0.6646	5.7941	10.2121	1.3807	0.014833

Test Identification	River Station	Q (cfs)	Reach Length (ft)	Cumulative Channel Length (ft)	Minimum Channel Elevation (ft)	WSE (ft)	Depth (ft)	Flow Area (ft ²)	Top Width, Tw (ft)	Velocity (ft/s)	Shear Stress (lb/ft ²)
W12	13.1357	8	4.03	137.96	97.2158	97.8796	0.6638	5.6138	14.2098	1.4251	0.015521
W12	12.763	8	4.03	133.93	97.2045	97.8717	0.6672	5.1979	14.1483	1.5391	0.018482
W12	12.3864	8	2.82	129.9	97.1884	97.8683	0.6799	5.1394	14.0957	1.5566	0.018953
W12	12.1228	8	2.82	127.08	97.2005	97.8691	0.6686	5.4026	10.0245	1.4808	0.017355
W12	11.8517	8	4.03	124.26	97.1668	97.8659	0.6991	5.2857	14.0966	1.5135	0.017742
W12	11.4712	8	4.03	120.23	97.154	97.8626	0.7086	5.2214	14.1062	1.5321	0.0182
W12	11.0903	8	2.82	116.21	97.1411	97.8616	0.7205	5.3398	14.0186	1.4982	0.017243
W12	10.8275	8	2.82	113.39	97.1465	97.8601	0.7136	5.3405	9.8923	1.498	0.017777
W12	10.5644	8	6.06	110.57	97.1593	97.8519	0.6926	4.9268	14.0543	1.6238	0.020817
W12	10	8	10.24	104.5	97.1868	97.8668	0.68	7.9032	14.1448	1.0122	0.007733
W12	9	8	10.52	94.26	97.1975	97.8563	0.6588	6.5547	11.9908	1.2205	0.011658
W12	8	8	8.16	83.74	97.1048	97.8463	0.7415	5.9693	10.4138	1.3402	0.013546
W12	7.24052	8	2.8	75.58	97.1137	97.7802	0.6665	3.6388	9.9768	2.1985	0.037637
W12	6.97849	8	2.8	72.78	97.1168	97.7794	0.6626	3.775	7.0734	2.1192	0.035868
W12	6.70431	8	7.34	69.98	97.1199	97.7631	0.6432	3.4781	9.8897	2.3001	0.041547
W12	5.98594	8	7.34	62.65	97.127	97.7707	0.6437	4.1079	9.9705	1.9475	0.029619
W12	5.30317	8	2.8	55.31	97.0887	97.7455	0.6568	3.6574	9.9694	2.1873	0.037214
W12	5.04255	8	2.8	52.51	97.0741	97.7493	0.6752	3.943	7.1767	2.0289	0.032568
W12	4.77162	8	7.36	49.71	97.068	97.7336	0.6656	3.6072	9.9532	2.2178	0.038279
W12	4.05535	8	7.31	42.35	97.0563	97.7232	0.6669	3.5697	9.8366	2.2411	0.038997
W12	3.36764	8	2.8	35.03	97.0534	97.7091	0.6557	3.4378	9.8329	2.3271	0.042687
W12	3.09985	8	2.8	32.23	97.0525	97.7143	0.6618	3.7466	7.0501	2.1352	0.03647
W12	2.84815	8	7.34	29.43	97.0496	97.7039	0.6543	3.5698	9.8796	2.241	0.039227
W12	2.18504	8	7.34	22.09	97.0382	97.6905	0.6523	3.4663	9.8105	2.3079	0.041824
W12	1.53099	8	2.8	14.76	97.0453	97.6742	0.6289	3.3199	9.6925	2.4097	0.04615
W12	1.29277	8	2.8	11.96	97.0505	97.6742	0.6237	3.4615	6.9007	2.3111	0.04351
W12	1.05453	8	4.58	9.16	97.0557	97.6556	0.5999	3.2	9.5396	2.5	0.050136
W12	0.529217	8	4.58	4.58	97.057	97.6904	0.6334	4.9479	9.841	1.6169	0.021051
W12	0	8			97.0571	97.688	0.6309	4.9871	9.9427	1.6041	0.020735

Test Identification	River Station	Q (cfs)	Reach Length (ft)	Cumulative Channel Length (ft)	Minimum Channel Elevation (ft)	WSE (ft)	Depth (ft)	Flow Area (ft ²)	Top Width, Tw (ft)	Velocity (ft/s)	Shear Stress (lb/ft ²)
W12	18	12	2.28	189.25	97.2192	98.1086	0.8894	11.3143	15.4613	1.0606	0.00799
W12	17.7859	12	2.27	186.97	97.2245	98.1069	0.8824	10.9659	15.4657	1.0943	0.008588
W12	17.5722	12	2.82	184.7	97.2299	98.1056	0.8757	10.7485	15.476	1.1164	0.008998
W12	17.3069	12	2.82	181.88	97.2366	98.0864	0.8498	7.8863	15.3598	1.5216	0.018576
W12	17.0415	12	4.03	179.06	97.2433	98.0965	0.8532	10.6586	15.3979	1.1258	0.009164
W12	16.6801	12	4.03	175.03	97.2329	98.0958	0.8629	10.7145	15.4271	1.12	0.009056
W12	16.3178	12	2.82	171	97.2199	98.0955	0.8756	10.9172	15.4496	1.0992	0.008674
W12	16.0643	12	2.82	168.18	97.2108	98.0805	0.8697	8.3934	15.3743	1.4297	0.016078
W12	15.7831	12	4.03	165.36	97.2155	98.0887	0.8732	11.0168	15.3993	1.0892	0.008487
W12	15.3834	12	4.03	161.33	97.2284	98.087	0.8586	10.7699	15.3354	1.1142	0.008934
W12	14.9854	12	2.82	157.3	97.2405	98.0853	0.8448	10.5593	15.2738	1.1364	0.009344
W12	14.7182	12	2.82	154.48	97.2358	98.0659	0.8301	7.7831	15.1957	1.5418	0.019095
W12	14.451	12	4.03	151.66	97.2312	98.0762	0.845	10.5548	15.2949	1.1369	0.009356
W12	14.0689	12	4.03	147.63	97.2246	98.0756	0.851	10.6423	15.3458	1.1276	0.009188
W12	13.6813	12	2.82	143.6	97.2206	98.0749	0.8543	10.7201	15.3608	1.1194	0.009036
W12	13.4085	12	2.82	140.78	97.2182	98.0561	0.8379	7.9147	15.257	1.5162	0.018387
W12	13.1357	12	4.03	137.96	97.2158	98.0661	0.8503	10.7073	15.3237	1.1207	0.009055
W12	12.763	12	4.03	133.93	97.2045	98.062	0.8575	9.9986	15.2697	1.2002	0.0106
W12	12.3864	12	2.82	129.9	97.1884	98.0593	0.8709	9.7116	15.2255	1.2356	0.01133
W12	12.1228	12	2.82	127.08	97.2005	98.0418	0.8414	7.6025	15.1166	1.5784	0.02013
W12	11.8517	12	4.03	124.26	97.1668	98.0535	0.8867	10.4284	15.1952	1.1507	0.0096
W12	11.4712	12	4.03	120.23	97.154	98.0528	0.8988	10.5171	15.1661	1.141	0.009407
W12	11.0903	12	2.82	116.21	97.1411	98.0524	0.9113	10.6971	15.0712	1.1218	0.009031
W12	10.8275	12	2.82	113.39	97.1465	98.03	0.8835	7.5656	14.9792	1.5861	0.020316
W12	10.5644	12	6.06	110.57	97.1593	98.0388	0.8795	9.6162	15.1089	1.2479	0.011566
W12	10	12	10.24	104.5	97.1868	98.0404	0.8536	10.6498	15.1244	1.1268	0.009131
W12	9	12	10.52	94.26	97.1975	98.0269	0.8295	8.6842	12.9692	1.3818	0.013981
W12	8	12	8.16	83.74	97.1048	98.0148	0.91	7.8829	11.4021	1.5223	0.016812
W12	7.24052	12	2.8	75.58	97.1137	98.0081	0.8944	7.6137	11.2652	1.5761	0.01815

Test Identification	River Station	Q (cfs)	Reach Length (ft)	Cumulative Channel Length (ft)	Minimum Channel Elevation (ft)	WSE (ft)	Depth (ft)	Flow Area (ft ²)	Top Width, Tw (ft)	Velocity (ft/s)	Shear Stress (lb/ft ²)
W12	6.97849	12	2.8	72.78	97.1168	97.9478	0.831	5.182	10.911	2.3157	0.044364
W12	6.70431	12	7.34	69.98	97.1199	97.9708	0.8509	7.1426	11.0574	1.6801	0.020932
W12	5.98594	12	7.34	62.65	97.127	97.9646	0.8376	6.9663	11.0736	1.7226	0.022191
W12	5.30317	12	2.8	55.31	97.0887	97.9649	0.8762	7.463	11.2504	1.6079	0.019005
W12	5.04255	12	2.8	52.51	97.0741	97.9255	0.8514	5.4924	11.0878	2.1848	0.038943
W12	4.77162	12	7.36	49.71	97.068	97.9448	0.8768	7.4031	11.2013	1.6209	0.019335
W12	4.05535	12	7.31	42.35	97.0563	97.9415	0.8852	7.4499	11.1317	1.6108	0.019024
W12	3.36764	12	2.8	35.03	97.0534	97.9353	0.8819	7.24	11.1574	1.6575	0.020331
W12	3.09985	12	2.8	32.23	97.0525	97.8898	0.8373	5.2243	10.9412	2.297	0.043575
W12	2.84815	12	7.34	29.43	97.0496	97.9155	0.8659	7.3116	11.1152	1.6412	0.019858
W12	2.18504	12	7.34	22.09	97.0382	97.9113	0.8731	7.2908	11.1146	1.6459	0.019987
W12	1.53099	12	2.8	14.76	97.0453	97.9049	0.8596	7.1052	11.0561	1.6889	0.02118
W12	1.29277	12	2.8	11.96	97.0505	97.8379	0.7874	4.6658	10.6423	2.5719	0.056189
W12	1.05453	12	4.58	9.16	97.0557	97.8724	0.8167	6.7535	10.8292	1.7769	0.023688
W12	0.529217	12	4.58	4.58	97.057	97.8701	0.8131	6.8112	10.9024	1.7618	0.023275
W12	0	12			97.0571	97.868	0.8109	6.8714	10.9929	1.7464	0.022864
W12	18	16	2.28	189.25	97.2192	98.2352	1.0161	13.3201	16.2134	1.2012	0.009339
W12	17.7859	16	2.27	186.97	97.2245	98.2335	1.0089	12.9704	16.2086	1.2336	0.009936
W12	17.5722	16	2.82	184.7	97.2299	98.2321	1.0022	12.7524	16.2089	1.2547	0.010342
W12	17.3069	16	2.82	181.88	97.2366	98.2131	0.9765	9.8801	16.1133	1.6194	0.018848
W12	17.0415	16	4.03	179.06	97.2433	98.2232	0.9799	12.6567	16.1634	1.2641	0.010495
W12	16.6801	16	4.03	175.03	97.2329	98.2224	0.9895	12.7157	16.1811	1.2583	0.010391
W12	16.3178	16	2.82	171	97.2199	98.2221	1.0022	12.9214	16.1943	1.2383	0.010019
W12	16.0643	16	2.82	168.18	97.2108	98.207	0.9962	10.3852	16.1126	1.5407	0.016796
W12	15.7831	16	4.03	165.36	97.2155	98.2154	0.9999	13.0142	16.1389	1.2294	0.009847
W12	15.3834	16	4.03	161.33	97.2284	98.2135	0.9851	12.757	16.0821	1.2542	0.010297
W12	14.9854	16	2.82	157.3	97.2405	98.2117	0.9712	12.5374	16.0275	1.2762	0.010706
W12	14.7182	16	2.82	154.48	97.2358	98.1926	0.9568	9.7566	15.9504	1.6399	0.019341
W12	14.451	16	4.03	151.66	97.2312	98.2029	0.9717	12.5398	16.0483	1.2759	0.010706

Test Identification	River Station	Q (cfs)	Reach Length (ft)	Cumulative Channel Length (ft)	Minimum Channel Elevation (ft)	WSE (ft)	Depth (ft)	Flow Area (ft ²)	Top Width, Tw (ft)	Velocity (ft/s)	Shear Stress (lb/ft ²)
W12	14.0689	16	4.03	147.63	97.2246	98.2022	0.9776	12.6339	16.0979	1.2664	0.010534
W12	13.6813	16	2.82	143.6	97.2206	98.2016	0.981	12.7135	16.1114	1.2585	0.010385
W12	13.4085	16	2.82	140.78	97.2182	98.1831	0.9649	9.8999	16.0083	1.6162	0.018722
W12	13.1357	16	4.03	137.96	97.2158	98.1931	0.9773	12.7004	16.0737	1.2598	0.010402
W12	12.763	16	4.03	133.93	97.2045	98.1887	0.9842	11.981	16.0169	1.3354	0.011897
W12	12.3864	16	2.82	129.9	97.1884	98.186	0.9976	11.6873	15.9669	1.369	0.012592
W12	12.1228	16	2.82	127.08	97.2005	98.1693	0.9688	9.5767	15.8621	1.6707	0.020168
W12	11.8517	16	4.03	124.26	97.1668	98.1807	1.0139	12.4084	15.9349	1.2895	0.010951
W12	11.4712	16	4.03	120.23	97.154	98.18	1.026	12.4928	15.8999	1.2807	0.010774
W12	11.0903	16	2.82	116.21	97.1411	98.1796	1.0385	12.6664	15.9109	1.2632	0.010367
W12	10.8275	16	2.82	113.39	97.1465	98.1576	1.0111	9.5271	15.7732	1.6794	0.020323
W12	10.5644	16	6.06	110.57	97.1593	98.1662	1.0069	11.5859	15.8283	1.381	0.012828
W12	10	16	10.24	104.5	97.1868	98.1679	0.9812	12.6236	15.8325	1.2675	0.01052
W12	9	16	10.52	94.26	97.1975	98.1518	0.9543	10.3515	13.7472	1.5457	0.015758
W12	8	16	8.16	83.74	97.1048	98.1363	1.0316	9.3121	12.1167	1.7182	0.019299
W12	7.24052	16	2.8	75.58	97.1137	98.129	1.0153	9.0174	11.9428	1.7744	0.020745
W12	6.97849	16	2.8	72.78	97.1168	98.0695	0.9527	6.5506	11.5825	2.4425	0.043741
W12	6.70431	16	7.34	69.98	97.1199	98.0921	0.9722	8.5252	11.7365	1.8768	0.023485
W12	5.98594	16	7.34	62.65	97.127	98.0859	0.9589	8.3521	11.7786	1.9157	0.02461
W12	5.30317	16	2.8	55.31	97.0887	98.0867	0.998	8.8755	11.9528	1.8027	0.021487
W12	5.04255	16	2.8	52.51	97.0741	98.0478	0.9737	6.8913	11.7942	2.3218	0.039009
W12	4.77162	16	7.36	49.71	97.068	98.067	0.999	8.8155	11.9093	1.815	0.021785
W12	4.05535	16	7.31	42.35	97.0563	98.0636	1.0073	8.8533	11.8567	1.8072	0.021507
W12	3.36764	16	2.8	35.03	97.0534	98.0573	1.0039	8.6452	11.8787	1.8507	0.022739
W12	3.09985	16	2.8	32.23	97.0525	98.0135	0.961	6.6222	11.6625	2.4161	0.04259
W12	2.84815	16	7.34	29.43	97.0496	98.0363	0.9867	8.6961	11.8206	1.8399	0.022434
W12	2.18504	16	7.34	22.09	97.0382	98.0319	0.9937	8.6746	11.8311	1.8445	0.022545
W12	1.53099	16	2.8	14.76	97.0453	98.0254	0.9801	8.4797	11.7715	1.8869	0.023718
W12	1.29277	16	2.8	11.96	97.0505	97.9633	0.9128	6.0467	11.3858	2.6461	0.052099

Test Identification	River Station	Q (cfs)	Reach Length (ft)	Cumulative Channel Length (ft)	Minimum Channel Elevation (ft)	WSE (ft)	Depth (ft)	Flow Area (ft ²)	Top Width, Tw (ft)	Velocity (ft/s)	Shear Stress (lb/ft ²)
W12	1.05453	16	4.58	9.16	97.0557	97.995	0.9393	8.1258	11.556	1.969	0.025998
W12	0.529217	16	4.58	4.58	97.057	97.9929	0.9359	8.1945	11.63	1.9525	0.025557
W12	0	16			97.0571	97.991	0.9339	8.2676	11.7106	1.9353	0.025125
W13	18	8	2.84	189.25	97.2192	97.9217	0.7025	8.5274	14.3644	0.9382	0.006697
W13	17.7328	8	2.84	186.4	97.2259	97.9185	0.6926	7.8582	14.3361	1.0181	0.007849
W13	17.4659	8	2.86	183.57	97.2326	97.8967	0.6641	5.3194	14.1959	1.5039	0.017551
W13	17.1969	8	2.86	180.71	97.2394	97.8972	0.6578	5.564	10.1973	1.4378	0.016286
W13	16.9342	8	5.44	177.85	97.242	97.8953	0.6533	5.5205	14.1615	1.4492	0.016168
W13	16.445	8	5.44	172.41	97.2244	97.8924	0.668	5.504	14.1978	1.4535	0.016209
W13	15.9431	8	2.82	166.97	97.2103	97.8918	0.6815	5.741	14.2612	1.3935	0.014685
W13	15.6634	8	2.82	164.15	97.2193	97.8916	0.6723	5.8782	10.1728	1.361	0.014328
W13	15.3837	8	5.44	161.33	97.2284	97.8865	0.6581	5.532	14.1095	1.4461	0.016005
W13	14.8519	8	5.44	155.89	97.2382	97.8831	0.6449	5.4615	14.0407	1.4648	0.016531
W13	14.3364	8	2.82	150.45	97.2292	97.8807	0.6515	5.4944	14.1203	1.456	0.016314
W13	14.0689	8	2.82	147.63	97.2246	97.8807	0.6561	5.6764	10.1681	1.4093	0.015536
W13	13.7986	8	5.86	144.81	97.2216	97.8775	0.6559	5.5226	14.1684	1.4486	0.016125
W13	13.2314	8	5.02	138.95	97.2166	97.8746	0.658	5.5186	14.1747	1.4496	0.016112
W13	12.7625	8	2.82	133.93	97.2045	97.8666	0.662	5.1483	14.1176	1.5539	0.01889
W13	12.4991	8	2.82	131.11	97.1932	97.866	0.6728	5.2678	10.0459	1.5187	0.018391
W13	12.2357	8	5.44	128.29	97.1819	97.8609	0.679	5.0565	14.0486	1.5821	0.019614
W13	11.718	8	5.44	122.85	97.1623	97.8586	0.6963	5.1515	14.0631	1.553	0.01876
W13	11.2042	8	2.82	117.41	97.1449	97.8557	0.7108	5.1731	14.0235	1.5465	0.018503
W13	10.9398	8	2.82	114.59	97.1516	97.8559	0.7043	5.3721	9.7863	1.4892	0.017465
W13	10.6768	8	7.27	111.77	97.1538	97.8464	0.6926	4.8812	13.9686	1.6389	0.021214
W13	10	8	10.24	104.5	97.1868	97.8612	0.6744	7.8296	14.1125	1.0218	0.007901
W13	9	8	10.52	94.26	97.1975	97.8503	0.6528	6.4834	11.9566	1.2339	0.011948
W13	8	8	6.19	83.74	97.1048	97.8411	0.7363	5.9908	10.3832	1.3354	0.013727
W13	7.42392	8	6.32	77.55	97.1115	97.835	0.7235	5.7004	10.2982	1.4034	0.015038
W13	6.8269	8	2.74	71.23	97.1185	97.7681	0.6496	3.5508	9.9152	2.253	0.039749

Test Identification	River Station	Q (cfs)	Reach Length (ft)	Cumulative Channel Length (ft)	Minimum Channel Elevation (ft)	WSE (ft)	Depth (ft)	Flow Area (ft ²)	Top Width, Tw (ft)	Velocity (ft/s)	Shear Stress (lb/ft ²)
W13	6.55876	8	2.74	68.49	97.1215	97.7687	0.6472	3.7107	7.0529	2.156	0.037274
W13	6.29035	8	10.35	65.76	97.1245	97.7563	0.6318	3.493	9.8683	2.2903	0.041302
W13	5.31188	8	10.35	55.4	97.0892	97.7459	0.6567	3.6064	9.9698	2.2183	0.0383
W13	4.31849	8	2.74	45.05	97.0606	97.7292	0.6686	3.5332	9.8933	2.2642	0.039919
W13	4.05183	8	2.74	42.31	97.0562	97.7339	0.6777	3.8345	7.0067	2.0863	0.034488
W13	3.80176	8	10.31	39.57	97.0547	97.7142	0.6595	3.4542	9.7982	2.316	0.042073
W13	2.8327	8	10.31	29.26	97.0493	97.7019	0.6526	3.4745	9.8674	2.3025	0.041505
W13	1.8881	8	2.74	18.95	97.0374	97.6864	0.649	3.4204	9.7874	2.3389	0.043049
W13	1.65508	8	2.74	16.21	97.0425	97.6866	0.6441	3.5639	6.9441	2.2447	0.040742
W13	1.42209	8	6.74	13.48	97.0476	97.6655	0.6179	3.2352	9.6344	2.4728	0.048852
W13	0.78293	8	6.74	6.74	97.0569	97.6763	0.6194	3.8957	9.7032	2.0536	0.03323
W13	0	8			97.0571	97.688	0.6309	4.9871	9.9427	1.6041	0.020735
W13	18	12	2.84	189.25	97.2192	98.0844	0.8652	10.9422	15.3196	1.0967	0.008611
W13	17.7328	12	2.84	186.4	97.2259	98.0822	0.8562	10.5239	15.3212	1.1403	0.009422
W13	17.4659	12	2.86	183.57	97.2326	98.0806	0.848	10.311	15.3301	1.1638	0.00988
W13	17.1969	12	2.86	180.71	97.2394	98.0586	0.8192	7.4744	15.1864	1.6055	0.020974
W13	16.9342	12	5.44	177.85	97.242	98.0703	0.8283	10.2876	15.2432	1.1665	0.009919
W13	16.445	12	5.44	172.41	97.2244	98.0694	0.845	10.4232	15.2884	1.1513	0.009628
W13	15.9431	12	2.82	166.97	97.2103	98.0692	0.8589	10.8121	15.3064	1.1099	0.008849
W13	15.6634	12	2.82	164.15	97.2193	98.0487	0.8294	7.7793	15.1478	1.5425	0.019098
W13	15.3837	12	5.44	161.33	97.2284	98.0585	0.8301	10.3351	15.1674	1.1611	0.009798
W13	14.8519	12	5.44	155.89	97.2382	98.0564	0.8182	10.1531	15.1202	1.1819	0.010203
W13	14.3364	12	2.82	150.45	97.2292	98.0554	0.8262	10.2662	15.1875	1.1689	0.009957
W13	14.0689	12	2.82	147.63	97.2246	98.0332	0.8086	7.4381	15.0943	1.6133	0.021175
W13	13.7986	12	5.86	144.81	97.2216	98.0449	0.8233	10.2361	15.1797	1.1723	0.010024
W13	13.2314	12	5.02	138.95	97.2166	98.0438	0.8272	10.3447	15.1889	1.16	0.009783
W13	12.7625	12	2.82	133.93	97.2045	98.039	0.8345	9.648	15.1339	1.2438	0.011485
W13	12.4991	12	2.82	131.11	97.1932	98.0143	0.8211	7.0196	14.9661	1.7095	0.024142
W13	12.2357	12	5.44	128.29	97.1819	98.027	0.8451	9.4069	15.0288	1.2757	0.012152

Test Identification	River Station	Q (cfs)	Reach Length (ft)	Cumulative Channel Length (ft)	Minimum Channel Elevation (ft)	WSE (ft)	Depth (ft)	Flow Area (ft ²)	Top Width, Tw (ft)	Velocity (ft/s)	Shear Stress (lb/ft ²)
W13	11.718	12	5.44	122.85	97.1623	98.0277	0.8654	10.0611	15.0467	1.1927	0.010402
W13	11.2042	12	2.82	117.41	97.1449	98.0269	0.882	10.2512	14.9545	1.1706	0.009944
W13	10.9398	12	2.82	114.59	97.1516	98.0023	0.8507	7.2399	14.7679	1.6575	0.022398
W13	10.6768	12	7.27	111.77	97.1538	98.0123	0.8585	9.3157	14.9301	1.2881	0.012407
W13	10	12	10.24	104.5	97.1868	98.0133	0.8265	10.2418	14.9739	1.1717	0.009968
W13	9	12	10.52	94.26	97.1975	97.9983	0.8009	8.3157	12.7961	1.4431	0.015398
W13	8	12	6.19	83.74	97.1048	97.9848	0.8801	7.5441	11.2262	1.5906	0.018527
W13	7.42392	12	6.32	77.55	97.1115	97.979	0.8675	7.3104	11.1206	1.6415	0.019864
W13	6.8269	12	2.74	71.23	97.1185	97.974	0.8555	7.1982	11.0664	1.6671	0.020565
W13	6.55876	12	2.74	68.49	97.1215	97.9117	0.7902	4.7901	10.734	2.5051	0.052985
W13	6.29035	12	10.35	65.76	97.1245	97.9428	0.8183	6.765	10.9258	1.7738	0.023654
W13	5.31188	12	10.35	55.4	97.0892	97.9407	0.8515	7.1862	11.1085	1.6699	0.020666
W13	4.31849	12	2.74	45.05	97.0606	97.9366	0.876	7.3198	11.1226	1.6394	0.019805
W13	4.05183	12	2.74	42.31	97.0562	97.8855	0.8293	5.0971	10.7989	2.3543	0.045946
W13	3.80176	12	10.31	39.57	97.0547	97.9087	0.854	6.96	10.9462	1.7241	0.022154
W13	2.8327	12	10.31	29.26	97.0493	97.905	0.8557	7.192	11.0541	1.6685	0.020597
W13	1.8881	12	2.74	18.95	97.0374	97.8983	0.8609	7.1486	11.0402	1.6787	0.02088
W13	1.65508	12	2.74	16.21	97.0425	97.827	0.7845	4.5906	10.6026	2.614	0.058274
W13	1.42209	12	6.74	13.48	97.0476	97.8624	0.8148	6.6254	10.7959	1.8112	0.024729
W13	0.78293	12	6.74	6.74	97.0569	97.8581	0.8012	6.6441	10.7829	1.8061	0.024571
W13	0	12			97.0571	97.8549	0.7978	6.7273	10.9162	1.7838	0.023965
W13	18	16	2.84	189.25	97.2192	98.2119	0.9928	12.9441	16.0732	1.2361	0.00995
W13	17.7328	16	2.84	186.4	97.2259	98.2096	0.9837	12.5245	16.0718	1.2775	0.010741
W13	17.4659	16	2.86	183.57	97.2326	98.208	0.9754	12.3116	16.0807	1.2996	0.011179
W13	17.1969	16	2.86	180.71	97.2394	98.1869	0.9475	9.4716	15.9538	1.6893	0.020712
W13	16.9342	16	5.44	177.85	97.242	98.1982	0.9562	12.2864	16.0157	1.3023	0.011204
W13	16.445	16	5.44	172.41	97.2244	98.1973	0.9729	12.4276	16.0453	1.2875	0.010925
W13	15.9431	16	2.82	166.97	97.2103	98.1972	0.9869	12.8185	16.0506	1.2482	0.010178
W13	15.6634	16	2.82	164.15	97.2193	98.1769	0.9576	9.7706	15.9	1.6376	0.019258

Test Identification	River Station	Q (cfs)	Reach Length (ft)	Cumulative Channel Length (ft)	Minimum Channel Elevation (ft)	WSE (ft)	Depth (ft)	Flow Area (ft ²)	Top Width, Tw (ft)	Velocity (ft/s)	Shear Stress (lb/ft ²)
W13	15.3837	16	5.44	161.33	97.2284	98.1866	0.9582	12.3262	15.9233	1.298	0.011108
W13	14.8519	16	5.44	155.89	97.2382	98.1844	0.9462	12.1375	15.883	1.3182	0.011501
W13	14.3364	16	2.82	150.45	97.2292	98.1835	0.9542	12.26	15.9487	1.3051	0.011253
W13	14.0689	16	2.82	147.63	97.2246	98.1624	0.9378	9.4383	15.8615	1.6952	0.020843
W13	13.7986	16	5.86	144.81	97.2216	98.1737	0.9521	12.2407	15.9433	1.3071	0.011291
W13	13.2314	16	5.02	138.95	97.2166	98.1726	0.956	12.3506	15.9504	1.2955	0.011062
W13	12.7625	16	2.82	133.93	97.2045	98.1676	0.9631	11.6443	15.8927	1.3741	0.012668
W13	12.4991	16	2.82	131.11	97.1932	98.145	0.9518	9.0257	15.7345	1.7727	0.023045
W13	12.2357	16	5.44	128.29	97.1819	98.1566	0.9747	11.4051	15.7905	1.4029	0.01326
W13	11.718	16	5.44	122.85	97.1623	98.1575	0.9951	12.0626	15.7975	1.3264	0.011651
W13	11.2042	16	2.82	117.41	97.1449	98.1567	1.0118	12.2409	15.7213	1.3071	0.011229
W13	10.9398	16	2.82	114.59	97.1516	98.1333	0.9817	9.2297	15.6073	1.7335	0.021736
W13	10.6768	16	7.27	111.77	97.1538	98.1428	0.989	11.3121	15.6911	1.4144	0.013484
W13	10	16	10.24	104.5	97.1868	98.144	0.9573	12.2468	15.6998	1.3065	0.011242
W13	9	16	10.52	94.26	97.1975	98.1264	0.929	10.0054	13.5894	1.5991	0.016963
W13	8	16	6.19	83.74	97.1048	98.1096	1.0049	8.9908	11.9598	1.7796	0.020806
W13	7.42392	16	6.32	77.55	97.1115	98.1034	0.9919	8.7381	11.8261	1.8311	0.022182
W13	6.8269	16	2.74	71.23	97.1185	98.0983	0.9798	8.6172	11.758	1.8567	0.022899
W13	6.55876	16	2.74	68.49	97.1215	98.0416	0.9201	6.2323	11.4669	2.5673	0.048722
W13	6.29035	16	10.35	65.76	97.1245	98.0697	0.9452	8.1983	11.6523	1.9516	0.025547
W13	5.31188	16	10.35	55.4	97.0892	98.0683	0.9791	8.65	11.8449	1.8497	0.02267
W13	4.31849	16	2.74	45.05	97.0606	98.0643	1.0037	8.7889	11.8761	1.8205	0.02183
W13	4.05183	16	2.74	42.31	97.0562	98.0169	0.9607	6.5665	11.5792	2.4366	0.043117
W13	3.80176	16	10.31	39.57	97.0547	98.0385	0.9838	8.4315	11.7231	1.8976	0.023876
W13	2.8327	16	10.31	29.26	97.0493	98.0352	0.9859	8.6809	11.8152	1.8431	0.022416
W13	1.8881	16	2.74	18.95	97.0374	98.0292	0.9918	8.6443	11.8194	1.8509	0.022604
W13	1.65508	16	2.74	16.21	97.0425	97.9691	0.9266	6.1567	11.4454	2.5988	0.049701
W13	1.42209	16	6.74	13.48	97.0476	97.9986	0.951	8.1506	11.6043	1.963	0.025668
W13	0.78293	16	6.74	6.74	97.0569	97.9947	0.9378	8.1724	11.5938	1.9578	0.025512

Test Identification	River Station	Q (cfs)	Reach Length (ft)	Cumulative Channel Length (ft)	Minimum Channel Elevation (ft)	WSE (ft)	Depth (ft)	Flow Area (ft ²)	Top Width, Tw (ft)	Velocity (ft/s)	Shear Stress (lb/ft ²)
W13	0	16			97.0571	97.992	0.9349	8.2793	11.7164	1.9325	0.02488
W14	18	8	2.39	189.25	97.2192	97.9299	0.7107	8.6452	14.4127	0.9254	0.006493
W14	17.7749	8	2.39	186.85	97.2248	97.927	0.7022	8.0077	14.388	0.999	0.007513
W14	17.5497	8	2.3	184.46	97.2305	97.9059	0.6754	5.4005	14.255	1.4813	0.016932
W14	17.3338	8	2.3	182.16	97.2359	97.9066	0.6707	5.6438	10.2933	1.4175	0.015793
W14	17.1176	8	4.68	179.87	97.2414	97.9038	0.6624	5.4993	14.219	1.4547	0.016301
W14	16.6946	8	4.68	175.19	97.2334	97.902	0.6686	5.5576	14.2266	1.4395	0.015893
W14	16.2737	8	2.3	170.51	97.2183	97.9008	0.6825	5.6718	14.2757	1.4105	0.01513
W14	16.0675	8	2.3	168.21	97.2109	97.9026	0.6917	6.0881	10.3199	1.314	0.013259
W14	15.8385	8	4.7	165.92	97.2137	97.8996	0.6859	5.8721	14.2859	1.3624	0.014006
W14	15.3726	8	4.66	161.22	97.2287	97.8957	0.667	5.671	14.1648	1.4107	0.015163
W14	14.9154	8	2.3	156.56	97.2393	97.8916	0.6523	5.4889	14.0825	1.4575	0.016312
W14	14.6975	8	2.3	154.26	97.2355	97.8922	0.6567	5.7174	10.1974	1.3992	0.015282
W14	14.48	8	4.68	151.97	97.2318	97.8886	0.6568	5.5121	14.1437	1.4514	0.016164
W14	14.0366	8	4.68	147.29	97.2241	97.8867	0.6626	5.5523	14.2097	1.4408	0.015913
W14	13.5858	8	2.3	142.61	97.2198	97.8851	0.6653	5.621	14.2239	1.4232	0.015487
W14	13.3636	8	2.3	140.32	97.2178	97.8857	0.6679	5.8431	10.2783	1.3691	0.014566
W14	13.1411	8	4.68	138.02	97.2158	97.8826	0.6668	5.644	14.2281	1.4174	0.015334
W14	12.7077	8	4.68	133.34	97.2021	97.8736	0.6715	5.1709	14.153	1.5471	0.018689
W14	12.2706	8	2.3	128.66	97.1834	97.8703	0.6869	5.148	14.1044	1.554	0.018843
W14	12.0557	8	2.3	126.37	97.2083	97.8721	0.6638	5.4786	10.0707	1.4602	0.016808
W14	11.833	8	4.68	124.07	97.1662	97.8674	0.7012	5.2344	14.107	1.5283	0.01809
W14	11.3912	8	4.68	119.39	97.1513	97.8651	0.7138	5.2645	14.1125	1.5196	0.017858
W14	10.9513	8	2.3	114.71	97.1404	97.863	0.7226	5.2982	13.9474	1.51	0.017542
W14	10.7368	8	2.3	112.42	97.1509	97.8619	0.711	5.3193	10.0068	1.504	0.017982
W14	10.5227	8	5.61	110.12	97.1613	97.8545	0.6931	4.9349	14.0767	1.6211	0.020732
W14	10	8	10.24	104.5	97.1868	97.8695	0.6828	7.9389	14.1604	1.0077	0.007654
W14	9	8	10.52	94.26	97.1975	97.8591	0.6617	6.5892	12.0073	1.2141	0.011521
W14	8	8	8.64	83.74	97.1048	97.8493	0.7445	5.9983	10.4311	1.3337	0.013398

Test Identifi- cation	River Station	Q (cfs)	Reach Length (ft)	Cumulative Channel Length (ft)	Minimum Channel Elevation (ft)	WSE (ft)	Depth (ft)	Flow Area (ft ²)	Top Width, Tw (ft)	Velocity (ft/s)	Shear Stress (lb/ft ²)
W14	7.196	8	2.34	75.1	97.1142	97.7774	0.6632	3.549	9.9604	2.2542	0.039661
W14	6.97653	8	2.34	72.76	97.1168	97.7787	0.6619	3.7691	7.1019	2.1225	0.036011
W14	6.74727	8	7.87	70.42	97.1194	97.764	0.6446	3.4944	9.8931	2.2893	0.041135
W14	5.97681	8	7.87	62.55	97.1265	97.7504	0.6239	3.4051	9.8531	2.3494	0.043594
W14	5.24437	8	2.34	54.67	97.0854	97.7495	0.6641	3.6783	10.0066	2.1749	0.036687
W14	5.02615	8	2.34	52.33	97.0732	97.7543	0.6811	3.984	7.2312	2.0081	0.031843
W14	4.7991	8	7.86	49.99	97.0684	97.7396	0.6712	3.6597	9.99	2.1859	0.037079
W14	4.03405	8	7.89	42.13	97.0559	97.7279	0.672	3.5965	9.8619	2.2244	0.038323
W14	3.29177	8	2.34	34.24	97.0531	97.7104	0.6573	3.399	9.8548	2.3537	0.043635
W14	3.06804	8	2.34	31.9	97.0524	97.7186	0.6662	3.7959	7.1049	2.1075	0.035436
W14	2.85952	8	7.87	29.56	97.0498	97.704	0.6542	3.5178	9.8801	2.2741	0.040425
W14	2.14792	8	7.87	21.68	97.0375	97.694	0.6565	3.5204	9.8325	2.2725	0.040451
W14	1.4504	8	2.34	13.81	97.047	97.6748	0.6278	3.3174	9.6911	2.4115	0.046228
W14	1.25113	8	2.34	11.47	97.0513	97.6758	0.6245	3.471	6.9335	2.3048	0.043261
W14	1.05195	8	4.56	9.13	97.0557	97.652	0.5963	3.1163	9.518	2.5672	0.053016
W14	0.527431	8	4.56	4.56	97.057	97.6904	0.6334	4.947	9.8414	1.6171	0.02101
W14	0	8			97.0571	97.688	0.6309	4.9871	9.9427	1.6041	0.020735
W14	18	12	2.39	189.25	97.2192	98.1178	0.8987	11.4578	15.5156	1.0473	0.007768
W14	17.7749	12	2.39	186.85	97.2248	98.1162	0.8914	11.096	15.5221	1.0815	0.008365
W14	17.5497	12	2.3	184.46	97.2305	98.1149	0.8844	10.8788	15.5318	1.1031	0.008759
W14	17.3338	12	2.3	182.16	97.2359	98.0972	0.8613	8.0696	15.4248	1.4871	0.017623
W14	17.1176	12	4.68	179.87	97.2414	98.1067	0.8653	10.7603	15.4673	1.1152	0.008976
W14	16.6946	12	4.68	175.19	97.2334	98.1059	0.8725	10.8669	15.486	1.1043	0.008774
W14	16.2737	12	2.3	170.51	97.2183	98.1056	0.8873	11.1121	15.5119	1.0799	0.008335
W14	16.0675	12	2.3	168.21	97.2109	98.0915	0.8806	8.5793	15.4386	1.3987	0.01529
W14	15.8385	12	4.7	165.92	97.2137	98.0995	0.8858	11.2151	15.4692	1.07	0.008154
W14	15.3726	12	4.66	161.22	97.2287	98.0976	0.8689	10.9264	15.3963	1.0983	0.00865
W14	14.9154	12	2.3	156.56	97.2393	98.0959	0.8566	10.739	15.3464	1.1174	0.008998
W14	14.6975	12	2.3	154.26	97.2355	98.0781	0.8426	7.9922	15.271	1.5015	0.01797

Test Identification	River Station	Q (cfs)	Reach Length (ft)	Cumulative Channel Length (ft)	Minimum Channel Elevation (ft)	WSE (ft)	Depth (ft)	Flow Area (ft ²)	Top Width, Tw (ft)	Velocity (ft/s)	Shear Stress (lb/ft ²)
W14	14.48	12	4.68	151.97	97.2318	98.0878	0.856	10.7249	15.3596	1.1189	0.009027
W14	14.0366	12	4.68	147.29	97.2241	98.0871	0.863	10.8277	15.4188	1.1083	0.00884
W14	13.5858	12	2.3	142.61	97.2198	98.0863	0.8665	10.9172	15.4312	1.0992	0.008674
W14	13.3636	12	2.3	140.32	97.2178	98.0693	0.8515	8.1432	15.3361	1.4736	0.017228
W14	13.1411	12	4.68	138.02	97.2158	98.0786	0.8628	10.8987	15.3975	1.101	0.008703
W14	12.7077	12	4.68	133.34	97.2021	98.0741	0.8719	10.0838	15.3352	1.19	0.010407
W14	12.2706	12	2.3	128.66	97.1834	98.0726	0.8892	10.0419	15.2989	1.195	0.010498
W14	12.0557	12	2.3	126.37	97.2083	98.0568	0.8485	7.8897	15.2069	1.521	0.018486
W14	11.833	12	4.68	124.07	97.1662	98.0673	0.9011	10.6416	15.2767	1.1277	0.009174
W14	11.3912	12	4.68	119.39	97.1513	98.0666	0.9153	10.7597	15.2308	1.1153	0.008934
W14	10.9513	12	2.3	114.71	97.1404	98.0657	0.9253	10.7744	15.173	1.1138	0.0089
W14	10.7368	12	2.3	112.42	97.1509	98.0451	0.8942	7.7472	15.0972	1.549	0.019253
W14	10.5227	12	5.61	110.12	97.1613	98.0538	0.8925	9.8321	15.2024	1.2205	0.011005
W14	10	12	10.24	104.5	97.1868	98.0554	0.8686	10.8773	15.2077	1.1032	0.008708
W14	9	12	10.52	94.26	97.1975	98.0427	0.8452	8.8891	13.0673	1.35	0.013275
W14	8	12	8.64	83.74	97.1048	98.0312	0.9264	8.0706	11.4986	1.4869	0.01596
W14	7.196	12	2.34	75.1	97.1142	98.0247	0.9105	7.7985	11.3534	1.5388	0.01721
W14	6.97653	12	2.34	72.76	97.1168	97.9737	0.8569	5.4703	11.0543	2.1937	0.039245
W14	6.74727	12	7.87	70.42	97.1194	97.9941	0.8747	7.4093	11.1846	1.6196	0.019293
W14	5.97681	12	7.87	62.55	97.1265	97.9883	0.8618	7.2371	11.2139	1.6581	0.02039
W14	5.24437	12	2.34	54.67	97.0854	97.9887	0.9032	7.7748	11.4023	1.5435	0.017355
W14	5.02615	12	2.34	52.33	97.0732	97.9558	0.8826	5.8444	11.2675	2.0533	0.033849
W14	4.7991	12	7.86	49.99	97.0684	97.9725	0.9041	7.7204	11.3635	1.5543	0.017619
W14	4.03405	12	7.89	42.13	97.0559	97.9694	0.9135	7.7711	11.2958	1.5442	0.017328
W14	3.29177	12	2.34	34.24	97.0531	97.9642	0.9111	7.6071	11.3397	1.5775	0.018219
W14	3.06804	12	2.34	31.9	97.0524	97.9289	0.8765	5.6815	11.1757	2.1121	0.036062
W14	2.85952	12	7.87	29.56	97.0498	97.9478	0.8979	7.6748	11.3033	1.5636	0.017837
W14	2.14792	12	7.87	21.68	97.0375	97.9439	0.9064	7.667	11.3105	1.5651	0.017881
W14	1.4504	12	2.34	13.81	97.047	97.938	0.891	7.4623	11.247	1.6081	0.019002

Test Identification	River Station	Q (cfs)	Reach Length (ft)	Cumulative Channel Length (ft)	Minimum Channel Elevation (ft)	WSE (ft)	Depth (ft)	Flow Area (ft ²)	Top Width, Tw (ft)	Velocity (ft/s)	Shear Stress (lb/ft ²)
W14	1.25113	12	2.34	11.47	97.0513	97.8906	0.8393	5.2361	10.952	2.2918	0.04332
W14	1.05195	12	4.56	9.13	97.0557	97.9135	0.8578	7.2051	11.0733	1.6655	0.020524
W14	0.527431	12	4.56	4.56	97.057	97.9117	0.8547	7.2703	11.1477	1.6505	0.020142
W14	0	12			97.0571	97.91	0.8529	7.3382	11.238	1.6353	0.019763
W14	18	16	2.39	189.25	97.2192	98.2352	1.016	13.3194	16.2131	1.2013	0.009372
W14	17.7749	16	2.39	186.85	97.2248	98.2333	1.0085	12.9552	16.2082	1.235	0.009999
W14	17.5497	16	2.3	184.46	97.2305	98.2319	1.0014	12.7364	16.2092	1.2562	0.010408
W14	17.3338	16	2.3	182.16	97.2359	98.2134	0.9775	9.9029	16.1152	1.6157	0.018801
W14	17.1176	16	4.68	179.87	97.2414	98.2233	0.9819	12.6056	16.1688	1.2693	0.010637
W14	16.6946	16	4.68	175.19	97.2334	98.2226	0.9892	12.7137	16.1811	1.2585	0.010433
W14	16.2737	16	2.3	170.51	97.2183	98.2222	1.0039	12.9618	16.196	1.2344	0.009985
W14	16.0675	16	2.3	168.21	97.2109	98.2072	0.9963	10.4045	16.1139	1.5378	0.016773
W14	15.8385	16	4.7	165.92	97.2137	98.2157	1.002	13.053	16.1468	1.2258	0.009819
W14	15.3726	16	4.66	161.22	97.2287	98.2136	0.9848	12.7519	16.081	1.2547	0.010347
W14	14.9154	16	2.3	156.56	97.2393	98.2117	0.9724	12.5561	16.0368	1.2743	0.010714
W14	14.6975	16	2.3	154.26	97.2355	98.193	0.9575	9.787	15.9556	1.6348	0.019266
W14	14.48	16	4.68	151.97	97.2318	98.2033	0.9715	12.5382	16.0466	1.2761	0.010753
W14	14.0366	16	4.68	147.29	97.2241	98.2025	0.9784	12.6474	16.1041	1.2651	0.010554
W14	13.5858	16	2.3	142.61	97.2198	98.2017	0.9819	12.7375	16.1146	1.2561	0.010384
W14	13.3636	16	2.3	140.32	97.2178	98.1837	0.9659	9.9368	16.0128	1.6102	0.018628
W14	13.1411	16	4.68	138.02	97.2158	98.1936	0.9778	12.7084	16.0769	1.259	0.010434
W14	12.7077	16	4.68	133.34	97.2021	98.1885	0.9864	11.8777	16.0088	1.3471	0.012191
W14	12.2706	16	2.3	128.66	97.1834	98.187	1.0036	11.83	15.9688	1.3525	0.012296
W14	12.0557	16	2.3	126.37	97.2083	98.1706	0.9623	9.6578	15.8701	1.6567	0.019851
W14	11.833	16	4.68	124.07	97.1662	98.1817	1.0155	12.4266	15.9406	1.2876	0.010967
W14	11.3912	16	4.68	119.39	97.1513	98.1809	1.0296	12.5383	15.8906	1.2761	0.010732
W14	10.9513	16	2.3	114.71	97.1404	98.1799	1.0395	12.5489	15.9021	1.275	0.010669
W14	10.7368	16	2.3	112.42	97.1509	98.1582	1.0073	9.4926	15.7832	1.6855	0.020601
W14	10.5227	16	5.61	110.12	97.1613	98.1673	1.006	11.5927	15.8322	1.3802	0.012884

Test Identification	River Station	Q (cfs)	Reach Length (ft)	Cumulative Channel Length (ft)	Minimum Channel Elevation (ft)	WSE (ft)	Depth (ft)	Flow Area (ft ²)	Top Width, Tw (ft)	Velocity (ft/s)	Shear Stress (lb/ft ²)
W14	10	16	10.24	104.5	97.1868	98.1691	0.9824	12.6426	15.8392	1.2656	0.010537
W14	9	16	10.52	94.26	97.1975	98.153	0.9556	10.3691	13.7552	1.543	0.015802
W14	8	16	8.64	83.74	97.1048	98.1377	1.0329	9.3283	12.1246	1.7152	0.019371
W14	7.196	16	2.34	75.1	97.1142	98.1301	1.0159	9.0256	11.9418	1.7727	0.020861
W14	6.97653	16	2.34	72.76	97.1168	98.0722	0.9554	6.586	11.5979	2.4294	0.043605
W14	6.74727	16	7.87	70.42	97.1194	98.0948	0.9754	8.5642	11.7472	1.8682	0.023482
W14	5.97681	16	7.87	62.55	97.1265	98.0883	0.9618	8.3878	11.7951	1.9075	0.02464
W14	5.24437	16	2.34	54.67	97.0854	98.0891	1.0037	8.9494	11.9814	1.7878	0.02132
W14	5.02615	16	2.34	52.33	97.0732	98.0512	0.978	6.9453	11.8185	2.3037	0.038761
W14	4.7991	16	7.86	49.99	97.0684	98.0703	1.0019	8.8589	11.9288	1.8061	0.021817
W14	4.03405	16	7.89	42.13	97.0559	98.0666	1.0107	8.8974	11.8734	1.7983	0.021545
W14	3.29177	16	2.34	34.24	97.0531	98.0606	1.0075	8.7273	11.9064	1.8333	0.022565
W14	3.06804	16	2.34	31.9	97.0524	98.0189	0.9665	6.7108	11.7005	2.3842	0.041934
W14	2.85952	16	7.87	29.56	97.0498	98.0409	0.9911	8.7525	11.8471	1.8281	0.022431
W14	2.14792	16	7.87	21.68	97.0375	98.0363	0.9988	8.7373	11.8602	1.8312	0.022516
W14	1.4504	16	2.34	13.81	97.047	98.0292	0.9822	8.5119	11.7881	1.8797	0.023883
W14	1.25113	16	2.34	11.47	97.0513	97.971	0.9197	6.1349	11.4283	2.608	0.051449
W14	1.05195	16	4.56	9.13	97.0557	98.0014	0.9457	8.2016	11.5943	1.9508	0.02594
W14	0.527431	16	4.56	4.56	97.057	97.9994	0.9424	8.2704	11.6693	1.9346	0.025502
W14	0	16			97.0571	97.9975	0.9404	8.3439	11.7485	1.9176	0.025072
W15	18	8	3.05	189.25	97.2192	97.9321	0.7129	8.6767	14.4257	0.922	0.00644
W15	17.713	8	3.05	186.19	97.2264	97.9288	0.7024	7.9583	14.3974	1.0052	0.007619
W15	17.4257	8	2.26	183.14	97.2336	97.9071	0.6735	5.3657	14.2592	1.4909	0.017176
W15	17.2134	8	2.26	180.89	97.239	97.9083	0.6693	5.6457	10.2363	1.417	0.015754
W15	17	8	6.11	178.63	97.2444	97.9069	0.6625	5.6052	14.23	1.4272	0.015596
W15	16.4541	8	6.11	172.51	97.2248	97.9041	0.6793	5.6161	14.2688	1.4245	0.015487
W15	15.8865	8	2.3	166.4	97.2121	97.9032	0.6911	5.8385	14.3177	1.3702	0.014141
W15	15.6588	8	2.3	164.1	97.2195	97.9032	0.6837	5.9688	10.2137	1.3403	0.013837
W15	15.4307	8	6.11	161.81	97.2268	97.8987	0.6719	5.6454	14.1956	1.4171	0.015273

Test Identification	River Station	Q (cfs)	Reach Length (ft)	Cumulative Channel Length (ft)	Minimum Channel Elevation (ft)	WSE (ft)	Depth (ft)	Flow Area (ft ²)	Top Width, Tw (ft)	Velocity (ft/s)	Shear Stress (lb/ft ²)
W15	14.833	8	6.11	155.69	97.2379	97.8947	0.6568	5.5253	14.1178	1.4479	0.016068
W15	14.2532	8	2.29	149.58	97.2279	97.8919	0.664	5.5453	14.2043	1.4427	0.015933
W15	14.0359	8	2.3	147.28	97.2241	97.8926	0.6685	5.777	10.2139	1.3848	0.014927
W15	13.8154	8	6.11	144.99	97.2218	97.8893	0.6675	5.5742	14.2392	1.4352	0.01575
W15	13.2237	8	6.11	138.87	97.2166	97.8862	0.6696	5.5626	14.2465	1.4382	0.01578
W15	12.6531	8	2.3	132.76	97.1998	97.8774	0.6776	5.1753	14.17	1.5458	0.018638
W15	12.4386	8	2.3	130.46	97.1906	97.878	0.6874	5.3748	10.0817	1.4884	0.017571
W15	12.2238	8	6.11	128.16	97.1814	97.8737	0.6923	5.1755	14.1241	1.5457	0.0186
W15	11.6423	8	6.11	122.05	97.1597	97.8704	0.7107	5.2026	14.1391	1.5377	0.018296
W15	11.065	8	2.3	115.94	97.1402	97.8688	0.7286	5.351	14.0453	1.4951	0.017107
W15	10.8511	8	2.3	113.64	97.1559	97.868	0.7121	5.3975	9.8952	1.4822	0.017332
W15	10.6367	8	6.84	111.34	97.1557	97.8588	0.7031	4.8993	14.0614	1.6329	0.020973
W15	10	8	10.24	104.5	97.1868	97.8741	0.6873	7.9984	14.1865	1.0002	0.007525
W15	9	8	10.52	94.26	97.1975	97.8639	0.6665	6.6467	12.0347	1.2036	0.011299
W15	8	8	10.74	83.74	97.1048	97.8552	0.7504	6.1378	10.4654	1.3034	0.013008
W15	7	8	2.16	73	97.1165	97.78	0.6635	3.5421	9.9751	2.2586	0.039784
W15	6.78821	8	2.34	70.84	97.1189	97.7769	0.658	3.528	9.9666	2.2676	0.040153
W15	6.55892	8	2.34	68.5	97.1215	97.7814	0.6599	3.7993	7.1327	2.1057	0.035384
W15	6.32985	8	10.83	66.16	97.1241	97.7665	0.6424	3.513	9.9277	2.2773	0.040661
W15	5.30521	8	10.83	55.33	97.0888	97.7573	0.6685	3.6726	10.0385	2.1783	0.036744
W15	4.26516	8	2.36	44.5	97.0597	97.7406	0.6809	3.5921	9.9561	2.2271	0.038411
W15	4.03506	8	2.36	42.14	97.0559	97.7462	0.6903	3.9248	7.0856	2.0383	0.032761
W15	3.82106	8	10.83	39.77	97.0548	97.7276	0.6728	3.5297	9.8744	2.2665	0.040036
W15	2.80386	8	10.83	28.94	97.0488	97.7172	0.6684	3.6065	9.9566	2.2182	0.038246
W15	1.81666	8	2.36	18.11	97.039	97.7003	0.6613	3.5014	9.8653	2.2848	0.040865
W15	1.6153	8	2.36	15.75	97.0434	97.7014	0.658	3.6611	7.0315	2.1851	0.038393
W15	1.41426	8	6.69	13.38	97.0478	97.6828	0.635	3.3384	9.7359	2.3964	0.045505
W15	0.777525	8	6.69	6.69	97.0569	97.7129	0.656	5.1261	9.9226	1.5607	0.019234
W15	0	8			97.0571	97.71	0.6529	5.2072	10.071	1.5363	0.018831

Test Identification	River Station	Q (cfs)	Reach Length (ft)	Cumulative Channel Length (ft)	Minimum Channel Elevation (ft)	WSE (ft)	Depth (ft)	Flow Area (ft ²)	Top Width, Tw (ft)	Velocity (ft/s)	Shear Stress (lb/ft ²)
W15	18	12	3.05	189.25	97.2192	98.1067	0.8875	11.2854	15.4504	1.0633	0.008036
W15	17.713	12	3.05	186.19	97.2264	98.1045	0.8781	10.8477	15.4573	1.1062	0.008805
W15	17.4257	12	2.26	183.14	97.2336	98.1031	0.8695	10.6464	15.4622	1.1271	0.009197
W15	17.2134	12	2.26	180.89	97.239	98.0839	0.8449	7.83	15.3388	1.5326	0.018872
W15	17	12	6.11	178.63	97.2444	98.0946	0.8502	10.6648	15.3808	1.1252	0.009149
W15	16.4541	12	6.11	172.51	97.2248	98.0936	0.8688	10.7887	15.4336	1.1123	0.008913
W15	15.8865	12	2.3	166.4	97.2121	98.0932	0.8811	11.1471	15.439	1.0765	0.008265
W15	15.6588	12	2.3	164.1	97.2195	98.0754	0.8559	8.1577	15.3045	1.471	0.017146
W15	15.4307	12	6.11	161.81	97.2268	98.0843	0.8575	10.7539	15.3263	1.1159	0.008963
W15	14.833	12	6.11	155.69	97.2379	98.0822	0.8443	10.5507	15.2769	1.1374	0.009362
W15	14.2532	12	2.29	149.58	97.2279	98.0812	0.8533	10.6818	15.353	1.1234	0.00911
W15	14.0359	12	2.3	147.28	97.2241	98.0623	0.8382	7.8631	15.2722	1.5261	0.018665
W15	13.8154	12	6.11	144.99	97.2218	98.0727	0.8509	10.6567	15.3439	1.1261	0.009159
W15	13.2237	12	6.11	138.87	97.2166	98.0716	0.855	10.7721	15.3539	1.114	0.008934
W15	12.6531	12	2.3	132.76	97.1998	98.0662	0.8664	9.8859	15.2837	1.2139	0.010885
W15	12.4386	12	2.3	130.46	97.1906	98.0468	0.8562	7.506	15.1544	1.5987	0.020735
W15	12.2238	12	6.11	128.16	97.1814	98.0577	0.8763	9.8922	15.2098	1.2131	0.010852
W15	11.6423	12	6.11	122.05	97.1597	98.0581	0.8984	10.5403	15.2188	1.1385	0.009369
W15	11.065	12	2.3	115.94	97.1402	98.0574	0.9172	10.7878	15.1047	1.1124	0.008862
W15	10.8511	12	2.3	113.64	97.1559	98.0356	0.8796	7.6312	15.0036	1.5725	0.01991
W15	10.6367	12	6.84	111.34	97.1557	98.0447	0.889	9.7559	15.1241	1.23	0.011189
W15	10	12	10.24	104.5	97.1868	98.0459	0.8591	10.7327	15.1548	1.1181	0.008974
W15	9	12	10.52	94.26	97.1975	98.0327	0.8352	8.7588	13.005	1.3701	0.013717
W15	8	12	10.74	83.74	97.1048	98.0208	0.916	7.9513	11.4374	1.5092	0.016494
W15	7	12	2.16	73	97.1165	98.0132	0.8967	7.665	11.2704	1.5656	0.017877
W15	6.78821	12	2.34	70.84	97.1189	98.0117	0.8928	7.6134	11.2795	1.5762	0.018161
W15	6.55892	12	2.34	68.5	97.1215	97.9685	0.847	5.4123	11.0544	2.2172	0.040222
W15	6.32985	12	10.83	66.16	97.1241	97.9888	0.8647	7.2811	11.1865	1.6481	0.02009
W15	5.30521	12	10.83	55.33	97.0888	97.987	0.8982	7.7114	11.3776	1.5561	0.017676

Test Identification	River Station	Q (cfs)	Reach Length (ft)	Cumulative Channel Length (ft)	Minimum Channel Elevation (ft)	WSE (ft)	Depth (ft)	Flow Area (ft ²)	Top Width, Tw (ft)	Velocity (ft/s)	Shear Stress (lb/ft ²)
W15	4.26516	12	2.36	44.5	97.0597	97.9835	0.9238	7.8595	11.3974	1.5268	0.016919
W15	4.03506	12	2.36	42.14	97.0559	97.9487	0.8928	5.7982	11.1727	2.0696	0.034384
W15	3.82106	12	10.83	39.77	97.0548	97.9654	0.9106	7.6014	11.2829	1.5787	0.018225
W15	2.80386	12	10.83	28.94	97.0488	97.9622	0.9134	7.8296	11.3895	1.5327	0.017068
W15	1.81666	12	2.36	18.11	97.039	97.9567	0.9177	7.7712	11.3828	1.5442	0.017363
W15	1.6153	12	2.36	15.75	97.0434	97.916	0.8726	5.5535	11.1276	2.1608	0.037959
W15	1.41426	12	6.69	13.38	97.0478	97.9352	0.8874	7.4265	11.2277	1.6158	0.019205
W15	0.777525	12	6.69	6.69	97.0569	97.9323	0.8754	7.4609	11.2231	1.6084	0.019008
W15	0	12			97.0571	97.93	0.8729	7.5643	11.3547	1.5864	0.018478
W15	18	16	3.05	189.25	97.2192	98.2164	0.9973	13.0163	16.1002	1.2292	0.009893
W15	17.713	16	3.05	186.19	97.2264	98.214	0.9875	12.5746	16.0982	1.2724	0.010722
W15	17.4257	16	2.26	183.14	97.2336	98.2124	0.9788	12.371	16.1076	1.2934	0.011134
W15	17.2134	16	2.26	180.89	97.239	98.1918	0.9528	9.5188	15.9833	1.6809	0.020613
W15	17	16	6.11	178.63	97.2444	98.2032	0.9588	12.3711	16.0395	1.2933	0.011112
W15	16.4541	16	6.11	172.51	97.2248	98.2021	0.9773	12.4987	16.0731	1.2801	0.010867
W15	15.8865	16	2.3	166.4	97.2121	98.2017	0.9896	12.8572	16.0709	1.2444	0.010184
W15	15.6588	16	2.3	164.1	97.2195	98.1821	0.9626	9.8241	15.9296	1.6286	0.019152
W15	15.4307	16	6.11	161.81	97.2268	98.1919	0.9651	12.4363	15.9602	1.2866	0.010974
W15	14.833	16	6.11	155.69	97.2379	98.1895	0.9516	12.2236	15.916	1.3089	0.01141
W15	14.2532	16	2.29	149.58	97.2279	98.1884	0.9605	12.3617	15.99	1.2943	0.011136
W15	14.0359	16	2.3	147.28	97.2241	98.1677	0.9436	9.5054	15.8978	1.6833	0.020668
W15	13.8154	16	6.11	144.99	97.2218	98.179	0.9572	12.3215	15.9742	1.2985	0.011222
W15	13.2237	16	6.11	138.87	97.2166	98.1779	0.9613	12.4363	15.9817	1.2866	0.010986
W15	12.6531	16	2.3	132.76	97.1998	98.1716	0.9717	11.5293	15.9029	1.3878	0.01308
W15	12.4386	16	2.3	130.46	97.1906	98.1508	0.9602	9.1145	15.7656	1.7555	0.022733
W15	12.2238	16	6.11	128.16	97.1814	98.1625	0.9811	11.5189	15.8244	1.389	0.013087
W15	11.6423	16	6.11	122.05	97.1597	98.163	1.0033	12.1697	15.8242	1.3147	0.011526
W15	11.065	16	2.3	115.94	97.1402	98.1623	1.0221	12.4081	15.7956	1.2895	0.010953
W15	10.8511	16	2.3	113.64	97.1559	98.1381	0.9822	9.2034	15.6491	1.7385	0.022138

Test Identification	River Station	Q (cfs)	Reach Length (ft)	Cumulative Channel Length (ft)	Minimum Channel Elevation (ft)	WSE (ft)	Depth (ft)	Flow Area (ft ²)	Top Width, Tw (ft)	Velocity (ft/s)	Shear Stress (lb/ft ²)
W15	10.6367	16	6.84	111.34	97.1557	98.1481	0.9924	11.3502	15.7239	1.4097	0.013526
W15	10	16	10.24	104.5	97.1868	98.1496	0.9628	12.3338	15.7306	1.2972	0.011174
W15	9	16	10.52	94.26	97.1975	98.1326	0.9351	10.0886	13.6275	1.586	0.016869
W15	8	16	10.74	83.74	97.1048	98.1161	1.0113	9.068	11.9977	1.7645	0.020727
W15	7	16	2.16	73	97.1165	98.1068	0.9903	8.7439	11.7862	1.8298	0.022501
W15	6.78821	16	2.34	70.84	97.1189	98.105	0.9861	8.6902	11.7996	1.8411	0.022822
W15	6.55892	16	2.34	68.5	97.1215	98.0528	0.9313	6.3645	11.53	2.514	0.047378
W15	6.32985	16	10.83	66.16	97.1241	98.0768	0.9527	8.2866	11.6885	1.9308	0.025441
W15	5.30521	16	10.83	55.33	97.0888	98.0749	0.9861	8.7338	11.8849	1.832	0.02264
W15	4.26516	16	2.36	44.5	97.0597	98.0708	1.0111	8.8766	11.9112	1.8025	0.021805
W15	4.03506	16	2.36	42.14	97.0559	98.0265	0.9706	6.686	11.6353	2.393	0.042419
W15	3.82106	16	10.83	39.77	97.0548	98.0472	0.9924	8.5443	11.7734	1.8726	0.023777
W15	2.80386	16	10.83	28.94	97.0488	98.0434	0.9946	8.7737	11.8645	1.8236	0.022457
W15	1.81666	16	2.36	18.11	97.039	98.0365	0.9975	8.6991	11.8581	1.8393	0.022898
W15	1.6153	16	2.36	15.75	97.0434	97.982	0.9386	6.3008	11.5199	2.5394	0.048836
W15	1.41426	16	6.69	13.38	97.0478	98.0094	0.9616	8.2765	11.6685	1.9332	0.025637
W15	0.777525	16	6.69	6.69	97.0569	98.0057	0.9488	8.3012	11.6604	1.9274	0.025478
W15	0	16			97.0571	98.003	0.9459	8.4086	11.7806	1.9028	0.024846

APPENDIX D STATISTICAL DATA

Table D.1: Model Parameters

Data Point	Test Number	Q (cfs)	Bend Location	P1	P2	P3	P4	P5	P6	P7
				$L_{arc}/L_{proj,w}$	y/h_w	$T_w/L_{proj,cw}$	$L_{proj,cw}/L_{cw}$	A_w/A_c	R_c/T_w	T_w/y
1	W01	8	Upstream	4.102	0.870	3.456	1.000	0.264	2.715	21.304
2	W01	8	Downstream	5.947	0.800	3.345	1.000	0.255	6.516	16.195
3	W01	12	Upstream	4.102	1.109	3.683	1.000	0.238	2.548	17.813
4	W01	12	Downstream	5.947	1.059	3.600	1.000	0.250	6.056	13.161
5	W01	16	Upstream	4.102	1.259	3.850	1.000	0.204	2.437	16.405
6	W01	16	Downstream	5.947	1.174	3.772	1.000	0.218	5.779	12.435
7	W02	8	Upstream	5.122	0.860	3.495	1.000	0.263	2.685	21.796
8	W02	8	Downstream	8.421	0.790	3.327	1.000	0.254	6.551	16.305
9	W02	12	Upstream	5.122	1.048	3.613	1.000	0.255	2.597	18.497
10	W02	12	Downstream	8.421	1.005	2.841	1.000	0.267	7.674	10.938
11	W02	16	Upstream	5.122	1.198	3.784	1.000	0.217	2.480	16.940
12	W02	16	Downstream	8.421	1.084	3.292	1.000	0.242	6.621	11.762
13	W03	8	Upstream	3.408	0.898	3.502	1.000	0.265	2.680	20.923
14	W03	8	Downstream	4.763	0.865	3.400	1.000	0.259	6.410	15.220
15	W03	12	Upstream	3.408	1.143	3.729	1.000	0.229	2.516	17.493
16	W03	12	Downstream	4.763	1.128	3.705	1.000	0.230	5.884	12.720
17	W03	16	Upstream	3.408	1.280	3.880	1.000	0.200	2.418	16.252
18	W03	16	Downstream	4.763	1.213	3.833	1.000	0.209	5.687	12.233
19	W04	8	Upstream	3.401	0.811	6.449	1.000	0.102	2.707	22.928
20	W04	8	Downstream	5.899	0.826	6.341	1.000	0.078	6.488	15.748
21	W04	12	Upstream	3.401	1.050	6.734	1.000	0.110	2.592	18.497
22	W04	12	Downstream	5.899	1.050	6.778	1.000	0.092	6.070	13.239
23	W04	16	Upstream	3.401	1.208	7.060	1.000	0.093	2.473	16.844
24	W04	16	Downstream	5.899	1.192	7.182	1.000	0.078	5.729	12.355
25	W05	8	Upstream	4.100	0.808	6.446	1.000	0.102	2.708	23.002
26	W05	8	Downstream	7.622	0.822	6.334	1.000	0.077	6.495	15.817
27	W05	12	Upstream	4.100	1.079	6.795	1.000	0.106	2.569	18.155

Data Point	Test Number	Q (cfs)	Bend Location	P1	P2	P3	P4	P5	P6	P7
				$L_{arc}/L_{proj,w}$	y/h_w	$T_w/L_{proj,cw}$	$L_{proj,cw}/L_{cw}$	A_w/A_c	R_c/T_w	T_w/y
28	W05	12	Downstream	7.622	1.109	6.942	1.000	0.086	5.927	12.836
29	W05	16	Upstream	4.100	1.236	7.113	1.000	0.090	2.454	16.599
30	W05	16	Downstream	7.622	1.249	7.338	1.000	0.074	5.607	12.054
31	W06	8	Upstream	3.403	0.840	4.428	1.000	0.190	2.693	22.241
32	W06	8	Downstream	5.898	0.826	4.318	1.000	0.172	6.488	15.753
33	W06	12	Upstream	3.403	1.074	4.639	1.000	0.183	2.570	18.239
34	W06	12	Downstream	5.898	1.043	4.395	1.000	0.178	6.374	12.695
35	W06	16	Upstream	3.403	1.216	4.839	1.000	0.157	2.464	16.795
36	W06	16	Downstream	5.898	1.137	4.780	1.000	0.159	5.861	12.666
37	W07	8	Upstream	4.102	0.841	4.421	1.000	0.190	2.697	22.198
38	W07	8	Downstream	7.620	0.826	4.344	1.000	0.172	6.449	15.839
39	W07	12	Upstream	4.102	1.078	4.641	1.000	0.182	2.569	18.166
40	W07	12	Downstream	7.620	1.073	4.666	1.000	0.172	6.004	13.101
41	W07	16	Upstream	4.102	1.211	4.827	1.000	0.158	2.470	16.819
42	W07	16	Downstream	7.620	1.156	4.824	1.000	0.156	5.807	12.572
43	W08	8	Upstream	3.404	0.807	6.187	0.866	0.106	2.699	23.117
44	W08	8	Downstream	5.895	0.821	5.971	0.866	0.084	6.462	15.918
45	W08	12	Upstream	3.404	1.063	6.467	0.866	0.112	2.582	18.342
46	W08	12	Downstream	5.895	1.073	6.417	0.866	0.096	6.013	13.084
47	W08	16	Upstream	3.404	1.226	6.787	0.866	0.094	2.460	16.690
48	W08	16	Downstream	5.895	1.218	6.803	0.866	0.081	5.672	12.220
49	W09	8	Upstream	4.103	0.805	6.187	0.866	0.106	2.699	23.171
50	W09	8	Downstream	7.617	0.822	5.973	0.866	0.084	6.460	15.901
51	W09	12	Upstream	4.103	1.052	6.446	0.866	0.113	2.590	18.471
52	W09	12	Downstream	7.617	1.064	6.389	0.866	0.097	6.040	13.135
53	W09	16	Upstream	4.103	1.219	6.772	0.866	0.095	2.465	16.745
54	W09	16	Downstream	7.617	1.216	6.795	0.866	0.081	5.678	12.219
55	W10	8	Upstream	3.400	0.837	4.419	0.866	0.185	2.700	22.277

Data Point	Test Number	Q (cfs)	Bend Location	P1	P2	P3	P4	P5	P6	P7
				$L_{arc}/L_{proj,w}$	y/h_w	$T_w/L_{proj,cw}$	$L_{proj,cw}/L_{cw}$	A_w/A_c	R_c/T_w	T_w/y
56	W10	8	Downstream	5.899	0.828	4.299	0.866	0.165	6.524	15.633
57	W10	12	Upstream	3.400	1.086	4.657	0.866	0.176	2.562	18.092
58	W10	12	Downstream	5.899	1.070	4.656	0.866	0.166	6.025	13.090
59	W10	16	Upstream	3.400	1.242	4.878	0.866	0.150	2.446	16.568
60	W10	16	Downstream	5.899	1.205	4.917	0.866	0.142	5.704	12.274
61	W11	8	Upstream	4.100	0.843	4.401	0.866	0.185	2.711	22.021
62	W11	8	Downstream	7.620	0.831	4.316	0.866	0.166	6.499	15.635
63	W11	12	Upstream	4.100	1.108	4.678	0.866	0.172	2.550	17.812
64	W11	12	Downstream	7.620	1.118	4.757	0.866	0.157	5.896	12.801
65	W11	16	Upstream	4.100	1.243	4.870	0.866	0.150	2.450	16.524
66	W11	16	Downstream	7.620	1.215	4.942	0.866	0.141	5.675	12.240
67	W12	8	Upstream	3.399	0.878	3.470	0.866	0.260	2.703	21.205
68	W12	8	Downstream	5.900	0.841	3.355	0.866	0.254	6.455	15.549
69	W12	12	Upstream	3.399	1.107	3.683	0.866	0.235	2.547	17.855
70	W12	12	Downstream	5.900	1.060	3.584	0.866	0.246	6.042	13.179
71	W12	16	Upstream	3.399	1.271	3.866	0.866	0.199	2.426	16.312
72	W12	16	Downstream	5.900	1.218	3.818	0.866	0.205	5.672	12.217
73	W13	8	Upstream	4.100	0.874	3.459	0.866	0.260	2.712	21.243
74	W13	8	Downstream	7.620	0.841	3.338	0.866	0.254	6.487	15.462
75	W13	12	Upstream	4.100	1.072	3.639	0.866	0.244	2.578	18.204
76	W13	12	Downstream	7.620	1.027	3.524	0.866	0.256	6.146	13.367
77	W13	16	Upstream	4.100	1.241	3.828	0.866	0.205	2.451	16.552
78	W13	16	Downstream	3.400	1.200	3.097	0.866	0.272	5.726	12.286
79	W14	8	Upstream	5.900	0.879	4.439	0.966	0.170	2.919	19.610
80	W14	8	Downstream	3.400	0.844	2.741	0.966	0.396	5.800	17.238
81	W14	12	Upstream	5.900	1.121	5.115	0.966	0.155	2.533	17.722
82	W14	12	Downstream	3.400	1.107	2.684	0.966	0.351	5.924	12.864
83	W14	16	Upstream	7.620	1.270	4.712	0.966	0.157	2.426	16.338

Data Point	Test Number	Q (cfs)	Bend Location	P1	P2	P3	P4	P5	P6	P7
				$L_{arc}/L_{proj,w}$	y/h_w	$T_w/L_{proj,cw}$	$L_{proj,cw}/L_{cw}$	A_w/A_c	R_c/T_w	T_w/y
84	W14	16	Downstream	5.900	1.224	3.891	0.966	0.202	5.657	12.186
85	W15	8	Upstream	4.100	0.889	3.466	0.966	0.264	2.700	20.977
86	W15	8	Downstream	7.620	0.858	3.404	0.966	0.254	6.466	15.208
87	W15	12	Upstream	4.100	1.110	3.674	0.966	0.237	2.547	17.796
88	W15	12	Downstream	7.620	1.116	3.718	0.966	0.229	5.921	12.768
89	W15	16	Upstream	4.100	1.247	3.826	0.966	0.206	2.446	16.501
90	W15	16	Downstream	7.620	1.214	3.866	0.966	0.205	5.694	12.211

Table D.2: Velocity Terms

Data Point	Test Number	Q (cfs)	Bend Location	MVR_{center}	MVR_{inner}	MVR_{tip}	V_{r-tip}	$V_{r-inner}$
1	W01	8	Upstream	1.302	1.370	1.186	0.891	1.143
2	W01	8	Downstream	1.670	1.461	1.452	1.048	1.141
3	W01	12	Upstream	1.270	1.433	1.189	0.962	1.240
4	W01	12	Downstream	1.751	1.553	1.488	1.153	1.291
5	W01	16	Upstream	1.251	1.451	1.125	0.941	1.214
6	W01	16	Downstream	1.697	1.615	1.593	1.195	1.278
7	W02	8	Upstream	1.368	0.000	1.225	1.002	0.000
8	W02	8	Downstream	1.652	1.252	1.377	1.065	0.957
9	W02	12	Upstream	1.297	0.000	1.182	0.932	0.000
10	W02	12	Downstream	1.541	1.316	1.391	1.031	0.964
11	W02	16	Upstream	1.282	0.000	1.250	0.988	0.000
12	W02	16	Downstream	1.753	1.452	1.590	1.126	0.988
13	W03	8	Upstream	1.321	1.187	1.355	1.135	1.017
14	W03	8	Downstream	1.706	1.419	1.509	1.246	1.192
15	W03	12	Upstream	1.297	1.284	1.463	1.284	1.149
16	W03	12	Downstream	1.632	1.444	1.465	1.339	1.320
17	W03	16	Upstream	1.275	1.502	1.111	0.989	1.293
18	W03	16	Downstream	1.678	1.554	1.442	1.198	1.306
19	W04	8	Upstream	1.093	1.342	1.095	1.008	1.236
20	W04	8	Downstream	1.288	1.145	1.242	1.229	1.133
21	W04	12	Upstream	1.210	1.332	1.160	1.032	1.267
22	W04	12	Downstream	1.356	1.279	1.174	1.121	1.215
23	W04	16	Upstream	1.220	1.312	1.148	1.071	1.226
24	W04	16	Downstream	1.382	1.329	1.255	1.177	1.246
25	W05	8	Upstream	1.117	1.304	1.078	0.988	1.196
26	W05	8	Downstream	1.187	1.128	1.237	1.225	1.047
27	W05	12	Upstream	1.152	1.307	1.107	1.034	1.278

Data Point	Test Number	Q (cfs)	Bend Location	MVR_{center}	MVR_{inner}	MVR_{tip}	V_{r-tip}	$V_{r-inner}$
28	W05	12	Downstream	1.283	1.201	1.122	1.194	1.223
29	W05	16	Upstream	1.252	1.362	1.161	1.091	1.304
30	W05	16	Downstream	1.520	1.332	1.345	1.369	1.308
31	W06	8	Upstream	1.203	1.271	1.189	0.961	1.136
32	W06	8	Downstream	1.467	1.236	1.268	1.135	1.076
33	W06	12	Upstream	1.277	1.461	1.187	1.000	1.336
34	W06	12	Downstream	1.482	1.408	1.308	1.143	1.207
35	W06	16	Upstream	1.268	1.466	1.226	1.028	1.261
36	W06	16	Downstream	1.426	1.491	1.320	1.071	1.209
37	W07	8	Upstream	1.302	1.351	1.178	0.983	1.232
38	W07	8	Downstream	1.540	1.228	1.383	1.247	1.082
39	W07	12	Upstream	1.239	1.456	1.101	1.000	1.262
40	W07	12	Downstream	1.436	1.279	1.229	1.155	1.205
41	W07	16	Upstream	1.267	1.480	1.142	1.012	1.249
42	W07	16	Downstream	1.553	1.433	1.356	1.172	1.238
43	W08	8	Upstream	1.157	1.264	1.086	0.952	1.131
44	W08	8	Downstream	1.436	1.345	1.261	1.178	1.256
45	W08	12	Upstream	1.213	1.377	1.122	1.044	1.280
46	W08	12	Downstream	1.275	1.122	1.082	1.044	1.140
47	W08	16	Upstream	1.172	1.345	1.120	1.063	1.245
48	W08	16	Downstream	1.409	1.307	1.324	1.238	1.289
49	W09	8	Upstream	1.140	1.350	1.099	1.003	1.232
50	W09	8	Downstream	1.320	1.161	1.211	1.201	1.099
51	W09	12	Upstream	1.170	1.307	1.102	1.013	1.239
52	W09	12	Downstream	1.379	1.150	1.224	1.222	1.159
53	W09	16	Upstream	1.179	1.323	1.094	1.007	1.222
54	W09	16	Downstream	1.447	1.367	1.228	1.199	1.285
55	W10	8	Upstream	1.247	1.358	1.205	1.003	1.213
56	W10	8	Downstream	1.548	1.334	1.513	1.281	1.152

Data Point	Test Number	Q (cfs)	Bend Location	MVR_{center}	MVR_{inner}	MVR_{tip}	V_{r-tip}	$V_{r-inner}$
57	W10	12	Upstream	1.260	1.284	1.099	0.988	1.195
58	W10	12	Downstream	1.485	1.417	1.326	1.211	1.264
59	W10	16	Upstream	1.250	1.409	1.180	1.089	1.299
60	W10	16	Downstream	1.543	1.499	1.511	1.313	1.313
61	W11	8	Upstream	1.201	1.315	1.164	0.950	1.200
62	W11	8	Downstream	1.518	1.354	1.438	1.282	1.177
63	W11	12	Upstream	1.260	1.379	1.140	1.016	1.307
64	W11	12	Downstream	1.530	1.356	1.449	1.363	1.350
65	W11	16	Upstream	1.256	1.364	1.107	1.020	1.261
66	W11	16	Downstream	1.656	1.481	1.559	1.327	1.365
67	W12	8	Upstream	1.286	1.328	1.231	0.967	1.151
68	W12	8	Downstream	1.747	1.449	1.568	1.254	1.224
69	W12	12	Upstream	1.256	1.371	1.159	0.987	1.226
70	W12	12	Downstream	1.597	1.479	1.569	1.244	1.275
71	W12	16	Upstream	1.258	1.408	1.251	1.039	1.228
72	W12	16	Downstream	1.674	1.643	1.559	1.341	1.341
73	W13	8	Upstream	1.258	1.260	1.188	0.943	1.061
74	W13	8	Downstream	1.566	1.253	1.466	1.204	1.029
75	W13	12	Upstream	1.211	1.274	1.141	0.909	1.031
76	W13	12	Downstream	1.449	1.441	1.363	1.094	1.157
77	W13	16	Upstream	1.376	1.350	1.243	0.997	1.108
78	W13	16	Downstream	1.755	1.639	1.572	1.277	1.329
79	W14	8	Upstream	1.274	1.397	1.183	0.977	1.219
80	W14	8	Downstream	1.695	1.473	1.527	1.247	1.257
81	W14	12	Upstream	1.276	1.367	1.145	0.990	1.250
82	W14	12	Downstream	1.560	1.518	1.410	1.274	1.398
83	W14	16	Upstream	1.317	1.425	1.151	0.984	1.212
84	W14	16	Downstream	1.611	1.516	1.593	1.287	1.339
85	W15	8	Upstream	1.346	1.463	1.241	0.964	1.251

Data Point	Test Number	Q (cfs)	Bend Location	MVR_{center}	MVR_{inner}	MVR_{tip}	V_{r-tip}	$V_{r-inner}$
86	W15	8	Downstream	1.630	1.227	1.497	1.173	0.998
87	W15	12	Upstream	1.272	1.352	1.115	0.951	1.176
88	W15	12	Downstream	1.433	1.398	1.327	1.212	1.277
89	W15	16	Upstream	1.327	1.351	1.156	0.964	1.143
90	W15	16	Downstream	1.544	1.511	1.450	1.234	1.286

Table D.3: Shear-stress Terms

Data Point	Test Number	Q (cfs)	Bend Location	MTR_{inner}	MTR_{tip}	MTR_{center}	V_{r-tip}	$V_{r-inner}$
1	W01	8	Upstream	1.672	1.458	1.811	1.381	1.541
2	W01	8	Downstream	1.894	2.589	2.991	2.150	1.680
3	W01	12	Upstream	1.881	1.482	1.754	1.337	1.780
4	W01	12	Downstream	2.240	2.404	3.172	2.179	1.798
5	W01	16	Upstream	2.765	1.922	1.844	1.706	1.653
6	W01	16	Downstream	2.605	2.643	2.924	2.122	2.116
7	W02	8	Upstream	0.000	1.690	2.234	1.702	0.000
8	W02	8	Downstream	1.927	2.468	3.091	1.990	1.682
9	W02	12	Upstream	0.000	1.592	2.014	1.295	0.000
10	W02	12	Downstream	1.628	2.016	2.360	1.593	1.251
11	W02	16	Upstream	0.000	1.770	1.833	1.391	0.000
12	W02	16	Downstream	2.103	2.824	2.979	1.910	1.099
13	W03	8	Upstream	1.777	1.942	2.034	1.942	1.839
14	W03	8	Downstream	1.576	2.003	2.466	2.014	1.676
15	W03	12	Upstream	1.678	1.501	1.633	1.576	1.741
16	W03	12	Downstream	1.802	2.279	2.651	2.585	2.019
17	W03	16	Upstream	2.010	1.502	1.893	1.453	1.905
18	W03	16	Downstream	2.393	2.693	2.333	2.292	2.037
19	W04	8	Upstream	2.800	2.761	2.619	1.750	3.272
20	W04	8	Downstream	2.025	1.526	1.559	2.164	3.271
21	W04	12	Upstream	3.173	2.606	2.635	3.042	3.661
22	W04	12	Downstream	2.268	2.096	2.583	2.826	3.120
23	W04	16	Upstream	3.211	2.913	2.633	3.203	3.480
24	W04	16	Downstream	2.114	2.141	2.566	2.388	2.564
25	W05	8	Upstream	3.015	2.814	2.784	3.187	3.573
26	W05	8	Downstream	1.841	1.926	2.080	2.602	2.690
27	W05	12	Upstream	3.156	2.470	2.575	3.156	4.096

Data Point	Test Number	Q (cfs)	Bend Location	MTR_{inner}	MTR_{tip}	MTR_{center}	V_{r-tip}	$V_{r-inner}$
28	W05	12	Downstream	1.578	1.825	2.171	2.960	3.275
29	W05	16	Upstream	3.052	2.902	2.871	3.396	3.577
30	W05	16	Downstream	2.151	2.534	3.070	3.236	2.750
31	W06	8	Upstream	3.005	2.958	5.232	3.135	3.526
32	W06	8	Downstream	2.367	2.397	2.950	2.851	2.686
33	W06	12	Upstream	3.513	2.981	3.176	2.981	4.028
34	W06	12	Downstream	2.000	2.314	2.459	2.534	2.135
35	W06	16	Upstream	3.153	2.806	3.175	2.934	3.017
36	W06	16	Downstream	2.061	2.322	2.581	2.104	1.701
37	W07	8	Upstream	2.975	3.166	3.052	3.321	3.445
38	W07	8	Downstream	2.229	2.475	2.792	3.032	2.466
39	W07	12	Upstream	3.541	2.904	3.827	3.034	3.616
40	W07	12	Downstream	2.097	2.193	2.842	2.674	2.313
41	W07	16	Upstream	3.072	2.991	3.185	2.782	2.803
42	W07	16	Downstream	2.503	2.864	2.808	2.726	2.226
43	W08	8	Upstream	2.679	2.672	2.622	3.075	3.236
44	W08	8	Downstream	2.079	2.629	2.643	3.362	2.975
45	W08	12	Upstream	3.508	2.356	2.487	2.919	4.199
46	W08	12	Downstream	2.140	2.204	2.710	2.873	3.133
47	W08	16	Upstream	3.511	2.558	2.684	2.910	4.051
48	W08	16	Downstream	2.384	2.488	2.362	2.819	3.046
49	W09	8	Upstream	2.823	2.759	2.603	3.113	3.393
50	W09	8	Downstream	2.042	2.205	2.593	3.085	2.691
51	W09	12	Upstream	2.629	2.298	2.410	2.684	3.236
52	W09	12	Downstream	1.891	2.056	2.144	2.961	2.630
53	W09	16	Upstream	2.857	2.577	2.666	2.714	3.189
54	W09	16	Downstream	2.642	2.063	2.563	2.577	3.029
55	W10	8	Upstream	2.883	3.234	3.077	3.329	3.127
56	W10	8	Downstream	2.211	3.033	2.868	3.029	2.459

Data Point	Test Number	Q (cfs)	Bend Location	MTR_{inner}	MTR_{tip}	MTR_{center}	V_{r-tip}	$V_{r-inner}$
57	W10	12	Upstream	2.513	2.637	2.597	2.769	2.881
58	W10	12	Downstream	2.024	2.237	2.405	2.382	2.310
59	W10	16	Upstream	3.059	2.800	2.967	2.794	3.151
60	W10	16	Downstream	2.671	2.782	2.931	2.808	2.697
61	W11	8	Upstream	2.804	2.808	2.797	2.856	3.137
62	W11	8	Downstream	2.344	2.994	3.327	3.572	2.796
63	W11	12	Upstream	2.723	2.650	2.829	2.869	3.113
64	W11	12	Downstream	2.105	2.630	2.812	3.643	2.915
65	W11	16	Upstream	3.194	2.720	3.003	2.732	3.055
66	W11	16	Downstream	2.501	2.965	2.745	2.983	2.681
79	W14	8	Upstream	0.430	0.965	0.998	0.807	0.424
80	W14	8	Downstream	2.167	2.438		2.366	2.103
81	W14	12	Upstream	0.876	1.887	1.060	1.706	0.885
82	W14	12	Downstream	1.866	1.629	2.664	1.763	2.020
83	W14	16	Upstream	1.175	1.128	1.077	1.011	1.084
84	W14	16	Downstream	2.515	2.468	2.665	2.270	2.257
85	W15	8	Upstream	1.145	1.366		1.485	1.245
86	W15	8	Downstream	1.719	1.884	0.527	1.789	1.804
87	W15	12	Upstream	0.997	1.001	1.142	0.923	0.930
88	W15	12	Downstream	1.572	1.358	1.407	1.542	1.785
89	W15	16	Upstream	1.754	1.167	1.443	0.938	1.513
90	W15	16	Downstream	2.027	2.247	2.606	2.053	1.736

APPENDIX E STATISTICAL THEORY

E.1 INTRODUCTION

This appendix is not meant to provide a complete treatise on statistical theory, nevertheless enough information is covered here to provide some explanation to statistical analysis present in the results.

E.2 REGRESSION AND CORRELATION

Regression, in general, uses relationships between one or more variables to provide an approximation of the mean of one of the variables by knowing values of the others (Devore, 1995). Using associations between a set of variables, a mathematical equation is developed to predict the value or condition of one variable given varying values or conditions of multiple predictor variables. In terms of simple linear regression, this mathematical equation takes the form of Equation E.1:

$$Y = \beta_0 + \beta_1x_1 + \beta_2x_2 + \beta_nx_n + \varepsilon \quad \text{Equation E.1}$$

where

- Y = prediction of population mean based on model parameters and an independent, x ;
- $\beta_1, \beta_2, \beta_n$ = change in mean value of Y for a unit change in x_n ;
- β_0 = mean value of Y if all 'x's are 0;
- x = independent variable; and
- ε = **error associated with the difference of the predicted mean and actual observations.**

Exact predictions of a dependent variable based on any model are virtually impossible even when using variables with high degree of association. An error term is included into Equation E.1 to account for error between the actual data and predicted mean using the mathematical model. Figure E.1 shows an example of a simple linear model used to correlate independent x values to dependent y values and the error associated with this correlation.

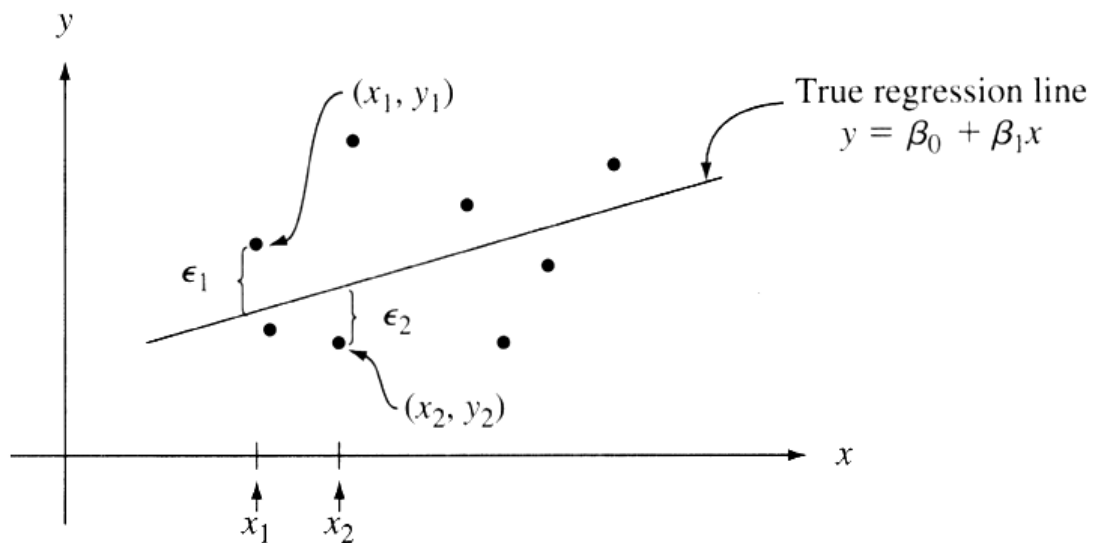


Figure E.1: Example of a Simple Linear Model Showing Error Associated with Predicted Values

Model error, ε , can be computed as the difference between the actual measurements, y , and the model prediction, Y , or $\varepsilon = y - Y$. Clearly, the error can either be negative or positive depending on whether the model overpredicts or underpredicts the actual value of y . For this reason, model error, ε , is typically squared to eliminate the sign. Estimation of the model parameters can then be made by minimizing the sum of the

squared errors associated with the model prediction. This least square estimate is the basis for regression analyses presented in this thesis.

Total error between the actual observed data (y_i) and the computed mean (\bar{y}) from the observed data is sometimes referred to as SS Total. Total error about the mean (\bar{y}) can be subdivided into a portion that is explained by the predictive regression model and a portion that is unexplained by the predictive model. Figure E.2 shows the subdivision of the total error about the mean graphically.

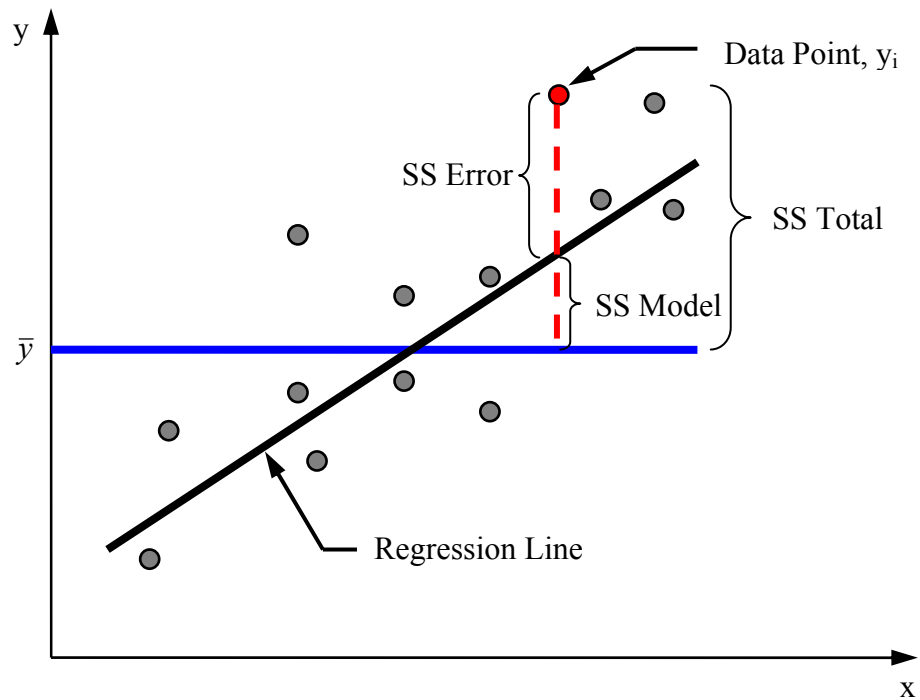


Figure E.2: Subdivision of the Total Error about the Mean (Chapman, 2006)

To estimate the validity of the resulting predictive regression model, the SS Model is compared to the SS Total, the ratio for which is sometimes referred to as the R^2 . The R^2 value increases as the variability explained by the regression model (SS Model) gets large, and the variability unexplained by the regression model, SS Error, gets small.

Note that for each data point there exists a distinct SS Model, SS Error, and SS Total. Like the sample set of data, the collection of errors has a sample mean, standard deviation, and distribution.

E.3 REGRESSION ASSUMPTIONS

Validity of a regression analysis for a specific set of data involves four basic assumptions in regard to the sample set of errors:

1. Linearity: the association between the variables is, in fact, linear, such that the expected error is 0 ($E(\varepsilon_i) = 0$) for all i ;
2. Homoscedasticity: all the errors have the same variance ($\text{Var}(\varepsilon_i) = \sigma_\varepsilon^2$), for all i ;
3. Independence: all errors are independent of each other; and
4. Normality: all errors are normally distributed (ε_i is normally distributed for all i) (Ott and Longnecker, 2001).

While esoteric at first glance, particular tests can be performed to assure each of the assumptions shown above are met.

Assumptions for regression analyses can be generally checked in two ways: 1) by plotting the error (ε_i) sometimes referred to as the residual with respect to the predicted values from the regression equation, and 2) plotting a quantile plot of the residuals which indicates the linearity of the error distribution (Ott and Longnecker, 2001). Linearity can be deduced from the scatter plot of the predicted versus observed plot, however sometimes linearity is difficult to definitively ascertain. Chapman (2006), however, recommends using the plot of the residuals versus the predicted values as a more robust

method to check regression assumptions. When plotted, the residuals should form a band of constant width about 0 (Chapman, 2006). Transformation may be necessary if the residuals do not maintain randomized scatter of constant width about 0. Plotting residuals against the individual x values can be a useful tool as well. Such a plot of residuals versus individual x 's should not have any curvature and constant variances. Linearity can be tested by plotting residuals versus the normal scores (QQ plot). A straight line in this plot indicates a normal distribution, however, transformation may be required if a straight line is not observed.

E.4 OUTLIER ANALYSIS

When data are taken from a natural system, or in a laboratory setting where natural systems are being simulated, there is a chance that collected data may fall outside what is expected or reasonable. Such suspect data might be statistically designated an outlier. Outliers can exist either because of natural random patterns in the tested system, erroneous testing equipment, or problems in the testing procedure. Checks for outliers include: 1) plotting the data identifying those data that fall outside a visible mean, 2) computing a studentized residual which establishes how many standard deviations the particular error is from the mean, 3) computing the R-studentized residual, which is an estimate of what the residual would be if the point was removed from the analysis, or 4) a combination of all three. When a point is an outlier, it tends to pull the regression line towards itself. As a result, the studentized residual might not correctly identify possible outliers. A R-studentized residual is an estimate of the change in the error if the point was removed from the analysis altogether. Once the point is removed, if the change in

error is significant then there is a possibility that the removed point is an outlier. An outlier analysis is best performed through the use of specialized computer software such as Statistical Analysis Software (SAS).

E.5 MODEL SELECTION

Simple linear regression attempts to develop a mathematical correlation between a dependent variable, y , and a single independent variable, x . Selection of an appropriate statistical model in the case of simple linear regression involves knowing what independent variable needs to be associated with a particular dependent variable. An extension of simple linear regression involves the use of multiple independent variables that have some predictive association with a single dependent variable. In all likelihood, research objectives may identify a number of variables that could exert some influence on a specific property or parameter, but at the onset of the research it may not be entirely clear which one or how many of the variables are significant. As a result, it is often desirable to systematically test combinations of variables known to exercise some influence on the dependent variable through the use of statistical principles. Model-selection methods have been developed to methodically test the predictive accuracy of regression equations for all possible combinations of independent variables. Performed manually, model-selection parameters can be tedious if not impossible. Statistical packages such as SAS are generally employed for standard model-selection procedures.

Model-selection methodology can be performed either by 1) testing each variable for significance, while stepping through a specific hierarchy, either forward, backward, or stepwise, or 2) by using a best-subsets selection criterion (Chapman, 2007). A forward

selecting hierarchy begins with the simplest form of regression equation adding one term at a time, comparing the significance of the added variable at each step. Once a variable is added that does not show significance (*i.e.*, the hypothesis test that the added model parameter (β) is 0 can not be rejected) then the selection procedure stops. This method runs the risk of stopping too soon, before all variables are tested. Backwards selection hierarchy begins with the most complicated model and analyzes the level of significance for each variable. At each step, the variable with the most significance (greatest p-value) is eliminated. When none of the variables have significant p-values based on the specified criteria (typically p-value > 0.05) then the procedure stops. Stepwise hierarchy is essentially a hybrid between forward and backward selection criteria where the procedure begins like a forward selection hierarchy and after the second variable is added, the first is re-evaluated.

Best-subsets selection criterion differs from a hierarchy procedure in that instead of systematically stepping through a series of models, best-subsets criteria computes all possible models at once and uses a goodness of fit parameter to evaluate predictive quality. Predictive quality may be based on:

1. maximizing R^2 ;
2. minimizing Mallows' C_p ; or
3. minimizing Akaike Information Criterion (AIC).

As discussed previously, the R^2 value is an estimate of the amount of error that is explained by the regression equations. Ideally, the chosen regression model should have the best overall ability for explanation of the error. However, R^2 can not be used to compare models of different sizes. Once a term is added to a model, the R^2 almost

always increases because more information is used to describe the variability. Mallow's Cp is another model-selection parameter that is commonly used in model selection. Sometimes referred to as an estimate of Total Standardized Expected Squared Prediction Error, Mallow's Cp is an estimate of the squared bias caused by omitting variables from the model. Including all possible parameters in the model is considered an unbiased model, however, since some of the model parameters (β s), may be poorly estimated, the variability of the predictions might be high. Mallow's Cp is an indication of which model has the least amount of prediction variability and, therefore, the model with the smallest Cp is desired.

Akaike Information Criterion is another method for evaluating model selection and is based on relating error variance to a penalty for including additional terms. Like Cp, selection is based on the model with the lowest AIC. Generally, the AIC and the Cp produce similar results, however, judgment based on plots of predicted data and validity of specific variables is required for final model selection. In the analyses provided here, hierarchical procedures were used as a check against the primary model-selection method of best-subset criteria.